Offshore Environment of the ROPME Sea Area after the War-Related Oil Spill-

Results of the 1993-94 Umitaka-Maru Cruises

Offshore Environment of the ROPME Sea Area after the War-Related Oil Spill-

Results of the 1993-94 Umitaka-Maru Cruises

Edited by
A. Otsuki, M. Y. Abdulraheem, and R. M. Reynolds

Terra Scientific Publishing Company, Tokyo

Offshore Environment of the ROPME Sea Area after the War–Related Oil Spill–
Results of the 1993–94 Umitaka-Maru Cruises
Edited by A. Otsuki, M. Y. Abdulraheem, and R. M. Reynolds
ISBN No. 4-88704-123-3

Published by Terra Scientific Publishing Company (TERRAPUB), 2003 Sansei Jiyuugaoka Haimu, 5-27-19 Okusawa, Setagaya-ku, Tokyo 158-0083, Japan.
Tel: +81-3-3718-7500 Fax: +81-3-3718-4406

This book is partly supported by Grant-in-Aid for Publication of Scientific Research Result, Grant-in-Aid for Scientific Research of the Ministry of Education, Science, Sports and Culture of Japan.

Printed in Japan

Preface

The ROPME Sea Area (RSA) is the area surrounded by eight Member States, namely, State of Bahrain, Islamic Republic of Iran, Republic of Iraq, State of Kuwait, Sultanate of Oman, State of Qatar, Kingdom of Saudi Arabia and the United Arab Emirates (U.A.E.). The discovery and large scale exploitation of oil and gas over the past six decades are largely responsible for the immense economic growth and the strategic importance of the ROPME Region. However, with such a growth came the increased rate of demand for natural resources in the area which coincided with the sudden and dramatic changes and boom in the Region.

Coastal habitats have been quickly converted to urban and industrial developments. Major ecological problems have arisen from loss/degradation of coastal habitats, caused by landfilling, dredging and sedimentation. Fisheries also came under significant pressure from over-exploitation of target species. Furthermore, the region is subjected to chronic release and more frequent oil spillages as tanker and ship traffic increased with time.

While Member States were learning how to cope with the environmental pressures of industrial and urban growth, war in the Region brought environmental degradation to catastrophic levels, first during the Iran-Iraq War (1980–1989) and then through the war over Kuwait (1990–1991). The last war was specially hard on the marine environment. About 10 million barrels of crude oil were released into the marine environment and 800 oil wells in the State of Kuwait remained burning for several months emitting huge quantities of pollutants to the atmosphere, while 60 millions of barrels of crude oil gushed from the burning wells creating oil lakes over a large area of desert.

In an attempt to assess the impacts of war and to improve knowledge on the large-scale dynamics of physical, chemical and biological processes in the RSA and their roles in the distribution, fate and flux of pollutants among different ecosystems, the open sea cruises were planned for the Region. The Mt. Mitchell cruise organized by ROPME with the assistance of the US National Oceanic and Atmospheric Administration (NOAA) and in association with the United Nations Intergovernmental Oceanographic Commission (IOC) and UNEP, as part of the international response to study the effects of the massive oil spills and oil fires. This cruise can be considered as the first major attempt to begin proper investigation of the marine condition in our Region with particular consideration for the Environmental catastrophe in the area due to premeditated assault on oil installations in Kuwait and spilling of millions of barrels of crude oil into the Sea Area.

This was followed by the three short cruises of the Tokyo University of Fisheries R/V Umitaka-Maru which were carried out in the inner part of the RSA

during 1993–94. These cruises were conducted under the umbrella ROPME/ UNEP/IOC/JAPAN. The findings reflected a significant efforts in following up the changes in the status of the marine environment with time. The text available hitherto are the results of the cruises which were presented at the International Symposium on the Status of the Marine Environment in the ROPME Sea Area after the 1990-91 Environmental Crisis with special emphasis to the Umitaka-Maru Cruises, Tokyo - Japan, 4–7 December, 1995.

It gives me special pleasure to express ROPME's appreciation to the Tokyo University of Fisheries and their scientists, IOC, UNEP and to the institutes and scientists from the Region who contributed to this excellent work.

Dr. Abdul Rahman Al-Awadi
Executive Secretarv of ROPME

Introduction

An urgent meeting to discuss an international investigation of the impact of the huge amount of spilled crude oil on the marine ecosystem of the Gulf as a result of the then recently terminated Gulf war, was held in Kuwait on 24-27 September 1991. The meeting was organized by the Intergovernmental Oceanographic Commission (IOC) and the Regional Organization for Protection of the Marine Environment (ROPME), in cooperation with the United Nations Environment Programme (UNEP). An Integrated Project Plan for the ROPME sea area was finalized at the meeting (Report of the Meeting of the ROPME-IOC Steering Committee on Oceanographic Cooperation in the ROPME Sea Area, organized in cooperation with UNEP).

Subsequently, IOC-ROPME requested the major IOC member nations to support the implementation of the Integrated Project Plan. The Japanese Government, through the Ministry of Education, Science, Sports and Culture, contacted the Tokyo University of Fisheries. The University decided to send a training/research vessel, the *Umitaka Maru*, to the ROPME sea area to conduct oceanographic surveys, because the activities could be done during training cruises and because the vessel had undertaken a survey cruise in the ROPME sea area in 1969 at the request of the Kuwait Government. This international research project was funded by the Japanese Ministry of Education, Science, Sports and Culture for 3 years, covering the fiscal years 1992-1994.

According to the Integrated Project Plan, the intention of the project was to use ship-based survey to obtain a synoptic view of oceanographic processes and to undertake interdisciplinary studies that would facilitate understanding of recent pollution events, as well as to provide a basis for future regional studies in support of the long-term objectives of ROPME. Also the survey cruises would provide opportunities for regional training and information exchange.

The cruise program had two parts: the synoptic oceanographic program, which was the main component, and a series of site-specific studies to evaluate the impact of the oil spills on the marine environment.

Studies suggested for the oceanographic program included: 1) synoptic-scale CTD surveys for defining baroclinic structure and water mass analysis; 2) investigation of localized physical processes to define exchange and sub-synoptic-scale current patterns in the Strait of Hormuz, NW coast, mid-sea sill, freshwater sources in the northeastern region and Salwa Bay; 3) determination of hydrocarbon loading by sediment interface research, including sediment trap, sediment sampling and hydrocarbon analysis, as well as benthic community sampling for future analysis; 4) biodegradation of hydrocarbons, through benthic sampling and metabolic studies; 5) water column sampling for future chemical

and biological analyses; 6) surveys of hard-bottom coral areas including a survey of offshore islands by diving; and 7) collection and analysis of commercial marine species—shrimp, fish and molluscs.

The first 100-day cruise by the research vessel *Mt. Mitchell* of the US National Oceanographic and Atmospheric Administration was successfully carried out from late February to early June 1992, following the two elements of the Integrated Project Plan. The results were published in a special issue of the *Marine Pollution Bulletin* in 1995.

The *Umitaka Maru* cruises took place in January and December 1993 and December 1994. Although they were planned in a similar manner, including regional training opportunities, each cruise was limited to 12 days because the activities were part of extensive training cruises for cadets. A major problem in these cruises was that the vessel could not enter Iranian territorial waters to take samples, despite diplomatic efforts by ROPME. Table 1 gives a summary of the *Umitaka Maru* cruises.

Dr. Ibrahim A. Alam, formerly associate professor at the Research Institute of King Fahd University of Petroleum and Minerals (now Vice-Mayor of Jeddah City, Kingdom of Saudi Arabia), was a team leader of the ROPME participants during the 3 cruises and made a great contribution to their success.

After these cruises, the "International Symposium on the Status of the Marine Environment in the ROPME Sea Area after the 1990-1991 Environmental Crisis, With Special Reference to the Umitaka-Maru Cruises", was held at the Tokyo University of Fisheries, 4-7 December 1995, with the support of UNEP and the Japanese Ministry of Education, Science, Sports and Culture. There were 31 oral and 16 poster papers presented, with 98 participants including invited speakers (Drs. Scott Fowler, Monaco; C. Michael Reynolds, USA; Charles C. Shepherd, UK; and Friedhelm Krupp, Germany), representatives of UNEP (Dr. Makram Gerges) and IOC (Dr. K. Kitazawa), and the coordinator and a representative of ROPME headquarters. As a result, we decided to publish this book.

The following persons were responsible for the various chapters including peer review:

Chapter 1—Dr. R.M. Reynolds, Brookhaven National Laboratory, USA, and Dr. J. Yoshida, Tokyo University of Fisheries;

Chapter 2—Dr. M. Maeda, Tokyo University of Fisheries, and Dr. L. Al-Omran, Kuwait University;

Chapter 3—Drs. T. Ishimaru, and K. Fujita, Tokyo University of Fisheries;

Chapter 4—Dr. I.A. Alam, Vice-Mayor, Jeddah City, and Dr. A. Otsuki, Tokyo University of Fisheries.

Table 1. Details of the *Umitaka-Maru* Cruises.

Dates	Departure Port	Arrival Port	Number and Status of Partici pants
First Cruise (6 sections, 21 sampling sites) 14-25 Jan. 1993	Dobayy, UAE	Dobayy, UAE	Japanese: 14 including 1 research associate and 7 graduate students. ROPME: 10, of whom 5 from Kuwait and 5 from Saudi Arabia.
Second Cruise (5 sections, 19 sampling sites) 15-26 Dec. 1993	Dobayy, UAE	Manama, Bahrain	Japanese: 18 including 8 graduate students and 3 underwater camera men. ROPME: 15, of whom 6 from Kuwait, 8 from Saudi Arabia and 1 from UAE.
Third Cruise (7 sections, 24 sampling sites) 15-26 Dec. 1994	Abu Dhabi, UAE	Shuwaikh, Kuwait	Japanese: 15 including 8 graduate students. ROPME: 14, of whom 4 from Kuwait, 8 from Saudi Arabia, 1 from UAE and 1 from Oman.

This book is dedicated to the Year of the Ocean 1998.

20 January 1998

Akira Otsuki
Chief Scientist
Department of Ocean Sciences
Tokyo University of Fisheries

Contents

Offshore Environment of the ROPME Sea Area after the War-Related Oil Spill, Eds. A. Otsuki *et al.*, pp. 1–22.

Hydrography in the RSA during the RT/V Umitaka-Maru Cruises

Jiro YOSHIDA[1], Masaji MATSUYAMA[1], Tomoharu SENJYU[2], Takashi ISHIMARU[1], Tsutomu MORINAGA[1], Hideyuki ARAKAWA[1], Akiyoshi KAMATANI[1], Masaru MAEDA[1], Akira OTSUKI[1], Shinya HASHIMOTO[1], Isao KASUGA[3], Yoshio KOIKE[3], Yuji MINE[3], Yoshinobu KURITA[3], Akira KITAZAWA[3], Akira NODA[3], Toshihumi HAYASHI[3], Tadashi MIYAZAKI[3] and Keiko TAKAHASHI[3]

[1]*Department of Ocean Sciences, Tokyo University of Fisheries, 5-7, Konan 4-chome, Minato-ku, Tokyo 108-8477, Japan*
[2]*Department of Fishery Science and Technology, National Fisheries University, 2-7-1, Nagatahonmachi, Shimonoseki, Yamaguchi 759-6595, Japan*
[3]*Research and Training Vessels, Tokyo University of Fisheries, 5-7, Konan 4-chome, Minato-ku, Tokyo 108, Japan*

Abstract—Oceanographic observations in the inner part of ROPME Sea Area (RSA) were carried out at three different periods: (1) Cruise I: January 15–24, 1993 (2) Cruise II: December 15–27, 1993 and (3) Cruise III: December 15–27, 1994. For each of observations, 20 to 25 stations were taken. Major results are summarized as follows:

(1) Temperature is lower and salinity is higher near the southern coast of the RSA. Temperatures are slightly lower in January (Cruise I) than those in December (Cruises II and III), and this should be due to the severe winter time cooling and evaporation in January.

(2) The patterns of horizontal distribution of temperature and salinity are almost identical to the previous results by Brewer and Dyrssen (1985) and Reynolds (1993). In the area near the Strait of Hormuz, low salinity water is found in the surface layer, and seems to extend westward to the inner area of the RSA. This water should have come from the Gulf of Oman.

(3) High salinity water (exceeding 40, in particular exceeding 44 off Bahrain in Cruise II) is often found in the bottom layer near the southern coast of the RSA. This water might be formed by the strong evaporation and winter time cooling inside the RSA.

(4) Surface salinity shows a minimum in the area northeast of Qatar, where is the proposed sinking region of water coming from the Gulf of Oman (Reynolds, 1993).

(5) Vertical cross sections perpendicular to the RSA axis near the Strait of Hormuz indicate the outward (eastward) flow of warmer and more saline water from the RSA to the Gulf of Oman through the Strait of Hormuz.

INTRODUCTION

The water bodies surrounded by United Arab Emirates, Qatar, Bahrain, Saudi Arabia, Kuwait, Iraq and Iran, are sometimes reterred as ROPME (Regional

Organization for the Protection of Marine Environment) Sea Area (abbreviated as RSA) (Fig. 1). The mean depth of the RSA is 25 m and the maximum depth does not exceed 100 m (Sugden, 1963). The RSA is connected to the Gulf of Oman facing towards the Indian Ocean by the narrow Strait of Hormuz.

In spite of the commercial or military importance of the RSA, only a few surveys have been done in this area. Emery (1956) did some pioneering intensive surveys in this area in the summer of 1948, and Brewer and Dyrssen (1985) reported the results of intensive survey by the Woods Hole Oceanographic Institution in the winter of 1976. The Research and Training Vessel (RT/V) Umitaka-Maru, Tokyo University of Fisheries (TUF) also conducted intensive scientific survey with collaboration of KISR (Kuwait Institute for Scientific Research) in the winter of 1968, and the reports are compiled in the Transactions of the Tokyo University of Fisheries (1974).

Most recently, after the environmental crisis in the RSA in 1991, several international programs to study the effects of the oil spill on the environment were implemented. During the period from February to June in 1992, an intensive expedition was conducted on the R/V Mt. Mitchell, operated by the U.S. National Oceanic and Atmospheric Administration (NOAA), from the Gulf of Oman to the far north-west off of the Kuwait coast. This was the first expedition to investigate winter and summer hydrography in the RSA. More than five-hundred CTD

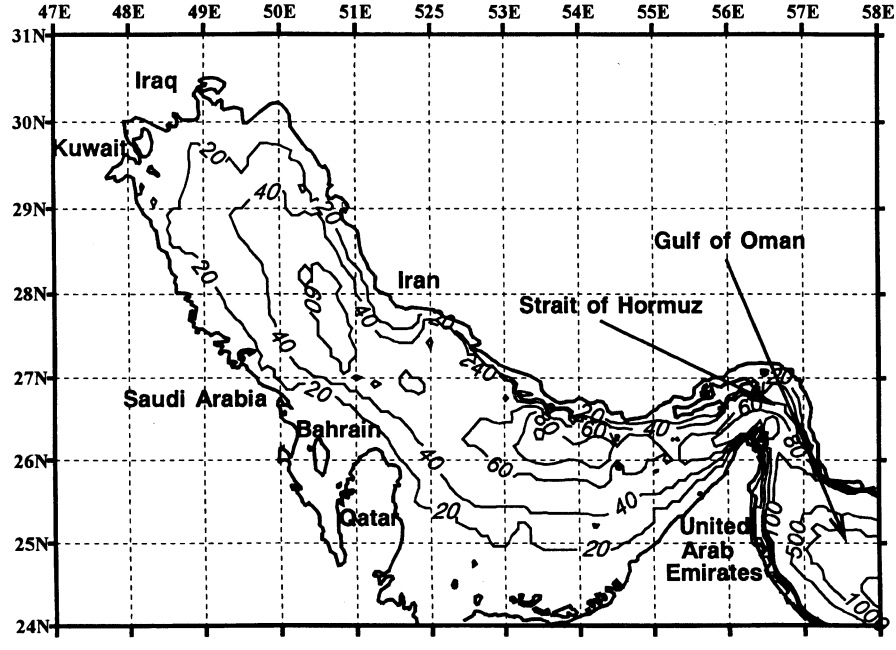

Fig. 1. Map showing the bathymetry of the ROPME Sea Area (RSA). Thin lines show the isobaths contoured at an interval of 20 m.

stations were occupied, some in very shallow areas with less than 10 m depth at mooring stations, seven current meters were deployed (two were not recovered), and thirty-six drifting buoys were deployed for investigating the physical oceanographic conditions in the RSA. Reynolds (1993) summarized the hydrography of this expedition in detail.

These previous investigations all pointed out that physical oceanographic conditions in the RSA are strongly controlled by the relative small input of the fresh water and intensive evaporation in addition to big difference in temperature between summer and winter. As a result, very high salinity waters exceeding 40 are sometimes found at the southern coast of the RSA. The proposed winter circulation process in the RSA is as follows (Reynolds, 1993): In the eastern half of the RSA (from Qatar to the Strait of Hormuz) is density driven with a surface current, having relatively low salinity and high temperature intruding from the Strait of Hormuz and flowing along the Iranian coast to the area off Qatar. The flow stagnates east of Qatar, where a strong evaporation and sinking form a dense bottom flow to the east and it flows out of the Strait of Hormuz. This flow pattern was matched with earlier view of Emery (1956) and Brewer and Dyrssen (1985),

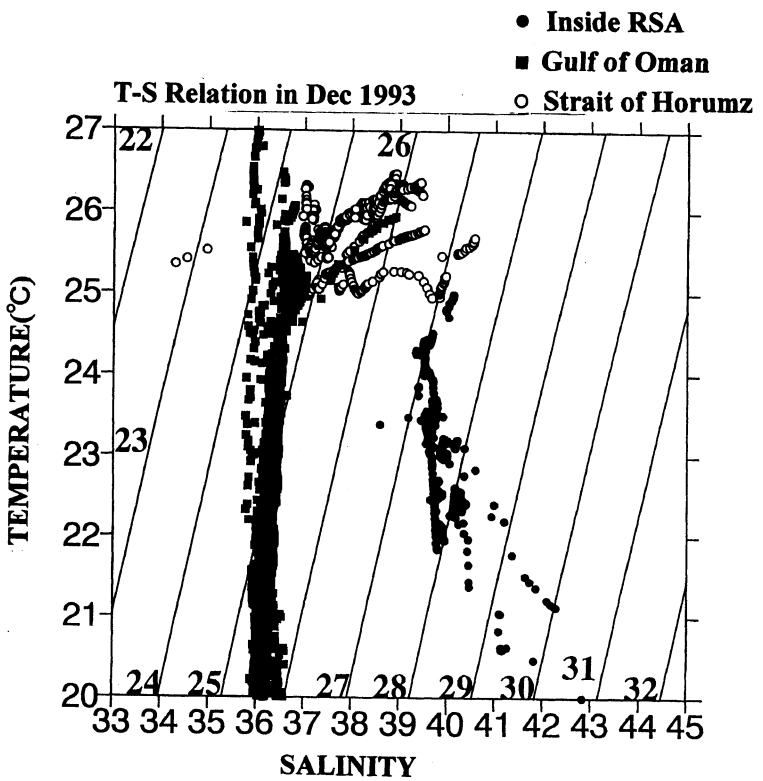

Fig. 2. Temperature-salinity diagram obtained at Umitaka-Maru Cruise II in December 1993.

and traditionally called a Mediterranean type circulation or a "negative estuary" meaning evaporation exceeds fresh water input from rain or river runoff. In the north-western half of the RSA circulation is predominantly wind driven. The surface current flows along both coasts in a southerly direction, and in the central region clockwise or anti-clockwise circulation (depending on the wind condition such as a strong NW wind called the Shamal) will be formed. As a result, the temperature-salinity diagram obtained in the RSA and the Gulf of Oman shows the maximum water temperature at the RSA mouth, and gradual decrease of temperature and increase of salinity (from 36 at the Gulf of Oman to exceeding 40 inside the RSA) by the winter cooling and evaporation (Brewer and Dyrssen, 1985). Temperature-salinity diagram obtained by the Umitaka-Maru cruise in December, 1993 is shown in Fig.2, which depicts the same characteristics as those obtained by Brewer and Dyrssen (1985).

After about a quarter century of interval, the Umitaka-Maru conducted three cruises in winter time from 1993 to 1994 with the scientific collaboration with ROPME countries. Totally, more than 30 people from ROPME countries and more than a hundred people from Japan joined the expedition. This research was widely planned for investigating the physical, chemical and biological conditions of the RSA. In this brief report, physical oceanographic conditions of the RSA are summarized.

OBSERVATION

Oceanographic observations in the RSA were conducted at three different periods: (1) Cruise I: January 15–24, 1993 (2) Cruise II: December 15–27, 1993 and (3) Cruise III: December 15–27, 1994. At each cruise, 20 to 25 stations were occupied after the previous observation by R/V Mt. Mitchell in 1992. However, due to the limitation of the time of observation, some stations made by Mt. Mitchell were not repeated. Stations at each cruise are shown in Fig. 3. At Cruise II, additional stations were occupied at the Strait of Hormuz and the Gulf of Oman to investigate the tidal front formed in this strait and the eddy structure originated from the Gulf. These data are analyzed by Matsuyama *et al.* (1998) and Senjyu *et al.* (1998; in this volume).

Conductivity-Temperature-Depth (CTD) profiler with dissolved oxygen sensor and Rosette Multi Sampler (RMS) was used at each station to measure temperature, salinity and dissolved oxygen structure. However, bottom depths at each station were usually very shallow (at most 100 m), and the response time of the oxygen sensor is too slow to detect the real change in oxygen field in such shallow depths, we did not use oxygen data in the following analysis. Neil Brown Mark IIIB CTD was used at Cruises I and III, and FSI (Falmouth Scientific Institute Inc.) ICTD (Integrated CTD) was used at Cruise II. CTD was lowered slowly to the depth of 3–4 m above bottom, and we sampled waters from three or four different levels while its recovering. Salinity of sample water was determined by using Guildline AUTOSAL or PORTASAL, and was used for calibrating the CTD salinity value.

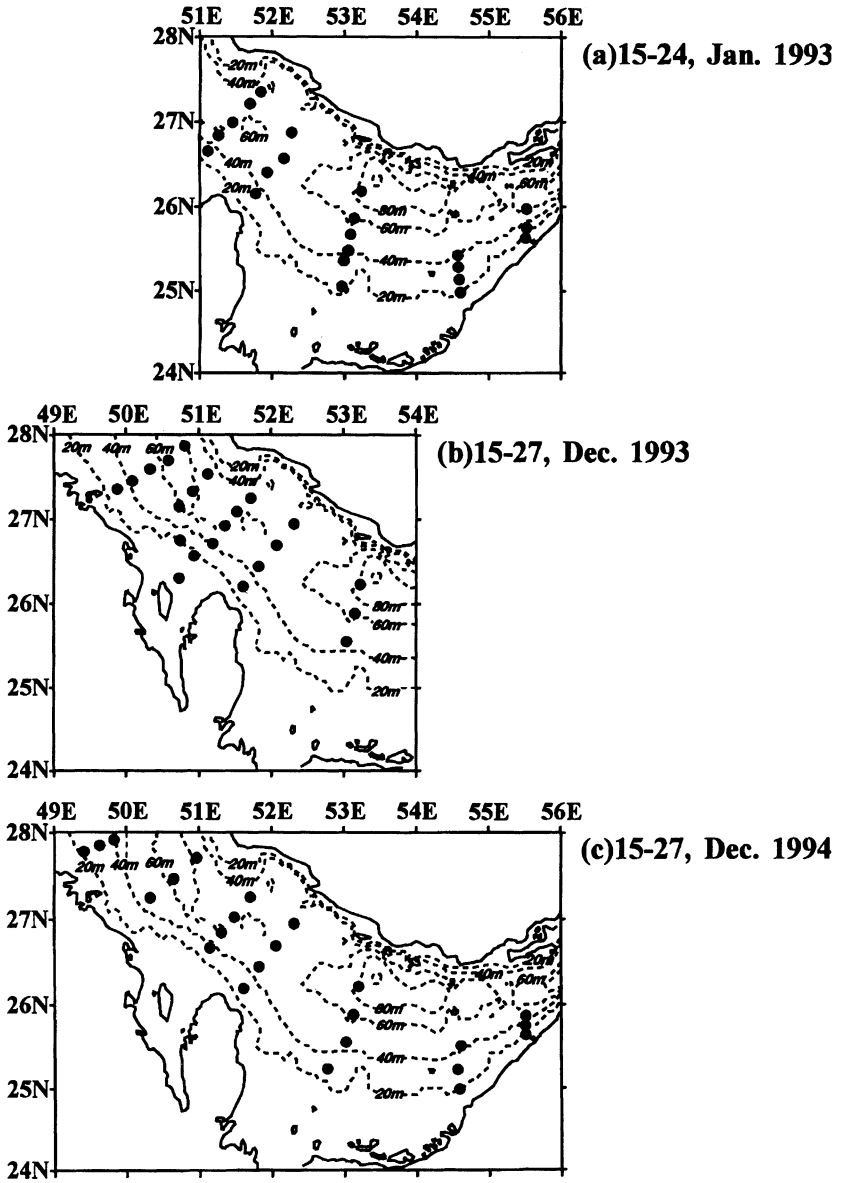

Fig. 3. Map showing occupied stations in (a) Cruise I (15–24, Jan. 1993), (b) Cruise II (15–27, Dec. 1993) and (c) Cruise III (15–27, Dec. 1994). Dashed lines show isobaths at an interval of 20 m. Solid circles show occupied stations.

RESULTS

Horizontal temperature, salinity and sigma-t distributions

Contour lines of temperature, salinity and sigma-t at the water surface obtained in Cruises I, II and III are shown in Fig. 4 (temperature), Fig. 5 (salinity)

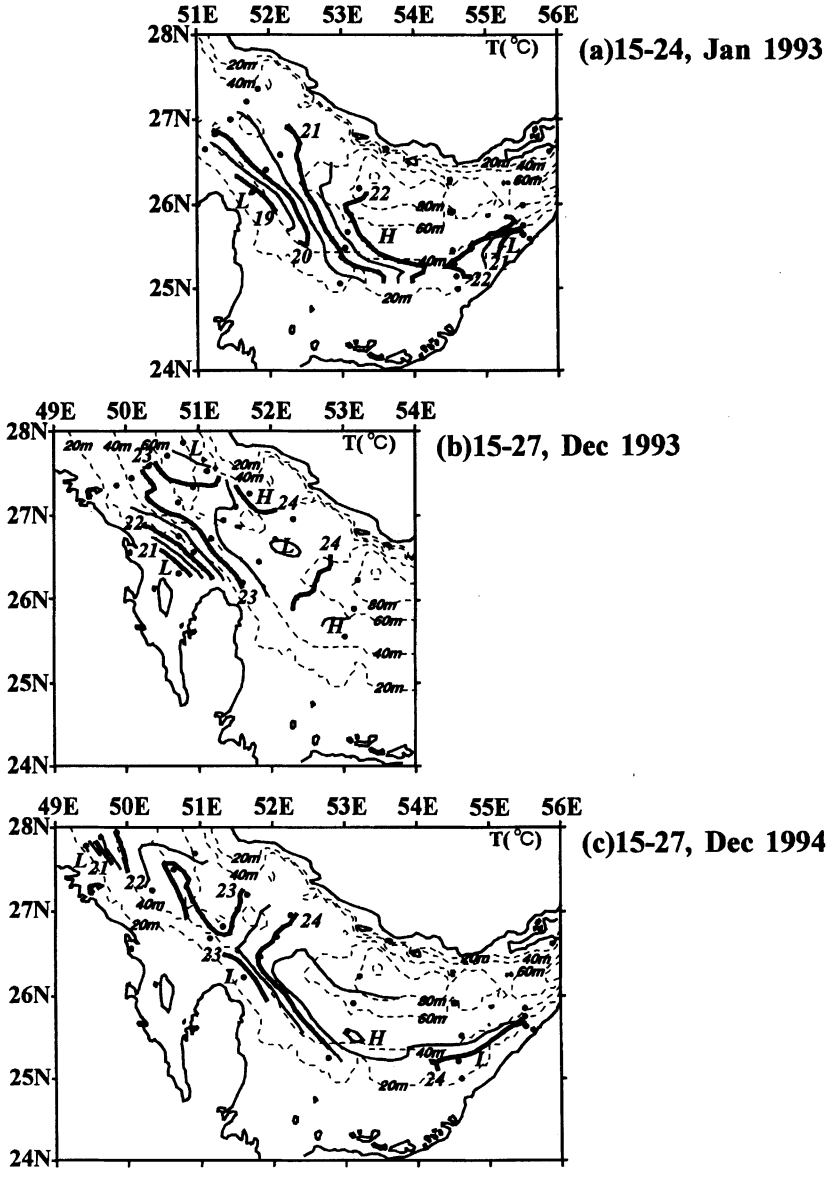

Fig. 4. Horizontal distribution of temperature (contour interval of 0.5°C) in (a) Cruise I (15–24, Jan. 1993), (b) Cruise II (15–27, Dec. 1993) and (c) Cruise III (15–27, Dec. 1994).

and Fig. 6 (sigma-t), respectively. Contour lines are almost parallel along the isobaths near the southern coast of the RSA. Generally, lower temperature and higher salinity exist near the southern coast of the RSA. Temperatures are slightly lower in January (Cruise I) than those obtained in December (Cruise II and Cruise III), and should be due to the fact that winter cooling was strongest in January.

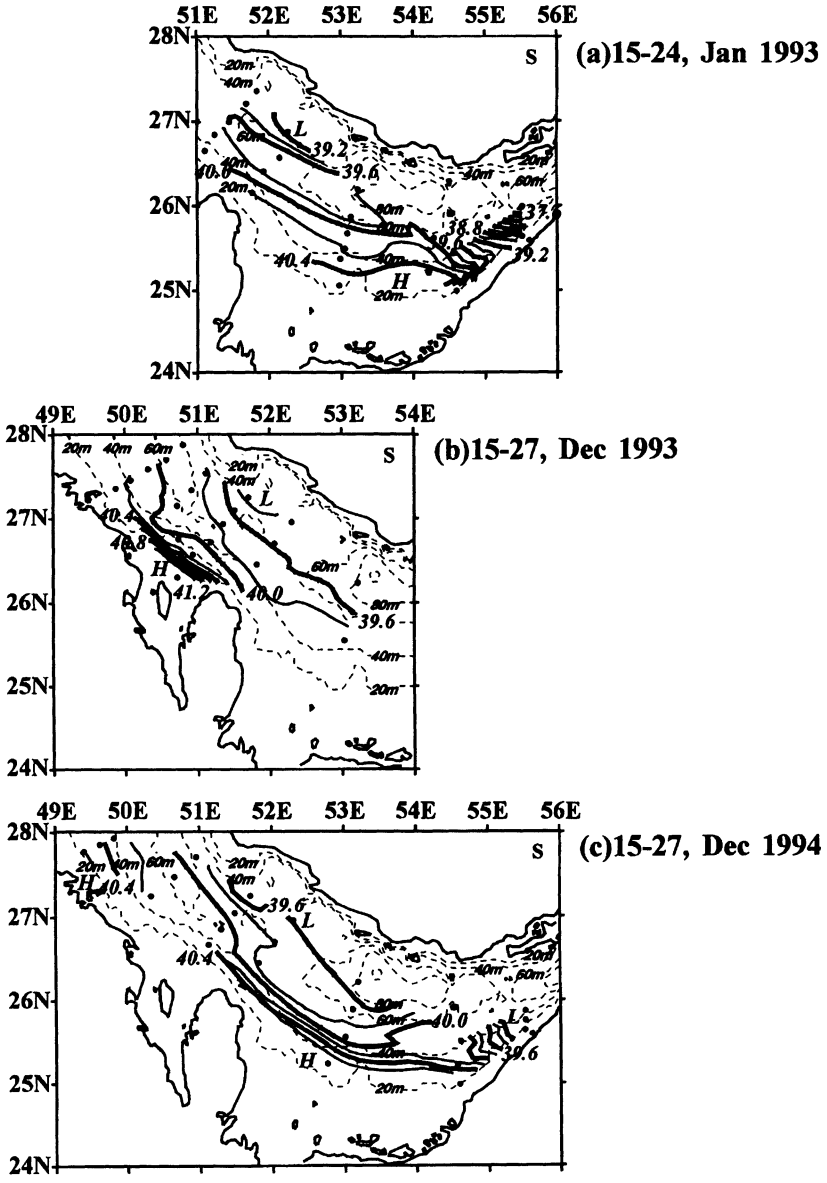

Fig. 5. Same as in Fig. 4, but for salinity (contour interval of 0.2).

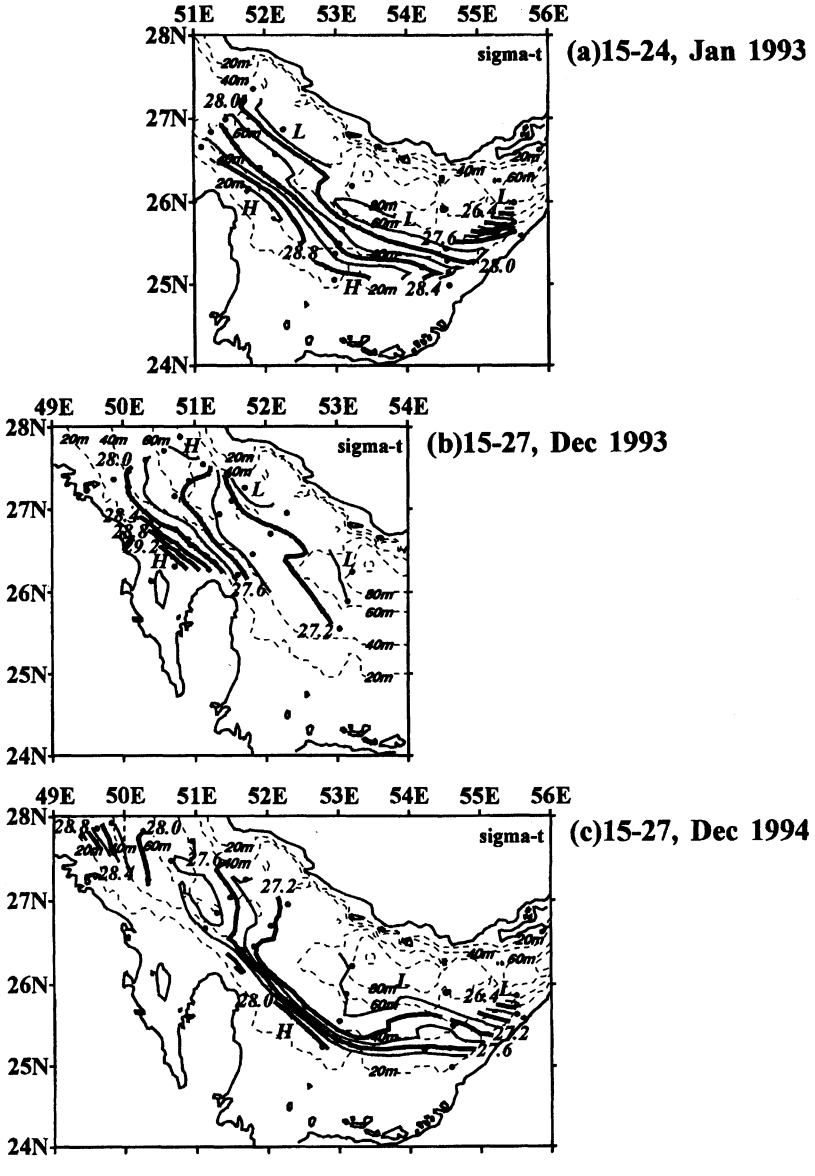

Fig. 6. Same as in Fig. 4, but for sigma-t (contour interval of 0.2).

Temperature in February (Reynolds, 1993) also decreased from January, about 2–3°C at the same locations in Cruise I. This feature is clearly seen by the temperature-salinity diagram obtained off Bahrain (Fig. 7). Salinity range is almost the same, but temperature decreases 2–3°C in January. Notice that

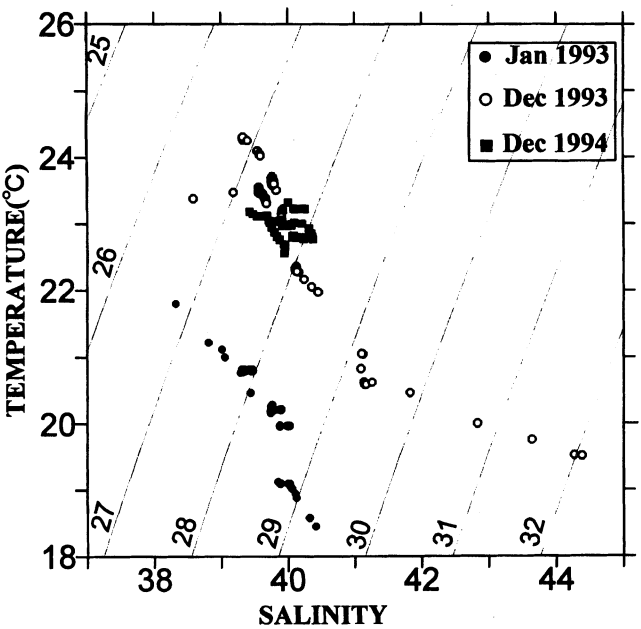

Fig. 7. Temperature-salinity diagram off Bahrain from three cruises.

extremely high salinity water (>44.0) is found in Cruise II at an observation point not covered in Cruises I and III.

In the area off UAE coast near the Strait of Hormuz, low salinity water (<37.4 in Cruise I and <39.2 in Cruise III) is found at the easternmost stations (55°30′ E, see Fig. 5). Fig.2 shows that the origin of this low salinity water may be associated with an inflow of water from the Gulf of Oman through the Strait of Hormuz (Reynolds, 1993). This low salinity water was also detected in Mt. Mitchell Cruise in winter, and salinity was less than 38.0 at that time. At the neighboring section (between 54°E and 55°E), salinity value is so high that a strong salinity front crossing the isobath are formed in this area. Horizontal salinity difference of this front is larger in Cruise I than that in Cruise III. In Cruise II, high salinity water (about 41.2) is found off Bahrain (26°20′ E, 50°30′ E) forming a strong salinity front which runs parallel to the isobaths. In Mt. Mitchell Cruise, such high salinity water of more than 43 was only found at the sea surface off UAE coast (24°30′ E, 52°30′ E).

Horizontal sigma-t distributions at all cruises show water of high density near the southern coast of the RSA. The distribution patterns are similar to those of salinity, indicating that density structure in winter is primarily determined by salinity (Reynolds, 1993).

Overall features of the horizontal distributions are almost identical to the winter observations of Brewer and Dyrssen (1985) and Reynolds (1993).

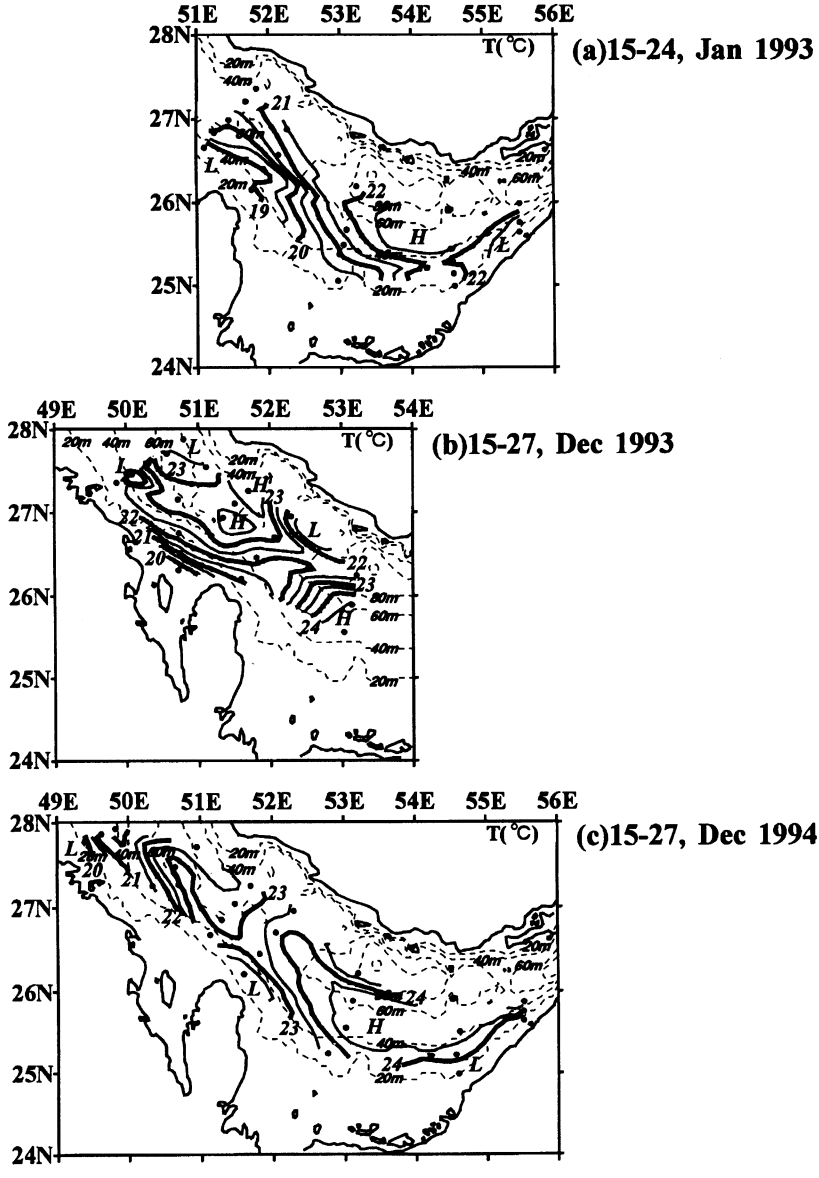

Fig. 8. Same as in Fig. 4, but are drawn from the deepest layer temperature.

Contour lines of temperature, salinity and sigma-t at the deepest depths of Cruises I, II and III are shown in Fig. 8 (temperature), Fig. 9 (salinity) and Fig. 10 (sigma-t) to show the distribution of high salinity waters near the bottom more clearly. In general, contour lines are also parallel along the isobaths and high

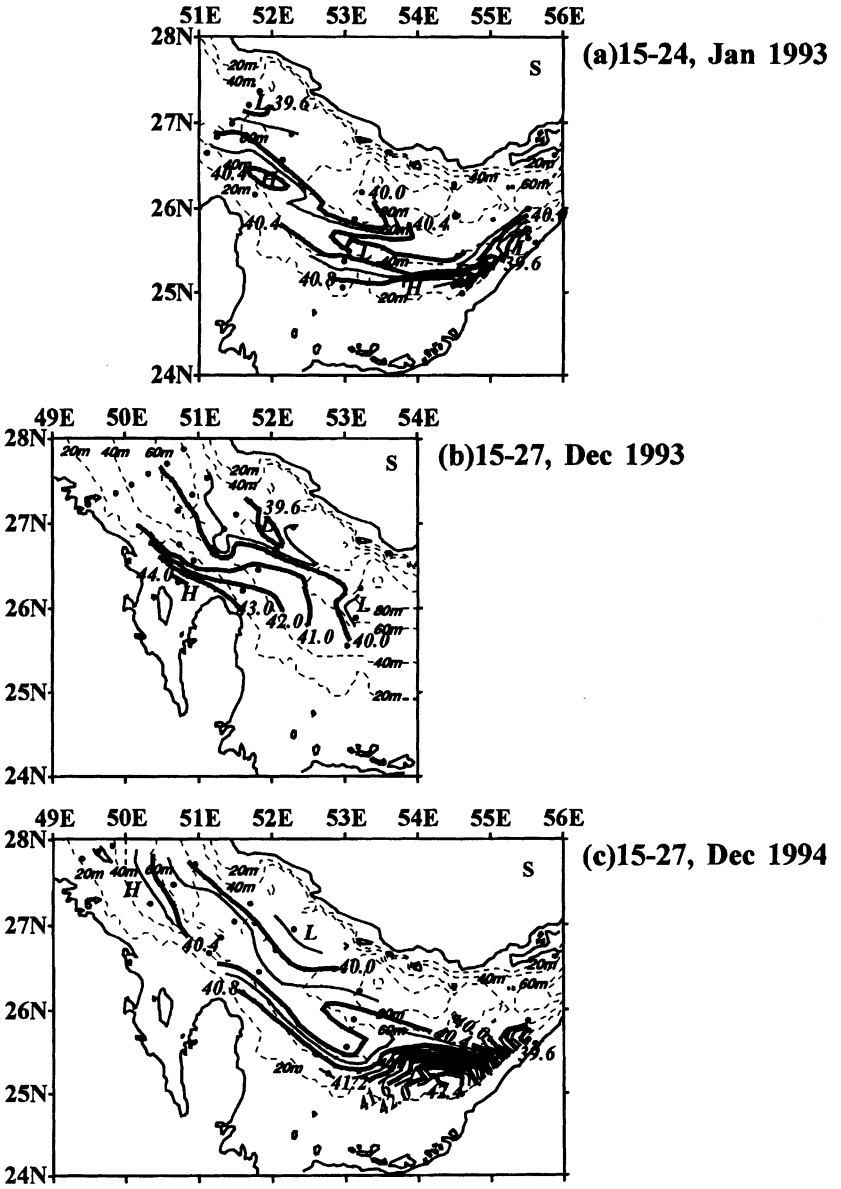

Fig. 9. Same as in Fig. 5, but are drawn from the deepest layer salinity. Notice that contour line interval exceeding 41.0 is set to 1.0.

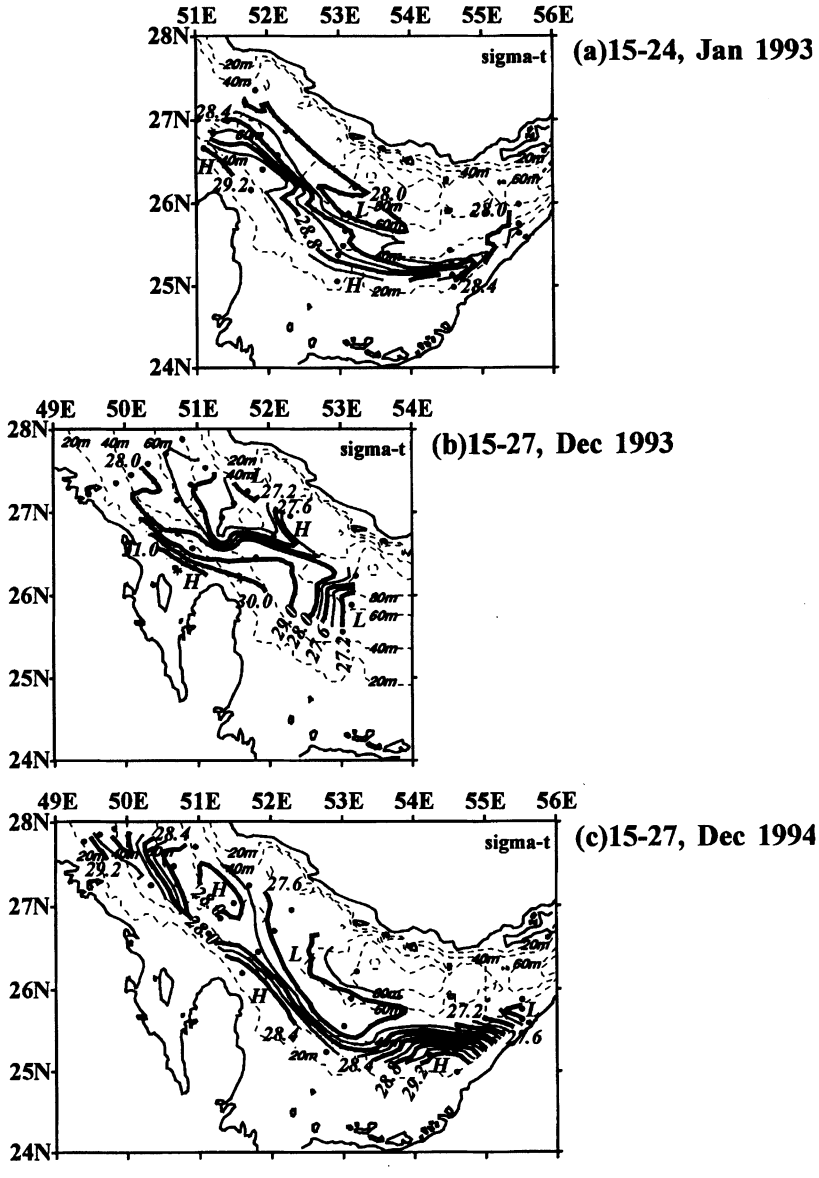

Fig. 10. Same as in Fig. 6, but are drawn from the deepest layer sigma-t.

salinity waters are found along the southern coast of the RSA. Low salinity (<39.6) water is also found at the easternmost stations in Cruises I and III at the surface and near the bottom, but the situations of the fronts are quite different between Cruises I and III. In Cruise I, salinity front seems to be weakened near

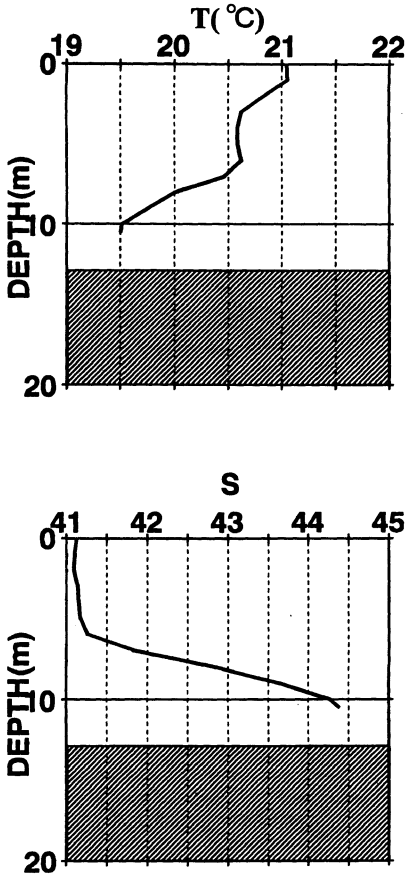

Fig. 11. Vertical profiles of temperature and salinity off Bahrain where an extremely high salinity water is found in Cruise II.

the bottom than at the surface and runs along the isobath. In Cruise III, however, high salinity water (>42.4) is found at the southernmost station between 54°E and 55°E, and another strong salinity front was formed showing the more complex structure in this area. In Cruise II, horizontal temperature gradient is large at the central eastern part of the RSA (52°E to 53°E). An extremely high salinity water (>44.0, also see Fig. 7) is found off Bahrain forming a strong salinity front. Vertical profiles of temperature and salinity at the station with the bottom of 13 m are shown in Fig. 11. Salinity increases from 41.2 at the depth of 7 m to 44.3 at the depth of 10 m forming a sharp bottom halocline, while temperature decreases by about 1 degree in this halocline. The origin of this high salinity water is believed to be formed by the strong evaporation in this area (Reynolds, 1993). The structure of this high salinity water will be discussed in the next section.

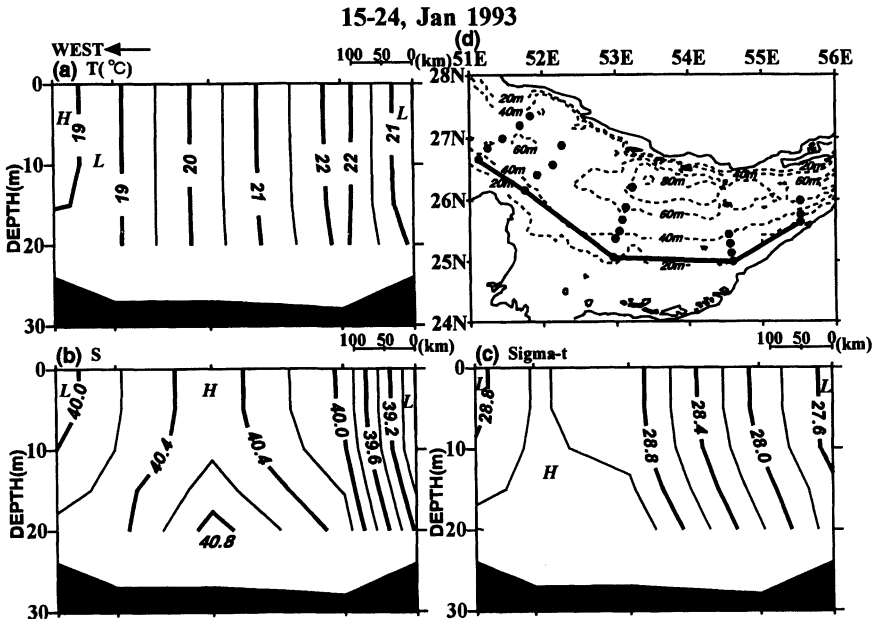

Fig. 12. Vertical cross sections along the Gulf axis at the southern stations in Cruise I. (a) temperature (contour interval of 0.5°C), (b) salinity (contour interval of 0.2) and (c) sigma-t (contour interval of 0.2). In the up-right corner (d) shows the position of stations by a thick line. Tick marks in the abscissa of each figure show the position of stations.

Vertical temperature, salinity and sigma-t distributions

Vertical cross sections along the axis of the RSA near the southern coast in Cruises I and III are shown in Figs. 12 and 13, respectively. The section along the axis of Gulf in Cruise II did not extend further to 55°E area, and will be omitted from this discussion. Generally, the temperature decreases and salinity increases as we go from the entrance to the central part of the RSA in both cruises. It is seen that water column is well mixed to the bottom, but salinity and density becomes slightly higher near bottom forming a weak two-layer structure between 52°E and 55°E in both cruises. This type of distribution also coincides with that obtained by Reynolds (1993).

Highest salinity water near bottom was found at 53°E (>40.8) in Cruise I (Fig. 12) and at 54°30′ E (>42.4) in Cruise III (Fig. 13). It is interesting that surface salinity reaches maximum at these longitude (about 40.4 at 53°E in Cruise I and 40.8 at 54°30′ E in Cruise III). In Cruise III, surface salinity approaches a minimum value (<40.2) north of Qatar (around 51°E). Surface temperature is maximum and sigma-t is minimum at this longitude. This area coincides with that where the density driven flow from the Strait of Hormuz stagnates sinks and eventually to a deep layer by high evaporation (Reynolds, 1993). In Cruise I,

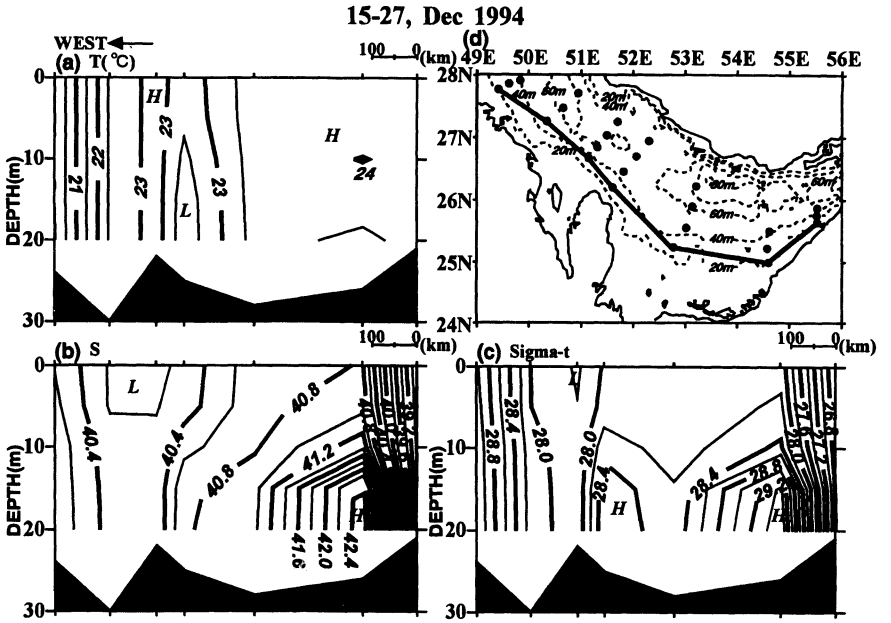

Fig. 13. Same as in Fig. 12, but for Cruise III.

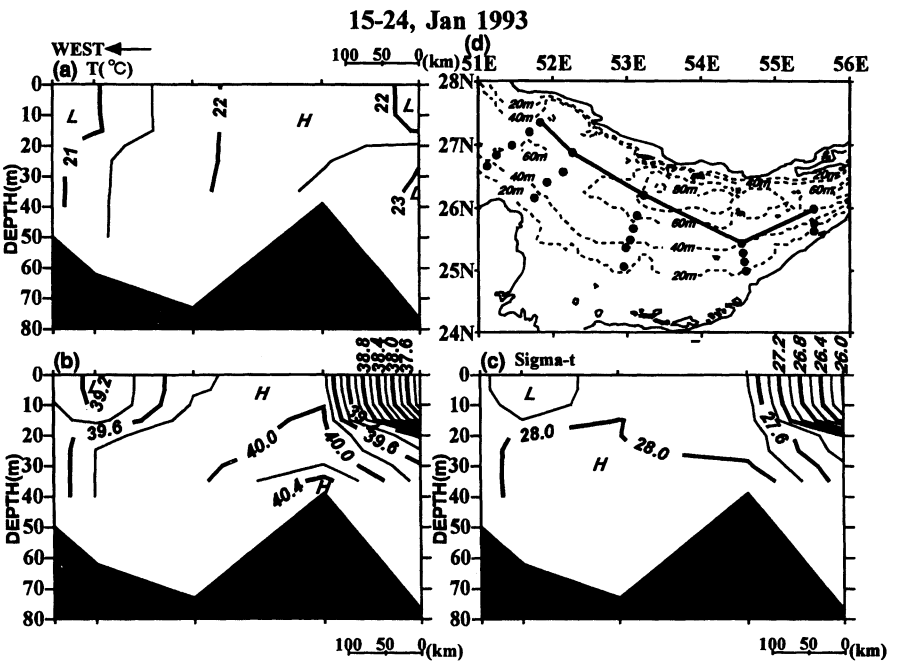

Fig. 14. Same as in Fig. 12, but for at the northern stations.

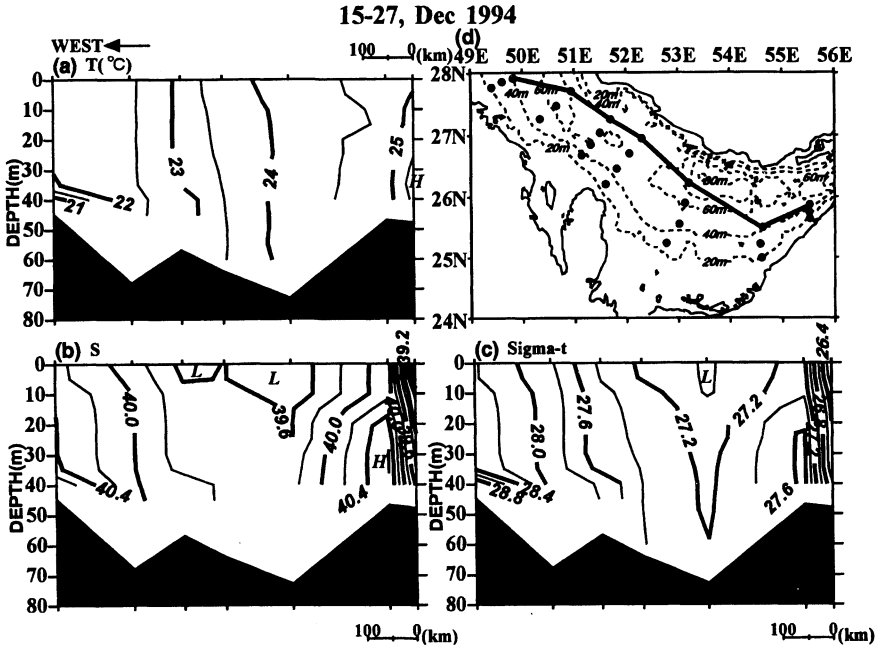

Fig. 15. Same as in Fig. 14, but for Cruise III.

unfortunately, the section was terminated off Bahrain, but, a salinity minimum might be formed at the surface off Bahrain.

Figures 14 and 15 show vertical properties sections along the northern coastal axis. In Cruise I (Fig. 14), surface salinity is lower (also sigma-t) than the southern section, and is quite low at 55°30′ E (<37.4). This water is believed to come from the Gulf of Oman (see Fig. 2). It is interesting that temperature in the upper layer is lower with a weak inversion layer. These features were also reported in Mt. Mitchell Cruise (Reynolds, 1993). The surface salinity shows a maximum value (>39.8) at 54°30′ E and bottom salinity value does (>40.4). This feature was also seen at the southernmost section but at different longitude (at 53°E, see Fig. 12). Surface salinity reaches a minimum value (<39.2) north-east of Qatar (around 52°E). As for Cruise III (Fig. 15), surface salinity at 55°30′ E was not so low as in Cruise I (Stations were not taken north of 26°N). Surface and bottom salinity maximum were also found at 54°30′ E as in southern section (Fig. 13), but having lower values (>40 at the surface and >40.4 at the bottom). Surface salinity has a minimum value (<39.6) around 52°E north-east of Qatar.

Vertical cross sections perpendicular to the RSA axis near the Strait of Hormuz (55°30′ E) in Cruises I and III are shown in Figs. 16 and 17, respectively. In Cruise I (Fig. 16), as was seen in the horizontal distribution on the surface salinity (Fig. 5), low salinity water occupies the surface layer in this section. At the northern two stations, surface salinity value falls below 38.0 while the

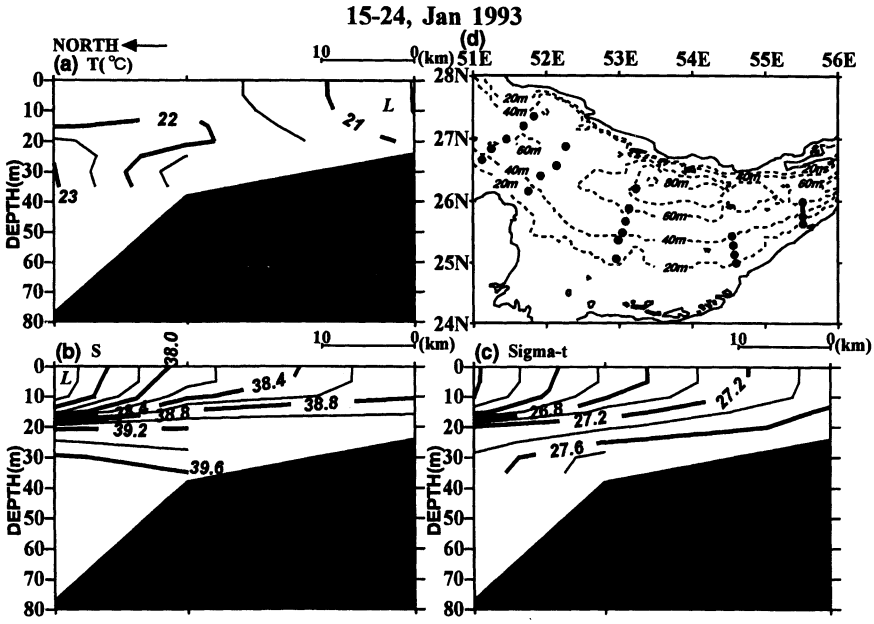

Fig. 16. Vertical cross sections perpendicular to the Gulf axis ear the Strait of Hormuz (55°30′ E) in Cruise I. (a) temperature (contour interval of 0.5°C), (b) salinity (contour interval of 0.2) and (c) sigma-t (contour interval of 0.2). In the up-right corner (d) shows the position of stations by a thick line. Tick marks in the abscissa of each figure show the position of stations.

salinity at the bottom is higher forming a strong halocline around 15 to 20 m depth. Bottom high salinity layer does not extend to the southernmost station. Temperature inversion exceeding 1°C (26°N) is found in this section. Such temperature inversions were also seen in the cross section along the RSA (Figs. 13, 14 and 15), and should be a characteristic feature of the intruding water from the Gulf of Oman. In Cruise III (Fig. 17), unfortunately, the section did not extended to 26°N, and such a low salinity water at the surface as in Cruise I is not observed in this section. Isopycnals in the bottom layer (<10 m depth) in both cruises slopes slightly upward toward the UAE coast;this means the semi-geostrophically balanced outward flow from the RSA suggesting the circulation model of the RSA presented by Reynolds (1993).

In Figs. 18 and 19, we show the vertical cross sections perpendicular to the RSA axis at 54°30′ E in Cruises I and III. In Cruise I (Fig. 18), temperature is almost homogeneous in this section, salinity is generally high (>40), and the highest salinity water below 20 m exceeding 40.8, is found at 25°20′ N. Surface salinity also shows maximum at this location. The structure of this high salinity water is similar to that found at 25°N and 53°E (see Fig. 12) which indicates that a high salinity water lies from 53°E to 54°30′ E (see Fig. 9). The slope of the

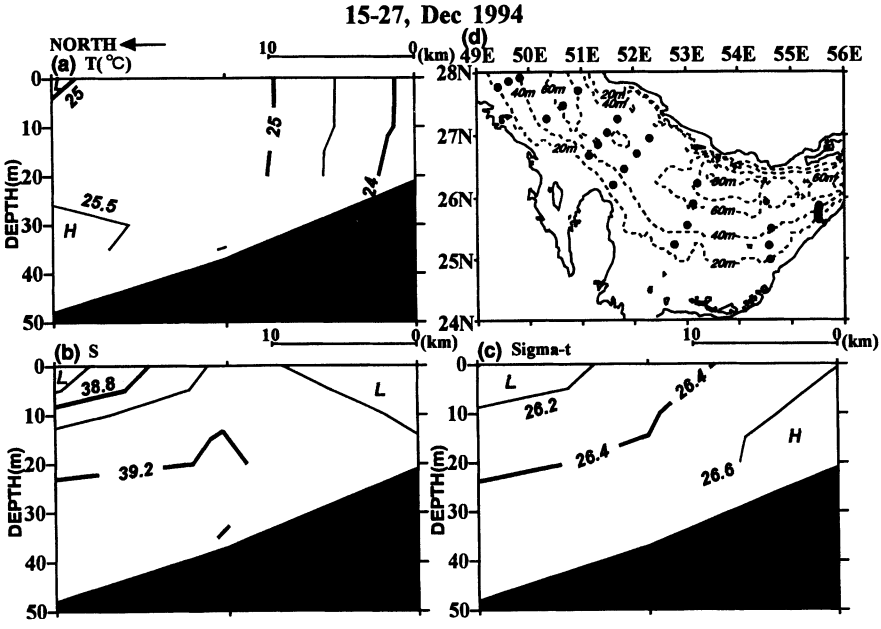

Fig. 17. Same as in Fig. 16, but for Cruise III.

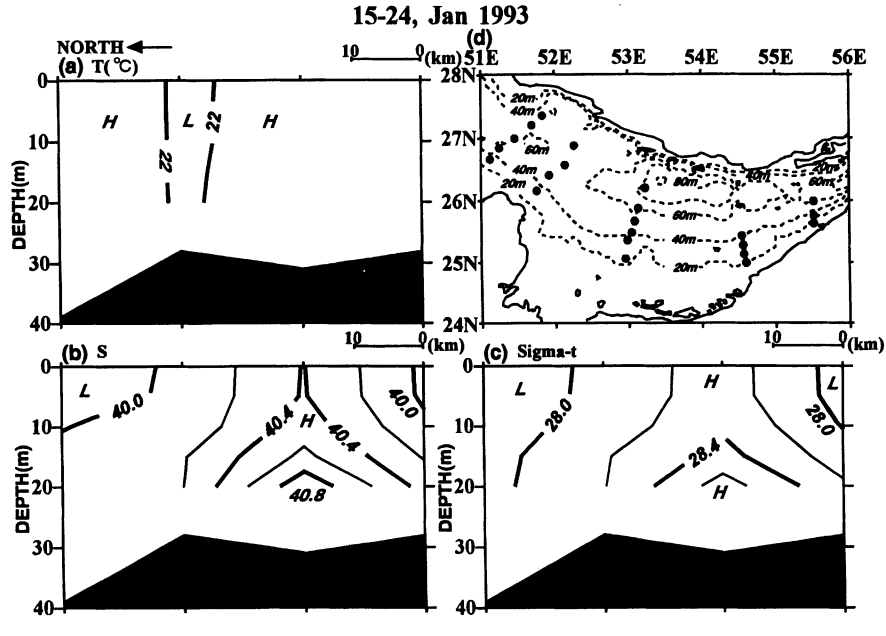

Fig. 18. Same as in Fig. 16, but obtained at 54°30′ E in Cruise I.

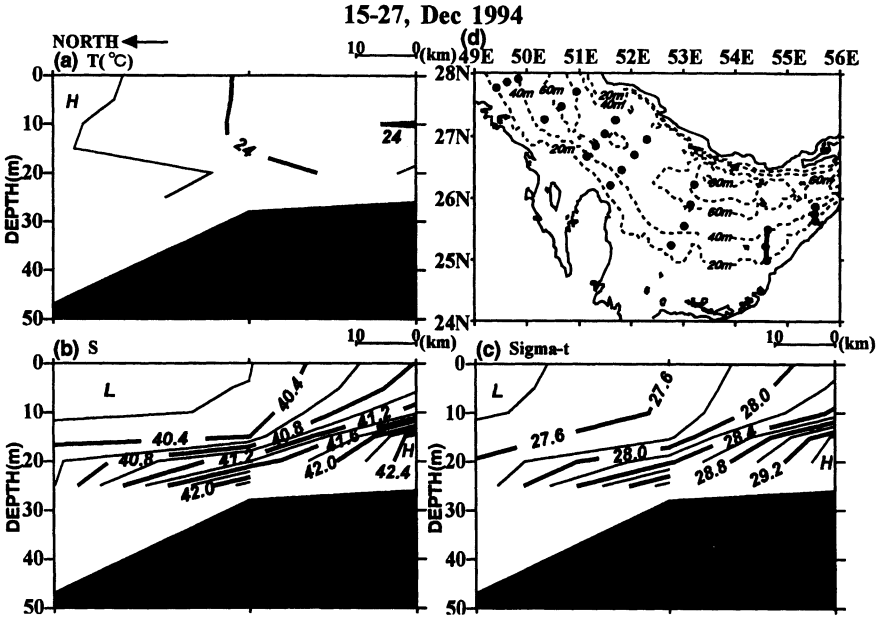

Fig. 19. Same as in Fig. 18, but for Cruise III.

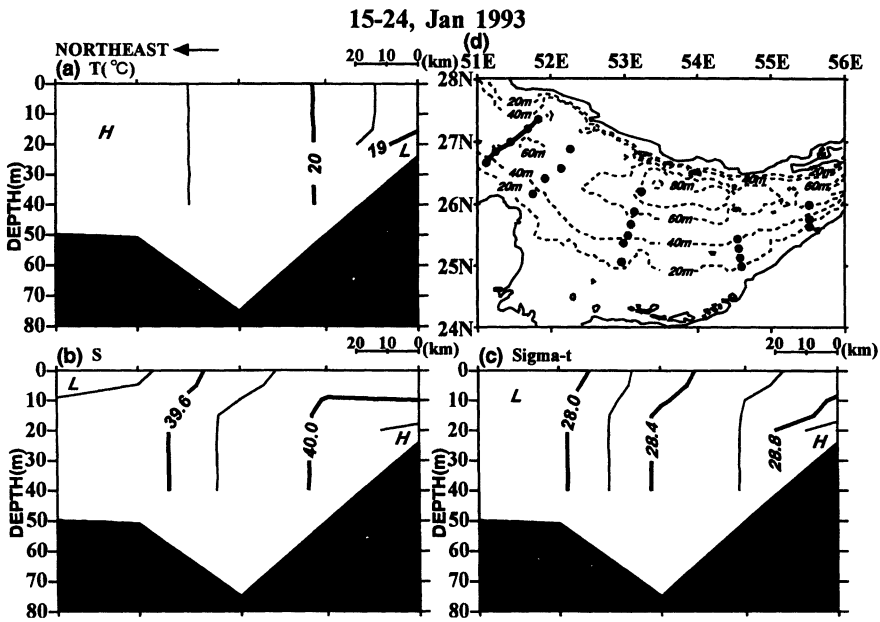

Fig. 20. Same as in Fig. 16, but obtained off Bahrain in Cruise I.

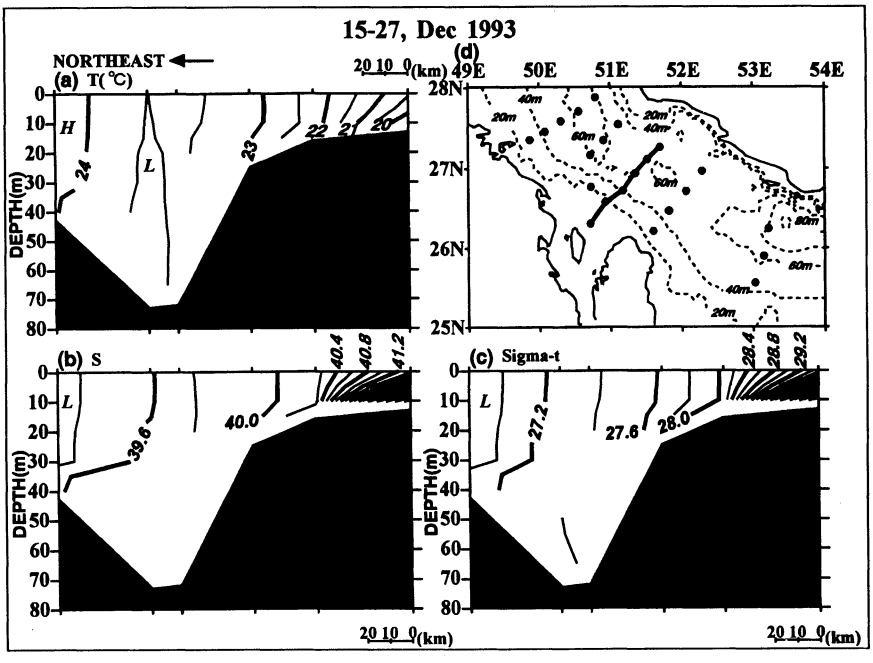

Fig. 21. Same as in Fig. 20, but for Cruise II.

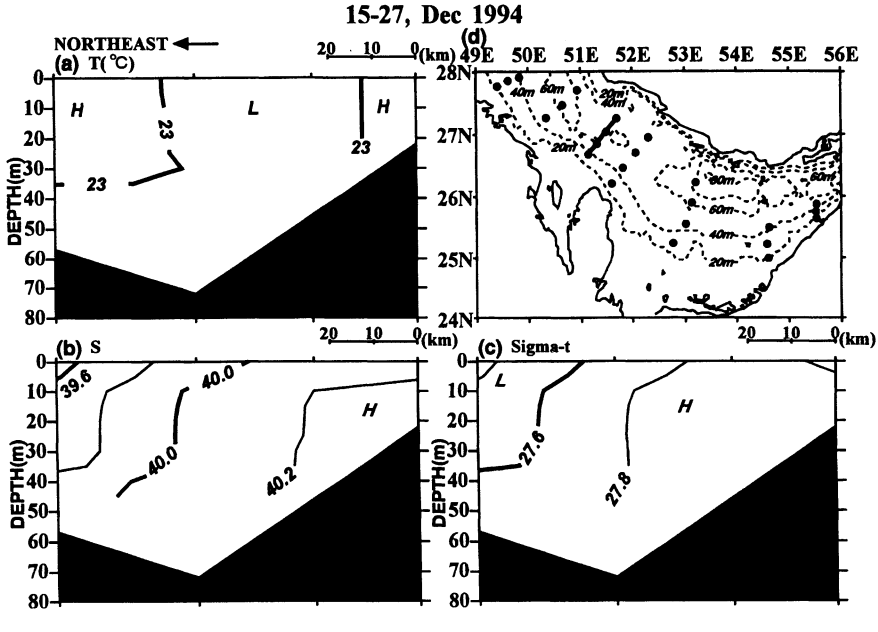

Fig. 22. Same as in Fig. 20, but for Cruise III.

isopycnals are downward to the UAE coast and upward to the north. A ridge of higher density water indicates a complex flow field, if the flow field in this section is geostrophically balanced. In Cruise III (Fig. 19), the temperature is also almost homogeneous, and, the salinity is high in the bottom layer than that at the surface. No ridges of high salinity (density) bottom water was found. A highest salinity water is found at 25°N (>42.4) forming a strong halocline near the bottom. Slope of the isopycnals is upward to the UAE coast, meaning the eastward (outward) flow from the RSA.

We show the vertical cross sections perpendicular to the RSA axis obtained off Bahrain in Cruise I (Fig. 20), Cruise II (Fig. 21) and Cruise III (Fig. 22). High salinity and low temperature water exists off the southern coast of the RSA. This feature is also observed at other inner sections of the RSA. In Cruise II, a station was occupied nearer to Bahrain, and highest salinity water (>44) in our cruises was found. Isopycnals slopes mean the eastward flow here.

The results summarized above are almost identical with those by Reynolds (1993). That is, in the eastern half of the RSA, the high temperature and relatively low salinity water originated from the Gulf of Oman comes through the Strait of Hormuz forming a surface density current. This water gradually increases its salinity by the strong evaporation and cooling by the winter time chill wind to sink off Qatar. This high salt water is distributed along the southern coast of the RSA and may flow out in the bottom layer through the Strait of Hormuz. In the present analysis, salinity value shows a minimum value in the proposed sinking area, which sounds curious for us. More intensive survey, especially to the northern half near to the Iranian coast should be done in the future.

Acknowledgements

The authors express their sincere thanks to the staff and crew members of the RT/V Umitaka-Maru. The cooperation with the scientists from the ROPME countries were of great help for us. Above all, we express our great thanks to Dr. Ibrahim Alam for his hospitality and efforts throughout the entire cruises. We also wish to thank Drs. Hideo Sudo, R. M. Reynolds and Amin Meshal for constructive reviews of preliminary draft. This work was supported by the Grand-in Aid for International Co-operative Research for "Studies on the Influence of Oil Spill to the ROPME Sea Area" by the Ministry of Science, Education, Science, Sports, and Culture in Japan.

REFERENCES

Arabian Gulf Fishery-Oceanography Survey by the Umitaka-Maru, Training-Research Vessel, Tokyo University of Fisheries with Collaboration of Kuwait Institute for Scientific Research, December 1968 (1974), Trans. Tokyo Univ. Fish, No. 1, 1–118.

Brewer, P. G. and D. Dyrssen (1985). Chemical oceanography of the Persian Gulf, *Prog. Oceanogr.*, **14**, 41–55.

Emery, K. O. (1956). Sediments and water pollution of Persian Gulf, *Bull. Amer. Ass. Petrol. Geol.*, **40**(10), 2354–2383.

Evans, G. (1966). Persian Gulf. In *The Encyclopedia of Oceanography: Encyclopedia of Earth Sciences Series*, Vol. 1, pp. 689–695, ed. by R. W. Fairbridge, Reihhold Publ. Co., New York.

Matsuyama, M., Y. Kitade, T. Senjyu, Y. Koike and T. Ishimaru (1997). Vertical structure of a current and density front in the strait of Hormuz. This volume.

Reynolds, R. M. (1993). Physical oceanography of the Gulf, Strait of Hormuz, and the Gulf of Oman—Results from the Mt. Mitchell Expedition, *Marine Pollution Bull.*, **27**, 35–59.

Senjyu, T., T. Ishimaru, M. Matsuyama and Y. Koike (1997). High salinity lens from the Gulf. This volume.

Sugden, W. (1963). The hydrology of the Persian Gulf in respect to evaporite condition, *Amer. J. Sci.*, **261**, 741–755.

Offshore Environment of the ROPME Sea Area after the War-Related Oil Spill, Eds. A. Otsuki *et al.*, pp. 23–34.

Vertical structure of a current and density front in the Strait of Hormuz

Masaji MATSUYAMA, Yujiro KITADE, Tomoharu SENJYU*,
Yoshio KOIKE and Takashi ISHIMARU

Tokyo University of Fisheries, Konan 4-5-7, Minato-ku, Tokyo 108-8477, Japan

Abstract—Current measurements by ADCP were made at a moored station near the Strait of Hormuz in the Arabian Gulf from December 16, 1993 to January 2, 1994. The measurements show that the vertical current structure and its time variations can be described as the sum of tidal and low frequency currents. The tidal currents are mostly due to the barotropic tide. The amplitudes of the tidal currents are 0.34 m/s for K_1 constituent, 0.22 m/s for M_2, 0.11 m/s for O_1, and 0.07 m/s for S_2, so the diurnal tidal currents dominate over the semidiurnal ones. During the first six days, low frequency current direction was outward at all depths, principally a barotropic structure. An inflow in the upper layer and outflow in the lower layer, a baroclinic structure, dominated the middle and last parts of the observation period. The baroclinic structure is consistent with the results obtained from the hydrography by R/V *Mt. Mitchell*, and is the classical structure of a negative estuary.

CTD measurements were made at nine stations along the bay-axis in the Strait of Hormuz on December 16, 1993. A density front was observed near the center of the strait. The front was formed by a pronounced salinity difference between the high salinity water in the Gulf and fresher water in the Arabian Sea. The parameter $\Gamma = H/U^3$, where H is the water depth, and U the tidal current amplitude, is 780 s^3/m^2 during the spring tide and 6000 s^3/m^2 during the neap tide for the diurnal tide. These values suggest that for diurnal tides the tidal front exists during the spring tide but disappears during the neap tide. On the other hand, for the semidiurnal tide, the front may not form, even for the spring tide. The data suggest that water exchange through the Strait of Hormuz occurs during the neap tide of the diurnal period when the tidal front disappears.

INTRODUCTION

The Strait of Hormuz, located at the mouth of the Arabian Gulf, has a width of about 70 km and depth of about 90 m. There is no sill in the strait. It is very important to understand the mechanism of water exchange between the Gulf and the Indian Ocean through the strait. The high salinity (dense) water formed in the Gulf flows out in the lower layer. The dense bottom water is formed by large excess of evaparation over both precipitation and river inflow (Reynolds, 1993). This region is one of the most important waterways in the world, and ship traffic

*Present address: National Fisheries University, Nagata-honmachi 2-7-1, Shimonoseki, Yamaguchi 759-65, Japan.

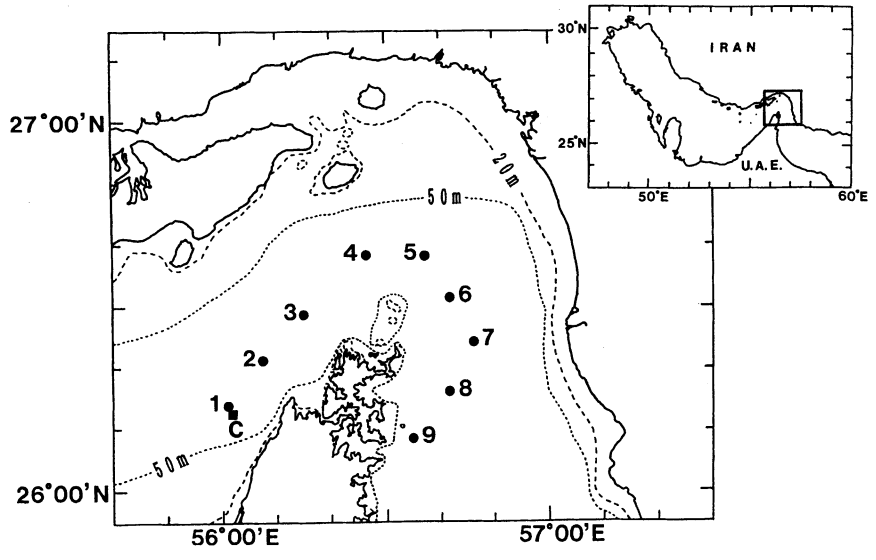

Fig. 1. The location of the moored current measurement (Stn. C) and locations of CTD casts (Stn. 1 through Stn. 9). Inset shows the figure location relative to the Arabian Gulf.

is crowded. As a result, the number of direct oceanographic observations from this region are small (Reynolds, 1993). As a result of the *Mt. Mitchell* Expedition from February to June 1992, Reynolds (1993) concluded that flow in and out of the Strait of Hormuz forms the estuarine exchange of the Gulf with the world's ocean. In addition, he emphasized that because very little is known of the currents here, it is essential to make direct current measurements in the Strait.

While training and research vessel *Umitaka-maru* (Tokyo University of Fisheries) operated in the Gulf region, we made the current measurements by ADCP (Acoustic Doppler Current Profiler) at the moored station and CTD casts along the Strait of Hormuz. The purpose of the observation is to determine the current structure and variation in the strait. The locations of current measurements and CTD casts are shown in Fig. 1. An ADCP (300 kHz, RD Company) was installed near the bottom (92 m), and the data were collected every 2 m from 80 m depth to the surface layer at 5 minute intervals from December 16, 1993 to January 2, 1994. Due to ship traffic in the strait, there was only one CTD observation on December 16, 1993.

RESULTS

Current variations

The current meter was deployed at Stn. C (Fig. 1). The vertical alongshore and onshore components of the current at 6 m intervals are shown in Fig. 2. The

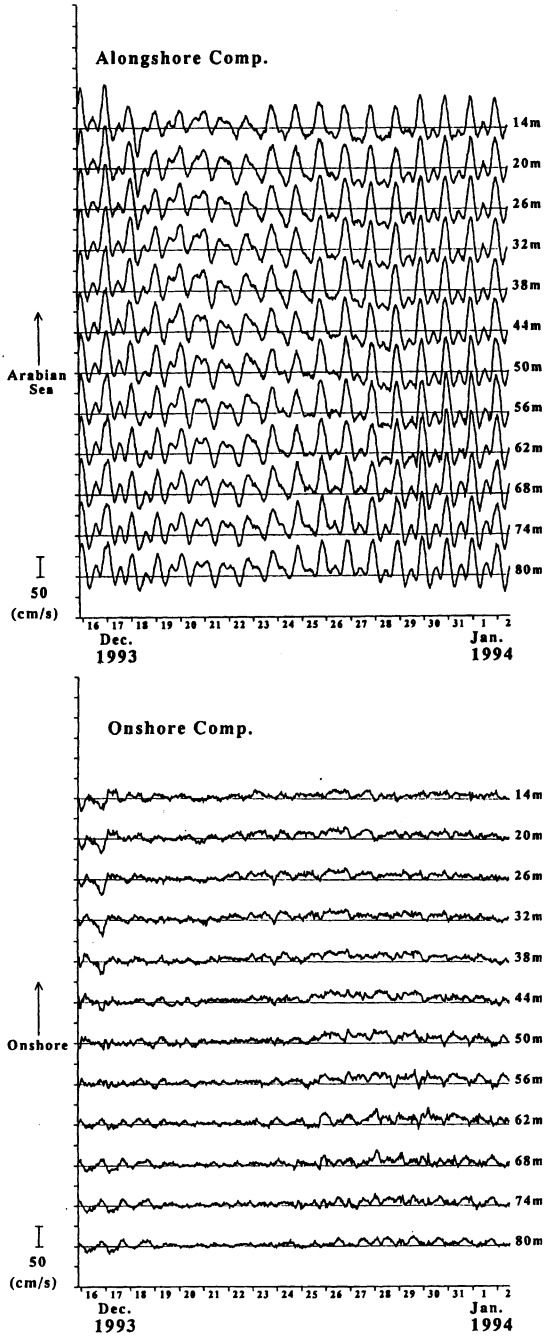

Fig. 2. Time variations of alongshore (upper) and onshore (lower) components of velocity at every 6 m interval at Stn. C. Attached numerals on vertical axis show speed in cm/s and slide the mark of each record by one step (50 cm/s) vertically.

positive alongshore and onshore components are taken as 60° true and 150° true, respectively. The deepest current data were obtained at 12 m above the sea bottom, i.e., 80 m depth. Due to acoustic noise in the upper layer, the shallowest measurements were from a depth of 14 m. Figure 2 shows the existence of strong tidal currents and low frequency currents. The tidal currents exhibit greater temporal than vertical variation which suggests that they are predominantly barotropic. From the vertical-mean current, the amplitudes of the four major constituents for the barotropic tidal current are estimated as O_1 of 11.0 cm/s, K_1 of 33.7 cm/s, M_2 of 21.6 cm/s and S_2 of 7.3 cm/s. The sum of the two diurnal components is greater than that for the semidiurnal components. Figure 3 shows the co-tidal and co-range charts of M_2 and K_1 constituents as representatives of the semidiurnal and diurnal constituents, respectively. Tides in the Gulf are

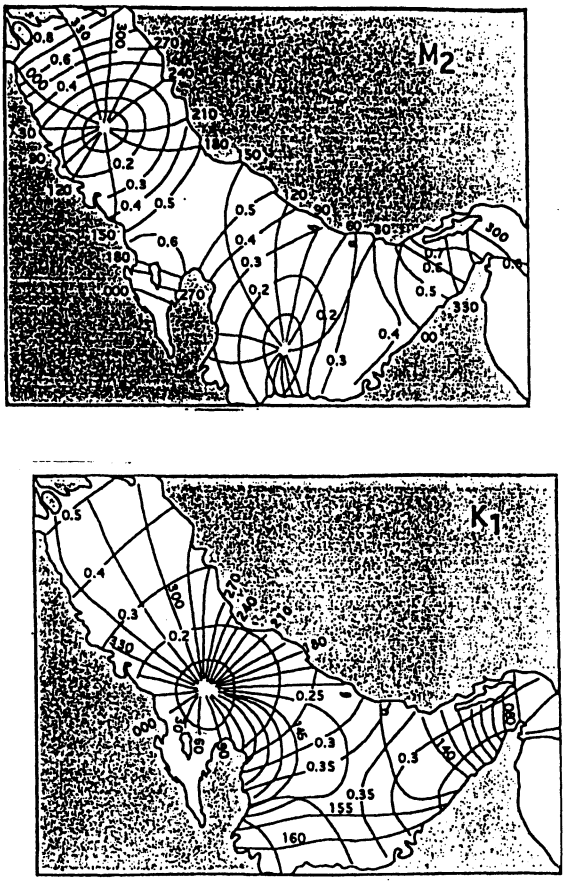

Fig. 3. Co-tidal and co-range charts of the M_2 and K_1 constituents in the Gulf (Lardner *et al.*,1982). The amplitudes are shown in meter.

complex standing waves and their dominant pattern varies from semidiurnal to diurnal by one or two amphidromic points (Reynolds, 1993). The sea level amplitude for the semidiurnal tide near the Strait of Hormuz is larger than that of the diurnal one. The difference in dominant period between sea level and current near the strait is important. A strong diurnal current is caused by the concentration of the co-phase lines near the strait (Fig. 3). As a result, although the sea level amplitude of about 30 cm is small in comparison with that of the semidiurnal component of 60 to 70 cm, the strong pressure gradient for the diurnal component

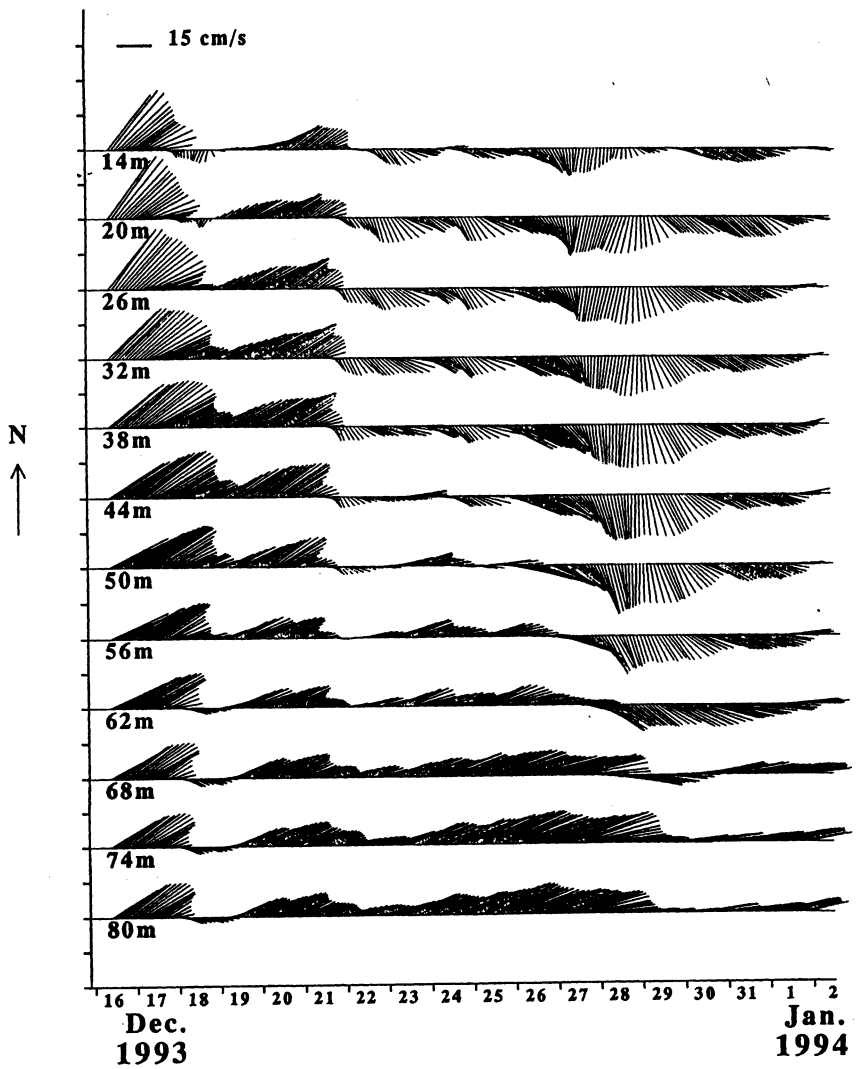

Fig. 4. Time series of low frequency velocity at every 6 m interval at Stn. C.

along the strait induces the tidal current. The predominance of the diurnal tidal current is predicted by the numerical modeling (Lardner *et al.*, 1982).

The residual currents computed from 25–hour running averages of velocity in 6m depth bins (Fig.4). The low frepuency residual currents are almost uniform in the vertical which indicates a strongly barotropic flow from the start of the time series until December 21. From December 22, the velocity shows inflow in the upper layer (above 38 m depth) and outflow in the lower layer, which is characteristic of the water exchange through the Strait of Hormuz, and can be inferred from the distribution of water properties, salinity, temperature, density, etc. The upper layer thickness of the inflow is about 50 m from December 22 to 26, but increases to 60 m to 70 m thereafter. The thickness appears to depend on the strength of the low-frequency current, which may in turn be influenced by such forcing effects as wind, tidal current and density current.

CTD casts

Profiles of the vertical variations in temperature, salinity and density, at Stns. 2, 7 and 9 are shown in Fig. 5. At Stn. 2, the inner station, the temperature and salinity are higher in the lower layer than in the upper layer. The vertical temperature change ranges from 25.5 to 26.4°C, which is in the narrow range for winter. The salinity varies greatly, from 37.9 at the surface to 39.5 at 80 m depth. The density is mostly stratified due to the salinity. The salinity distribution is composed of the surface mixed layer, halocline and bottom mixed layer. The depths of strong salinity gradients in the halocline are 15 m and 50 m, the boundary between the various water masses. At Stn. 7, near the narrowest part of the strait, the three profiles show a uniform water with a temperature of 25.6°C and salinity of 37.1. Near the bottom, a slight increase in temperature and salinity is found, indicating the existence of outflow. At Stn. 9, the salinity varies from 36.9 at the sea surface to 38.5 at 90 m depth, and the density varies in the same manner as the salinity. A sharp change of the salinity in the upper layer is found near 10 m depth. A thin surface mixed layer is found at Stn. 9 and Stn. 2, but the temperature is higher and the salinity are lower at Stn. 9.

An interesting observation is the existence of a density front near the center of the strait. A detailed view of the front is given by the vertical section along the strait axis (Figs. 6(a) to 6(c)). The salinity distribution (Fig. 6(a)) clearly shows the existence of the front between Stns. 3 and 4, and its vertically uniform structure between Stns. 4 and 7. The outside front near Stn. 8 appears to lean to the offshore, but the process by which it extends to the sea surface cannot be confirmed. The high value for salinity is 38.0 inside the front (Stns. 1 to 3), especially in the lower layer, and a high salinity region is also found in the lower layer from Stns. 8 to 9. The low salinity water near the center appears to be related to that in the upper layer at the outside of the strait. It is significant that the salinity in the lower layer is higher at Stns. 8 and 9 than at Stns. 4 to 7. Although the temperature is less variable through the strait during winter observations (Fig. 6(b)), the weak temperature front exists at the same location as the salinity front

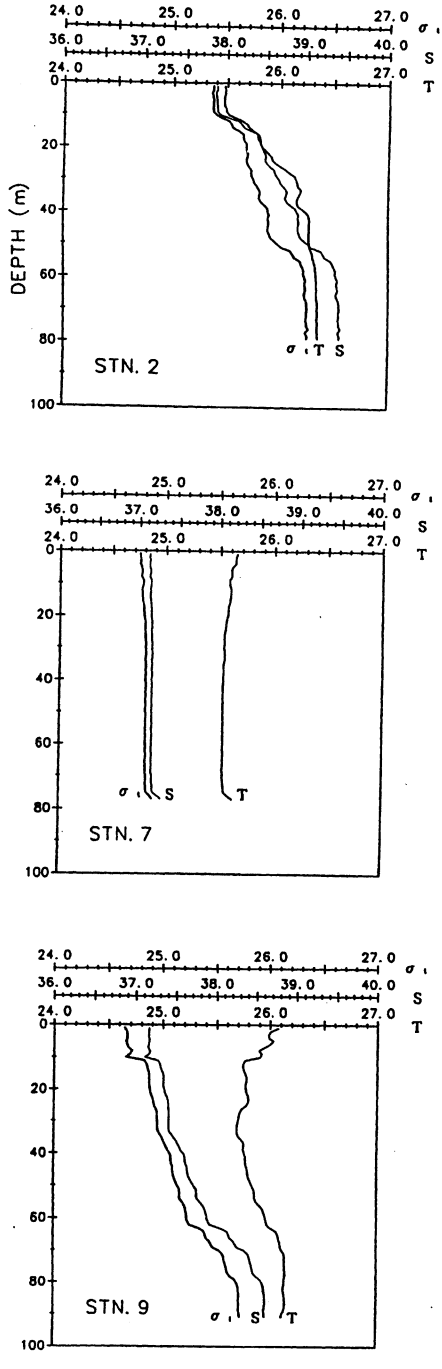

Fig. 5. Vertical profiles of temperature, salinity and sigma-t at Stns. 2, 7 and 9. T: Temperature (°C), S: Salinity (psu), σ_t: Sigma-t (kg/m^3).

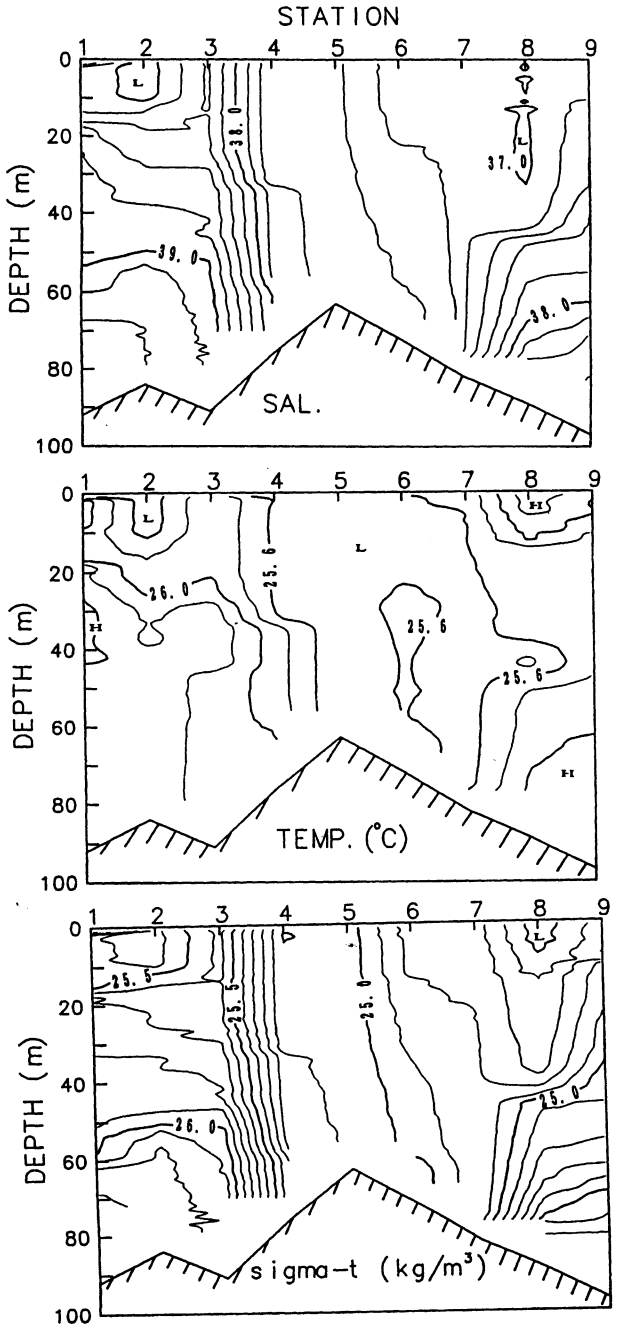

Fig. 6. Vertical sections of salinity (upper), temperature (middle) and density (lower) along the Strait of Hormuz.

between Stns. 3 and 4. The density distribution is very similar to that for salinity because during winter change in density is caused primarily by change in salinity. Consequently, the density front is formed at the same location as the salinity front. The high density water exists in the lower layer inside the front, and the low density water occupies the area from the surface to bottom between Stns. 4 and 7. This distribution indicates a strong density gradient along the axis, and is responsible for the formation and continuation of the density front in this region.

DISCUSSION

The current and CTD observations in the Strait of Hormuz was carried out to clarify the process of water exchange between the Arabian Sea water and Gulf water. The main mechanism of water exchange may be similar to estuarine circulation, that is, the outflow of Gulf water in the lower layer and inflow of Arabian Sea water in the upper layer. It is very important to clarify how the exchange process occurs or does not occur at any given time. So, the density front will be discussed here.

The density front is due to the difference in salinity between Stns. 3 and 4, near the center of the strait. A density front observed in strong tidal current regions is mostly a tidal front (Simpson and Hunter, 1974; Simpson and James, 1986), because it is naturally maintained by the strong tidal mixing. The criterion for existence of the tidal front is justified by parameter $\Gamma = H/U^3$, where H is the water depth and U the tidal current amplitude. When Γ is small, the tidal front is formed for strong tidal currents. The critical value of Γ for the existence of the tidal front is different in the world ocean, where it ranges from 100 to 3000 s^3/m^2 (e.g., Yanagi and Ohba, 1985), although Simpson and Hunter (1974) first showed about 500 s^3/m^2.

Table 1 shows the amplitude, orientation of the main axis, and value of Γ for the four major barotropic tidal currents obtained at Stn. C, where the water depth, H, is taken as 70 m. The value of Γ is, as a whole, large in comparison with that in the world sea. The K_1 constituent alone is 1800 s^3/m^2, within the range indicated by Yanagi and Ohba (1985).

Recently, Hibiya and LeBlond (1993) theoretically indicated that the effec-

Table 1. Harmonic constants and Γ for four major tidal constituents.

	O_1	K_1	M_2	S_2
Amplitude (cm/s)	11.0	33.7	21.6	7.3
Orientation	58.1°	57.6°	58.0°	61.5°
Γ (s^3/m^2)	5.3×10^4	1.8×10^3	6.9×10^3	1.8×10^5

$\Gamma = H/U^3$, H: water depth, U: tidal current amplitude.

Table 2. Tidal current amplitude and Γ for spring and neap tides.

	Diurnal Component		Semidiurnal Component	
	Spring	Neap	Spring	Neap
Current amplitude (cm/s)	44.7	22.7	28.9	14.3
$\Gamma(=H/U^3)(s^3/m^2)$	784	5984	2900	23940

tive water exchange in a fjord is developed during the neap tide for the weakened tidal mixing. Previously, Takeoka and Yoshimura (1988) showed that the water exchange in Uwajima Bay in Japan is due to the density current during the neap tide as well. In both cases, the strong tidal currents and density front are observed during the spring tide. This suggests the possibility of effective water exchange through the Strait of Hormuz during the neap tide as well, while the density front exists during the spring tide. The CTD observations were made on December 16, 1993 during the near-spring tide. Current amplitudes and Γ of the fortnight period tide are estimated at both the spring and neap tides of the diurnal and semidiurnal components, as indicated in Table 2. As the value of Γ is less than 1000 s^3/m^2 for the spring tide in relation to the diurnal tide, the density front may be formed and maintained in the near spring stage. On the other hand, it is less likely that the fortnight period in relation to the semidiurnal tide will form the density front for the small current amplitude, even at spring tide.

The density front and water exchange between the Gulf water and the Arabian Sea water are consistent to the estuarine circulation obtained in the world ocean. A schematic representation of this finding, which may be extremely important in understanding the dynamics of the strait, is shown in Fig. 7. Density front formation depends on the strength of the density stratification under the same tidal current because the vertical mixing due to the tidal current is suppressed by the strong density stratification. The strength of summer stratification is evident for heating at the sea surface (Reynolds, 1993). We hypothesize that because density front formation is more difficult in summer than in winter, water exchange through the Strait of Hormuz between the Gulf and Arabian Sea is strong in summer. Reynolds (1993) showed that the inflow along the Iranian coast is related to *Shamal* winds (NW winds), which are strong in winter, resulting in an inflow that is weak in winter but strong in summer. On the other hand, the seasonal inflow variations can also be explained qualitatively by the density front and strength of the density stratification. We conclude that the summer strength of the inflow is due to both *Shamal* winds and the density front.

An important phenomenon, the barotropic current structure of the low-frequency current observed from December 16 to 22, cannot be explained by this analysis. We speculate that the barotropic coastal current is induced by the strong wind, *Shamal*, although our data cannot justify this conclusion. Our information on the current and hydrography in the strait is insufficient to elucidate the detailed mechanism of the water exchange, as indicated by Reynolds (1993). We cannot

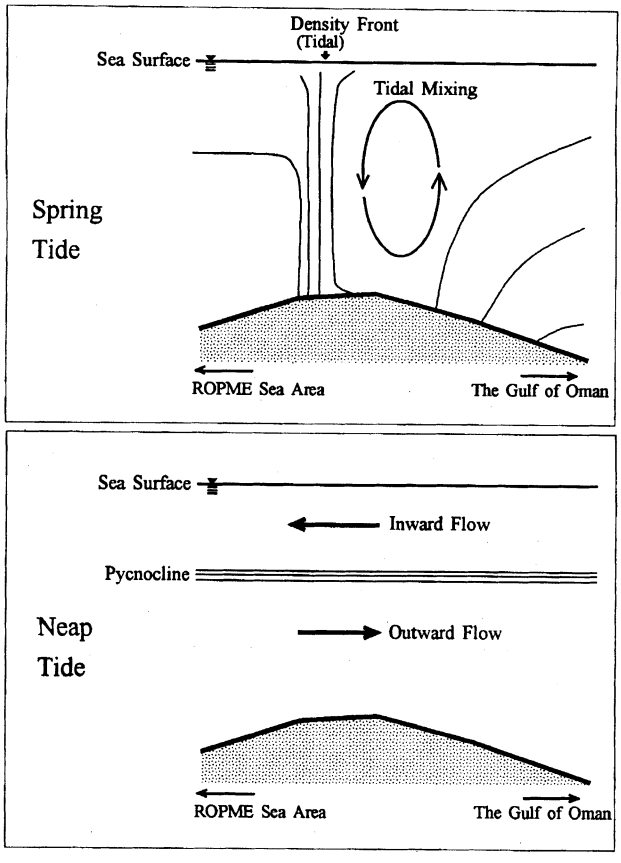

Fig. 7. Schematic view of water exchange model in the Strait of Hormuz.

see clearly that the inflow is evident in the current data. The reason is considered that the position of our moored station is not center of the strait, but near the southern coast to see the inflow in the upper layer and outflow in the lower layer. We therefore recommend additional current measurements and CTD observations in and around the Strait of Hormuz.

SUMMARY

The current measurements by ADCP were made at the moored station near the Strait of Hormuz in the Gulf from December 16, 1993 to January 2, 1994. The current data are indicated as the sum of the tidal and low frequency currents. The tidal currents are mainly due to the barotropic tide from the current data. Their amplitudes are 0.34 m/s for K_1 tidal current amplitude, 0.22 m/s for M_2, 0.11 m/s for O_1, and 0.07 m/s for S_2, leading to the conclusion that diurnal tidal

currents dominate over semidiurnal tidal currents. During the first six days, the low frequency currents indicated the outflow at all depths (barotropic structure) while during the middle and latter part of the observation period they indicated the inflow in the upper layer and outflow in the lower layer (baroclinic structure). The baroclinic structure is consistent to estuarine circulation obtained from the hydrography by the *Mt. Mitchell* Expedition.

The CTD measurements were made at 9 stations along the bay-axis in the Strait of Hormuz on December 16, 1993. The density front was observed near the center of the strait, and consisted of a pronounced salinity difference between the high saline water in the Gulf and the fresher water in the Arabian Sea. The parameter $\Gamma = H/U^3$, where H is the water depth, and U the tidal current amplitude, is the value of 780 s^3/m^2 during the spring tide and 6000 s^3/m^2 during the neap tide. The critical value for formation of the tidal front is frequently chosen as 100 to 3000 s^3/m^2(Yanagi and Ohba, 1985). This suggests that a tidal front exists during the spring tide for the diurnal tide in the Strait of Hormuz, but disappears during the neap tide for the diurnal tide. However, the front may be not formed even for the spring tide for the semidiurnal tide. The Gulf water is speculated to flow out in the upper layer for the neap tide of the diurnal period when the tidal front disappears.

Acknowledgements

The field work was accomplished on R.V. *Umitaka-maru* through the cooperation of Captain T. Isouchi, his crew, and Japan and ROPME scientists joining the cruise. The authors thank them greatly. We also wish to thank Dr. Reynolds for his valuable discussion and comments.

REFERENCES

Hibiya T. and P. H. LeBlond (1993): The control of fjord circulation by fortnightly modulation of the tidal mixing process. *J. Phys. Oceanogr.*, **23**, 2034–2052.

Lardner, R. W., M. S. Belen and H. M. Cekige (1982): Finite difference model for tidal flows in the Arabian Gulf. *Comp. Maths. Appls.*, **8**(6), 425–444.

Reynolds, R. M. (1993): Physical oceanography of the Gulf, Strait of Hormuz, and the Gulf Oman—Results from the *Mt. Mitchell* expedition. *Mar. Pol. Bull.*, **27**, 35–59.

Simpson, J. H. and J. R. Hunter (1974): Fronts in the Irish Sea. *Nature*, **250**, 404–406.

Simpson, J. H. and J. D. James (1986): Coastal and estuarine fronts. In *Baroclinic Process on Continental Shelf*, ed. by C. N. K. Mooers, American Geophy. Union, Washington, D.C., pp. 63–94.

Takeoka, H. and T. Yoshimura (1988): The Kyucho in Uwajima Bay. *J. Oceanogr. Soc. Japan*, **44**, 6–16.

Yanagi, T. and T. Ohba (1985): Tidal front in Bungo Channel. *Bull. Coast. Oceanogr. Japan*, **23**, 29–25 (in Japanese with English abstract).

Offshore Environment of the ROPME Sea Area after the War-Related Oil Spill, Eds. A. Otsuki *et al.*, pp. 35–48.

High salinity lens from the Strait of Hormuz

Tomoharu SENJYU*, Takashi ISHIMARU, Masaji MATSUYAMA and Yoshio KOIKE

Tokyo University of Fisheries, 5-7, Konan 4, Minato-ku, Tokyo 108-8477, Japan

Abstract—An isolated saline water lens was observed at depth in the Gulf of Oman in January 2–3, 1994. We named the anomalous water mass "Peddy" after Mediterranean "Meddy". The Peddy was 250–400 m deep, and had horizontal and vertical scales of 50 km and 150 m, respectively. The core of the Peddy had a temperature of 18–19°C, a salinity of >36.8, σ_θ of about 26.5 and dissolved oxygen content of >0.5 ml l^{-1}. Anticyclonic circulation in the Peddy reached >35 cm s^{-1} of geostrophic velocity at the sea surface southeast of its core. At the edge of the Peddy, finestructures with vertical scales of 10 m or more were found; this indicates mixing with surrounding waters by thermohaline intrusions. Water similar to the Peddy's core was found just east of the Strait of Hormuz, and it is considered to be an initial stage of the Peddy formation. A pulse of outflow from the Strait of Hormuz was suggested by the ADCP data moored near the Strait; this supports Matsuyama *et al.*'s (1998) hypothesis that the water exchange through the Strait of Hormuz is blocked during spring tide period. These results suggest that the formation of Peddy depends on the intermittent outflow through the Strait of Hormuz.

INTRODUCTION

In the Arabian Sea a vertical salinity maximum from water originating from the Red Sea and the ROPME Sea Area (RSA) is commonly seen. (In this paper, we refer to so-called the Persian or Arabian Gulf as the RSA.) Although water characteristics of the two source waters are slightly different (the RSA shows somewhat higher temperature and higher dissolved oxygen content than the Red Sea), the two water masses are often regarded as one (Tomczak and Godfrey, 1994). These high salinity waters spread into the Arabian Sea at an intermediate level, mainly at depths of 400–800 m, and occasionally reach as far south as 30°S (Gründlingh, 1985).

For the process of outflow from adjacent seas to open oceans, the flow from the Mediterranean to the Atlantic Ocean has been studied in detail. A part of the saline Mediterranean water injected through the Strait of Gibraltar forms lens-shaped eddies of about 50–100 km in diameter (Armi and Zenk, 1984; Hebert, 1988a; Armi *et al.*, 1989; Hebert *et al.*, 1990). Such an eddy is called "Meddy".

*Present address: National Fisheries University, 2-7-1, Nagata-honmachi, Shimonoseki, Yamaguchi 759-6595, Japan.

Meddy shows anticyclonic circulation with a period of rotation of about 5 days and moves south to southwestward with mean speed of 1–2 cm s^{-1} (Richardson *et al.*, 1989). Meddies are considered to an important agent on transport of salinity and heat to the Gulf of Cadiz and Canary Basin region (Hebert, 1988a).

Similar eddies, originating from the Red Sea, are found in the Arabian Sea and are called "Reddy" (Shapiro and Meschanov, 1991). A similar eddy originating from the RSA is expected, but there is no available data to confirm it.

International surveys to study the effects of oil spills on the marine environment were carried out in 1993–1994 in the RSA as a cooperative study of Tokyo University of Fisheries (TUF) and Regional Organization for the Protection of the Marine Environment (ROPME). As a part of the program hydrographic observations were made in the Strait of Hormuz and the Gulf of Oman from December 1993 to January 1994. In this survey a lens-shaped saline water mass was observed in the Gulf of Oman. This anomalous water mass was named "Peddy" after the Mediterranean Meddy. In this paper we describe oceanographic structures of the Peddy and discuss the process of its formation. The largest and the third largest oil spill occurred in the RSA during the Gulf War in 1991 and the Iran-Iraq war in 1982–1983, respectively. These eddies may be one of the important agents of transport of 0:1 pollutants, as well as salt and heat, from the RSA to the Indian Ocean.

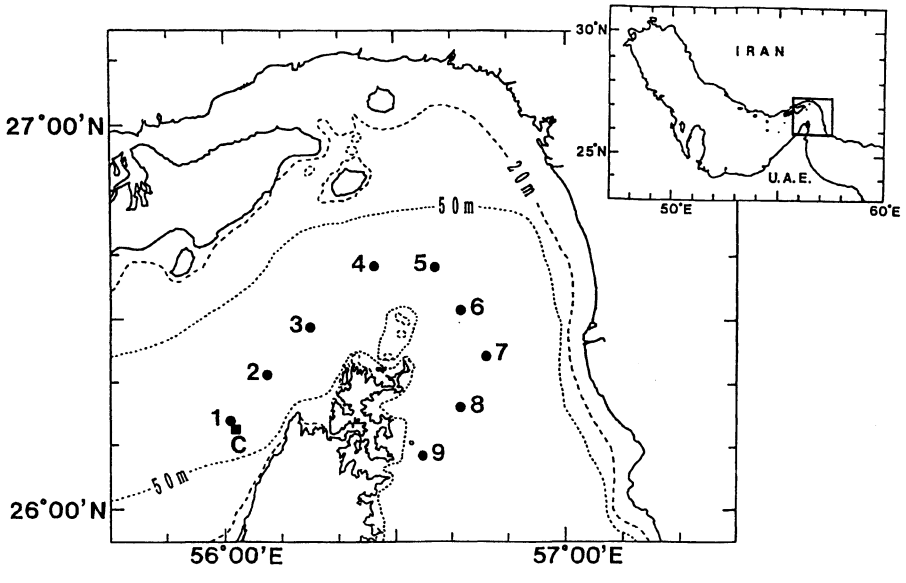

Fig. 1. Map of CTD stations (solid circles) in Leg 1 (December 15–16, 1993). Solid square in the map (Sta. C) denotes the ADCP mooring point.

OBSERVATIONS

Observations in the Strait of Hormuz and the Gulf of Oman were carried out in December 1993–January 1994 by RT/V *Umitaka-Maru* belonging to TUF. CTD casts along the Strait of Hormuz were made in December 15–16, 1993 (Fig. 1; Leg 1). Leg 2 of the cruise (December 17–27, 1993) was devoted to the survey in the RSA. Hydrographic observation in the Gulf of Oman was made in Leg 3 (January 2–3, 1994). Figure 2 shows bottom topography in the observation area and location of CTD and XBT stations in Leg 3.

An ICTD (Integrated CTD; Falmouth Scientific Institute Inc.) with a dissolved oxygen sensor was used at each CTD station. CTD observations were carried out down to 500 m depth or the bottom at shallower stations.

An ADCP (Acoustic Doppler Current Profiler; RD Instrument Co., 300 kHz) was upward installed near the bottom at Sta. C in Fig. 1 (26°13.1′ N 56°00.0′ E, 92 m of bottom depth) on December 15, 1993 and recovered on January 2, 1994. Current data were obtained from 80 m depth to the surface at every 2 m with 5 minutes interval. The data in upper few depths were somewhat noisy due to rough sea conditions.

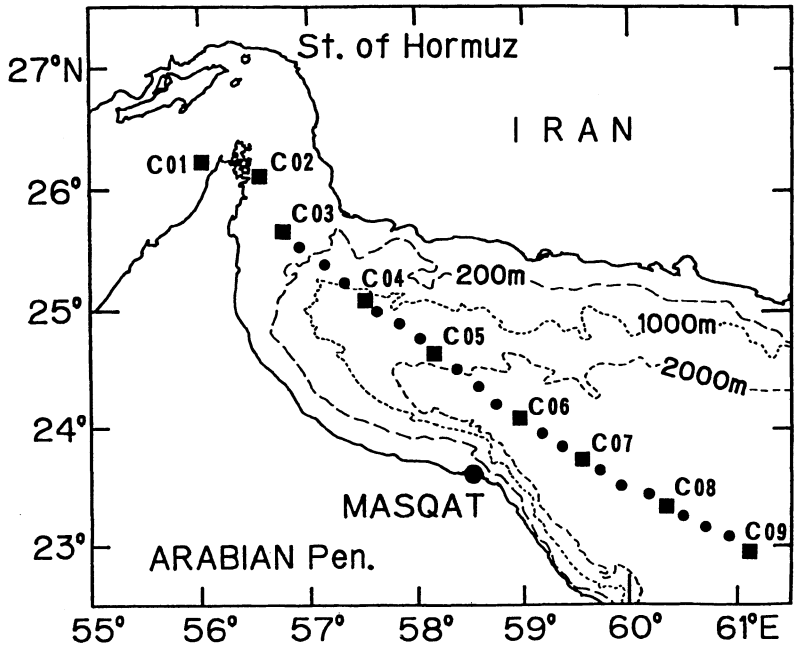

Fig. 2. Bottom topography in the observation area and location of CTD (solid squares) and XBT (solid circles) stations in Leg 3 (January 2–3, 1994).

This paper relates the CTD measurements taken during Legs 1 and 3 and the ADCP current data. Physical aspects in the RSA obtained from Leg 2 and other cruises are reported in Yoshida *et al.* (1998).

STRUCTURE OF THE PEDDY

Temperature, salinity and dissolved oxygen sections along the observation line in Fig. 2 are shown in Fig. 3. The Peddy is found clearly in the salinity section (Fig. 3(b)). An isolated saline water more than 36.6 is seen at about 300 m depth around Sta. C07. The Peddy bordered by the isohaline of 36.6 has a vertical extent of about 150m. The core of the Peddy shows a salinity of more than 36.8. In the temperature section (Fig. 3(a)) the Peddy is identified as a thermostad between the isotherms of 18 and 19°C at 180–350 m depth. Closer examination can be made on the temperature section obtained from CTD and XBT data. The center of the Peddy (the thickest thermostad) is seen 21 km northwest of Sta. C07 showing 185 m of thickness, and the horizontal scale of the Peddy is estimated to be about 50 km. The Peddy must be originated from the RSA; this is supported by the dissolved oxygen distribution (Fig. 3(c)). An isolated high oxygen water with more than 0.4 ml l^{-1} is seen at Sta. C07, the center of the Peddy. The high oxygen content in the Peddy indicates that its origin is in the RSA where vertical

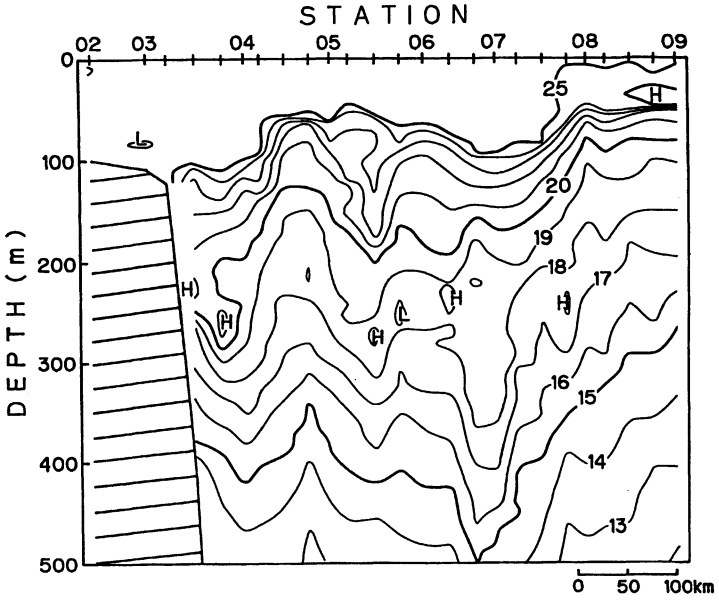

(a)

Fig. 3. (a) Temperature (°C), (b) salinity and (c) dissolved oxygen (ml l^{-1}) sections along the observation line in Fig. 2.

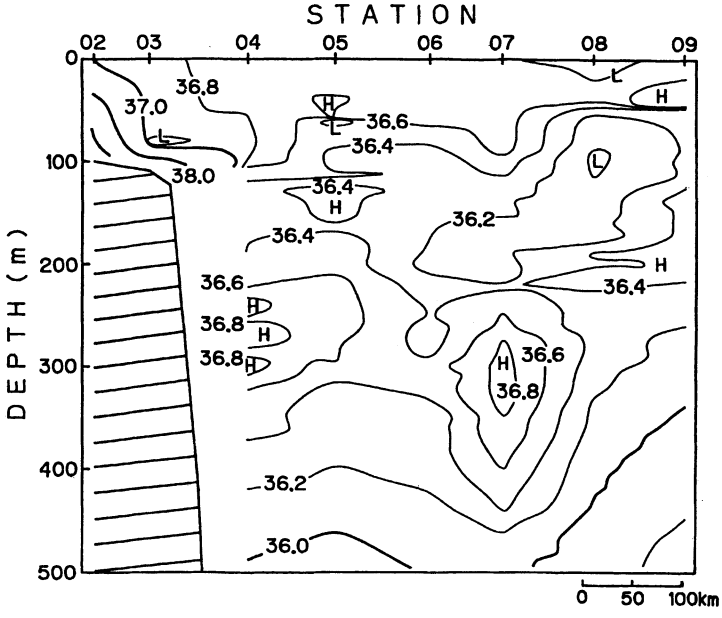

(b)

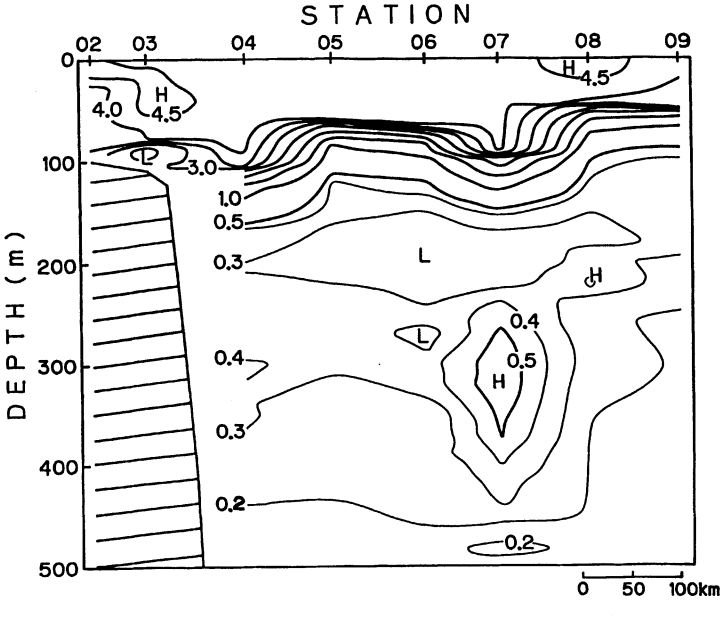

(c)

Fig. 3. (continued).

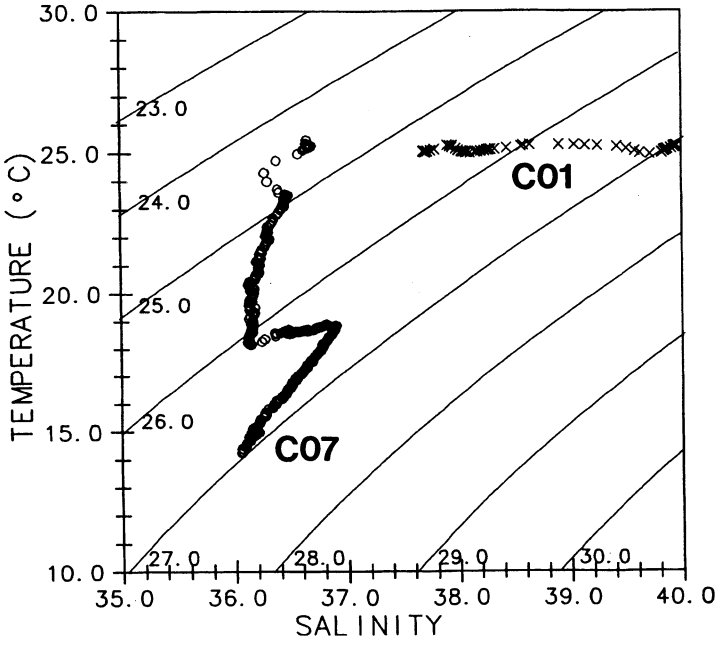

Fig. 4. T-S diagram at Sta. C01 (in the RSA) and Sta. C07 (at the center of Peddy). Open circles denote at Sta. C07 and crosses are at Sta. C01.

convection is active and the residence time is short (Brewer and Dyrssen, 1985; Tomczak and Godfrey, 1994).

Temperature-Salinity relationship at Sta. C01 (in the RSA) and Sta. C07 (near the center of the Peddy) are shown in Fig. 4. The core of the Peddy has a temperature of 18.89°C and a salinity of 36.91 which are significantly lower than those observed in the RSA in the same period. At Sta. C01, the water column has a temperature of nearly 25°C and a salinity range of 37.69–39.96. The Peddy must undergo a mixing with surrounding waters after leaving the Strait of Hormuz.

Salinity profiles at Sta.C07 near the center of the Peddy and at adjacent stations C06 and C08 are shown in Fig. 5. In the core of the Peddy, 220–460 m depth at Sta. C07, salinity reaches its maximum at 310 m depth. Its vertical variation shows less fluctuations compared to those at the adjacent stations which show finestructures with vertical scales of 10 m or more. These finestructures are also seen in the upper and lower layers of the Peddy's core. Similar thermohaline structures are found in the data collected by the *Mt. Mitchell* Expedition in the Gulf of Oman in 1992 (Sultan and Elghribi, 1996). Such finestructures are common to Meddies in the Atlantic Ocean (Armi *et al.*, 1989) and Reddies in the Indian Ocean (Gründlingh, 1985), and considered to be thermohaline intrusions

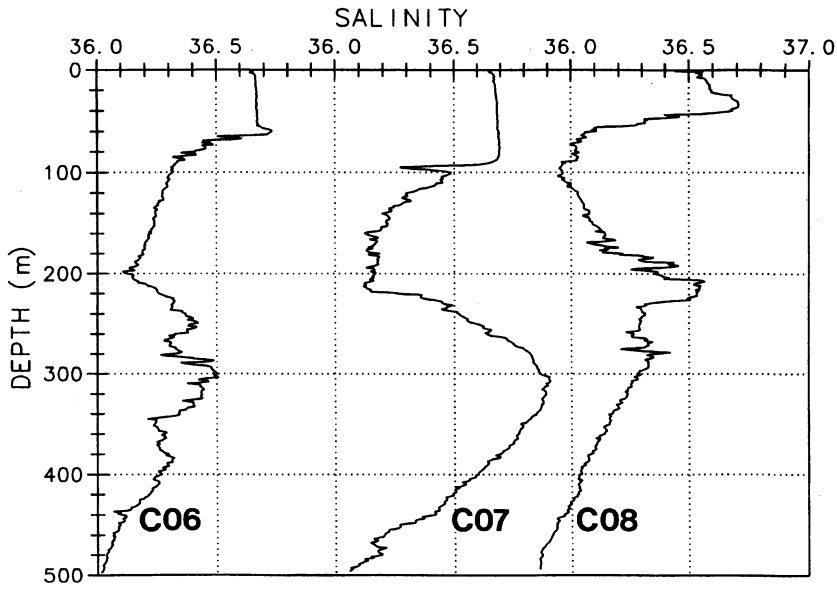

Fig. 5. Salinity profiles at the center of the Peddy (Sta. C07) and at adjacent stations (Stas. C06 and C08).

caused by double diffusion (Hebert, 1988b; Ruddick, 1992).

Figure 6 shows potential density and geostrophic velocity sections referred to 500 db (1 db equal to 10 kPa). Negative values in the velocity section (Fig. 6(b), hatched area) denote southwestward flow. The current east of the Peddy's center (about 25 km northwest of Sta. C07) is southwestward, while northeastward flow is found west of it in accordance with the density distribution (Fig. 6(a)). This flow pattern indicates an anticyclonic circulation in the Peddy. The maximum velocity with 35 cm s^{-1} or more is found at the sea surface southeast of the Peddy, though the core of the Peddy is located at about 300 m depth (Fig. 3). One of Argos-tracked drifting buoys in the Gulf of Oman deployed during the *Mt. Mitchell* Expedition in 1992 drew an anticyclonic trajectory about 80 km of diameter with the mean scaler speed of 21.07 cm s^{-1} (ID9450; Reynolds, 1993). This buoy might be trapped in a Peddy.

DENSITY FRONT IN THE STRAIT OF HORMUZ AND PEDDY FORMATION

Another water mass having almost the same salinity and dissolved oxygen content as the core of the Peddy is seen in 250–300 m depths at Sta. C04 (Figs. 3(b) and 3(c)). The water shows higher temperature (more than 20°C northwest of Sta. C04, Fig. 3(a)) than that of the Peddy's core. This is the outflow water from the RSA through the Strait of Hormuz. The water is separated from the Peddy over 150 km by colder, less saline and lower oxygen content water. This separation

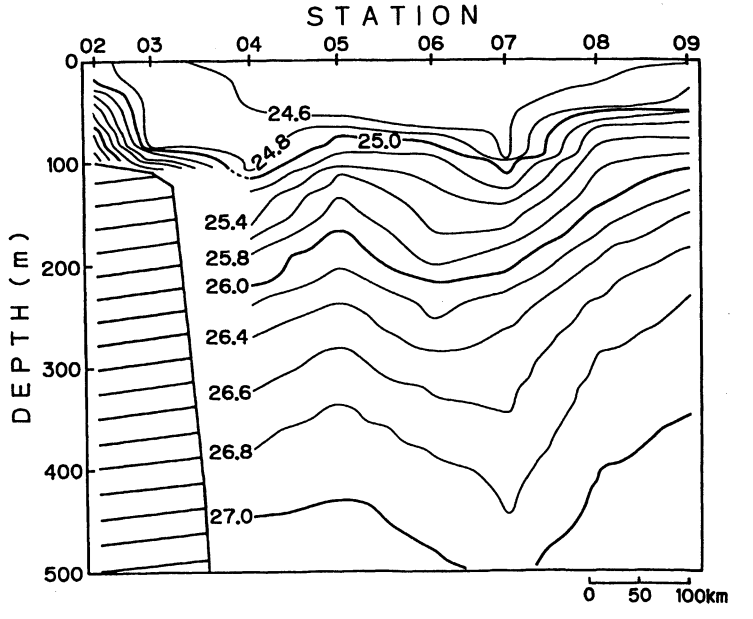

(a)

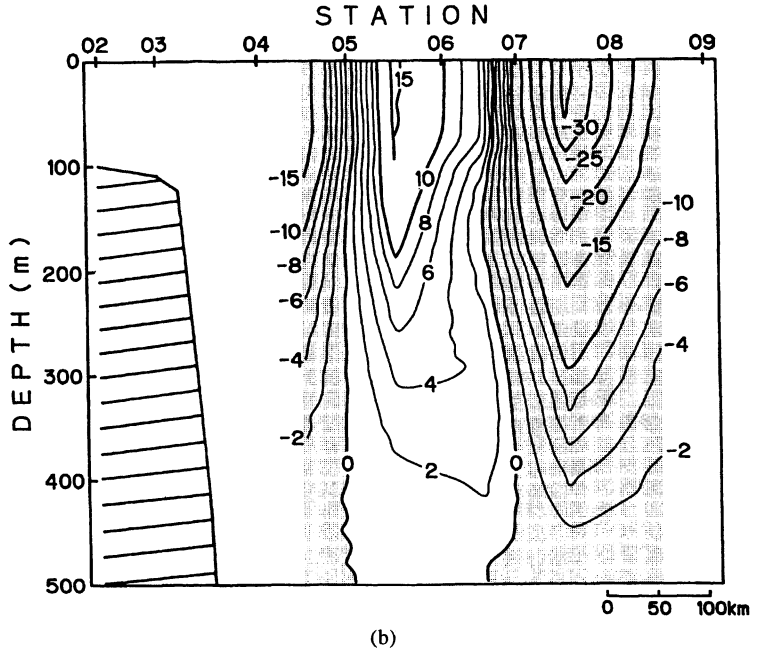

(b)

Fig. 6. (a) Potential density (σ_θ) and (b) geostrophic velocity (cm s^{-1}) sections referred to 500 db. Hatched areas in the velocity section show southwestward flow.

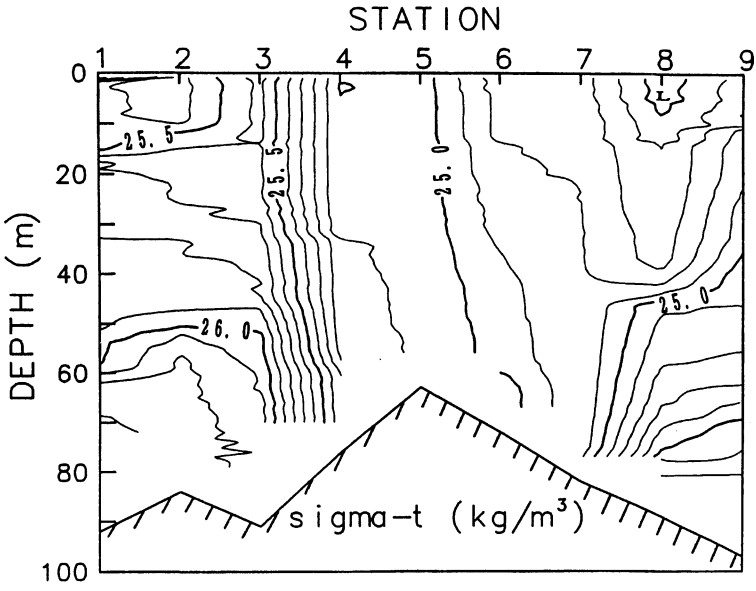

Fig. 7. Density (σ_t) section along the Strait of Hormuz.

suggests an intermittency of the outflow from the Strait of Hormuz.

CTD observation along the Strait of Hormuz in December 15–16, 1993 (Fig. 1) shows a density front in the Strait of Hormuz. The density section along the observation line is shown in Fig. 7. Strong stratifications are found in the RSA (Stas. 1–3 in Fig. 7) and in the Gulf of Oman out of the Strait (Stas. 8 and 9), but almost homogeneous water is found at the center of the Strait (Stas. 4–7) forming a steep density front between Stas. 3 and 4. The wintertime density distribution depends strongly on the salinity distribution. Matsuyama *et al.* (1998) explained the density structure in the Strait of Hormuz as a tidal front caused by strong tidal currents and discussed the water exchange between the RSA and the Arabian Sea through the Strait. They speculated that a mixing due to the strong tidal current in spring tide period forms a steep density front, but at other times the density front disappears and an active water exchange occurs through the Strait.

Figure 8 shows mean velocity profiles obtained by the ADCP moored at Sta. C (see Fig.1). The current data are filtered out by 25-hours running mean to remove tidal currents, and then each component of mean velocities (along and cross strait directions) is calculated for the neap (December 20–24, 1993) and the spring tide period (December 15–16 and 27–31, 1993), respectively. As previously stated, the data above 12 m depth are omitted.

The along strait component in the neap tide period shows outflow direction at all depths. The component in the spring tide period is also outflow except for the depths between 16 and 24 m. However, it is reported that the water exchange

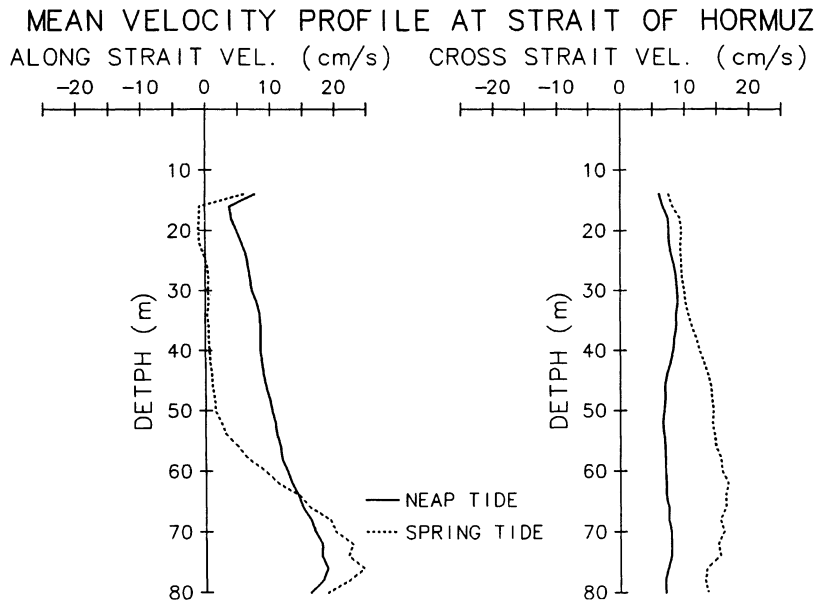

Fig. 8. Mean velocity profiles obtained by the ADCP moored at Sta. C. Along strait denotes northeast-southwest direction (positive northeast) and cross strait is northwest-southeast direction (positive northwest). Mean velocities are separately calculated for the neap (December 20–24, 1993) and the spring tide period (December 15–16 and 27–31, 1993), respectively.

through the Strait of Hormuz has a two-layer flow system throughout the year; relatively low salinity water enters into the RSA in the upper layer and a high-salinity dense water flows to the Gulf of Oman in the deeper portion of the Strait of Hormuz (Reynolds, 1993). This reverse estuary flow is also suggested by residual currents based on the current meter data taken during the *Mt. Mitchell* expedition (Abdelrahman and Ahmad, 1995). Our ADCP fails to show any evidence of surface inflow. The all inflow might be confined in upper 12 m depths.

The profile of along strait component shows a maximum near the bottom in both the neap and spring tide periods. This maximum is more clear in the spring tide period. Velocities above 62 m depth in the neap tide period are greater than those in the spring tide (the velocities at 22–44 m depths in the spring tide are less than 1.0 cm s^{-1}), but below that depth velocities in the spring tide period exceed those in the neap tide. Table 1 shows volume transports integrated from 14 to 80 m depths in vertical for each component. The along strait component of volume flow in the neap tide period is 62% greater than the spring tide (2.72 m^3s^{-1}). If this current structure is maintained over the width of the Strait (56 km), the difference of volume transport between the neap and spring tide periods amounts to 0.15 ×

Table 1. Volume transports integrated 14–80 m depths in the Strait of Hormuz.

	Cross strait (m^3/s)	Along strait (m^3/s)
Spring tide	8.53	4.36
Neap tide	5.05	7.08
All period	6.76	6.95

10^6 m^3s^{-1}. On the other hand, cross strait velocities in the spring tide period are larger than those in the neap tide at all depths. Its volume transport is larger than that in the neap tide period by 3.48 m^3s^{-1} (Table 1). This suggests that a part of dense water in the RSA flows northwestward along the steep density front west of the Strait of Hormuz in the spring tide period. These facts agree with the Matsuyama *et al.*'s (1998) hypothesis.

From the distribution of water characteristics along with the ADCP current data, it is suggested that the formation of a Peddy depends on the pulse of outflow from the RSA through the Strait of Hormuz. In the Mediterranean, bottom topographic effects and baroclinic instability are proposed as causes of Meddy formation (McWilliams, 1985; Hebert, 1988a). This study shows that the local condition in the strait, such as the existence of tidal front, can be one of the important factors of eddy formation as well as topographic effects and baroclinic instability.

DISCUSSION

In previous sections, we pointed out that the Peddy must undergo a mixing with surrounding waters after outflowing from the Strait of Hormuz. We can make a rough estimation of mixing ratio of the RSA Water to surrounding waters by

$$\frac{V_S}{V_G} = \frac{S_G - S_P}{S_P - S_S},$$

where V_G and S_G are volume and salinity of the RSA Water, V_S and S_S are those of surrounding waters and S_P denotes salinity in the Peddy. If we take S_G, S_S and S_P to be 39.8, 36.3 and 36.7 as typical values respectively, the ratio is 7.8. This means that the outflow water from the RSA entrained about eight times of volume of surrounding waters. Most of the entrainment or mixing with surrounding waters must occur immediately after the outflow from the Strait because the outflow water just east of the Strait has almost the same properties as the core of

the Peddy (Fig. 3).

We can make a rough estimation of salt transport by Peddies in the western Gulf of Oman. Salinity flux is evaluated by $V_P \Delta S(n/t)$, where V_P denotes volume of the Peddy, ΔS ($=S_P - S_S$) is salt anomaly relative to surrounding waters (kg m^{-3}) and (n/t) the number of Peddies per unit time passing through the Gulf of Oman. The horizontal and vertical scales of the Peddy were estimated to be 50 km and 150 m, respectively (Fig. 3). If the Peddy is approximated by a cylinder with 50 km of diameter and 150 m of thickness, the volume V_P is 2.9×10^{11} m^3. If ΔS is taken to be 0.4 kg m^{-3} as above and a Peddy is formed every 15 days according to neap and spring tide period, the salt flux by Peddies is estimated to be 8.95×10^4 kg s^{-1}.

On the other hand, salinity flux through the Strait of Hormuz is estimated by

$$V_i + V_o + V_e = 0,$$

$$V_i S_S + V_o S_G = 0$$

or

$$V_o(S_G - S_S) = V_e S_S,$$

where V_i, V_o and V_e denote water volumes of inflow and outflow through the Strait of Hormuz and evaporation in the RSA, assuming river runoff is negligible. If the evaporation in the RSA is taken to be 2–5 m year^{-1} and the area of the RSA is 2.39×10^5 km^2, then the salt flux from the RSA is 0.55×10^6–1.38×10^6 kg s^{-1}. These

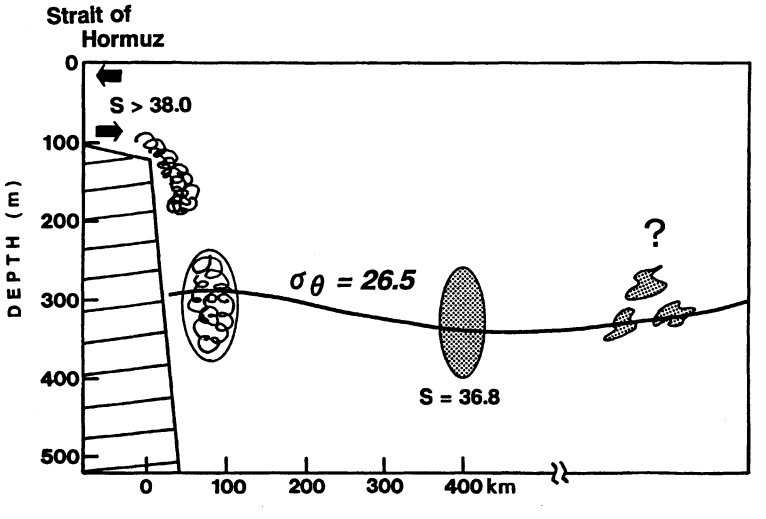

Fig. 9. Cartoon of the life cycle of a Peddy.

figures indicate that about 10% of the salt flux from the RSA are transported by Peddies. Though the rate shows that Peddies are not the dominant transport mechanism of salt in the Gulf of Oman, they are probably an important one for the Arabian Sea because Peddies can transport its salt anomaly to remote places. The rate is probably not maintained through the year because a strong stratification is formed in the Strait of Hormuz in summer (Reynolds, 1993). The formation of tidal front depends strongly on the condition of stratification. Moreover, flows in the Strait are greatly affected by winds, such as *Shamal* (Matsuyama *et al.* ,1998).

Salinity (Fig. 3(b)) and potential density distributions (Fig. 6(a)) show that the core of the Peddy lies at about $26.5\sigma_\theta$ (see also Fig. 4). On the other hand, the high salinity water at Sta. C04 near the Strait of Hormuz is also seen at 26.2–$26.5\sigma_\theta$. This saline water is considered to be an initial stage of Peddy formation. Therefore, the Peddy must have migrated along the isopycnal surface of $26.5\sigma_\theta$ in the Gulf of Oman.

After McWilliams (1985), we show a cartoon of the life cycle of a Peddy in Fig. 9. At first a saline water more than 38.0 enters the Gulf of Oman through the Strait of Hormuz. Since the water is denser than surrounding waters, sinking down to the depth of $26.5\sigma_\theta$ occurs. The water characteristics of Peddy must be determined through the sinking process accompanying convection, entrainment and mixing with surrounding waters because the water characteristics in this stage are almost the same as Peddy's core. The depth of $26.5\sigma_\theta$ is gravitationally stable for the diluted RSA Water. After an inertial period the water mass acquires an anticyclonic circulation through the geostrophic adjustment process; a Peddy is formed. Then the Peddy migrates to the Arabian Sea along the $26.5\sigma_\theta$ surface in the Gulf of Oman. Mixing with surrounding waters by thermohaline intrusions continues throughout the migration. Eventually, the Peddy disappears and forms a salinity maximum layer in the Arabian Sea together with the Red Sea water. This last stage is highly speculative.

Acknowledgements

We wish to thank Captain T. Isouchi and crew of RT/V *Umitaka-Maru*. Thanks are also due to ROPME and Japanese scientists joining the cruise. Valuable comments and discussion from Drs. R. M. Reynolds and H. Sudo are greatly acknowledged. The ADCP observation in this study was supported by Mr. T. Nakagawa, S.E.A. Co.

REFERENCES

Abdelrahman, S. M. and Ahmad, F. (1995). A note on the residual currents in the Arabian Gulf, *Continent. Shelf Res.* **15**, 1015–1022.

Armi, L. and Zenk, W. (1984). Large lenses of highly saline Mediterranean Water, *J. Phys. Oceanogr.* **14**, 1560–1576.

Armi, L., Hebert, D., Oakey, N., Price, J. F., Richardson, P. L., Rossby, H. T. and Ruddick, B. (1989). Two years in the life of a Mediterranean salt lens, *J. Phys. Oceanogr.* **19**, 354–370.

Brewer, P. G. and Dyrssen, D. (1985). Chemical oceanography of the Persian Gulf, *Prog. Oceanogr.* **14**, 41–55.

Gründlingh, M. L. (1985). Occurrence of Red Sea Water in the southwestern Indian Ocean, 1981,

J. Phys. Oceanogr. **15**, 207–212.

Hebert, D. (1988a). Mediterranean salt lenses. In *Small-Scale Turbulence and Mixing in the Ocean* (J. C. J. Nihoul and B. M. Jamart, eds.), pp. 229–237, Elseviar.

Hebert, D. (1988b). Estimates of salt-finger fluxes, *Deep-Sea Res.* **35**, 1887–1901.

Hebert, D., Oakey, N. and Ruddick, B. (1990). Evolution of a Mediterranean salt lens: Scalar properties, *J. Phys. Oceanogr.* **20**, 1468–1483.

Matsuyama, M., Kitade, Y., Senjyu, T., Koike Y. and Ishimaru, T. (1998). Vertical structure of a current and density front in the Strait of Hormuz. This volume.

McWilliams, J. C. (1985). Submesoscale, coherent vortices in the ocean, *Rev. Geophys.* **23**, 165–182.

Reynolds, R. M. (1993). Physical oceanography of the Gulf, Strait of Hormuz, and the Gulf of Oman—Results from the *Mt. Mitchell* expedition, *Mar. Pollution Bull.* **27**, 35–59.

Richardson, P. L., Walsh, D., Armi, L., Schroder, M. and Price, J. F. (1989). Tracking three Meddies with SOFAR floats, *J. Phys. Oceanogr.* **19**, 371–383.

Ruddick, B. (1992). Intrusive mixing in a Mediterranean salt lens—Intrusion slopes and dynamical mechanisms, *J. Phys. Oceanogr.* **22**, 1274–1285.

Shapiro, G. I. and Meschanov, S. L. (1991). Distribution and spreading of Red Sea Water and salt lens formation in the northwest Indian Ocean, *Deep-Sea Res.* **38**, 21–34.

Sultan, S. A. R. and Elghribi, N. M. (1996). Temperature inversion in the Arabian Gulf and the Gulf of Oman, *Continent. Shelf Res.* **16**, 1521–1544.

Tomczak, M. and Godfrey, J. S. (1994). *Regional Oceanography: An Introduction*, 422 pp., Pergamon Press.

Yoshida, J., Matsuyama, M., Senjyu, T., Ishimaru, T., Hashimoto, S., Morinaga, T., Otsuki, A., Kamatani, A., Maeda, M., Arakawa, H., Kasuga, I., Koike, Y., Mine, Y., Kurita, Y., Kitazawa, A., Noda, A., Hayashi, T., Miyazaki, T. and Takahashi, K. (1998). Hydrography in the Gulf during the RT/V *Umitaka-Maru* Cruises. This volume.

Offshore Environment of the ROPME Sea Area after the War-Related Oil Spill, Eds. A. Otsuki *et al.*, pp.49–63.

Distribution of Turbidity in the ROPME Sea Area

Hisayuki ARAKAWA, Toru HIRAWAKE and Tsutomu MORINAGA

Department of Ocean Sciences, Tokyo University of Fisheries, 5-7, Konan-4, Minato-ku, Tokyo 108-8477, *Japan*

Abstract—Through three cruises in the ROPME Sea Area, a water of low turbidity, of which the beam attenuation coefficient was 0.2–0.4 m^{-1}, could be seen in the surface layer. This low turbidity water had a width of approximately 15–25 miles and extended along the Gulf axis from near the Strait of Hormuz to off the Peninsula of Qatar. Also, it generally distributed in the layer from surface to near the seabed. While the high turbidity water was seen in the shallow water, and appeared near the seabed. Moreover, the annual variation of transparency was broad. In Jan. 1993, the largest value of transparency was more over 12 m, and the smallest one was less than 4 m. The water color ranged between 4 and 8, and the colors, which appeared most frequently, were 5 and 6. The correlation between the beam attenuation coefficient and SS (Suspended solid) is shown as follows;

$$C = 0.416G + 0.18 \quad (r = 0.779),$$

where C and G are beam attenuation coefficient and SS, respectively.

INTRODUCTION

This study was conducted as a part of the project "Studies on the oil spills in the ROPME Sea Area". ROPME Sea Area (hereafter abbreviated as RSA) means the region surrounded by United Arab Emirates, Qatar, Bahrain, Saudi Arabia, Kuwait, Iraq and Iran, and suffered a environmental disaster by a destruction of oil wells in Kuwait in 1991. In this volume, thorough cooperative investigations by RT/V Umitaka-Maru, Tokyo University of Fisheries with ROPME countries are presented from physical, chemical and biological oceanographic point of view.

With respect to the physical and chemical oceanographic conditions in the RSA, only a few surveys have been done by Emery (1956), Brewer and Dyrssen (1985), and Reynolds (1991), however, a study on turbidity in the RSA was not conducted in these studies.

The turbidity of seawater resulting from the existence of suspended and/or dissolved matters is considered to be one of the most important factors for the environment from the viewpoint of contamination and its protection of the ocean (Matsuike *et al.*,1986). Also, it is considered to be of great help for classifying the water mass distribution (Morinaga,1983).

The study of turbidity in the RSA is only a few, and as far as we know, Oshite(1974) first investigated the transparency and suspended solid (hereafter

abbreviated as SS) as indices of turbidity in this area. 40 stations were covered from the area off Kuwait to the Strait of Hormuz in December 1968. The ranges of transparency and SS obtained were 8 to 16 m and 0.2 to 1.8 mg/l, respectively. In this brief report, we present the latest results of turbidity observation in winter time. The observations were conducted three times over two years. More than 60 stations were occupied and horizontal and vertical distributions of turbidity are presented.

METHODS AND INSTRUMENTS

The observations were carried out in Jan. 1993, Dec. 1993, and Dec. 1994, aboard RT/V Umitaka-Maru travelling through the RSA. Observation stations are shown in Figs. 1 a, b, and c. The items of water properties measured were turbidity, transparency, water color, SS, ignition loss, temperature and salinity, respectively. The turbidity of the seawater at each station was continuously recorded from the surface to near the seabed, with an in situ beam transmittance meter (XMS transmisso meter: Martek inc.; light path length: 1 m; measured wavelength: 486 nm). As an indicator of turbidity, the beam attenuation coefficient (C, unit is m^{-1}) is calculated as $C=1/r \cdot \ln(1/T)$, where r and T are light path length and beam transmittance, respectively. To estimate transparency and water color, Secchi disc and Forel's color scale were used. SS was obtained by the following method. Sample seawater at each station was collected from several layers (surface, 10 m, 20 m and bottom) by use of Van Dorn water samplers in Dec. 1993 and Dec. 1994 cruises, and was filtrated with millipore HA filters of the pore size of 0.45 μm. After the filtration, the filters were dried with oven for three days at 60°C, and the weight was estimated. Ignition loss was to measure the weight of cinders made by means of burning the filters for 4 hr at 450°C after measuring SS. In order to measure the temperature and salinity, Neil Brown Mark IIIB CTD was used in Jan. 1993 and Dec. 1994, and FSI (Falmouth Scientific Institute Inc.) ICTD (Integrated CTD) was used in Dec. 1993.

RESULTS

Distribution of turbidity

Horizontal distribution of turbidity in the surface layer in Jan. 1993 can be seen in Fig. 2 a. The area of low turbidity, beam attenuation coefficient (C) of 0.5 m^{-1}, occupied a great part of RSA. Especially, the lowest value less than 0.4 m^{-1} appeared in the center of gulf. The width of this area is approximately 15 miles, and extended along the Gulf axis from the Strait of Hormuz to off the Peninsula of Qatar. Along the Iran and UAE sides of this area, turbidity gradually increased towards the coast.

The vertical distribution of turbidity along Section K in Jan. 1993 is shown in Fig. 3. The low turbidity water ($C < 0.5$ m^{-1}) was generally distributed in the layer from surface to near the seabed, while the muddy or turbid water ($C > 0.5$ m^{-1}) was seen in the shallow water. Moreover, in shallow water region, a value of beam attenuation coefficient is so high ($C > 0.9$ m^{-1}) near the bottom, and may

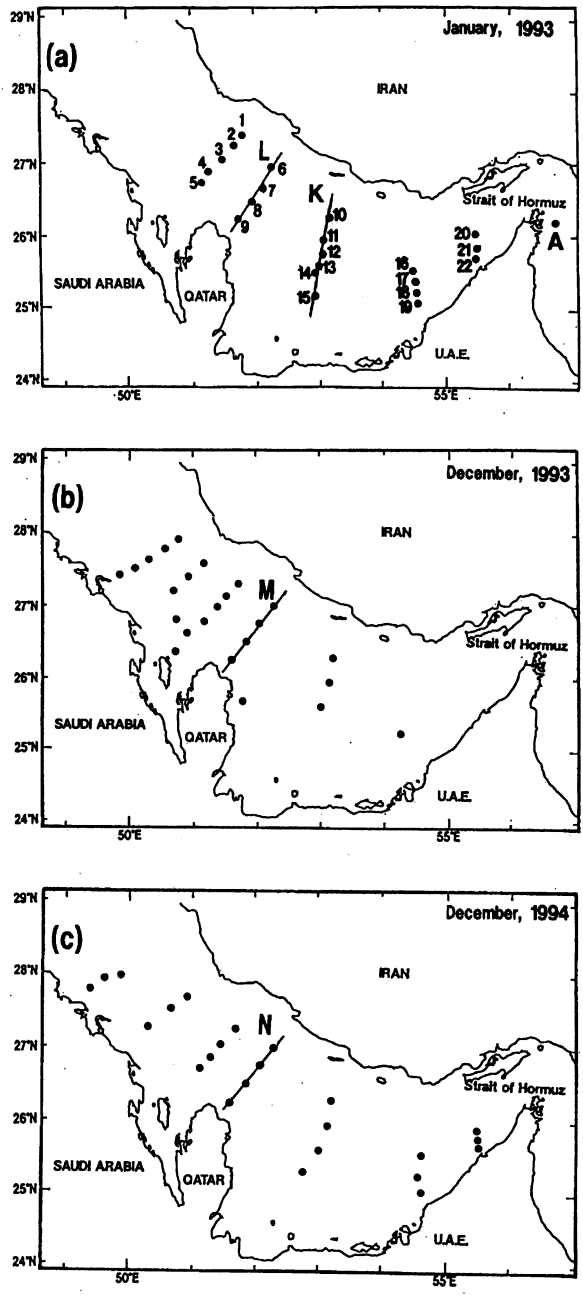

Fig. 1. Observation stations in (a) Jan. 1993, (b) Dec. 1993, and (c) Dec. 1994 are shown in solid circles. The numerals are station numbers from 1 to 22, are referred in Fig. 11. The vertical sections of turbidity along lines K, L, M, and N are shown in Fig. 3, Figs. 5 a, 5 b, and 5 c, respectively. The vertical distribution of turbidity at station A is shown in Fig. 4.

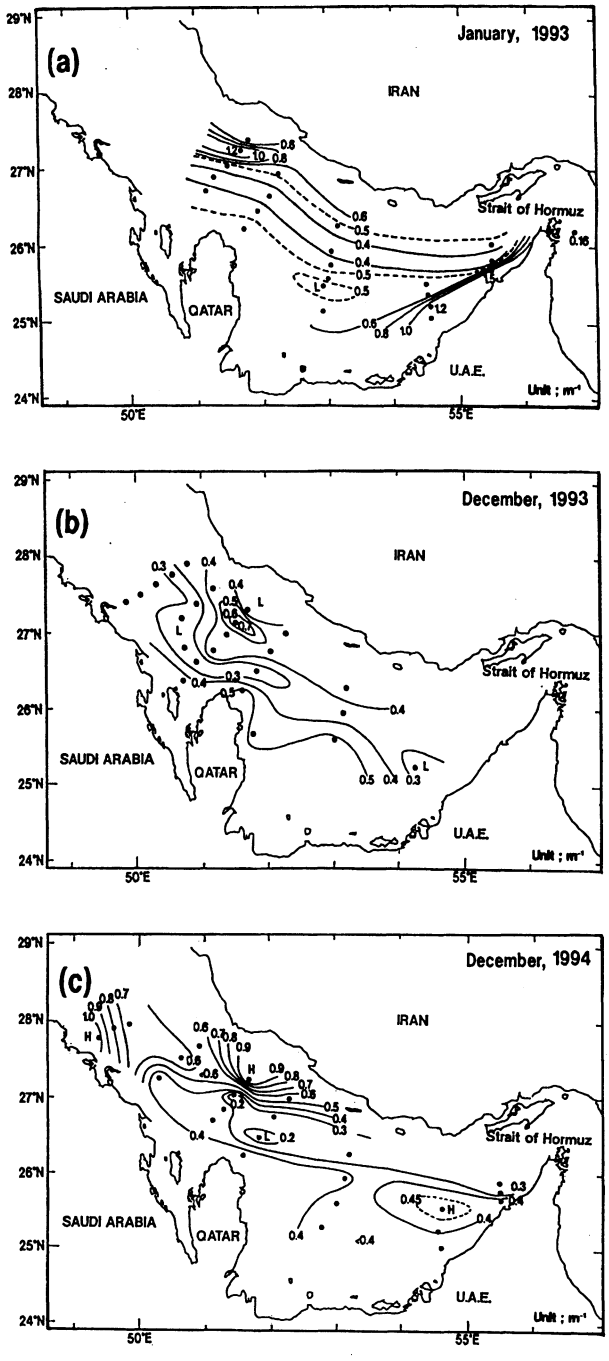

Fig. 2. Horizontal distribution of turbidity (Beam attenuation coefficient; C) in (a) Jan. 1993, (b) Dec. 1993, and (c) Dec. 1994. Unit of turbidity is m^{-1}, and contour interval is 0.1 m^{-1}.

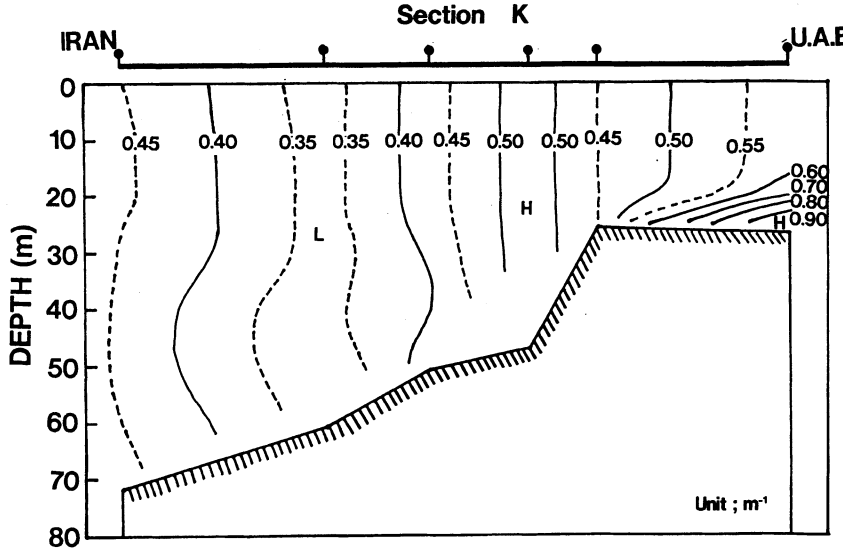

Fig. 3. Vertical distribution of turbidity along Section K in Jan. 1993. A Contour interval is 0.05 m^{-1}.

be due to the effect of bottom sediment.

Subsequently, the vertical profile of turbidity at station A (see the position in Fig. 1 a) in the Strait of Hormuz is shown in Fig. 4. The turbidity is almost homogeneous ($C \fallingdotseq 0.2\ m^{-1}$) from surface to a depth of 50 m, and is increased with the depth increased below 50 m depth. At a depth of 65 m, the turbidity reached its maximum value ($C \fallingdotseq 0.9\ m^{-1}$). This low turbidity water in the surface layer was never seen in the RSA. Thus, the extremely low turbidity water ($C < 0.2\ m^{-1}$) in the layer shallower than a depth of 50 m is generally seen in the open ocean. (for example; Central pacific $C = 0.09\ m^{-1}$ (at 440 nm), Jerlov (1951); Indian Ocean $C = 0.11$–$0.22\ m^{-1}$ (at 486 nm), Morinaga *et al.* (1992)) Also, the value of this high turbidity at a depth of 65 m is similar to that of the water near the coast of UAE and the near seabed in the RSA.

Annual variation of turbidity

The annual variation of turbidity has been examined in this section. Figs. 2 a, b, and c show the horizontal distributions of turbidity at the surface layer in Jan. 1993, Dec. 1993, and Dec. 1994, respectively. In Dec. 1993, the values of C in the center of the RSA were less than $0.4\ m^{-1}$. This low turbidity water was deviated toward the south off Qatar. Also, the extremely low turbidity water ($C < 0.3\ m^{-1}$) which was observed in Dec. 1993 reached to an inner part of the gulf. In Dec. 1994, the low turbidity water, less than $0.4\ m^{-1}$, occupied most of the Gulf. This region was the widest through three cruises. Also, the lowest value

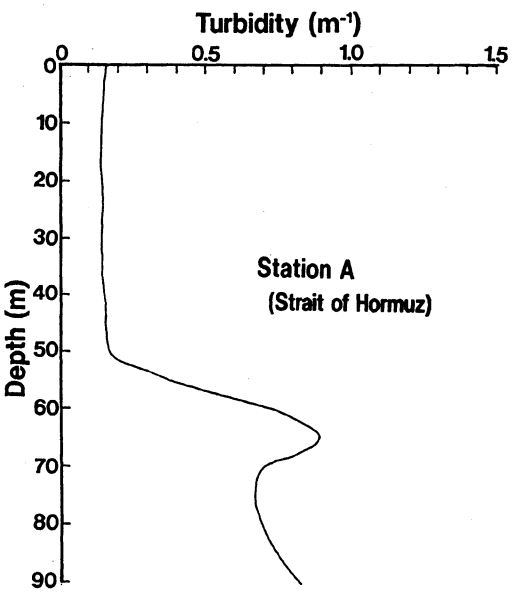

Fig. 4. Vertical distribution of turbidity at station A in the Gulf of Oman (Near the Strait of Hormuz) in Jan. 1993.

of turbidity, of which C was less than 0.2 m^{-1} was found off Qatar. This value was close to that observed at the Strait of Hormuz (see Fig. 4) in Jan. 1993.

In addition, the vertical distributions of turbidity on Section L, M, and N off Qatar can be seen in Figs. 5 a, b, and c, respectively. At Section L (Jan. 1993), the low turbidity water ($C < 0.4$ m^{-1}) appeared in the layer from surface to near the seabed at the center of the RSA, and in the layer between 20 m and 30 m depths in the region from the center of the Gulf to the coast of Iran. Also, the high turbid water (0.6 $m^{-1} < C < 1.0$ m^{-1}) appeared near the seabed on Iranian side.

Along Section M (Dec. 1993), the low turbidity water ($C < 0.4$ m^{-1}) showed a belt-shaped distribution between the surface at the center of the RSA and the layer from a depth of 20 to 50 m toward the coast of Iran. Also, it was found that the high turbidity water ($C > 0.5$ m^{-1}) extended along the sea floor from Qatar to Iranian coast. The value of turbidity is the highest off Qatar.

Along Section N (Dec. 1994), the low turbidity water ($C < 0.4$ m^{-1}) occupied the widest area among three cruises. Besides, the lowest value of C (< 0.2 m^{-1}) among three cruises appeared in the center of the RSA. The turbidity distribution in the gulf was coaxial semicircles in shape with a center at the middle of the gulf. Low turbidity area, of which C was less than 0.3 m^{-1} had a width of about 45 miles and thickness of about 30 m. The high turbid water appeared near the bottom from Qatar to Iran. The largest value of turbidity, of which C was

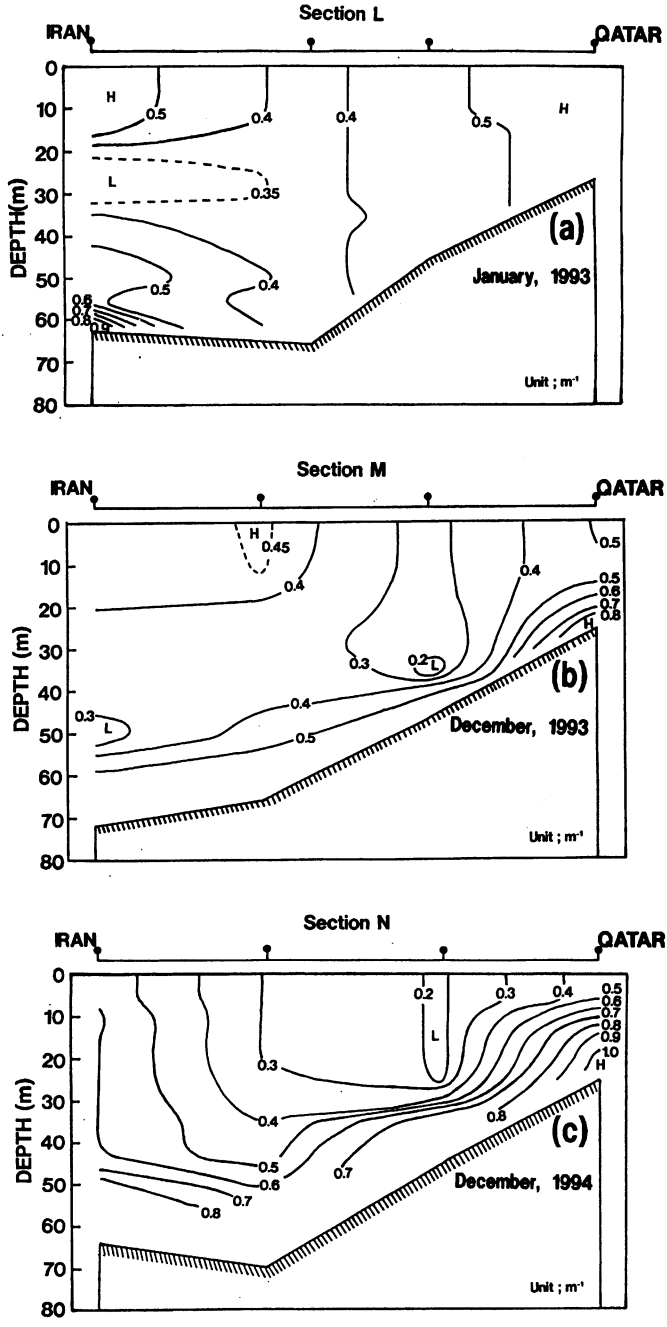

Fig. 5. Annual variation of horizontal distribution of turbidity on the surface layer in (a) Jan. 1993, (b) Dec. 1993, and (c) Dec. 1994. A Contour interval is 0.1 m^{-1}.

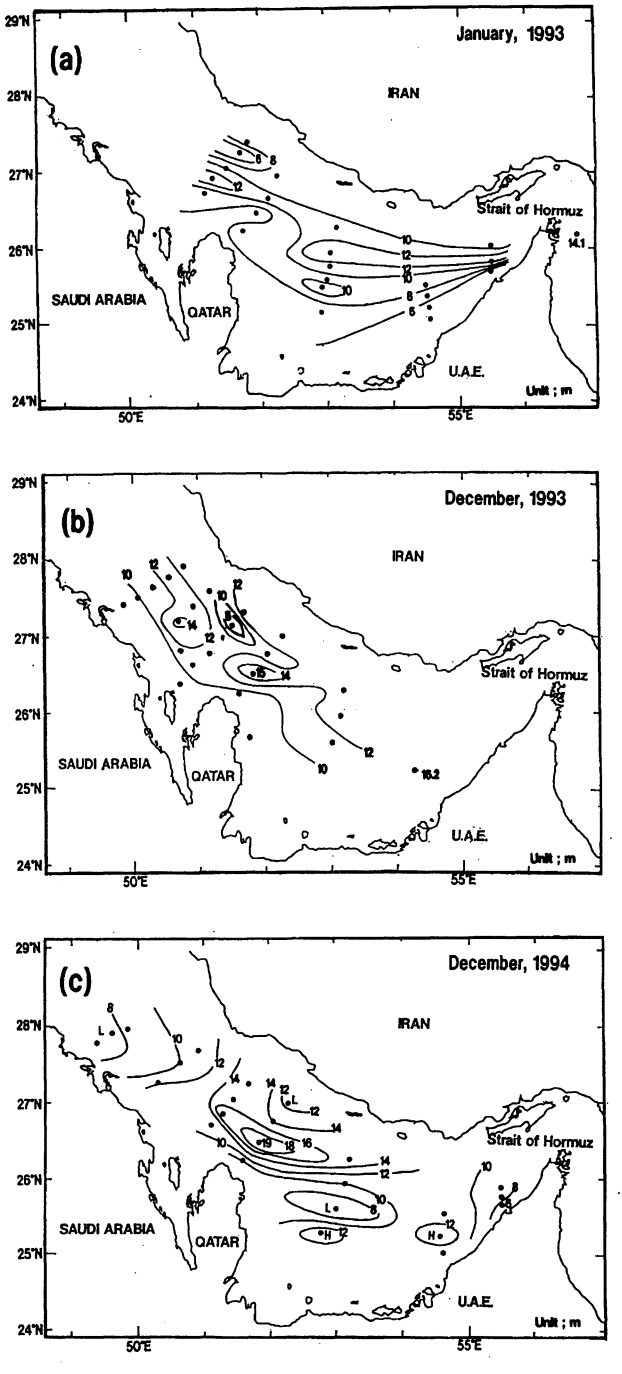

Fig. 6. Annual variation of distribution of transparency in (a) Jan. 1993, (b) Dec. 1993, and (c) Dec. 1994. Unit of transparency is m. A contour interval is 2 m.

more than 1.0 m^{-1} indicated the bottom off Qatar. Thus, it is found that the low turbidity seawater ($C < 0.4\ m^{-1}$) covered a wide area in the center of the RSA, and the high turbidity water covered near the sea bottom in December.

Distributions of transparency and water color

Figures 6 a, b, and c show the distribution of transparency in Jan. 1993, Dec. 1993, and Dec. 1994, respectively. In Jan. 1993, the clear area above 10 m at transparency was in the center of the RSA, and distributed along the Gulf axis from the Strait of Hormuz to off the Peninsula of Qatar, and its values gradually decreased toward the coast. The value of transparency in the inner of gulf and off UAE showed less than 6 m. In Dec. 1993 and Dec. 1994, the high values of transparency appeared in the center of the gulf. In particular, that in Dec. 1994 showed the largest value at 19 m. This distribution of transparency is similar to that of turbidity in Fig. 2.

Distribution of water color in Jan. 1993, Dec. 1993, and Dec. 1994 can be seen in Figs. 7 a, b, and c, respectively. The water color is the discrete value. However, we draw the contour line for convenience. In Jan. 1993, the area where water color was between 4 and 5, appeared in the center of the RSA from near the Strait of Hormuz to off the Peninsula of Qatar. Along the north and south sides of this area, the values of water color ranged from 6 to 8. In Dec. 1993 and Dec. 1994, the most part of gulf was occupied by the water of water color 5 to 6 and 4 to 5, respectively. The relationship between water color and turbidity was not obviously rather than that between transparency and turbidity.

DISCUSSIONS

Correlation between turbidity and SS

From the results in this study, a detailed distribution of turbidity were shown in the RSA in winter. At first, we examined the relationship between the turbidity and quantity of suspended matter.

The value of SS in Dec. 1993 and Dec. 1994 cruises ranged from the largest value of 2.2 mg/l to its smallest one of 0.2 mg/l. The correlation between C and SS can be seen by following formula (Fig. 8): $C = 0.416\ G + 0.180$ ($r = 0.779$); where, C and G are beam attenuation coefficient and SS, respectively. The correlation coefficient (r) is high. From the correlation and the turbidity distribution in Fig. 2, we can estimate the distribution of SS in the RSA.

Further, it shows the ratio of inorganic matter contained SS. The distribution of ratios of inorganic matter can be seen in Fig. 9. The ratios of inorganic matter corresponding to SS indicated a range from 18 to 65%, and its mean value was approximately 45 %. Examining the relationship between the rates of inorganic particle suspension and the turbidity distribution, the ratios of inorganic matter had a tendency to decrease in the area of low turbidity water. Generally speaking, the ratio of inorganic matter content is higher in the coastal sea, and that is lower in the open ocean. (Gibbs, 1974) It can be assumed that the low turbidity water in the center of gulf originates from the water outside the RSA.

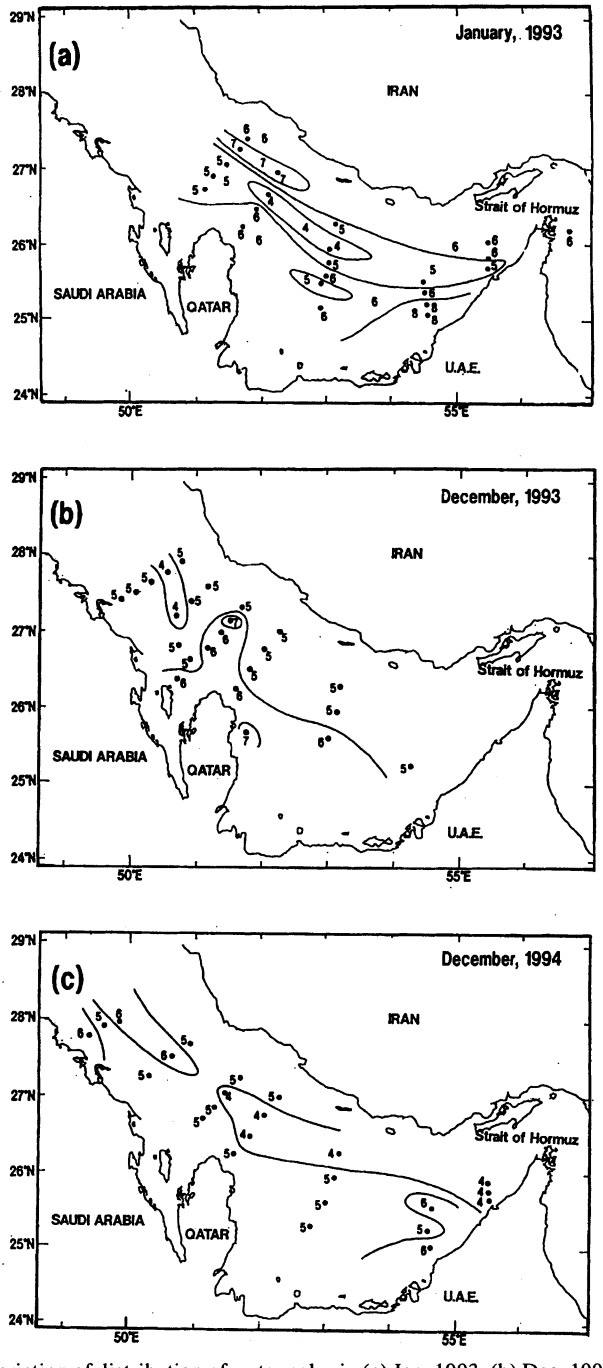

Fig. 7. Annual variation of distribution of water color in (a) Jan. 1993, (b) Dec. 1993, and (c) Dec. 1994. A contour interval is 1.

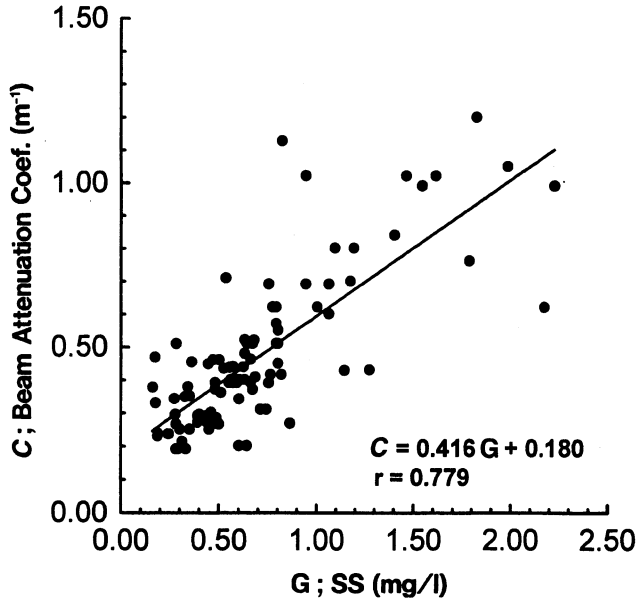

Fig. 8. Correlation between turbidity (C; Beam attenuation coefficient) and SS (G; Suspended solid). Solid line shows the line fit of data points.

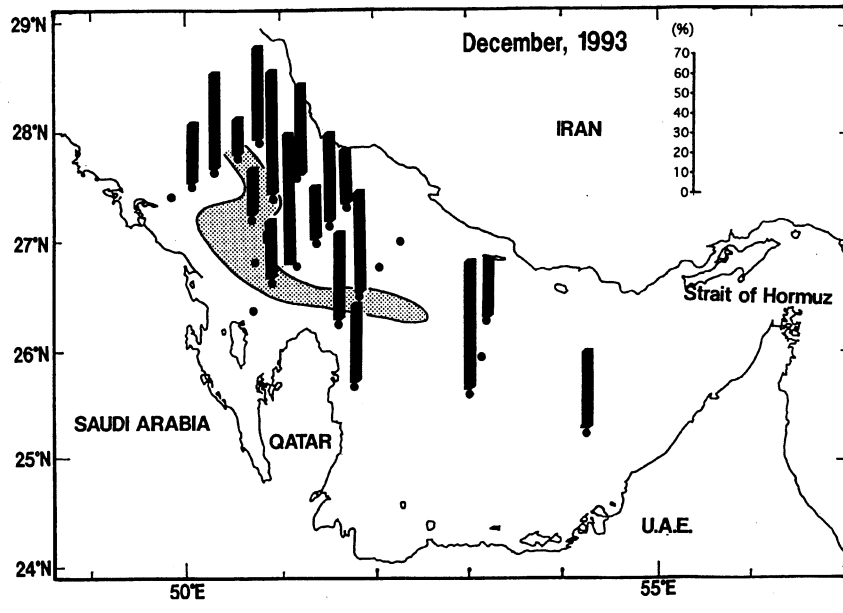

Fig. 9. Horizontal distribution of rate of inorganic matter contents in Dec. 1993. Vertical bars indicate the ratio of inorganic matter contained in suspended particles. Hatched area shows the region where C was less than 0.3 m^{-1}.

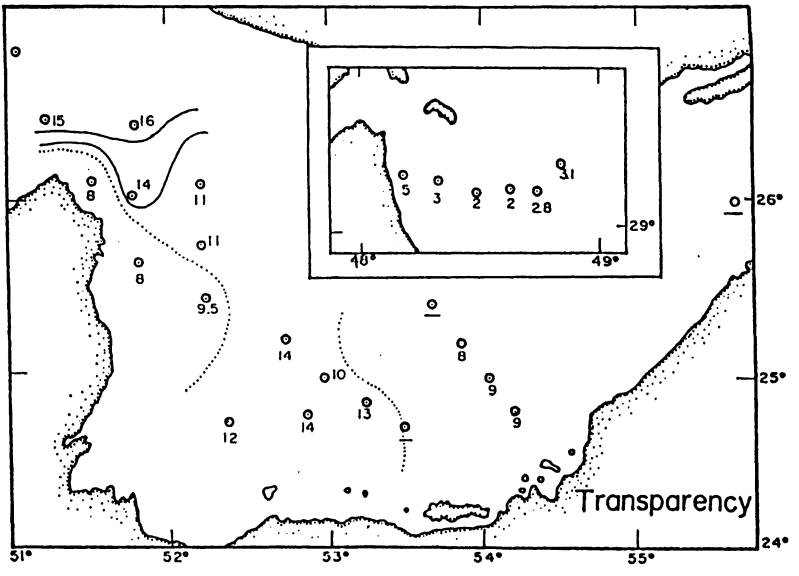

Fig. 10. Distribution of transparency in Dec. 1968 obtained by Oshite (1974). Inserted map shows the value of transparency off kuwait. Numerals at each station indicate values of transparency in meter.

Turbidity distribution in 1968

Figure 10 shows the distributions of transparency illustrated by Oshite (1974). The range of transparency off Qatar and UAE was 8 to 16 m. The largest value (16 m) of transparency appeared off Qatar. Area where transparency is larger than 10 m extended from the center of the gulf to the UAE coast. This result is similar to that obtained from our two cruises in December, 1993 and 1994. Also, the value of SS off Qatar and UAE measured by Oshite (1974) ranged from 0.2 to 1.8 mg/l, which roughly coincided with our result ranged from 0.2 to 2.2 mg/l.

Movement of the low turbidity water

In order to discuss the origin and movement of the low turbidity water in the RSA, turbidity-salinity diagrams in Jan. 1993 is shown in Fig. 11.

Water was classified into three groups; (A) the water of low salinity and low turbidity, (B) high salinity and low turbidity, and (C) high salinity and high turbidity. The group (A) water existed in the Strait of Hormuz (station A) and near the mouth (stations 20, 21) of RSA. The group (B) water existed in the center of the gulf (stations 1, 3, 4, 5, 6, 7, 8, 9, 10, 11, 12, 13, 14, 15, 16 and 17). The group (C) water existed near the southern coast (stations 18, 19 and 22) and inner part of RSA (station 2).

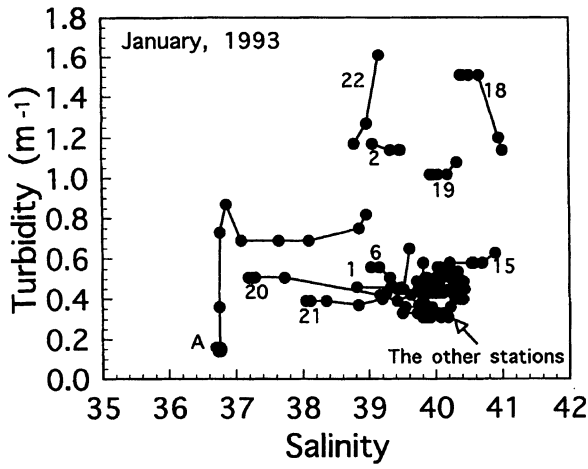

Fig. 11. Turbidity-Salinity diagrams through the cruise in Jan. 1993. Numerals in the figure indicate observation position in Jan. 1993 (refer to Fig. 1a).

The water of low salinity near the mouth of the gulf was also detected through Mt. Mitchell cruise in winter. Reynolds (1993) reported that the origin of this low salinity water may be associated with an inflow of water from the Gulf of Oman through the Strait of Hormuz. Also, Yoshida *et al.* (1998) concluded that the relatively low salinity water in the eastern half of the RSA originated from the Gulf of Oman come through the Strait of Hormuz.

On the other hand, the authors found that the turbidity of water in low salinity shown near the mouth of gulf was approximately similar to that of the Gulf of Oman (Fig. 4). Besides, the low turbidity water near the mouth of gulf distributed continuously to the inner part of gulf.

From the fact as described above, it is suggested that the low turbidity water in the center and mouth of the gulf, of which salinity was low, had its origin in the inflow water from the Gulf of Oman. Also, we found that the inflow water into the gulf covered a wide area, and reached to off the Qatar.

Finally, we refer to the movement of the low turbidity water into the RSA. It is considered that the extremely low turbidity water ($C < 0.2$) inflows from the Gulf of Oman through the Strait of Hormuz before December. (refer to Fig. 2 and Fig. 3) In December, this low turbidity water reaches off the Peninsula of Qatar. In January, the turbidity of this water increases slightly. Then after, the low turbidity water ($C < 0.4$) generally distributes in the layer from surface to near the seabed. This reason might be due to the vertical mixing of water. Besides, a part of this low turbidity water distribute in the layer of 20 to 35 m deep toward the Iranian coast. In order to know an accurate movement of the clear water in the RSA, however, we must investigate the distribution of turbidity during other seasons in the future.

SUMMARY

Distributions of turbidity, transparency, water color, and SS were investigated in the ROPME Sea Area, in Jan. 1993, Dec. 1993, and Dec. 1994, aboard RT/V Umitaka-Maru.

1. In the first cruise (Jan., 1993), for example, a water of low turbidity, of which the beam attenuation coefficient was 0.4 m^{-1}, could be seen in the surface layer. This low turbidity water of the surveyed area had a width of approximately 15 miles and extended along the Gulf axis from near the Strait of Hormuz to off the Peninsula of Qatar. Along the Iran and UAE sides of the RSA, however, the values of the beam attenuation coefficients gradually increased towards the coast, indicating a sign of turbidity occurring.

2. Referring to the vertical distribution of turbidity, the low turbidity water generally distributed in the layer from surface to near the seabed in the center of gulf, while the high turbidity water was seen in the shallow water. In addition, in the shallow water region, a large value of beam attenuation coefficient due to the effect of bottom sediment appeared in the layer near the seabed. The area of low turbidity water was the widest in Dec. 1994.

3. The annual variation of transparency was broad. The largest value of transparency in Jan. 1993 was more than 12 m, and the smallest one was less than 4 m. Especially, the transparency in the center of gulf appeared as the largest value of 19 m in Dec. 1994. The distribution pattern of the transparency was a fairly good approximation with that of turbidity.

4. The range of water color was between 4 and 8, and the colors, which appeared most frequently, are 5 and 6.

5. The value of SS ranged from the largest value of 2.2 mg/l to its smallest one of 0.2 mg/l. The distribution of SS was similar to that of turbidity. The correlation between SS and the beam attenuation coefficient is shown as follows : $C = 0.416\ G + 0.18$ ($r = 0.779$), where C and G are beam attenuation coefficient and SS, respectively. Also, these suspended particles contained approximately 45% inorganic matter.

6. In regard to the origin of the low turbidity water in the RSA, It is estimated that this water has its origin in the inflow water from the Gulf of Oman, and reaches to off the Qatar.

Acknowledgments

The authors are pleased to acknowledge the considerable assistance of Prof. and Dr. A. Otsuki who was a leader of this research, and also would like to thank Profs. Y. Saotome, T. Isouchi, and K. Kasuga, captains of the RT/V Umitaka-Maru of Tokyo Univ. of Fish., and their staff.

REFERENCES

Brewer, P.G. and D. Dyrssen (1985); Chemical oceanography of the Persian Gulf, *Prog. Oceanogr.*, 14, 41–55.

Emery, K.O. (1956); Sediments and water pollution of Persian Gulf, *Bull. Amer. Ass. Petrol. Geol.*, 40(10), 2354–2383.

Gibbs, R. J. (Editor, 1974); Suspended solids in water. *Marine Science Series*, 4. Plenum Press, New York, N. Y., 320 pp.

Jerlov, N. G. (1951); Optical studies of ocean water. *Rep. Swedish Deep-Sea Expad.* 3, 1–59.

Matsuike, K., T. Morinaga and T. Hiraoka (1986); Turbidity distributions in Tokyo Bay and movement of the turbid water. *J. Tokyo Univ. Fish.*, 73(2), 97–114.

Morinaga, T. (1983); Distribution of temperature, salinity and turbidity in the Antarctic Ocean. *La mer*, 21(3), 123–132.

Morinaga, T., A. Imazeki, S. Takeda, and H. Arakawa (1992) ; The environmental conditions of the tunas' maneuvering sphere in the Bay of Bengal. *La mer*, 30(1), 5–16.

Oshite, K.(1974); Suspension collected in the Arabian Gulf. Arabian Gulf Fishery-Oceanography Survey, December 1968., *Trans. Tokyo Univ. Fish.*, Vol. 61, No. 1.

Reynolds, R. M. (1993); Physical Oceanography of the Gulf, Strait of Hormuz, and the Gulf of Oman-Results from the Mt. Mitchell Expedition, *Marine Pollution Bull.*, Vol. 27, 35–59.

Yoshida, J., M. Matsuyama, T. Senjyu, T. Ishimaru, T. Morinaga, H. Arakawa, A. Kamatani, M. Maeda, A. Otsuki, S. Hashimoto, I. Kasuga, Y. Koike, Y. Mine, Y. Kurita, A. Kitazawa, A. Noda, T. Hayashi, T. Miyazaki, and K. Takahashi (1998); Hydrography in the RSA during the RT/V Umitaka-Maru Cruises. This volume.

Offshore Environment of the ROPME Sea Area after the War-Related Oil Spill, Eds. A. Otsuki *et al.*, pp. 65–88.

Mineralogy, genesis and sources of surficial sediments in ROPME Sea Area

A. N. AL-GHADBAN[1], A. M. AL-DOUSARI[1], A. AL-KADI[2], M. BEHBEHANI[1] and P. CACERES[1]

[1]*Environmental Sciences Department, Kuwait Institute for Scientific Research, P.O. Box 24885, 13109 Safat, Kuwait*
[2]*Scanning Electron Microscopy, Kuwait University, Kuwait*

Abstract—The main objective of this study is to determine the sediment sources of the ROPME Sea Area and to define their relative importance. Heavy and light minerals in the very fine sand and coarse silt fractions were determined microscopically. These size fractions were selected for heavy mineral analysis because they represent a large proportion of the total sediment budget and their results will be readily comparable with the published results of the potential sources (wind-borne and river-borne sediments). X-ray diffraction was utilized to determine the mineralogical composition of the "whole sediment" and the mineral constituents of the clay-size fraction.

The light minerals are chiefly composed of carbonates, quartz, feldspars with lesser quantities of chert, gypsum, and mica. Dolomite was found to be the most common heavy minerals followed by amphiboles, topaz, opaques, mica and epidotes.

The gross mineralogy is biased toward carbonates, clay minerals, and a small amount of quartz and feldspars. Carbonates are represented by low-Mg calcite, high-Mg calcite, dolomite, and aragonite. Low and high-Mg calcites were found to be the most common carbonate species in the study area. In the case of dolomite, they are thought to be of detrital origin carried into the study area primarily as dust fallout and as a result of direct biochemical precipitation with respect to high-Mg calcite. Clay minerals are composed of illite, palygorskite, illite-montmorillonite mixed layer, kaolinite, and chlorite. Illite, palygorskite, and illite-montmorillonite mixed layer are the most important clay minerals, forming more than 70% of the clay-size fraction. It is suggested that palygorskite is most probably developed as a diagenetic mineral in the lower Mesopotamian plain and transported to the study area by eolian processes. Other clay minerals are thought to be of detrital origin derived from many sources.

Comparison of the average frequency percentage of light minerals with those of the dust fallout and the Tigris-Euphrates basin sediments shows close resemblance in the light minerals constituents of the dust fallout and the study area environments. This resemblance suggests that substantial quantities of the very fine sand and coarse silt fractions of the ROPME Sea Area are of detrital origin, derived from the dust fallout.

X-ray diffraction analyses of the "whole sediment" revealed that the

carbonates, in general average about 75% of the non clay constituents while terrigenous minerals (quartz and feldspars) form about 25% in average. The relativelly stable phases (low-Mg calcite and to some extent dolomite) are the dominant carbonate minerals in the study area and were generally found to decrease in abundance in a north-south direction.

The results show that the dust storms which originate in southern Iraq by the prevailing northwestern wind are a major contributor to the total sediment budget, particularly with respect to dolomite, palygorskite, and low-Mg calcite. Other sources which have impact upon the study area are direct precipitation from the water body, Shatt Al-Arab river and other rivers from the Iranian side. The distribution of some heavy and clay minerals infer the effect of the counter-clockwise water circulation and a north-south transport from the northern part, parallel to the axis of area is also inferred.

INTRODUCTION

ROPME Sea Area is a marginal sea measuring some 1,000 km in length and 200–300 km in width, covering an area of approximately 226,000 km^2. The entire basin lies on the continental shelf whose margin and slope occur in the Gulf of Oman. At the head of the Gulf is the Tigris-Euphrates delta which extends for about 100 km seaward from the river mouth (Larsen and Evans, 1978). In addition to Shatt Al-Arab, rivers into the Gulf occur primarily on the Iranian northeastern side, the estuary of major rivers such as the Hendijan, the Hilleh and the Mand (Fig. 1). The bathymetry of the Inner sea shallows to the northwest and to the west coasts. The floor of the sea basin is asymmetric, with its axis lying close to the Iranian coast. It slopes gradually from the shallow deltaic northern part to deeper waters in the south. However, the depth rarely exceeds 100 m and is only 36 m on average (Purser and Seibold, 1978; Reynolds, 1993).

Between 19 and 30 January 1991, an estimated 10.8 million barrels (Mbbls) of oil were spilled in ROPME Sea Area deliberately by Iraqi troops mainly from seven abandoned tankers and the Al-Ahmadi Sea Island terminal near the Coast of Kuwait in addition to smaller discharges from the Iraqi Mina Al-Baker terminal and nearly sunken tankers, and the Saudi Ras Al-Zor refinery at Mina Saud (Tawfig and Oslen, 1993). Oil fallout from the smoke, plumes of the over 600 oil well blowouts and fires, started in late February 1991, has also doubled the size of the oil slick and made this event the largest of its kind in the history of marine pollution (Reynolds, 1993).

Later, in the same year, an international programme was planned and sponsored by the Regional Organization for the Protection of the Marine Environment (ROPME), Intergovernmental Oceanographic Commission (IOC), United Nation Environment Programme (UNEP) and US National Oceanic and Atmospheric Administration (NOAA) to study the fate and effects of the Kuwait oil slick on the region's marine environment. As part of this programme, arrangements were made for 140 scientists from 15 nations to cruise in the area between February and June 1992 aboard the NOAA Research Vessel "Mt. Mitchell".

As part of this programme, detailed sedimentological and geochemical studies have been carried out recently on 112 grab samples collected in 1992 from

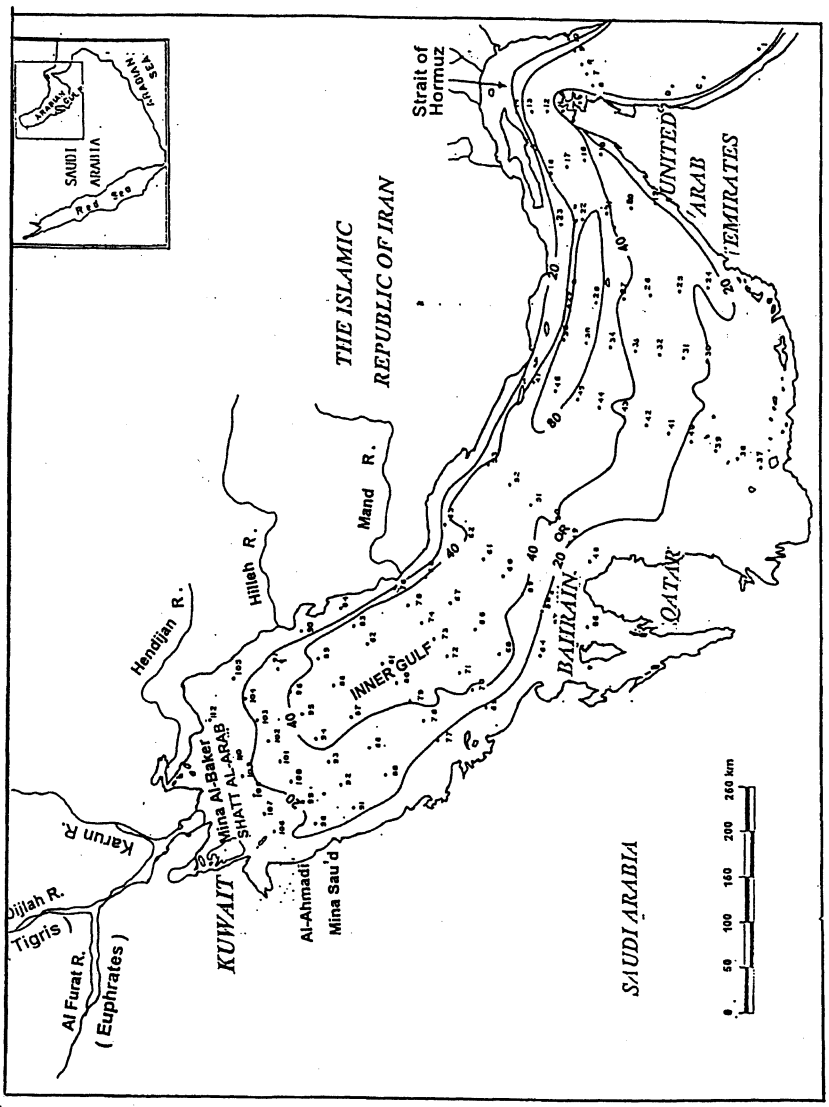

Fig. 1. Map showing the bathymetry of ROPME Sea Area and the station of collected sediments in 1992.

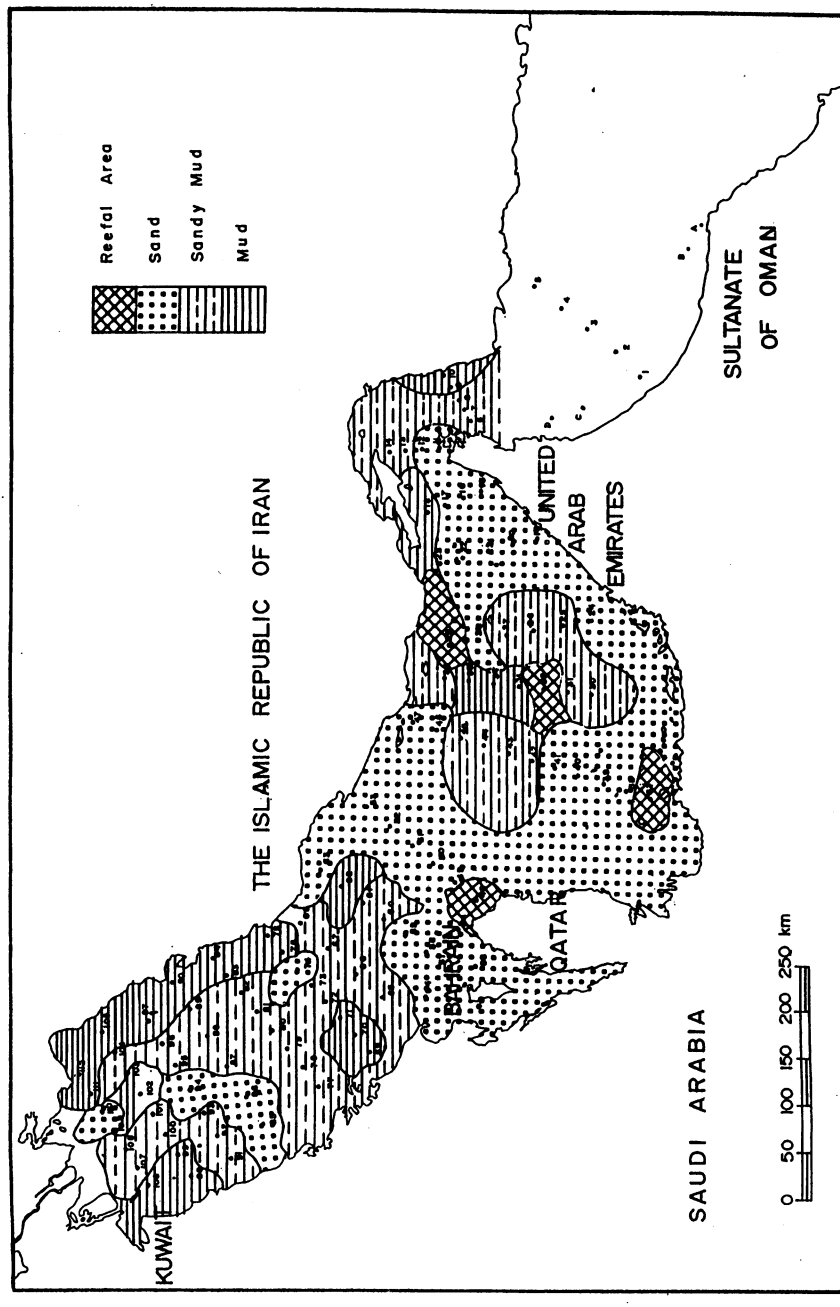

Fig. 2. Regional sediment distribution of textural classes of bottom sediments (after Al-Ghadban et al., 1996).

the bottom sediments of the area to investigate the petroleum hydrocarbon and heavy metals pollutants that were transfered through the water column from the Kuwait Oil slick to the sea bed to reside in offshore bottom sediments (Al-Ghadban *et al.*, 1996; Al-Abdali *et al.*, 1996; Massoud *et al.*, 1996).

Regional distribution of bottom sediments

The textural characteristics and regional grain-size distribution of bottom sediments in the study area were discussed in detail by Al-Ghadban *et al.*, 1996. Most of the study area is covered with fine-grained sediments (mud and sandy mud) which occupy the deeper offshore areas as well as the sheltered depressions in coastal areas. On the other hand, coarse-grained sediments (sandy and muddy sand) occur mainly in narrow belts in the western area (offshore Bahrain, Qatar and United Arab Emirates (U.A.E.)) and as patches on and around islands and the

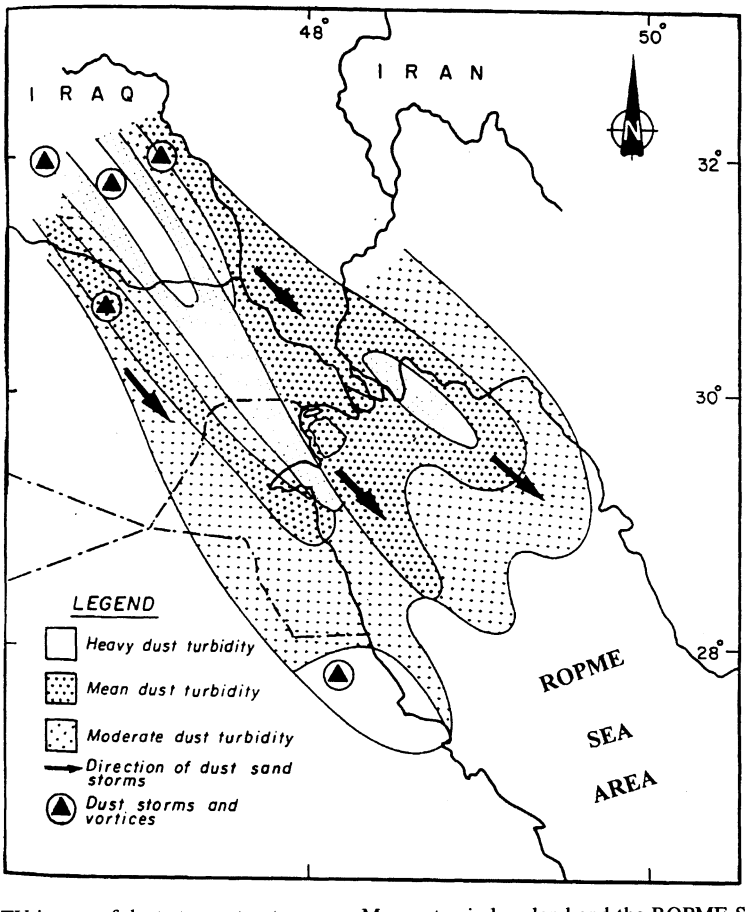

Fig. 3. TV image of dust storm structure over Mesopotamia low-land and the ROPME Sea Area (after Vinogradov, 1973).

rocky bottoms of the bathymetric highs (Fig. 2). The deposition of finer sediments along the eastern Iranian side compared with the western side is attributed to the counter clockwise circulation from the Indian ocean, whilst the deposition of poorly sorted sediments near the eastern side and in the northwestern area is probably due to the effect of tidal currents, river-borne sediments and deposition of aeolian sediments. Suspension is thought to be the most important process of transportation and deposition, and hence low energy conditions prevail in the area, particularly in the northern part which could be described as a low energy zone with low sediment movement. In contrast, the southern part represents a relatively moderate to high energy zone with higher sediment movement. A north-south sediment transport from the northern part is inferred, with net movement parallel to the axis of the study area (Al-Ghadban *et al.*,1996).

The present work is a further step toward the proper understanding of the bottom sediment transport in the Gulf. The objective of this work was to provide baseline information needed for the overall assessment of the marine environment of the area and to contribute towards the understanding of the concentration and behavior of the various pollutants in the offshore sediments. In this article, the results of a detailed mineralogical investigation of the surface sediments covering the bottom of the area are presented and the genesis of the main mineral species is described and discussed. The specific objectives of the paper were to understand the mineralogical characteristics and to define the relative importance of the potential sediment sources of the study area.

Climate of ROPME Sea Area

A dry hot climate dominates the northern part of the study area. The region is mainly controlled by three factor; the atmospheric pressure distribution, the distribution of sea and land, and the regional topography. The region is affected by four main semi-permanent pressure systems: the cold Siberian anticyclone, travelling depressions, an extension of the Sudan depression and the Indian monsoon depression (Al-Ghadban and Salman, 1993).

Temperatures during summer reach 45°C on most days in June and July in the northern part of the region. Winter is cool and the temperature may drop to 7°C in January. Rainfall is scanty and begins in October and ends in May. December and January are the rainiest months of the year. The mean amount of precipitation is about 115 mm (Al-Ajmi and Safar, 1987).

The winds affecting the region are the prevailing north westerly winds, Shamal, and, to a lesser extent, the south easterly winds, Kaus Winds from the other direction are less frequent and of shorter duration. Dust phenomena, are characteristic features of the climate in the northwestern regions (Al-Khulaib, 1981). Dust may occur in any month of the year but it is more frequent and severe in summer, particularly in June and July. Meteorological records in Arabia and Mesopotamia indicates that dust in general, and the dust storms in particular, are strongly associated with NW winds. A good example is Kuwait where for the period 1970–77, the frequency of the observations of the various types of dust revealed that about 85% of the observations were associated with NW winds, 10%

with SE winds, and less than 5% with other winds (Safar, 1980). The association of dust with the Shamal is also confirmed by a satellite image of the region taken during severe summer dust storms (Fig. 3). This dust storm originated in southern Iraq and advanced over Kuwait and the Northern part (Vinogradov *et al.*, 1973).

Methods of study

A total of 92 sediments samples from the region (Inner Gulf) were used for mineralogical investigations (Fig. 1). Very fine sand and coarse silt fractions were chosen to study the heavy and light mineral assemblages using the methodology described by Bush, 1973. These size fractions were selected for heavy mineral analysis because mechanical analysis revealed that a large proportion of the collected samples belong to these size fractions, and, hence, that would give a good representation of the heavy mineral content of the studied sediments. In addition, results from these size fractions would be readily comparable with the published results from potential sediment sources (wind and river borne sediments). The relative frequency percentage of the various mineral grains in both heavy and light mineral fractions was determined by counting about 300 grains in each slide.

For the study of "whole sediment" mineralogy, a portion of the dried sample was finely crushed and analyzed by X-ray powder diffraction. Semiquantitative estimation of the minerals present in the "whole sediment" samples was made by measuring the integral intensities of the (101) quartz, (040) feldspars, and (104) dolomite as detailed in Schultz (1964) and Bush (1971). A suction-onto-ceramic disc method (Shaw, 1971) was employed for the preparation of oriented clay samples for X-ray diffraction analysis. The identification of clay minerals involved the standard pretreatments of glyceration and heating at 550°C in the range (2O) from 4 to 32 degrees. The semiquantitative estimates of the relative amount of clay minerals were calculated by measuring the integral intensities of the peaks located at 10A, 7A and 3.5A in the untreated air-dried samples and the peak at 10A in the glycerated samples, as detailed in Schultz (1964). Because of the semi quantative nature of the X-ray analysis, the relative content of the various minerals in the clay fraction and the "whole sediment" were only quoted to the nearest 5%.

RESULTS

Light minerals

Texturally, most of the region is covered with mud and muddy sediments (>50% material finer than 63 microns) while sand and sandy sediments (<50% material finer than 63 microns) are found mainly restricted to the topographic highs and the western coastal areas.

Light minerals of both the very fine sand and coarse silt fractions are chiefly composed of carbonate grains, quartz, and feldspars. Chert, gypsum, and mica were recorded in lesser quantities (Table 1).

The average relative frequency percentages of the carbonate grains in the very fine sand and coarse silt fractions account for about 48% and 38% of the total

Table 1. Summary statistics of the relative frequency percentages of light minerals in the bottom sediments of ROPME Sea Area.

Light Minerals	Very Fine Sand (n = 52)		Coarse Silt (n = 44)	
	Mean	Standard Deviation	Mean	Standard Deviation
Carbonates	47.8	22.5	38.4	12.3
Quartz	24.0	7.2	29.7	12.1
Feldspar	12.0	9.3	14.0	8.8
Chert	6.0	3.3	8.8	6.1
Gypsum	2.6	1.3	5.3	0.9
Mica	7.6	3.9	3.8	0.9

n = number of samples.

light minerals, respectively. Carbonate grains are mainly represented by detrital calcite and biogenic grains. The latter are composed of whole microfaunal shells, mostly of foraminifera and ostracoda, and shell fragments of macrofaunna (bivalves, gastropodes and echinoids). The detrital calcite was found to be in the form of rounded to subrounded monocrystalline grains and rounded polycrystalline grains (micrite lumps). The micritic calcite grains are thought to be produced as a result of mechanical breakdown of the micritic envelopes of recent shell fragments. Rhombohedral calcite grains were occasionally recorded in the sediments. They are thought to be of detrital origin.

The relative frequency percentage of the quartz grains varies from 16.2 to 52.6% with an average of about 29.7% in the coarse silt fraction and between 9.2 and 42% with an average of about 24% in the very fine sand fraction. These grains are commonly found as irregularly shaped, subrounded to angular, and slightly turbid with microlite inclusions and vacuoles.

Feldspars are represented by plagioclase and potash feldspars (orthoclase and microcline). Most of these grains are rounded and show partial alteration to kaolinite and calcareous material. Their frequency percentages range between 4.1 and 38.2% with an average of 12% in the very fine sand and between 8.0 and 49.2% with an average of 14% in the coarse silt fraction.

Chert and gypsum grains were found to form a small portion of the light minerals with an average frequency percentage, in both size fractions, of about 6% and 2%, respectively. Separation of mica was rather inaccurate because of its flaky nature and its specific gravity (2.80–2.93), which straddles that of Bromoform. For this reason, micaceous minerals were recorded in both light and heavy fractions. In the light fraction, they were represented by muscovite and leached chlorite. Relative frequency percentages in both size fractions were found to average about 6 and 4%,respectively, of the light minerals.

Heavy minerals

Heavy mineral fractions average about 10.2 and 13.6% by weight of the very

Table 2. Summary statistics of the relative frequency percentages of heavy minerals.

Heavy Minerals	Very Fine Sand (n = 52)		Coarse Silt (n = 44)	
	Mean	Standard deviation	Mean	Standard deviation
Opaque	11.7	3.9	32.8	16.8
Dolomite	20.5	14.2	22.8	11.0
Transp. heavy mineral	67.8	8.2	44.4	7.3
Transparent heavy mineral (100%)				
Amphiboles	33.7	12.8	25.0	2.0
Pyroxenes	20.0	9.2	16.0	7.9
Epidotes	6.5	3.4	4.9	3.4
Mica	9.0	1.7	7.9	1.3
Garnet	3.6	2.3	8.0	4.2
Topaz	14.6	6.6	10.0	8.0
Aragonite	4.3	1.9	5.2	2.8
Zircon	2.3	1.2	17.5	9.6
Tourmaline	0.8	0.4	2.0	0.6
Others	5.2	2.2	3.5	1.9
weight percentages of heavy fractions	10.2	4.6	13.6	5.2

Others = Kyanite, rutile, sillimanite, andalusite, apatite, sphene, staurolite and barite.
n = number of samples.

fine sand and coarse silt fractions, respectively. Both size fractions are characterized by the same heavy mineral association (Table 2). This association is marked by the predominance of dolomite, amphiboles, pyroxenes, topaz, opaques, mica, and epidotes. Garnet, aragonite, zircon, tourmaline, and "others" occur less frequently. As shown in Table 2, the opaques and dolomite frequencies were given as percentages of the total heavy mineral fraction while the rest of the heavy minerals were expressed as percentages of the total transparent population.

Opaques

Magnetite, ilemenite, hematite, spinel, and some pyrite grains were found to represent the opaque constituents in the studied sediments. In most of the study area, the opaques form only a small portion (<5%) of the heavy mineral content, and their areal distribution shows no distinct trends. In the sediments of the eastern part, however, the opaques are more common with frequency percentages reaching up to 30%. The excess of opaque minerals in the eastern part of the study area probably reflects the influence of river-borne sediments as an important source.

Dolomite

Dolomite is commonly present as irregular grains with varying degrees of

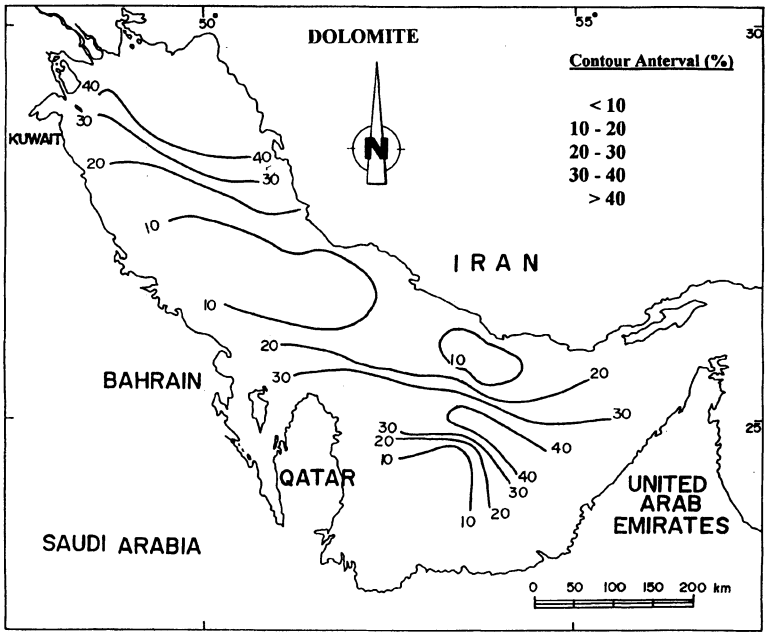

Fig. 4. Areal distribution of dolomite in 125–31 μ fraction.

roundness and sometimes as individuals rhombs with black cores of organic matter. Dolomite is an abundant heavy minerals in both very fine sand and coarse silt fractions with average frequency percentages of about 21% and 23%, respectively. Its areal distribution indicates definite general distribution pattern in which the average frequency percentage decrease towards the central part of the region, i.e.; offshore of Qatar (Fig. 4). Its percentage reaches a maximum of about 40% in the northeastern and south western corners of the area and falls gradually to about 10% with a northwesterly-southeasterly trend in the central region.

Amphiboles

Amphiboles represent the most frequent transparent heavy mineral group with frequency percentages ranging from 9% to 35%. Hornblende is by far the most abundant mineral species in this group followed by tremolite-actinolite and anthophyllite. Most of the amphibole grains are subrounded to rounded and several grains showed ragged ends as evidence of weathering.

Pyroxenes

In general, pyroxenes form the second most abundant group in the transparent fraction with values ranging between 8% and 26%. Pyroxene grains usually occur as euhedral to subhedral prismatic crystals with subrounded terminations. Pyroxene grains are represented by augite, diopside, enstatite, and hypersthene.

Epidotes

Pistacite is the main constituents of this group, forming more than 70% of all epidotes in most of the samples. Epidotes usually occur as subrounded to well rounded grains and are yellow to yellowish green in color. Zoisite grains were recorded less frequently and were found as angular to subangular colorless grains.

Mica

This group is represented by muscovite, chlorite and biotite. Both muscovite and chlorite occur abundantly; biotite was recorded less frequently. The average percentages of mica for both size fractions were found to vary from 4% to about 20% of the transparent heavy components.

Aragonite

Irregularly shaped fragments with the characteristic "twinkling" of a carbonate and acicular structure were ascribed to aragonite. These grains were recorded in appreciable quantities in most of the analyzed samples. Their frequency percentage varies from 2% to 12% in the coarse silt fraction and from 2.5% to 10% in the very fine sand fraction.

Garnet

Garnet is present as colorless, reddish brown and pinkish grains in most of the studied samples. Its average frequency percentage varies from 1% to 15% in the coarse silt fraction and from 2% to 7% in the very fine sand fraction.

Zircon

Small amounts of zircon grains were recorded in the majority of analyzed samples but were absent in a few. Their frequency percentages range, when present, from 2% to 30.0% in the coarse silt and from 0.5% to 6.0% in the very fine sand fraction.

Tourmaline

Tourmaline was only positively identified in some of the samples with maximum percentages of 2% of the transparent minerals.

Others

All the transparent heavy minerals which occur sporadically and in trace quantities in the sediments were included under the heading "others". These include: Kyanite, rutile, sillimanite, andalusite, staurolite, sphene, apatite and barite.

WHOLE SEDIMENT MINERALOGY

The estimated relative percentages of the different minerals in the "whole sediment" were computed on the basis of 100% nonclay minerals. The nonclay

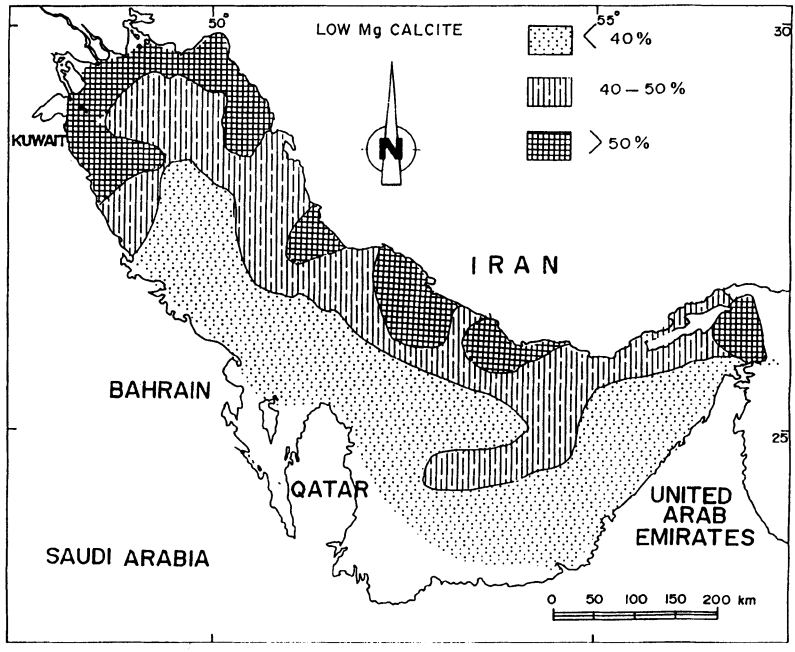

Fig. 5. Areal distribution of low-Mg calcite of the "whole sediments" fraction.

mineral fraction is mainly composed of carbonates, quartz, and feldspars. The carbonates were found to form the bulk of the nonclay constituents, averaging about 75% of the "whole sediment." Their main constituents, arranged in a descending order of abundance, are low-Mg calcite, high-Mg calcite,dolomite, and aragonite.

Low-Mg calcite was recorded as the most frequent individual mineral species in the nonclay components. Its relative percentages range from 13% to 67% with an average of about 50%. The spatial distribution pattern of this mineral shows a tendency to decrease southward, especially towards the Arabian side. Zones of high concentration (75%) were identified in the eastern parts of the region, suggesting the supply of the Iranian river inputs southward. A zone of low concentration (<40%) was identified in the southern quarter of the area (Fig. 5).

High Mg calcite was found to represent the second frequent carbonate mineral in most of the analyzed samples. Its relative percentage ranges from 6% to 38% with an average of about 18%. The areal distribution of high Mg calcete shows a definite trend of increasing abundance from north to south (Fig. 6). The lowest value, less than 10%, were recorded in two areas: 1) at the northeast corner, and 2) at the Iranian side. The concentration increases southward to reach a maximum of about 40%. A zone of high concentration is also identified off the northern coast of United Arab Emirates.

Dolomite was found to represent the third most frequent carbonate mineral in most of the analyzed samples. Its relative percentage ranges from 6% to 26%

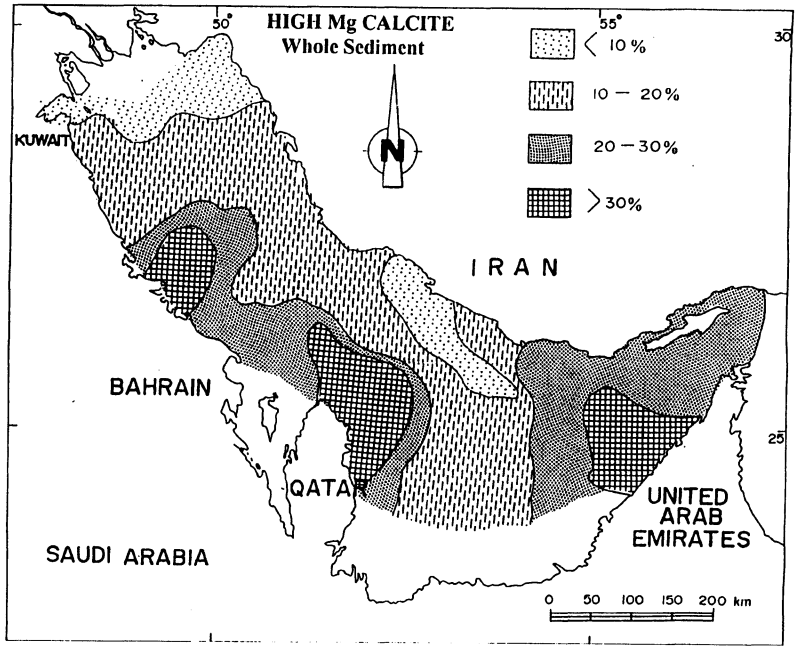

Fig. 6. Areal distribution of high-Mg calcite "whole sediment" fraction.

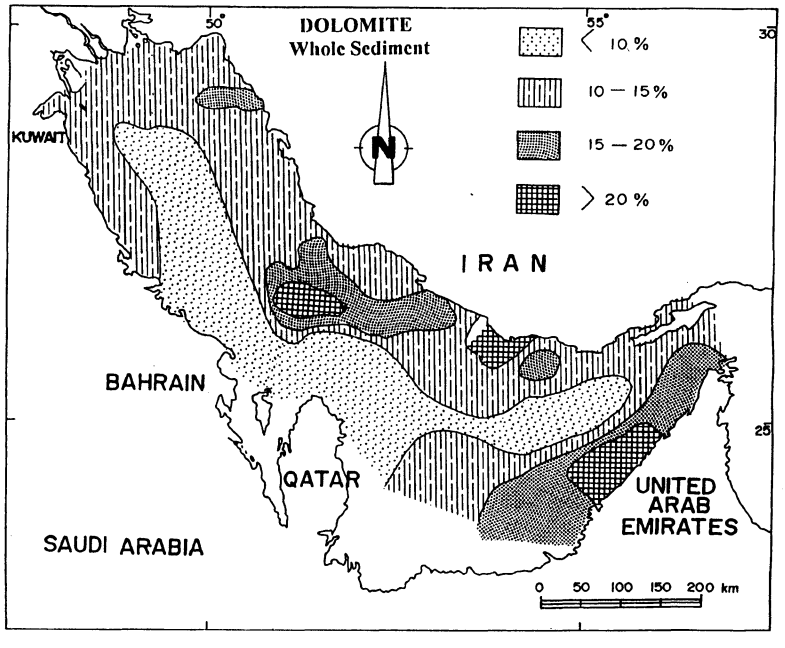

Fig. 7. Areal distribution of dolomite "whole sediment" fraction.

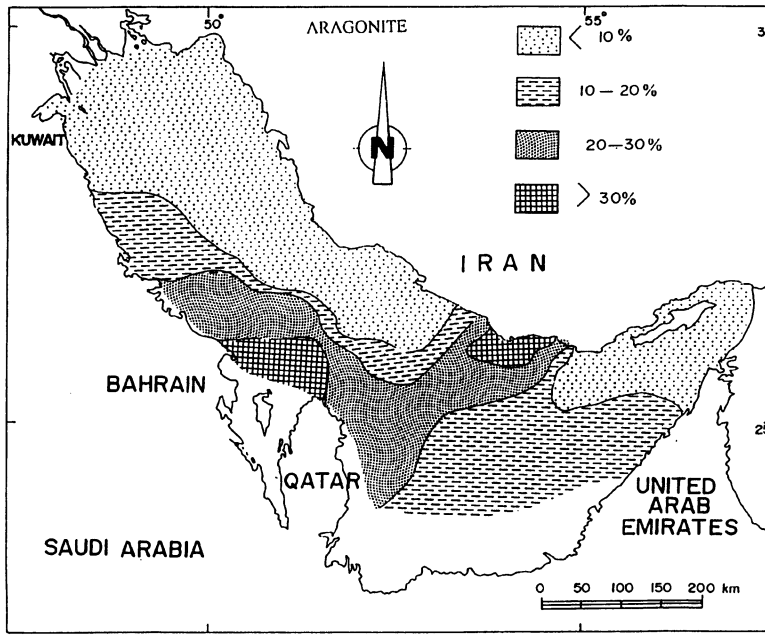

Fig. 8. Areal distribution of aragonite "whole sediment" fraction.

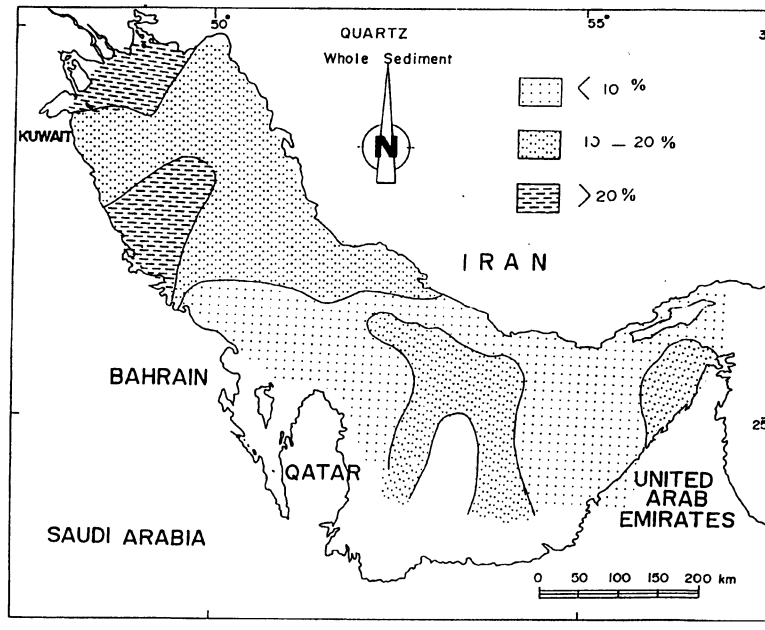

Fig. 9. Areal distribution of quartz "whole sediment" fraction.

with an average of about 15%. With the exception of some discrepancies, the distribution of dolomite shows a progressive decrease in a southward direction (Fig. 7). In general, its pattern of distribution is possitively correlated with that of the low-Mg calcite.

Aragonite is present in small quantities in some of the studied samples. It has an average frequency percentage of about 1% to 32% with an average of about 14%. Again the areal distribution of aragonite shows general agreement with the high Mg calcite's distribution (Fig. 8). The northern part of the region is characterized by low values of arogonite (less then 10%), whilst the southern area has more abundance of aragonite. Two zones of high concentrations are identified: 1) area off Bahrain, and 2) area off the Iranian coast. This distribution clearly demonstrates that the western part of the Gulf is more effected by chemical precipitation compared to the eastern part.

The noncarbonate minerals (quartz and feldspars) generally form about 25% of the nonclay minerals. Quartz percentage ranges from 5%–20% with an average of about 15%. Feldspars (albite and K-feldspars) are present in all samples, but are less frequent than quartz. Relative percentages range between 3% and 23%, with an average of about 10%. Although the areal distribution of both clastic minerals did not exhibit distinctive trends, the northern parts, in general, tend to be richer in clastic minerals (such as quartz) than the southern parts of the study area (Fig. 9). This distribution implies that the northern part of ROPME Sea Area "from Kuwait to the area offshore of Qatar" is generally receiving more aeolian input compared to the southern area.

CLAY MINERALS

The clay mineral suite consists of illite, palygorskite, an illite-montmorillonite mixed layer, kaolinite, and chlorite. Illite is present in most of the analyzed samples as the most common clay mineral, with values ranging from 18% to 30% and with an average of about 25% of the whole clay-mineral fraction. It was noticed that the general distribution pattern of illite shows that its relative frequency reaches a maximum of 28% in the northwestern and southeastern corners of the region. Two zones of high concentrations were also observed at east-west and north-south directions in the northern and southern parts of the region, respectively. The concentrations gradually decrease in a northeasterly and southwesterly direction. This pattern of distribution suggests that the main source of illite is laying to the north of the study area" Shatt Al-Arab" as well as from the Iranian rivers at the northeastern part of Gulf. The supply from the Indian Ocean into the area is also possible (Fig. 10).

Palygorskite was found to represent the second most common clay mineral in the majority of the analyzed samples. Its percentages range from 10% to 33% with an average of about 20% of the clay-mineral content. Areal distribution of palygorskite shows that the bottom sediments of the northwesterly part of the region "Offshore of Qatar to Kuwait" are having more concentration compared to the southeasterly region (Fig. 11). This, however, might suggests the effect of dust fallout approaching the area from the northwestern corner of the region.

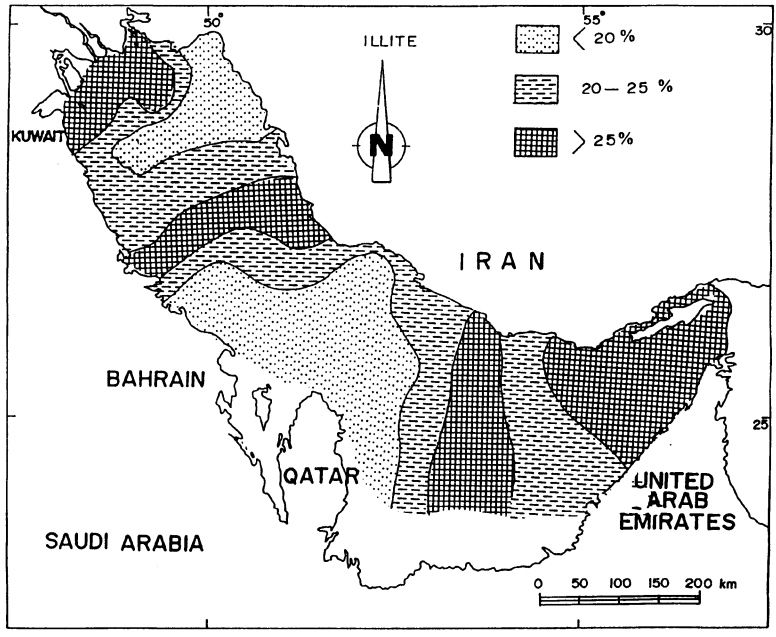

Fig. 10. Areal distribution of illite.

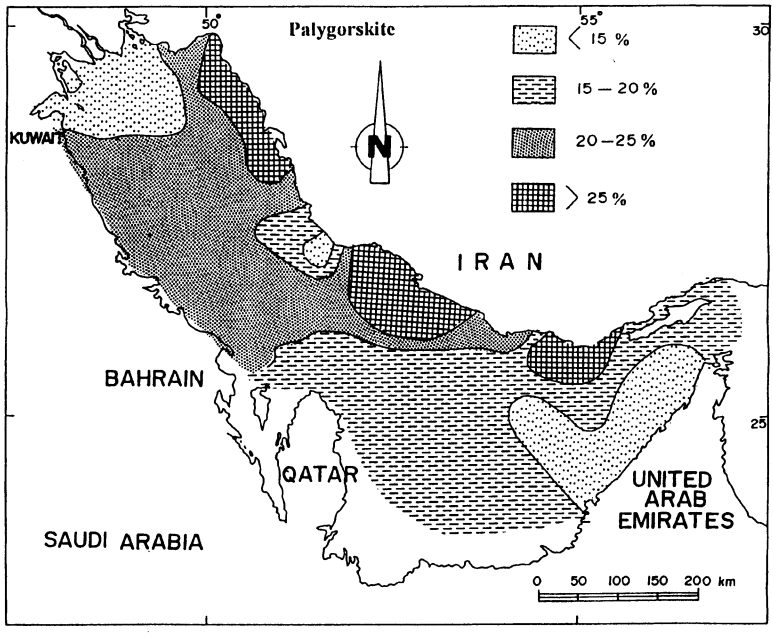

Fig. 11. Areal distribution of palygorskite.

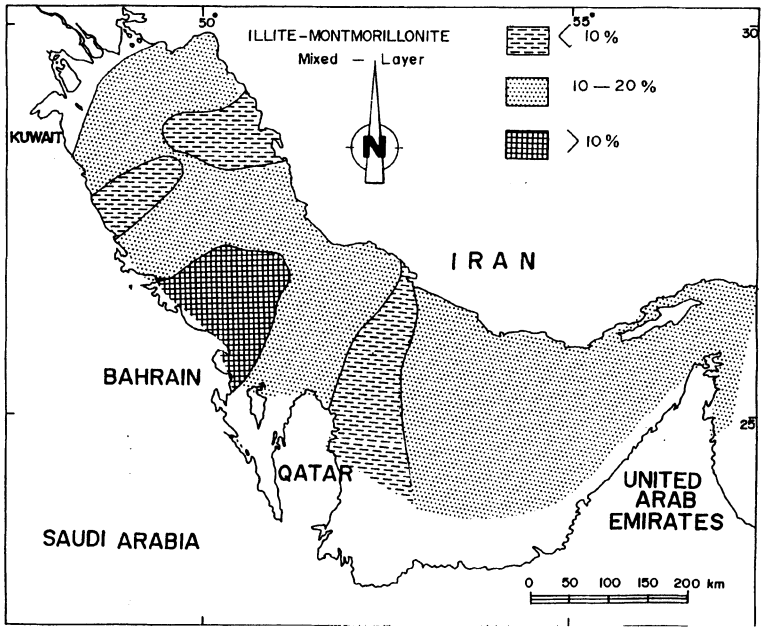

Fig. 12. Areal distribution of the illite montmorillonite mixed-layer clay.

Three zones of high concentrations are also identified at the eastern side of the study area, which clearly demonstrate the supply of Iranian rivers into this region.

The illite-montmorillonite mixed layer clay was recorded less frequently than illite and palygorskite minerals with relative percentages ranging from 8% to 20% with an average of about 14%. The regional distribution of this mineral shows a general tendency of abundance in the study area, with more abundance in the western part of the Gulf "southern offshore area of Saudi Arabia" (Fig. 12). Samples were found to be relatively deficient in kaolinite. Unlike kaolinite, chlorite was found to have a relatively greater abundance. In general, the relative percentage of each mineral never exceeded 20% of the clay mineral suite, with an average of about 8%.

DISCUSSION AND CONCLUSION

Detailed mineralogical investigation of the very fine sand and coarse silt fractions revealed that the light mineral suites in both fractions are characterized by the predominance of carbonates and the occurrence of quartz and feldspars in substantial amounts. Gypsum, chert, and mica grains are present in lesser quantities. Carbonates are primarily represented by rounded to subrounded and often pitted calcite grains. Comparision of the average frequency percentage of light minerals with those of the dust fallout and Tigris-Euphrates basins (Table 3) shows close resemblance in the light mineral constituents of the study area and the dust fallout environments. This resemblance suggests that substantial quan-

Table 3. Average frequency percentages of light minerals in the ROPME bottom sediments, dust fall out and Tigris-Euphrates basins.

Light Mineral	Location/Size Fraction				
	ROPME Sea Area		Dust fall out sediments (Khalaf et. al. 1980)		Tigris/Euphrates Delta (Darmoion and Lindqvist 1988)
	v.f.s	c.s.	v.f.s	c.s	Whole Sediment
Carbonates	47.8	38.4	32.42	46.83	60.0
Quartz	24.0	24.7	30.2	20.3	34.5
Feldspars	12.0	14.0	12.7	10.4	3.3
Gypsum	6.0	8.8	6.9	6.6	
Chert	2.6	5.3	4.9	3.4	
Mica	7.6	3.8	1.9	2.2	

Note: v.f.s. = very fine sand; c.s. = coarse silt.

tities of the very fine sand and coarse silt fractions of marine bottom sediments of ROPME Sea Area are of detrital origin, derived from the dust fallout and the Tigris-Euphrates basins.

The heavy mineral association is marked by the abundance of dolomite amphiboles, pyroxenes, topaz, opaques, and mica, with subordinate amounts of aragonite, garnet, epidotes and zircon. Tourmaline, kyanite, rutile, sillimanite, staurolite, andulusite, sphene, apatite, and barite were recorded in trace quantities. Microscopic examination revealed that most dolomite grains are irregular in shape, exhibit varying degrees of roundness and surface pitting, while fresh, angular rhombic grains are less frequent. A comparison of the heavy minerals of the studied sediments with those from potential sources, as shown in Table 4 and Fig. 13, indicates that the heavy mineral content of the study area is very similar to that of the dust fallout (particularly with respect to dolomite) and Tigris-Euphrates basin sediments. The studied sediments and the Tigris-Euphrates Recent sediments (Ali, 1976) show some resemblance in their classic heavy mineral suite. It is evident, therefore, that the wind-borne sediments carried into the study during dust storms are the primary contributor of dolomite. On the other hand, the classic heavy minerals are thought to have originated from the surface deposits of the areas lying to the north and to the west of the region zone and to have been transported to the study area as wind-borne and river-borne sediments.

The contribution of dust fallout to the bottom sediments of the study area has been reported in a number of previous studies. Sugden (1963) estimated that one third of the region's bottom sediment is eolian in origin. Pilkey and Nobel (1966) and Kukal and Saadallah (1973) reported that the wind-transported sediment is a

Table 4. Average relative frequency percentages of heavy minerals in ROPME bottom sediments, dust fall out and Tigris-Euphrates basin.

Heavy Mineral	Location/Size Fraction				
	ROPME Bottom Sediments		Dust fall out sediments (Khalaf et. al. 1980)		Tigris/Euphrates Delta (Darmoian and Lindqvist 1988)
	v.f.s	c.s.	v.f.s	c.s	(0.25-0.06 mm)
Opaques	11.7	32.8	20.0	21.5	9.6
Dolomite	20.5	22.8	25.3	30.6	2.8
Amphiboles	25.7	17.0	18.4	15.7	11.0
Pyroxenes	15.4	6.7	19.6	15.0	17.3
Epidotes	5.4	3.2	4.8	4.1	18.8
Mica	10.0	5.9	7.9	6.2	16.0
Garnet	2.0	4.2	2.6	2.3	6.5
Aragonite	3.5	2.8	-	-	-
Zircon	1.5	1.0	0.7	1.6	2.6
Tourmaline	0.4	1.6	0.5	0.9	1.8
Others	3.8	2.0	1.0	1.7	13.4

Note: v.f.s. = very fine sand; c.s. = coarse silt.

major contributor to the detrital sediment in the northern parts of the region. Emery (1956) and Khalaf *et al.* (1980) stated that ROPME Sea Area dust fallout is composed mainly of calcareous silt, rich in dolomite. On the other hand, the greatest part of the Tigris-Euphrates suspended material is deposited in Iraq, and only about 10% of the material that passes Baghdad City can reach the study area (Wilson, 1952). These statements and the climatic data given earlier strongly suggest that the dust and dust storms, which are commonly derived from the prevailing NW winds which pass over sourthern Iraq are far more important than the Tigris-Euphrates River system as a source of detrital sediments in the study area.

X-ray diffraction analyses of the "whole sediment" revealed that the carbonates, in general, average about 75% of the nonclay constituents while terrigenous minerals (quartz and feldspars) form about 25% in average. The relatively stable phases (low-Mg calcite and to some extent dolomite) are the dominant carbonate minerals in the study area and were found to decrease in abundance in a north-south direction (Figs. 5 and 7). The less stable carbonates (high-Mg calcite and aragonite), on the other hand, increase in relative percentage towards the western part of the Gulf (Figs. 6 and 8). This distribution pattern is primarily a function of the relative contribution of the local and regional sources to the study area. Submerged calcareous hard layers, oolitic limestone ridges along the western flank of the region, and beach rocks are potential sources for the less stable

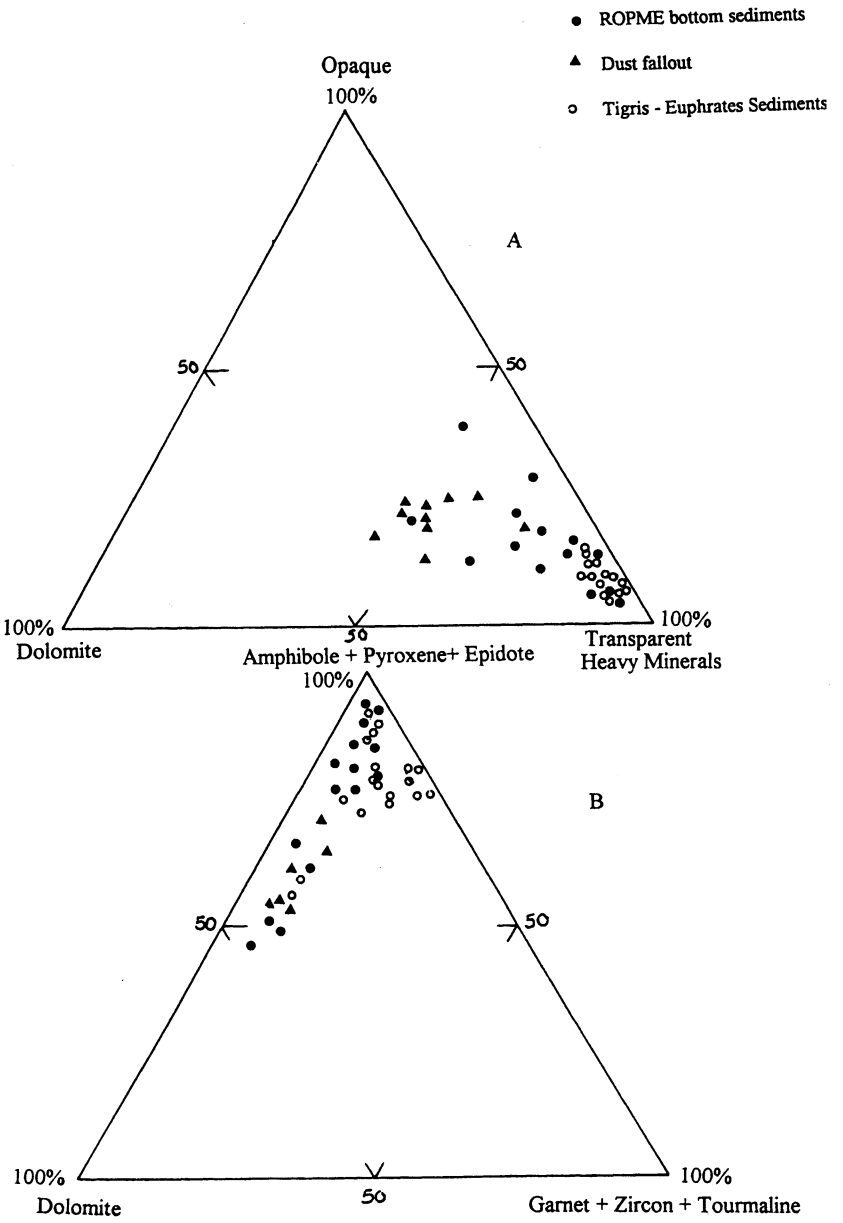

Fig. 13. Ternary diagrams of the correlation of heavy mineral association in the sediments of ROPME Sea Area environment, Tigris-Euphrates, and dust fall out.

carbonates. These coastal sediments are subjected to biological and mechanical breakdown, producing fine material rich in aragonite and high-Mg calcite, which are available for transportation to the nearby offshore area. Another potential source of aragonite and high-Mg calcite is the biochemical precipitation from seawater in the form of shells of microorganisms, mostly foraminifera and ostracoda.

The stable carbonates are believed to be of detrital origin derived from the surface sediments to the north and west of the study area. This view is supported by evidence deduced from the microscopic examination of the very fine sand and coarse silt fractions. Most of the low-Mg calcite and dolomite are believed to be derived ultimately from the ancient limestone and dolomite rocks exposed in the southern and southwestern parts of Iraq (Al-Naqib, 1967) and from the sabkhas along the shores of the northern region (Patterson and Kinsman, 1982). Stable carbonates from both sources are transported to the study area mostly as wind-borne sediment, by the NW winds, and as river-borne sediment, by the Shatt-Al-Arab River (Philip, 1968; Kinsman, 1964).

Based on the foregoing discussion, it can be concluded that the relative abundance of high-Mg calcite and aragonite on the western side of the Gulf is primarily due to the fact that the nearby coastal sediments are rich in these minerals and that their in situ production from seawater increases westward as the supply of the detrital carbonates decreases in this direction. On the other hand the abundance of low-Mg calcite and dolomite in the north is due to its proximity to the sources of detrital carbonates (i.e., source of dust and river discharge).

The clay mineral suite of the marine bottom sediments of the Gulf is chiefly composed of illite, palygorskite, and the illite-montmorillonite mixed layer while kaolinite and chlorite are found in small amounts, it seems that so many factors are influencing the distribution of the clay minerals in the study area that it is almost impossible to note anything but the most general trends. The heterogenous nature of the clay mineralogy is a strong indication of a primary detrital origin for the clay-fraction constituents. Suspended sediments of Shatt-Al-Arab and its submerged Pleistocene estuarine deposits are important sources of illite, the illite-montmorillonite mixed layer, and chlorites (Pilkey and Nobel, 1966; Berry *et al.*, 1970). The deficiency of kaolinite in the study area could be attributed to the lack of a potential source in the nearby areas. The absence of palygorskite in the suspended sediments of the Shatt-Al-Arab and its occurrence in the dust-fallout sediments (Khalaf *et al.*, 1980; Khalaf *et al.*, 1984) suggests that this mineral has been developed as a diagenetic mineral. Palygorskite can result from the reaction of hypersaline water with other detrital clay minerals in the sabkhatized flood plain of the lower Mesopotamian plain in southern Iraq (Grim, 1953; Bonython, 1956). Therefore, it is suggested that the palygorskite is most probably derived from the ancient Mesopotamian flood plain and carried into the region by dust storms. Another source of palygorskite is the submerged ancient estuarine sediments of the Shatt-Al-Arab. This view is supported by the fact that palygorskite was reported in core samples taken about 2 m below the sea bed (Stoffers and Ross, 1979).

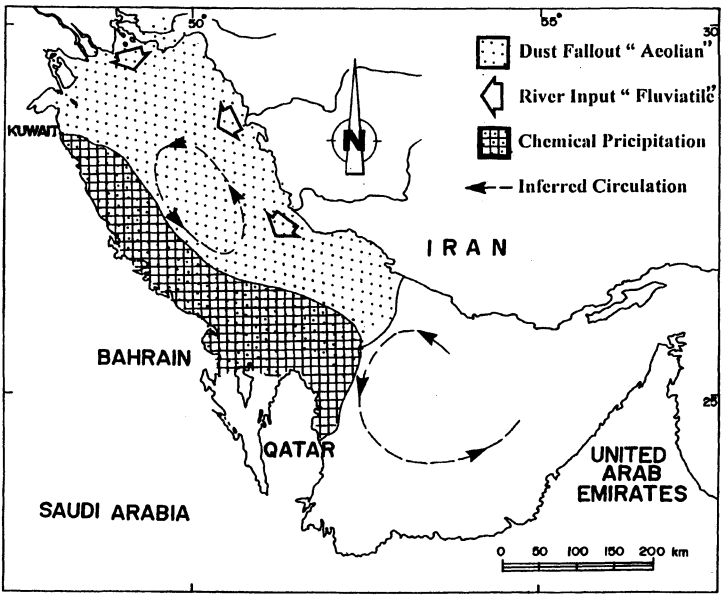

Fig. 14. Generalized model showing the potential sources of bottom sediment.

Based on the mineralogical characteristics of the various size fractions, it can be concluded that the studied sediments are mostly of detrital origin and that they are polygenetic, that is, derived from different sources. A generalized model showing the potential sources of these sediments is shown in Fig. 14. The distributions of most of the heavy as well as the clay minerals infer that the bottom of the ROPME Sea Area is impacted by the general counter-clockwise water circulation. This information might however, contribute to a better understanding of the nature of the bottom sediment and the transport of its associated pollutants in the study area. Al-Ghadban *et al.* (1996) suggested that the sedimentological characteristics of bottom sediments in ROPME Sea Area reflect the interaction between autochthonous calcareous fragments, mostly of biogenic origin, rock fragments derived from beachrocks and submerged reef flats, and allochthonous terrigenous detritus supplied to the area mainly by dust storms and river deltas in the far northern area and along the Iranian side. They used carbonate ($CaCO_3$) measurements made in whole core sediment samples (Al-Ghadban and Jacob, 1993) to draw a map showing the regional distribution of carbonates in the area. Al-Abdali *et al.* (1996) and Massoud *et al.* (1996) noted positive correlation between the presence of high concentrations of trace metals and total petroleum hydrocarbons (contaminants) and low carbonate-finer sediments. As seen from Fig. 2., ROPME Sea Area is heavily occupied by finer bottom sediments and therefore, would be susabtable to oil and non-oil pollution. These findings infers the needs for more information about the nature of bottom sediments and the

sediment transport regime in the area.

The following are the main potential sources of the Recent marine bottom sediment of ROPME Sea Area, arranged in approximate order of importance:

1) dust fallout originated from Southern Iraq and transported by the prevailing NW winds;

2) river-borne sediments from the Shatt Al-Arab River and the Iranian rivers;

3) direct biochemical precipitation from sea water;

4) submerged ancient sediments occupying the bottom of the area.

Acknowledgements

The paper is an integral part of a major study implemented by the Environment and Earth Sciences Department of the Kuwait Institute for Scientific Research (KISR). The authors would like to thank KISR management for supporting this work. Appreciation is extended to ROPME/IOC/UNEP for implementing the cruise of the NOAA R/V Mt. Mitchell. Thanks are also due to the crew staff of R/V Mt. Mitchell and to Mr. Mahmoud from Qatar University for helping in the sample collection. Many thanks are extended to Dr. S. Massoud from Kuwait University for reviewing the manuscript. Thanks are also due to Mohamed Ibrahim for drafting the maps and to Ms. Shikha Johar for typing the Manuscript.

REFERENCES

Al-Abdali, F., Massoud, M. S. and Al-Ghadban, A. N., 1996, Bottom sediments of the Arabian Gulf; III. Trace metal contents as indicators of pollution and implications for the effect and fate of Kuwait oil slick. Environmental Pollution, 93(3), 285–301.

Al-Ajmi, D. and Safar, M., 1987, An *Introduction to Climate and Geographical Climatology*. Al-Falah Puplishing Co., Kuwait.

Al-Ghadban, A. N. and Jacob, P. G., 1993, Total organic carbon in the sediments of the Arabian Gulf and need for biological productivity investigations. *Marine Pollution Bullentin*, 28(6), 356–362.

Al-Ghadban, A. N. and Salman, A. S., 1993, Preliminary *Assessment of the Suspended Sediment and Associated Pollutants in Kuwait Bay*. Kuwait Institute of Scientific Research, KISR 4213, Kuwait.

Al-Ghadban, A. N., Massoud, M. S. and Al-Abdali, F., 1996, Bottom sediments of the Arabian Gulf; I. Sedimentological characteristics. J. Univ. Kuwait. *(Sci.)*, 23, 71–88.

Al-Khulaib, A. A., 1981, Climate of Kuwait. Meteorological Department, Directorate General of civil Aviation, Kuwait, 195 pp.

Al-Naqib, K.M., 1967, Geology of the Arabian Peninsula, southwestern Iraq. U.S. Survey, Prof. Pap., 560-G, 54 pp.

Ali, A. J., 1976, Heavy mineral provinces of the recent sediments of the Euphrates-Tigris basin. J. *Geol. Soc. Iraq*, 10, 33–46.

Berry, R. W., Brophy, G. P. and Nagas, A., 1970, Mineralogy of the suspended sediment in the Tigris-Euphrates and Shatt Al-Arab rivers of Iraq and the recent history of the Mesopotamian plain. *J. Sed. Petrology*, 40, 131–139.

Bonython, C. W., 1956, The Salt of Lake Eyre, its occurrence in Modigar Gulf and its possible origin. Trans. R. Soc. S. Aust., 79, 6–92.

Bush, P. R., 1973, Sedimentology and groundwater chemistry of some Recent coastal sediments. Abu-Dhabi, Trucial Coast, Persian Gulf, Ph.D. Thesis, Univ. London, London, 365 pp.

Darmoian, S. A. and Lindqvist, K., 1988, Sediments in the estuarine environment of the Tigris/Euphrates delta; Iraq; Arabian Gulf. *Geological J.*, 23, 15–23.

Emery, E. O., 1956, Sediments and water of the Persian Gulf. Bull. Amer. Assoc. Petrol. Geol., 40, 2354–2383.

Grim, R. E., 1953, *Clay Mineralogy*. McGraw Hill, New York, 348 pp.

Khalaf, F. I., Kadib, L., Gharib, I., Al-Hashash, M., Al-Saleh, S. and Al-Kadi, A., 1980, Dust fallout in Kuwait. Kuwait Institute for Scientific Research, Technical Report, Kuwait, KISR/PPI 108/ EES-RF-8016.

Khalaf, F., Al-Bakri, D. and Al-Ghadban, A. N., 1984, Sedimentological characteristics of the surficial sediments of the Kuwaiti marine environment, northern Arabian Gulf. Sedimentology, 31, 531–545.

Kinsman, D. J. J., 1964, Recent carbonate sedimentation near Abu-Dhabi. Trucial Coast. Persian Gulf, Ph.D. Thesis, Univ. London, London.

Kukal, Z. and Saadallah, A., 1973, Aeolian admixtures in the sediments of the Northern Persian Gulf, in The Persian Gulf, B. H. Purser, ed., Springer-Verlag, Berlin, 471 pp.

Larsen, C. E. and Evans, C., 1978, The Holocene geological history of the Tigris-Euphrates-Karun Delta, in The *Environmental History of the Near and Middle East*, W. C. Brice, ed., Academic Press, London, 384 pp.

Massoud, M. S., Al-Abdali, F., Al-Ghadban, A. N. and Al-Sarawi, M., 1996, Bottom sediments of the Arabian Gulf; II, TPH and TOC contents as indicators of oil pollution and implications for the effect and fate of Kuwait oil slick. *Environmental Pollution* (in press).

Patterson, R. J. and Kinsman, D. J. J., 1982, Formation of diagenetic dolomite in coastal sabkha along Arabian (Persian) Gulf. Am. Assoc. Petroleum Geologists Bull., 66, 28–43.

Philip, G., 1968, Mineralogy of recent sediments of Tigris-Euphrates rivers and some of the older detrital deposit. J. *Sed. Petrology*, 38, 35–44.

Pilkey, O. H. and Nobel, D., 1966, Carbonate and clay mineralogy of the Persian Gulf. Deep-Sea Res., 13, 1–16.

Purser, B. H. and Seibold, E., 1973, The principal environmental factors influencing Holocene sedimentation and diagenesis, in The Persian Gulf, B. H. Purser, ed., Springer-Verlag, Berlin, 471 pp.

Reynolds, R. M., 1993, Physical oceanography of the Gulf, Strait of Hormuz and the Gulf of Oman: results from the Mt. Mitchell Expedition. Mar. Pollut. Bull., 27, 35–59.

Safar, M. I., 1980, Frequency of *Dust in Day-Time Summer in Kuwait*. Kuwait Meteorological Department, Kuwait International Airport, Kuwait.

Schultz, L. G., 1964, Analytical methods in geochemical investigations of the Pierre Shale, quantitative interpretation of mineralogical composition from X-ray and chemical data for the Pierre Shale, U.S. Geol. Surv. Prof. Pap., 39(C), 1–39.

Shaw, H. F., 1971, The mineralogy of Recent sediments in the Wash, eastern England, Ph.D. Thesis, Univ. London, London.

Stoffers, P. and Ross, D. A., 1979, Late Pleistocene and Holocene sedimentation in the Persian Gulf-Gulf of Oman. Sediment. *Geol.*, 23, 181–208.

Sugden, W., 1963, Some aspects of sedimentation in the Persian Gulf. J. *Sed. Petrology*, 33, 355–364.

Tawfig, N. and Oslen, D. A., 1993, Saudi Arabia's response to the 1991 Gulf oil spill. Mar. Pollut. Bull., 27, 333–345.

Vinogradov, B. V., Grigoryev, A. A. and Lipatov, V. B., 1973, Structure of dust storms from ITOS-I.T.V. images obtained over Iraq and the Gulf of Persia. Proc. 8th Int. S*ymposium on Remote Sensing of Environment*, Univ. of Mich., Ann Arbor.

Wilson, A. T., 1925, The delta of the Shatt Al-Arab and proposals for dredging the bar. *Geograph. J.*, 65, 225–239.

Offshore Environment of the ROPME Sea Area after the War-Related Oil Spill, Eds. A. Otsuki *et al.*, pp. 89–98.

Concentrations of bromide and chloride ions and their relationships with salinity in the central region of the ROPME Sea Area

A. OTSUKI[1], K. NAGAOKA[1], S. HASHIMOTO[1], R. TSUJIMOTO[2], T. SENJYU[3] and Y. KOIKE[4]

[1]*Tokyo University of Fisheries, Department of Ocean Sciences, 5-7 Konan 4, Minato-ku, Tokyo 108-8477, Japan*
[2]*Toyama Prefectural Fisheries Research Institute, 2373 Takatsuka, Namerikawa, Toyama 936, Japan*
[3]*National Fishery University, Department of Fishery Science and Technology, 2-7-1 Nagatahonmachi, Shimonoseki Yamaguchi 759-65, Japan*
[4]*Tokyo University of Fisheries, Research and Training Vessels, 5-7 Konan 4, Minato-ku, Tokyo 108-8477, Japan*

Abstract—The concentrations of chloride and bromide ions in seawater samples from the central region of the Regional Organization for the Protection of the Marine Environment (ROPME) Sea Area were determined by ion chromatography after 100-fold dilution with ultra-pure water. The calibration curves were highly linear between 0 and 500 mg l^{-1} for chloride and between 0 and 1 mg l^{-1} for bromide with correlation coefficients for both of greater than 0. 999. The relative standard deviations at salinity 39. 861 were ±0.53% for chloride ion and ±0.91% for bromide ion (n = 5), respectively.

The concentrations of chloride and bromide ions in open seawater in the central region of the ROPME Sea Area ranged from 21.70 to 23.56 g kg^{-1} with an average value of 22.20 g kg^{-1} and from 76.4 to 81.4 mg kg^{-1} with an average value of 78.3 mg kg^{-1}, respectively, while the salinity range was from 39.551 to 42.314 PSU. These average concentrations were 14.7% higher for chloride ion and 16.3% higher for bromide ion than those in ocean water of average salinity, 35 PSU.

An excellent linear relationship between salinity and chloride ion concentration in the salinity range to 42.314 PSU with correlation coefficient of 0.981 was confirmed in open seawater samples in this region. The ratios of bromide to chloride were distributed nearly normal with an average value of 0. 00353, which is the highest value reported for the oceans and seas with one exception, the Red Sea.

INTRODUCTION

The ROPME Sea Area, which does not have a large river water input except for the Shatt al-Arab River, is located in the desert zone in the Middle East, and evaporation there far exceeds freshwater input (Abuzinada and Krupp, 1994). Although some authors have reported salinities (38–42 PSU) in open seawater of the ROPME Sea Area higher than the average salinity of 35 for the world's oceans

(Brewer and Dyrssen, 1985; Samra, 1988), the concentrations of chloride and bromide ions in the open sea area of this region had not been previously determined.

However, the salinity measurement range of commercially available CTD systems is limited to between 2. 0 and 42. 0. Examination of the relationship between salinity and chloride ion concentration for our oceanographic survey of the ROPME Sea Area was necessary, because salinity there was known to often exceed their measurement range over 42 PSU (Brewer and Dyrssen, 1985; Samra, 1988).

The classic silver nitrate titration method has been widely used as a precise method for determination of chloride ion in seawater samples. For the determination of bromide ion in saline water samples, 2 methods have commonly been applied. One is the iodine titration method, based on thiosulfate titration of iodine liberated by addition of iodide after oxidation of bromide to bromic acid, and the other is the colorimetric method, based mainly on the bromination of phenol red in the presence of chloramine-T after oxidation of bromide to bromine. However, it is always necessary to check and correct for the presence of other interfering halogen ions when analyzing water sample of high salinity. With the recent development of analytical instruments, ion chromatography offers a simple and reliable tool to quantify these halogen ions in highly saline waters, because chloride, bromide, fluoride and iodide ions can be easily separated using an anion exchange resin column with low exchange capacity and a carbonate mobile phase.

The purposes of the present study were to precisely determine the concentration of bromide ion in open seawater of the ROPME Sea Area using ion chromatography, to examine a linearity between salinity and chloride ion concentrations in high salinity samples, and to compare the ratio of bromide to chloride ions with the other marine values to characterize the ROPME Sea Area.

MATERIALS AND METHODS

Sampling station

Figure 1 shows the sampling stations in the central region of the ROPME Sea Area and also in Sagami Bay near Tokyo. The latter served as reference stations. Samples were collected in Niskin bottles on a CTD/Rosette system 18 to 24 December, 1993 during the second R/V Umitaka-Maru cruise. The number of sampling stations in the central region was 18 and the total number of sea water samples was 91.

Reagents

All reagents used were of analytical grade, and pure water was prepared with a Milli-Q system (Millipore Co., USA). This pure water was used for the preparation of all solutions.

Apparatus

A Dionex DX-100 ion chromatograph with an autosampler (model DAS-50)

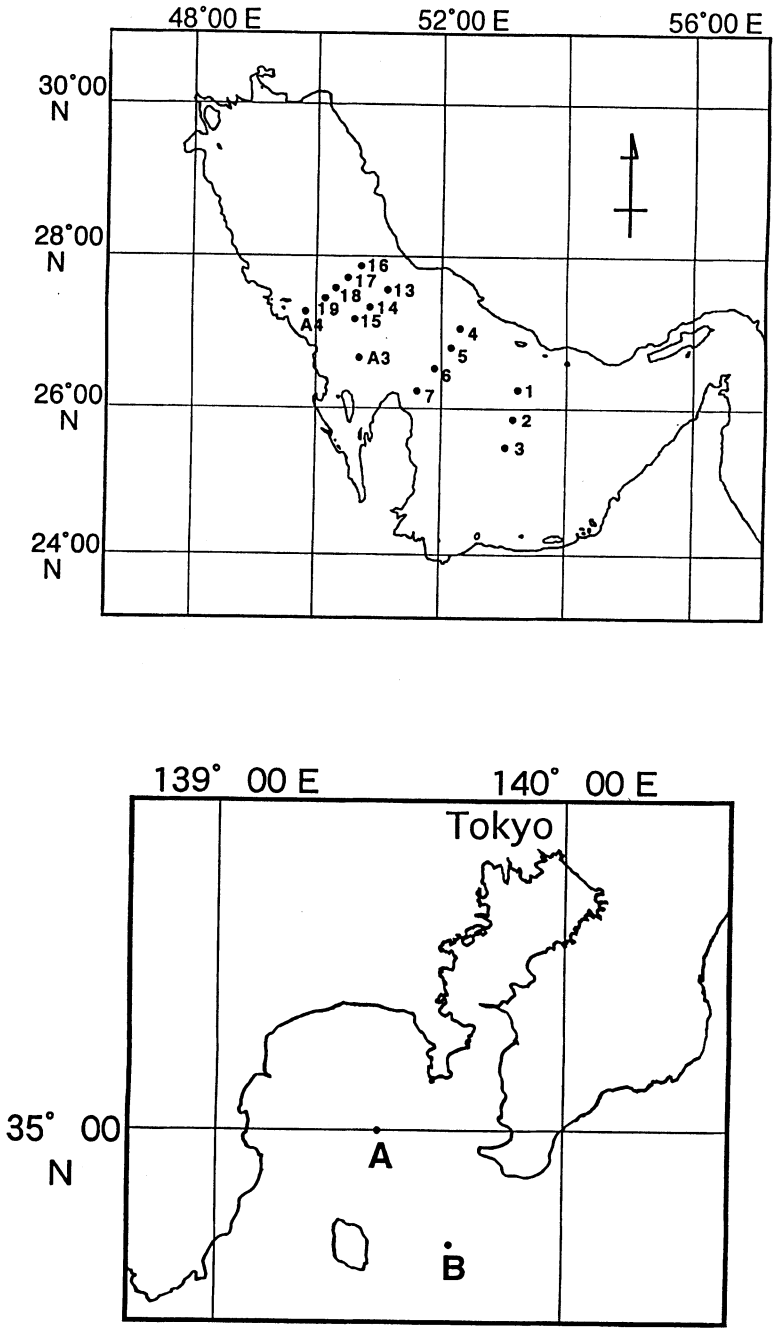

Fig. 1. Sampling stations in the ROPME Sea Area (upper) and in Sagami Bay, Japan (lower).

with a IonPac AG4A-SC column (4 mm I.D. × 25 cm in length) connected to a guard column, IonPac AG4A (4 mm I.D. × 5 cm in length), was used. Detection was via a conductivity meter. Data was acquired with a Shimadzu Chromatopak C-R6A integrator.

Analytical conditions

The mobile phase was a 1.8 mM Na_2CO_3-1.7 mM $NaHCO_3$ solution. The flow rate was 1.0 ml min^{-1} and injection volume was 25 μl. The sensitivities of the conductivity meter were set at 300 μS for chloride ion and 3 μS for bromide ion, respectively. Calibration curves were prepared with standards between 0 and 500 mg l^{-1} for chloride ion and between 0 and 1 mg l^{-1} for bromide ion, respectively.

Analytical method

After 100-fold dilution of each seawater sample with pure water, 25 μl of the diluted samples were automatically injected into the ion chromatograph and the area of each chloride and bromide ion peak was measured. Each sample was analyzed in triplicate. After the determination of both ions on a weight per volume basis, their concentrations were converted to a weight basis using the density at each sampling depth.

Salinity was determined with a Guildline AUTOSAL. Values from this salinometer were used to calibrate the CTD salinity value.

RESULTS AND DISCUSSION

The useful chromatograms for both chloride and bromide ions after 100-fold ions dilution were achieved by changing detection sensitivities (Fig. 2). When a low sensitivity of 300 μS for full scale was used to determine the concentration of chloride ion in diluted seawater, only one peak, for chloride ion was observed on the ion chromatogram, but when the sensitivity was elevated to 3 μS, a sharp peak for bromide ion appeared after the large peak for chloride ion. These results confirm that 100-fold dilution of seawater samples with pure water is appropriate for ion chromatographic determination of both ions in the seawaters of this region. Calibrations were highly linear between 0 and 500 mg l^{-1} for chloride ion and between 0 and 1 mg l^{-1} for bromide ion with correlation coefficients for both of greater than 0.999. The relative standard deviations at salinity 39.861 were ±0.53% for chloride ion and ±0.91% for bromide ion (n = 5), respectively. Recoveries of additions of 10.0 mg chloride and 0.10 mg bromide ions to 100 ml of 100-fold dilution of seawater sample at ST14-40 m were 99. 92% for chloride ion and 99.59% for bromide ion, respectively. The bromide ion peak was confirmed by the increased one caused by this addition of bromide.

The concentrations of chloride and bromide ions in open seawaters of the central region of the ROPME Sea Area ranged from 21.70 to 23.56 g kg^{-1} with an average value of 22.20 g kg^{-1} and from 76.4 to 81.4 mg kg^{-1} with an average value of 78.3 mg kg^{-1}, respectively, while the salinity range was from 39.551 to 42.314 PSU (Table 1). These average concentrations were 14.7% and 16.3% higher than

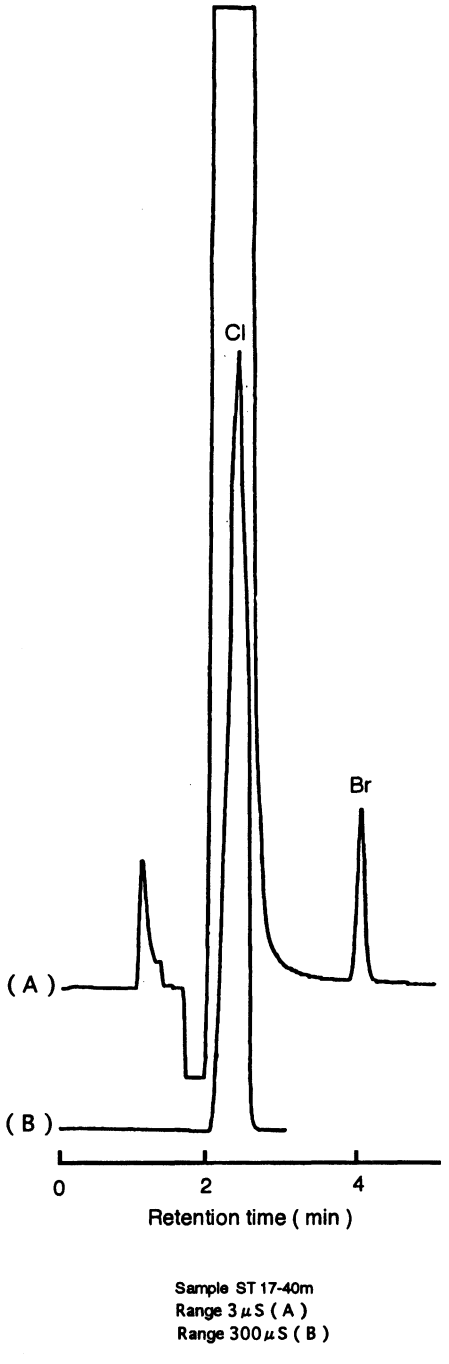

Fig. 2. Ion chromatograms of chloride and bromide ions in a diluted seawater sample achieved by changing the detection sensitivity of the conductivity meter.

Table 1. The concentrations of chloride and bromide ions in open seawaters at some sampling stations in the central region of the ROPME Sea Area.

Station	Latitude N	Longitude E	Sampling depth (m)	Temperature (℃)	Salinity (PSU)	Chloride ion (g kg^{-1})	Bromide ion (mg kg^{-1})
ST-2	25° 54.40'	53° 07.90'	4	24.40	39.596	21.98	76.4
			8	24.42	39.596	21.98	78.8
			20	24.37	39.596	21.98	79.5
			30	24.40	39.629	21.98	78.8
			40	24.43	39.642	21.98	78.8
			50	24.51	39.683	21.98	78.8
			59	24.52	39.689	21.98	78.8
ST-6	26° 27.90'	51° 48.50'	5	23.70	39.700	21.86	78.7
			10	23.69	39.698	22.05	79.5
			20	23.62	39.695	22.22	76.4
			30	23.60	39.698	22.23	77.1
			41	22.19	41.218	22.99	79.3
ST-7	26° 13.00'	51° 35.20'	4	23.05	40.000	22.23	77.9
			9	23.04	40.000	22.23	77.1
			23	21.12	42.314	23.56	81.4
ST-15	27° 09.80'	50° 41.70'	4	23.26	39.943	22.45	80.2
			10	23.21	39.942	22.45	80.2
			20	23.20	39.939	22.26	79.2
			30	23.21	39.953	22.45	79.5
			40	23.17	39.953	22.45	79.5
			50	23.17	39.960	22.26	80.2
			62	23.20	40.198	22.45	80.2
ST-18	27° 36.00'	50° 17.80'	4	23.18	40.147	22.26	77.9
			10	23.13	40.145	22.04	77.9
			20	23.14	40.146	22.04	77.9
			30	23.14	40.147	22.04	78.7
			40	23.13	40.152	22.04	77.9
			50	23.13	40.170	22.04	77.9
			60	23.15	40.186	22.04	77.9

the 19.354 g kg^{-1} and 67.3 mg kg^{-1} of chloride and bromide ions concentrations, respectively, in ocean water of average salinity, 35 PSU. In contrast, in Sagami Bay the concentrations of chloride ion ranged from 18.64 g kg^{-1} at 1,200 m depth to 18.86 g kg^{-1} at 100 m depth, and that of bromide ion from 64.9 mg kg^{-1} at 2,000 m depth to 65.8 mg kg^{-1} at 100 m depth, respectively, 18–20% lower than those in the central region of the ROPME Sea Area.

The frequency distribution of bromide to chloride ratios in open seawaters of this region is nearly normal distribution (Fig. 3), with a maximum value between 0.003525 and 0.00355. The mean value, 0.00353, was higher than any other values for the world oceans and seas shown in Table 2 (Morris and Riley, 1966).

Figures 4(a), 4(b) and 4(c) show three examples of vertical distributions of the bromide to chloride ratio at ST-2, ST-6 and ST-14, suggesting that the behavior of bromide ion in this region is not always identical to the same as that of chloride ion. Although the relationship between salinity and chloride ion concentrations (Fig. 5) was completely linear, that between chloride and bromide

Table 2. Concentrations of bromide ion in world sea waters.

Reference	Ocean or Sea etc.	Br(g/kg){for S=35‰}	Br/Cl
BERGLUND(1885)	North	0.0638-0.0665	0.00330-0.00334
	Atlantic	0.0652-0.0660	0.00337-0.00341
	Gulf of Mexico	0.0660	0.00341
	Mediterranean	0.0663	0.00343
	Adriatic	0.0660	0.00341
MAKIN(1898)	Atlantic	0.0628	0.00325
WINKLER(1916)	Adriatic	0.0670	0.00347
CAMERON(1922)	Departure Bay	0.0693	0.00358
VASIL'EV(1937)	Japan	0.0643	0.00333
RATMANOFF(1937)	Bering	0.0668	0.00345
MIYAKE(1939)	W.Pacific	0.0640	0.0033
THOMPSON and KORPI(1942)	N.E.Pacific	0.0673	0.00348
	Antarctic	0.0667	0.00345
	Bering	0.0670	0.00347
MATIDA and YAMAUCHI(1951)	Japan	0.0670	0.00347
HASLAM and GIBSON(1950)	British Coastal Waters	0.0667	0.00345
THIS STUDY(1994)	ROPME Sea Area*	0.0783	0.00353
	Sagami Bay Japan*	0.0650	0.00348

*ROPME Sea Area {S = 39.395–42.314‰}, Sagami Bay Japan {S = 34.266–34.586‰}. Morris, A. W. and J. P. Riley, 1966.

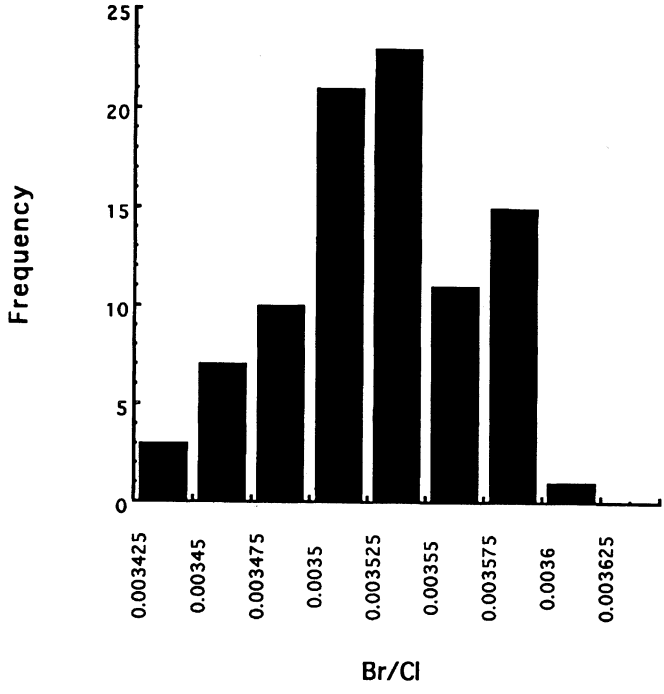

Fig. 3. Histogram of bromide to chloride ratios in open seawaters of the central region of the ROPME Sea Area.

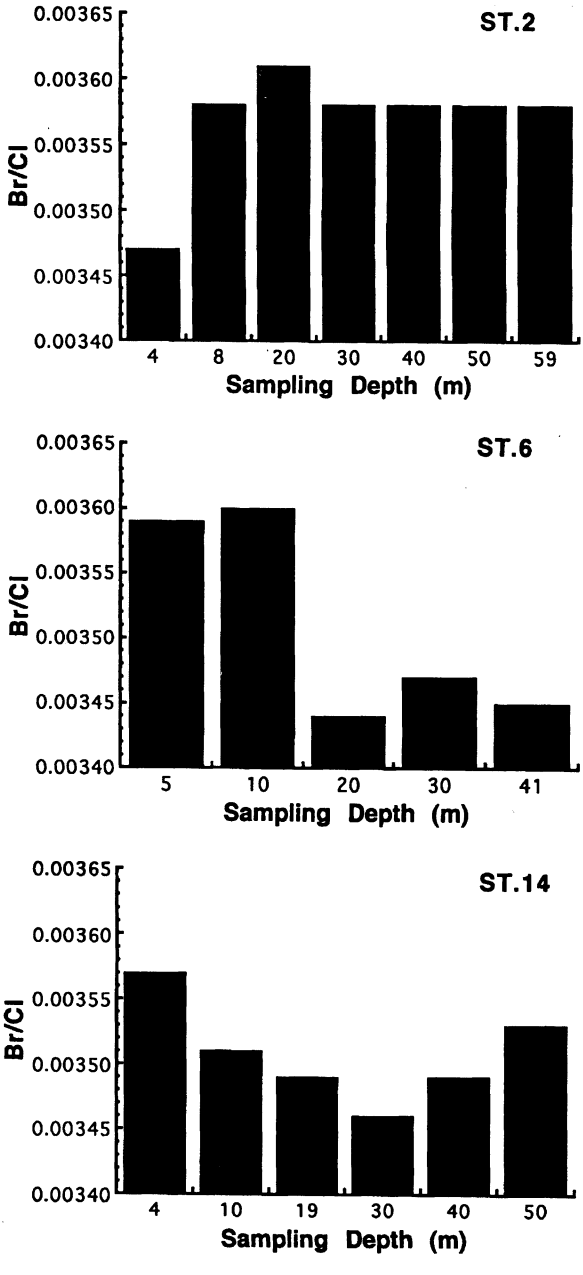

Fig. 4. Vertical distributions of bromide to chloride ratios at ST-2 (a), ST-6 (b) and ST-14 (c).

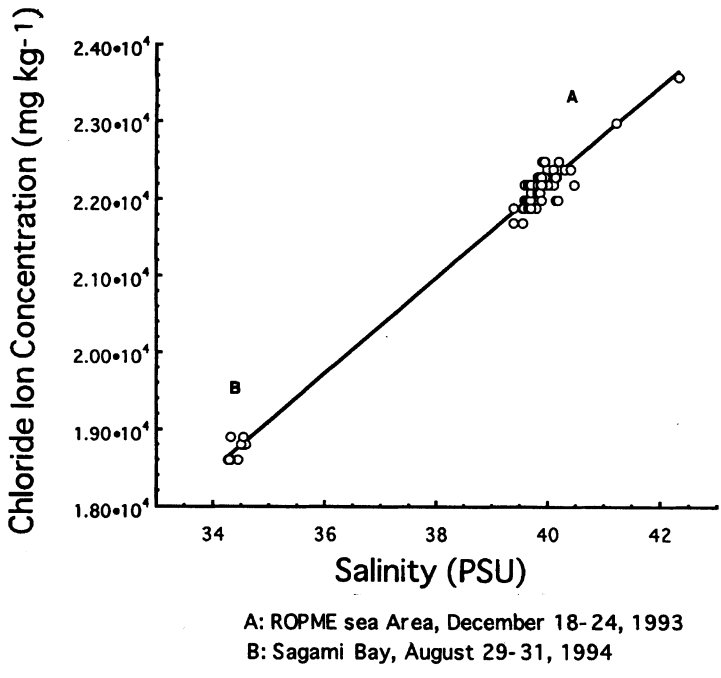

Fig. 5. Relationship between salinity and chloride ion concentration in the central region of the ROPME Sea Area.

ions concentrations (Fig. 6) deviated from linearity near the chloride ion concentration of 23.00 g kg^{-1} for unknown reasons. These results suggest that the ratio of chloride ion concentration to salinity as well as the density may be tracers of water masses in the ROPME Sea Area.

CONCLUSIONS

The present study was the first to report the precise concentrations of chloride and bromide ions in open seawater of the central region of the ROPME Sea Area using ion chromatography. Chloride ion concentration ranged from 21.71 to 23.56 g kg^{-1} with an average of 22.20 g kg^{-1} and bromide ion ranged from 76.4 to 81.4 mg kg^{-1} with an average of 78.3 mg kg^{-1}. We confirmed the linear relationship between chloride ion concentrations and salinity up to salinities of 42.314 PSU.

The ratios of bromide to chloride ions in open seawaters of the central region of the ROPME Sea Area had a nearly normal frequency distribution with an average value of 0.00353, which was the highest value reported for the oceans and

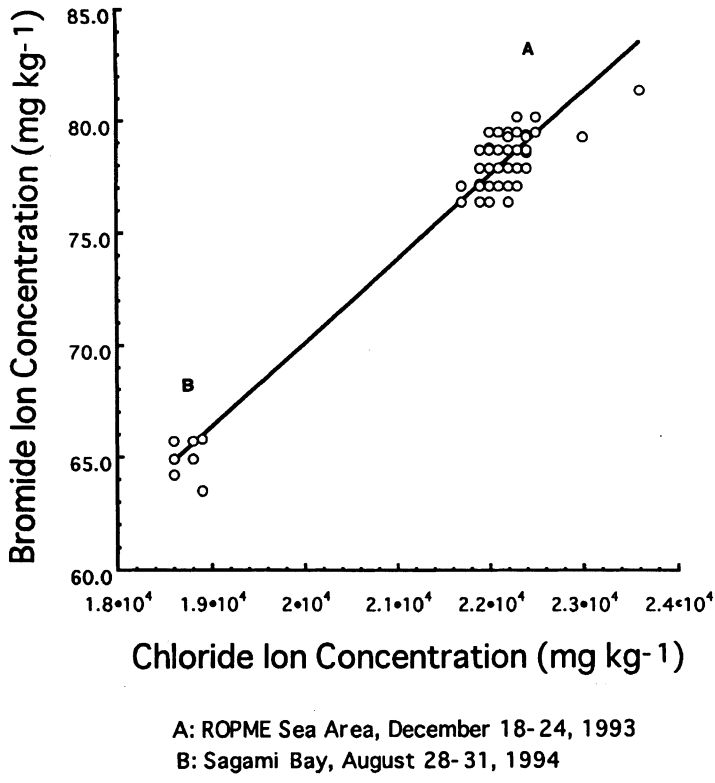

Fig. 6. Relationship between chloride and bromide ions in the central region of the ROPME Sea Area.

seas with the one exception of the Red Sea.

Acknowledgements

We thank Captain and Prof. T. Isouchi and the crew of the R/V Umitaka-Maru for their cooperation during this cruise.

REFERENCES

Abdulaziz A. H. and Krupp, F. (1994). The Arabian Gulf environment and the consequences of the 1991 oil spill. Cour. Forsch.-*Inst. Senckenberg*. 166, 3–10.

Brewer, P. G. and Dyrssen, D. (1985). Chemical oceanography of the Persian Gulf. Prog. Oceanogr. 14, 14–55.

Morris, A. M. and Riley, J. P. (1966). The bromide/chlorinity and sulphate/chlorinity ratio in seawater. Deep-Sea *Res*. 13, 699–705.

Samra, M. I. El (1988). Chemical observations in the Arabian Gulf and the Gulf of Oman. Arab Gulf *J. Scient. Res. Math. Phys. Sci*., A6, 204–215.

Offshore Environment of the ROPME Sea Area after the War-Related Oil Spill, Eds. A. Otsuki *et al.*, pp. 99–124.

Distribution of nutrient, nitrous oxide and chlorophyll a of RSA: Extremely high ratios of nitrite to nitrate in whole water column

S. HASHIMOTO[1], R. TSUJIMOTO[2], M. MAEDA[1], T. ISHIMARU[1], J. YOSHIDA[1], Y. TAKASU[3], Y. KOIKE[3], Y. MINE[3], A. KAMATANI[1] and A. OTSUKI[1]

[1]*Department of Ocean Sciences, Tokyo University of Fisheries, 4-5-7 Konan, Minato-ku, Tokyo 108-8477, Japan*
[2]*Toyama Prefectural Fisheries Research Institute, 364, Takatsuka, Namerikawa, Toyama 936, Japan*
[3]*Research and Training Vessels, Tokyo University of Fisheries, 4-5-7 Konan, Minato-ku, Tokyo 108-8477, Japan*

Abstract—Observations of chemical properties such as nutrients, chlorophyll a, phaeopigments and dissolved nitrous oxide (N_2O) were made on 22–25 stations between 28°N and the Strait of Hormuz in ROPME sea area on RV Umitaka-Maru cruises during January and December 1993, and December 1994. Generally, nitrite concentrations were much lower than those of nitrate, so its contribution to the marine nitrogen cycle is not considered to be as important as that of nitrate (Kamykowski and Zentara, 1991). However, we found that nitrite concentrations in the RSA were relatively high compared to those of nitrate. Average molar ratios of nitrite to nitrate during three cruises were 0.73 (n = 74), 0.59 (n = 133), and 0.78 (n = 114). Nitrification in oxic waters is probably the source of the observed nitrite.

The distribution of dissolved nitrous oxide concentrations was measured to evaluate the shallow gulf, without any anaerobic layer, as a natural nitrous oxide emission source. Nitrous oxide concentrations in excess of saturation were detected in all samples from the RSA and there were no large vertical differences in the concentrations in samples collected in December 1994. Levels of oxygen were generally near saturation, however the lowest oxygen value measured during the three cruises was 1.00 ml/l at 71 m depth near the bottom (73 m). These results suggest that nitrous oxide was produced in the RSA, and that nitrification in oxic waters can be invoked as its source. The concentrations of dissolved nitrous oxide in surface water ranged from 6.99 nM to 11.7 nM, or 107 to 184% saturation, with an average of 134%. The RSA may be a natural source of nitrous oxide to the atmosphere in winter.

The range and average concentrations of phosphate, silicate, nitrate, nitrite, ammonium (all in μM), and chlorophyll a (μg l^{-1}) for the three cruises were: <0.06–1.23, 0.41; 0.34–15.5, 3.65; <0.09–14.3, 1.56; <0.09–1.78, 0.62; 0.32–2.64, 1.12; and 0.06–3.83, 0.94, respectively. High concentrations of nitrate, phosphate, and silicate were observed along the Iranian coast, while concentrations of nitrate and nitrite were depleted in surface waters along the coasts of Saudi Arabia and the United Arab Emirates (UAE). Chlorophyll a concentrations were also high at stations along the Iranian coast with high nutrient concentrations. However, the distribution of ammonium appeared to

be different. These results show that nutrient-rich water entered from the Gulf of Oman and flowed northwards along the Iranian coast, increasing in chlorophyll a concentration as it went. As the concentrations and distributions of nitrogenous nutrients were similar during the three cruises, we speculate that a region of high nitrite exists in winter and that the remarkably high ratios of nitrite to nitrate observed may be "normal" in the RSA during this season.

INTRODUCTION

Nutrients in the RSA had been measured only a few times in the past: March to April 1965 (Rabsch, 1972), December 1968 (Transactions of the Tokyo University of Fisheries, 1974), February to March 1977 (Brewer and Dyrssen, 1985) and September to November 1984–86 (El Samra, 1988). Surface nitrate values were below the detection limit from February to March 1977, and productivity in the RSA appeared to be limited by nitrogenous nutrients (Brewer and Dyrssen, 1985). However, ammonium concentrations were not measured during that cruise. Based on available information, the simultaneous observation of nitrogenous nutrients such as nitrate, nitrite and ammonium at offshore stations in the RSA had not previously been conducted. We here describe the results of hydrochemical study undertaken during three successive cruises of RV *Umitaka-Maru* to the RSA in the winter months during January 14–26 and December 15–27, 1993 and December 15–27, 1994. The aim of the present study was to carry out extensive sampling for the chemical properties of the water column in RSA, looking into the distributions of dissolved oxygen, nutrients, chlorophyll a and phaeopigments, with particular emphasis on nitrous oxide. The later was examined to judge on the potential of this shallow gulf with no anaerobic layer to be a natural source of nitrous oxide.

MATERIALS AND METHODS

Sampling

The research was carried out during the three cruises on the RV *Umitaka-Maru* during January 14–26 and December 15–27, 1993, and December 15–27, 1994 in the RSA, an area characterized by strong evaporation and high salinity in the water column. Sampling sites were 22–25 stations along 5–7 sections between 28°N and the Strait of Hormuz (Fig. 1). Water samples were collected from 3–9 depths at each station with 1.5 L Niskin bottles and a 20 L Van Dorn sampler. Analyses for dissolved oxygen, nutrients, chlorophyll a and phaeopigments were carried out on board within 12 h of sampling. Water samples for the measurement of dissolved nitrous oxide were collected in 50 ml glass bottles. After overflow of more than 100 ml of water, 0.5 ml of $HgCl_2$ was added to inhibit microbial activity. The bottles were then immediately capped with a hand-clipper, taking care to exclude air bubbles, and stored at 4°C. Samples containing air bubbles were discarded. The final concentration of $HgCl_2$ in solution was about 350 mg l^{-1}.

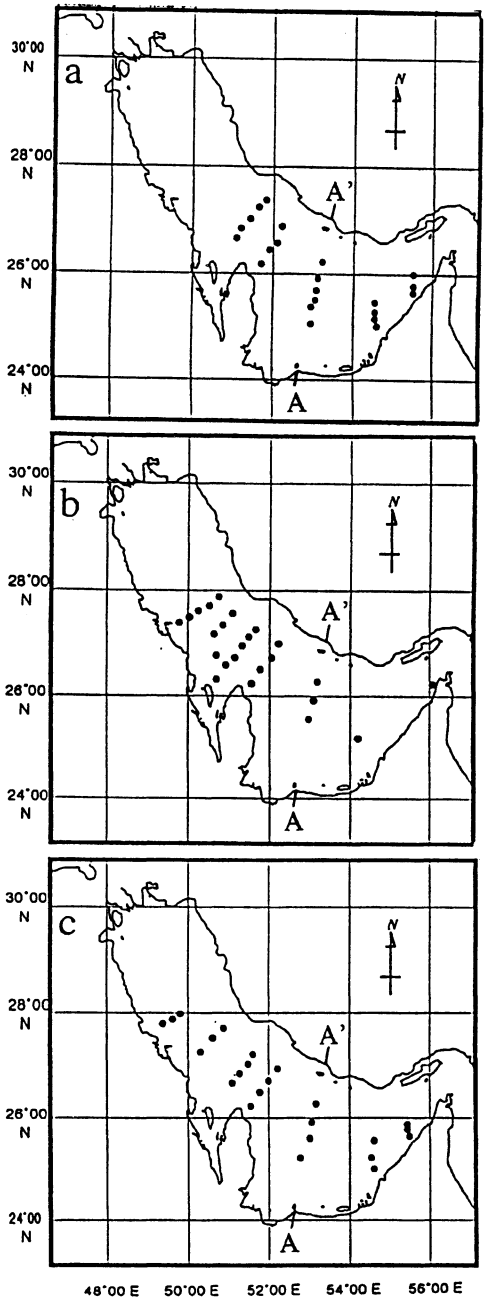

Fig. 1. Sampling stations in the RSA. Cruise: (a) Jan. 1993, (b) Dec. 1993, (c) Dec. 1994.

Measurement

Modified standard procedures (Parsons *et al.*, 1984) were used to determine nutrient concentrations. Details of the methods are described in the Cruise Report of Tokyo University of Fisheries (Tokyo University of Fisheries, 1995). Nitrate, nitrite and ammonium were determined on board with a Technicon Auto-Analyzer AAII. Phosphate and silicate were determined by colorimetry with a double beam spectrophotometer (Shimadzu model UV-140-01). Calibrations for each nutrient were carried out daily with CSK standard solutions (guaranteed by the Sagami Chemical Research Center) for nitrite (0, 0.5, 1, and 2 μM nitrite), nitrate (0, 5, 10, and 20 μM nitrate dissolved in 30.5% NaCl), phosphate (0, 0.5, 1, and 2 μM phosphate dissolved in 30.5% NaCl), and silicate (0, 5, 10, and 50 μM silicate dissolved in 30.5% NaCl). No salt effect on the analysis of nitrite by this method was observed. The detection limits for both nitrite and nitrate was about 0.1 μM. Reproducibility of sample measurements was about ±5%. Ultrapure water (Milli-Q water) was used to decrease the background level. All reagents used were of analytical grade.

For the measurements of chlorophyll a and phaeopigments, 250 ml of water was filtered through a glass fiber filter (Whatman GF/F, nominal pore size 0.7 μm) and the filter was extracted with N,N′-dimethylformamide (Suzuki and Ishimaru, 1990). Chlorophyll a and phaeopigments were determined with a fluorometer. Dissolved oxygen was determined by the standard Winkler method. Salinity was measured with a temperature controlled conductivity salinometer.

Analysis of dissolved nitrous oxide was performed in the laboratory one month after the cruise with an automatic analyzer consisting of a sample injection system, a purging chamber, adsorption and desorption columns with a cooling and heating system, a GC-ECD detector, and a calibration system (Hashimoto *et al.*, 1993). The stability of stored dissolved nitrous oxide samples was confirmed by analyzing a portion of the replicate water samples on both 10 January and 27 April. The average difference between replicate samples measured on both these dates was 5.4%, within analytical precision. Dissolved nitrous oxide sampled from Tokyo Bay and stored in the same way was stable for at least five months. The analytical system was modified in three ways from that reported previously (Hashimoto *et al.*, 1993). A system of back-flushing the precolumn prevented column memory due to tailing compounds. A 10 × 40 mm magnesium perchlorate (Wako Pure Chemical Industries, Ltd., Japan) in-line trap was used to remove water vapor from the carrier gas leaving the purging chamber containing the water sample. A 20°C oven (AO-30C, Shodex, Japan) prevented the co-elution of carbon dioxide and nitrous oxide from a 1 m Porapak Q column. The sample volume was approximately 14 ml and the weights of purged water samples were measured gravimetrically. We checked the concentration of the standard gas (9.9 ppm nitrous oxide in nitrogen produced by Nippon Sanso Corporation, Japan) with another standard gas (2.0 ppm nitrous oxide in nitrogen produced by Taiyo Toyo Sanso Co. Ltd., Japan). Agreement between the two was within 1.2%. Five replicate measurements using 14 ml samples containing 8 nM of nitrous oxide were reproducible to within about ± 5%. The detection limit of this system was

about 2 nM.

Nitrous oxide concentrations in the air were not measured during our cruise. We estimated the average mixing ratio of nitrous oxide in the air at the time of the cruise in December, 1994 as 310.7 ppb, accounting for an annual 0.2% increase and a 307 ppb value tropospheric nitrous oxide in 1988 (Butler and Elkins, 1991). The equilibrium nitrous oxide concentrations in surface water was calculated from this value and the solubility equation of Weiss and Price (1980).

RESULTS

Distribution of nutrients, nitrous oxide and chlorophyll a in the RSA

Horizontal and vertical profiles of nitrate, nitrite, and ammonium are shown in Figs. 2–7. During the three cruises, high concentrations of nitrate and nitrite were observed along the Iranian coast, while nitrate was severely depleted (<0.09 μM) in the southern part of the RSA. However, the pattern of ammonium distribution appeared to be different. The range and average of nitrate, nitrite, the ratio of nitrite:nitrate, ammonium, dissolved nitrous oxide, phosphate, silicate, chlorophyll a, phaeopigments and dissolved oxygen during the three cruises are shown in Table 1. Ammonium was measured in all samples and its concentration was relatively constant. Nutrient concentrations during these gulf cruises, especially those of ammonium in surface waters, were relatively high. The high concentration of nitrite, compared to that of nitrate, was a noteworthy characteristic.

Table 1. Summary of measurements during three winter seasons in the RSA.

sampling period	Jan., 1993	Dec., 1993	Dec., 1994
number of samples	82	143	129
		(minimum-maximum, average)	
nitrate (μM)	<0.09-5.22, 1.37	0.10-14.3, 2.10	<0.09-9.98, 1.07
nitrite (μM)	0.09-1.38, 0.41	<0.09-1.78, 0.70	<0.09-1.39, 0.67
ratio of nitrite/nitrate	0.057-3.25, 0.73	0.007-1.46, 0.59	0.04-2.12, 0.78
ammonium (μM)	1.13-2.64, 1.91	0.32-1.56, 1.00	0.53-1.60, 0.75
nitrous oxide (nM)	not measured	not measured	6.24-11.7, 9.02
phosphate (μM)	0.18-0.65, 0.38	<0.06-1.23, 0.34	0.38-1.18, 0.51
silicate (μM)	0.34-4.06, 1.93	2.30-15.5, 4.74	1.67-14.1, 3.53
chlorophyll (μg l^{-1})	0.45-2.98, 1.35	0.06-3.83, 0.80	0.08-2.56, 0.84
phaeopigments (μg l^{-1})	0.030-1.71, 0.29	0.003-0.050, 0.009	0.064-2.2, 0.38
dissolved oxygen (ml l^{-1})	3.63-5.35, 4.80	1.12-4.75, 4.18	1.00-5.06, 4.38

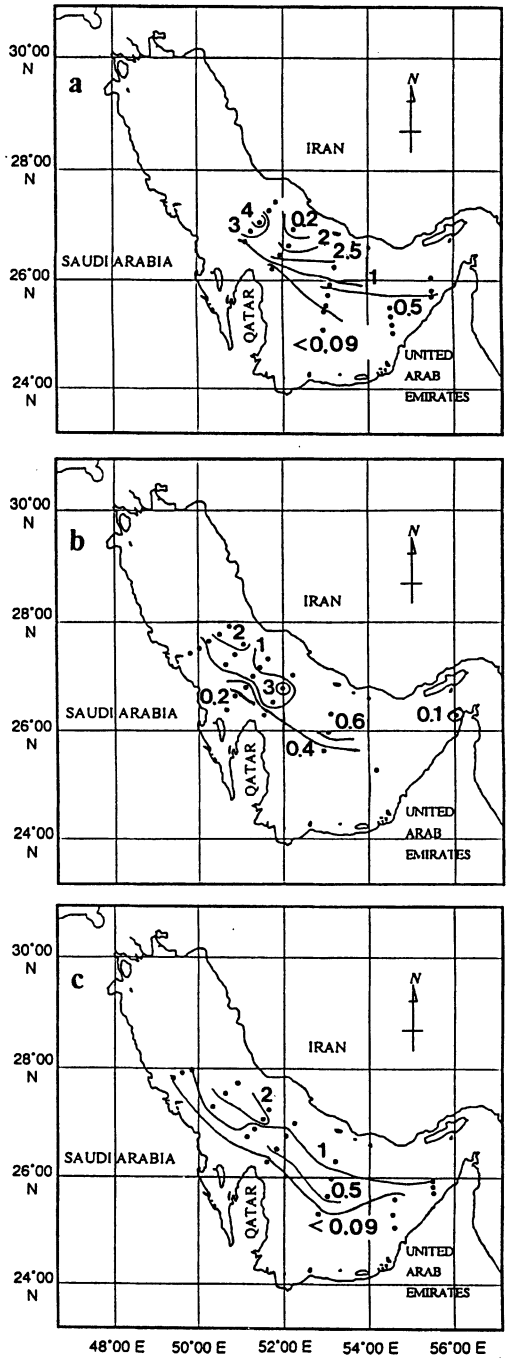

Fig. 2. Distribution of surface nitrate (μM) in the RSA. Cruise: (a) Jan. 1993, (b) Dec. 1993, (c) Dec. 1994.

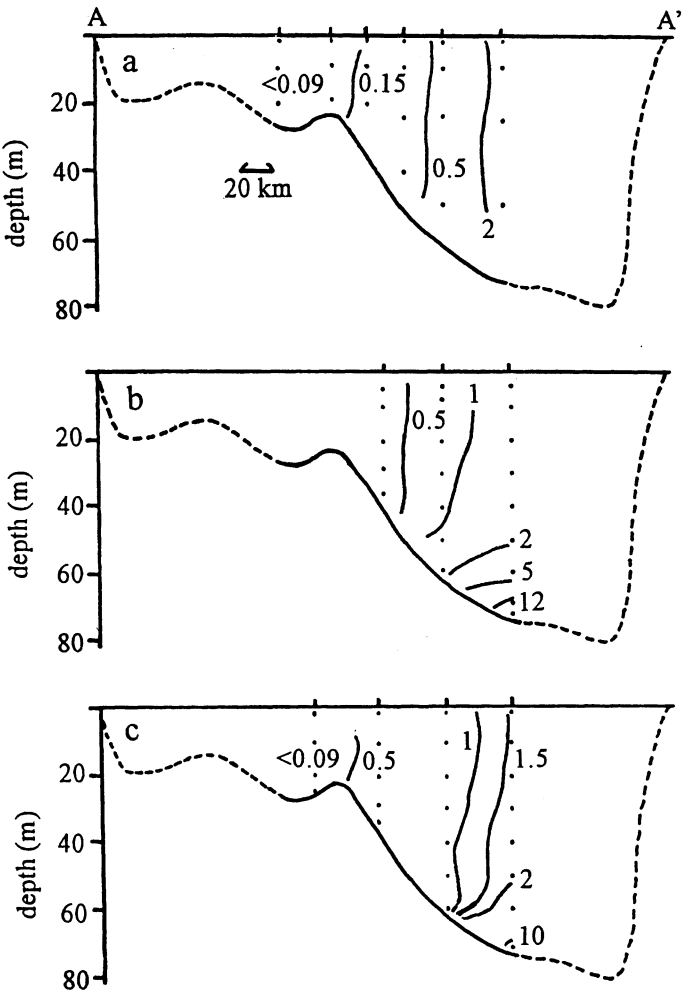

Fig. 3. Vertical nitrate (μM) section along line A-A' shown in Fig. 1. Cruise: (a) Jan. 1993, (b) Dec. 1993, (c) Dec. 1994.

The horizontal and vertical distributions of nitrous oxide were also relatively constant as was that of ammonium (Figs. 8 and 9). The dissolved nitrous oxide concentrations and saturation state of surface waters (Table 2) suggest that the dissolved nitrous oxide levels there exceeded the concentrations expected from equilibrium with the air.

High concentrations of phosphate were observed along the Iranian coast, while lower values were observed along the coasts of Saudi Arabia and UAE (Figs. 10 and 11). The highest observed silicate concentration was sampled at the outflow from the Shatt al Arab waterway at the northern end of the RSA (6 μM:

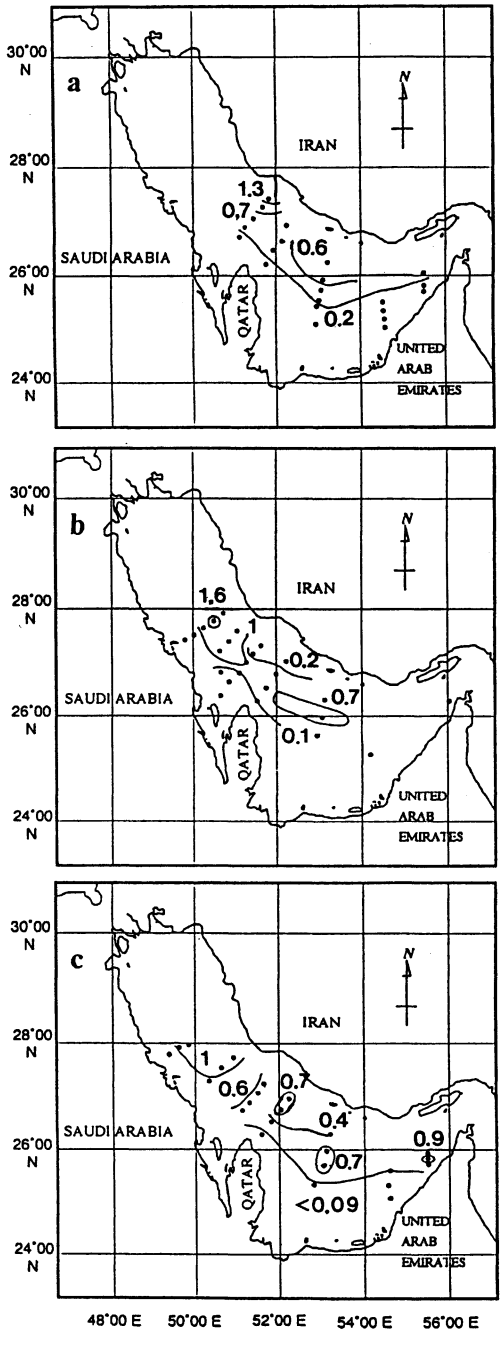

Fig. 4. Distribution of surface nitrite (μM) in the RSA. Cruise: (a) Jan. 1993, (b) Dec. 1993, (c) Dec. 1994.

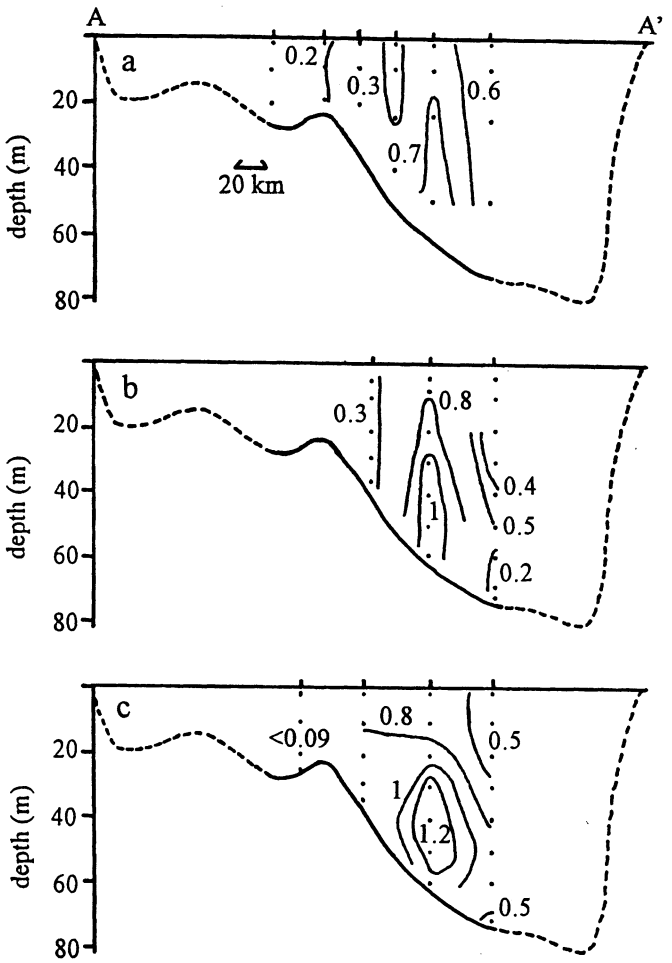

Fig. 5. Vertical nitrite (μM) section along line A-A' shown in Fig. 1. Cruise: (a) Jan. 1993, (b) Dec. 1993, (c) Dec. 1994.

Brewer and Dyrssen, 1985; 20 μM: El Samra, 1988). Higher silicate concentrations were also sampled at the inner part of the RSA (north of the Qatar peninsula) and lower values were sampled along the coast of UAE (Figs. 12 and 13).

The concentrations of chlorophyll a were also relatively high at the stations on the Iranian coast (Figs. 14 and 15), corresponding with the distributions of nutrients. Average molar ratios of phaeopigments to chlorophyll a during the three cruises carried out in January and December 1993, and in December 1994 were 0.25 (n = 66), 0.02 (n = 137), and 0.54 (n = 126), respectively.

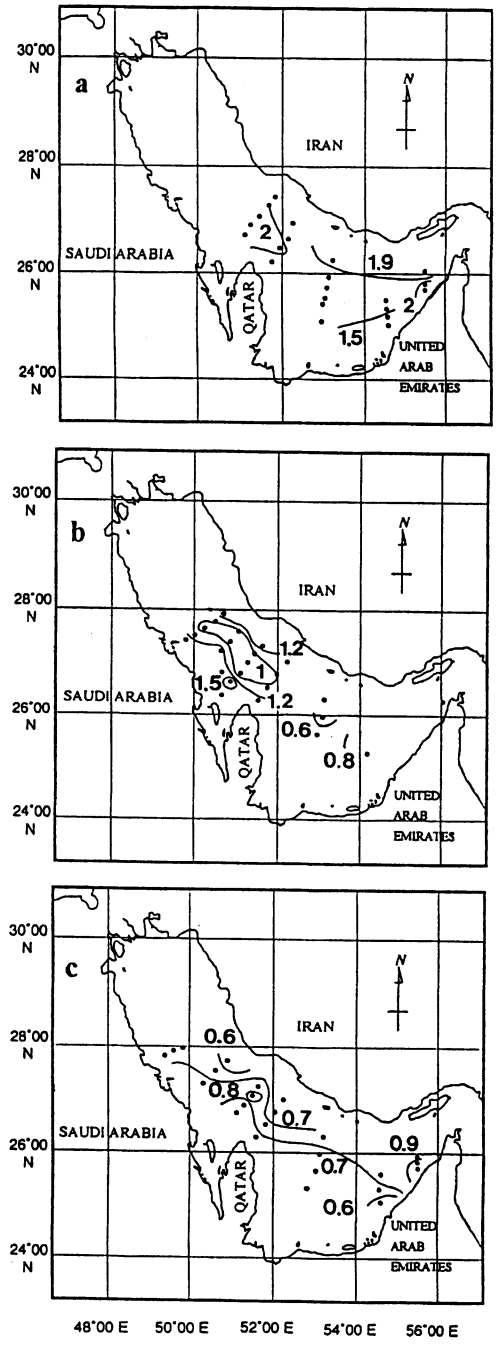

Fig. 6. Distribution of surface ammonium (μM) in the RSA. Cruise: (a) Jan. 1993, (b) Dec. 1993, (c) Dec. 1994.

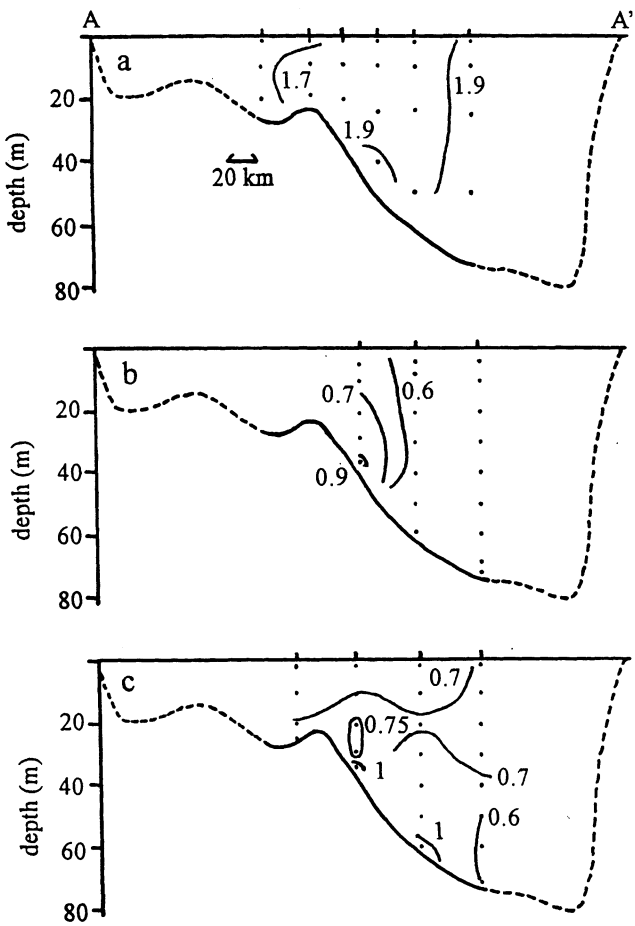

Fig. 7. Vertical ammonium (μM) section along line A-A' shown in Fig. 1. Cruise: (a) Jan. 1993, (b) Dec. 1993, (c) Dec. 1994.

Salinity, temperature, and dissolved oxygen

The surface water temperature and salinity in December 1994 ranged from 20.8 to 25.8°C and from 38.493 to 40.889 PSU, respectively. The average wind speed was 7.4 m sec^{-1}. The vertical distributions of salinity and temperature at most stations indicate that the upper waters (shallower than about 20 m) in the RSA were vertically well mixed by strong winds. The salinity data show that Gulf of Oman water entered the Strait of Hormuz and flowed northwards along the Iranian coast, circulated counterclockwise around the Qatar Peninsula, and then part flowed back toward the mouth of the RSA along the coast of Saudi Arabia with increasing salinity (similar to the data of Reynolds (1993)). As shown in

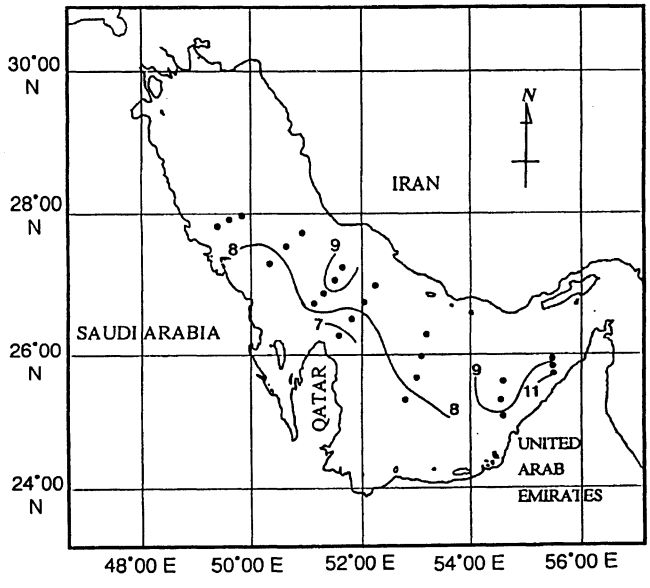

Fig. 8. Distribution of surface dissolved nitrous oxide (nM) in the RSA during December 1994.

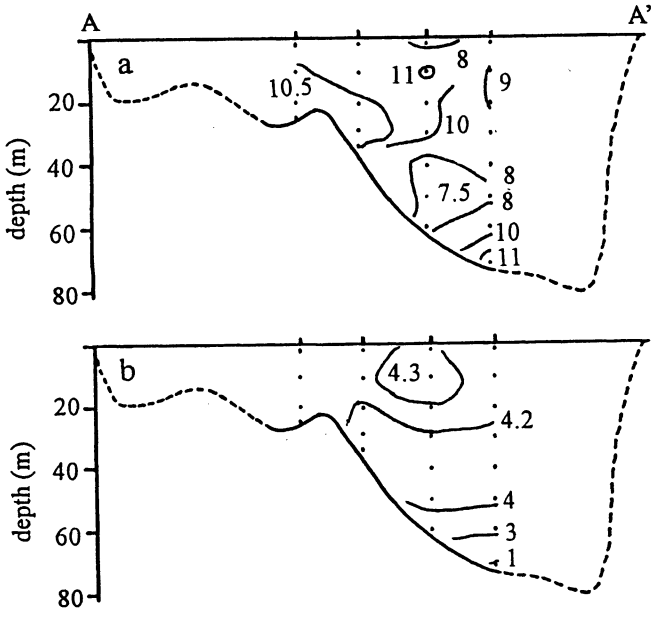

Fig. 9. Vertical distribution of dissolved nitrous oxide (nM) and dissolved oxygen (ml l^{-1}) along line A-A' shown in figure 1. Cruise: Dec. 1994. (a) dissolved nitrous oxide, (b) dissolved oxygen.

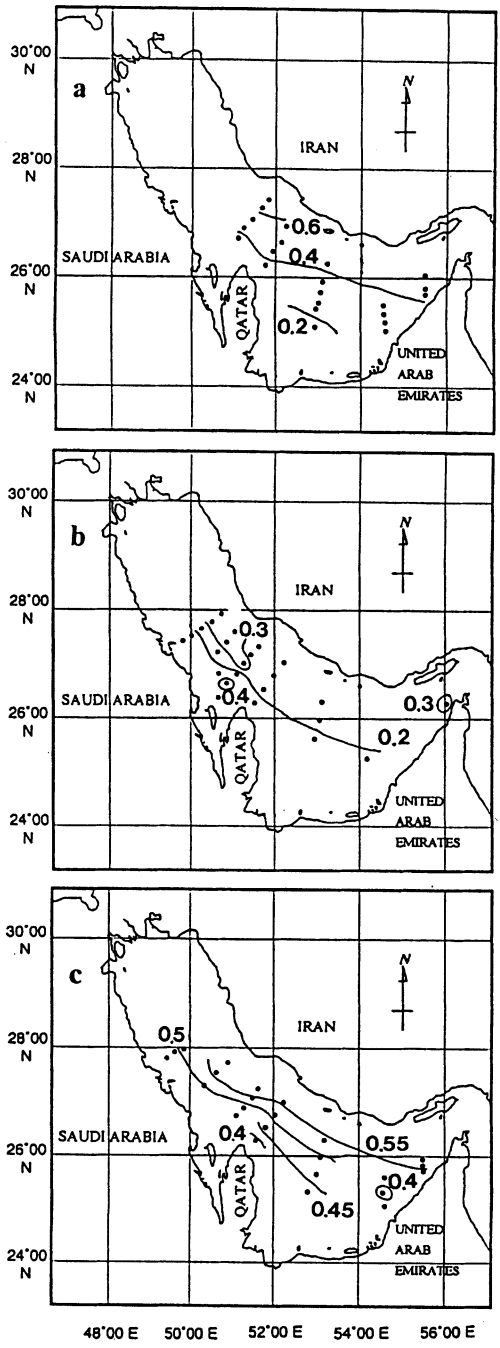

Fig. 10. Distribution of surface phosphate (μM) in the RSA. Cruise: (a) Jan. 1993, (b) Dec. 1993, (c) Dec. 1994.

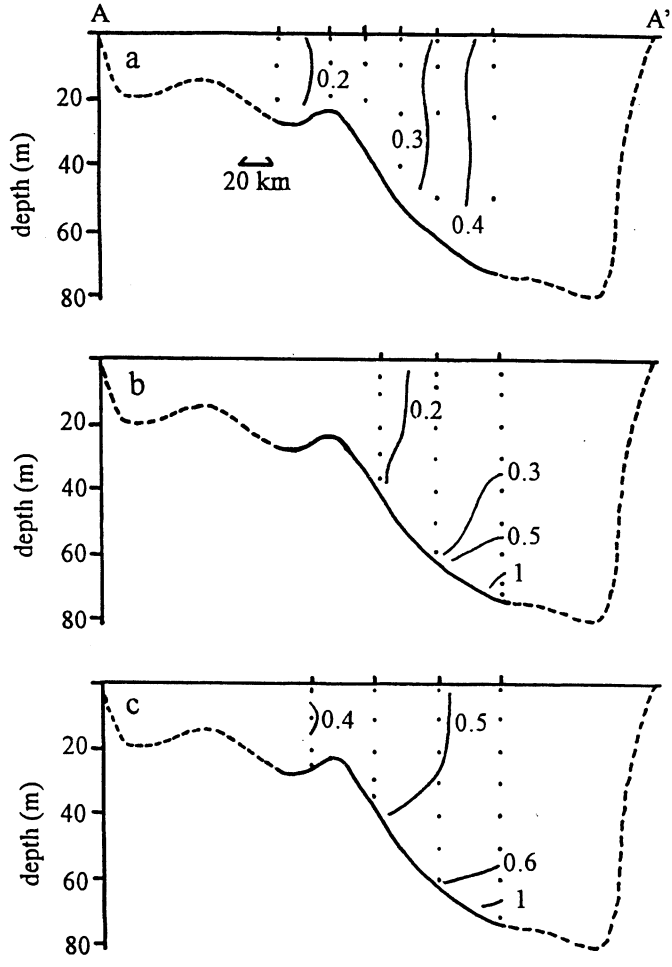

Fig. 11. Vertical phosphate (μM) section along line A-A' shown in Fig. 1. Cruise: (a) Jan. 1993, (b) Dec. 1993, (c) Dec. 1994.

Table 1 and Fig. 9, levels of oxygen were generally near saturation and the lowest oxygen value we observed was 1.00 ml/l at 71 m depth.

DISCUSSION

Comparison of nutrients and chlorophyll a among stations

Similar to the results of earlier studies (Brewer and Dyrssen, 1985; El Samra, 1988), we found a negative linear relationship between surface phosphate and

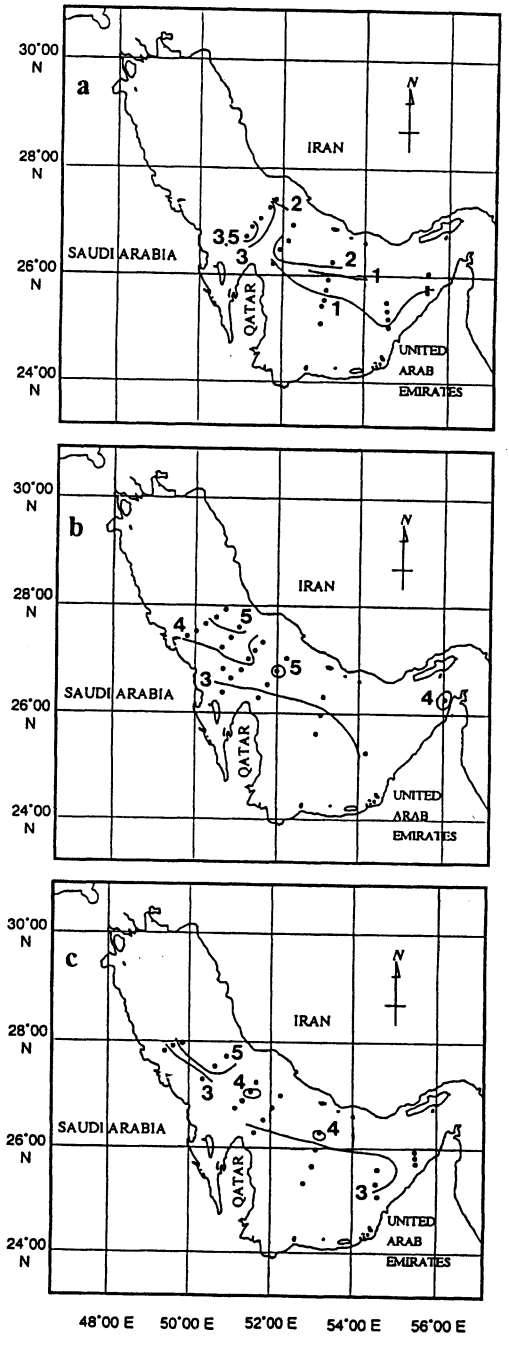

Fig. 12. Distribution of surface silicate (μM) in the RSA. Cruise: (a) Jan. 1993, (b) Dec. 1993, (c) Dec. 1994.

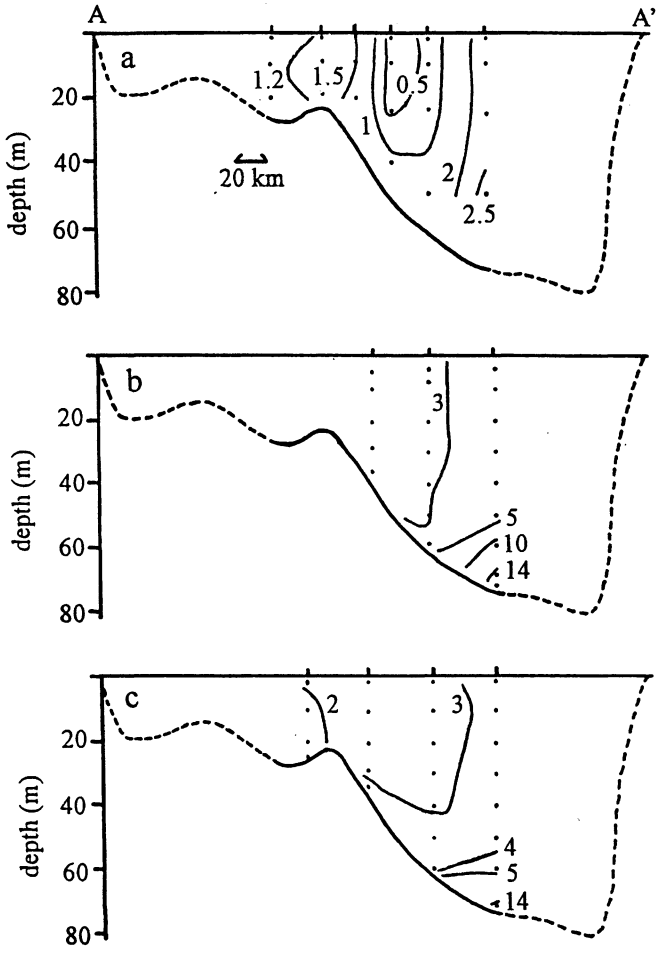

Fig. 13. Vertical silicate (μM) section along line A-A' shown in Fig. 1. Cruise: (a) Jan. 1993, (b) Dec. 1993, (c) Dec. 1994.

surface salinity (Fig. 16), suggesting that the surface water entering the RSA from the Gulf of Oman contained high concentrations of phosphate. High phosphate concentrations along the Iranian coast, due to upwelling induced by the northeast monsoon, were observed in the inflowing surface waters (Rabsch, 1972; Transactions of the Tokyo University of Fisheries, 1974; Brewer and Dyrssen, 1985; El Samra, 1988). The distributions of phosphate observed in the RSA during the three cruises were similar (see Figs. 10, 11 and 16) to those observed on earlier cruises. Phosphorus was observed in all samples, suggesting that it is not a limiting nutrient during this season.

In contrast, nitrate and nitrite were not detected in some water samples along

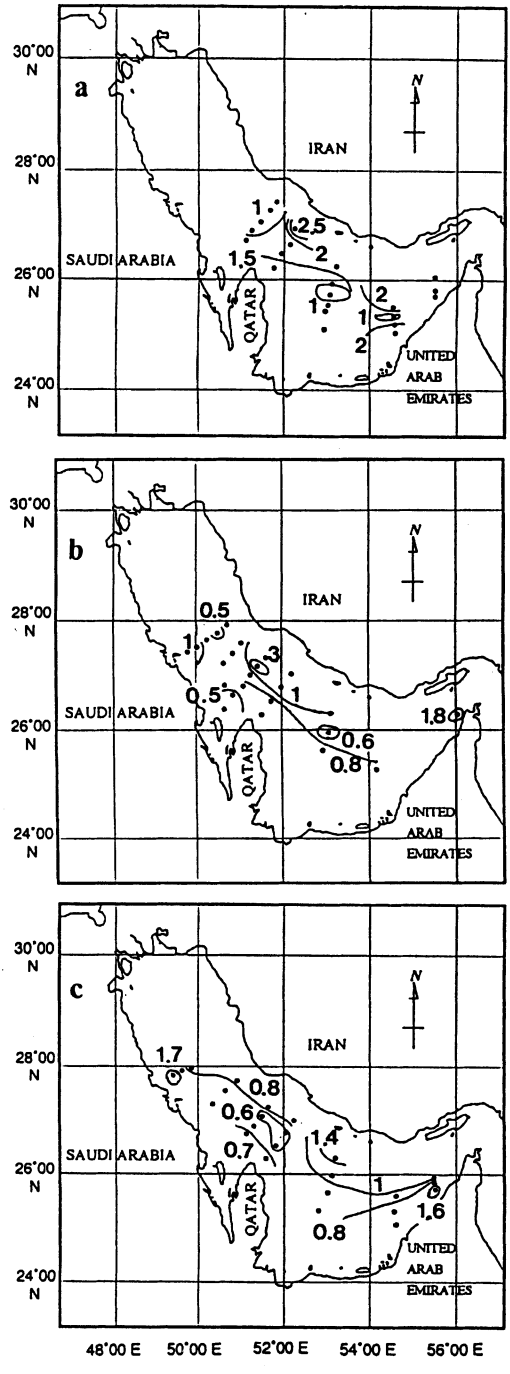

Fig. 14. Distribution of surface chlorophyll a ($\mu g\ l^{-1}$) in the RSA. Cruise: (a) Jan. 1993, (b) Dec. 1993, (c) Dec. 1994.

Table 2. Surface nitrous oxide concentrations and saturation state.

latitude	longitude	salinity	water temp.	N_2O (observed)	N_2O (equilibrium)	saturation
(N)	(E)	(PSU)	(°C)	(nM)	(nM)	(%)
25° 00.30'	54° 35.80'	40.849	23.9	8.43	6.25	135
25° 14.00'	54° 33.00'	40.432	24.0	9.10	6.25	146
25° 31.94'	54° 35.92'	40.282	24.9	9.04	6.09	148
25° 52.38'	55° 28.99'	38.493	25.0	9.13	6.12	149
25° 46.14'	55° 29.49'	39.138	25.6	10.3	6.00	172
25° 39.00'	55° 30.25'	38.904	24.0	11.7	6.30	186
26° 14.63'	53° 11.73'	38.546	24.2	8.13	6.28	130
25° 55.40'	53° 05.93'	39.792	24.7	7.86	6.13	128
25° 35.53'	53° 00.98'	39.994	24.9	8.33	6.09	137
25° 15.73'	52° 45.24'	40.889	23.8	7.94	6.26	127
26° 13.85'	51° 34.89'	40.405	22.8	6.99	6.48	108
26° 28.12'	51° 48.45'	39.879	24.1	7.71	6.25	123
26° 42.69'	52° 02.18'	39.906	24.1	8.28	6.25	133
26° 57.34'	52° 14.41'	39.716	24.0	8.13	6.27	130
26° 41.69'	51° 07.20'	40.236	23.3	8.63	6.39	135
26° 50.37'	51° 17.43'	40.196	22.8	8.60	6.47	133
27° 01.82'	51° 29.74'	40.028	23.0	9.29	6.44	144
27° 12.43'	50° 19.29'	39.643	23.1	9.03	6.43	140
27° 15.14'	51° 38.31'	40.306	22.6	7.84	6.52	120
27° 30.81'	50° 37.23'	40.249	23.1	8.08	6.42	126
27° 42.44'	50° 54.50'	39.969	22.4	8.11	6.56	124
27° 56.99'	49° 49.77'	40.388	22.0	8.10	6.62	122
27° 47.88'	49° 23.70'	40.721	20.0	8.60	7.04	122
average ± standard deviation				8.58 ± 0.96		136 ± 17

the Saudi Arabian coast. We divided the data into four regions (Fig. 17) based on the currents and water circulation processes in the RSA (Reynolds, 1993; Yoshida *et al.*, this volume) to compare the levels of dissolved oxygen, nutrients, nitrous oxide, and chlorophyll a in the euphotic zone (0–35 m depth) among stations (Table 3). Nitrate and nitrite concentrations along the Saudi Arabian coast (region B) were the lowest among the four areas, suggesting the following processes of nitrate consumption in the RSA. The inflowing surface water that entered from the Gulf of Oman was high in nitrate due to upwelling there and flowed northwards along the Iranian coast, and then counterclockwise around the Qatar peninsula. Part of this water then flowed southwards along the southern part of RSA (Reynolds, 1993). Nitrate in the water entering the RSA decreased with

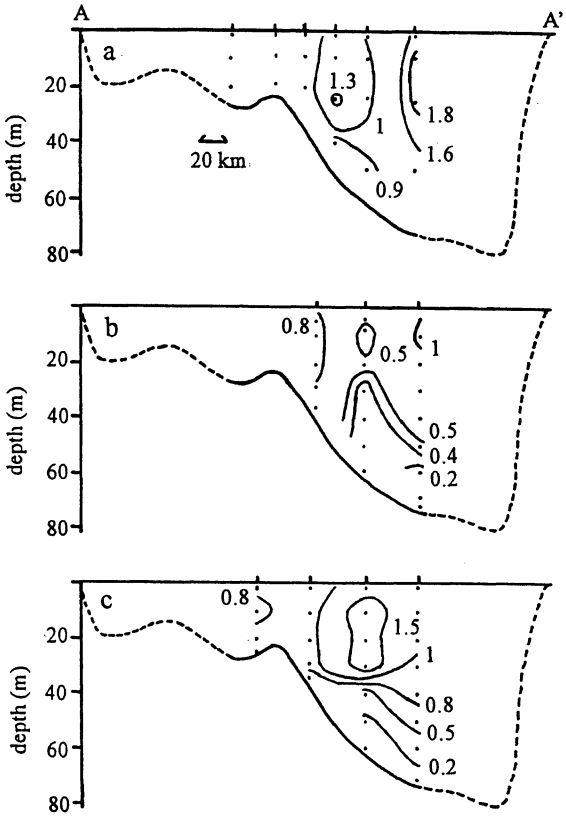

Fig. 15. Vertical chlorophyll a ($\mu g\ l^{-1}$) section along line A-A' shown in Fig. 1. Cruise: (a) Jan. 1993, (b) Dec. 1993, (c) Dec. 1994.

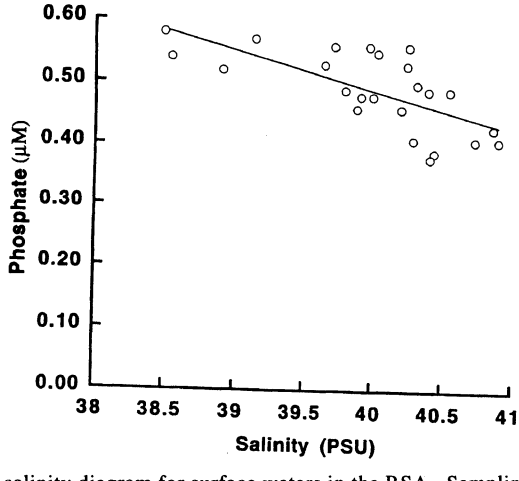

Fig. 16. Phosphate-salinity diagram for surface waters in the RSA. Sampling period: Dec. 1994.

Table 3. Summary of salinity, dissolved oxygen, nutrients, nitrous oxide and chlorophyll a in the euphotic zone of the four regions shown in Fig. 17.

region	A	B	C	D
	(minimum-maximum, average)			
salinity (PSU)	38.546-40.042, 39.750	40.282-42.628, 41.073	38.493-39.251, 38.992	39.643-40.722, 40.214
dissolved oxygen (ml l^{-1})	4.07-4.48, 4.30	3.75-4.75, 4.45	3.97-4.68, 4.23	4.43-5.06, 4.65
phosphate (μM)	0.44-0.56, 0.50	0.38-0.49, 0.42	0.52-0.62, 0.57	0.39-0.59, 0.51
silicate (μM)	2.27-4.07, 2.95	1.67-3.13, 2.38	2.86-3.79, 3.53	2.40-5.87, 4.00
nitrate (μM)	0.30-1.74, 0.90	<0.09-0.42, 0.11	0.12-1.75, 1.06	<0.09-2.23, 1.19
nitrite (μM)	0.37-1.25, 0.73	<0.09-0.18, 0.11	0.14-1.10, 0.68	0.10-1.23, 0.75
ratio*	0-1.75, 0.94	0.34-0.84, 0.60	0-1.09, 0.64	0.26-1.56, 0.76
ammonium (μM)	0.64-0.83, 0.71	0.53-1.22, 0.74	0.76-1.60, 0.98	0.55-0.85, 0.67
nitrous oxide (nM)	7.71-11.1, 9.22	6.99-10.7, 8.66	7.50-11.7, 9.04	6.68-9.29, 8.25
chlorophyll (μg l^{-1})	0.29-1.85, 0.99	0.59-1.17, 0.82	0.50-2.00, 1.00	0.25-2.56, 1.00

*Ratio of nitrite to nitrate.

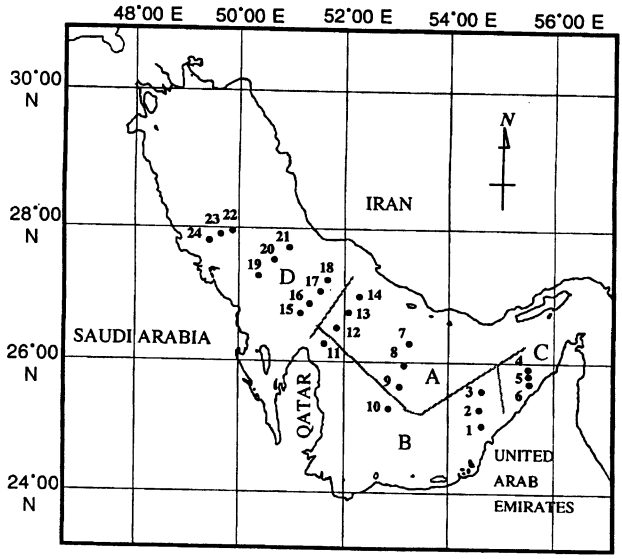

Fig. 17. Sampling stations in the RSA in December, 1994. A, B, C, D: the four regions used in Table 3.

flow northwards along the Iranian coast, as chlorophyll a gradually increased. Consequently, nitrate was not detected at some stations along the southern part of RSA. The concentration of chlorophyll a was also relatively high at the stations along the Iranian coast corresponding to the distributions of nitrate and phosphate. The high chlorophyll a concentrations measured along the Iranian coast are consistent with the relatively high levels of primary production (Hirawake *et al.*, this volume) and zooplankton production (Nomura *et al.*, this volume) measured there at the same times.

The maximums of nitrate, phosphate, and silicate were observed from the water sampled near the bottom at station 7 near the Iranian coast (region A) (Tables 1 and 4). In contrast, water with the maximum ammonium concentration was sampled at 20 m at station 6 (bottom: depth: 21 m) near the UAE coast (region C), where high concentrations of organotin compounds (Watanabe *et al.*, this volume) and normal alkanes (Tsujimoto *et al.*, this volume) were also measured. Generally ammonium concentrations are relatively high in the regions B and C, where nitrous oxide and chlorophyll a are also high. This implies that ammonium might be used as primary nitrogenous nutrient due to nitrate deficiency in the region.

In February and March 1977, nitrogen seemed to be the limiting element in the RSA (Brewer and Dyrssen, 1985). However, at least one of the three nitrogenous nutrients, nitrate, nitrite, and ammonium, was observed at all stations during our three cruises, suggesting that nitrogenous nutrients were not limiting phytoplankton biomass in this season.

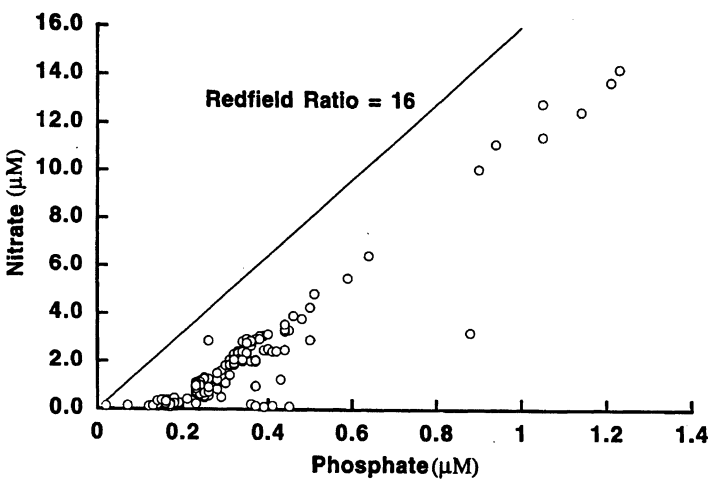

Fig. 18. Nitrate-phosphate diagram for all Dec. 1993 water samples from the RSA. We have no reason to suspect the outlier on the lower right other than its distance from all other points.

Table 4. Concentrations of nutrients, nitrous oxide, and chlorophyll a along section 7-10 across the RSA.

station*	depth (m)	nitrate (μM)	nitrite (μM)	ratio**	ammonium (μM)	phosphate (μM)	silicate (μM)	nitrous oxide (nM)	chlorophyll (μg l^{-1})
7	0	1.50	0.37	0.25	0.71	0.54	4.07	8.13	1.56
	10	1.50	0.37	0.25	0.72	0.54	3.40	9.08	1.06
	20	1.53	0.37	0.24	0.74	0.54	3.40	9.10	1.19
	30	1.74	0.56	0.32	0.74	0.56	3.60	8.86	0.89
	40	1.78	0.77	0.43	0.67	0.56	3.53	8.98	0.89
	50	1.86	0.87	0.47	0.60	0.56	3.60	7.68	0.66
	60	2.70	0.87	0.32	0.58	0.62	4.53	9.65	0.30
	70	9.98	0.40	0.04	0.60	1.18	14.1	11.5	0.08
bottom	73								
8	0	0.60	0.68	1.14	0.65	0.49	2.27	7.86	1.28
	10	0.50	0.68	1.36	0.65	0.48	2.33	11.1	1.79
	20	0.68	0.90	1.33	0.71	0.49	2.67	10.2	1.62
	30	0.71	1.25	1.75	0.64	0.50	2.73	10.3	1.85
	40	0.84	1.37	1.62	0.62	0.51	2.80	7.52	0.45
	50	0.72	1.39	1.92	0.61	0.52	2.80	7.53	0.24
	61	0.52	1.10	2.12	1.26	0.53	3.33	7.52	0.73
bottom	63								
9	0	0.68	0.79	1.17	0.66	0.48	2.87	8.33	0.81
	10	0.63	0.79	1.26	0.70	0.47	2.87	9.92	0.90
	20	0.76	0.95	1.25	0.75	0.48	2.90	10.6	0.89
	30	0.71	0.95	1.34	0.76	0.49	2.80	10.8	0.84
	37	0.56	0.55	0.97	1.15	0.49	3.13	10.7	0.73
bottom	39								
10	0	<0.09	<0.09		0.65	0.41	2.13	7.94	0.82
	10	<0.09	<0.09		0.62	0.39	1.67	10.7	0.77
	20	<0.09	<0.09		0.70	0.41	1.73	no data	0.85
	26	0.18	<0.09		0.74	0.41	1.73	9.89	0.90
bottom	28								

* Stations are shown in Fig. 17.

** Ratio of nitrite to nitrate.

Relationship among nutrients in the RSA

The relationship between nitrate and phosphate for all samples collected from the RSA in December 1993 was linear (Fig. 18). Similar results were found for the January 1993 and December 1994 cruises. The phosphate intercept at around 0.2 μM suggests nitrate limitation for the surface waters along the Saudi Arabian coast. Outflow of nitrate-depleted water was also observed outside of the RSA near the Strait of Hormuz (Mantoura *et al.*, 1993) suggesting that nitrogen was the limiting element in February and March 1977 (Brewer and Dyrssen, 1985). Dissimilatory nitrate reduction (denitrification) in the Arabian Sea was suggested by the break in the slope of the phosphate-nitrate diagram (Mantoura *et al.*, 1993). However, we found no breaks in the slope of nitrate-phosphate plots of the RSA waters in winter (e.g., Fig. 18), suggesting that essentially no denitrification was occurring in winter in this shallow water column with no

anaerobic layer.

The relationships among nutrients such as nitrate, nitrite, ammonium, phosphate and silicate were also examined. During our three cruises, significant positive relationships were observed among nitrate, phosphate and silicate in all samples, but no significant relationship was observed between ammonium and the other nutrients. No significant relationship was also observed between nitrite and the other nutrients.

Relatively high nitrite to nitrate ratio

The ratios of nitrite to nitrate concentrations observed in the RSA were significantly higher (see Figs. 2–6 and Tables 1, 3 and 4) than those for other oceanic regions, like the northwestern Indian Ocean where nitrite levels were generally one order of magnitude lower than those of nitrate except at the nitrite peak (Mantoura *et al.*, 1993). Generally water column nitrite is thought to originate from three different biological mechanisms, assimilatory nitrate reduction, denitrification, and nitrification (principally ammonium-based). When nitrite production from these processes exceed nitrite uptake by phytoplankton and bacteria, accumulation of nitrite in the water column occurs.

Assimilatory nitrate reduction may be carried out by phytoplankton in the euphotic zone. However, the potential for uptake of nitrite by phytoplankton is usually larger than that for production of nitrite in the euphotic zone (Olsen, 1981). In the case of the nitrite maximum usually associated with the chlorophyll a maximum at the bottom of the euphotic zone, the nitrite is produced mainly by assimilatory nitrate reduction by phytoplankton (Kiefer *et al.*, 1976; French *et al.*, 1983). However, the chlorophyll a maximum in the RSA (Fig. 15) was shallower than 30 m, and did not coincide with the nitrite maximum (Fig. 5).

Another type of nitrite maximum, often called a "secondary nitrite maximum", is usually observed in oxygen deficient waters, and denitrification is generally the major mechanism of nitrite production (Codispoti and Packard, 1980; Codispoti and Christensen, 1985; Mantoura *et al.*, 1993). However, the levels of oxygen in the RSA during our three cruises were typically about 4 ml/l with a minimum of 1.00 ml/l at 71 m depth (Fig. 9(b)) and we found no breaks in the slopes of the nitrate-phosphate relationship (Fig. 18); in other words, we found no indication of denitrification in the gulf's water column, suggesting that the high concentration of nitrite there cannot be explained by denitrification alone.

Two types of bacterial population are responsible to ammonium oxidation to nitrate, i.e., ammonium oxidizer and nitrite oxidizer (Olsen, 1981). Nitrite oxidizers are more light-sensitive than ammonium oxidizers and this difference can produce primary nitrite maxima near the bottom of the euphotic zone, particularly in stratified water columns (Olsen, 1981). The depth of the 1% light level in the RSA was about 35–40 m and there is a possibility that ammonium oxidation in deeper waters was the main reason for the existence of a nitrite maximum below the euphotic zone (Fig. 5).

The ratios of nitrite to nitrate were very variable at different stations in the RSA, however, they were almost constant in the water column at each station (Table 4). This suggests that nitrite produced below the euphotic zone at each station would be transported to the upper waters by physical diffusion such as the vertical mixing by strong wind in the shallow RSA.

The concentrations of ammonium were almost constant and relatively high at each station. Phytoplankton preferencely utilize ammonium to nitrate. The decreased potential for nitrate uptake by phytoplankton in the euphotic zone caused by high ammonium concentrations would facilitate the accumulation of nitrate in the upper waters.

Dissolved nitrous oxide in the RSA

Nitrous oxide is one of the causal compounds of several global climatic processes. It is involved in stratospheric ozone depletion and is a greenhouse gas. Although identification of the emission sources of nitrous oxide is important, a significant portion of these sources remain to be identified (Benarde, 1992). We examined the distribution of dissolved nitrous oxide concentrations in the RSA to determine whether a shallow gulf lacking an anaerobic layer in the water column could be a significant natural nitrous oxide emission source. All stations in the RSA were supersaturated with nitrous oxide. Surface nitrous oxide concentrations and saturation states ranged from 6.99 to 11.7 nM and from 108 to 186% (average: 136%), respectively. These values gives an indication that nitrous oxide was produced there despite the lack of an anaerobic layer, and the RSA could be a natural source of nitrous oxide to the atmosphere at least in December.

In the oxic water column of the Indian Ocean, nitrous oxide could originate from nitrification (Mantoura *et al.*, 1993). Generally, ammonium concentrations in surface waters are extremely low (Mantoura *et al.*, 1993) due to rapid consumption by phytoplankton. Consequently, the production of nitrous oxide by nitrification would be limited by the lack of ammonium. Since, the RSA in this season has an ammonium-rich shallow water column without an anaerobic layer, a portion of ammonium there might be nitrified to produce nitrous oxide.

To study the possibility that both nitrite and nitrous oxide in the RSA were produced from ammonium, we check the relationship between the ratio of nitrite to nitrate and the apparent nitrous oxide production below the euphotic zone (Fig. 19). As shown in this figure, we found a negative linear relationship between the ratio of nitrite to nitrate and the apparent nitrous oxide production in sea water samples below the euphotic zone. An enhanced production of nitrous oxide at low ratio of nitrite to nitrate is presumably due to that the nitrous oxide is a by-product in the process of nitrification (ammonium oxidation). The extent of nitrous oxide supersaturation we observed in the RSA also supports this hypothesis and suggests that ammonium oxidation occurred and produced at least part of nitrous oxide found there.

The present data are insufficient to discuss the biogeochemical nitrogen

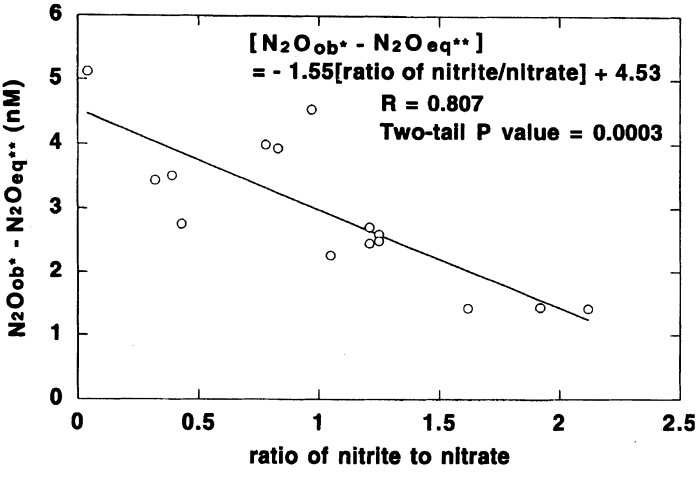

Fig. 19. Relationship between the ratio of nitrite to nitrate and the apparent nitrous oxide production below the euphotic zone. Sample: all Dec. 1994 water samples collected in 40-71 m depth.
*: observed nitrous oxide, **: calculated nitrous oxide.

cycle of the RSA in detail. The nitrogen cycle including the relatively high concentration of ammonium and the high ratio of nitrite to nitrate in the whole water column has been observed in the RSA. The future works on the sources of high ammonium concentration in the whole RSA, for example the dry fall out transported by wind from desert, are needed. The high concentration of ammonium may introduce the production of nitrite and nitrous oxide below the euphotic zone (Figs. 5 and 19). The production of nitrous oxide in the sediment are also needed to examine (Table 4: Sta. 7, 70 m). The research using isotope (Yoshida, 1988; Kim and Craig, 1990) would be a logical solution.

Acknowledgements

We are deeply grateful to Dr. Isao Koike (Ocean Research Institute, University of Tokyo) for his constructive review of this manuscript. We wish to thank the captain and crew of the RV Umitaka-Maru for their help in sampling. The authors also thank the ROPME scientists for their cooperation and helpful discussion.

REFERENCES

Benarde, M. A. (1992). Global *Warning*. John Wiley & Sons, pp. 84–85.

Brewer, P. G. and Dyrssen, D. (1985). Chemical oceanography of the Persian Gulf. Prog. Oceanog., 14, 41–55.

Butler, J. H. and Elkins, J. W. (1991). An automated technique for the measurement of dissolved N_2O in natural waters. Mar. Chem., 34, 47–61.

Codispoti, L. A. and Christensen, J. P. (1985). Nitrification, denitrification and nitrous oxide cycling in the eastern tropical South Pacific Ocean. Mar. *Chem.*, 16, 277–300.

Codispoti, L. A. and Packard, T. T. (1980). Denitrification rates in the eastern tropical South Pacific. J. *Mar. Res.*, 38, 453–477.

Cruise Report (1995). Survey report in the Persian Gulf. Tokyo University of *Fisheries*, 4, 108–113.

El Samra, M. I. (1988). Chemical observations in the Arabian Gulf and the Gulf of Oman. Arab Gulf *J. Scient. Res., Math. Phys. Sci.*, A6(2), 205–215.

French, D. P., Furnas, M. J. and Smayda, T. J. (1983). Diel changes in nitrite concentration in the chlorophyll maximum in the Gulf of Mexico. Deep-Sea Res., 30, 707–722.

Hashimoto, S., Sun, H. Y., Nakamura, T., Nojiri, Y. and Otsuki, A. (1993). Seasonal variations in dissolved nitrous oxide concentrations in a eutrophic shallow lake without anaerobic layer. Geochem. J., 27, 117–123.

Hirawake *et al.*, this volume.

Kamykowski, D. and Zentara, S. (1991). Spatio-temporal and process-oriented views of nitrite in the world ocean as recorded in the historical data set. Deep-Sea Res., 38, 445–464.

Kiefer, D. A., Olson, R. J. and Holm-Hansen, O. (1976). Another look at the nitrite and chlorophyll maxima in the central North Pacific. Deep-Sea *Res.*, 23, 1199–1208.

Kim, Kyung-Ryul and Craig, H. (1990). Two-isotope characterization of N_2O in the Pacific Ocean and constraints on its origin in deep water. Nature, 347, 58–61.

Mantoura, R. F. C., Law, C. S., Owens, N. J. P., Burkill, P. H., Woodward, E. M. S., Howland, R. J. M. and Llewellyn, C. A. (1993). Nitrogen biogeochemical cycling in the northwestern Indian Ocean. Deep-Sea Res., 40, 651–671.

Nomura et al., this volume.

Olsen R. J. (1981). 15N Tracer studies of the primary nitrite maximum. J. *Mar. Res.*, 39, 203–226.

Parsons, T. R., Maita, Y. and Lalli, C. M. (1984). A *Manual of Chemical and Biological Methods for Seawater Analysis*. Pergamon Press.

Rabsch, U. (1972). Zur Verteilung von Sauerstoff und von Nährstoffen im Persischen Golf auf Grund von Beobachtungen von F. S. "Meteor" im Frühjahr 1965. *"Meteor" Forsch. Ergebnisse*, 11, 74–88.

Reynolds, R. M. (1993). Physical oceanography of the gulf, Strait of Hormuz, and the Gulf of Oman-results from the Mt. Mitchell expedition. Mar. Pollut. Bull., 27, 35–59.

Suzuki, R. and Ishimaru, T. (1990). An improved method for the determination of phytoplankton chlorophyll using N,N-dimethylformamide. J. Oceanogr. *Soc. Japan*, 46, 190–194.

Transactions of the Tokyo University of Fisheries (1974). Arabian Gulf fishery-oceanography survey by the Umitaka-maru, training-research vessel, Tokyo University of Fisheries with collaboration of Kuwait Institute for Scientific Research, December 1968, 1, 113–118.

Tsujimoto et al., this volume.

Watanabe et al., this volume.

Weiss, R. F. and Price, B. A. (1980). Nitrous oxide solubility in water and seawater. Mar. *Chem.*, 8, 347–359.

Yoshida, N. (1988). 15N-depleted N_2O as a product of nitrification. Nature, 335, 528–529.

Yoshida *et al.*, this volume.

Offshore Environment of the ROPME Sea Area after the War-Related Oil Spill, Eds. A. Otsuki *et al.*, pp. 125–147.

Levels of mercury in the marine environment of the ROPME area

Nahida B. AL-MAJED and Wajdi A. RAJAB

Environment Protection Department, Ministry of Health, P.O. Box 24395 Safat, Postal Code 13104 Kuwait

Abstract—The purpose of this study is to determine the levels of total and methyl mercury (MeHg) in different fish species and sediment samples from ROPME Sea Area. Samples were collected as a part of Umitaka Maru Cruises through the period 1993–1994. The cruises were organized by ROPME and Tokyo University of Fisheries, Japan.

A total of 72 fish samples of different species and 42 sediment samples were collected during the two cruises. Fish and sediment were prepared in accordance with The Manual of Oceanographic Observation and Pollutant Analyses Methods (MOOPAM,1989) for the analysis of total mercury. The final determination was obtained by a Gold Film Mercury Analyzer. Whereas, fish samples were prepared and analyzed in accordance with IAEA/UNEP/FAO/IOC: Reference Methods for Marine Pollution Studies No. 13, Rev. 1 UNEP 1991, for determination of MeHg. The level of MeHg was obtained by gas chromatograph provided with electron capture detector.

The obtained mean value of total Hg based on dry weight in fish samples was 0.80 μg/g with standard deviation of ±0.52. The minimum obtained value was 0.250 μg/g recorded in two species *Pelates quadrilineatus* (Yamyam) and *Platax orbicularis* (Bent Alnokhetha). The maximum obtained value was 3.201 μg/g recorded in *Therapon thraps* (Theeb). While, the mean value of MeHg based on dry weight was 0.76 μg/g with standard deviation of ±0.54. The minimum value was 0.144 μg/g recorded in *Saurida unvosqamis* (Hasoom). The maximum obtained value was 2.944 μg/g recorded in *Therapon thraps* (Theeb). MeHg was linearly correlated with total Hg. MeHg values averaged between 85.5% to 101.9% of the total Hg content. The Hg levels detected in the edible species are almost close to the permissible value set by different international organization.

The results of sediment samples analysis show that the levels of total Hg varied between 0.042 μg/g and 0.375 μg/g with an overall mean value of 0.169 ± 0.070 μg/g. The obtained levels of Hg in sediment does not reflect the levels in fish.

INTRODUCTION

Mercury (Hg) is recognized as a potentially hazardous pollutant and it is considered one of the most dangerous pollutants to man and a nonessential micro-elements in the marine environment. Hg is widely distributed in the form of various inorganic and organic compounds of different toxicity to aquatic organisms (GESAMP, 1986).

Hg compounds have been used by Arab and Greek physicians since the 4th century B.C. and they are still being used effectively and safely to treat a variety of infections and disorders today. In the 13th century Italian assassins used to pour Hg into the ear of sleeping victims from whence it would diffuse into the brain causing a very unpleasant death (Freiand and Hutzinger 1975).

The essential point to remember is that Hg has certain characteristics which ensure that it will be distributed naturally through all parts of the environment. It is the only metal which is liquid at room temperature and it boils at 375°C compared to 212°C of silver. It is ten thousand time more volatile than DDT and has a vapor pressure of 1.2×10^{-3} compared to 1.5×10^{-7} for DDT.

Mercury has three oxidation states: Hg^0, Hg^+ and Hg^{2+} and it is capable of making covalent bonds. Whereas, organomercury compounds such as methyl mercury CH_3Hg^+ and ethyl mercury $(CH_3)_2Hg^+$ are formed by biochemically mediated or chemical conversion and they are highly bioaccumulated in tissues organisms.

Sources of mercury

Mercury has two main sources in the environment:

1 - Natural sources: Rain water collected at various places and times containes between 0.05 and 0.48 μg/L of mercury and an average of 0.5 μg/g of Hg, and sedimentary rocks contain more mercury than igneous rocks.

2 - Anthropogenic sources: Mercury is used in the chlor-alkali industry as a catalyst, dental preparations, electrical apparatus such as batteries, paint industry, for general laboratory use, pharmaceutical, and pulp and paper industry. The chlor-alkali industry is the most common, dangerous, and localized source at which high concentration of mercury is used in this industry. It has been estimated that about 0.35 to 0.5 lb of Hg can be lost to the environment from every 100 ton of produced chlorine (Study Group on Mercury Hazards, 1970).

Hg is also present in the non-ferrous metal industries in certain sulphur ores of zinc and lead, copper but only at 0.0–10.0 ppm range. The chief losses of Hg occurred when metals are heated or alloyed. The sulphuric acid made from these gases produced by such operations may contain 1.0–3.0 mg Hg/L (American Chemical Society, 1981).

Mercury in the marine environment

Mercury enters the marine environment with the dumping of sewage sludge and by direct discharge of industrial effluents. Under suitable conditions, some metals associated with sediments and suspended particles are returned to the overlying water following remobilization and upward diffusion (Bryan, 1976). This process may act as a significant source of trace metal contamination. MeHg, the most toxic form, is formed mainly by methylation of Hg by methanogenic bacteria which is widely distributed in sediment of rivers and canals and in sludge of sewage beds. The biological cycle of mercury in the environment has been explained earlier by Wood (1972) as shown in Fig. 1. It has been increasingly

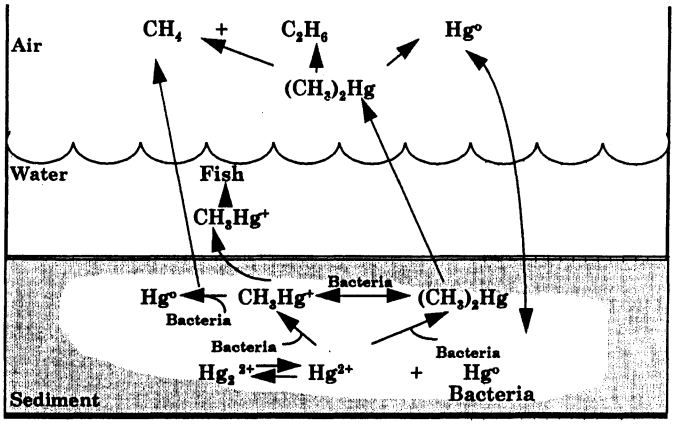

Fig. 1. Biological cycle for mercury.

realized that eolian input of mercury into the marine represents a major source of contamination in the marine environment where, dust particles in the air will normally carry more than the expected amount of Hg, due to the ability of Hg to absorb on any and all surfaces (Williston, 1968). Whereas, large quantities of Hg are released into the atmosphere from anthropogenic sources. Gadner (1975) found that the mean mercury content of north Atlantic waters under the north jet stream to be 26.5 ng/L compared with an average of 15.9 ng/L in the southern hemisphere.

Toxicity of mercury compounds

Toxic properties of mercury compounds have also been known for a long time, and they have been used at time for murder and suicide. Mercury can be toxic to biological organisms and thus its presence in the marine environment is generally considered undesirable.

The initial uptake of mercury and other metals by the aquatic organisms can be considered in terms of three main processes; from water through respiratory surface, adsorption from water onto body and from ingested food particles through the digestive system (Des *et al.*, 1984).

The toxicity of mercury chloride has been reported by Walker, (1989) using LD_{50} or EC_{50} values of <0.05–50 mg dm^{-3} in various biological system. The toxic effect of methyl mercury on man is primarily the form of damage to the central nervous system. Research data suggest that methyl mercury chlorides are more toxic than any of the inorganic mercury compounds. For example, the lethal concentration for *Lemna minor* is 4 mg dm^{-3} $HgCl_2$ or 0.01 mg dm^{-3} CH_3HgCl. Methyl mercurial chloride is specially poisonous because it can penetrate the membranes separating the blood stream from the brain (Subhadra, 1991).

Methyl mercury uptake appears to be detoxified to some degree by

demethylation and storage in tissues as less toxic inorganic forms. MeHg concentrations and their ratios to total Hg concentrations in water, air, sediment and soil are dependent on environmental factors such as species and concentrations of methyl donor, forms and concentration of inorganic mercury, pH, redox potential, temperature, microflora etc. (Des and Gergory, 1984). There is still a lack of reliable data with respect to the ecotoxicological effects of other organomercurial compounds.

Major mercury poisoning episodes

The toxicity of Hg has caused wide spread public human concern as a result of several widely publicized disasters. These incidents took place in a limited areas where there had been very heavy localized pollution with mercurial compounds.

The main source of the human mercury intake will be the consumption of fish and other marine animals. Consumption of fish containing high levels of methyl mercury can have serious consequences, as demonstrated in Minamata disaster in Japan in 1950. This was the first incident by a mercury compound. Over one hundred people were poisoned after eating sea food containing high levels (27.0–102.0 μg/g dry weight of methyl mercury) as a result of direct discharge of industrial effluent in Minamata Bay (Patricia *et al.*, 1975). In 1964–1965 a similar epidemic in Niigata, Japan, occurred when 26 people were poisoned after eating food contaminated with MeHg compounds and five died (Fukunaga and Tsukano, 1969).

Commercial fishing was banned on some lakes and rivers in Sweden in 1967, when fish were found to contain more than 1.0 μg/g of Hg. Similarly, commercial fishing was banned on many lakes and rivers in North America when mercury residues greater than 0.5 μg/g were found (Patricia *et al.*, 1975).

THE R/V UMITAKA MARU CRUISES IN THE ROPME SEA AREA

The Umitaka Maru cruises were organized by the Regional Organization of the Marine Protection Environment (ROPME) in collaboration with Tokyo University of Fisheries, Japan. The first cruise was conducted in the period from 15–25 January 1993, while the second cruise was conducted in the period from 14–26 December 1993. Sampling locations of the Umitaka Maru cruises in the ROPME Sea Area are shown in Fig. 2.

The main objective of these cruises was to follow the impact of the largest oil spill in ROPME Sea Area history as a result of the Gulf War in January 1991, where an estimated 6–8 million barrels of oil were spilled into the ROPME Sea Area. The oil was dumped from Iraqi tankers near Mina Al-Baker in the Iraqi territorial waters but the main discharge was from Al-Ahmadi Sea Island terminal and from tankers located near Mina Al-Ahmadi port in the southern beach of Kuwait. Fallout in the from of small oil droplets and oily soot from the burning

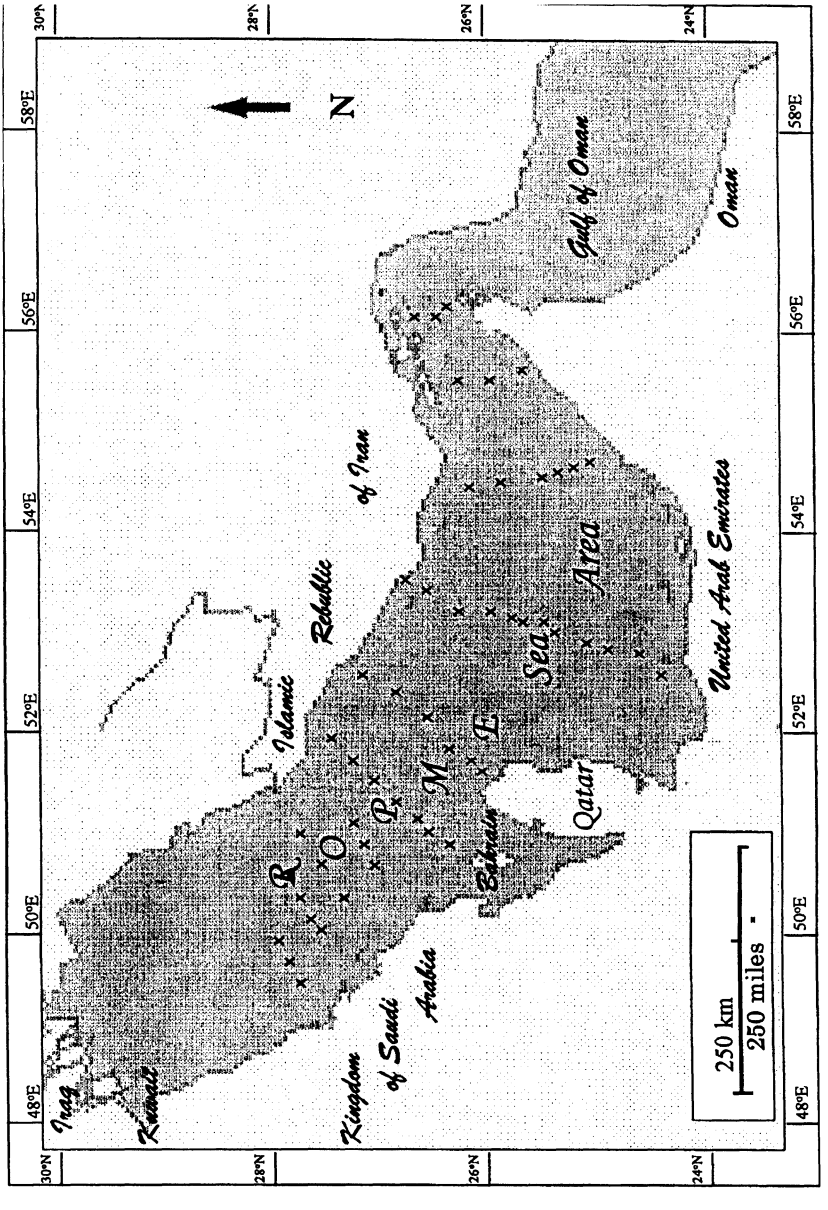

Fig. 2. Sampling stations of the Umitaka Maru Cruises in the ROPME Sea Area (1993–1994).

Kuwait oil wells represent an additional source of input of contamination into the ROPME Sea Area.

It is worth noting here that the first cruise in the region was conducted by USA—NOAA Ship Mt. Mitchell—the 100 Day Cruise organized by ROPME in collaboration with the National Oceanic and Atmospheric Administration (NOAA) and the Intergovernmental Oceanographic Commission (IOC) in the period from February–June 1992. Samples of fish and sediment analyzed in this study were collected during the Umitaka Maru cruises.

MATERIALS AND METHODS

Sampling

Fish

A total of 72 fish samples representing 28 species was collected from 17 stations during the two R/V Umitaka Maru cruises. *Lethrinus kallpoterus* and *Caranx leptolepis* species represent 29% of the total analyzed fish samples, while a total of 11 samples of *Lethrinus kallpoterus* and 10 samples of *Caranx leptolepis* was analyzed. Other samples include different numbers of other species such as 6 samples of *Pelates quadrilineatus*, 5 samples of *Loxodon macrorhinus*, 4 samples of *Arius thalassinus* and *Therapon thraps*, 3 samples of *Trachrurus trachrurus*, *Saurida lndosquamis* and *Tylosurus leiurus*, 2 samples from each of *Dentex nufar*, *Etrumeas tera*, *Nemitterus tolu*, *Scolopsis phaeops* and *Therapon jarbua*. Adding to those, each 1 sample from other species such as *Argyrops filamentosus*, *Argyrops spinifer*, *Cephalopholis miniatus*, *Gnathandon speciosus*, *Lethrinus horak*, *Parupeneus cyclostomus*, *Platax orbicularis*, *Platycephalus indicus*, *Plectorhynchus cincuts*, *Rochycentron canadus*, *Saurida unvosqamis*, *Scolopsis bimaculatus* and *Scolopsis ghanam*, was included.

Fishing was carried out usually from sun-set to sun-rise, using fishing gears (long line, traps, rod and line and gill-net) that were available on the vessel. The total catch was randomly distributed among the concerned scientists. Total weight, total length, fork length and standard length were carried out on board for all species. Taxonomy tasks for identification of the scientific and local name and sex were also carried on board (Katsuzo and Yoshitaka, 1986). Samples were also dissected for fillets, then the fillets were wrapped with sterilized aluminum foil labelled and stored in deep freezer (at –20°C) until the time of analysis.

The species name, length expressed in centimeters (cm), fresh weight expressed in grams (g), dry weight/fresh weight ratio, sex and location for the analyzed fish samples are summarized in Table 1a for the first cruise and in Table 1b for the second cruise.

Sediment

Samples were collected from different stations as shown in Fig. 2, using a Smith Macintyre grab sampler, kept in pre-treated glass bottles and stored in deep freezer (at –20°C) until the time of analysis. Water depth in meter (m) was recorded for each station in addition to the date and sampling location. These data are shown in Table 2.

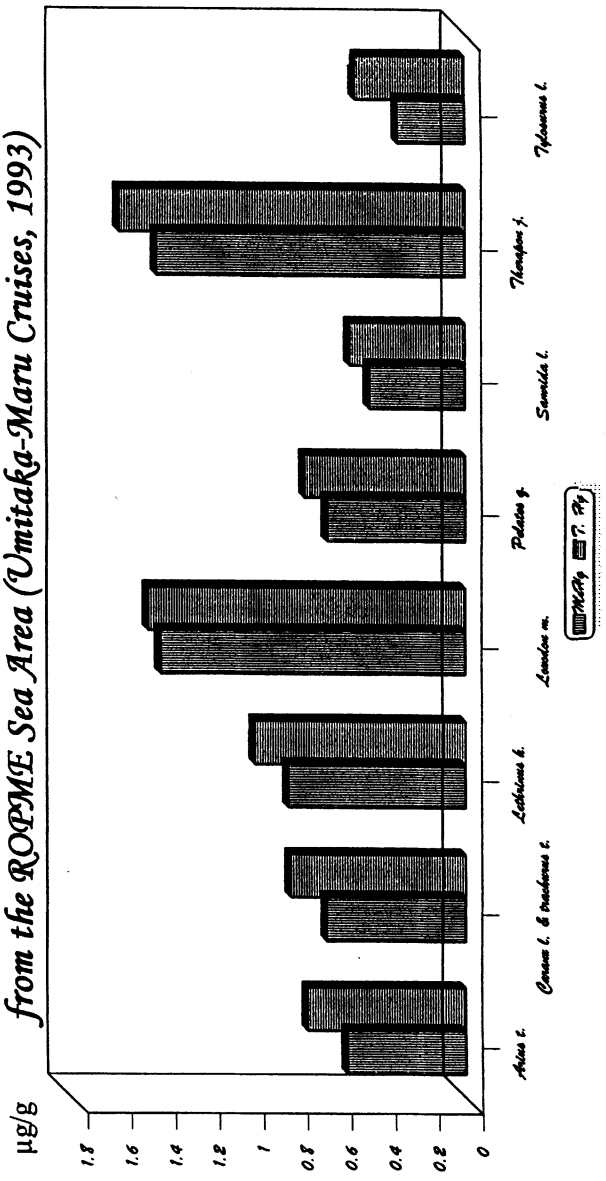

Fig. 3. Overall mean levels of mercury in fish species from the ROPME Sea Area (Umita Maru Cruises, 1993).

Table 1(a). Characteristics and location of fish species collected from ROPME Sea Area (Umitaka Maru Cruise No. 1, 14–26 January 1993).

Sample Code	Species Name		Length (cm)		Fresh wt. (gm)		DW/FW	Sex	Location	
	Latin	Local	Total	Fork	Fish	Fillets			Long.	Lat
11FC1	*Arius thalassinus*	Chim	38	31	424	89	0.27	F	52°56.10′E	25°37.60′N
38FC1	*Arius thalassinus*	Chim	56	48	1700	511	0.14	F	55°30.20′E	25°39.20′N
15FC1	*Caranx leptolepis*	Curfa	20	17	74	19	0.25	F	52°56.10′E	25°37.60′N
26FC1	*Caranx leptolepis*	Curfa	20	17	80	21	0.23	F	51°39.90′E	26°40.59′N
31FC1	*Caranx leptolepis*	Curfa	20	18	88	23	0.23	F	51°23.10′E	26°44.60′N
19FC1	*Caranx leptolepis*	Curfa	20	18	98	17	0.26	M	52°56.10′E	25°37.60′N
09FC1	*Caranx leptolepis*	Curfa	21	18	101	28	0.25	M	53°15.27′E	25°51.85′N
25FC1	*Caranx leptolepis*	Curfa	21	19	96	26	0.24	F	51°39.90′E	26°40.59′N
17FC1	*Caranx leptolepis*	Curfa	21	18	104	26	0.26	F	52°56.10′E	25°37.60′N
08FC1	*Cephalopholis miniatus*	Shananwa	27	*	273	82	0.21	F	53°15.27′E	25°51.85′N
27FC1	*Dentex nufar*	Nahash	15	13	46	12	0.22	F	51°39.90′E	26°40.59′N
29FC1	*Dentex nufar*	Nahash	18	16	90	22	0.19	F	51°23.10′E	26°44.60′N
14FC1	*Etrumeas tera*	Oom	16	15	38	12	0.24	F	52°56.10′E	25°37.60′N
16FC1	*Etrumeas tera*	Oom	18	17	56	12	0.24	F	52°56.10′E	25°37.60′N
10FC1	*Lethrinus horak*	Sha'ary	30	28	392	130	0.23	F	53°15.27′E	25°51.85′N
06FC1	*Lethrinus kallopterus*	Sha'ary	28	26	360	131	0.22	M	53°15.27′E	25°51.85′N
07FC1	*Lethrinus kallopterus*	Sha'ary	36	33	530	185	0.23	F	53°15.27′E	25°51.85′N
32FC1	*Loxodon macrorhinus*	Jarjoor	51	48	592	88	0.26	F	51°40.00′E	26°10.00′N
35FC1	*Loxodon macrorhinus*	Jarjoor	57	44	534	77	0.26	F	51°44.00′E	26°09.70′N
28FC1	*Loxodon macrorhinus*	Jarjoor	59	46	692	69	0.26	F	51°23.10′E	26°44.60′N
01FC1	*Loxodon macrorhinus*	Jarjoor	65	52	1212	302	0.26	M	54°34.70′E	25°09.18′N
13FC1	*Loxodon macrorhinus*	Jarjoor	65	51	966	121	0.25	F	52°56.10′E	25°37.60′N
30FC1	*Nemipetrus tolu*	Bassy	20	17	86	24	0.21	F	51°23.10′E	26°44.60′N
33FC1	*Pelates quadrilineatus*	Yamyam	16	15	56	11	0.21	F	51°40.00′E	26°10.00′N
02FC1	*Pelates quadrilineatus*	Yamyam	18	17	90	19	0.23	M	54°34.70′E	25°09.18′N
05FC1	*Pelates quadrilineatus*	Yamyam	19	18	102	20	0.22	M	54°34.70′E	25°09.18′N
04FC1	*Pelates quadrilineatus*	Yamyam	20	19	110	24	0.22	F	54°34.70′E	25°09.18′N
03FC1	*Pelates quadrilineatus*	Yamyam	20	19	120	28	0.21	F	54°34.70′E	25°09.18′N
39FC1	*Pelates quadrilineatus*	Yamyam	20	19	102	28	0.21	F	55°30.20′E	25°39.20′N
34FC1	*Saurida lndosquamis*	Turr	21	20	70	21	0.22	M	51°40.00′E	26°10.00′N
37FC1	*Saurida lndosquamis*	Turr	30	28	152	144	0.20	F	51°44.00′E	26°09.70′N
36FC1	*Saurida lndosquamis*	Turr	31	29	184	48	0.20	F	51°44.00′E	26°09.70′N
12FC1	*Therapon thraps*	Theeb	20	19	120	29	0.23	F	52°56.10′E	25°37.60′N
24FC1	*Therapon thraps*	Theeb	17	16	86	20	0.22	F	51°39.90′E	26°40.59′N
22FC1	*Therapon thraps*	Theeb	26	24	244	66	0.24	F	52°09.50′E	25°57.05′N
21FC1	*Therapon thraps*	Theeb	27	24	230	62	0.22	F	52°09.50′E	25°57.05′N
18FC1	*Trachrurus trachrurus*	Curfa	20	17	74	19	0.22	F	52°56.10′E	25°37.60′N
20FC1	*Trachrurus trachrurus*	Curfa	20	18	76	21	0.22	F	52°56.10′E	25°37.60′N
23FC1	*Trachrurus trachrurus*	Curfa	20	18	72	21	0.21	M	51°39.90′E	26°40.59′N

* : missing data

Table 1(b). Characteristics and location of fish species collected from ROPME Sea Area (Umitaka Maru Cruise No. 2, 14–26 December 1993).

Sample	Species Name		Length (cm)		Fresh wt. (gm)		DW/FW	Sex	Location	
Code	*Latin*	Local	Total	Fork	Fish	Fillets			Long.	Lat.
10FC2	*Aegyrops filamentosus*	Andug	28	25	420	92	0.22	M	49°50.60'E	27°22.10'N
08FC2	*Argyrops spinifer*	Andug	35	32	750	158	0.23	F	54°14.80'E	25°12.80'N
34FC2	*Arius thalassinus*	Chim	43	35	700	101	0.23	M	50°54.90'E	26°34.90'N
09FC2	*Arius thalassinus*	Chim	58	48	1540	299	0.22	M	55°00.00'E	25°59.80'N
02FC2	*Caranx leptolepis*	Curfa	21	19	110	20	0.24	M	49°50.60'E	27°22.10'N
04FC2	*Caranx leptolepis*	Curfa	23	19	100	23	0.23	M	49°50.60'E	27°22.10'N
14FC2	*Caranx leptolepis*	Curfa	24	21	150	39	0.24		51°45.40'E	25°36.20'N
18FC2	*Gnathandon speciosus*	Rebeeb	23	20	150	39	0.21		51°45.40'E	25°36.20'N
26FC2	*Lethrinus kallopterus*	Sha'ary	22	20	160	28	0.22	M	51°26.00'E	26°09.50'N
05FC2	*Lethrinus kallopterus*	Sha'ary	22	20	150	30	0.22	M	50°42.80'E	26°45.60'N
28FC2	*Lethrinus kallopterus*	Sha'ary	22	24	190	39	0.22	M	51°26.00'E	26°09.50'N
01FC2	*Lethrinus kallopterus*	Sha'ary	22	20	170	134	0.81	M	50°42.80'E	26°45.60'N
27FC2	*Lethrinus kallopterus*	Sha'ary	23	21	195	15	0.25	M	51°26.00'E	26°09.50'N
31FC2	*Lethrinus kallopterus*	Sha'ary	23	21	200	31	0.19	M	51°26.00'E	26°09.50'N
29FC2	*Lethrinus kallopterus*	Sha'ary	23	22	210	19	0.23	M	51°26.00'E	26°09.50'N
30FC2	*Lethrinus kallopterus*	Sha'ary	24	21	205	32	0.23	M	51°26.00'E	26°09.50'N
03FC2	*Lethrinus kallopterus*	Sha'ary	24	22	200	39	0.22	M	49°50.60'E	27°22.10'N
15FC2	*Nemitterus tolu*	Bassy	21	19	125	26	0.23		51°45.40'E	25°36.20'N
13FC2	*Parupeneus cyclostomus*	Heddi	22	20	140	35	0.23	M	49°50.60'E	27°22.10'N
33FC2	*Platax orbicularis*	Bent Alnokhetha	13	13	100	17	0.24	FM	50°54.90'E	26°34.90'N
23FC2	*Platycephalus indicus*	Wahra	34	34	250	41	0.23	M	51°45.40'E	25°36.20'N
11FC2	*Plectorhynchus cincuts*	Fersh	21	21	140	23	0.23	M	49°50.60'E	27°22.10'N
06FC2	*Rochycentron canadus*	Sikin	70	62	2300	350	0.23	M	49°50.60'E	27°22.10'N
16FC2	*Saurida unvosqamis*	Hasoom	28	26	190	30	0.24	M	51°45.40'E	25°36.20'N
20FC2	*Scolopsis bimaculatus*	Bzeemi	24	21	140	18	0.22		55°00.00'E	25°59.80'N
12FC2	*Scolopsis ghanam*	Bzeemi	25	22	180	43	0.21	M	49°50.60'E	27°22.10'N
32FC2	*Scolopsis phaeops*	Bzeemi	23	203	140	15	0.21	F	51°26.00'E	26°09.50'N
35FC2	*Scolopsis phaeops*	Bzeemi	24	21	160	22	0.21	M	50°54.90'E	26°34.90'N
22FC2	*Therapon jarbua*	Theeb	23	21	190	24	0.23		51°45.40'E	25°36.20'N
17FC2	*Therapon jarbua*	Theeb	31	30	420	83	0.23	F	51°45.40'E	25°36.20'N
07FC2	*Tylosurus leiurus*	Hagool	62	51	300	82	0.24	M	54°14.80'E	25°12.80'N
25FC2	*Tylosurus leiurus*	Hagool	103	88	1650	377	0.26	FM	51°45.40'E	25°36.20'N
24FC2	*Tylosurus leiurus*	Hagool	105	93	1600	304	0.25	F	51°45.40'E	25°36.20'N

Table 2. Geographical distribution and physical characteristics of sediment samples collected at ROPME Sea Area (Umitaka Maru Cruise No. 1 and No. 2, 1993).

Station		Water Depth	Date of	Location		Sediment Characteristics
Code	Transect	(m)	Sampling	Long.	Lat.	
16SC1	5	25	21-Jan-93	51° 05.79 'E	26° 39.66 'N	Sandy
15SC1	5	50	21-Jan-93	51° 13.79 'E	26° 50.78 'N	Silty Sand
14SC1	5	76	21-Jan-93	51° 26.41 'E	27° 00.54 'N	Muddy
04SC1	2	38	16-Jan-93	51° 31.84 'E	25° 27.24 'N	Silty Sand
17SC1	4	27	21-Jan-93	51° 44.09 'E	26° 09.69 'N	Sandy with shells
13SC1	5	50	20-Jan-93	51° 49.51 'E	27° 22.46 'N	Muddy
18SC1	4	46	22-Jan-93	51° 55.43 'E	26° 25.23 'N	Silty Sand with shell fragments
11SC1	4	66	19-Jan-93	52° 08.30 'E	26° 35.25 'N	Silty to muddy
12SC1	4	62	19-Jan-93	52° 14.89 'E	26° 53.10 'N	Muddy core
10SC1	3	27	18-Jan-93	52° 56.90 'E	25° 03.94 'N	Sandy / Clay shells
08SC1	3	48	18-Jan-93	53° 01.97 'E	25° 29.89 'N	Silty Sand
07SC1	3	51	17-Jan-93	53° 04.28 'E	25° 41.26 'N	Silty with coral fragments
06SC1	3	61	17-Jan-93	53° 06.97 'E	25° 52.87 'N	Silty / Clay
05SC1	3	73	17-Jan-93	53° 13.45 'E	26° 11.93 'N	Silty Sand
01SC1	2	28	15-Jan-93	54° 21.20 'E	25° 00.00 'N	Sandy with shell fragments
03SC1	2	28	16-Jan-93	54° 33.00 'E	25° 18.20 'N	Silty Sand
02SC1	2	30	15-Jan-93	54° 34.30 'E	25° 09.25 'N	Sandy with shell fragments
20SC1	1	77	24-Jan-93	55° 30.11 'E	26° 00.20 'N	Silty Sand
19SC1	1	38	24-Jan-93	55° 30.15 'E	25° 46.06 'N	Silty Sand
09SC2	8	57	24-Dec-93	50° 03.70 'E	27° 27.70 'N	Muddy - tar ball at bottom
08SC2	8	60	24-Dec-93	50° 17.80 'E	27° 36.00 'N	Sand muddy
11SC2	8	55	24-Dec-93	50° 33.20 'E	27° 43.50 'N	Sand muddy
05SC2	6	60	23-Dec-93	50° 41.70 'E	27° 07.80 'N	Muddy sand - tar ball at 60 cm
03SC2	8	60	24-Dec-93	50° 46.70 'E	27° 52.60 'N	Sand muddy
07SC2	6	50	23-Dec-93	50° 54.50 'E	27° 20.80 'N	Sand mud
02SC2	5	15	22-Dec-93	50° 54.90 'E	26° 34.90 'N	Muddy sand shell
10SC2	5	16	21-Dec-93	50° 55.00 'E	26° 34.90 'N	
06SC2	6	65	23-Dec-93	51° 06.50 'E	27° 32.60 'N	Sandy mud shell
04SC2	5	23	21-Dec-93	51° 09.70 'E	26° 44.50 'N	Sandy shell
01SC2	5	68	21-Dec-93	51° 19.90 'E	26° 56.90 'N	Sandy shell and coral
18SC2	5	70	21-Dec-93	51° 29.70 'E	27° 06.60 'N	Sandy silt
15SC2	4	20	20-Dec-93	51° 35.20 'E	26° 13.00 'N	Sandy muddy shells
16SC2	5	40	21-Dec-93	51° 41.40 'E	27° 16.10 'N	Silty clay
21SC2	4	13	19-Dec-93	51° 45.70 'E	25° 36.40 'N	Muddy sandy shell
13SC2	4	40	20-Dec-93	51° 48.50 'E	26° 27.90 'N	Muddy sand - heavy tar ball
14SC2	4	60	20-Dec-93	52° 02.70 'E	27° 43.50 'N	Muddy sand - tar ball
12SC2	4	65	20-Dec-93	52° 17.20 'E	26° 58.10 'N	Muddy sand
22SC2	3	35	18-Dec-93	53° 00.86 'E	25° 34.19 'N	Clay muddy sand
19SC2	3	60	18-Dec-93	53° 07.86 'E	25° 54.38 'N	Silty clay
23SC2	3	70	18-Dec-93	53° 11.60 'E	26° 14.60 'N	Silty clay
20SC2	2	20	17-Dec-93	54° 14.90 'E	25° 12.70 'N	Sandy
17SC2	0	93	15-Dec-93	56° 00.70 'E	26° 13.30 'N	Sand shell

Analysis

Fish and sediment samples were freeze-dried, ground and homogenized before the chemical analysis. Total mercury in fish and sediment samples were carried in accordance with the Manual of Oceanographic Observation and Pollutant Analyses Methods (MOOPAM,1989). The final determination was obtained by a Jerome Gold Film Mercury Analyzer Model 511. Whereas, for MeHg in fish, samples were prepared and analyzed in accordance with IAEA/

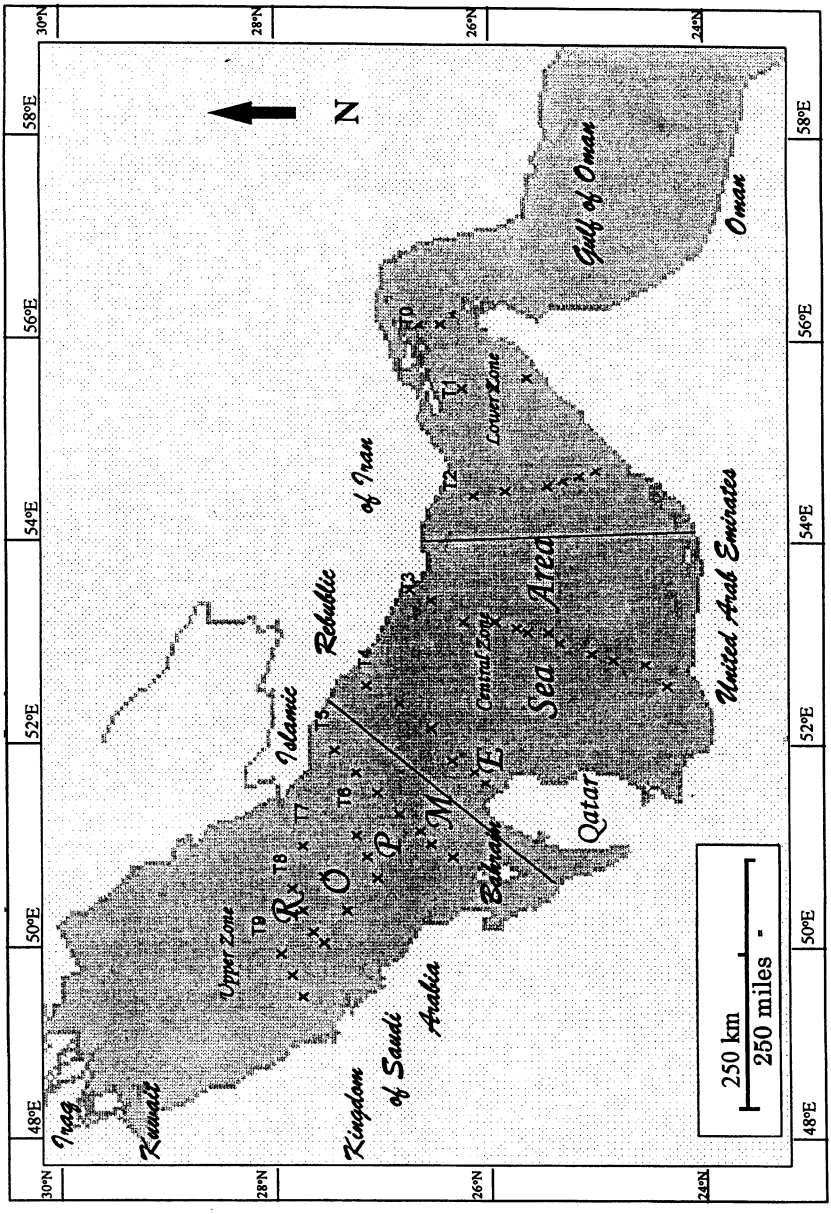

Fig. 4. The distribution of the main sampling transects in the area ROPME Sea Area (1993–1994).

Table 3(a). Levels of mercury (μg/g) dry weight in fish species collected from ROPME Sea Area (Umitaka Maru Cruise No. 1, 14–26 January 1993).

Sample Code	Species Name		Length	Weight	DW/FW	MeHg	Total Hg	% MeHg
	Latin	Local	(cm)	(gm)		(μg/gm)	(μg/gm)	
11FC1	*Arius thalassinus*	Chim	38	424	0.27	0.619	0.735	84.2
38FC1	*Arius thalassinus*	Chim	56	1700	0.14	0.401	0.750	53.5
15FC1	*Caranx leptolepis*	Curfa	20	74	0.25	0.292	0.375	77.9
26FC1	*Caranx leptolepis*	Curfa	20	80	0.23	0.615	0.750	82.0
31FC1	*Caranx leptolepis*	Curfa	20	88	0.23	0.889	0.920	96.6
19FC1	*Caranx leptolepis*	Curfa	20	98	0.26	0.321	0.564	56.9
09FC1	*Caranx leptolepis*	Curfa	21	101	0.25	0.520	0.750	69.3
25FC1	*Caranx leptolepis*	Curfa	21	96	0.24	0.412	0.564	73.0
17FC1	*Caranx leptolepis*	Curfa	21	104	0.26	0.430	0.750	57.3
08FC1	*Cephalopholis miniatus*	Shananwa	27	273	0.21	0.520	0.750	69.3
27FC1	*Dentex nufar*	Nahash	15	46	0.22	1.320	1.500	88.0
29FC1	*Dentex nufar*	Nahash	18	90	0.19	2.021	2.064	97.9
14FC1	*Etrumeas tera*	Oom	16	38	0.24	0.841	0.931	90.3
16FC1	*Etrumeas tera*	Oom	18	56	0.24	0.304	0.375	81.1
10FC1	*Lethrinus horak*	Sha'ary	30	392	0.23	0.597	0.600	99.5
06FC1	*Lethrinus kallopterus*	Sha'ary	28	360	0.22	0.375	0.474	79.1
07FC1	*Lethrinus kallopterus*	Sha'ary	36	530	0.23	1.010	1.125	89.8
32FC1	*Loxodon macrorhinus*	Jarjoor	51	592	0.26	0.957	0.939	101.9
35FC1	*Loxodon macrorhinus*	Jarjoor	57	534	0.26	0.427	0.564	75.7
28FC1	*Loxodon macrorhinus*	Jarjoor	59	692	0.26	2.430	2.490	97.6
01FC1	*Loxodon macrorhinus*	Jarjoor	65	1212	0.26	1.450	1.525	95.1
13FC1	*Loxodon macrorhinus*	Jarjoor	65	966	0.25	1.676	1.700	98.6
30FC1	*Nemipetrus tolu*	Bassy	20	86	0.21	0.700	0.750	93.3
33FC1	*Pelates quadrilineatus*	Yamyam	16	56	0.21	0.871	0.900	96.8
02FC1	*Pelates quadrilineatus*	Yamyam	18	90	0.23	0.640	0.750	85.3
05FC1	*Pelates quadrilineatus*	Yamyam	19	102	0.22	0.749	0.750	99.9
04FC1	*Pelates quadrilineatus*	Yamyam	20	110	0.22	0.814	0.939	86.7
03FC1	*Pelates quadrilineatus*	Yamyam	20	120	0.21	0.520	0.750	69.3
39FC1	*Pelates quadrilineatus*	Yamyam	20	102	0.21	0.192	0.250	76.8
34FC1	*Saurida Indosquamis*	Turr	21	70	0.22	0.298	0.375	79.5
37FC1	*Saurida Indosquamis*	Turr	30	152	0.20	0.356	0.450	79.1
36FG93	*Saurida Indosquamis*	Turr	31	184	0.20	0.661	0.754	87.7
12FC1	*Therapon thraps*	Theeb	20	120	0.23	0.499	0.750	66.5
24FC1	*Therapon thraps*	Theeb	17	86	0.22	2.011	2.066	97.3
22FC1	*Therapon thraps*	Theeb	26	244	0.24	0.961	1.210	79.4
21FC1	*Therapon thraps*	Theeb	27	230	0.22	2.944	3.201	92.0
18FC1	*Trachrurus trachrurus*	Curfa	20	74	0.22	0.754	0.939	80.3
20FC1	*Trachrurus trachrurus*	Curfa	20	76	0.22	0.800	0.939	85.2
23FC1	*Trachrurus trachrurus*	Curfa	20	72	0.21	0.614	0.781	78.6

Table 3(b). Levels of mercury (μg/g) dry weight in fish species collected from ROPME Sea Area (Umitaka Maru Cruise No. 2, 14–26 December 1993).

Sample Code	Species Name		Length	Weight	DW/FW	MeHg	Total Hg	% MeHg
	Latin	Local	(cm)	(gm)		(μg/gm)	(μg/gm)	
10FC2	*Aegyrops filamentosus*	Andug	28	420	0.22	0.323	0.450	71.8
08FC2	*Argyrops spinifer*	Andug	35	750	0.23	0.303	0.450	67.3
34FC2	*Arius thalassinus*	Chim	43	700	0.23	0.535	0.650	82.3
09FC2	*Arius thalassinus*	Chim	58	1540	0.22	0.610	0.750	81.3
02FC2	*Caranx leptolepis*	Curfa	21	110	0.24	0.725	0.750	96.7
04FC2	*Caranx leptolepis*	Curfa	23	100	0.23	0.255	0.302	84.4
14FC2	*Caranx leptolepis*	Curfa	24	150	0.24	1.007	1.350	74.6
18FC2	*Gnathandon speciosus*	Rebeeb	23	150	0.21	0.628	0.650	96.6
26FC2	*Lethrinus kallopterus*	Sha'ary	22	160	0.22	0.623	0.650	95.8
05FC2	*Lethrinus kallopterus*	Sha'ary	22	150	0.22	0.605	1.350	44.8
28FC2	*Lethrinus kallopterus*	Sha'ary	22	190	0.22	0.779	1.020	76.4
01FC2	*Lethrinus kallopterus*	Sha'ary	22	170	0.81	0.871	0.993	87.7
27FC2	*Lethrinus kallopterus*	Sha'ary	23	195	0.25	0.798	0.846	94.3
31FC2	*Lethrinus kallopterus*	Sha'ary	23	200	0.19	0.729	0.750	97.2
29FC2	*Lethrinus kallopterus*	Sha'ary	23	210	0.23	0.749	0.801	93.5
30FC2	*Lethrinus kallopterus*	Sha'ary	24	205	0.23	0.846	0.900	94.0
03FC2	*Lethrinus kallopterus*	Sha'ary	24	200	0.22	0.900	1.050	85.7
15FC2	*Nemitterus tolu*	Bassy	21	125	0.23	0.615	1.050	58.6
13FC2	*Parupeneus cyclostomus*	Heddi	22	140	0.23	0.237	0.300	79.0
33FC2	*Platax orbicularis*	Bent Alnokhetha	13	100	0.24	0.230	0.250	92.0
23FC2	*Platycephalus indicus*	Wahra	34	250	0.23	1.022	1.350	75.7
11FC2	*Plectorhynchus cincuts*	Fersh	21	140	0.23	0.352	0.350	100.6
06FC2	*Rochycentron canadus*	Sikin	70	2300	0.23	0.375	0.450	83.3
16FC2	*Saurida unvosqamis*	Hasoom	28	190	0.24	0.144	0.350	41.1
20FC2	*Scolopsis bimaculatus*	Bzeemi	24	140	0.22	0.556	0.602	92.4
12FC2	*Scolopsis ghanam*	Bzeemi	25	180	0.21	0.275	0.450	61.1
32FC2	*Scolopsis phaeops*	Bzeemi	23	140	0.21	1.294	1.323	97.8
35FC2	*Scolopsis phaeops*	Bzeemi	24	160	0.21	1.110	1.298	85.5
22FC2	*Therapon jarbua*	Theeb	23	190	0.23	0.612	0.652	93.9
17FC2	*Therapon jarbua*	Theeb	31	420	0.23	2.384	2.500	95.4
07FC2	*Tylosurus leiurus*	Hagool	62	300	0.24	0.304	0.600	50.7
25FC2	*Tylosurus leiurus*	Hagool	103	1650	0.26	0.402	0.500	80.4
24FC2	*Tylosurus leiurus*	Hagool	105	1600	0.25	0.218	0.400	54.5

UNEP/FAO/IOC: Reference Method for Marine Pollution Studies No. 13, Rev. 1 UNEP 1991. Determination of MeHg was carried out using a Hewlett Packard Series II Model 5890 gas chromatograph provided with electron capture detector.

Quality control

Duplicate analyses were carried out for each sample to determine the concentration of total mercury. Quality control was also carried out with each set of samples to check the performance of the analysis by running blanks and reference standard material. The International Atomic Energy Agency (IAEA) reference sample (Trace Metals In Tuna Fish, IAEA 350) was analyzed with each set of fish samples. Reference samples (SD-M-2/TM) and (IAEA 356) were analyzed with each set of sediment samples. The reference material analysis gave results within ±5% of the certified values.

RESULTS AND DISCUSSION

Fish

Results of methyl and total mercury analysis in fish sampled in cruise No. 1 and No. 2 are summarized in Tables 3a and 3b, respectively. Of the various types of fish collected *Pelates quadrilineatus* (Yamyam) and *Platax orbicularis* (Bent Alnokhetha) recorded the lowest concentration of total Hg 0.250 μg/g (DW). While, *Therapon thraps* (Theeb) recorded the highest concentration of Hg 3.201 μg/g. The mean values of total Hg was 0.76 μg/g with standard deviation of ±0.540. The lowest concentration of MeHg 0.144 μg/g recorded in *Saurida unvosqamis* (Hasoom) species and the highest concentration 2.944 μg/g was recorded also in *Therapon thraps* (Theeb) species. The percentage of MeHg was varied between 85.5% to 101.9% of the total Hg content.

Fish species from at least 3 samples were collected, and grouped as shown in Table 4. The results show that MeHg and total Hg were the highest levels in the non edible fish species, *Therapon jarbua* and *Therapon thraps* (Theeb). Whereas, the range varied between 0.499–2.944 μg/g for MeHg and between 0.652–3.201 μg/g for total Hg. Followed by *Loxodon macrorhinus* (Jarjoor) species in which MeHg ranged from 0.427–2.430 μg/g, while total Hg ranged between 0.564–2.490 μg/g and the result could be attributed to the feeding behaviour for the fish species which is considered carnivorous species. *Caranx leptolepis* (Curfa) species recorded total Hg ranging from 0.375–1.350 μg/g, while MeHg ranged between 0.292–1.007 μg/g. *Pelates quadrilineutus* (Yamyam) species recorded total Hg ranging between 0.250–0.939 μg/g and MeHg ranging between 0.192–0.871 μg/g. The overall mean value for methyl and total Hg for 11 analyzed species are shown in Fig. 3.

The levels of Hg in more commonly caught species was also correlated with the length and weight. The results show insignificant correlation. Biological factors were excluded from this study due to the limitation in the number of samples analyzed. The level of Hg in fish species was found to be independent of the geographical distribution. Moreover, no statistical difference could be

Table 4. Levels of mercury (μg/g) dry weight in some frequently sampled fish species collected from ROPME Sea Area (Umitaka Maru Cruise No. 1 and No. 2, 1993).

Species Name *Latin*	Local	No. of Samples	Length (cm)	Weight (gm)	MeHg (μg/gm)	Total Hg (μg/gm)
Arius thalassinus	Chim	4	38 - 58	424 - 1700	0.401 - 0.619	0.650 - 0.750
Caranx leptolepis & *Trachurus trachurus*	Curfa	13	20 - 24	72 - 150	0.255 - 1.007	0.302 - 1.350
Lethrinus kallopterus	Sha'ary	11	22 - 36	150 - 530	0.375 - 1.010	0.474 - 1.350
Loxodon macrorhinus	Jarjoor	5	51 - 65	534 - 1212	0.427 - 2.430	0.564 - 2.490
Pelates quadrilineatus	Yamyam	6	16 - 20	56 - 120	0.192 - 0.870	0.250 - 0.939
Samrida landosquamis	Turr	3	21 - 31	70 - 184	0.298 - 0.661	0.375 - 0.754
Therapon jarbua & *Therapon thraps*	Theeb	6	17 - 31	86 - 244	0.499 - 2.944	0.652 - 3.201
Tylosurus leiurus	Haggol	3	62 - 105	300 - 1650	0.218 - 0.402	0.400 - 0.600

Table 5. Levels of mercury (μg/g) dry weight in fish species collected from Kuwait (EPD Water Monitoring Programme, 1992–1993).

Species Name		Length	Weight	DW/FW	MeHg	Total Hg	% MeHg
Latin	Local	(cm)	(g)		(μg/g)	(μg/g)	
Argyrops filamentosus	Andug (3)*	21	193	0.23	0.768	1.019	75.37
Amphiprion clarki	Bzazyi (5)*	30	420	0.26	0.450	0.455	98.90
Arius thalassinus	Chim	24	200	0.22	0.720	0.792	90.91
Arius thalassinus	Chim	30	400	0.24	0.538	1.125	47.82
Arius thalassinus	Chim	39	800	0.25	1.000	1.060	94.34
Arius thalassinus	Chim (3)*	36	717	0.25	0.452	0.457	98.91
Chirocentrus dorab	Hiff (2)*	65	975	0.25	0.512	0.542	94.46
Dentex Nufar	Nahash	21	110	0.22	0.476	0.502	94.82
Epinephelus chlorostigma	Hamoor (2)*	40	1400	0.22	1.150	0.941	122.21
Epinephelus tauvina	Ballool	34	500	0.21	0.404	0.710	56.90
Epinephelus tauvina	Ballool	40	1000	0.23	0.450	0.449	100.22
Epinephelus tauvina	Ballool	41	900	0.23	0.350	0.371	94.34
Hcanthopagrus bifasciatus	Fasker (4)*	22	150	0.22	1.120	1.127	99.38
Hilso ilisha	Suboor	35	450	0.27	0.015	0.123	12.20
Himantura uarnak	Lokhmah	31	1600	0.26	1.000	1.065	93.90
Liza macrolepis	Maid (10)*	16	70	0.27	0.190	0.191	99.48
Loxodon macrorhinus	Jarjoor	32	1000	0.25	4.900	4.960	98.79
Loxodon macrorhinus	Jarjoor	47	2200	0.27	1.300	1.269	102.44
Loxodon macrorhinus	Jarjoor	53	750	0.16	0.598	1.286	46.50
Lutjanus coccineus	Hamrah	48	1600	0.22	0.700	0.722	96.95
Lutjanus coccineus	Hamrah	60	2750	0.20	1.735	1.667	104.08
Otolithes argenteus	Newaiby	28	150	0.22	0.352	0.417	84.41
Otolithes argenteus	Newaiby	30	250	0.22	0.374	0.389	96.14
Otolithes argenteus	Newaiby	31	400	0.21	0.785	0.833	94.24
Otolithes argenteus	Newaiby	32	350	0.23	0.352	0.375	93.87
Otolithes argenteus	Newaiby	32	350	0.24	0.382	0.417	91.61
Otolithes argenteus	Newaiby	39	600	0.22	0.274	0.585	46.84
Otolithes argenteus	Newaiby	40	700	0.22	0.418	0.875	47.77
Otolithes argenteus	Newaiby	41	700	0.20	0.895	1.250	71.60
Otolithes argenteus	Newaiby	42	800	0.23	0.700	0.721	97.09
Otolithes argenteus	Newaiby	46	900	0.22	0.880	1.000	88.00
Otolithes argenteus	Newaiby	47	1100	0.22	0.458	1.333	34.36
Otolithes argenteus	Newaiby (2)*	38	250	0.22	0.550	0.556	98.92
Otolithes argenteus	Newaiby (3)*	34	365	0.22	0.575	0.592	97.13
Pampus argenteus	Zobaidy (15)*	25	220	0.22	0.175	0.177	98.87
Platycephalus indicus	Wahar	47	1200	0.23	3.862	4.500	85.82
Platycephalus indicus	Wahra	50	900	0.26	0.335	2.659	12.60
Plectorhinchus schotaf	Yanem	33	650	0.23	0.814	1.417	57.45
Plectorhinchus schotaf	Yanem	34	650	0.23	1.276	1.470	86.80
Plectorhynchus cincuts	Fersh	58	2800	0.23	1.470	1.500	98.00
Rochycentron canadus	Sikin	58	1600	0.23	0.320	0.316	101.27
Sardinellas fimbriata	Oom (30)*	18	90	0.15	0.125	0.126	99.21
Scomberoides commersonianus	Thelah	65	2000	0.26	1.250	1.246	100.32
Scomberoides commersonianus	Thelah	83	3100	0.26	12.012	12.412	96.78
Sphyraena jello	Dwailmy	103	1010	0.26	0.720	0.730	98.63
Sphyraena jello	Dwailmy	104	1800	0.24	0.899	0.905	99.34

* Composite sample, the number in parentheses refer to the number used for the composite sample

Table 6. Comparison of the levels of mercury reported in various regional seas.

Year	Country	Area	Marine Organism	Hg Level		Reference
1972	Bombay	Indean Ocean	Fish Tissues	0.04-0.42	fw	Somayajulu & Rama, 1972
1973		Irish Sea	Fish	0.21-0.53	dw	Gradner & Riley, 1973
1975	Australia	North East	Black Marlin	7.5	fw	Mackay *et al*, 1975
1975	Mexican Coast	Veracrus	Fish	0.01-0.61	fw	Reimer & Rimer, 1975
1975	Sweden	Hakifa & Akko Bays	Carnivorous Fish	> 0.05	fw	Levitan *et al*, 1974
1976	India	Pacific Oceans	yellow fish tuna	0.23	fw	Ueda *et al*, 1976
1976	Korea	Han River	Fresh water Fish	0.03-.063	fw	Kim *et al*, 1976
1981	New Zealand	Pacific Ocean	Fish	> 0.35	fw	Van den B. et al, 1981
1981	California		Fish	< 0.02-4.30	dw	Young *et al*, 1981
1981	England	Baltic Sea	Fish	26.6-30.1	dw	Giblin *et al*, 1981
1981		Baltic Sea	Fish	0.40-1.70	dw	Furr *et al*, 1981
1981		Baltic Sea	Fish	0.08-2.40	dw	Brigmann, 1981
1982	Australia	Victoria lake (fresh water)	Axial Muscle	0.17-0.60	fw	Beumer & Bacher, 1982
1983	Kuwait		Fish (Lutjanus c.)	0.50-4.00	dw	Anderlini *et al*, 1983
1984	Israel	Haifa Bay	Muscle(Diplodus sargus)	0.66	fw	Hornung & Krumgalz, 1984
1985	Finland	Lake (fersh water)	Fish Tissue	1.0-4.1	fw	Verta *et al*, 1985
1986	Norway	Kammerfoss River	Fish(Salmo trutta &	0.5	fw	Norheim *et al*, 1986
			Perca fluviatilis	0.5	fw	
1986	Australia	Prince Royal harbour	Fish (8 different species)	0.01-3.30	fw	Michael et al, 1986
1986	Finland		Grey sea Phocahipidal	0.31-1.03	fw	Matti *et al*, 1986
			Halichoerus grypus	0.20-4.90	fw	
1989	Russia	Acidic Lake	Fish Muscle	0.50-1.10	fw	Haines *et al*, 1992
		Alkaline Lake		0.10-0.20	fw	
1989	Maldives	Indian Ocean	Skipjack tuna	0.36-0.91	fw	Renzoni, 1989
1989	Italy	Tyrrhenian Sea	Fish (Flat fish)	0.45-3.60	dw	Pellegrini, 1989
1990	Australia	Sydney	Snapper Muscle Tissues	0.01-1.66	fw	Chovjka, 1990
1990	Yugoslavia	Rijeka Bay	Fish	0.05-1.06	fw	Bartolo *et al*, 1990
1991	Pakistan	Arabian Sea	Fish (picnic seabream)	0.046	fw	Tariq & Jaffar, 1991
			Fish (Cornet)	0.269	fw	
1992	Australia	Prince Royal Harbour	Fish Tissue	10.3	fw	Francesconi & Lenanton, 1992
1992	Canada	North Atlantic	Cod, *Gadus mohum* muscle	0.11-1.30	dw	Hellou, 1992
1993	Florida	Alkaline Lake	Axial Muscle	0.04-1.53	fw	Lange *et al*, 1993
1993	New Zealand	North Island	Cardinalfish	0.59-2.15	fw	Tracey, 1993
1993	Meyen	Mediterranean	Dolphines	7-155	dw	Augier, 1993
1993	England	Liverpool Bay	Plaice Muscle Tissue	0.2	fw	Leah, 1993
1993	Italy	Tyrrhenian Sea	Fish	> 0.7	fw	Rossi, 1993
1993	Pakistan	Arabian Sea	Fish	0.01-0.16	fw	Jaleel *et al* , 1993
1994	England	North coast	Fish Tissues	0.03-0.14	fw	Rupert, 1994
1994	Netherland	Rhine delta	Aquatic Biota	0.01-2.95	fw	Hendrik, 1994
1994	Spain	Mediterranean	Marine Organism	.04-0.50	fw	Pastor *et al*, 1994
1995	England	Scotland (Frith of Clyde)	Fish Tissues	0.014-0.124	fw	Scot, 1995

Table 7. National primissible limits for mercury content in fish tissue expressed as (μg/g) fresh weight.

Year	Country / Organization	Hg Level	Reference
1967	Sweden	1.0	Berglund *et al*, 1971
1968	Canada	0.5	Sachinath, 1986
1968	USA / FDA	0.5	Sachinath, 1986
1970	Yougoslavia	0.5-1.0	Bartolo *et al*, 1990
1973	Japan / MPH	0.4	Sachinath, 1986
1974	FAO / WHO	0.3	WHO, 1974
1976	Europe / EQS	0.3	CEC, 1976
1976	UNEP / WHO	0.2-0.5	Sachinath, 1986
1980	Australia / NHMRC	0.5	Chvojka *et al*, 1990

tected between fish caught in cruise No. 1 and No. 2.

The obtained Hg levels in this study are found to be comparable with Hg level recorded in different fish species collected from Kuwait territorial waters, as a part of the Environment Protection Department (EPD)—Water Monitoring Programme, in 1992 and 1993. The results obtained in this programme are summarized in Table 5. The levels of Hg are also found to be comparable with the previously recorded levels in different fish species collected along the ROPME sea area, as a part of the μg/g and 1.320 μg/g both were recorded for *Letherinus kallopterus* (Sha'ary) species (Habashi *et al.*, 1993). Whereas, MeHg which was measured recently varied between 0.297 μg/g and 1.142 μg/g for each *Epinephelus chlorostigma* (Hamoor) and *Letherinus kallopterus* species, respectively.

The percentage of MeHg varied between 82% and 98.7% of the total Hg content. Results of MeHg% to the total Hg content were comparable with previously obtained data reported for other regions. Cappon and Smith (1981) reported the proportion of MeHg to the total mercury ranging from 59% to 93% in the analyzed fish samples. Kyle (1981) reported a range value varied from 78% to 98% for broad-snouted catfish. Chvojka (1990) reported an averaged of 94.7% of MeHg to the total Hg content of Sydney snapper and 91.3% of MeHg to the total Hg for Nowra snapper.

The reported levels of Hg in fish species from ROPME sea area was also found to be comparable with other regions as shown in Table 6. Somyajulu and Rama (1972) reported Hg levels ranging from 0.04–0.42 mg/g (FW) in ten different edible fish species collected from the Indian Ocean. Reimer and Reimer (1975) reported an average value for Hg ranging from 0.01–0.61 mg/g (FW) in fish caught from Veracruz and Coatzacoalcos, Mexican Coast. Ueda and Takeda (1976) reported an average MeHg level of 0.23 mg/g (FW) in muscle tissue of yellow fin tuna sampled from the mid of Pacific and east Indian Oceans.

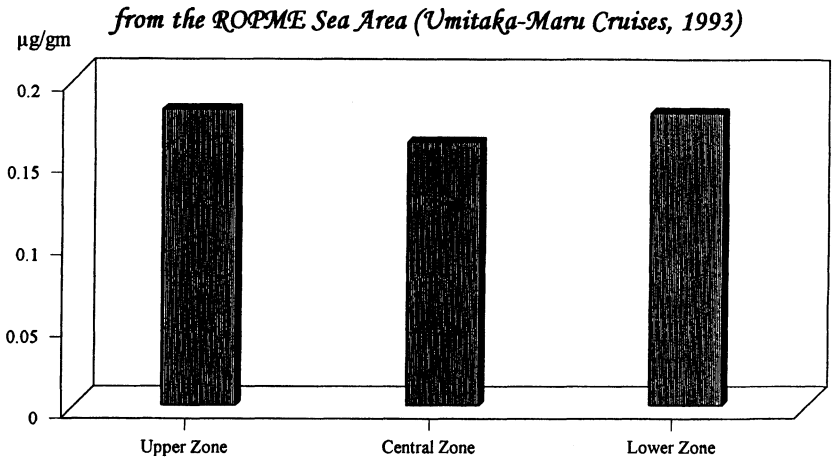

Fig. 5. The distribution of mercury in sediment from the ROPME Sea Area (Umita Maru Cruises, 1993).

Beumer and Bacher (1982) reported an average Hg levels ranged from 0.17–0.60 mg/g (FW) for axial muscle collected from Victoria Lake (fresh water), Australia. Anderlini *et al.* (1983) reported a relatively high levels of Hg varied between 0.50–4.00 µg/g (DW) for *Lutjanus coccineus.* (Hamrah) species, collected from Kuwait Fish Market, where Salt and Chlorine Plant represent the main source of Hg pollution in Kuwait Bay. Pellegrini (1989) reported an average Hg levels varied between 0.45–3.60 mg/g (DW) for flat fish tissues of various species, collected from Tyrrehenian Sea, Italy. While Rossi *et al.* (1993) reported Hg levels >0.70 mg/g (FW) for fish species collected from the same location. Jaleel *et al.* (1993) reported an average levels of Hg ranging from 0.01–0.16 mg/g (FW) for different edible fish species collected from Arabian Sea.

The upper value for the daily intake of Hg from fish species have been limited recently by several international organizations, as shown in Table 7. Whereas, the limited value for mercury was varied between 0.3–1.0 mg/g fresh weight. Referring to these international limited values, the detectable levels of Hg (fresh weight basis) in 20% of the analyzed fish species in the present study are considered harmful to the human health based on a regular consumption of these species as a main source of human food.

Sediment

The sampling stations are mainly located between 49°00.00′ E–56°30.00′ E longitude and 24°00.00′ N–28°00.00′ N latitude. The analytical results of the total Hg levels based on dry weight in sediment samples are summarized in Table 8. Results show that total Hg levels varied between 0.050 mg/g at station 3SC1 (54°33.00′ E and 25°18.20′ N) and 0.375 mg/g at station 13SC2 (51°48.50′ E and 26°27.90′ N) with an overall mean 0.169 ± 0.070 mg/g. The obtained levels

Table 8. Levels of mercury in sediment samples collected at ROPME Sea Area (Umitaka Maru Cruise No. 1 and No. 2, 1993).

Station		Water Depth	Hg	Location	
Code	Transect	(m)	(µg/gm)	Long.	Lat.
01SC1	2	28	0.113	54° 21.20 'E	25° 00.00 'N
02SC1	2	30	0.100	54° 34.30 'E	25° 09.25 'N
03SC1	2	28	0.042	54° 33.00 'E	25° 18.20 'N
04SC1	2	38	0.146	51° 31.84 'E	25° 27.24 'N
05SC1	3	73	0.145	53° 13.45 'E	26° 11.93 'N
06SC1	3	61	0.129	53° 06.97 'E	25° 52.87 'N
07SC1	3	51	0.196	53° 04.28 'E	25° 41.26 'N
08SC1	3	48	0.139	53° 01.97 'E	25° 29.89 'N
10SC1	3	27	0.200	52° 56.90 'E	25° 03.94 'N
11SC1	4	66	0.188	52° 08.30 'E	26° 35.25 'N
12SC1	4	62	0.048	52° 14.89 'E	26° 53.10 'N
13SC1	5	50	0.175	51° 49.51 'E	27° 22.46 'N
14SC1	5	76	0.138	51° 26.41 'E	27° 00.54 'N
15SC1	5	50	0.075	51° 13.79 'E	26° 50.78 'N
16SC1	5	25	0.146	51° 05.79 'E	26° 39.66 'N
17SC1	4	27	0.183	51° 44.09 'E	26° 09.69 'N
18SC1	4	46	0.063	51° 55.43 'E	26° 25.23 'N
19SC1	1	38	0.179	55° 30.15 'E	25° 46.06 'N
20SC1	1	77	0.187	55° 30.11 'E	26° 00.20 'N
17SC2	0	93	0.225	56° 00.70 'E	26° 13.30 'N
20SC2	2	20	0.250	54° 14.90 'E	25° 12.70 'N
19SC2	3	60	0.050	53° 07.86 'E	25° 54.38 'N
22SC2	3	35	0.125	53° 00.86 'E	25° 34.19 'N
23SC2	3	70	0.175	53° 11.60 'E	26° 14.60 'N
21SC2	4	13	0.125	51° 45.70 'E	25° 36.40 'N
12SC2	4	65	0.125	52° 17.20 'E	26° 58.10 'N
13SC2	4	40	0.375	51° 48.50 'E	26° 27.90 'N
14SC2	4	60	0.166	52° 02.70 'E	27° 43.50 'N
15SC2	4	20	0.313	51° 35.20 'E	26° 13.00 'N
01SC2	5	68	0.250	51° 19.90 'E	26° 56.90 'N
04SC2	5	23	0.188	51° 09.70 'E	26° 44.50 'N
10SC2	5	16	0.250	50° 55.00 'E	26° 34.90 'N
16SC2	5	40	0.250	51° 41.40 'E	27° 16.10 'N
18SC2	5	70	0.188	51° 29.70 'E	27° 06.60 'N
02SC2	5	15	0.250	50° 54.90 'E	26° 34.90 'N
05SC2	6	60	0.188	50° 41.70 'E	27° 07.80 'N
06SC2	6	65	0.250	51° 06.50 'E	27° 32.60 'N
07SC2	6	50	0.125	50° 54.50 'E	27° 20.80 'N
03SC2	8	60	0.188	50° 46.70 'E	27° 52.60 'N
08SC2	8	60	0.125	50° 17.80 'E	27° 36.00 'N
09SC2	8	57	0.125	50° 03.70 'E	27° 27.70 'N
11SC2	8	55	0.188	50° 33.20 'E	27° 43.50 'N

fluctuated around the mean value.

For further investigation, sampling area was divided into three main zones, upper, central and lower from west to east. Results as shown in Fig. 5 do not indicate any significant difference in the obtained levels of total Hg. The levels of total Hg in sediment sampled from ROPME Sea Area are considered very low in comparison with other reported Hg levels in other regions. Iglesias and Penchaszadeh (1983) reported high Hg levels up to 3.0 mg/g (DW) for sediment

collected from Trise Gulf in Venezuela. Hornung and Krumgaiz (1984) reported 0.99 mg Hg/g (DW) in sediment collected from Haifa Bay. Baldi and Bargagli (1984) reported high Hg level 4.06 mg/g (DW) in sediment sampled from Tyrrhenian sea, Italy. Jackson *et al.* (1986), reported Hg levels of 1.7 mg/g (FW) in sediment sampled from Princess Royal Harbour in western Australia. The result of Hg levels in sediment for the present study does not reflect the significantly high levels of Hg recorded in fish tissues of different species. A comprehensive monitoring for Hg levels in fish species from ROPME Sea Area should be carried out due to their priority in the food chain for most of the population in this region.

Acknowledgements

We would like to acknowledge the Environment Protection Council and ROPME for the financial support to conducting this study. We would like to thank Fuad Al-Safar and Mohameed Shahath for their participation in the cruise and collecting the fish and sediment samples used for this study. We also appreciate the contribution of Eqbal Al-Rugaab for her great help in preparing the samples for analysis.

REFERENCES

American Chemical Society (1981): Environmental Science Technology.

Anderlini *et al.* (1983): Annual Report, Kuwait Institute for Science Research.

Augier, H., Park, W. and Rommeau, C. (1993): Mercury contamination of the striped dolphin *Stenella coeruleoalba Meyen* from the French Meditrranean coasts, *Mar. Pollt. Bull.*, 26, 306–311.

Baldi, F. and Bargagli, R. (1982): Chemical leaching and specific surface area measurements of marine sediments in the evaluation of mercury contamination near Cinnabar deposits. *Mar. Environ. Res.*, 6, 69–82.

Bartolo, O., Mirjana, K., Jasana J. *et al.* (1990): As, Cd, Pb, Hg in benthic animals from the Kvarner – Rijeka Bay Region. *Yugoslavia. Mar. Pollut. Bull.*, 21, 595–598.

Bcrglund, F. M., Berlin, G., Birke, V. *et al.* (1971): Report of the Expert Group Nordisk Hygiensk Tidskrift, Sulement.

Bcumer, J. and Bacher, G. (1982): Species of *Anguilla* as indicators of mercury in the coastal rivers and lakes of Victoria. *Australia J. Fish Biol.*, 21, 87–94.

Bryan, G. W. (1976): Heavy Metals Concentration in the Sea. Marine Pollution, Academic Press, London. 185–302.

Cappon, C. and Smith, J. (1982): Chemical form and distribution of mercury and selenium in canned tuna. *J. Appl. Toxicol.*, 2, 181–189.

CEC (1976): Commission of the European Communities, Official Journal of the EuroPean Community, L129, 23–29.

Chovojka, R., William, R. and Fredrickson, S. (1990): Methyl mercury, total mercury, and sclcnium in snapper from two areas of the New South Wales Coast. *Australia. Mar. Pollut. Bull.*, 21, 570–573.

David, W., David, K. and Peter, J. (1993): Trace element concentrations in fish livers: implications of variations with fish size pollution monitoring. *Mar. Pollut. Bull.*, 26. 329–334.

Des, W. C. and Gregory J. M. (1984): Chemistry and Ecotoxicology of Pollution. Educational Committee of the Society of toxicology (1978): Editorial the Education of Toxicologist. *Toxicol. Al. Pharmacol.*, 45, 375–382.

Elisel, R. (1981): Trace Metal Concentration in Marinc Organisms. Pergamon Press, New York. p. 687.

EPD (1993): Environment Protection Department Annual Report. European Community Diretives Nos. 82/176 and 84/156.

Francesconi, K. and Lenanton, R. (1992): Mercury contamination in a semi–enclosed marine embayment: organic and inorganic mercury content of biota, and factors influencing mercury levels in fish. *Mar. Environ. Res.*, 33, 189–212.

Frei, R. W. and Hutzinger, O. (1975): Analytical Aspects of Mercury and other Heavy Metals in the Environment. (Gordon and Breach: London), 210p.

Fukano, K. and Tsukano, Y. (1969): *Residue Review*, 26, 1.

Furr, A. *et al.*, (1981): Concentrations of elements in a marine food chain cultured in sewege wastewater. *Bull. Environ. Contam. Toxicol.*, 26, 54–59.

Gardner, D. and Riley, J. (1973): Distribution of dissolved mercury in the Irish Sea. *Nature*, 241, 526–527.

GESAMP (1986): IMO/FAO/UNESCO/WMO/WHO/IAEA/UN/UNEP, Joint Group of Experts on the Scientific Aspects of Marine Pollution. Review of Potentially Harmful Substances: Arsenic, Mercury and Selenium. *Rep. Stud.* 28.

Habashi, B., AL–Majed, N. and Borhama, A. (1993): Levels of trace metals in ROPME sea area. Technical Report presented to the Scientific Workshop on Results of the Mt. Mitchell Cruise, Kuwait.

Haines, T., Komov, V. and Jagoe, C. (1992): Lake acidity and mercury content of fish in Darwin National Reserve, *Russia. Environ. Pollut.*, 78, 107–113.

Hellou, J., Warren, W. *et al.* (1992): Heavy metals and other elements in three tissues of cod, *Gadus morhua* from the Northwest Atlantic. *Mar. Pollut. Bull.*, 24, 452–458.

Hornung, H. and Krumgalz, B. (1984): Mercury pollution in sediments, benthic organisms and inshore fishes of Haifa Bay, Israel. *Mar. Environ. Res.*, 12, 191–208.

IAEA/UNEP/FOA/IOC (1991): Reference Method For Marine Pollution Studies No. 13, Rev. 1 – UNEP.

Iglesias, N. and Penchaszadeh, P. (1983): Mercury in sea stars from Golfo Triste, Venezuela. *Mar. Pollut. Bull.*, 14, 396–398.

Jackson, M., Hancock, D., *et al.* (1986): Rock phosphate: the source of mercury pollution in a marine ecosystem at Albany, Western Australia. *Mar. Environ. Res.*, 18, 185–202.

Jaleel, T., Jaffar, M. *et al.* (1993): Heavy metal concentrations in fish, shrimp, seaweed, sediment, and water from the Arabian Sea, Pakistan. *Mar. Pollut. Bull.*, 26, 11, 644–647.

Jalili, M. A. and Abbasi, A. H. (1961): Poisoning by ethylmercuritoluene sulfonamide. *Brit. J. Ind. Med.* 18, 303–308.

Katsuzo, K. and Yoshitaka, A. (1986): Fishes of Arabian Gulf. Kuwait Institute for Scientific Research.

Kim, N. B., Lee C. and Back, H. (1976): A study on the present levels of mercury and other trace elements in some freshwater fish by neutron activation analysis. *J. Korean Nucl. Soc.*, 8, 41–47.

Kyle, J. (1981): Waigni–Papua–New–Guinca–Office on Environment and Conservation, 59.

Lange, T. R., Royals, H. E. and Connor, L. L. (1993): Influence of water chemistry on mercury concentration in largemouth bass from Florida lakes. *Trans. Am. Fish. Soc.*, 122, 74–84.

Leah, R., Collings, S. *et al.* (1993): Mercury in plaice *(Plew onectes platessa)* from the sludge disposal ground of Liverpool Bay. *Mar. Pollut. Bull.*, 26, 436–439.

Matti, P., Olavi, S. *et al.* (1986): Heavy metals and organochlorine compounds in seals in the Gulf of Finland. *Mar. Environ. Res.*, 18, 43–59.

MOOPAM (1989): Manual of Oceanographic Observation and Pollutant Analysis Methods. Regional Organization for the Protection of the Marine Environment.

Norheim, G., Haestein. T. and Wassjoe, E. (1986): Nord. Veterinaermed., 38, 298.

Pastor, A., Hernandez, F. *et al.* (1994): Levels of heavy metals in some marine organisms from the Western Mediterranean Area (Spain). *Mar. Pollut. Bull.*, 28, 50–53.

Patricia A. Ditri and Frank M. Ditri (1975): Mercury Contamination – *A Human Tragedy.*

Pellegrini, D. and Barghigiani, D. (1989): Feeding behaviour and mercury content in two flat fish in the Northern Tyrrhenian Sea. *Mar. Pollut. Bull.*, 20, 443–447.

Reimer, A. A. and Reimer, R. D. (1975): Total mercury in some fish and shellfish along the Mexican coast. *Bull. Environ. Contam. Toxicol.*, 14, 105-111.

Renzoni, A. (1989): Mercury in scalp hair of Maldivians. *Mar. Pollut. Bull.*, 20, 93–94.

Rossi, A., Pellegrini, D. *et al.* (1993): Mercury in *Eledone cirrhosa* from the Northern Tyrrhenian Sea: contents and relations with life cycle. *Mar. Pollut. Bull.*, 26, 683–686.

Rupert, D. and Brayn, T. (1994): Mercury concentrations in stomach contents and musele of five fish species from the north east coast of England. *Mar. Pollut. Bull.*, 28, 741–745.

Sachinath, M. (1986): Mercury in the Ecosystem, Its Dispersion and Pollution Today.

Scot, M. and Donalds, S. (1995): Inter – species variation of mercury in skeletal muscle of five fish species from inshore waters of the Firth of Clyde, Scotland. *Mar. Pollut. Bull.*, 30, 283–286.

Study Group on Mercury Hazards (1970): Hazards of Mercury, Special Report to the Secretary s Pesticide Advisory, US Department of Health and Welfare, Public Health Service, National Air Pollution Control Administration.

Tariq, J., Jaffar, M. and Ashraf, M. (1991): Levcls of selected heavy metals in commercial fish from five freshwater lakes, Pakistan. *Toxicol. Environ. Chem.*, 34, 57–60.

Ueda, T. and Takeda, M. (1977): On mercury and selenium contained in tuna fish tisues – IV Methylmercury level in muscles and liver of yellowfin tuna. *Nippon Suisan Gakkaishi*, 43, 1115–1121.

Verta, M., Rekolainen, S. and Kinnunen, K. (1985): Vesientukimuslait Julk., Helsinki – Publ. Water – Res. Inst. Helsinki, 65, 44.

WHO/FAO (1974): WHO Technical Report Series No. 555.

Williston, S. H. (1968): Mercury in the atmosphere. *J. Geophys. Res.*, 73, 7051–7055.

Wood, J. M. (1974): Biological cycle for toxic elements in the environment. *Science*, 183, 1049–1052.

Offshore Environment of the ROPME Sea Area after the War-Related Oil Spill, Eds. A. Otsuki *et al.*, pp. 149–159.

Metal concentrations in sediment samples collected during Umitaka-Maru Cruises in 1993–1994

I. ALAM[1]*, A. A. AL-ARFAJ[2] and M. SADIQ[3]

[1]*Deputy Mayor for Municipal Services, Jeddah Municipality, Saudi Arabia*
[2]*Department of Chemistry, King Fahd University of Petroleum and Minerals, Dhahran, 31261, Saudi Arabia*
[3]*Water Resources and Environment Division, The Research Institute, King Fahd University of Petroleum and Minerals, Dhahran, 31261, Saudi Arabia*

Abstract—Surface sediment samples were collected from 36 locations during Umitaka-Maru cruises during 1993–1994. Concentrations of Ba, Cd, Co, Cr, Cu, Fe, Mn, Ni, P, Pb, Ti, V, and Zn were determined using an inductively coupled argon plasma analyzer. Significant ($p < 0.01$) variations in metal concentrations in the sediment samples were observed. Except for Ba, muddy sediments were significantly ($p < 0.01$) enriched with metals than the sandy and sandy-silt/clay texture sediments. Concentrations of metals, other than Pb, were not significantly ($p < 0.01$) influenced by the sampling date. Over 90% variations in metals concentrations, other than Ba, P, and Ti, could be explained by Fe in the sediment samples. The contouring technique indicated a west (lower) to east (higher) gradient in metal concentrations, but the number of sampling stations were limited. A comparison with the information in the literature indicated relatively higher concentrations of Cd, Ni, Mn, Pb, and Ba, and similar concentrations of Cr, Cu, V, and Zn in the sediments of this study. However, none of the metals was exceptionally high to be of environmental concerns.

INTRODUCTION

The Gulf War of 1991 was indeed an environmental tragedy of unprecedented ecological destruction (Sadiq and McCain, 1993). As a result of the War activities, about 7 million barrels of oil was spilled into the ROPME Sea Area (Tawfiq, 1991). Marine life in the coastal zone of the oil-impacted area was adversely affected. Short-term impact of the Gulf War oil spill has been well documented (Sadiq and McCain, 1993; Marine Pollution Bulletin, 1993). However, the long-term effects on the marine environment and marine life of the ROPME Sea Area (RSA) could not be predicted.

The international, regional, and local scientific communities started long-term studies to evaluate the impact of the 1991 Oil Spill on the RSA marine environment. The Mt. Mitchell cruise of 1992, organized jointly by the Regional Organization for the Protection of Marine Environment (ROPME), International Oceanic Committee (IOC-UNESCO), and National Oceanic and Atmospheric

* Secretary General of Saudi Environmental Society..

Organization (NOAA) and was the first international consorted effort to collect scientific data in the RSA. The Umitaka-Maru, cruises during 1993 and 1994, was another research vessel which conducted scientific studies in the RSA. These cruises were organized by ROPME, IOC (UNESCO), and TUF (Tokyo University of Fisheries). The ship undertook three cruises and collected physical and chemical oceanographic data. Samples of marine biota, seawater, and sediment were also collected during these cruises (ROPME Scientific Team Members, 1993a, 1993b, 1994). The collected sediment samples were analyzed for heavy metals in the Water Resources and Environment Division of the Research Institute of the King Fahd University of Petroleum and Minerals (KFUPM/RI). This paper summarizes the results of these analyses. Other details of the cruises can be found in reports of ROPME Scientific Team Members (1993a, 1993b, 1994).

MATERIALS AND METHODS

The Japanese Research Vessel Umitaka-Maru cruised through the RSA from 14th to 25th January 1993, 15th to 27th December 1993, and 15th to 27th December, 1994. Along with other studies, surface sediment samples were collected from many locations using a Smith McKintyre grab sampler. Different sample identification systems were adopted for sediment sampling locations during all three cruises (ROPME Scientific Team Members, 1993a, 1993b, 1994). However, sediment sampling locations for all three cruises were unified and are shown in Fig. 1. Information on sample identification and visual texture of the collected sediment samples are given in Table 1. Sediment textural classes are based on visual observations only (more information on sediment texture can be seen in a paper by Al-Ghadban et al. (this volume). Geographical locations of sampling stations in Fig. 1 are our best estimates and may vary from actual locations in the field.

Surface sediment samples collected during Umitaka-Maru cruises were stored in a deep freezer and later transported to the laboratory. In the laboratory, the sediment samples were air dried, hand crushed, sieved, mixed thoroughly, and stored in plastic containers. Two grams of the air dried sediment samples was taken in the 125 ml digestion tubes. The sediment samples were calcareous (containing calcium carbonate > 70%), therefore, concentrated nitric acid was added dropwise giving sufficient time to subside CO_2 gas effervescence. An additional 10 ml concentrated nitric acid were added to each tube after all the carbonates were exhausted. Later the content of the tube was digested at 120°C for three hours. After cooling, about 20 ml double distilled water was added to each tube, the content was filtered, and the volume was increased to 50 ml with distilled water. Concentrations of barium (Ba), cadmium (Cd), cobalt (Co), chromium (Cr), Copper (Cu), iron (Fe), lead (Pb), manganese (Mn), nickel (Ni), phosphorus (P), titanium (Ti), vanadium (V), and zinc (Zn) were determined in these aliquot samples using an Inductively Coupled argon Plasma Analyzer (ICAP).

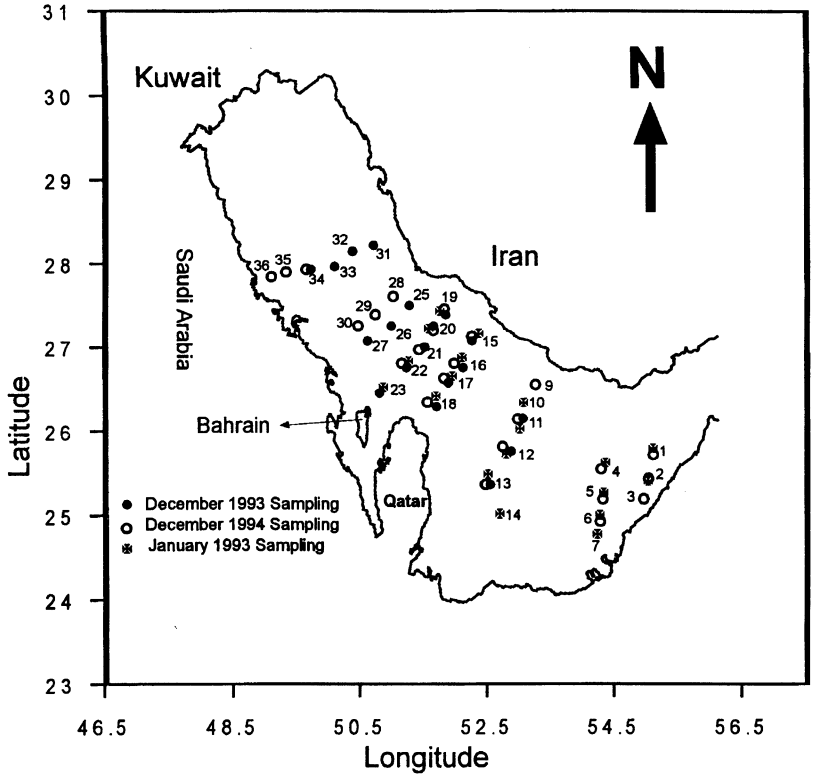

Fig. 1. Sediment sampling locations. Identification numbers given during cruises have been changed.

To ensure high quality of the analytical results, reagent blanks and reference standard materials (estuarine and river sediment standard reference material samples from US NIST) were included in the analytical scheme. Nitric acid and water were doubly distilled. All glassware was cleaned with 20% nitric acid. The chemicals used in the study were of the highest purity. Instrumental readings with relative standard deviation less 10% were only accepted. The analytical data were statistically evaluated using analysis of variance, correlation, and regression techniques. Contributions of various parameters to variations in metal concentrations were investigated using stepwise regression technique. The geographical trends in metal concentrations were investigated by using contour mapping technique.

RESULTS AND DISCUSSION

The analytical data of this study are summarized in Table 2 which shows that metal concentrations in the sediment samples varied widely ($p < 0.01$). Sediment

Table 1. Sediment sampling locations and type of sediment at these locations.

This paper Sample No	January 1993 Sample No	December 1993 Sample No	December 1994 Sample No	Sediment Texture
1	84		RO9404	Muddy sediment
2	83		RO9405	Muddy sediment
3			RO9406	Muddy sediment
4	79		RO9403	Sandy-silt/clay sediment
5	78		RO9402	Sandy-silt/clay sediment
6	77		RO9401	Sandy sediment
7	76			Sandy sediment
9			RO9407	Muddy sediment
10	67			Sandy-silt/clay sediment
11	66	ST1	RO9408	Muddy sediment
12	65	ST2	RO9409	Sandy-silt/clay sediment
13	64	ST3	RO9410	Sandy-silt/clay sediment
14	61			Muddy sediment
15	52	ST4	RO9414	Muddy sediment
16	51	ST5	RO9413	Sand sediment
17	50	ST6	RO9412	Sandy-silt/clay sediment
18	49	ST7	RO9411	Sandy sediment
19	47	ST8	RO9418	Muddy sediment
20	45	ST9	RO9417	Muddy sediment
21		ST10	RO9416	Sandy sediment
22	44	ST11	RO9415	Sandy sediment
23	43	ST12		Sandy sediment
25		ST13		Sandy sediment
26		ST14		Sandy-silt/clay sediment
27		ST15		Muddy sediment
28			RO9421	Sandy-silt/clay sediment
29			RO9420	Muddy sediment
30			RO9419	Sandy-silt/clay sediment
31		ST16		Sandy-silt/clay sediment
32		ST17		Sandy-silt/clay sediment
33		ST18		Sandy-silt/clay sediment
34		ST19	RO9422	Muddy sediment
35			RO9423	Muddy sediment
36			RO9424	Muddy sediment

Table 2. A summary of metal concentrations in the sediment samples collected during Umitaka-Maru cruises 1993–1994.

Metal	No of Samples	Mean (mg/kg)	Standard Deviation	Minimum (mg/kg)	Maximum (mg/kg)
Sediment Sampling Date: January 1993					
Barium	19	16.7		11.1	40.4
Cadmium	19	6.4	3.9	2.4	12.9
Cobalt	19	5.9	3.6	2.4	12.2
Chromium	19	22.5	17.1	6.2	54.8
Copper	19	6.1	4.9	1.7	16.3
Iron	19	5653	4713	951	13706
Manganese	19	129.0	108.0	29.0	321.5
Nickel	19	29.7	26.1	6.0	81.2
Phosphorus	19	671	154	440	967
Lead	19	32.2	9.7	21.3	48.7
Titanium	19	54.3	36.2	13.1	143.2
Vanadium	19	14.2	6.6	7.0	27.0
Zinc	19	16.1	12.5	3.5	39.6
Sediment Sampling Date: December 1993					
Barium	18	15.0	2.5	9.8	20.1
Cadmium	18	9.7	4.1	2.2	15.2
Cobalt	18	8.7	3.5	2.4	12.8
Chromium	18	32.7	16.1	2.4	55.9
Copper	18	9.5	4.6	1.8	17.4
Iron	18	8622	4455	344	14402
Manganese	18	229.8	114.9	11.2	366.4
Nickel	18	48.4	25.3	5.6	84.2
Phosphorus	18	712	137	372	895
Lead	18	37.0	9.1	20.7	50.1
Titanium	18	53.8	36.0	4.4	127.7
Vanadium	18	19.0	5.9	6.8	26.2
Zinc	18	25.0	12.7	2.3	43.4
Sediment sampling Date: December 1994					
Barium	21	18.4	10.5	11.8	62.7
Cadmium	21	6.7	4.0	1.9	14.7
Cobalt	21	5.6	3.4	1.8	11.7
Chromium	21	20.6	16.8	2.9	56.1
Copper	21	6.0	4.3	0.7	15.1
Iron	21	5913	4367	987	15598
Manganese	21	146.8	110.4	26.0	343.8
Nickel	21	28.9	23.5	6.6	81.6
Phosphorus	21	652	154	417	1066
Lead	21	27.2	10.6	14.3	48.0
Titanium	21	69.0	47.0	16.8	191.1
Vanadium	21	16.4	7.3	8.2	31.1
Zinc	21	15.9	11.9	3.6	42.1

samples were collected from many locations during three Umitaka-Maru cruises. Moreover, the texture of the samples was also variable. Geographical location, texture, and date of sampling might have contributed to the variations in metal concentrations in Table 2.

Analysis of variance technique was used to investigate the impact of the sampling date on metal concentrations. The date of collection had significantly ($p < 0.05$) affected concentrations of Cd, Co, Cr, Cu, Fe, Mn, Ni, Pb, V, and Zn in the sediments but influence appears to be weak (F values were close to the significant limits). The Duncan multiple range test indicated that concentrations of Cd, Co, Cr, Cu, Fe, Mn, Ni, V, and Zn were significantly ($p < 0.01$) higher in the sediment samples collected during December 1993 cruise than in the samples collected during other two cruises. The sampling date had no affect on P and Ti concentrations in sediment samples. Concentrations of Pb and Ba were significantly ($p < 0.01$) different in the samples collected during all cruises. Reasons for the influence of sampling date on metal concentrations could not be ascertained.

Texture of sediment could be the most important parameter that influence metal concentrations (Filipek and Owen, 1979; Basaham and Lihaibi, 1993). Field observations on sediment texture were available in reports of ROPME Scientific Team Members (1993a, 1993b, 1994). Based on this information, sediment samples were sorted into three textural classes; sandy, sandy-silt/clay, and muddy sediments. The results of analysis of variance and Duncan multiple range test revealed that concentrations of Cd, Co, Cr, Cu, Fe, Mn, Ni, P, Pb, V, and Zn were significantly ($p < 0.01$) higher in the muddy sediments than concentrations found in the sandy or sandy-silt/clay sediment samples. A reverse trend in Ba concentrations was observed. It seems that sediment texture was not influencing Ti concentrations in the sediment samples. Statistically similar concentration of metals were found in the sandy and sandy-silt/clay sediments.

Mean concentrations of metals in different textural types were computed and are plotted in Fig. 2. Basaham and Lihaibi (1993) also reported significant effect of particle size on metal concentrations in sediments from the coastal areas of Kuwait and Saudi Arabia. Filipek and Owen (1979) also reported that heavy metals were largely associated with the clay fraction of lacustrine sediments. Concentrations of Ba, P, and Ti in the sediment samples were not influenced by sediment texture.

Inter-elemental associations were investigated using correlation and regression techniques. Except for Ba, all other metals were significantly ($p < 0.0001$) correlated to Fe concentrations in the sediments, however, associations between Fe-P and Fe-Ti were less stronger than other metals. Some of the associations with Fe are shown in Fig. 3. Stepwise regression analysis technique was used to investigate factors that contribute to the observed variations in metals concentrations in the sediment samples. Over 90% variations in Cd, Co, Cr, Cu, Mn, Ni, Pb, V, and Zn concentrations could be accounted for by Fe concentrations alone. In addition to Fe concentrations, sampling date was also important in explaining variations in Ti and P concentrations. Variations in Ba concentrations could not

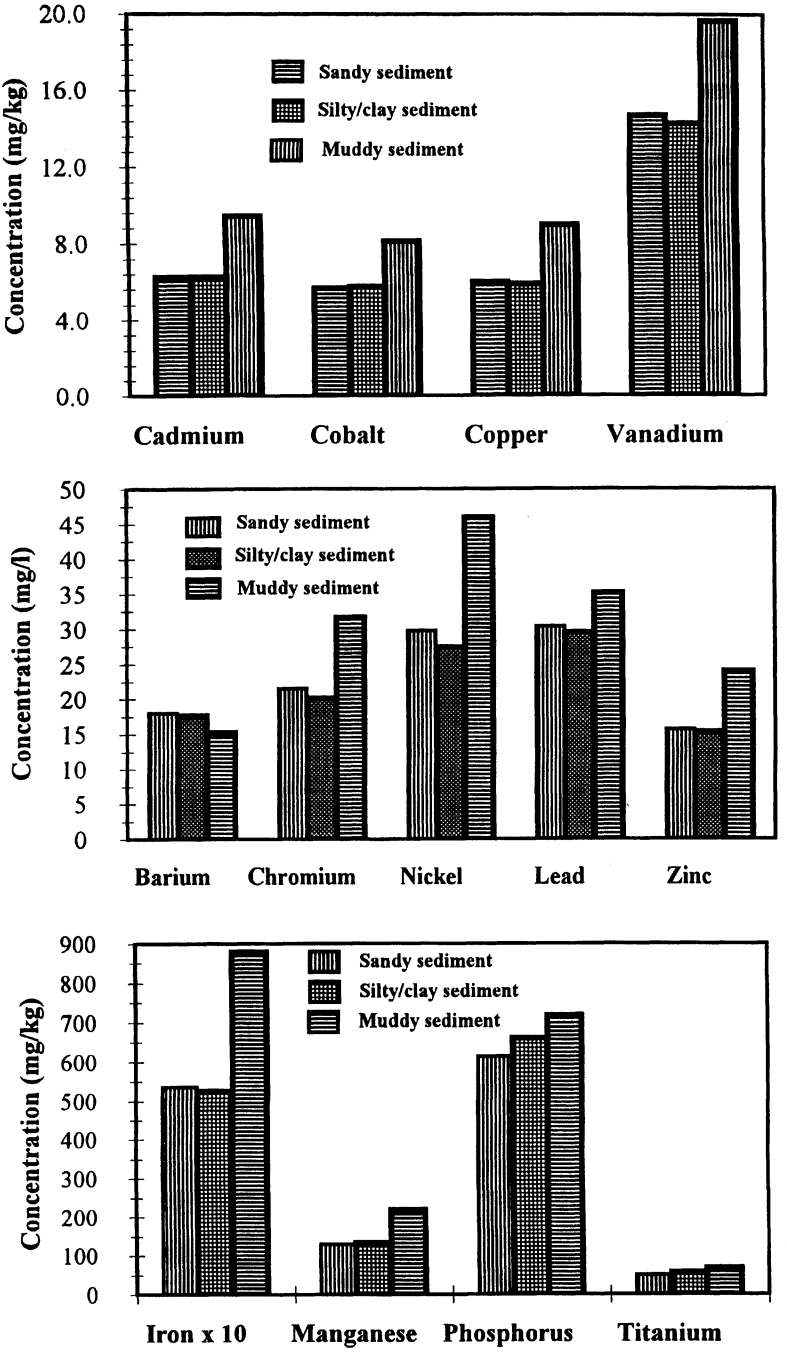

Fig. 2. Metal concentrations in different types of dry sediments.

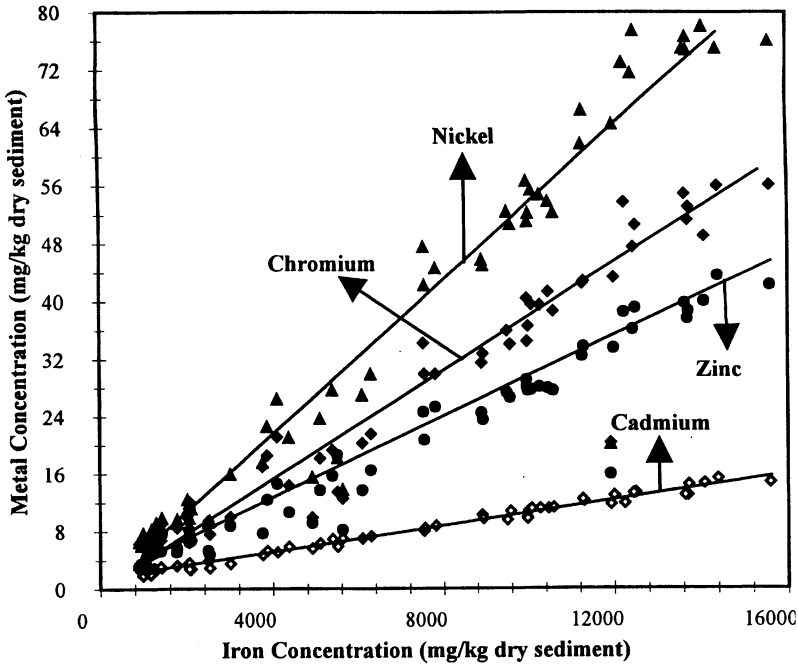

Fig. 3. Iron-metal associations in the sediment samples collected during the cruises.

be accounted for by the parameters investigated in this study. It has been reported that Fe oxides and hydroxides play an important role in the sorption of metals in marine environments (Sadiq, 1992). The sorption affinity of Fe oxides for metals may be responsible for very strong associations ($p < 0.0001$) between Fe and metals in the sediment samples of this study.

Sediment samples were collected from 36 locations (many sampling stations were similar in all three cruises, see Fig. 1). These many sampling stations are relatively too few with respect to the area to investigate regional trends. With the foregoing limitation in mind, the geographic trends in metal concentrations in the sediment samples were evaluated using contouring technique. Contour maps of Ba, Fe, and Ni concentrations are shown in Fig. 4. The highest Ba concentrations was found near Qatar coast. Another high Ba concentration area could be seen in the eastern part of the study area. Except for Ba, P, and Ti, contour maps of other metals were similar to that of Fe. As an example, contour map of Ni concentrations in the sediment samples is included in Fig. 4. In general, metal concentrations increased from the western coast (Saudi Arabia, Qatar, UAE) to the eastern coast (Iran). As mentioned earlier, the number of sampling stations are limited, therefore, the contour maps of metal concentrations should be carefully interpreted.

The analytical data of this study are compared with metal concentrations in

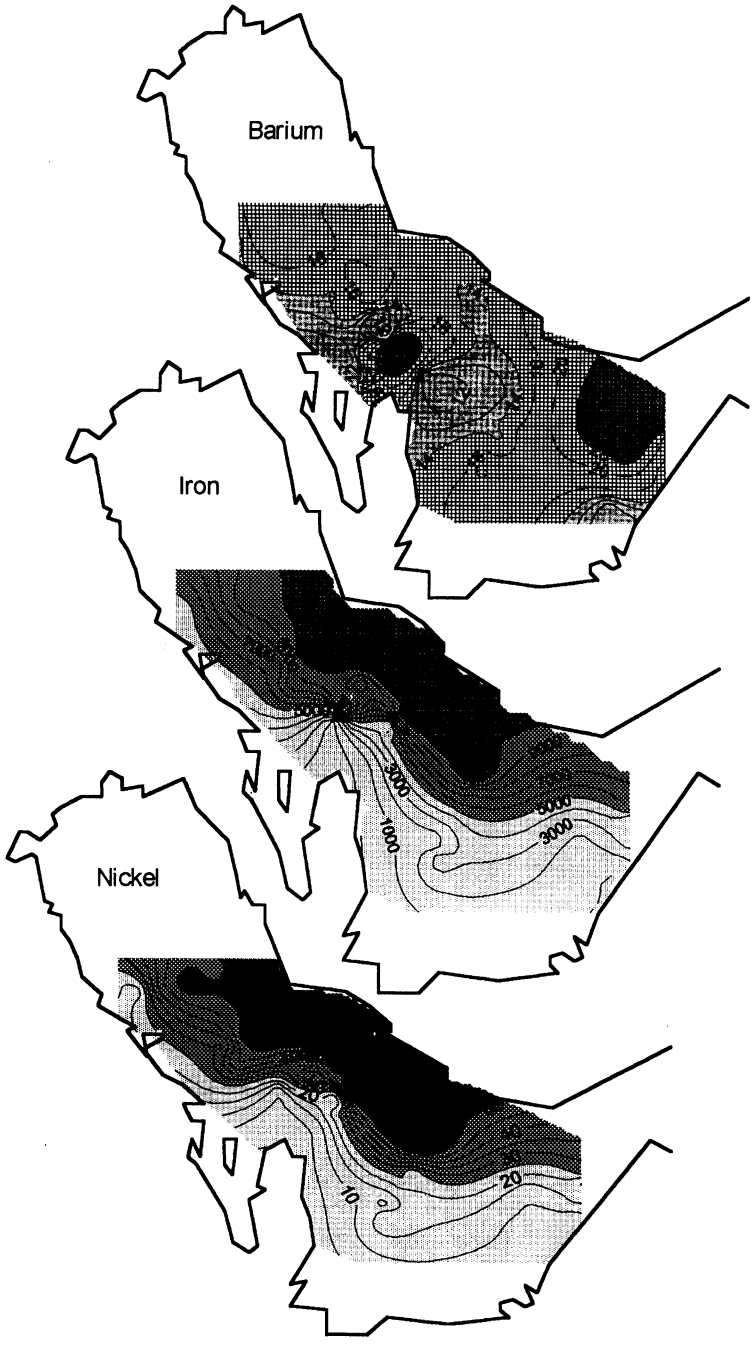

Fig. 4. Contour map of barium, iron, and nickel concentrations (mg/kg dry sediment) in the study area. Darker colors correspond to higher concentrations.

Table 3. A comparison of metal concentrations (mg/kg) in the sediment from the ROPME Sea Area.

Metal	Al-Arfaj & Alam (1993)	Sadiq & Zaidi (1985)	Basaham & Lihaibi (1993)*	Linden et al. (1990)*	This Study
Barium	6.0-27.7				9.7-62.7
Cadmium	<1-6.9	2.5-5.0		0.02-5.0	1.9-15.2
Cobalt	<1-7.1		1-27		1.8-12.8
Chromium	4.7-24.2	3.4-53.0	4-63		2.4-56.1
Copper	2.5-7.9	5.6-16.6	3-16	1.3-16.6	0.7-17.4
Iron*			553-9925		344-15598
Manganese	28.7-149.5	10.1-177.0	34-238		11.2-366.4
Nickel	3.2-39.1	20.5-64.6	6-54	0.4-65	5.6-84.2
Lead	8.4-35.8	0.6-4.2		0.6-15.1	14.3-50.1
Titanium	65.4-266.6				4.4-191.1
Vanadium	4.5-31.1	3.4-29.3	3-36	0.1-56.4	6.8-31.1
Zinc	2.4-20.1	4.2-22.6	13-65	1-51	2.3-43.4

*Data for Iraq and Kuwait were excluded.

sediments from the area in Table 3. Most of the literature information pertains to the coastal areas. Concentrations of Ba, Cd, Mn, Ni, and Pb were relatively higher in the sediments from this study than respective concentrations reported in the literature. However, concentration range of these elements in Table 3 are overlapping. Concentrations of Cr, Cu, V, and Zn of this study were comparable with those reported in the literature.

Acknowledgements

The authors gratefully acknowledge the support of the Research Institute of King Fahd University of Petroleum and Minerals in carrying out this study. Technical help of Messrs. T. H. Zaidi, A. A. Mian, and Hassan Al-Muhanna in analyzing sediment samples is appreciated. The crew and scientists of Umitaka-Maru cruises are highly appreciated for their cooperation in collecting the sediment samples. The role of ROPME and Tokyo University of Fisheries in organizing the Umitaka-Maru cruises is acknowledged.

REFERENCES

Al-Arfaj, A. A. and Alam, I. (1992). Chemical characterization of sediments from the Gulf area after the 1991 Oil Spill. *Mar. Pollut. Bull.* 27, 97–102.

Basaham, A. S. and Al-Lihaibi, S. S. (1993). Trace elements in sediments of the western Gulf. *Mar. Pollut. Bull.* 27, 103–107.

Filipek, L. H. and Owen, R. M. (1979). Geochemical associations and grain-size partitioning of heavy metals in lacustrine sediments. *Chem. Geol.* 26, 105–117.

Linden, O., Abdulraheem, M. Y., Gerges, M. A., Alam, I., Behbehani, M., Borhan, M. A. and Al-Kassab, L. F. (1990). State of the marine environment in the ROPME Sea Area. UNEP Regional Seas Report and Studies No 112, 34 pp.

Marine Pollution Bulettin (1993). The Gulf War. *Coastal and Marine Environmental Consequences.*

Vol. 27, 238 pp.
ROPME Scientific Team Members (1993a). Report on Research Vessel Umitaka-Maru cruise in the ROPME Sea area, from 14th to 25th January, 1993. Regional Organization for the Protection of Marine Environment (ROPME), Kuwait.
ROPME Scientific Team Members (1993b). Report on Research Vessel Umitaka-Maru cruise in the ROPME Sea area, from 15th to 27th January, 1993. Regional Organization for the Protection of Marine Environment (ROPME), Kuwait.
ROPME Scientific Team Members (1994). Report on Research Vessel Umitaka-Maru cruise in the ROPME Sea area, from 15th to 27th January, 1994. Regional Organization for the Protection of Marine Environment (ROPME), Kuwait.
Sadiq, M. (1992). Toxic Metal Chemistry in Marine Environments. Marcel Dekker, New York, 340 pp.
Sadiq, M. and McCain, J. C. (1993). The Gulf War Aftermath—*An Environmental Tragedy*. Kluwer Academic Publishers, Holland, 298 pp.
Sadiq, M. and Zaidi, T. H. (1985). Metal concentrations in the sediments from the ROPME Sea Area coast of Saudi Arabia. *Bull. Environ. Contam. Toxicol.* 34, 565–571.
Tawfiq, N. I. (1991). Response by Saudi Arabia to the environmental crisis caused by the Gulf War, pp. 40–43. In: The Environmental and Health Impacts of the Kuwaiti Oil Fires, ed. by A. K. S. Al Shatti and J. M. Harrington, Proc. Int. Symp., Univ. Birmingham, 17 October.

Offshore Environment of the ROPME Sea Area after the War-Related Oil Spill, Eds. A. Otsuki *et al.*, pp. 161–180.

Trace metals in the finest fraction of surface sediments from the inner part of ROPME Sea Area

Masaru MAEDA, Hiroki AKITAKE, Itaru KAMIYA, Fuyuki SHIBATA and Akiyoshi KAMATANI

Department of Ocean Sciences, Tokyo University of Fisheries, 4-5-7 Konan, Minato-ku, Tokyo 108-8477, *Japan*

Abstract—Trace (Co, Cu, Mn, V, Zn) and major (Al, Ca, Fe, K, Na, Ti) metals in surface sediments from the inner part of the ROPME Sea Area (RSA) were measured to provide basic data of and evaluate impacts of human activities on the concentrations and distributions of trace metals in the region. Short core samples were taken from surface sediments collected by a grab sampler. Surface layers of 2.5 cm thickness were wet-sieved and fractions composed of fine sand, silt and clay (<63 μm) were analyzed for their total metal concentrations. For some samples fractions of >2000, 2000–200, and 200–63 μm were also analyzed.

The concentrations of metals except Ca were far highest in the finest fraction but that of Ca was lowest in the same fraction. High correlation coefficients (r = 0.86–0.95) between the total concentration of each metal and the rate of the finest fraction in the whole sediments suggest the importance of the textural composition of host sediment in controlling the metal concentrations in the RSA sediments.

In the finest fraction ranges of the trace metal concentrations were <1.7–14.7, 6.7–25.3, 101–499, 16.3–72,8 and 15.4–64.5 μg g^{-1} for Co, Cu, Mn, V and Zn, respectively. The concentrations were in the ranges reported for undisturbed estuarine and coastal sediments. In case of the major metals following ranges were obtained; 10.2–39.3, 166–330, 6.3–28.6, 2.1 -13.1, 16.8–37.6, 4.09–6.38 and 0.76–2.79 mg g^{-1} for Al, Ca, Fe, K, Mg, Na and Ti, respectively. Even in the finest fraction Ca concentrations were extremely high and corresponded to 42–83% of the fraction as $CaCO_3$. Higher concentrations of Ca were found along the southwestern coastal area of the inner part of RSA, while for the other metals except Cu a southwest (lower) to northeast (higher) gradient in each metal concentration was observed. Copper distribution was complicated somewhat in the northern part of the study area where the distribution of the finest fraction was also intricate.

In addition to large Mg/Al ratios high positive correlations between Al, Fe and Mg (r = 0.95–0.97) and high but negative ones between Ca and each of Al, Fe and Mg (r = -0.91–0.92) suggest that carbonates, and aluminosilicate and ferromagnesian minerals are main components of the finest fraction. Furthermore there are high positive correlations between the trace metals except Cu and each of Al, Fe and Mg (r = 0.83–0.97), and high negative correlations between the trace metals and Ca (r = -0.79–0.89). These relationships demonstrate that the aluminosilicate and ferromagnesian minerals play a role of carriers of the trace metals and the carbonates act as diluents of the metals. In

the inner part of RSA the mixing ratio of these two components of host sediment seems to be controlling the trace metal concentrations of the finest fraction and so far of the whole sediment.

To evaluate the impact of human activities the correlation between the total concentration of each metal and that of the major metal (Al, Fe, Mg) in the fraction <63 um was examined. Of the trace metal examined Co, Mn, V, and Zn showed the high degree of correlations with Al as well as with Fe and Mg, and any anomalously high concentrations of these metals far from their regression lines with Al were not observed. The ratios of metals (Mn, V, Zn) to Al were also similar to those in the average crust. These suggest that the trace metals except Cu are mostly incorporated in the aluminosilicate and ferromagnesian minerals and the impact of human activities is minimal in the region. For Cu, further study is required to evaluate its concentrations.

In the RSA the concentration of Ca is extremely high and its carbonates act as diluents of trace metals. So it is very important to measure Ca or carbonate concentrations as well as that of Al to evaluate trace metal data in the sediments.

INTRODUCTION

The Sea Area of the Regional Organization for the Protection of Marine Environment (ROPME) is one of the globally largest area in oil production and transport. During the 1991 Gulf War the Regional Sea Area (RSA) suffered from extensive oil spill and oil-well fires. Therefore, and following the war several national and international scientific communities conducted multidisciplinary surveys and preliminary assessment of the marine environment (Marine Pollution Bulletin,

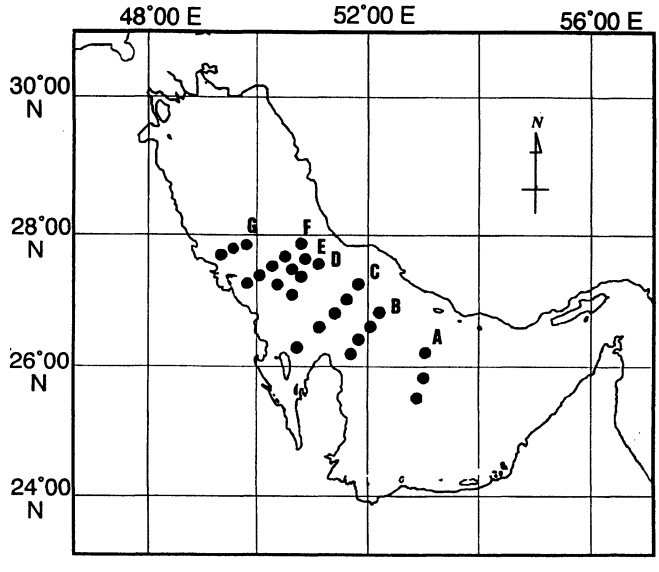

Fig. 1. A map showing the sampling locations. An alphabetical presentation of traverses is used in this study.

1993). Investigations with respect to trace elements showed signs of slight high levels of oil-related metals such as Ni and V in the sediments of the heavily oiled sites at the western coast of the RSA (Fowler *et al.*, 1993; Al-Arfaj and Alam, 1993). The levels in general decreased towards the south, attaining their lowest concentrations in Qatar (Basaham and Al-Lihaibi, 1993) to Oman (Fowler *et al.*, 1993). The trace metal contents were found to reflect the variations of fine materials in the host sediments significantly, and the effect of anthropogenic enrichment was minimum (Basaham and Al-Lihaibi, 1993).

Most of the surveys undertaken in the area were largely focused on the coastal and near-shore environment, while information on the impact of the War on the off-shore areas are scarce. As a part of the scientific program of the sea cruises of the Research and Training Vessel Umintaka-Maru in the inner part of RSA, this study was undertaken aimed to provide data on the major and trace metal contents in surface sediments to evaluate the oil impact on the off-shore region. The study has adopted the method of Windom *et al.* (1989), Luoma (1990) coupled to the method of Salomons and Förstner (1984), to provide a surveillance strategy based on the detection of the anomalous metal concentrations in the fine fraction of sediments (< 63 μm) and then normalized to a conservative element. The study also looked into the effect of textural composition on the distribution of metals in the surface sediments.

MATERIALS AND METHODS

Samples of surface sediments were collected from the inner part of RSA in December 1993 and December 1994 during the second and third cruises of the Research and Training Vessel Umitaka-Maru (Table 1). Twenty six stations located along 7 traverses across the main axis of the RSA were sampled for this study (Fig. 1). Sediments were collected with a Smith-MacIntyre grab sampler and the short cores (ca. 10 cm in length, 8.5 cm in diameter) were obtained from the retrieved sampler using polyethylene containers. The containers were put in polyethylene bags and then frozen until analyses. Measures were taken to avoid contamination during sample collection and handling.

In laboratory the frozen cores were thawed, and then cut into segments of 2.5 cm thickness. The upper most segments (0–2.5 cm) were size-fractionated into the fraction classes of coarse > 2000 μm, FC; medium 2000–200 μm, FM; fine 200–63 μm, FF; and finest < 63 μm, FEF, following the wet-sieving method. Each sediment sample was passed with Milli Q water consecutively through nylon sieves 2000, 200 and 63 μm mesh size. The finest fraction was recovered by centrifugation (3000 rpm, 10 min.). Each fraction was air-dried at room temperature and then powdered in an agate mortar for metal analyses. The amount of leachable metals from samples during the wet sieving procedure was estimated less than 5% (Abaychi and Douabul, 1986, Abu-Hilal, 1993) and ignored in this work.

The metals were extracted following a modified method of Haraguchi (1986). A known and representative amount (ca. 0.5 g) of the powdered material was digested with 10 ml conc. HNO_3 acid (overnight) to semi-dryness,followed

Table 1. Sampling locations of surface sediments in the inner part of RSA.

Traverse No.	Station No.	Location N	Location E	Water Depth m	Sediment Temp. °C	Sampling Date
A	RO9301	24°14.6'	53°11.6'	75	22.0	Dec. 18, 1993
	RO9302	25°55.4'	53°07.9'	63	24.3	Dec. 18, 1993
	RO9303	25°34.2'	53°00.9'	41	24.9	Dec. 18, 1993
B	RO9304	26°58.1'	52°17.2'	69	21.9	Dec. 20, 1993
	RO9305	26°43.5'	52°02.7'	72	23.0	Dec. 20, 1993
	RO9306	26°27.9'	51°48.5'	45	22.4	Dec. 20, 1993
	RO9307	26°13.0'	51°35.2'	25	21.4	Dec. 20, 1993
C	RO9308	27°16.1'	51°41.4'	43	24.1	Dec. 21, 1993
	RO9309	27°06.6'	51°29.7'	73	23.3	Dec. 21, 1993
	RO9310	26°56.9'	51°19.9'	70	23.4	Dec. 21, 1993
	RO9415	26°41.7'	51°07.4'	22	23.3	Dec. 21, 1994
	RO93A2	26°19.0'	50°42.4'	12	19.8	Dec. 22, 1993
D	RO9313	27°32.6'	51°06.5'	71	22.5	Dec. 23, 1993
	RO9314	27°20.8'	50°54.5'	62	22.9	Dec. 23, 1993
	RO9315	27°09.8'	50°41.7'	64	23.0	Dec. 23, 1993
E	RO9421	27°41.9'	50°54.7'	68	22.3	Dec. 24, 1994
	RO9420	27°30.3'	50°37.2'	56	23.3	Dec. 24, 1994
	RO9419	27°15.2'	50°19.1'	53	22.0	Dec. 24, 1994
F	RO9316	27°52.6'	50°46.7'	64	22.0	Dec. 24, 1993
	RO9317	27°43.5'	50°33.2'	57	22.5	Dec. 24, 1993
	RO9318	27°36.0'	50°17.8'	63	22.7	Dec. 24, 1993
	RO9319	27°27.7'	50°03.7'	59	21.7	Dec. 24, 1993
	RO93A4	27°22.1'	49°50.6'	19	22.2	Dec. 24, 1993
G	RO9422	27°56.1'	49°49.9'	57	21.0	Dec. 25, 1994
	RO9423	27°53.4'	49°36.4'	34	22.0	Dec. 25, 1994
	RO9424	27°47.7'	49°23.6'	20	19.8	Dec. 25, 1994

by successive digestion with 5 ml conc. HF acid and 15 ml of a mixture of (2:1, v/v) conc. HNO_3/ $HClO_4$ acids, to decompose the silica-like material and residual organic matter, respectively. The residue was then re-digested with conc. HCl acid to semi-dryness. Finally the digested residue was re-dissolved and made up 50 ml with 0.1 M HCl acid for ICP-AES determination. Only high quality acids and Milli Q water were used throughout the present work. In most cases

laboratory wares made of Teflon or polyethylene were used after being cleaned with acids and Milli Q water. One or two blanks were attached to each batch of samples to correct metal concentrations. It was found that the addition of $HClO_4$ acid to digest extract did not significantly affect the total metals concentration present in the samples.

An ICP-AES system of Hitachi model P-5200 was used for the determination of metal concentrations. The samples were analyzed for trace (Co, Cu, Mn, V and Zn) and major (Al, Ca, Fe, K, Mg, Na and Ti) metals. The reproducibility of the methodology was determined by analyzing replicate aliquots of the same sample. The coefficients of variation were found in the range between 0.7 to 5.7%. The accuracy of the method was established by comparing the analytical results of a standard reference material of coastal sediment (BCSS-1, National Research Council Canada) with its certified values. Deviations found were less than 10% for all metals.

RESULTS AND DISCUSSION

Textural composition

The textural composition of surface sediments and the lateral distribution pattern of FEF are presented in Figs. 2 and 3, respectively. It can be seen in the figures that the southern region of RSA by United Arab of Emirate and the eastern side by Iran, the sediments are essentially very fine sand to clayish deposits. While in the western region by Qatar and Saudi Arabia, the sediments are of fine to medium sandy deposit material. In the central region the distribution pattern shows rather coarser deposits in the north-westerly direction. The characteristics of the textural distribution pattern agree well with those reported by Al-Ghadban *et al.* (1993). Microscopic observations of medium and coarse materials revealed the dominance of shells and shell fragments in the western and southern regions.

Metal distribution in textural fractions

The concentrations of metals in the different fraction classes of six samples are given in Table 2 with estimated total concentrations. The total concentration was calculated using the textural compositions and the metal concentrations in the four fractions. Calcium was the most dominant metal in all fractions. It occupies 55–80% of the whole sedimentary material as $CaCO_3$. This could be attributed to the biogenic nature of the sediments produced from micro-organisms, mainly the Foraminifera (Sheppard, 1993).

The concentrations of Al, Co, Cu, V and Zn were far highest in the finest fraction FEF among the four textural fractions (Table 2). On the contrary the lowest concentrations of Ca and Sr were found in the same fraction in most cases. Figure 4 shows relationship between the total metal concentration and the rate of FEF to the whole sediment weight. The total concentration of each metal is highly correlated with the FEF fraction positively (Al, Co, Cu, V and Zn; $r = 0.86$–0.95) or negatively (Ca and Sr; $r = -0.85$–0.91). This clearly confirm the significance of the fine texture materials in the distribution of trace metal in the sediments, as

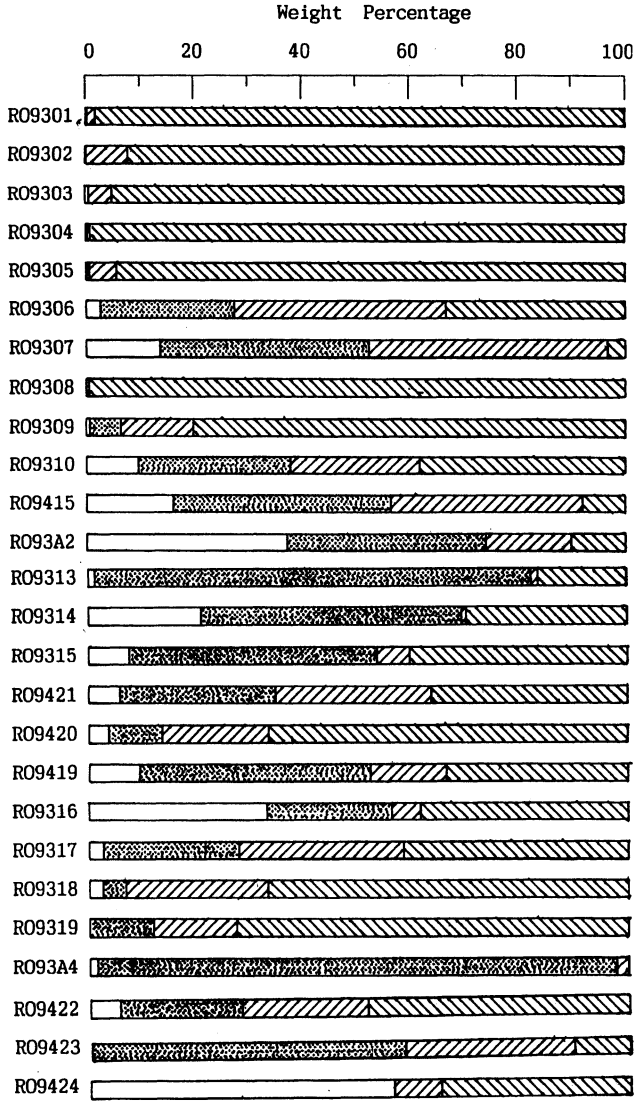

Fig. 2. Textural compositions of sediment samples from the inner part of RSA. Correspondence between patterns and grain sizes is as follows;
□ , > 2000 μm; ▒ , 2000–200 μm; ▨ , 200–63 μm; ▧ , < 63 μm.

consistently has been shown in other estuarine and marine areas (Williams *et al.*, 1978; Ackerman, 1980; Förstner and Salomons, 1980; Wheeler *et al.*, 1980; Loring, 1982; Ackerman *et al.*, 1983).

Even in the same textural fraction significant differences in the metal

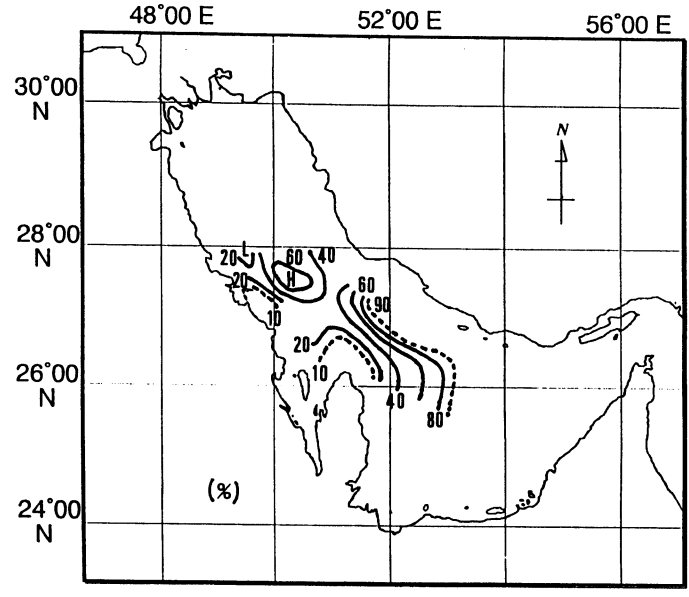

Fig. 3. Distribution of the finest fraction (<63 μm) of sediments in the inner part of RSA. Unit; weight percentage to whole sediment.

concentrations were observed among the stations. The concentrations of Co, Cu, V and Zn changed similarly to the amount of terrigenous aluminosilicate mineral represented by Al concentration present. However, they were inversely related to the changes occur in the amount of calcareous mineral as represented by the measured Ca concentration in the fraction. The relationship found consistently shows up in other fraction classes, which consequently was reflected in the whole sedimentary mineral. Figure 5 shows examples of the relationship between the concentrations of Al and Ca with trace metals. This presumably indicates the importance of the component composition of the host sedimentary material on the distribution of trace metals.

Distribution of the metals in the finest fraction

Table 3 compiles the concentrations of trace and major metals in FEF of the sediments from the inner part of the RSA. Ranges of the trace metals were <1.7–14.7, 6.69–25.3, 101–499, 16.3–72.8 and 15.4–64.6 μg g^{-1} dry weight for Co, Cu, Mn, V and Zn, respectively. In the case of major metals following ranges were found; 10.2–39.3, 166–330, 6.3–28.6, 2.07–13.1, 16.8–37.6, 4.09–6.49 and 0.76–2.79 mg g^{-1} dry weight for Al, Ca, Fe, K, Mg, Na and Ti, respectively. As pointed previously the concentrations of metals ranged widely among the stations and Ca concentrations were extremely high throughout the study area.

The concentrations were compared with those reported by Abaychi and

Table 2. The metal concentrations in textural fractions and whole sediments.

Trav. No.	Sta. No.	Grain Size*	Al mg g^{-1}	Ca mg g^{-1}	Sr mg g^{-1}	Co μg g^{-1}	Cu μg g^{-1}	V μg g^{-1}	Zn μg g^{-1}
E	RO9421	FC	3.6	315	1.36	4.0	3.2	8.0	6.6
		FM	8.6	246	0.96	3.3	4.1	7.7	7.2
		FF	10.2	286	0.72	3.4	4.3	14.9	15.1
		FEF	33.3	166	0.17	13.5	21.6	63.5	54.4
		W	17.8	232	0.63	7.1	10.3	30.1	26.6
	RO9420	FC	2.2	291	1.54	2.1	2.3	4.3	5.1
		FM	7.2	308	0.93	2.0	3.0	6.4	5.3
		FF	8.5	285	0.42	2.4	3.6	11.9	10.1
		FEF	26.0	181	0.50	12.0	18.5	53.9	43.4
		W	19.8	218	0.57	8.7	13.4	39.1	31.7
	RO9419	FC	0.9	313	2.23	5.2	1.6	3.7	2.3
		FM	1.0	254	1.92	5.9	1.1	3.9	5.6
		FF	4.7	221	1.08	6.4	1.3	5.8	8.5
		FEF	20.0	231	1.09	9.4	16.5	33.8	32.7
		W	8.6	247	1.55	7.1	6.4	14.2	14.8
F	RO9317	FC	2.8	371	1.67	5.3	3.3	10.2	8.8
		FM	15.4	262	1.31	6.5	4.9	19.8	14.1
		FF	16.3	267	1.05	6.2	4.6	17.0	12.6
		FEF	32.0	196	0.79	12.3	19.9	57.5	53.0
		W	22.2	239	1.02	8.8	11.0	34.3	29.7
	RO9318	FC	3.6	328	1.52	6.3	2.4	5.4	7.0
		FM	4.3	327	1.30	7.2	3.5	12.4	11.6
		FF	7.6	302	1.31	6.5	2.8	9.9	9.5
		FEF	29.4	185	0.72	10.8	17.7	45.2	37.1
		W	21.9	226	0.92	9.4	12.8	33.5	28.0
	RO93A4	FC	0.1	329	5.21	2.9	1.3	3.2	4.9
		FM	0.3	322	4.92	3.6	0.3	4.1	5.3
		FF	1.4	320	2.54	3.3	0.5	4.6	3.4
		FEF**	----	---	---	----	----	----	----
		W	0.3	322	4.87	3.6	0.3	4.1	5.2

* FC, >2000 μm; FM, 2000-200 μm; FF, 200-63 μm; FEF, <63 μm; W, whole sediments. The procedure to estimate whole sediments concentrations is described in the text.

** Measurable amount of the finest fraction (<63 μm) was not recovered in this sample.

Douabul (1986). They analyzed total metal concentrations in the same fraction as ours (<0.63 μm) of the sediments from the Shatt al-Arab River and the north-western part of the RSA (Table 4). They concluded that the effect of man-made enrichment upon the absolute concentrations of trace elements was minimal. There are not much differences in the ranges and averages of Cu and Zn between the north-western and the inner parts of the RSA. Lower concentrations of Mn and

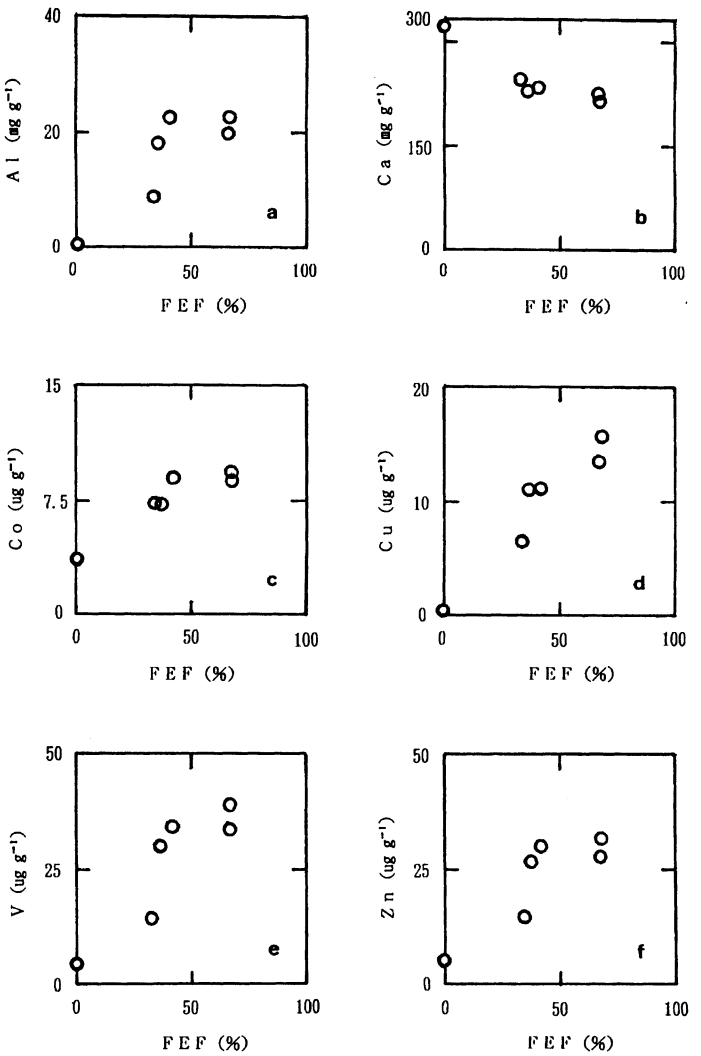

Fig. 4. Relationships between the rate of the finest fraction and the estimated total concentration of whole sediment. The procedure to estimate the concentrations is described in the text.

V, however, were found in the inner part, where Fe concentrations were higher than those in the north-western part. Though the reason why the trends are different among metals is not clear, the levels of trace metals found in this work are in general not high that of environmental concern.

Figure 6 shows the lateral distribution of the metals in the study area. Higher concentrations of Ca were observed along the southwest coastal area of the inner part of RSA and decreased toward the Iranian side (Fig. 6b). On the contrary Al concentration increased toward the deep Iranian side (Fig. 6a). Among the major

Table 3. The metal concentrations in the finest fraction (<63 μm) of surface sediments of the inner part of RSA.

Trav. No.	Sta. No.	Al mg g^{-1}	Ca mg g^{-1}	Fe mg g^{-1}	K mg g^{-1}	Mg mg g^{-1}	Na mg g^{-1}	Ti mg g^{-1}	Co μg g^{-1}	Cu μg g^{-1}	Mn μg g^{-1}	V μg g^{-1}	Zn μg g^{-1}
A	RO9301	34.8	185	23.9	12.1	35.3	----*	----	10.7	25.3	499	59.7	55.6
	RO9302	23.8	224	15.3	6.60	26.0	----	----	6.84	16.5	325	40.6	35.9
	RO9303	10.5	295	6.03	3.41	18.3	----	----	2.18	6.69	138	16.3	15.4
B	RO9304	35.8	174	25.0	10.8	37.6	----	----	11.6	25.1	479	62.2	50.8
	RO9305	34.4	182	23.6	10.0	30.8	----	----	8.70	18.3	396	53.6	47.1
	RO9306	22.1	243	14.9	6.08	23.8	----	----	4.55	13.1	279	33.7	33.3
	RO9307	10.2	299	7.07	2.07	17.0	----	----	<1.7	8.97	108	22.4	25.4
C	RO9308	37.8	169	27.8		35.6	----	----	9.36	17.1	425	68.5	55.4
	RO9309	35.2	181	24.1	5.62	31.0	----	----	9.62	19.4	423	57.5	52.0
	RO9310	29.2	192	19.8	4.20	28.4	----	----	8.40	19.1	383	48.7	45.3
	RO9415	17.5	258	13.4	5.44	24.4	4.64	1.31	8.25	20.8	244	37.5	40.9
	RO93A2	10.2	330	7.20	3.06	16.8	4.09	0.76	3.37	9.51	101	25.3	18.1
D	RO9313	39.3	170	26.8	13.1	37.0	4.92	2.44	13.5	23.0	416	72.8	63.6
	RO9314	32.1	197	21.3	10.0	32.3	6.49	2.47	11.2	19.5	392	57.3	48.4
	RO9315	25.4	237	18.7	8.20	28.5	5.76	2.07	9.60	20.7	343	47.5	41.4
E	RO9421	33.3	166	28.6	11.5	36.0	5.09	2.58	13.5	21.2	473	63.5	54.4
	RO9420	26.0	181	22.6	10.3	33.1	6.38	2.46	12.0	18.5	462	53.9	43.4
	RO9419	20.0	231	15.9	6.58	25.0	5.23	1.76	9.40	16.5	348	33.8	32.7
F	RO9316	36.2	192	27.5	11.9	35.6	5.34	2.58	14.6	24.7	416	72.4	64.6
	RO9317	32.0	196	24.1	9.98	33.1	5.99	2.79	12.3	19.3	415	57.5	53.0
	RO9318	29.4	185	19.9	8.72	30.8	6.06	2.29	10.8	17.7	429	45.2	37.1
	RO9319	20.6	261	15.0	5.84	23.2	4.62	1.48	8.80	20.7	309	36.1	32.5
G	RO9422	26.2	263	17.4	6.70	28.1	5.71	1.80	8.45	18.2	357	37.9	32.2
	RO9423	25.2	264	17.6	6.45	27.3	4.42	1.64	8.95	21.1	346	40.1	35.1
	RO9425	23.5	278	17.1	5.86	24.9	5.28	1.54	8.62	19.4	352	39.0	32.6

*Sodium and Ti were not measured in the samples of RO9301 - RO9310.

Table 4. Comparison of total metl concentrations in the fraction smaller than 63 μm of sediments of the RSA.

Area in the Gulf	Cu μg g^{-1}	Fe mg g^{-1}	Mn μg g^{-1}	V μg g^{-1}	Zn μg g^{-1}
Northwest* (coastal)	17.3 - 37.1 (25 ± 5)	4.45 - 9.37 (5.87 ± 1.26)	915 - 1643 (1160 ± 203)	150 - 186 (166 ± 10)	27 - 43 (33 ± 4)
Inner part** (off-shore)	6.69 - 25.3 (18 ± 5)	6.30 - 28.6 (19 ± 6)	101 - 499 (354 ± 110)	16.3 - 72.8 (47 ± 15)	15.4 - 64.6 (42 ± 13)

* Abaychi & Douable (1986).

** This study.

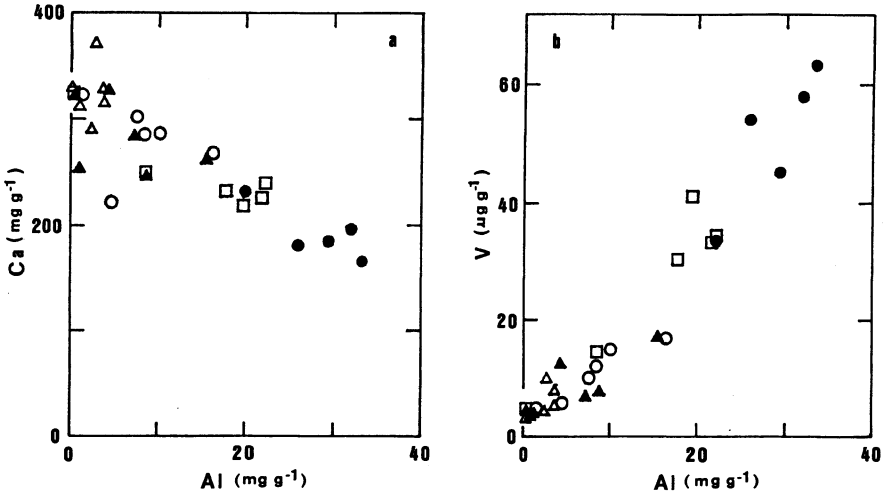

Fig. 5. Relationships between Al and Ca (a), and Al and V (b) within the textural fractions and the whole sediment. Correspondence between symbols and the fractions is as follows;
△, > 2000 μm; ▲, 2000–200 μm; ○, 200–63 μm; ●, < 63 μm; □, whole sediment.

Table 5. Correlation coefficients between metals in the finest fraction(<63 μm) of sediments from the inner part of RSA.

Metal	Ca	Fe	K	Mg	Na	Ti	Co	Cu	Mn	V	Zn
Al	-0.91	0.97	0.84	0.95	0.48	0.90	0.83	0.77	0.91	0.95	0.91
Ca		-0.92	-0.80	-0.92	-0.60	-0.93	-0.79	-0.65	-0.90	-0.89	-0.87
Fe			0.88	0.97	0.47	0.93	0.89	0.77	0.93	0.97	0.94
K				0.92	0.50	0.93	0.87	0.75	0.82	0.89	0.84
Mg					0.55	0.95	0.90	0.80	0.93	0.96	0.92
Na						0.71	0.49	0.15	0.66	0.39	0.39
Ti							0.93	0.57	0.90	0.88	0.83
Co								0.86	0.88	0.87	0.85
Cu									0.82	0.77	0.77
Mn										0.85	0.81
V											0.96

metals, Fe, K, Mg and Ti distributed similarly to Al. The distribution patterns of the trace metals except Cu were also similar to that of Al (Fig. 6c, 6e, 6f), that is, the southwest (lower) to northeast (higher) gradient in each metal distribution was observed. Copper distribution was somewhat different from the other trace metals (Fig. 6d). In the southern part of the study area (Traverses A and B) the element distributed similarly to the other metals, while its distribution pattern in the northern part (Traverses C to G) was more complicated.

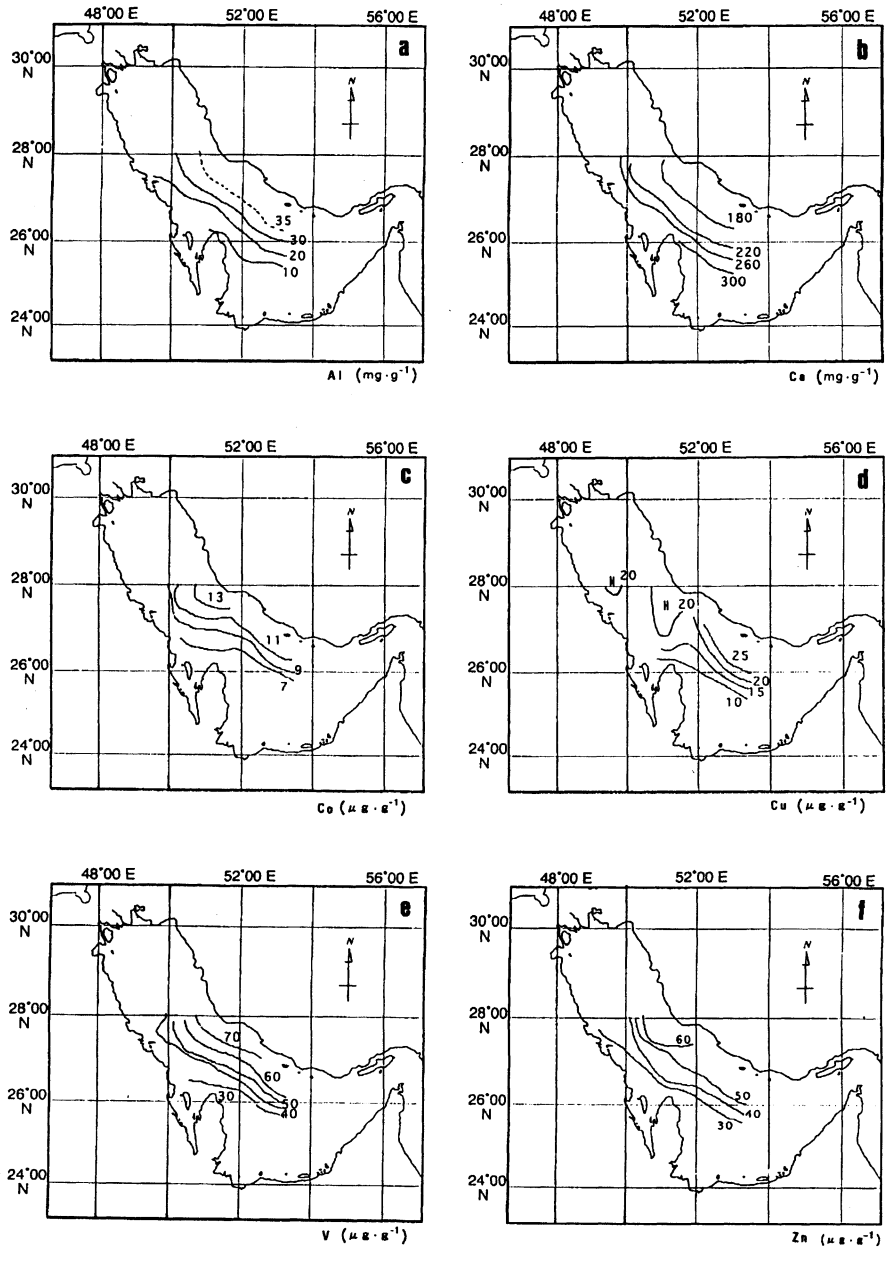

Fig. 6. Distribution of the etals in the finest fraction (<63 μm) of the sediments from the inner part of RSA.

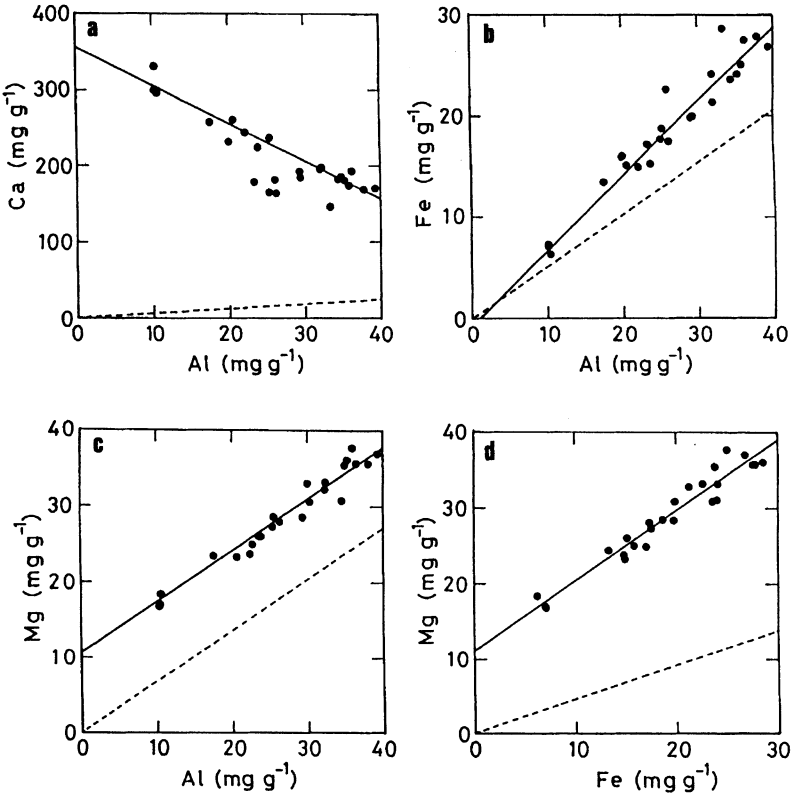

Fig. 7. Relationships between major metals in the finest fraction (<63 μm) of sediments from the inner part of RSA. In each figure solid line is a regression one between the metals in the sediments, while dashed line shows a concentration ratio of the metals drawn by assuming that the average crust (Chester, 1990) is mixed with materials free from the metals.

Relationship between the major metals in the finest fraction

Figure 7 indicates the relationships between Al and each of Ca, Fe and Mg in the fraction FEF with the concentration ratios of metals to Al in the continental crust (Chester, 1990). The correlation coefficients between the metals are also tabulated in Table 5. High negative correlation between Al and Ca and high positive one between Fe and Al can be seen. Magnesium also shows very high positive correlation to Al. However, the regression line between Mg and Al locates high above the crustal ratio and intersects the Mg-axis at very high concentration, suggesting occurrence of Mg-rich carbonates. These relationships suggest that in the inner part of RSA the finest fraction of the sediments is mainly composed of carbonates, and aluminosilicate and ferromagnesian minerals. This

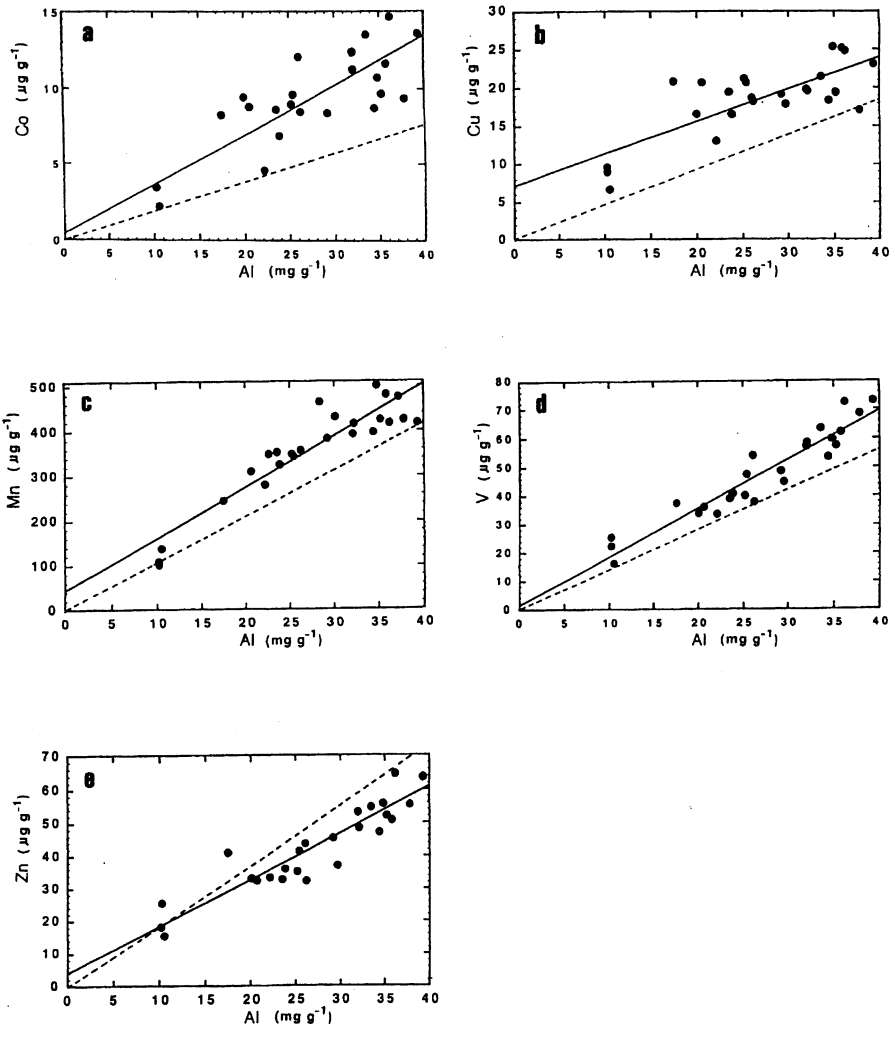

Fig. 8. Relationships between Al and each of trace metals in the finest fraction (<63 μm) of sediments from the inner part of RSA. In each figure solid line is a regression one between the metals in the sediments, while dashed line shows a concentration ratio of the metals drawn by assuming that the average crust (Chester, 1990) is mixed with materials free from the metals.

suggestion agrees well with mineralogical characteristics of the RSA sediments observed by Al-Ghadban *et al.* (1993, 1995). They found that the gross mineralogy is biased toward carbonates and clay minerals followed by a small amount of quartz and feldsper.

The sediments of the inner part of RSA are unique in their high Mg/Al ratios.

The ratios ranged from 0.88 to 1.74 (weight concentration basis) and are much higher than those of many kinds of geochemical materials such as shelf and hemipelagic sediments (Poldervaart, 1955; Calvert, 1976), oceanic clays and carbonates (Graf, 1960; Chester and Aston, 1976), shales and sandstones (Wedopohl, 1969–1974), coastal sediment-related materials (Chester, 1990) and igneous rocks (Poldervaart, 1955; Bowen, 1979). In Fig. 7a and 7d extrapolated concentrations of Ca and Mg to an Al concentration of 0 mg g^{-1} are 357 and 10.6 mg g^{-1}, respectively. Magnesium occupies 4% (molar basis) of carbonates if we assume that Ca and Mg occur as carbonates in a sediment free from Al. Al-Ghadban *et al.* (1993, 1995) suggested the occurrence of low-Mg-calcite and dolomite of detrital origin carried as dust fallout into the northern area, and fine debris of shells and shell fragments abraded by current and wave action or broken down biologically in the southern part of the RSA. In this context Kinsman (1966) found dolomite in an evaporation-exceeded salt flat (sabkha) along the Trucial coast of RSA as a result of dolomitization during early diagenesis. Furhtermore Foraminifera, the predominant component of biogenic sediment of the RSA (Sheppard, 1993), has calcite exoskeletons and contains higher concentration of Mg than aragonite ones do (Chave, 1954). It was also observed that the Mg concentration in Foraminifera increased with increase of water temperature (Chave, 1954). These conditions of the RSA and the surrounding lands might cause the relative enrichment of Mg compared to Al in the study area.

Evaluation of human impacts on the trace metal contents

To evaluate the impact of human activities to the trace metal contents of sediments of the inner part of RSA, the relationship between each trace metal and Al, which is one of conservative elements of aluminosilicates, was examined (Fig. 8). Of the trace metals, Co, Mn, V and Zn showed positive correlations of high degree (r = 0.83–0.95; Table 5), and any extremely high concentration of these metals far above their regression lines with Al was not observed. Moreover the concentration ratios of the metals (Mn, V, Zn) to Al are similar to those of average continental crust (Table 6). These findings suggest that the trace metals except Cu are mostly incorporated in the minerals and the impact of human activities is minimal in the region over a period of years, though our sampling technique of taking surface sediments of 2.5 cm thickness is not so valid to detect the impact of an event such as the 1991 Gulf War. For Cu, the concentrations found in the FEF and estimated for the whole sediments in this study are not much different from those reported previously and evaluated to be affected by minimal anthropogenic impact (Abaychi and Douabul, 1986; Basaham and Al-Lihaibi, 1993; Fowler *et al.*, 1993).

Factors controlling the trace metal concentrations

As mentioned above the correlations between Al and each of the trace metals except Cu are positive and very high (Fig. 8; Table 5), while those between Ca and the trace metals are also very high but negative(r = –0.79–0.90). Moreover the

Table 6. Concentration ratios of the trace metals to Al in the continental crust and sediments of the ROPME Sea Area.

Concentration ratio	Sediments of ROPME Sea Area*1	Continental Crust*2
Co/Al	3.4 x 10-4	1.9 x 10-4
	(3.2 x 10-4)	
Cu/Al	6.7 x 10-4	4.6 x 10-4
	(4.2 x 10-4)	
Mn/Al	1.3 x 10-2	1.0 x 10-2
	(1.1 x 10-2)	
V/Al	1.7 x 10-3	1.4 x 10-3
	(1.7 x 10-3)	
Zn/Al	1.6 x 10-3	1.8 x 10-3
	(1.4 x 10-3)	

*1 This study. Figures in parentheses are slopes of regression lines of the trace metals with Al.
*2 Martin & Whitfield (1983) cited in Chester (1990).

Table 7. Metal contents of exoskeletons of coral and molluscan (unit, $\mu g\ g^{-1}$ -dry) extracted from Eisler (1981).

Metal	Exoskeleton of coral	Shell of molluscs
Al	<125	3.0 - 470 (180)
Ca	---	---
Fe	<5 - 880	4.5 - 2600 (450)
K	---	---
Mg	---	---
Na	---	---
Ti	<20 - 80	---
Co	0.001 - 0.012	0.03 - 11 (0.89)
Cu	<2.0 - 20	0.1 - 117 (13)
Mn	2.0 - 130	1.0 - 227 (19)
V	<10	49 - 290 (115)
Zn	2.0 - 7.0	0.04 - 210 (21)

trace metal concentrations change corresponding to Al/Ca, Fe/Ca and Mg/Ca ratios in the fraction with high correlation coefficients (r = 0.79–0.96). These relationships between the trace metals and Al or Ca demonstrate strongly that the aluminosilicate and ferromagnesian minerals and the carbonates, which are suggested in the previous section to be the main components of the samples, play important roles in controlling the trace metal concentrations in the sediments of the RSA.

Exoskeletons of coral contain the trace metals at low concentrations, but molluscan shells show a wide range of the trace metal concentrations (Eisler, 1981; Table 7). So the biogenic carbonates may act as diluents of the trace metals in the RSA sediments, though they were grouped as carriers of non-detrital Cu in the Bay of Fundy sediment of Canada (Loring, 1982). On the other hand the aluminosilicate and ferromagnesian minerals are known to play roles of carriers and/or concentrators of many kinds of metals (Loring, 1982). The concentrations of trace metals in the FEF and whole sediments of the RSA might be controlled by the mixing ratio of the aluminosilicates and the ferromagnesian minerals, and the carbonates.

Eventually overall distribution of most trace metals in the inner part of the RSA seems to be governed by the grain size and mineral speciation of host components, as well as by the dynamic and hydraulic depositional conditions in the RSA (Reynolds, 1993; Al-Ghadban *et al.*, 1993).

Copper, which is somewhat different from the other trace metals in its lateral distribution pattern, has unique characteristics in the relationship with Al, too. In the southern part of the study area, where Cu distribution is similar to those of the other metals, it shows extremely high correlation with Al (r = 0.95; Fig. 8b) suggesting that Cu concentration is controlled by the same factors as those for the other metals. In the northern part, however, Cu concentration increases little with the increase in Al concentration and the data scattered rather broadly at both sides of the regression line. In the area the distribution pattern of FEF is also complicated. Further studies, however, are needed to make clear the factors controlling the complicated distribution pattern of Cu and its relationship to Al.

Even in the same textural fraction of FEF the concentrations of trace metals ranged broadly by factors of 4 to 9 depending on the metals in the study area. Following three factors could be considered to explain this finding; (1) textural composition in the fraction of <63 μm, (2) component composition of the host sediments, and (3) impact of human activities. The last one is eliminated by the reason discussed above. Concerning the first factor some researchers (Ackermann, 1980; Thorne and Nickless, 1981; Ackermann *et al.*, 1983) reported that fine fractions smaller than 20 μm contain much higher concentration of many kinds of metals than those of 20–60 μm do in estuarine sediments. As we did not separate the fraction smaller than 63 μm further, possibility of the factor (1) still remains to explain the wide range of trace metal concentrations. The high correlations, however, between the metals in the FEF suggest that the wide variation in mixing ratio of the sediment components, which are supposed to be

Table 8. Metal contents of coastal sedients and related materials (unit, $\mu g\ g^{-1}$) extracted from Chester (1990).

Metal	RSA sediment*	Near-shore mud	Continental crust	River Suspension	Crustal dust
Al	26800	84000	69300	94000	82000
Ca	222000	29000	45000	21500	---
Fe	19200	65000	35000	48000	48000
K	7690	25000	24000	20000	20000
Mg	28800	21000	16400	11800	---
Na	5330	40000	14200	5300	5100
Ti	2000	5000	3800	5600	5700
Co	9.1	13	13	20	23
Cu	18.4	56	32	100	47
Mn	354	850	720	1050	865
V	47.3	145	97	3	120
Zn	41.8	92	127	250	75

* Sediments of the ROPME Sea Area (<63 μm fraction).

aluminosilicate and ferromagnesian minerals and carbonates in the RSA, is the principal factor causing the wide range of variation in the trace metal concentrations.

Importance of Ca determination in the sediments of RSA

Particularly in the RSA, as our data showed that the trace metal concentrations are greatly affected by the contribution of carbonate fractions, it is very important to measure and evaluate Ca or carbonates concentrations as well as that of Al to compare trace metal data locally or temporally in the RSA and with other estuaries and coastal areas in the world. The concentrations of Co, Cu, Mn, V and Zn found in the fraction FEF in this study, which would be higher than those for the whole sediments, are still lower than any data for near-shore mud, crustal dust, river particulate material and continental crust compiled by Chester (1990) and shown in Table 8. This might be attributed to the diluting effect of the carbonates.

CONCLUSIONS

The analysis of trace and major metals in the textural fractions of sediments from the inner part of RSA has demonstrated that Co, Mn, V and Zn were mostly incorporated in the aluminosilicate and ferromagnesian minerals and the impact of human activities to the metal was minimal in the region. This conclusion is supported by the strong positive correlations between Al and each of Fe, Mg and the trace metals, and strong but negative correlations of Ca with Al, Fe, Mg and

the trace metals.

The trace metal concentrations in the finest fraction (<63 μm) varied considerably by factors 4 to 9 corresponding the changes in Al/Ca, Fe/Ca and Mg/Ca ratios. Higher concentrations of the trace metals were found in the eastern Iranian side where the sediment texture was muddy. In the RSA the trace metal concentrations are controlled basically by, in addition to the textural composition, the mixing ratio of the aluminosilicate and ferromagnesian minerals, and carbonates, which play roles of carriers and diluents of the trace metals, respectively.

Calcium concentrations were far highest among the metals examined even in the finest fraction throughout the study area. It is very important to measure Ca or carbonate concentration as well as that of Al for the charcterization of the sediment samples and evaluation of trace metal data in the sediments of the RSA.

Acknowledgments

The ROPME scientists on board the R-T/V Umitaka-Maru, Dr. A. A. Ibrahim as the team leader, and Dr. Otsuki and his team members of Japanese scientists from Tokyo University of Fisheries are highly appreciated for their cooperation in collecting sediment samples. Special thanks are extended to Messrs. K. Shimada, T. Hashimoto and T. Arai, Tokyo University of Fisheries, for their technical practice in operating the sampling gears. Captains Y. Saotome, T. Isouchi and K. Kasuga, their crew and the cadets on board the Umitaka-Maru are greatly thanked for their efforts to complete the stations as many as possible in spite of tough conditions. The necessary financial support was provided by the Ministry of Education, Culture, Science and Sport in Japan.

REFERENCES

Abaychi, L. K. & Douabul, A. A. Z. (1986). Trace element geochemical association in the Arabian Gulf. *Mar. Pollut. Bull.*, 8, 353–356.

Abu-Hilal, A. (1993). Observations on heavy metal geochemical association in marine sediments of the Jordan Gulf of Aqaba. *Mar. Pollut. Bull.*, 26, 85–90.

Ackermann, F. (1980). A procedure for correcting the grain size effect in heavy metal analyses of estuarine and coastal sediments. *Environ. Technol. Lett.*, 1, 518–527.

Ackermann, F., Bergmann, H. & Schleichert, U. (1983). Monitoring of heavy metals in coastal and estuarine sediments—A question of grain-size: <20 μm versus <60 μm. *Environ. Technol. Lett.*, 1, 317–328.

Al-Afraj, A. A. & Ibrahim, A. A. (1993). Chemical characterization of sediments from the Gulf area after the 1991 oil spill. *Mar. Pollut. Bull.*, 27, 97–101.

Al-Ghadban, A. N., Al-Dousari, A., Jacob, P. G., Behbehani, M. & Caceres, P. (1995). Mineralogy, genesis and sources of surficial sediments in the ROPME Sea Area. In *International Symposium on the Status of the Marine Environment in the ROPME Sea Area after the 1990–1991 Environmental Crisis with Special Emphasis to the Umitala-Maru Cruises* (A. Otsuki, ed.), pp. 11–12, 4–7 December, 1995, Tokyo University of Fisheries, Tokyo.

Al-Ghadban, A. N., Karam, H. & Al-Wayel, H. (1993). Textural characteristics of ROPME Sea Area bottom sediments. In *Final Report of the Scientific Workshop on Results of the R/V Mt. Mitchell Cruises in the ROPME Sea Area, vol. 1,* pp. 95–115. 24-28 January, 1993, ROPME/IOC(UNESCO)/UNEP/NOAA/EPC(Kuwait), Kuwait.

Basaham, A. & Al-Lihaibi, S. S. (1993). Trace elements in sediments of the western Gulf. *Mar.*

Pollut. Bull., 27, 103–107.

Bowen, H. J. M. (1979). In *Environmental Chemistry of the Elements,* Academic Press, London.

Calvert, S. E. (1976). The mineralogy and geochemistry of near-shore sediments. In *Chemical Oceanography, vol. 6* (J. P. Riley & R. Chester ed.), pp.187–280. Academic Press, London.

Chave, K. E. (1954). Aspects of the biogeochemistry of magnesium, 1. Calcareous marine organisms. *J. Geol.*, 62, 587–599.

Chester, R. (1990). *Marine Geochemistry.* Unwin-Hyman Ltd., London.

Chester, R. & Aston, S. R. (1976). The geochemistry of deep-sea sediments. In *Chemical Oceanography, vol. 6* (J. P. Riley & R. Chester eds.), pp.281–390. Academic Press, London.

Eisler, R. (1981). *Trace Metal Concentrations in Marine Organisms.* Pergamon Press, New York.

Förstner, U. & Salomons, W. (1980). Trace metal analysis on polluted sediments. Part I: Assessment of sources and intensities. *Environ. Technol. Lett.*, 1, 494–505.

Fowler, S. W., Readman, L. W., Oregioni, B., Villeneuve, J. -P. & McKay, K. (1993). Petroleum hydrocarbons and trace metals in nearshore Gulf sediments and biota before and after the 1991 War: An assessment of temporal and spatial trends. *Mar. Pollut. Bull.*, 27, 171–182.

Graf, D. L. (1960). Geochemistry of carbonate sediments and sedimentary rocks. Part III. *Illinois State Geol. Survey Circ.*, No. 309, 71p.

Haraguchi, H. (1986). *Fundamentals and Applications of ICP Atomic Emission Spectrometry.* Kodansha Ltd., Tokyo.

Kinsmann, D. J. J. (1966). Gypsum and anhydrite of recent age, Trucial Coast, Persian Gulf. In *Second Symposium on Salt, vol. 1* (J. L. Rau, ed.), 302–326, The Northern Ohio Geological Society.

Loring, D. H. (1982). Geochemical factors controlling the accumulation and dispersal of heavy metals in the Bay of Fundy sediments. *Can. J. Earth Sci.*, 19, 930–944.

Luoma, S. N. (1990). Processes affecting metal concentrations in estuarine and coastal marine sediments. In *Heavy Metals in Marine Environment* (R. W. Furness & P. S. Rainbow, eds.), 51–66, CRC Press, Boca Raton, Florida.

Marine Pollution Bulletin (1993). *The 1991 Gulf War: Coastal and Marine Environmental Consequences,* Pergamon Press, Oxford.

Poldervaart, A. (1955). Chemistry of the earth's crust. In *Crust of the Earth* (A. Poldervaart, ed.), 119–144, Geol. Soc. Amer., Special Paper 62.

Reynolds, R. M. (1993). Physical oceanography of the Gulf of Oman—Results from the Mt Mitchell expedition. *Mar. Pollut. Bull.*, 27, 35–59.

Salomons, W. & Förstner, U. (1980). Trace metal analysis on polluted sediments. Part II: Evaluation of environmental impact. *Environ. Technol. Lett.*, 1, 506–517.

Sheppard, C. R. C. (1993). Physical environment of the Gulf relevant to marine pollution: An overview. *Mar. Pollut. Bull.*, 27, 3–8.

Thorne, L. T. & Nickless, G. (1981). The relation between heavy metals and particle size fractions within the Severn Estuary (U. K.) inter-tidal sediments. *Sci. Total Environ.*, 19, 207–213.

Wedepohl, K. H. (1969–1974). *Handbook of Geochemistry.* Springer Verlag, Berlin.

Wheeler, R. B., Anderson, J. B., Schwarzer, R. R. & Hokanson, C. L. (1980). Sedimentary processes and trace metal contaminants in the Buccaneer oil/gas field, northwestern Gulf of Mexico. *Environ. Geol.*, 3, 163–175.

Williams, S. C., Simpson, H. J., Olsen, C. R. & Bopp, R. F. (1978). Sources of heavy metals in sediments of the Hudson River estuary. *Mar. Chem.*, 6, 195–201.

Windom, H. L., Schropp, S. J., Calder, F. D., Ryan, J. D., Smith Jr., R. G., Burney, L. C., Lewis, F. G. and Rawlinson, C. H. (1989). Natural trace metal concentrations in estuarine and coastal sediments of the southeastern United States. *Environ. Sci. Tech.*, 23, 314–320.

Offshore Environment of the ROPME Sea Area after the War-Related Oil Spill, Eds. A. Otsuki *et al.*, pp. 181–191.

Primary production in the ROPME Sea Area

T. HIRAWAKE[1]*, K. TOBITA[2]**, T. ISHIMARU[2], H. SATOH[1] and T. MORINAGA[1]

[1]*Department of Marine Science and Technology, Tokyo University of Fisheries, 5-7, Konan 4, Minato-ku, Tokyo 108-8477, Japan*
[2]*Department of Aquatic Biosciences, Tokyo University of Fisheries, 5-7, Konan 4, Minato-ku, Tokyo 108-8477, Japan*

Abstract—Primary production of phytoplankton was measured at 22 stations in the ROPME Sea Area (RSA) during the cruises of T/V Umitaka-Maru III in January 1993, December 1993, and December 1994.

Maximum photosynthetic rate at each station ranged from 2.6 to 8.5 mg C (mg chl.*a*)$^{-1}$h^{-1}. Chlorophyll *a* concentrations at sea surface in the investigated sites were within the range from 0.44 to 2.84 mg m^{-3} and their vertical distribution were homogeneous. Mean daily primary production in this area was estimated to be 0.51 gC m^{-2}day^{-1} with the range of 0.12–1.27 gC m^{-2} day^{-1}. The highest value (1.27 gC m^{-2}day^{-1}) was observed in the water off Hendorabi Island as well as the concentration of chlorophyll *a*. The primary production was high in the water off Iran near the entrance of the RSA, while the water off Qatar Peninsula to U.A.E. was low productive. It can be explained that the high primary productivity in the Iran side was attributed to the presence of high concentration of nitrate supplied from bottom of a basin off Iran, and the nitrate was consumed in the process of transport to U.A.E. side by currents within the RSA.

INTRODUCTION

The ROPME Sea Area (RSA) is enclosed by desert and has a shallow basin with no sill separating it from the open ocean. It has strong insolation through most of the year and the sea waters are warm and highly saline, but no remarkable vertical gradients have been observed (Seibold, 1973; Steinitz, 1973). The RSA was classified as one of the highest productive regions of the world ocean (Koblentz-Mishke *et al.*, 1970). A detailed information on primary production in this large sea area with extreme circumstances, however, has apparently not been reported to date. During the cruises of T/V Umitaka-Maru III of Tokyo University of Fisheries in January 1993, December 1993 and December 1994, a series of investigations for estimating primary production in this area were carried out. This paper summarizes the primary production data and attempts to explain it by relating to chemical and hydrographic features in studied area.

* Present address: National Institute of Polar Research, 9-10, Kaga 1, Itabashi-ku, Tokyo 173-8515, Japan.
** Present address: Tsukiji Market, Tokyo Metropolitan Central Wholesale Market, 2-1, Tsukiji 4, Tyuo-ku, Tokyo 104-0045, Japan.

MATERIALS AND METHODS

Photosynthetic productivity of phytoplankton was measured at 21 stations (Fig. 1) on the three cruises in the RSA. Seawater samples for photosynthetic productivity were collected using Van Dorn bottles from the sea surface and from 20 m and/or the depth at which 2–4% of surface light penetrated. Additional water samples were collected using a Rossete multi sampler equipped with a CTD system for measurement of chlorophyll *a* standing stock of phytoplankton.

For measurement of phytoplankton chlorophyll *a*, 200 ml of water sample was filtered through glass fiber filter (Whatman GF/F). The filter was immediately soaked in N,N-Dimethylformamide (DMF) and extracted pigments in the dark (Suzuki and Ishimaru, 1990). Concentration of chlorophyll a was determined fluorometrically with Turner Designs 10-005R fluorometer within a few days after the soaking (Parsons *et al.*, 1984).

Photosynthetic activity of phytoplankton was measured by the stable ^{13}C isotope method (Satoh *et al.*, 1985). Water samples were transferred into a 1000 ml clear poly carbonate bottles. After adding $NaH^{13}CO_3$ (approximately 10% of total carbonate, ISOTEC Inc.), the samples were incubated for 4 hours in a water bath controlled at surface water temperature under natural light (full sunlight, 46, 21, 11, 6% and dark). After the incubation, the water samples were filtered through glass fiber filters (Whatman GF/F) precombusted at 450°C for 4 hours. The filters were treated with HCl vapors to remove traces of inorganic carbon, and the isotope ratios of ^{12}C and ^{13}C were determined by infrared absorption spectrometry with a ^{13}C analyzer (EX-130, JASCO). The photosynthetic activity was

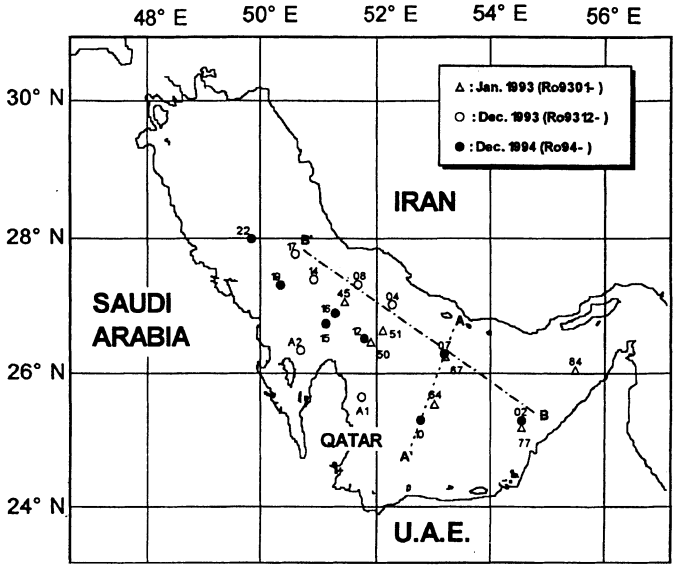

Fig. 1. Chart of the ROPME Sea Area showing the locations of sampling stations on the three cruises.

calculated by the equation of Hama *et al.* (1983), and the rate at each depth was calculated on the basis of P-I curve drawn by the model of Eilers and Peeters (1988).

Photosynthetically available radiation (PAR) was measured with an LI-190SB air quantum sensor and an LI-192SB underwater quantum sensor (LI.COR Inc.), and recorded with an LI-1000 (LI.COR Inc.) quantum meter.

Primary production in water column was estimated by integrating the value multiplied the photosynthetic rate by chlorophyll *a* concentration at each depth over the entire euphotic zone. Daily values of production were calculated on the basis of integrated PAR during the incubation period and during the whole day (Wetzel and Likens, 1991).

Nutrients were determined by the modified methods of standard procedures (Parsons *et al.*, 1984). The details of water sampling and the method were described by Hashimoto *et al.* (this volume).

Water temperature and salinity were measured with a CTD system. The sensor of salinity was calibrated with salinometer.

RESULTS AND DISCUSSION

Hydrographic condition

Values of surface temperature and salinity of each cruise are shown in Table 1. Water temperature in January 1993 (19.5–21.6°C) was lower than that in December 1993 (21.1–24.1°C) and 1994 (21.7–23.9°C). Water was well mixed throughout the water column except the stratified water at station Ro9301-84 as shown in Fig. 2. In general the salinity in this area was very high (37.24–40.89 PSU at surface) and water of more than 40 PSU was observed at most stations. At the surface layer of station Ro9301-84, the salinity was lowest (37.24 PSU) and the temperature was warmer (21.5°C) than at the other stations in January 1993. The low saline and warm water may have come from the Arabian Sea, because this station is located near the entrance of the RSA.

Chlorophyll a concentration

The ranges of chlorophyll *a* concentration and integrated value of chlorophyll *a* in water column for each cruise are shown in Table 2, respectively. Chlorophyll a concentrations at sea surface in this area were within the range from 0.44 at station Ro9412-12 to 2.84 mg m^{-3} at station Ro9301-84. The vertical

Table 1. Summary of temperature, salinity and surface nitrate concentration at the sampling stations during three cruises. Numbers in parenthesis represent the average values.

Cruise	Air Temp. (°C)	Water Temp. (°C)	Salinity (PSU)	Nitrate (μmol/l)
Jan. 1993	15.6 - 25.0 (18.5)	19.5 - 21.6 (20.7)	37.24 - 40.41 (39.55)	0.17 - 4.55 (2.00)
Dec. 1993	20.0 - 22.5 (21.7)	21.1 - 24.1 (22.9)	39.33 - 41.18 (39.99)	0.48 - 2.49 (1.36)
Dec. 1994	15.9 - 24.2 (21.2)	21.7 - 23.9 (22.9)	38.55 - 40.89 (40.11)	0.00 - 1.50 (0.72)

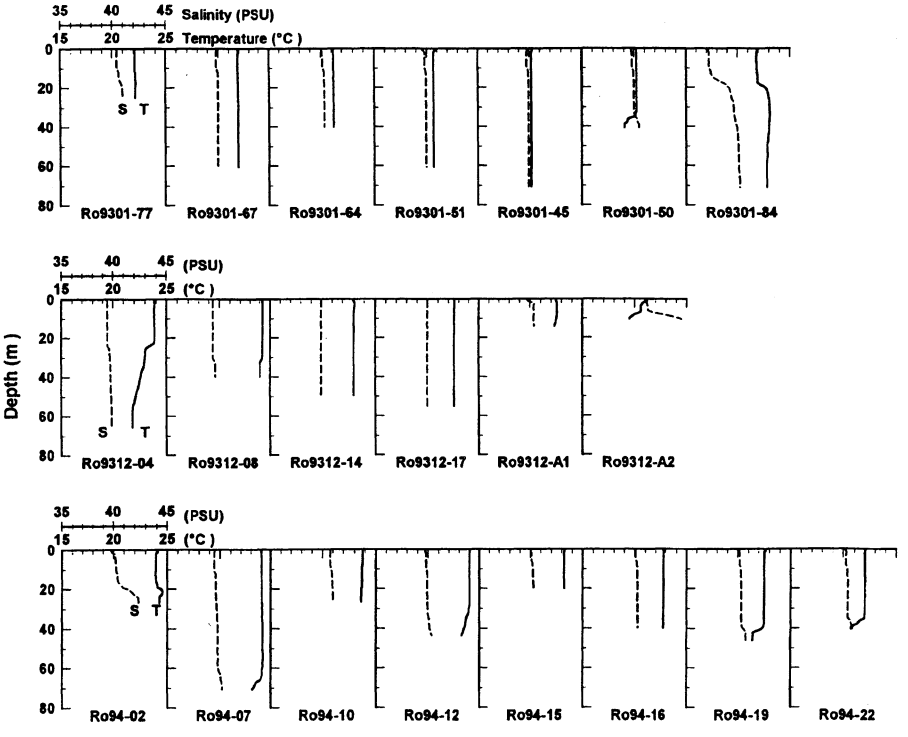

Fig. 2. Vertical profiles of water temperature (T) and salinity (S) at the sampling stations.

Table 2. Comparisons of values of chlorophyll *a* concentration, depth at which 1% of incident light penetrated, maximum photosynthetic rate, and daily primary production during three cruises. Numbers in parenthesis represent the average values.

Cruise	Number of Stations	Chlorophyll *a* Surface ($mg\ m^{-3}$)	Chlorophyll *a* Integrated ($mg\ m^{-2}$)	1 % Light Depth (m)	Maximum Photosynthetic Rate ($mg\ C \cdot mg\ chl.a^{-1} \cdot h^{-1}$)	Daily Primary Production ($g\ C \cdot m^{-2} \cdot day^{-1}$)
Jan. 1993	7	0.87 - 2.84 (1.74)	42.0 - 122.7 (77.6)	28	3.0 - 7.0 (5.3)	0.26 - 1.14 (0.55)
Dec. 1993	6	0.45 - 1.70 (0.85)	3.5 - 58.6 (30.2)	37	2.6 - 6.0 (4.5)	0.12 - 0.90 (0.33)
Dec. 1994	8	0.44 - 1.56 (0.86)	14.9 - 57.8 (32.0)	36	4.6 - 8.4 (6.3)	0.30 - 1.27 (0.62)
	Total 21	Average 1.15	46.7	34	5.5	0.51

distribution (Fig. 3) was homogeneous at most of stations. Integrated chlorophyll *a* in the water column ranged from 3.5 at station Ro9312-A2 to 122.7 mg m^{-2} at station Ro9301-67, and its highest value was observed in the water off Hendorabi Island (off Iran near the entrance of the RSA).

As shown in Table 1, water temperatures in January 1993 were lower than in December, so that a mixing of water in January was stronger than that in

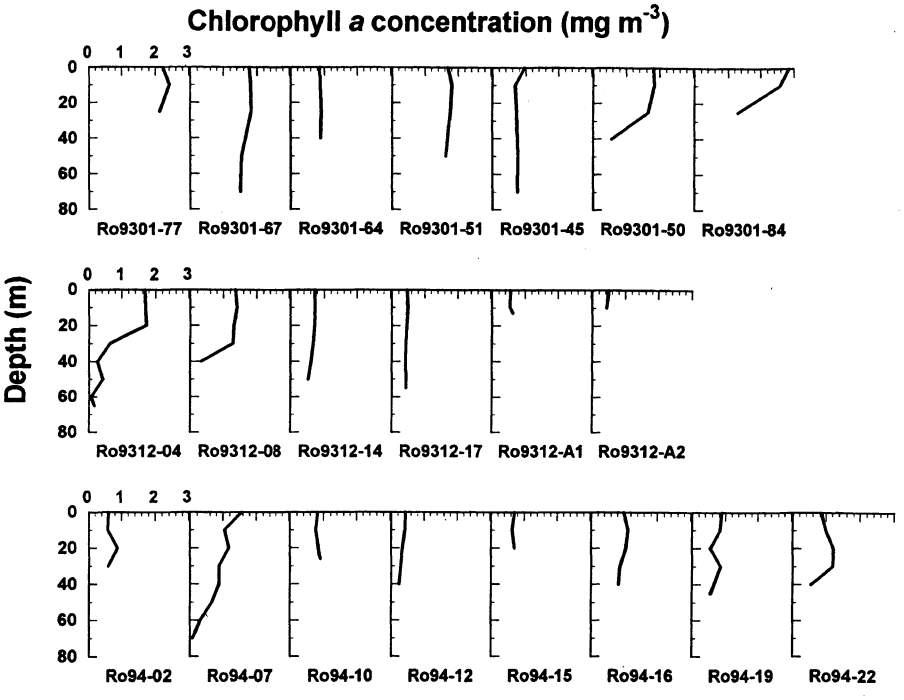

Fig. 3. Vertical distributions of chlorophyll *a* concentration (mg m^{-3}) at the sampling stations.

December. The strong mixing of water in January 1993 could transport rich nitrate (Table 1) up to the sea surface from the bottom. Accordingly, chlorophyll *a* concentrations in January 1993 were remarkably higher than the values of December.

Photosynthetic rates and P-I curves

Maximum photosynthetic rate (P_{max}) calculated from photosynthesis-Irradiance (PAR) curve (P-I curve) at each station, as shown in Table 2, ranged from 2.6 to 8.4 mg C (mg chl.*a*)$^{-1}h^{-1}$ with the mean value of 5.5 mg C (mg chl.*a*)$^{-1}$ h^{-1}. The highest value was observed at the station Ro94-07 in the waters off Hendorabi Island and the lowest was observed at Ro9312-A1 in the waters off east of Qatar Peninsula. These values are higher than the value of oligotrophic oceanic waters, e.g.: 2.09 mg C (mg chl.*a*)$^{-1}h^{-1}$ in the winter convection area of the eastern Arabian Sea (Goes *et al.*, 1993), 0.3–0.7 mg C (mg chl.*a*)$^{-1}h^{-1}$ in the Kuroshio in summer (Ichimura and Aruga, 1964), 1.4–2.0 mg C (mg chl.*a*)$^{-1}h^{-1}$ in western part of the North Pacific (Takahashi *et al.*, 1972), and same level compared with some bays and coastal regions in Japan (2–6 mg C (mg chl.*a*)$^{-1}$ h^{-1}; Ichimura and Aruga, 1964).

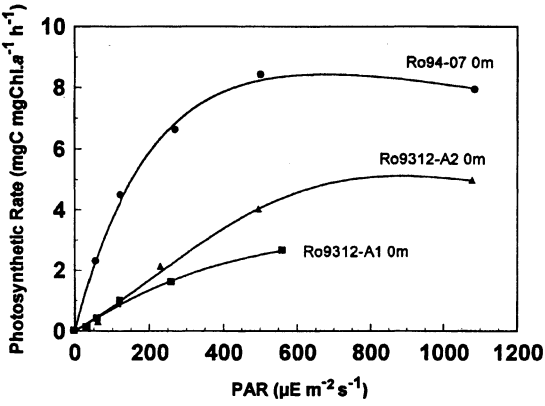

Fig. 4. Photosynthesis-Irradiance curves of phytoplankton collected from surface waters at the station of Ro94-07, Ro9312-A1, and Ro9312-A2.

P-I curves of phytoplankton at the surface of typical three stations are shown in Fig. 4. As shown by P-I curve of the surface water at Ro94-07, photosynthetic rate was saturated at the light intensity between 150 and 450 μE $m^{-2}s^{-1}$ at most stations. In the waters off Qatar Peninsula (Ro9312-A1, A2), saturated intensity was high at the range 500 to 600 μE $m^{-2}s^{-1}$, but the P_{max} was lower than other stations. This is probably due to loss of photosynthetic activity.

Primary production

The regional distributions of primary production in the studied area for each survey are shown in Figs. 5(a), 5(b) and 5(c). The levels of production are classified as four wide ranges, viz.: <0.26, 0.26–0.50, 0.51–1.00, and >1.00 gC $m^{-2}day^{-1}$.

In January 1993 (Fig. 5(a)), highest value of production (1.14 gC $m^{-2}day^{-1}$) was observed in the entrance of the RSA. The water off Iran was more productive rather than the water off U.A.E.

Primary production in December 1993 (Fig. 5(b)) was low in comparison with values obtained during other cruises. This is caused by low solar radiation during the incubation in this cruise. The highest value (0.90 gC $m^{-2}day^{-1}$) was observed in the waters off west of Hendorabi Island. While the low productive areas (<0.26) were observed in the waters off Qatar Peninsula and northern part of the RSA off Iran. Two low areas were separated by a band of a little high productive water.

In December (Fig. 5(c)), high productive area (>1.00 gC $m^{-2}day^{-1}$) and the highest value (1.27 gC $m^{-2}day^{-1}$) were observed in the waters off south of Hendorabi Island as well as the distribution of chlorophyll *a* concentration. The area was expanded toward northern part of the RSA and somewhat along the isobathymetric line. The waters of Iran side was higher in productivity than the waters of the other side.

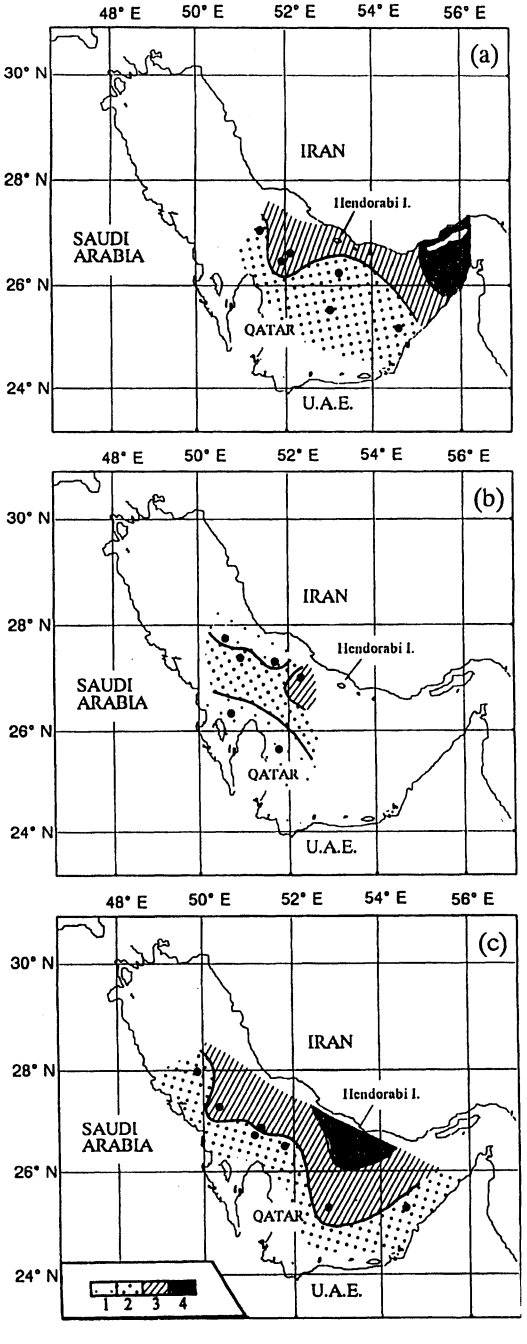

Fig. 5. Horizontal distributions of daily primary production of phytoplankton (gC m^{-2} day^{-1}) in January 1993 (a), December 1993 (b), and December 1994 (c). (1) Less than 0.26; (2) 0.26–0.50; (3) 0.51–1.00; (4) more than 1.00 gC m^{-2} day^{-1}.

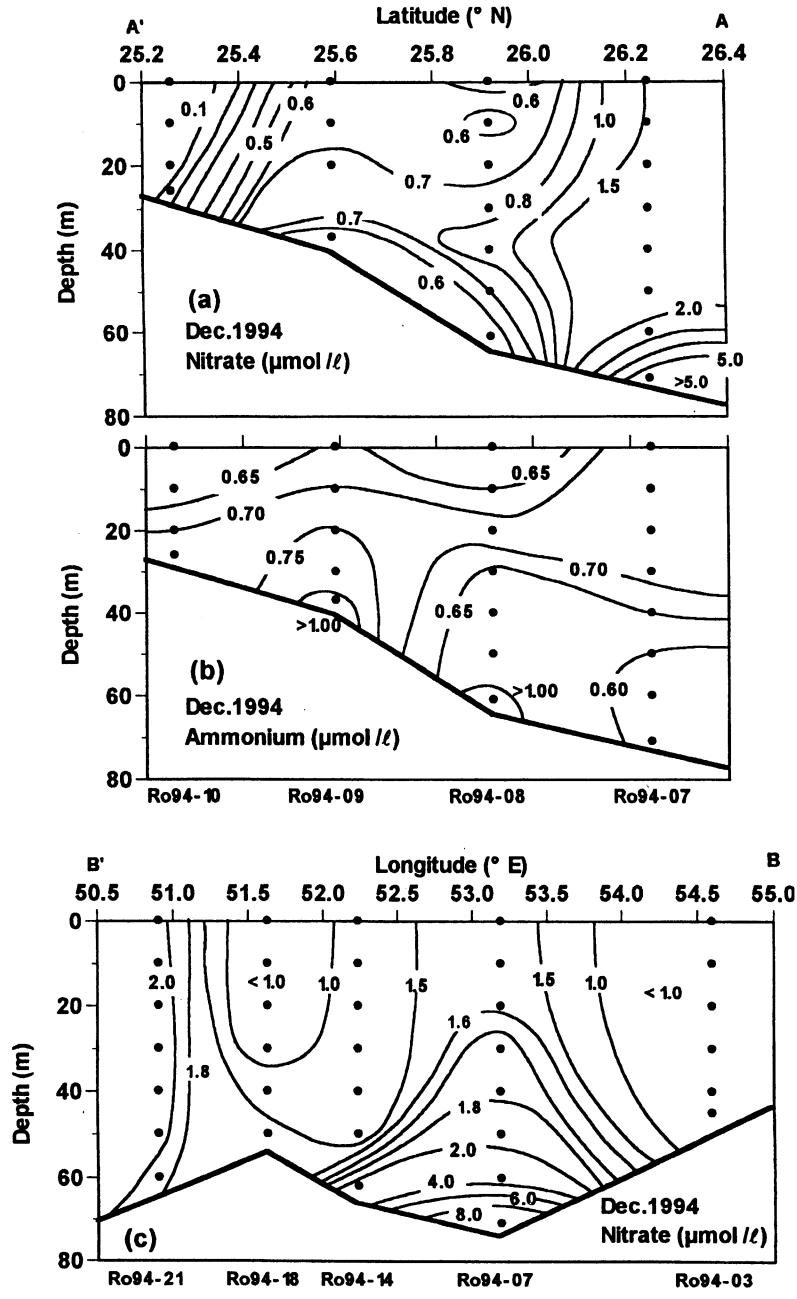

Fig. 6. Spatial distribution of nitrate (a) and ammonium (b) along the observation line A-A' shown in figure 1. (c) Spatial distribution of nitrate along the observation line B-B' shown in figure 1.

In most cases, horizontal distributions of primary production were geographically consistent over relatively large areas and corresponded with chemical and physical conditions. Spatial distributions of nitrate and ammonium (Hashimoto *et al.*, this volume) in December 1994 along the line A-A′ passed the station Ro94-07 (Fig. 1) and nitrate distribution along the line B-B′ are shown in Figs. 6(a), 6(b) and 6(c), respectively. High concentrations of nitrate (more than 5.0 μmol/l) were distributed at near the bottom of the Central Basin (depths to 105 m near station Ro94-07). The value on the Iran side was higher than on U.A.E. side (Fig. 6(a)). However, the value of ammonium was relatively constant (Fig. 6(b)). This rich nitrate at the bottom are supplied to the surface by vertical mixing or weak upwelling induced to NE monsoon (Fig. 6(b)). Furthermore, the low saline and warm oceanic water from Arabian Sea flows into the RSA and moves along the coast of Iran, as reported by Reynolds (1993). The oceanic water encounters with the high nitrate water and forms high productive water (Fig. 7). The nitrate in the high productive water mass is consumed in the process of approaching to the northern part of the RSA. The current turns in the northern part or center of the RSA and the low nitrate water (left side of Fig. 6(a)) flow toward the entrance. Therefore it is suggested that the primary production is high in the water off Iran near the entrance of the RSA, while the water off Qatar Peninsula to U.A.E. is low in productivity. Because of the lack of nitrate off Qatar Peninsula and U.A.E., it

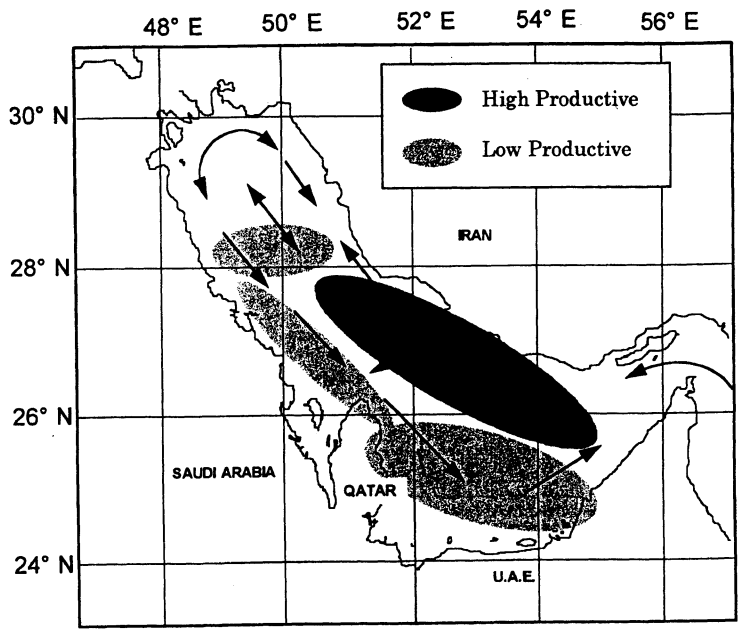

Fig. 7. Shematic figure of surface currents in ROPME Sea Area (after Reynolds, 1993), and high and low productive areas in the RSA.

is more assumed that the primary production of the U.A.E. side is "regenerated production" associated with ammonium (regenerated nitrogen), as proposed by Dugdale and Goering (1967) and Eppley and Peterson (1979).

The values of daily primary production in the RSA are summarized in Table 2. Mean daily primary production in the present study was estimated to be 0.51 gC $m^{-2}day^{-1}$. The value for this region as illustrated by Koblentz-Mishke *et al.* (1970) was more than 0.5 gC $m^{-2}day^{-1}$. Our results show the wide range of 0.12–1.27 gC $m^{-2}day^{-1}$. These values are almost the same as compared with value obtained from the Gulf of Elat (Aqaba), Red Sea which is also desert-enclosed sea and as the same latitude, and its highest recorded value in winter is 1.12 gC $m^{-2}day^{-1}$ (Levanon-Spanier *et al.*, 1979).

CONCLUSION

We were able to determine the level of the primary production in the RSA and to relate the distribution to nutrient and current pattern during the NE monsoon season. However, the measurements in this survey were made in the waters from the entrance towards the center of the RSA in January and December. It is considered that the distribution pattern and the level of the primary production directly influenced by seasonal change in the direction of the flow of water. As is generally well known, the currents in this area are determined by the monsoons, NE monsoon during the months of October to March and SW one during May to October. Therefore, it is necessary to continue the survey of the primary production in the whole of the RSA and during all seasons to estimate the annual primary production and to better establish the relationship between production and nutrients.

Acknowledgements

We are grateful to Capt. Y. Saotome, Capt. T. Isouchi, Capt. I. Kasuga, and the officers and crew of the T/V Umitaka Maru III, Tokyo Univ. of Fish. (T.U.F.) for their cooperation during the cruises. Thanks are also due to Prof. A. Otsuki, the leader of T.U.F. team and Dr. Ibrahim Alam, the leader of the Regional Organization for the Protection of the Marine Environment (ROPME) team, for good conduct of the cruises. We thank members of ROPME and T.U.F., for help provided on board the ship. We would like to thank Dr. Takeda, Central Institute of Electric Power Industry, for his support during the analysis of ^{13}C.

REFERENCES

Dugdale, R. C. and Goering, J. J. (1967). Uptake of new and regenerated forms of nitrogen in primary productivity. *Limnol. Oceanogr.* **12**, 196–206.

Eilers, P. H. C. and Peeters, J. C. H. (1988). A model for relationship between light intensity and the rate of photosynthesis in phytoplankton. *Ecol. Modeling* **42**, 199–215.

Eppley, R. W. and Peterson, B. J. (1979). Particulate organic matter flux and planktonic new production in the deep ocean. *Nature* **282**, 677–680.

Goes, J. I., Gomes, H. do R., Kumar, A., Gouveia, A., Devassy, V. P., Parulekar, A. H. and Rao, L. V. G. (1993). Satellite and ship studies of phytoplankton along the west coast of India. In

Oceanography of the Indian Ocean (B. N. Desai, ed.), pp. 67–80. A.A. Balkema, Rotterdam.

Hashimoto, S., Tsujimoto, R., Maeda, M., Ishimaru, T., Yoshida, J., Takasu, Y., Koike, Y., Mine, Y., Kamatani, A. and Otsuki, A. (1998). Distribution of nutrients, chlorophyll *a* and nitrous oxide in the ROPME Sea Area in winter of 1993–94. this volume.

Hama, T., Miyazaki, T., Ogawa, Y., Iwakuma, T., Takahashi, M., Otuki, A. and Ichimura, S. (1983). Measurement of photosynthetic production of marine phytoplankton population using a stable ^{13}C isotope. *Mar. Biol.* **73**, 31–36.

Ichimura, S. and Aruga, Y. (1964). Photosynthetic natures of natural algal communities in Japanese waters. In Recent R*esearches in the Fields of Hydrosphere, Atmosphere and Nuclear Geochemistry* (Y. Miyake and T. Koyama, eds.), pp. 13–37. Maruzen, Tokyo.

Koblentz-Mishke, O. J., Volkovinsky, V. V. and Kabanova, J. G. (1970). Plankton primary production of the world ocean. In *Scientific Exploration of the South Pacific* (W. S. Wooster, ed.), pp. 183–193. National Academy of Sciences, Washington.

Levanon-Spanier, I., Padan, E. and Reiss, Z. (1979). Primary production in a desert-enclosed sea—the Gulf of Elat (Aqaba), Red Sea. *Deep-Sea Res.* **26**(6a), 673–685.

Parsons, T. R., Maita, Y. and Lalli, C. M. (1984). *A Manual of Chemical and Biological Methods for Seawater Analysis*. Pergamon Press.

Reynolds, R. M. (1993). Physical oceanography of the Gulf, Strait of Hormuz, and the Gulf of Oman—Results from the *Mt Mitchell* expedition. *Mar. Pollut. Bull.* **27**, 35–59.

Satoh, H., Yamaguchi, Y., Kokubun, N. and Aruga, Y. (1985). Application of infrared absorption spectrometry for measuring photosynthetic production of phytoplankton by the stable ^{13}C isotope method. *La mer* **23**(4), 171–176.

Seibold, E. (1973). Biogenic sedimentation of the Persian Gulf. In *The Biology of the Indian Ocean* (B. Zeitzschel, ed.), pp. 103–114. Springer-Verlag, Berlin/Heidelberg/New York.

Steinitz, H. (1973). Fish ecology of the Red Sea and Persian Gulf. In *The Biology of the Indian Ocean* (B. Zeitzschel, ed.), pp. 465–466. Springer-Verlag, Berlin/Heidelberg/New York.

Suzuki, R. and Ishimaru, T. (1990). An improved method for the determination of phytoplankton chlorophyll using N,N-Dimethylformamide. *J. Oceanogr. Soc. Japan* **46**, 190–194.

Takahashi, M., Satake, K. and Nakamoto, N. (1972). Chlorophyll profile and photosynthetic activity in the north and equatorial Pacific Ocean. *J. Oceanogr. Soc. Japan* **28**, 27–36.

Wetzel, R. G. and Likens G. E. (1991). Primary productivity of phytoplankton. In *Limnological Analysis Second Edition* (R. G. Wetzel and G. E. Likens, eds.), pp. 207–226. Springer-Verlag.

Offshore Environment of the ROPME Sea Area after the War-Related Oil Spill, Eds. A. Otsuki *et al.*, pp. 193–202.

Post-spill spatial distribution of zooplankton in the ROPME Sea Area

Faiza AL-YAMANI, Kholood AL-RIFAIE, Hussain AL-MUTAIRI and Wafa ISMAIL

Kuwait Institute for Scientific Research, Kuwait

Abstract—The ROPME Sea Area is a rich habitat for numerous species of marine flora and fauna. Zooplankton play a major role in the marine food chain leading to the production of organisms of economical value such as shrimp and fish.

The Gulf crisis in 1991 resulted in a massive oil spill of 6–8 million barrels of crude oil that was spilled in the Gulf, therefore, threatening its environment and resources. During 18–24 December 1993, 19 Gulf stations were sampled for plankton and key oceanographic variables. Zooplankton samples were obtained from vertical hauls with a 110 μm NORPAC nets. The samples were preserved in 5% buffered formaldehyde, enumerated and identified to the lowest taxon possible. The objectives of this short-term study were to determine the zooplankton community structure, abundance, and the spatial distribution of the different kinds of zooplankton.

Over 75 genera and species of zooplankton were identified in the Gulf samples collected, and abundance of major groups as well as identified genera and species are reported.

Copepods dominated the zooplankton followed by nauplii. Copepods and nauplii composed more than 64% of the total zooplankton. Mollusc larvae, ostracods and chordates followed copepods and nauplii in abundance. The southern stations displayed higher numbers of ostracods, especially along the eastern coast of the Gulf. In general, total zooplankton abundance was higher on the western side of the Gulf than on the eastern side.

In general, calanoid and cyclopoid copepods were equally abundant. The three most abundant copepod genera were *Oithona*, *Onceae* and *Paracalanus*. The most abundant ostracod species was *Euconchoecia aculeata*, while the most abundant cladoceran was *Penillia avirostris*. *Oikopleura* spp. dominated the larvacean population.

The evaluation of the data on hydrographic conditions during this study, indicate no major differences in temperature and salinity values among the different stations during the period of the study, however, some regional differences in the abundance and distribution of the different kinds of zooplankton are evident.

In general, distribution and dominance of key zooplankton species obtained from this post-spill study resemble the pre-spill results reported by previous studies.

INTRODUCTION

The Gulf crisis in 1991 resulted in a massive oil spill of 6–8 million barrels of crude oil that was spilled in the Gulf, therefore, threatening its environment and

resources. Following the above massive oil spill, two research vessels surveyed the ROPME Sea Area following the crisis, namely, the *Mt. Mitchell* and the *Umitaka Maru* where several studies on the physical, chemical, and biological characteristics as well as on potential pollution impacts were conducted.

A considerable body of information is available on the zooplankton of the Gulf for the pre-spill period (Frontier, 1963; Kimor, 1973; Yamazi, 1974; Basson *et al.*, 1977; Gibson *et al.*, 1980; Halim, 1984; Michel *et al.*, 1986; Al-Yamani, 1989; Sheppard *et al.*, 1992). For the post-spill period, Al-Yamani *et al.* (1993) and Al-Aidaroos (1993) reported on the plankton distribution of the post-spill period during spring (April and May, 1992) as part of the *Mt. Mitchell* Gulf cruise studies. The mesh sizes of the plankton nets used in the *Mt. Mitchell* study were 64 μm and 335 μm.This study, which is part of the Umitaka-Maru cruises to survey inner ROPME Sea Area, constitutes a short-term post-spill investigation of the Gulf during winter (December 1993) to assess the possible effect of the above pollution on the distribution of the Gulf plankton population. It presents comparative abundance and spatial distribution patterns of different groups of zooplankton between the post-spill Umitaka-Maru survey and pre-spill results.

MATERIALS AND METHODS

Physicochemical oceanographic variables were measured during 18–24 December 1993, at 19 Gulf stations (Table 1, Fig. 1). Zooplankton samples were obtained from vertical hauls with a 100 μm NORPAC nets of 45 cm diameter ring. The samples were preserved in 5% formaldehyde buffered with sodium borate, enumerated and identified at Kuwait Institute for Scientific Research Plankton

Table 1. Sampling station information (NORPAC net).

St.	Sampling depth (m)	Date	Latitude (°N)	Longitude (°E)	Total depth (m)
1	64	18-12-93	26 14.60	53 11.60	74.4
2	57	18-12-93	25 54.38	53 07.86	63.3
3	38	19-12-93	25 34.19	53 00.86	41
4	59	20-12-93	26 58.10	52 17.20	69.5
5	58	20-12-93	27 43.50	52 02.70	66.9
6	42.3	20-12-93	26 27.90	51 48.50	46
7	23	20-12-93	26 13.00	51 35.20	25.6
8	38	21-12-93	27 16.10	51 41.40	42.5
9	70	21-12-93	27 06.60	51 29.70	72.2
10	64	21-12-93	26 56.90	51 19.90	72.2
11	23	21-12-93	26 44.50	51 09.70	25
12	15	21-12-93	26 34.90	50 54.90	15.9
13	64	23-12-93	27 32.60	51 06.50	67.8
14	50	23-12-93	27 20.80	50 54.50	52
15	64	23-12-93	27 07.80	50 41.70	65.2
16	62	24-12-93	27 52.60	60 46.70	63.2
17	54	24-12-93	27 43.50	50 33.20	56.9
18	59	24-12-93	27 36.00	50 17.80	61.7
19	62	24-12-93	27 27.70	50 03.70	57.3

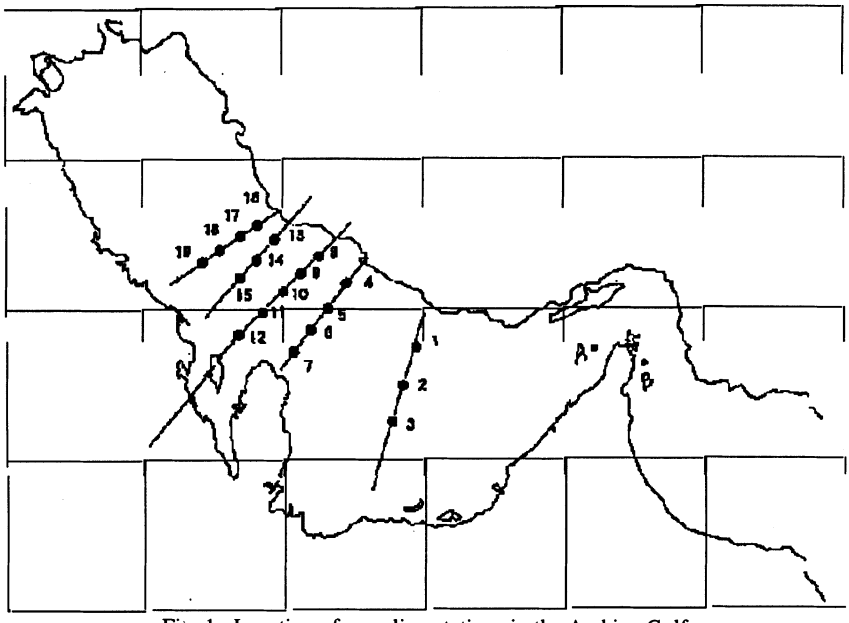

Fig. 1. Location of sampling stations in the Arabian Gulf.

Laboratory, to the lowest taxon possible.

Major zooplankton groups were enumerated and identified from the *Umitaka-Maru* Gulf samples to describe the spatial distribution of these groups and their most abundant species, during the December 1993 sampling period.

Descriptive statistics were applied to the data, and all mean values are reported with ±S.E. Sampled stations were identified on different transects, extending from the Iranian coast to the Arabian coast (roughly in an east-west manner, considering south being the entrance of the Gulf off the Strait of Hormuz, while north of the Gulf, being at the other end off Shatt al-Arab). Stations 1–3 fall on transect 1 (T1), 4–7 on transect 2 (T2), 8–12 on transect 3 (T3), 13–15 on transect 4 (T4), and stations 16–19 fall on transect 5 (T5) (Fig. 1).

The objectives of this short-term study were to determine the post-spill zooplankton community structure during the December 1993 cruise, zooplankton abundance (no./m^3), and the spatial distribution of the different kinds of zooplankton, with comparative reference to previous pre–spill Gulf studies.

RESULTS AND DISCUSSION

Physico-chemical parameters

Physico-chemical oceanographic variables were measured on board the *Umitaka-Maru* by the cruise team of Tokyo University of Fisheries. These data [temperature (°C), salinity (‰), dissolved oxygen (ml/l), phosphate (μmol/l),

silicate (μmol/l), nitrate (μmol/l), and chlorophyll-*a* (μg/l)] were made available to cruise participants (Dr. Otsuki, personal communication, December 1995). The use of these data in this study is merely to indicate any significant spatial pattern of these variables and their relevance to the zooplankton population distribution.

Mean surface temperature during the cruise period was 23.38°C (±0.18), while mean bottom temperature was 22.83 (±0.23). Temperature did not show a marked difference (<2°C) amongst the 19 stations sampled. A slight difference in temperature between surface and bottom layers, was evident at stations 1 (range = 2.22°C), 4 (range = 2.04°C), 6 (range = 1.51°C), 7 (range = 1.93°C), and 19 (range = 1.17°C).

Mean surface salinity was 39.80‰ (±0.18), while bottom salinity had a mean of 40.13 (±0.15). A slight vertical stratification (surface having lower values) was evident at stations 6 (range = 1.52‰), and 7 (range = 2.31‰).

Mean value of surface dissolved oxygen was 4.44 ml/l (±0.04), while mean value of bottom layer was 3.87 (±0.25). Difference between surface and bottom values was evident at stations 1 (range = 2.90 ml/l), 4 (range = 3.31 ml/l) and 8 (range = 2.20 ml/l), where surface values were higher than bottom values.

Mean surface value of phosphate was 0.28 μmol/l (±0.02), while mean bottom concentration was 0.43μmol/l (±0.07). Appreciable difference in concentration between surface and bottom (bottom being higher in concentration) was evident at stations 1 (range = 0.85 μmol/l), 4 (range = 0.96 μmol/l), and 8 (range = 0.66 μmol/l).

Mean surface concentration for silicate was 3.92 μmol/l (±0.22), while mean bottom concentration was 5.97 μmol/l (±0.87). Marked difference between surface and bottom values (bottom values being higher) was found at stations 1 (range = 11.00 μmol/l), 4 (range = 12.50 μmol/l), and 8 (range = 7.70 μmol/l).

Mean nitrate concentration was 1.22 μmol/l (±0.25) at the surface, and 3.56 μmol/l (±1.13) for mean bottom concentration. High bottom concentrations were found at stations 1 (17.51 μmol/l), 4 (13.74 μmol/l), and 8 (10.08 μmol/l).

Mean surface chlorophyll-*a* value was 1.09 μg/l (±0.16), while bottom concentration was 0.53 μg/l (±0.06). Relatively high (>1.0 μg/l) surface chlorophyll-*a* values were found at stations 4 (1.70 μg/l), 5 (1.84 μg/l), and 9 (3.36 μg/l).

ZOOPLANKTON COMMUNITY ANALYSIS

Mean abundance of zooplankton was 20,645/m³ (±3282) with a minimum of 9,363/m³ recorded at station 13, and a maximum abundance of 72,260/m³ at station 11. Four stations displayed zooplankton abundance greater than 25,000/m³, namely, stations 11 (72,260/m³), station 7 off Qatar (34,701/m³), station 3 (30,267/m³), and station 19 (26,361/m³).

Results of the previous studies in the Gulf (Table 2) indicated that copepods are the most numerous zooplankton group in the ROPME Sea Area. In the present study, the most abundant zooplankton groups (>1%) in terms of percentage

Table 2. Percentage composition of the 7 most abundant zooplankton groups in the ROPME Sea Area based on estimates of three zooplankton studies.

Yamazi, 1974 December 1968 Net size = 330 μm	**Michel et al., 1986** November 1979 Net size = 110 μm	**Present study, 1993** December 1993 Net size = 100 μm
Group (% composition)	Group (% composition)	Group (% composition)
Copepods (52.4%)	Copepods (74%)	Copepods (51.7%)
Cladocerans (15.3%)	Molluscs (13.3%)	Molluscs (10.7%)
Ostracods (9%)	Chordates (7.5%)	Ostracods (8.8%)
Chordates (6.2%)	Ostracods (2.2%)	Chordates (5.0%)
Chaetognaths (5.8%)	Cladocerans (1.6%)	Protozoans (4%)
Protozoans (3.7%)	Chaetognaths (0.8%)	Chaetognaths (1.4%)
Molluscs (2.4%)	Decapods (0.2%)	Polychaete Larvae (0.9%)

composition of the total zooplankton are copepods constituting 51.7% (67% of including copepodites and nauplii), molluscs (11%), ostracods (9%), chordates (5%), protozoans (4%), and chaetognaths (1%), while all other zooplankton groups constituted a total of 3%. In the category of the other zooplankton groups, polychaete larvae composed 0.9% of total zooplankton, followed by decapod larvae (0.5%), cnidarians (0.3%), cladocerans (0.1%), and fish larvae (0.02%). In general, copepods, mollusc larvae, ostracods and chordates were within the four most abundant zooplankton groups in this study as well as in Michel *et al.*'s (1986) study (Table 2). Emphasis in this study was placed on copepods, molluscs, ostracods, chordates, chaetognaths, and cladocerans.

Copepods

Adult copepods had a mean abundance of 10680 ± 1383, and were the most dominant group at all stations, with a percentage composition ranging from 41.3 to 62.7 of total zooplankton abundance. Copepods and copepod nauplii, on the average, composed more than 64% of the total zooplankton. In general, copepods were more abundant at stations along the western side of the ROPME Sea Area (on all the five transects), than on the eastern side.

On the average, calanoids composed 49% of total copepod population, followed by cyclopoids (46%) and harpacticoids (5%). Michel *et al.* (1986) found that cyclopoid abundance approximated calanoid abundance in the Gulf waters south of Kuwait. In our samples, calanoids and cyclopoids were equally abundant at all stations sampled, except at station 11, where calanoids were 2.5 times more abundant than cyclopoids, and at station 4, where cyclopoids were 2.5 times more abundant than calanoids. Yamazi (1974) found that the distribution of cyclopoids in the Gulf was apparently uniform whereas the present study show a marked increase in numbers of cyclopoids at the western stations of the ROPME Sea Area.

The most abundant calanoids were *Paracalanus crassirostris* (770.6/m^3),

Table 3. Dominant copepod genera, their percentage composition out of the total copepod population, their abundance (no./m^3), total copepod abundance (no./m^3), and total zooplankton abundance (no./m^3) at each sampled station along the different transects (T).

Stn	Depth (m)	Location	Dominant Copepod	% Composition	Abundance of genera	Total Copepod Abundance	Zooplankton Abundance
1	74.4	T1	Oncaea	30.0	2484	8294	13764
			Oithona	15.6	1993		
			Corycaeus	3.8	317		
			Paracalanus	3.7	304		
2	63.3	T1	Oithona	36.1	1765	4896	9411
			Oncaea	11.9	583		
			Paracalanus	3.9	192		
			Corycaeus	2.2	105		
3	41.0	T1	Oithona	37.9	6047	15973	30267
			Paracalanus	14.5	2320		
			Oncaea	7.6	1213		
			Euterpina	7.0	1113		
4	69.5	T2	Oithona	56.7	5358	9446	18906
			Paracalanus	8.7	818		
			Oncaea	7.6	716		
			Macrosetella	6.1	574		
5	66.9	T2	Oithona	31.4	2405	7671	16229
			Oncaea	7.4	570		
			Paracalanus	5.7	437		
			Corycaeus	3.6	272		
6	46.0	T2	Oithona	37.5	3340	8917	14691
			Paracalanus	10.1	899		
			Oncaea	5.0	450		
			Corycaeus	1.9	165		
7	25.6	T2	Oithona	22.7	3261	14354	34701
			Paracalanus	16.0	2295		
			Oncaea	13.3	1913		
			Corycaeus	7.5	1075		
			Euterpina	4.3	619		
8	42.5	T3	Oithona	59.3	3531	5951	14319
			Oncaea	5.8	346		
			Paracalanus	5.0	296		
			Corycaeus	1.5	86		
			Microsetella	1.5	86		
			Euchaeta	1.1	62		
9	72.2	T3	Oithona	25.2	3429	13610	25078
			Oncaea	8.9	1210		
			Paracalanus	4.8	648		
			Euterpina	2.1	286		
10	72.2	T3	Oithona	32.7	2324	7108	12574
			Oncaea	17.0	1206		
			Paracalanus	6.5	461		
			Corycaeus	2.5	177		
			Euchaeta	1.2	88		
11	25.0	T3	Paracalanus	20.9	6521	31173	72260
			Oncaea	10.2	3163		
			Corycaeus	9.5	2968		
			Oithona	6.9	2141		

Table 3. (continued)

Stn	Depth (m)	Location	Dominant Copepod	% Composition	Abundance of genera	Total Copepod Abundance	Zooplankton Abundance
12	15.9	T3	Oithona	25.4	3071	12095	19267
			Oncaea	22.6	2738		
			Paracalanus	14.6	1762		
			Corycaeus	3.9	476		
13	67.8	T4	Oithona	27.6	1609	5837	9363
			Oncaea	15.9	926		
			Paracalanus	11.2	655		
			Microsetella	2.9	168		
14	52.0	T4	Paracalanus	20.5	1556	7587	12341
			Oncaea	26.0	1975		
			Oithona	17.1	1301		
			Corycaeus	3.1	232		
15	65.2	T4	Oithona	25.3	2526	9987	16585
			Oncaea	25.1	2509		
			Paracalanus	15.4	1535		
			Corycaeus	5.	543		
			Microsetella	4.8	474		
16	63.2	T5	Oithona	29.3	2560	8737	17095
			Oncaea	22.3	1948		
			Paracalanus	20.5	1793		
			Corycaeus	2.3	197		
			Microsetella	2.3	197		
17	56.9	T5	Oithona	25.7	1409	5475	10093
			Oncaea	20.6	1125		
			Paracalanus	16.8	921		
			Corycaeus	4.6	250		
18	61.7	T5	Oncaea	27.9	2724	9767	18944
			Oithona	16.2	1585		
			Paracalanus	16.8	1642		
			Corycaeus	6.2	610		
19	57.3	T5	Oithona	28.1	4500	16040	26361
			Oncaea	15.2	2441		
			Paracalanus	12.2	1951		
			Corycaeus	7.0	1128		

and *Paracalanus aculeatus* (650.7/m³); most abundant cyclopoids were *Oithona* spp. (2850.2/m³), followed by *Oncaea* spp. (1591.5/m³); and the most abundant harpacticoids were *Euterpina acutifrons* (213/m³), followed by *Microsetella rosea* (187/m³), and *Macrosetella gracilis* (95/m³).

Several genera dominated the copepod population at the different stations sampled (Table 3). *Oithona* was the most abundant genus at all stations except stations 1 (*Oncaea* was the most abundant), 11 (*Paracalanus* was the most abundant), and 14 (*Paracalanus* was the most abundant). In general, *Oithona* spp. was found to be the dominant genus in this study, in Michel *et al.*'s study and in Yamazi's study.

The seven most abundant copepod genera and species constituting a mean abundance of more than 100/m³ in the December 1993 study are: *Oithona* spp. (2,850.2/m³), *Oncaea* spp. (1,591.5/m³), *Paracalanus crassirostris* (770.6/m³), *Paracalanus aculeatus* (650.7/m³), *Euterpina acutifrons* (213/m³), *Corycaeus speciosus* (191/m³) and *Microsetella rosea* (187/m³). Michel *et al.* (1986) listed the following seven most abundant species in terms of numerical order during November 1979: *Paracalanus crassirostris* (3,985/m³), *Oithona* spp. (2,350/m³), *Oncaea* spp. (1,970/m³), *Paracalanus aculeatus* (668/m³), *Corycaeus* spp. (259/m³), *Euterpina acutifrons* (173/m³), and *Microsetella rosea* (18/m³). The above two lists of species appear similar, however, there are differences in terms of their numerical dominance, probably due to monthly and inter-annual variabilities of the physico-chemical characteristics of the Gulf marine environment.

Large size copepods such as *Labidocera minuta* (438/m³), *Canthocalanus pauper* (341/m³), *Clausocalanus furcatus* (195/m³), and *Eucalanus subcrassus* (97/m³) were numerous at station 11, where other zooplankton groups also displayed maximum abundance. *Euchaeta concinna* (mean abundance = 36/m³) were in general more numerous at the eastern and central stations (maximum abundance of 88/m³ was found at station 10) along each of the five sampled transects than at the western stations.

Acartia spp. (mean abundance = 35.4/m³) were more numerous at stations 3 (146.7/m³) and 11 (340.6/m³). The most uncommon species, encountered only once, were *Undinula vulgaris* at station 11 (an expatriate from oceanic populations outside the Gulf), and *Pontellina plumata* at station 3. Another rare species that was found a couple of times was *Acrocalanus longicornis* at stations 1 and 2.

Mollusc Larvae

Mollusc larvae (mean abundance = 2,214/m³) were the second most abundant group in the study area (following copepods and their nauplii). Pelecypod larvae (bivalves) composed 53% of the total mollusc population, and were much more numerous than gastropod larvae (36.4%). The third most abundant mollusc was *Creseis acicula* (7.8%). Pelecypod larvae were also found to be the most dominant molluscan group in the studies of Michel *et al.* (1986) and Yamazi (1974). In the present study, pelecypod larvae were more numerous at stations 7 (5,993/m³), 11 (2,336/m³), 18 (2,179/m³), 16 (1,762/m³), 4 (1,635/m³), 3 (1,367/m³), and 15 (1,310/m³). Gastropod larvae were more numerous at stations 7 (5,646/m³), 16 (1,358/m³), and 19 (1,167/m³). Other mollusc groups were present but were much lower in abundance than the previous three. *Desmopterus papilio* was most abundant at station 15 (mean = 241/m³), followed by stations 9 (mean = 181/m³) and 4 (mean = 162/m³). *Carolina longirostris* were observed at station 17 only (mean = 0.1/m³).

Ostracods

The third most abundant zooplankton group was ostracods (mean abundance = 1,894/m³) which were represented by two species, *Euconchoecia aculeata* (mean = 1,698/m³) and *Cypridina* sp. (mean = 123/m³), with the first one (*Euconchoecia aculeata*) being the most abundant in the present study and in the

studies of Yamazi and Michel *et al.* Ostracods were less abundant at the western stations along transects 1, 2 and 3. However, similar abundance values were found at the eastern and western stations of transects 4 and 5. Highest abundance values for ostracods were found at stations 11, 8, 4 and 1.

Chordates

Three chordates (mean abundance = 1,007/m^3) were observed in our samples, *Oikopleura* spp. (97% of all chordates), *Doliolum* spp. (1.7%) and lancelets (1.3%). *Oikopleura* spp. were also the most dominant chordate in the studies of Michel *et al.* (1986) and Yamazi (1974). Highest density of *Oikopleura* was found at station 11 (mean = 4,477/m^3), followed by stations 3 (mean = 2,787/m^3), 8 (mean = 1,963/m^3), 12 (mean = 1,762/m^3) and 5 (mean = 1,715/m^3). No chordates were found at station 6. *Doliolum* spp. were most abundant at stations 19 (mean = 148/m^3) and 18 (mean = 58/m^3), while lancelets were most abundant at station 2 (mean = 97/m^3), followed by station 3 (mean = 60/m^3).

Chaetognaths

Chaetognaths (mean abundance = 289/m^3) were dominated by *Flaccisagitta enflata* (*Sagitta enflata*) in our study as well as the studies of Michel *et al.* (1986) and Yamazi (1974). Chaetognaths were more numerous at stations 11 (mean abundance = 1,168/m^3), and 19 (mean abundance = 1,078/m^3).

Cladocerans

Cladocerans were not abundant in the samples of the present study. Three species of cladocerans (mean abundance = 28/m^3) were observed in our samples, *Penilia avirostris* (mean abundance = 25/m^3), *Evadne tergestina* (mean abundance = 3/m^3), and *Podon polyphemoides* (mean abundance = 0.34/m^3). *P. avirostris* was the most dominant cladoceran group in this study as well as in the studies of Michel *et al.* (1986) and Yamazi (1974). *P. avirostris* was most numerous at stations 18 and 19, where it exclusively occurred at these stations. *Evadne tergestina* was encountered twice at stations 5 and 6, while, *Podon polyphemoides* was rare, and occurred only once at station 1.

CONCLUSIONS

Distribution and dominance of key zooplankton species obtained from this post-spill study resemble, in general, the pre-spill results reported by Michel *et al.* (1986) and Yamazi (1974). Copepods were most numerous at stations along the western side of the ROPME Sea Area, than the eastern side. Calanoids and cyclopoids were equally abundant at all stations sampled. *Oithona* spp. were the most numerous copepod species followed by *Oncaea* spp. and *Paracalanus* spp. Ostracods were more abundant at stations along the eastern coast of the ROPME Sea Area.

The evaluation of the data on hydrographic conditions during this study, indicates no major differences in temperature and salinity values among the different stations sampled during the period of the study. However, some regional differences in the abundance and distribution of the different kinds of zooplankton were evident. Station 11 was peculiar, due to the high abundance of plank-

tonic herbivores and carnivores. Highest densities of nauplii, total copepods, *Paracalanus* spp., *Corycaeus* spp., *Microsetella rosea*, *Labidocera minuta*, *Eucalanus subcrassus*, *Canthocalanus pauper*, *Clausocalanus furcatus*, ostracods, chordates, chaetognaths, and decapod larvae occurred at station 11, which makes it an interesting area to conduct a trophodynamic study.

REFERENCES

Al-Aidaroos, A. M. 1993. Planktonic decapoda from the western coast of the Gulf. *Marine Pollution Bulletin* 27: 245–249.

Al-Yamani, F. Y. 1989. Plankton Studies in the ROPME Sea Area, Present Status and Future Prospects. Regional Organization for the Protection of the Marine Environment, Kuwait. ROPME/GC-6/004.

Al-Yamani, F. Y., K. Al-Rifaie and W. Ismail. 1993. Post-spill zooplankton distribution in the NW Arabian Gulf. *Marine Pollution Bulletin* 27: 239–243.

Basson, P. W., Burchard, J. E., Hardy, J. T. and Price, A. R. G. 1977. Biotopes of the Western Arabian Gulf. Aramco, Dhahran. 284 pp.

Frontier, S. 1963. Zooplankton Recolte'en Her d'Arabic, Golfe Persique et Golfe d'Aden. Cahiers-ORSTOM Oceanographic 3: 17–30.

Gibson, V. R., Grice, G. D. and Graham, S. J. 1980. Zooplankton investigations in Gulf waters north and south of the Strait of Hormuz. Proceedings of a Symposium on Coastal and Marine Environment of the Red Sea, Gulf of Aden and Tropical Western Indian Ocean 3: 17–30.

Halim, Y. 1984. Plankton of the Red Sea and the Arabian Gulf. *Deep Sea Res.* 34(A6-8): 969–982.

Kimor, B. 1973. Plankton relations of the Red Sea, persian Gulf and Arabian sea. In *The Biology of the Indian Ocean* (B. Zeitzschel, ed.), pp. 221–232. Springer-Verlag, New York.

Michel, H. B., Behbehani, M., Herring, D., Arar, M., Shoushani, M. and Brakoniecki, T. 1986. Zooplankton of the western Arabian Gulf south of Kuwait waters. *Kuwait Bull. Mar. Sci.* 8: 1–36.

Sheppard, C., Price, A. and Roberts, C. 1992. *Marine Ecology of the Arabian Region.* Academic Press, London. 359 pp.

Yamazi, I. 1974. Analyses of the data on temperature, salinity and chemical properties of the surface water, and the zooplankton communities in the Arabian Gulf in December 1968. *Transactions of the Tokyo University of Fisheries* 1: 26–51.

Offshore Environment of the ROPME Sea Area after the War-Related Oil Spill, Eds. A. Otsuki *et al.*, pp. 203–214.

Aspects of reproduction in the pearl oyster, *Pinctada radiata* (Leach)

S. A. A. KHAMDAN

Environmental Affairs, P.O.Box 26909, Bahrain

Abstract—This study provides fundamental information regarding the reproductive biology of the ROPME Sea Area pearl oyster *P. radiata* monitored from January 1992 to December 1993. In this study and also that of Herdman (1903) and Tranter (1959), the gonad colour is shown to be an unreliable character for sex determination in *P. radiata*. The morphology of the gonad of *P.radiata* from Bahrain is similar to other populations or other species of the genus (Herdman, 1903; Tranter, 1958a, b, c, d; 1959; Rose *et al.*, 1990). The sequence of events of gametogenesis reported in this study is identical to that observed by Rose *et al.* (1990) on *P.maxima*. Gametogenesis takes place in winter and spring. Young *P. radiata* have been found settled on the shells of adults all year round, very little spawning activity out of season was noticeable and two distinct spawning maxima were found in summer/autumn. These observations are in agreement with those of Herdman (1903), Malpas (1931) and Tranter (1959) on the same species.

INTRODUCTION

There have been several studies conducted on the reproductive biology of different species of the genus *Pinctada; P. radiata* (Herdman & Hornell, 1906; Malpas, 1933; Tranter, 1959), *P. margaritifera* (Nicholls, 1931; Galtsoff, 1933; Tranter, 1958d), *P. albina* (Tranter, 1958a, b, c), *P. maxima* (Rose *et al.*,1990), *P. martensii* (Ojima & Maeki, 1955). The biology of pearl oysters is poorly understood, considering the importance of both natural and cultured pearl, and shell fisheries (Gervis & Sims, 1992).

No published work is available on the subject for the ROPME Sea Area population. This paper details some aspects of the reproductive biology of the Al-Jadoum, Bahrain, population of pearl oysters studied over a 2 year period. The results presented were determined from monthly histological sectioned gonads, and smears.

MATERIALS AND METHODS

Samples of the pearl oyster *Pinctada radiata*, were collected regularly on monthly visits between January 1992 and December 1993, from a single shallow (5m depth) population called Al-Jadoum, situated to the North of Bahrain, Long: 050 30 00 E; Lat: 26 20 00. Sample size was (on each sampling period) about 100

oysters (except September 1992 N=53). Oysters were collected and brought to the Laboratory of the Environmental Affairs.

Macroscopic examination of the gonads

For each specimen, information on gonad development, sex and colour of gonad. Gonad development was estimated by taking a small sample of tissue from an area next to the urogenital pore using a clean glass pipette and smearing the sample on a slide. Smears were examined under a compound Zeiss microscope at ×400 and/or ×1600. Four stages were recognised; stage 0; designates indeterminate or resorbed, stage 1; developing, stage 2; ripe and stage 3; spawning, and a gonad index based on the overall mean of these numbers was calculated for each month.

Histological examination of the gonads

Fifty animals from the monthly sample were fixed in Bouin's fluid (75 ml of Picric acid, saturated in filtered seawater; 25 ml formalin: –40 HCHO; 5 ml glacial acetic acid) at room temperature for 24 hours prior to dehydration through a series of alcohols: –30%, 50%, and 70%, allowing 2 hours between each change. Samples were then preserved in 70% alcohol for 1–2 weeks awaiting further treatment.

A piece of gonadal tissue, approximately 5 mm × 5 mm, from the gut loop, was excised from each fixed animal with a clean sharp scalpel. This tissue was preserved in Methyl benzoate at room temperature over-night. It was then suspended in a small tube closed at the bottom by 2 mm mesh and immersed in 1:1 of toluene-wax v/v in a 200 ml glass beaker at 60°C in an oven for 2 hours. The tube containing the tissue was given two changes of molten wax using a 200 ml glass beaker held in the oven at 60°C, for two hours at each transfer. The tissue was then embedded in fresh wax and allowed to cool.

Sections were cut at 7 m on a conventional Leitz rotary microtome fitted with a disposable blade. Ribbons of wax containing gonadal tissue were spread on a microscope slide and a few drops of glycerin-albumen solution (15 drops of concentrated stock in 100 ml distilled water) were added to ease the spreading and to glue the tissue onto the slide. Each slide accommodated a double track ribbon of 10–20 sections. Two slides were made from each wax block, labelled with a diamond knife and placed on a hot plate at 35°C for 6–8 hours, and then left standing at room temperature over-night.

For dewaxing, staining and counter-staining, slides were held in a slide holder immersed in a 250 ml container of histo-clear solvent for 4 minutes; transferred into a series of alcohols; 100%, 70% and 50% for 2 minutes between each transfer. They were then placed in distilled water for 1/2 to 1 minute, followed by immersion in a concentrated solution of lithium carbonate for 1 minute, to remove picric acid, and stained with Ehrlich's haematoxylin for 15 minutes. The slides were blued in tap water for 30 seconds, counter-stained with aqueous eosin for 30 seconds, and again placed under tap water for 30 seconds. The slides were then transferred immediately into a series of alcohols (90%,

100% and 100%), and finally, histo-clear, allowing 2 minutes at each change.

The slides were mounted with a few drops of DPX mountant and covered immediately but gently with a rectangular 64 × 22 mm (thickness = 1) cover-slip. The slides were placed on a hot plate at 35°C for 8 hours and then left at room temperature over-night.

Rose *et al.* (1990) developed a simple staging scheme for *Pinctada maxima* based on several schemes first proposed by Tranter (1958a,b,c,d; 1959) for several species within the genus *Pinctada*. Following initial observations Rose *et al.*'s (1990) scheme was found to be the most reliable staging procedure for *P. radiata* and it has been adopted without modification in this study. Sections were examined and photographed on a Zeiss photomicroscope II. A gonad index was produced based on the frequency of each stage for each month.

RESULTS

Morphology of the gonad

The gonad in *P. radiata* is not a discrete organ. The gonad is paired but assymetrical. The pair covers the stomach, liver and parts of the intestine. The byssal gland divides the gonad into a dorsal, larger part, and a ventral, smaller part. The gonad is bordered by the foot anteriorly and by the pericardium posteriorly both of which are free from gonad. No portion of the gonad extends into the foot or into the mantle, as is the case in *Mytilus edulis* (Seed & Suchanek, 1992).

Table1 shows the relationship between the colour of gonads in adult oysters and their gender. The χ^2 test confirms that the ratios of m:f:x are significantly different between colours and demonstrates that the gonad colour is an unreliable indicator of sex.

The reproductive follicles originate near the urogenital papilla proximal to the retractor muscle and proliferate within the connective tissue between the epithelium and viscera. The morphology of the gonad in *P. radiata* resembles that reported for *P. vulgaris* (= *P. radiata*) from Sri Lanka [Ceylon], (Herdman, 1903), the Australian Pearl oysters; *P.albina* (Tranter, 1958 a,b,c), *P. margaritifera* (Tranter, 1958d), *P. fucata* (= *P.radiata*),(Tranter, 1959) , and *P. maxima* (Rose *et al.*, 1990).

Spermatogenesis

Plate I shows the sequence of events of spermatogenesis based on histological preparations of gonads of 50 oysters per month. Plate I (B & C) illustrate the early spermatogenesis of stage 1 where stem cells and spermatogonia (Sg) reside in the follicle wall. The volume of the follicle is gradually filled up and spermatogonia develop to spermatocytes (Sc). Plate I (C) shows that the spermatocytes are accommodated in a condensed dark band beneath the layer of spermatogonia which is attached to the follicle wall. There is a difference in the staining intensity (basophilic) within the band and this indicates that spermatocytes are undergoing maturation to give rise to secondary spermatocytes. Two major differences between the stem cells and spermatogonia are recognised.

Table 1. *P. radiata*: (2 contingency table, DF (3-1) x (3-1) on colour of gonad in relation to gender in adults. Abbreviations: c = cream; w = white; y = yellow; F = females; M = males; X = indeterminates. Figures in brackets are percentages (Pct).

	Colour			
Count **Row Pct**				
Sex	**c**	**w**	**y**	**Row Total**
F	464 (55.1)	109 (12.9)	269 (31.9)	842 (35.7)
M	491 (70.6)	81 (11.7)	123 (17.7)	695 (29.5)
X	455 (55.6)	317 (38.7)	47 (5.7)	819 (34.8)
Column Total	1410 (59.8)	507 (21.5)	439 (18.6)	2356 (100.0)

Chi-Square	Value	DF	Significance
Pearson	345.34	4	<0.00001

First, the nuclear chromatin staining is darker in spermatogonia, and second the spermatogonia are usually free from the follicle wall. The difference between the primary and secondary spermatocytes is distinguishable because the primary spermatocytes undergo cytoplasmic and nuclear growth producing a darker nucleus a suggestion of meiosis I prophase in the secondary spermatocytes. Plate I (D) shows actively developing testis of stage 2 where spermatids, which are in the centre with developed cytoplasm, are transformed to spermatozoa giving a characteristic river or stream-like pattern filling the core of the follicle. This event is followed by a corresponding decrease in the number of spermatogonia at the earlier stages and around the periphery of the follicle wall. Plate I (E) shows a near-ripe phase of stage 2 where the spermatozoa are condensed to a dark band in the lumen of the follicle. Plate I (F) illustrates that the follicles are enlarged as the spermatozoa continuously increase in number and this gives rise to stage 3 of spawning-ripe event. Plate I (G & H) show the partially spawned to spent phase of stage 4 where a gap between the follicular wall and the mass of spermatozoa has occurred indicating a spawning event. Thereafter, the follicle has shrunk with isolated pockets of spermatids. Plate I (A) illustrates stage 0 of indeterminate or inactive gonad where the follicles are collapsed and noticeably reduced in volume.

Plate I. Various stages of spermatogenesis in *P. radiata.*

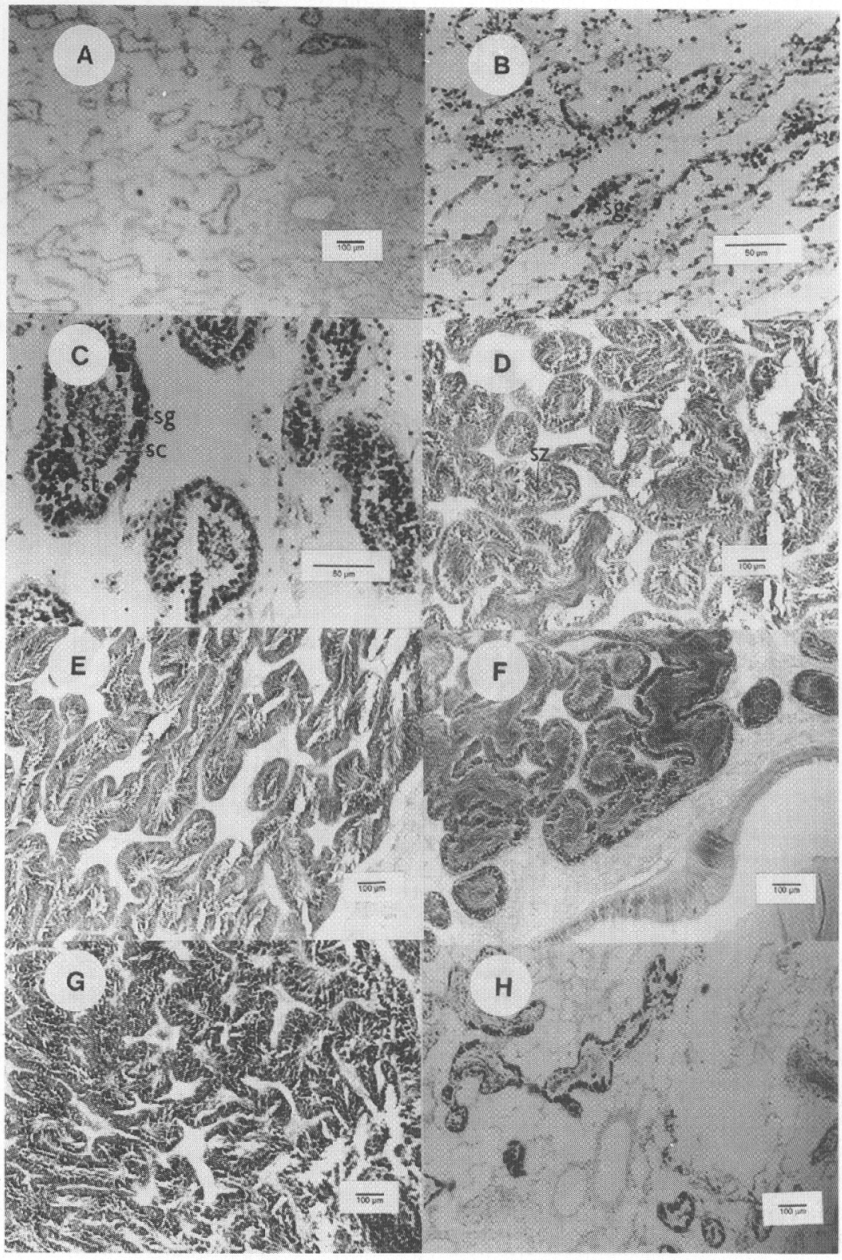

(A) Indeterminate stage (0). (B) Beginning of spermatogenesis (stage 1); (Sg), Spermatogonia. (C) Advanced stage of early spermatogenesis, (SC) spermatocytes, (St) spermatids. (D) Actively developing testis (stage 2), (Sz) spermatozoa. (E) Near ripe testis (stage 2). (F) Spawning-ripe testis (stage 3). (G) Partially spawned testis (stage 4). (H) Spent testis (stage 4).

Oogenesis

Plate II illustrates the events of oogenesis. Plate II (A) shows early oogenesis of stage 1 where stem cells (St C) undergo mitotic division and give rise to oogonia (og) both of which reside on the wall of the follicle. Plate II (B) illustrates an advanced stage 1 where oogonia growing along the wall of the follicle are entering meiosis I "prophase" and it appears that some oogonia are at various stages of maturity while some are in the resting stage. Plate II (C) is an actively developing ovary of stage 2 where the connected oocytes, those which are still joined to the follicle wall, are undergoing cytoplasmic maturation. Mature free oocytes then accumulate in the lumen of the follicle. Plate II (D) is a near-ripe ovary of stage 2 where free oocytes are gradually filling the lumen of the follicle with a corresponding reduction in the numbers of earlier stage oogonia. Plate II (E) is a spawning-ripe ovary of stage 3 where free oocytes are increasing in their number and the follicle volume has expanded. A characteristic feature of the ova at this stage is their polygonal shape which results from the pressure exerted by the follicle wall. Plate II (F) is a spawning-ripe ovary of stage 4 in a transitional phase where the shape of the ova has changed to pear-shape, an indication of relief from the pressure and commencement of partial spawning. Plate II (G & H) are advanced stages of spawning stage 4 where the volume of the follicle has reduced and regressed or collapsed. It should be noted here that there are no yolk nuclei visible in the cytoplasm of the oocytes or ova as in *P. margaritifera* (Tranter, 1958d), *P. maxima* (Rose *et al.*, 1990). The functions of these organelles which appear as circles, crescents or saucers are not yet understood (Rose *et al.*, 1990).

To summarize, the timing of events of gametogenesis is similar in both sexes, i.e. commences in winter and continues through spring. However, as will be discussed in a later section on the breeding season, spawning of adult *P. radiata* is continuous in the sense that there are always at least a few spawning individuals present throughout the year. It follows that redevelopment, too, is continuous.

Breeding seasons

Figure 1 summarizes the histological data from monthly gonad preparations for the two years monitoring period. It can be seen in the figure that early gametogenesis, as judged by the development stage 1, took place during January, February, March, April and December 1992, and January through March and December 1993. During May and June 1992 the gonad underwent a rapid transition to ripe and spawning stages and then maintained a nearly 100% spawning stage through July 1992 followed by an abrupt decline in August of the same year with a corresponding increase in the spent stage up to 25% suggesting the commencement of the summer peak spawning. In September 1993, there was a noticeable decline in the percentage of oysters in the spawning stage followed by a corresponding increase in the proportion of the spent individuals up to about 35%. The oysters continued to spawn intermittently but with redeveloping follicles and gametes. In November 1992, a noticeable increase to 80% in the

Plate II. Various stages of oogenesis in *P. radiata*.

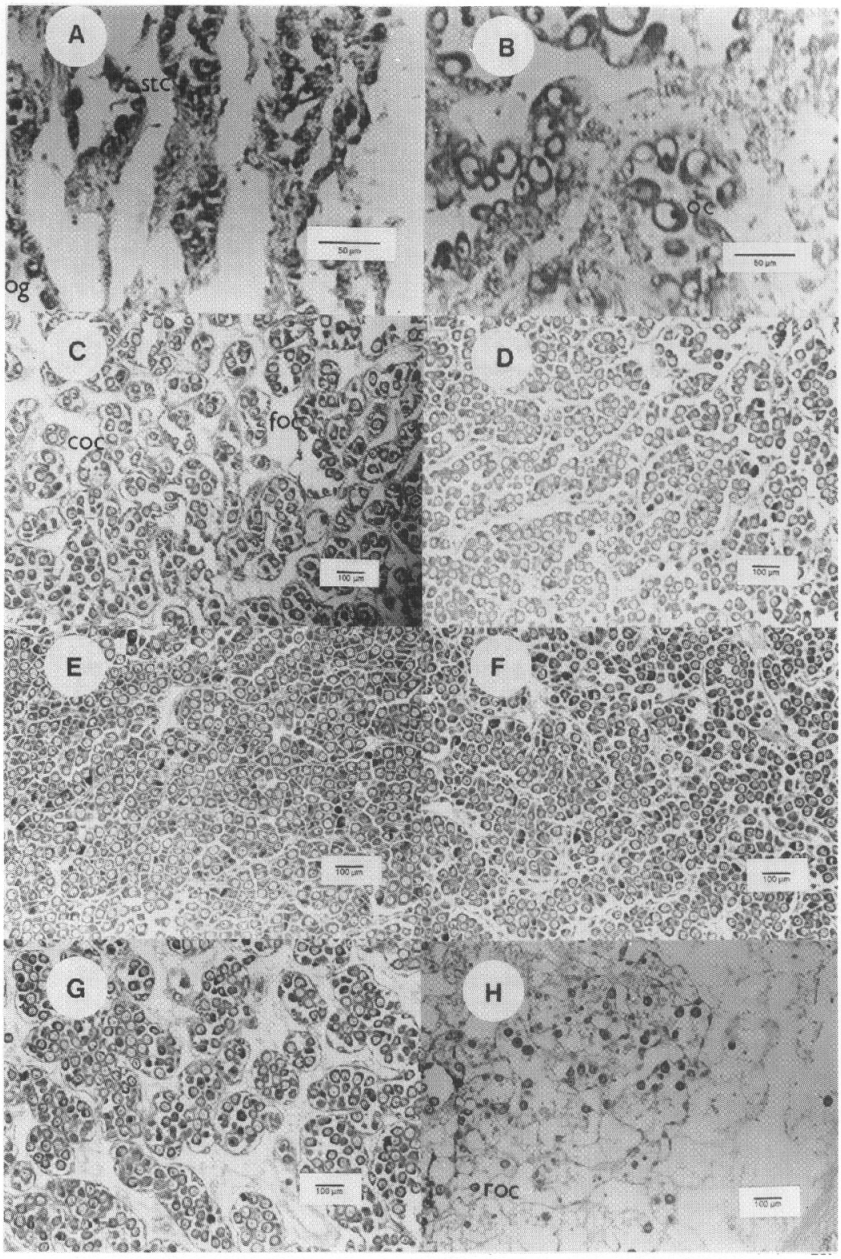

(A) Beginning of oogenesis with stem cells (St C) and oogonia (Og). (B) Advanced stage of early oogenesis (stage 1) with larger oocytes (OC). (C) Actively developing ovary (stage 2) with connected oocytes (C OC) and free oocytes (F OC). (D) Near-ripe ovary (stage 3). (E) Spawning-ripe ovary (stage 3). (F) Partially spawned ovary (stage 4). (G) Advanced stage of partially spawned ovary. (H) Spent ovary (stage 4) with residual oocytes (r oc).

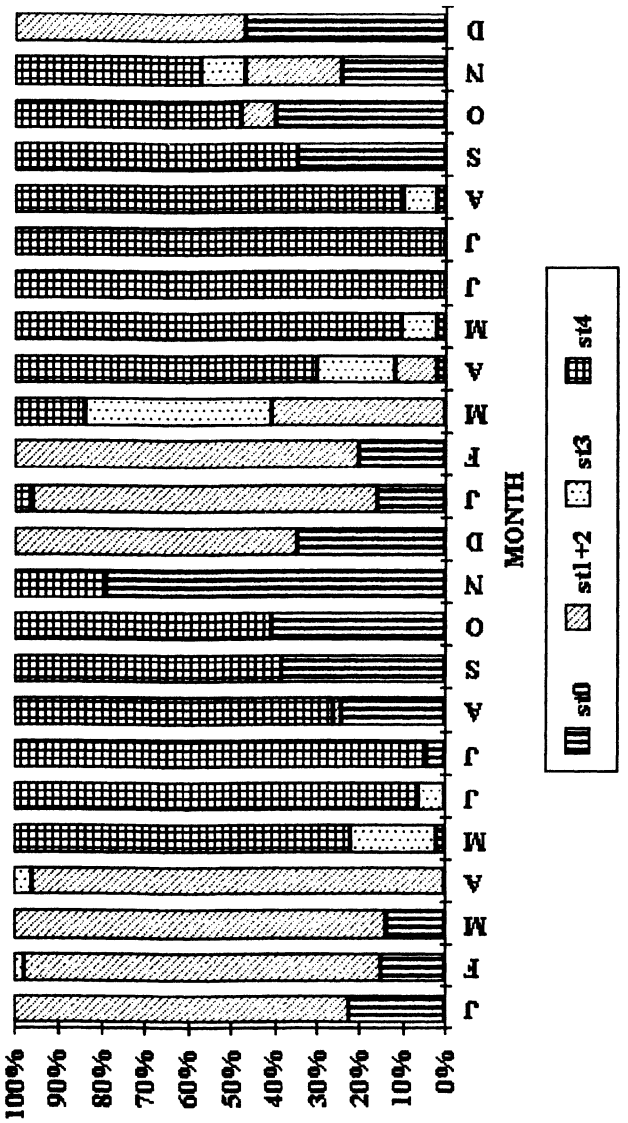

Fig. 1. Annual reproductive cycle of P. radiata studies between January 1992 and December 1993. Abbreviations, st0=stage 0 (spent); st1+2 = stages1 and 2(developing); st3= stage3(ripe) and st4=stage4(spawning).

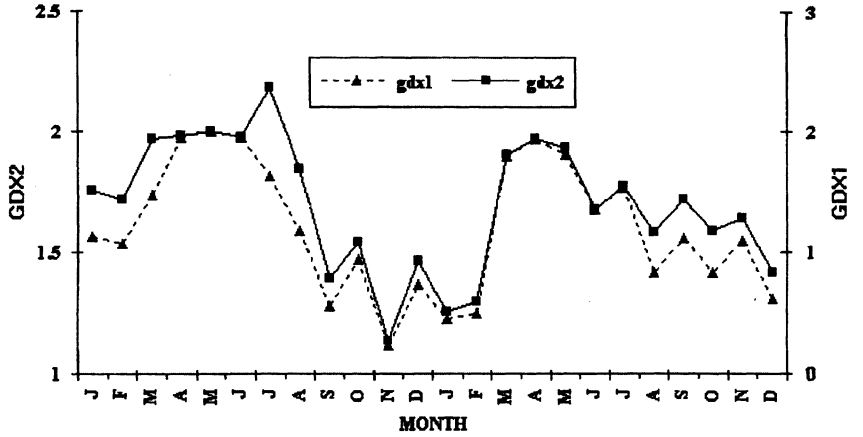

Fig. 2. *P. radiata*, macroscopic monthly gonadal indices (GDX1 and GDX2, see text) based on examining live gemete smears for the period January 1992 and December 1993.

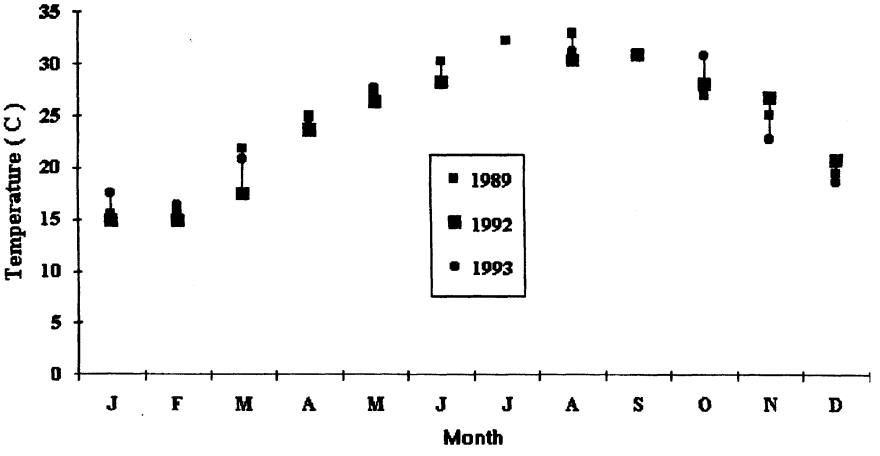

Fig. 3. Mean monthly seawater temperature around the Island State of Bahrain (ROPME Sea Area) for 1989, 1992, and 1993.

percentage of spent individuals is evident while a similar pattern (50%) was found in December 1993 and this event signalled an autumn peak spawning. The majority of gonads after this second spawning were collapsed (Plate IA), and they entered a resting phase for 3 to 4 months during winter when early gametogenesis took place. However, insignificant partial spawning is noticeable in Fig. 1 which had taken place in January and March 1993.

Figure 2 shows the macroscopic gonadal maturation indices (GDX1 and GDX2) based on live smears. GDX1 is based on 4 values given to 4 stages as follows, spent = 0, developing = 1, ripe = 2, and spawned = 3. GDX2 is simpler

than GDX1 where both spent and developing are given a combined value = 1, and the ripe and spawned stages are given a pooled value = 2.

Both indices give similar patterns to that obtained from histological preparations and are clear enough to suggest that there exist two spawning events, firstly, in summer; August/September and secondly, in autumn; November/December.

Figure 3 shows the mean monthly seawater temperature around the Island State of Bahrain for the years 1989, 1992 and 1993 (kindly supplied by the Meteorology office, Civil Aviation Directorate). The coldest months are December, January, February and March where the temperature is within the range 15–20°C. In April the temperature starts to rise to 25°C to reach its maximum above 30°C in August and then drops in September.

To summarize, the breeding cycle in this species is seasonal with two peak spawnings in summer (August/September) and autumn (November/December) and this correlates with the temperature regime prevailing in the ROPME SEA AREA . However, partial spawning was found to have taken place in January and March 1993. Indices developed from both histological preparations and from simple gonad smears gave similar general annual patterns of gonadal maturation. There were slight but noticeable differences in the timings of the spawnings between years.

DISCUSSION

Morphology of the gonad

Sexual dimorphism is absent in *P. radiata* and the colour of the gonad is an unreliable aid in sex determination. Gonad colouration distinguishes sex in the Australian *P. margaritifera* being pinkish, creamy or yellow in females and white in males, with an error of less than 5% (Tranter, 1958d). Gonad colour has also been found to be reliable in determining sex in *P. albina* (Tranter, 1958a) and *P. maxima* (Rose *et al.*,1990). In this study and also that of Herdman (1903) on *P. vulgaris* (= *P. radiata*), and Tranter (1959) on *P. fucata* (= *P. radiata*) gonad colour is an unreliable character in sex determination. The morphology of the gonad of this population of *P. radiata* is similar to other populations of this species and other species of the genus (Herdman, 1903; Tranter 1958a, b, c, d;1959; Rose *et al.*,1990).

Gametogensis

A ripe oyster is identifiable superficially by the size of the gonad and macroscopically by examining live gamete smears, and microscopically by examining histological preparations of gonads. Rose *et al.* (1990) simplified Tranter's (1958a, b, c, d; 1959) several schemes on histological gonad indices and in this study, Rose *et al.*'s (1990) scheme was found to be reliable. Furthermore, the sequence of events of gametogensis depicted, in this study (plates I and II) is identical to that produced by Rose *et al.* (1990).

Breeding seasons

In Sri Lanka, Herdman and Hornell (1906) studied *P. vulgaris* (= *P. radiata*) and found that spawning occurs all year round with two distinct maxima; May/July and November/January. Malpas (1933) re-examined the species in Sri Lanka and found it to spawn both in summer (July/August) and winter (December/January). The summer peak coincided with the south-west monsoon when there is influx of high salinity water from the Indian Ocean into the Gulf of Mannar, where major pearl oyster beds are situated. The winter spawning coincided with the north-east monsoon which produces significant rainfall and a reduction of salinity. He suggested that spawning is controlled by salinity.

The Australian *P. fucata* (= *P. radiata*) was studied by Tranter (1959) and the species was found spawning all year round with two distinct peaks being in the southern hemisphere summer (January/February) and autumn (April/May). Gametogensis took place in winter and ripening in spring. In this study, young *P. radiata* have been found settled on the shells of adults all year round, very little spawning activity out of season was noticeable (in January, March 1993) and two distinct spawning maxima were found in summer/autumn. Gametogenesis took place in winter and spring and this corresponds well with the Australian and the Sri Lankan populations of the same species of pearl oysters.

In Hawaii, *P. galtsoffi* (= *P. margaritifera*) spawns once a year in July/August (Galtsoff,1933). In New Zealand direct observation of spawning in the field was reported in August by Bullivant (1962). Nicholls (1931) during the Great Barrier Reef expedition (1928-1929) reported that *P. margaritifera* spawns twice a year once in November and again in May. However, Tranter (1958 d) criticized the work of Nicholls (1931) as being incomplete because there were no consecutive samples for a full year and stated instead that in Australia, the species spawns all year round with two spawning maxima being in summer (January) and winter (July). Crossland (1957) studied the *P. margaritifera* in the Sudanese Dongonab Bay, the Red Sea, and suggested that spawning took place between July to October with gonad development from March to June. Nicholls (1931), Galtsoff (1933), Crossland (1957), Tranter (1958d) and Bullivant (1962) considered that the temperature (26–28°C) was the spawning inducer in *P. margaritifera*. Tranter (1958a,b,c) studied *P.albina* from Australia and found it breeding continuously all year round but with one peak spawning in winter (May/April) coinciding with the drop in seawater temperature.

Recently Rose *et al.* (1990) studied the reproductive biology of the silver or gold-lipped pearl oyster, *P.maxima*, from Australia and found it breeding in winter/spring (September/October) and summer/autumn (March/April). They suggested temperature as the major spawning controller.

Considering the biogeographical distribution of the species of *Pinctada* being between 30° north and south of the equator (Galtsoff, 1933; Tranter, 1958d) and the experience gained from a previous study (Khamdan,1993) on the spawning, fertilization and larval rearing , it seems that the temperature is more likely to be the controlling factor for spawning at least for the summer peak. However it is of interest to ascertain the cause(s) of the autumn peak which perhaps is more

likely controlled by food availability as judged from redevelopment of gonad after summer spawning and variation of weight of a standard oyster (Khamdan ,in prep.).

REFERENCES

Bullivant, J.S. (1962): Direct observation of spawning in the black shell oyster (*Pinctada margaritifera*) and the Thorny oyster (*Spondyllus* sp.). *Nature*, 193:700–701.

Crossland, C. (1957): The cultivation of the mother-of-pearl oyster in the Red Sea. *Aust. J. Mar. Freshw. Res.*, 8: 111–130.

Galtsoff, P. S. (1933): Pearl and Hermes Reef , Hawaii , Hydrographical and biological observations. *Bernice P. Bishop Museum*, 107: 49 pp.

Gervis, M. H. & Sims, N. A. (1992): The biology and culture of pearl oysters (Bivalvia : *Pteriidae*). *The International Center for Living Aquatic Resources Management (ICLARM), Stud. Rev.*, 21: 49pp.

Herdman, W.A. (1903): Observations and experiments on the life history and habits of the pearl oyster. In: (Ed. Herdman, W.A.), the pearl oyster fisheries of the Gulf of Mannar. *Report to the Ceylon Govt. Royal Soc. London*, I: 125–146.

Herdman, W.A. & Hornell, J. (1906): General summary and recommendations. III. Reproduction and life-history of the Pearl Oyster. In: (Ed. Herdman, W.A.), the Pearl Oyster Fisheries of the Gulf of Mannar.*Report to the Government of Ceylon. Royal Soc. London*, V: 114–118.

Khamdan, S.A.A. (1993): The reproduction, Larval rearing and production of triploid embryos and spat of the pearl oyster, *Pinctada radiata*. In : *The proceeding of second Arab conference on perspective of modern biotechnology*, 24–28 April 1993 - Amman Jordan. Bio Dynamics International, San Diego , California USA., pp. 190–207.

Malpas, A. H. (1933): Further observations on the age and growth-rate of the Ceylon pearl oyster, *Margaritifera vulgaris*, with special reference to oysters of Donnan's Muttuvarattu paar. *Ceylon J. Sci.*(C), V: 21–48.

Nicholls, A. G. (1931): On the breeding and growth rate of the black lip pearl oyster (*Pinctada margaritifera*). *Rep. Gt. Barrier Reef Comm.*, 2: 26–31.

Ojima, Y. & Maeki, K. (1955): Some cytological account of the maturation of the gonad in the Pearl Oyster, *Pinctada martensii* (Dunker). *Kwansei Gakuin Univ. Ann. Studies*, 3: 1–4.

Rose, R. A. ; Dybdahl, R. E. & Harders, S. (1990): Reproductive cycle of the Western Australian silverlip pearl oyster , *Pinctada maxima* (Jameson) (Mollusca: *Pteriidae*). *J. Shellfish. Res.*, 9: 261–272.

Seed, R. & Suchanek, T. H. (1992): Population and community ecology of Mytilus. In: *The mussel Mytilus : Ecology , Physiology , Genetics and Culture*. (Ed. Gosling, E.). Elsevier, pp. 87–169.

Tranter, D.J. (1958a): Reproduction in Australian Pearl Oysters (Lamellibranchia).I. *Pinctada albina* (Lamarck): Primary gonad development. *Aust. J. Mar. Freshw. Res.*, 9: 135–143.

Tranter, D.J. (1958b): Reproduction in Australian Pearl Oysters (Lamellibranchia). II. *Pinctada albina* (Lamarck): gametogenesis. *Aust. J. Mar Freshw. Res.*, 9: 144–158.

Tranter, D.J. (1958c): Reproduction in Australian Pearl Oysters (Lamellibranchia).III. *Pinctada albina* (Lamarck):breeding season and sexuality. *Aust. J. Mar. Freshw. Res.*, 9: 191–216.

Tranter, D.J. (1958d): Reproduction in Australian Pearl Oysters (Lamellibranchia).IV. *Pinctada margaritifera* (Linnaeus). *Aust. J. Mar. Freshw. Res.*, 9: 509–525.

Tranter, D.J. (1959): Reproduction in Australian Pearl Oysters (Lamellibranchia) V. *Pinctada fucata* (Gould). *Aust. J. Mar. Freshw. Res.*, 10: 45–66.

Offshore Environment of the ROPME Sea Area after the War-Related Oil Spill, Eds. A. Otsuki *et al.*, pp. 215–230.

Distribution of n-alkanes and heterocyclic sulfur compounds in the central region of the ROPME Sea Area (Persian Gulf)

R. TSUJIMOTO[1], S. HASHIMOTO[2] and A. OTSUKI[2]

[1]*Toyama Prefectural Fisheries Institute, 364 Takatsuka, Namerikawa, Toyama 936, Japan*
[2]*Department of Ocean Sciences, Tokyo University of Fisheries, 4-5-7 Konan, Minato-ku, Tokyo 108-8477, Japan*

Abstract—Total n-alkane (C_{12}–C_{30}) concentrations in open seawater of the central region of the ROPME sea area (Persian Gulf) ranged from 29.8 to 859 ng l^{-1} in 1993 and from 49.4 to 652 ng l^{-1} in 1994. Mean concentrations in 1993 and 1994 were 150.9 and 146.2 ng l^{-1}, respectively. Although benzothiophene was below the detection limit (<0.5 ng l^{-1}) at all sampling stations, dibenzothiophene concentrations in 1993 and 1994 ranged from undetectable to 3.0 ng l^{-1} and undetectable to 2.1 ng l^{-1} with mean concentrations of 0.5 and 0.7 ng l^{-1}, respectively. The present results indicate that the horizontal distribution of total n-alkanes at 4–5 m depth did not relate to the northeast shore of Saudi Arabia which was contaminated with crude oil during the Gulf War spill in 1991 and that the crude oil contamination caused by that oil spill did not have serious long term impacts on the open seawaters of the central region. A linear relationship between total n-alkanes and dibenzothiophene concentrations ($r = 0.66$, $P < 0.01$) suggests that oil pollution by successive inputs such as oil well leakage and illegal ballast and bilge water discharges are still continuing in the central region of the ROPME sea area and that mineralization of total n-alkanes by bacteria was not significant in open seawater in this region.

INTRODUCTION

On 17 January 1991, the Gulf War broke out and a huge volume of crude oil was spilled in the northwestern part of the ROPME sea area (the Gulf). The spill volume was estimated to have been about 10 million barrels, and it has been presumed that about 40% of the spilled crude oil evaporated, about 30% landed on beaches, and the rest changed to dissolved and suspended forms that might be subjected to bacterial mineralization and/or sink to the bottom as tar balls (Tawfiq, 1993). In addition, this area is highly contaminated by illegal discharges of ballast and bilge waters from oil tankers, oil well leakage, and minor accidents at oil terminals (El Samra, 1986, 1988; Emara, 1990).

In December, January 1993 and December 1994 (2 and 3 years after the spill), cruises by the Japanese R/V Umitaka-Maru were conducted to follow up Mt. Mitchell cruise (NOAA, USA) in response to a request from UNESCO

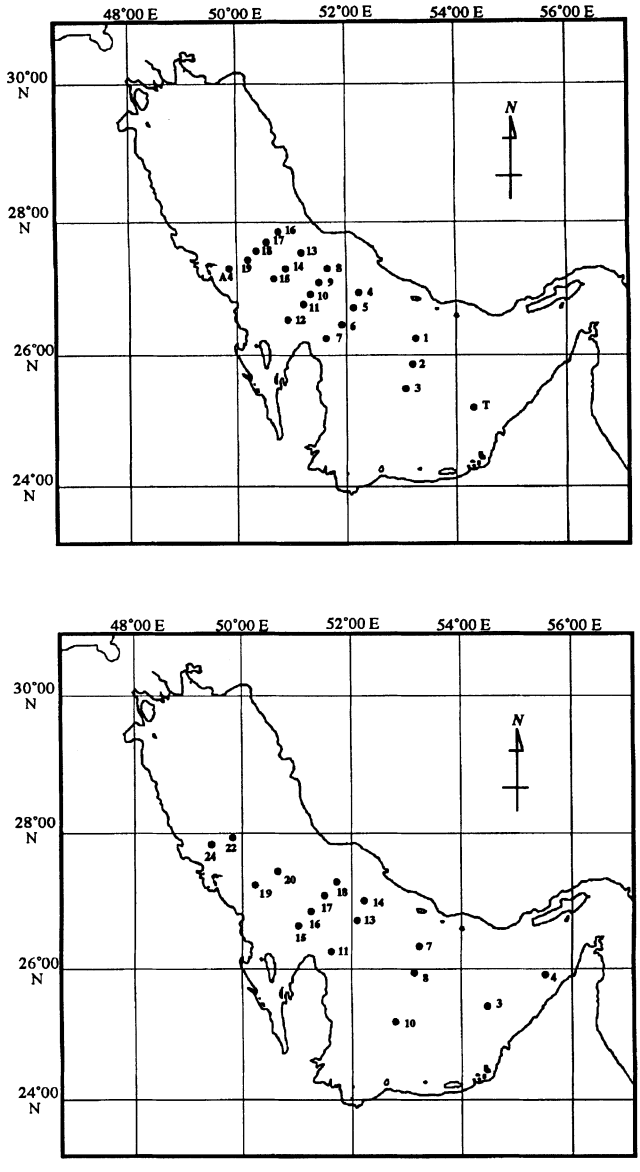

Fig. 1. Sampling stations in the RSA in Dec. 1993 (a) and Dec. 1994(b).

Intergovernmental Oceanographic Commission (IOC), and ROPME (Alam, 1993).

The main purposes of the present study were to analyze the impact of the crude oil spill on the open sea area of the Gulf and to evaluate the extent of crude oil pollution there through analysis of several hydrocarbons of crude oil (C_{12}–C_{30} n-alkanes, benzothiophene and dibenzothiophene) in open seawater. We selected

benzothiophene and dibenzothiophene as important indices of crude oil pollution, because the thiophenes are persistent in the marine environment and highly toxic to many marine organisms (Ogata *et al.*, 1981).

MATERIALS AND METHODS

The sampling stations selected during the December 1993 and December 1994 cruises are shown in Figs. 1(a) and 1(b), respectively, and their locations are listed in Tables 1(a) and 1(b). Seawaters were sampled during these 2 R/V Umitaka-Maru cruises with a Teflon lined GO/FLO samplers (General Oceanics) fixed to a greaseless Kevler line. Whole seawater samples without filtration were transferred into pre-washed (3 times with acetone) 1.2 liter SPC glass bottles, and then 20 g of sodium chloride and the first internal standard (Anthracene-d_{10} for recovery check) were immediately added. Extraction was done by adding 3 ml n-hexane to the sample and stirring magnetically for 15 min. The resulting mixture was allowed to stand for 15 min. and the organic layer formed was collected with a Pasteur pipette. A second extraction was repeated with the same volume of n-hexane. The extracts were combined and centrifuged at 2,500 rpm for 15 min. to separate traces of seawater (Desideri *et al.*, 1992). Water in the centrifuged extract was removed by passage through an anhydrous sodium sulfate column. The dried extract was immersed in a 15°C water bath and concentrated to 0.5 ml by flushing with nitrogen gas. Although the concentrates might have contained

Table. 1a. Location of sampling stations in Dec. 1993.

Station	Latitude(°N)	Longitude(°E)
T	25 12.70	54 14.90
1	26 14.60	53 11.60
2	25 54.38	53 07.86
3	25 34.19	53 00.86
4	26 58.10	52 17.20
5	26 43.50	52 02.70
6	26 27.90	51 48.50
7	26 13.00	51 35.20
8	27 16.10	51 41.40
9	27 06.60	51 29.70
10	26 56.90	51 19.90
11	26 44.50	51 09.70
12	26 34.90	50 54.90
13	27 32.60	51 06.50
14	27 20.80	50 54.50
15	27 09.80	50 41.70
16	27 52.60	50 46.70
17	27 43.50	50 33.20
18	27 36.00	50 17.80
19	27 27.70	50 03.70
A4	27 22.10	49 50.60

Table 1b. Location of sampling stations in Dec. 1994.

Station	Latitude(°N)	Longitude(°E)
3	25 31.94	54 35.92
4	25 52.38	55 28.99
7	26 14.63	53 11.73
8	25 55.40	53 05.93
10	25 15.73	52 45.24
11	26 13.85	51 34.89
13	26 42.69	52 02.18
14	26 57.34	51 14.41
15	26 41.69	51 07.20
16	26 50.37	51 17.43
17	27 01.82	51 29.74
18	27 12.43	51 38.30
19	27 15.14	50 19.29
20	27 30.81	50 37.23
22	27 56.99	49 49.77
24	27 47.88	49 23.70

Table 2. Gas chromatography/mass spectrometer operating parameters.

Gas chromatography	Varian 3400
sample amount	1μl
column	DB-5ms, 0.25mm i.d. x30m,
	0.25μm 5%diphenyl 95%dimetylpolysiloxane
	bonded phase (J&W Scientific Folsom, CA)
carrier gas	helium at 15psig
injector	split/splitless in splitless mode,
	1min. splitless time, temp. 250°C
transfer line	300°C
temp. programs	
initial temp.	50°C
initial hold	1min.
ramp rate	10°C/min.
final temp.	300°C
final hold	24min.
run time	50min.
Mass spectrometer	
scan range	84.8–85.2m/z
	127.8–128.2m/z
	133.8–134.2m/z
	135.8–136.2m/z
	183.8–184.2m/z
	187.8–188.2m/z
	243.8–244.2m/z
	263.8–264.2m/z
start time	18min.
scan cycle	0.1min.
ionization	EI(electron impact)
electron energy	70eV
emission curent	200μA

small amounts of polar compounds, no clean-up pretreatment with silica gel or alumina was not performed. Additional internal standards (Naphthalene-d_8, Phenanthrene-d_{10}, p-Terphenyl-d_{14}, and Perylene-d_{12}) for GC/MS analysis were then added to the concentrates.

Determination of n-alkanes and thiophenes was done on a Varian 3400 capillary gas chromatograph interfaced to a Finnigan Mat Mass Spectrometer SSQ 700 at Selective Ion Monitoring (SIM) mode. The gas chromatography/mass spectrometric condition is shown in Table 2. The ions monitored were m/z 85,

134, and 184 for n-alkanes, and two parent ions m/z 134 and 184 for benzothiophene and dibenzothiophene, respectively.

For recovery test, each 200 ng of n-alkanes (C_{12} to C_{30}), benzothiophene, and dibenzothiopene was added to 1.2 l seawater samples. Both n-alkanes and thiophenes were extracted in the same manner described above. Quantification was done by the internal standard method. Recovery efficiencies for 5 runs of C_{24}–C_{12} or C_{30}–C_{25} in n-alkanes were 68–82% and 52–64%, respectively, while those of benzothiophene and dibenzothhiopene were 76%, and 88%, respectively. Relative coefficients of variation for each compound were less than ±16%. A Kuwait standard crude oil, kindly supplied by Dr. Lila Al-Omran of Kuwait University, was used for comparison.

RESULTS AND DISCUSSION

Total n-alkane (ΣC_{12}–C_{30}) and dibenzothiophene concentrations in December 1993 and December 1994 were given in Tables 3a,b and 4a,b. In both years, benzothiophene concentration was below detection limit (<0.5 ng l^{-1}) at all stations. Total n-alkane concentrations did not exceed 1 $\mu g\ l^{-1}$ at any stations, and

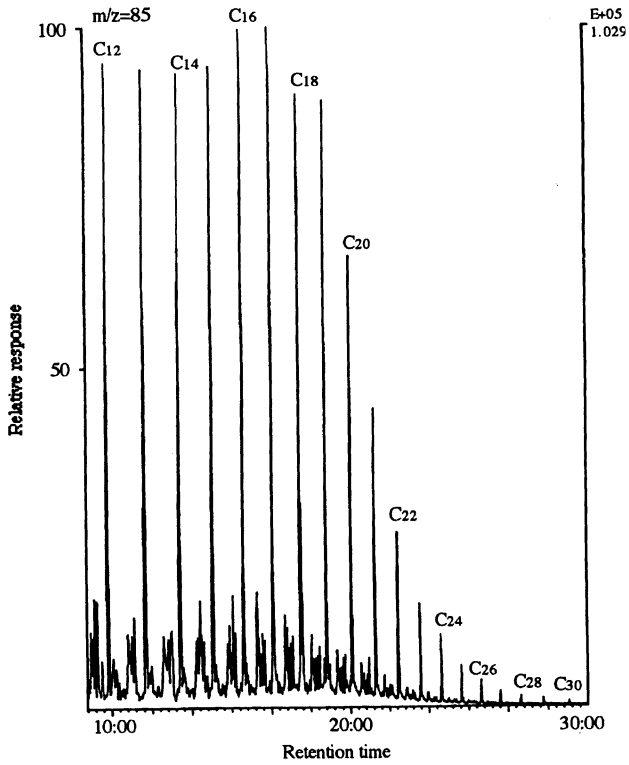

Fig. 2. Normal-alkanes SIM chromatogram of the Kuwaiti Crude Oil.

Table 3a. Total n-alkane and dibenzothiophene concentrations in seawater in Dec. 1993.

station No.	sampling depth (m)	total n-alkanes (ng l^{-1})	dibenzothiophene (ng l^{-1})
T	0	367.6	1.1
	10	259.5	0.8
	20	215.0	0.6
1	0	95.0	1.1
	10	143.1	1.2
	20	58.2	0.7
	40	423.1	0.6
	60	146.7	0.5
2	0	69.1	0.7
	10	129.1	0.6
	25	121.1	0.5
	50	133.6	0.6
3	0	46.9	nd
	10	161.7	0.6
	20	115.6	nd
	30	96.5	0.5
4	0	858.8	3.0
	10	386.3	0.9
	20	212.1	0.7
	40	94.1	nd
	60	76.8	nd
5	0	29.8	nd
	10	69.3	nd
	20	45.2	0.5
	40	419.6	1.8
	60	414.5	1.7
6	0	100.8	0.7
	10	79.6	0.6
	20	80.2	nd
	40	67.8	nd
7	0	89.6	nd
	10	144.2	0.6
	20	62.9	nd
8	0	86.6	0.8
	10	126.2	0.7
	20	164.3	0.5
	40	229.3	0.8
9	0	100.7	0.6
	10	60.2	nd
	20	164.3	0.5
	40	70.5	0.6
	60	83.7	0.5

ranged from 29.8 to 858.8 ng l^{-1} in 1993 and 49.4 to 652.4 ng l^{-1} in 1994. The mean concentrations of total n-alkane in 1993 and 1994 were 150.9 ng l^{-1} and 146.2 ng l^{-1}, respectively. Dibenzothiophene concentrations ranged from below the detection limit (<0.5 ng l^{-1}) to 3.0 ng l^{-1} in 1993, and below the detection limit to 2.1 ng l^{-1} in 1994 with the mean concentrations of 0.5 ng l^{-1} in 1993, and 0.7

Table 3a. (continued)

station No.	sampling depth (m)	total n-alkanes (ng l^{-1})	dibenzothiophene (ng l^{-1})
10	0	95.6	nd
	10	61.3	nd
	20	489.6	1.2
	40	54.5	nd
	60	87.6	nd
11	0	102.8	nd
	10	132.4	nd
	20	445.2	2.1
12	0	119.6	nd
	10	155.7	0.6
13	0	152.5	0.7
	10	136.2	0.6
	20	99.6	nd
	40	93.8	nd
	60	141.9	nd
14	0	85.0	nd
	10	73.6	nd
	20	82.1	nd
15	0	88.0	nd
	10	87.2	nd
	40	96.9	0.5
16	0	90.5	0.7
	10	94.2	0.5
	20	184.3	0.7
	50	273.5	0.8
17	0	51.5	nd
	10	78.7	nd
	20	250.3	0.6
	50	484.7	0.7
18	0	67.7	nd
	10	165.3	0.5
	20	70.8	0.6
	50	61.3	0.5
A4	0	143.8	0.7
	10	128.5	0.6

ng l^{-1} in 1994. In 1986 before the Gulf War crude oil spill occurred, Ehrhardt and Douabul (1989) reported a dibenzothiophene concentration of 0.8 ng l^{-1} in the northern part of the Gulf (29°05′ N, 48°25′ E). Thus, the dibenzothiophene concentrations we measured were similar to that measured before the Gulf War crude oil spill.

The relative concentration distribution of n-alkanes in the Kuwait standard crude oil, as revealed in an ion chromatogram (Fig. 2), was nearly constant between C_{12} and C_{19}, and then rapidly decreased from C_{20} to C_{30}. The typical distribution pattern of n-alkanes in seawater samples, in contrast that in Kuwait standard crude oil, had a normal distribution curve with a peak at C_{18-19} between

Table 3b. Total n-alkane and dibenzothiophene concentrations in seawater in Dec. 1994.

station No	sampling depth (m)	total n-alkanes (ng l^{-1})	dibenzothiophene (ng l^{-1})
3	0	652.4	0.9
4	0	308.3	2.1
	15	500.0	1.7
	30	434.8	1.5
	40	305.0	2.0
7	0	300.7	1.3
	10	175.7	0.5
	30	152.0	1.2
	50	172.3	0.6
	70	247.6	0.9
8	0	182.4	1.4
	10	244.8	1.3
	30	121.3	1.0
	60	104.6	1.1
10	0	99.7	0.5
	10	62.2	nd
	26	101.3	nd
11	0	97.2	0.8
	10	87.5	nd
	24	101.3	nd
13	0	144.3	nd
	10	125.1	nd
	30	77.5	0.7
	68	72.0	nd
14	0	59.2	nd
	10	60.1	0.5
	30	60.4	nd
	62	86.2	nd
15	0	184.9	1.3
	20	76.6	nd
16	0	136.0	1.0
	30	124.2	0.5
	40	167.9	0.5
17	0	220.7	0.8
	30	204.4	0.5
	50	49.4	nd
18	0	61.9	0.5
	30	66.0	1.0
	50	89.2	1.5

C_{12} and C_{30} (Fig. 3).

The distribution patterns of n-alkane concentrations in almost all seawater samples had a nearly normal distribution curve for chain lengths between C_{12} and C_{24} with a peak at C_{18-19} (for example, see Fig. 4). Individual n-alkane concentrations ranged from a few ng to several hundreds ng l^{-1}. Although Ehrhardt and Burns (1993) reported that coastal water samples collected at northern Abu Ali peninsula in early 1992 showed odd carbon number predominance of C_{15}, C_{17}, and C_{19} n-alkanes suggesting biosynthetic origin, a nearly normal distribution

Table 3b. (continued)

station No.	sampling depth (m)	total n-alkanes (ng l^{-1})	dibenzothiophene (ng l^{-1})
19	0	115.2	0.6
	30	96.3	1.5
	45	67.2	1.5
20	0	66.8	0.7
	50	207.2	1.3
	60	83.4	1.2
22	0	73.7	0.5
	30	76.4	0.5
	40	61.0	0.5
24	0	87.7	nd
	22	110.4	nd

pattern of n-alkane concentrations was common in the open seawater in the central region in the present study. These normal distribution patterns may be reasonably interpreted by assuming that the concentrations of n-alkanes shorter than C_{12} decreased due to rapid volatilization and/or bacterial mineralization, whereas the concentrations of high molecular weight n-alkanes with longer than C_{25} were limited by their low solubility in seawater. However, reported solubilities of dodecane (C_{12}) and hexacosane (C_{26}) in seawater are 31 nM (5270 ng l^{-1}) and 1.0 nM (366 ng l^{-1}), respectively (Sutton and Calder, 1974). The concentrations of individual n-alkanes we measured in open seawaters of the ROPME sea area in the central region were lower than their respective solubilities, at least for in the range of C_{12} to C_{26}. Thus, the present n-alkane concentrations would have been undersaturated and not limited by their solubilities. The proportions of low molecular weight n-alkanes (shorter than C_{12}) in crude oils are known to be much higher than those of high molecular weight n-alkanes (longer than C_{25}) and we have experienced declines in n-alkane concentrations in seawater samples 3 months after storage on the January 1993 cruise, despite the addition of mercuric chloride on board to all seawater samples to final concentrations of about 40 mg Hg l^{-1}. These results suggest that the seawater in the ROPME sea area may have high mineralization activity of n-alkanes by bacteria.

The n-alkanes in the seawater sample collected at 10 m depth of Station 4 in 1993 were distributed with odd carbon number predominance (Fig. 5), suggesting a phytoplankton origin (Clark and Blumer, 1967). However, we found no other seawater samples with odd carbon predominance. Thus, although we directly extracted n-alkanes with n-hexane from all seawater samples without filtration, the present data on n-alkanes implies that they were not over-estimated.

The Carbon Preference Indexes (CPI) of n-alkanes from almost all stations showing normal distribution patterns of n-alkanes with a peak at C_{18}–C_{19} were near unity, suggesting origin mainly from crude oil (Mille *et al.*, 1992; Ehrhardt and Burns, 1993; Ehrhardt and Petrick, 1993). Also, the Unresolved Complex Mixture (UCM) was clearly apparent in the ion chromatograms of the relatively high n-alkane concentration samples, suggesting that these n-alkanes originated

Table 4a. Total n-alkane and dibenzothiophene concentrations in the seawater at Dec. 1994.

station No.	sampling depth(m)	total n-alkanes(ng l^{-1})	dibenzothiophene(ng l^{-1})
3	0	652.4	0.9
4	0	308.3	2.1
	15	500.0	1.7
	30	434.8	1.5
	40	305.0	2.0
7	0	300.7	1.3
	10	175.7	0.5
	30	152.0	1.2
	50	172.3	0.6
	70	247.6	0.9
8	0	182.4	1.4
	10	244.8	1.3
	30	121.3	1.0
	60	104.6	1.1
10	0	99.7	0.5
	10	62.2	nd
	26	101.3	nd
11	0	97.2	0.8
	10	87.5	nd
	24	101.3	nd
13	0	144.3	nd
	10	125.1	nd
	30	77.5	0.7
	68	72.0	nd
14	0	59.2	nd
	10	60.1	0.5
	30	60.4	nd
	62	86.2	nd
15	0	184.9	1.3
	20	76.6	nd
16	0	136.0	1.0
	30	124.2	0.5
	40	167.9	0.5
17	0	220.7	0.8
	30	204.4	0.5
	50	49.4	nd
18	0	61.9	0.5
	30	66.0	1.0
	50	89.2	1.5

from spilled crude oils. These sampling stations would have frequently been contaminated by successive crude oil leakages and discharges (Al-Saad, 1990; Morel *et al.*, 1991).

In 1993 and 1994, high concentrations of total n-alkanes were not observed in the northern part of the ROPME sea area (Figs. 6 and 7), which was heavily contaminated by the Gulf War oil spill in 1991. On the other hand, relatively high concentrations of total n-alkanes were observed in the ROPME sea area near the Strait of Hormuz. These results are consistent with the results of a study of

Table 4b.

station No.	sampling depth(m)	total n-alkanes(ng l^{-1})	dibenzothiophene(ng l^{-1})
19	0	115.2	0.6
	30	96.3	1.5
	45	67.2	1.5
20	0	66.8	0.7
	50	207.2	1.3
	60	83.4	1.2
22	0	73.7	0.5
	30	76.4	0.5
	40	61.0	0.5
24	0	87.7	nd
	22	110.4	nd

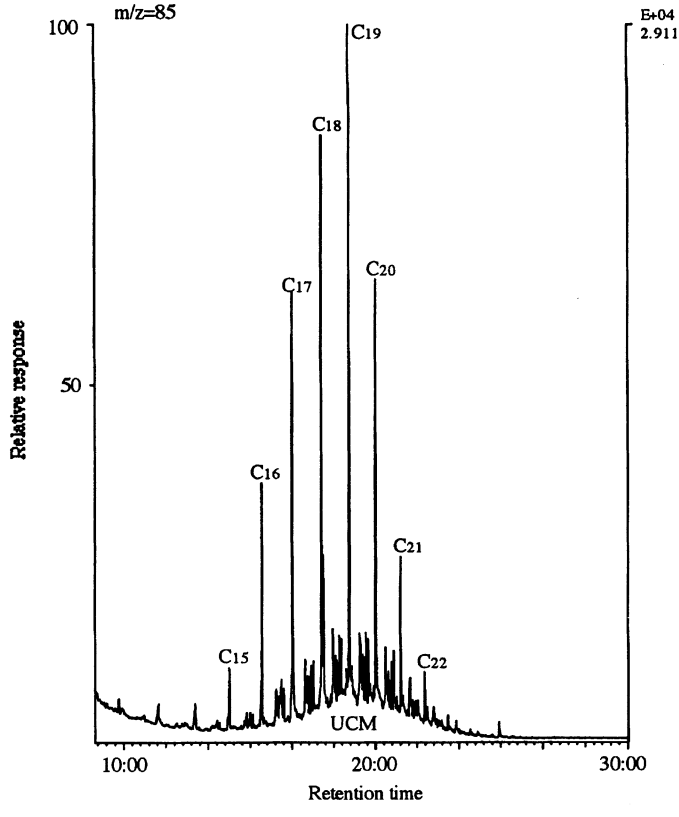

Fig. 3. Normal-alkanes SIM chromatogram of 40 m seawater sample from Sta. 5 in Dec. 1993.

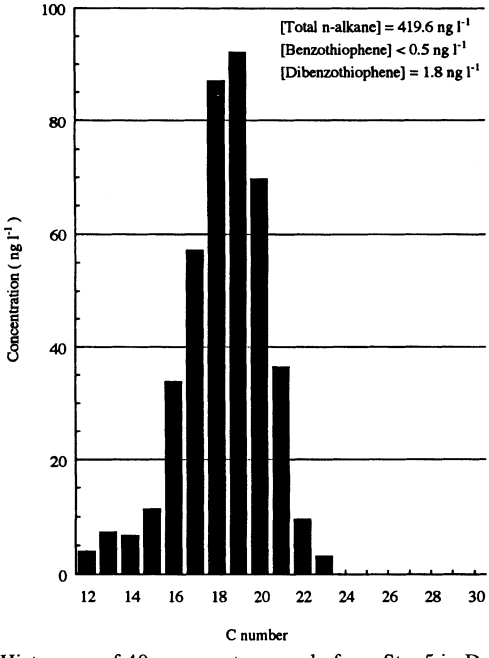

Fig. 4. Histogram of 40 m seawater sample from Sta. 5 in Dec. 1993.

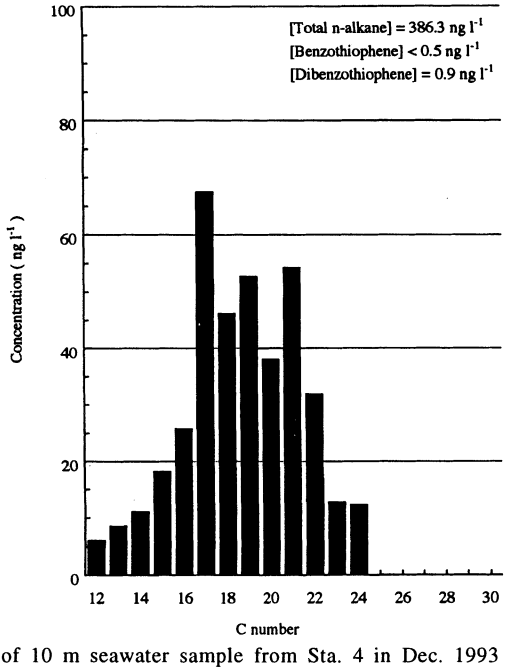

Fig. 5. Histogram of 10 m seawater sample from Sta. 4 in Dec. 1993 (odd carbon number predominance).

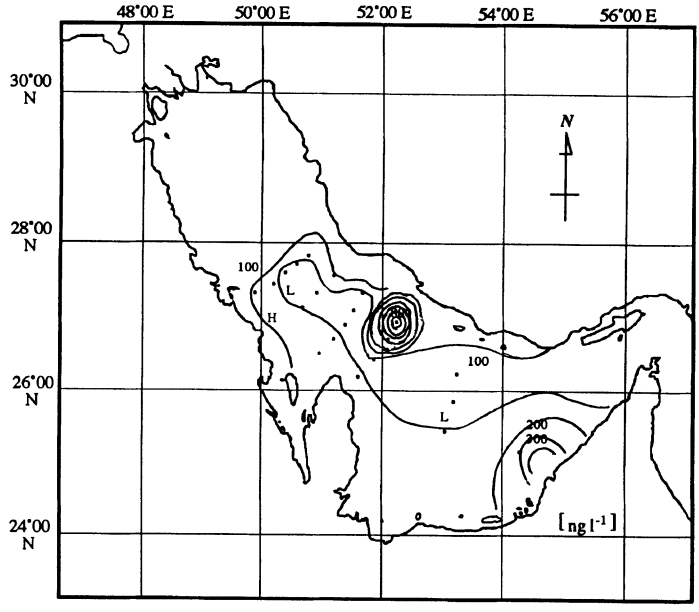

Fig. 6. Distribution of total n-alkanes(ng l^{-1}) in the RSA surface water in Dec. 1993.

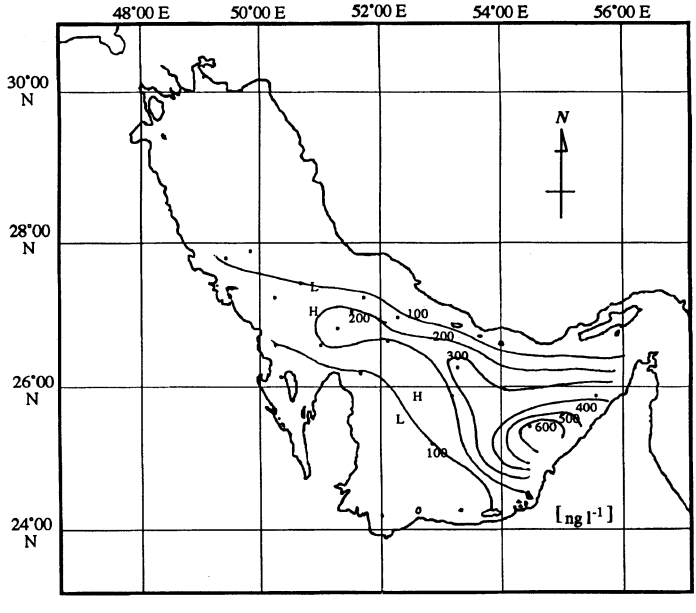

Fig. 7. Distribution of total n-alkanes(ng l^{-1}) in the RSA surface water in Dec. 1994.

organotin compounds contamination in fish (Watanabe *et al.*, 1997).

The bottom waters in the central part in the ROPME sea area have relatively higher total n-alkane concentrations than those in surface waters at stations 5, 8, 11, 16 and 17 in 1993 (Table 3a and b), and at stations 10, 14, 16, 18 and 24 in 1994 (Table 4a and b). These results were in agreement with those observed by El Samra (1988) and Emara (1990), and also suggest that oil pollution in this area is extending not only to surface water, but also to middle and bottom waters. In other words, surface seawater contaminated with crude oil spill in shallow area may flow southeast along Saudi Arabian coast, increase in density with time, and sink into the middle and bottom water along the west side of the Qatar peninsula.

Dibenzothiophene was detected at low concentrations at many sampling stations. Dibenzothiophene is one of the most persistent components in crude oil and the most toxic to marine organisms (Ogata *et al.*, 1977, 1979, 1980, 1981; Berthou *et al.*, 1981; Clark, 1992). Although benzothiophene in open seawater should be present at levels similar to those of dibenzothiophene, as in crude oils, benzothiophene was not detected in any seawater samples. These results were probably due to rapid bacterial degradation of benzothiophene, rather than low solubility in seawater, because although the solubility of dibenzothiophene in seawater is lower than that of benzothiophene, dibenzothiophene was detected in most seawater samples.

The linear relationship between dibenzothiophene and total n-alkane concentrations suggests that the latter total n-alkane can be a reliable index of crude oil spills (Fig. 8). This linear relationship implies that fresh crude oil spill into seawater was occurring, because, among crude oils components, n-alkanes are the most degradable and dibenzothiophene is persistent in the environment. Further, this linear relationship also suggested that the contributions of phy-

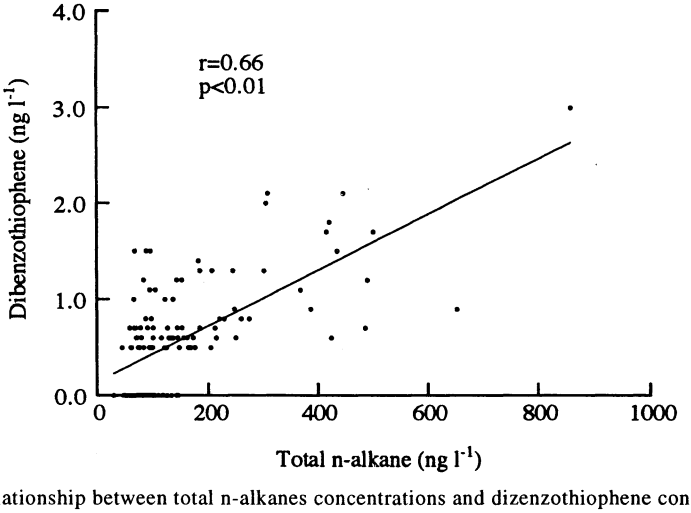

Fig. 8. Relationship between total n-alkanes concentrations and dizenzothiophene concentrations in the RSA in 1993 and 1994.

toplankton and zooplankton to the n-alkanes in open seawaters of the central region of the ROPME sea area was insignificant.

The present study suggested that the main source of the present crude oil pollution in the central part in the ROPME sea area was successive crude oil inputs from sources such as discharges of ballast and bilge waters by tanker, pipeline failure, and small accidents at marine oil terminals, rather than the Gulf War oil spill in January 1991. The impact of the Gulf War crude oil spill on the offshore ecosystem would not have lasted, even if there had been serious impact on the offshore ecosystem at the time. This study confirmed the results of some previous reports (Readman, 1992; Ehrhardt and Burns, 1993; Gupta *et al.*, 1993).

CONCLUSIONS

Total n-alkane concentrations (ΣC_{12}–C_{30}) in open seawater samples from the central region of the ROPME sea area ranged from 29.8 to 859 ng l^{-1} in 1993 and from 49.4 to 652 ng l^{-1} in 1994. Total n-alkane concentrations in the northern part of the ROPME sea area, where the crude oil spill occurred in 1991, were lower than those in the southern part. The results of the present study suggested that the impact of the Gulf War oil spill on the offshore ecosystem in the central region of the ROPME sea area did not persist 2–3 years after the crisis. The linear relationship between total n-alkane and dibenzothiophene concentrations suggested that offshore ecosystem in the central region of the ROPME sea area is being affected by successive inputs of crude oils such as discharges of ballast and bilge waters from tankers and oil well leakage.

Acknowledgements

We would like to thank Captain I. Kasuga, the officers, and the crews of R/V Umitaka-Maru for their cooperation in samplings.

REFERENCES

Alam, I. A. H. (1993). The 1991 Gulf War Oil Spill-Lessons from the past and a warning for the future. Mar. Pollut. Bull. 27, 357–360.

Berthou, F., Gourmelun, Y., Dreano, Y. and Friocourt, M. P. (1981). Application of gas chromatography on glass capillary columns to the analysis of hydrocarbon pollutants from the Amoco Cadis Oil Spill. J. Chromatogr. 203, 279–292.

Clark, R. B. (1992). Marine Pollution third edition, Clarendon Press, Oxford. pp. 28–52.

Clark, R. C., Jr. and Blumer, M. (1967). Distribution of n-paraffins in marine organisms and sediment. Limnol. Oceanogr. 12, 79–87.

Desideri, P. G., Lepri, L. and Checchini, L. (1992). A new apparatus for the extraction of organic compounds from aqueous solution. Microchim. Acta 107, 55–63.

Ehrhardt, M. and Burns, K. A. (1993). Hydrocarbons and related photo-oxidation products in Saudi Arabian Gulf coastal waters and hydrocarbons in underlying sediments and bioindicator bivalves. Mar. Pollut. Bull. 27, 187–197.

Ehrhardt, M. and Douabul, A. (1989). Dissolved petroleum residues and alkylbenzene photo-oxidation products in the upper Arabian Gulf. Mar. Chem. 26, 363–370.

Ehrhardt, M. and Petrick, G. (1993). On the composition of dissolved and particle-associated fossil fuel residues in Mediterranean surface water. Mar. Chem. 42, 57–70.

El Samra, M. I. and El Deeb, K. Z. (1988). Horizontal and vertical distribution of oil pollution in the

Arabian Gulf and the Gulf of Oman. Mar. Pollut. Bull. 19, 14–18.
El Samra, M. I., Emara, H. I. and Shunbo, F. (1986). Dissolved petroleum hydrocarbon in the northwestern Arabian Gulf. Mar. Pollut. Bull. 17, 65–68.
Emara, H. I. (1990). Oil pollution in the southern Arabian Gulf and Gulf of Oman. Mar. Pollut. Bull. 21, 399–401.
Mille, G., Rivet, L., Jawad A. I. and Bertrand J. C. (1992). Hydrocarbon distribution in low polluted surface sediments from Kuwait, Bahrain and Oman coastal zones (before the Gulf War). Mar. Pollut. Bull. 24, 622–626.
Morel, G., Samhan, O. et al. (1991). Evaluation of chromatographic and spectroscopic methods for the analysis of petroleum-derived compounds in the environment. Frescenius J. Anal. Chem. 339, 669–715.
Ogata, M. and Miyake, Y. (1979). Identification of organic sulfur compounds transferred to fish from petroleum suspension by mass chromatography. Water Res. 13, 1179–1185.
Ogata, M. and Miyake, Y. (1981). Identification of organic sulfur compounds and poly cyclic hydrocarbons transferred to shellfish from petroleum suspension by capillary mass chromatography. Water Res. 15, 257–266.
Ogata, M., Miyake, Y. and Kira, S. (1977). Transfer to fish of petroleum paraffins and organic sulfur compounds. Water Res. 11, 333–338.
Ogata, M., Miyake, Y., Fujisawa, K., Kira, S. and Yoshida, Y. (1980). Accumulation and dissipation of organosulfur compounds in short-necked clam and eel. Bull. Environm. Contam. Toxicol. 25, 130–135.
Readman, J. W., Fowler, S. W., Villeneuve, J. P., Cattini, C., Oregioni, B. and Mee, L. D. (1992). Oil combustion-product contamination of the Gulf marine environment following the war. Nature 358, 662–665.
Sen Gupta, R., Fondekar, S. P. and Alagarsamy, R. (1993). State of oil pollution in the northern Arabian sea after the 1991 Gulf oil spill. Mar. Pollut. Bull. 27, 85–91.
Sutton, C. and Calder, J. A. (1974). Solubility of higher-molecular-weight n-paraffins in distilled water and seawater. Environ. Sci. *Tech.* 8, 654–657.
Tawfiq, N. I. and Olsen, D. A. (1993). Saudi Arabia's response to the 1991 Gulf Oil Spill. Mar. Pollut. Bull. 27, 333–345.
Watanabe, M., Hashimoto, S., Fujita, K. and Otsuki, A. (1998). Organotin compounds contamination of fish in the ROPME sea area. in this book.

Offshore Environment of the ROPME Sea Area after the War-Related Oil Spill, Eds. A. Otsuki *et al.*, pp. 231–244.

Distribution of organotin compounds in fish and the ratio of phenyl-tin to total organic-tin in the ROPME Sea Area

Masami WATANABE[1], Shinya HASHIMOTO[1], Kiyoshi FUJITA[2] and Akira OTSUKI[1]

[1]*Department of Marine Science & Technology, Tokyo University of Fisheries, 4-5-7 Konan, Minato-ku, Tokyo 108-8477, Japan*
[2]*Department of Aquatic Biosciences, Tokyo University of Fisheries, 4-5-7 Konan, Minato-ku, Tokyo 108-8477, Japan*

Abstract—Organotin compounds, particularly tributyltin (TBT), have been widely used as antifouling agents in various paints for ships, boats and aquaculture nets. These organotin compounds are known to be persistent in the aquatic environment for long time, and to have high toxicity against shellfish. Although many countries started to regulate the use of antifouling paints containing TBT, their use on large vessels is not regulated yet. Thus, it remains necessary to monitor organotin contamination from large vessels.

The ROPME Sea Area has heavy oil tankers traffic to and from the oil-producing countries along the coast. Therefore, the ROPME Sea Area should provide the best area to evaluate the organotin contamination from large vessels. This study reports the contamination of organotin compounds from oil tankers in the ROPME Sea Area through analysis of fish samples.

Organotin compounds in muscle and liver samples of fish were detected throughout the ROPME Sea Area. The distribution of butyltin compounds in fish increased along Arabian shore north from the inner part to the Strait of Hormuz. Although the concentrations of phenyltin compounds were extremely low compared to those of butyltin compounds, they were also detected throughout the ROPME Sea Area.

The main emission source of organotin compounds in the ROPME Sea Area is oil tankers and since the use of triphenyltin compounds as antifouling agent is limited to Japan, large vessels built in Japan may be the sole source of phenyltin compounds there. Assuming that the ratio of phenyl-tin (PTs) to total organictins (TOTs, total phenyltin plus total butyltin) in fish samples can be an index of organotin contamination caused by oil tankers built in Japan, we estimated that about 60% of total organotin contamination in the ROPME Sea Area might be from oil tankers built in Japan.

INTRODUCTION

Tributyltin compounds (TBT) have been widely used as one of antifouling agents in paints for ships, boats and aquaculture nets since mid-1960s to control the attachment and growth of periphyton such as barnacles and mussels (Huggett *et al.*, 1992). This is particularly true for large vessels, because these fouling organisms produce turbulent flow and increase resistance across the hulls of

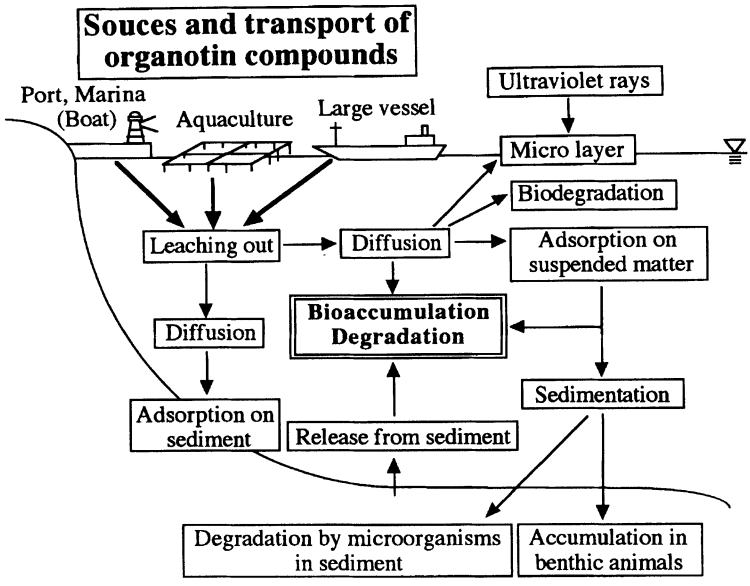

Fig.1. Source and transport of organotin compounds in aquatic environment.

ships, leading to increased fuel consumption and decreased speed (Huggett *et al.*, 1992). Antifouling prevent the attachment of marine organisms by releasing TBT from the paint film slowly. Therefore, it was inevitable that the aquatic environment is contaminated with TBT and/or its decomposition products.

Since a French scientist reported marine pollution by organotin compounds (Alzieu, 1991), many studies have been done. France was the first country to prohibit the use of antifouling paints containing TBT on boats shorter than 25 m in 1982. Later, several advanced countries regulated their use (Huggett *et al.*, 1992). However, the use of antifouling paints containing TBT for large vessels is not yet internationally regulated. Thus, it remains necessary to monitor the organotin contamination from the large vessels.

Figure 1 shows the routes of organotin compounds into aquatic environment. The main sources of TBT are antifouling paints on ships, boats, and aquaculture nets. TBT released from these sources are diffused by tidal movements and ocean currents. The concentrations of TBT in coastal seawaters are usually reported to be at ppt levels (Gabrielides *et al.*, 1990). The concentrations of TBT in seawater near shore are variable due to the distance from their sources, ship activity and exchange rates of seawater in enclosed bays.

Since alkyltin compounds are hydrophobic, they easily adsorb onto suspended matters, and then sink to the bottom. Thus, the concentrations of TBT in sediments have been reported to reach levels of a few hundred ppb. Although the half life of TBT in seawaters is in the range of several days to 2 weeks (Seligman *et al.*, 1988; Lee *et al.*, 1989; Adelman *et al.*, 1990), that of TBT in the sediments

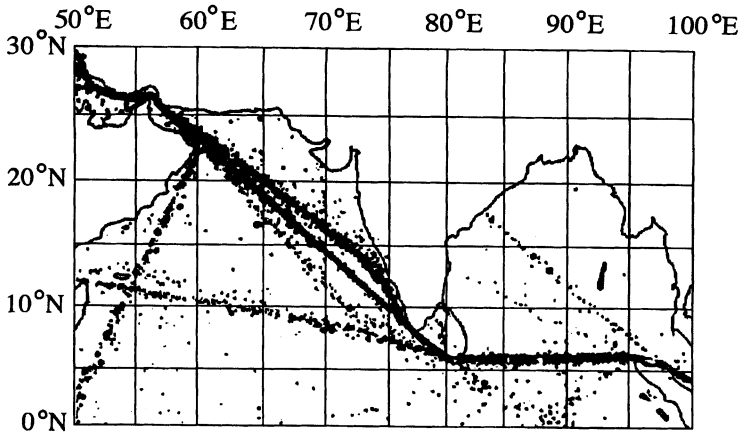

Fig. 2. Oil tanker routes and shipping lanes in the Indian Ocean (Gupta & Kureishy, 1981).

is reported to be in the range of 1/2 to 2 years (Wade *et al.*, 1990; Sarradin *et al.*, 1994; de Mora *et al.*, 1995). Organotin compounds are also well known to be easily accumulated by shellfish through biomagnification (Alzieu, 1991).

Although TBT has been shown to be an extremely effective biocide, TBT is also known to be the most toxic in organotin compounds, and causes oyster shell anomalies (Alzieu *et al.*, 1986, 1989; Dyrynda, 1992), imposex in gastropods (Bryan *et al.*, 1989; Stewart *et al.*, 1992; Evans *et al.*, 1995), and reduced growth in bivalves. Further, the minimum concentration at which TBT causes imposex for gastropods has been reported to be 2 ng l^{-1} in seawater (Bryan *et al.*, 1989; Dyrynda, 1992); such low concentrations in seawater are difficult to quantify.

Recently, it was reported that organotin contamination has been declining since regulations on the use of antifouling paints containing TBT have come into force. Specifically, ambient levels of TBT are decreasing in the water column, sediments and soft tissues of molluscs, and recoveries of imposex in dogwhelks and oyster shell anomalies were observed (Alzieu *et al.*, 1986; Wade and Garcia-Romero, 1991; Dowson *et al.*, 1993; Evans *et al.*, 1995; Minchin *et al.*, 1995). However, the release of organotin compounds from large vessels still continues.

The ROPME Sea Area has heavy oil tankers (large vessels) traffic, because there are several oil-producing countries along the coast (Fig. 2) (Gupta and Kureishy, 1981). The main emission source of organotin compounds in this area would be oil tankers. However, there is little information about organotin contamination in this area. This study reports the concentrations of organotin compounds in fish samples and phenyltin contamination of this area.

MATERIALS AND METHODS

Fish muscle and liver samples were analyzed for tributyltin (TBT), Triphenyltin (TPT), and their degradation products such as dibutyltin (DBT),

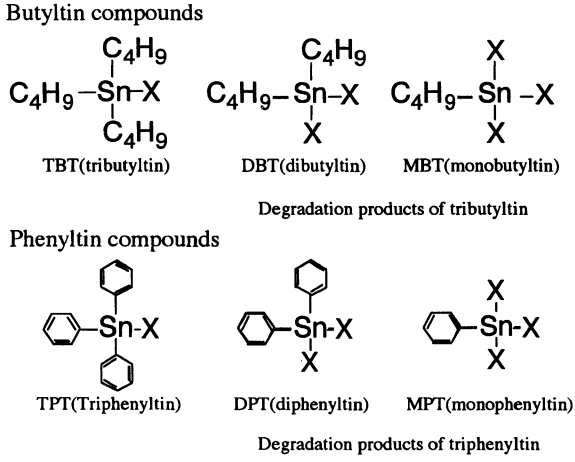

Fig. 3. Chemical structures of organotin compounds.

monobutyltin (MBT), diphenyltin (DPT) and monophenyltin (MPT) (Fig. 3). The use of TBT and TPT as the most effective antifouling agents for paints are not officially prohibited, but their production has been regulated in Japan.

Sampling

Figure 4 shows the sampling stations in the ROPME Sea Area. Bigeye scad (*Selar crumenophthalmus*), roundherring (*Etrumeus teres*), seacatfish (*Arius thalassinus*), lizardfish (*Saurida undosquamis*), barracuda (*Sphyraena putnamiae*), butterfly breams (*Nemipterus* spp.), and lined piggy (*Pomadasys stridens*) were caught by gill net and/or line in December 1993 and 1994 (Table 1). They were stored at –20°C until analysis.

Table 1. Fish species caught in the RSA in December 1993 and 1994.

English name	Scientific name
Bigeye scad	*Selar crumenophthalmus*
Roundherring	*Etrumeus teres*
Seacatfish	*Arius thalassinus*
Lizardfish	*Saurida undosquamis*
Barracuda	*Sphyraena putnamiae*
Butterfly breams	*Nemipterus* spp.
Lined piggy	*Pomadasys stridens*

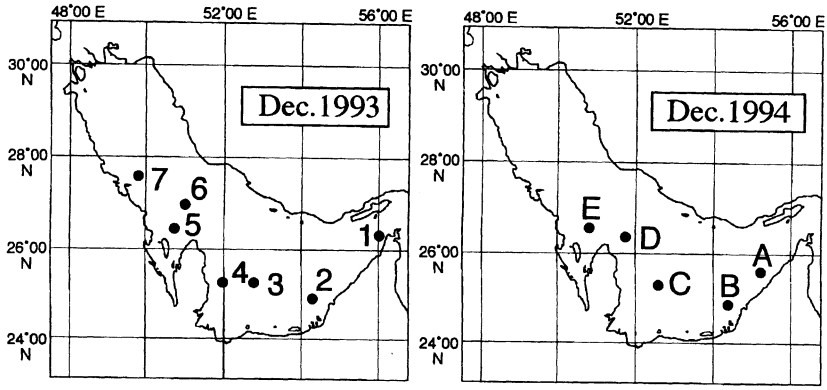

Fig. 4. Sampling stations in the RSA in December 1993 and 1994.

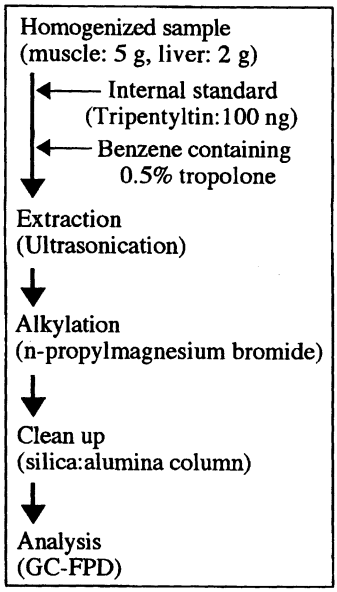

Fig. 5. Flow chart of analytical method for organotin compounds.

Analytical procedure

Figure 5 shows the analytical method of organotin compounds used. To about 5 g of homogenized muscle or 2 g of homogenized liver samples, 100 ng of tripentyltin as an internal standard, 0.1 g ascorbic acid, 10 ml 1 N hydrochloric acid/ethanol (9:1), and 10 ml benzene containing 0.5% tropolone were added. The mixture was then ultrasonicated for 30 min. and centrifuged at 3,000 rpm for 10

Table 2. GC-FPD analytical conditions for determination of organotin compounds.

Capillary column	DB-1 30 m, 0.25 mm i.d., Film 1 μm
Sample volume	2 μl
Injector temperature	270℃
Oven	
Initial oven temperature	80℃ (1 min)
Temperature program	40℃/min to 160℃
	2.5℃/min to 195℃
	15℃/min to 270℃
Final oven temperature	270℃ (25min)
Detector temperature	280℃
Carrier gas (He)	
Total flow	60 ml/min
Septum purge	1 ml/min
Column head pressure	20 psi
FPD	
Hydrogen flow rate	200 ml/min
Air (oxygen, 21%; nitrogen, 79%) flow rate	100 ml/min
Nitrogen flow rate	20 ml/min

min. to separate the benzene layer. After the benzene layer was collected, a further 8 ml benzene containing 0.5% tropolone and 2 ml ethanol were added to the residue. After ultrasonication and centrifugation, this second benzene layer was collected and combined with the first extract. The combined benzene extract was washed with 10% sodium chloride solution to remove soluble proteins. After removal of water with dehydrated sodium sulfate, the benzene extract was concentrated to about 5 ml in a rotary evaporator at 40°C and further concentrated to 1 ml by evaporation under a nitrogen gas flow. After displacement to *n*–hexane, extracted organotin compounds were converted into their *n*-propyl derivatives by reaction with 1 ml n-propylmagnesium bromide for 30 min. at room temperature. After the excess reagent was decomposed by addition of 4 ml 10% ammonium chloride solution and it was centrifuged to separate *n*–hexane layer, the extract was collected and clean-upped by passage through a silica/alumina column. After elution from the column in 50 ml n-hexane:benzene (1:1), the eluent was concentrated to 5 ml in a rotary evaporator at 40°C, and further concentrated to 0.25 ml by evaporation under a nitrogen gas flow. The concentrates were analyzed by a GC-FPD. Table 2 shows the GC-FPD analytical conditions. The detection limit of this method was about 1 ng g^{-1} wet weight.

RESULTS AND DISCUSSION

Organotin compounds were detected in most fish muscle and liver samples, TBT in 51 out of 55 samples and TPT in 42 out of 55 samples. The concentrations of TBT and TPT in fish muscle samples were in the range from below the detection limit to 21 and below the detection limit to 7 ppb (ng chloride g^{-1} wet

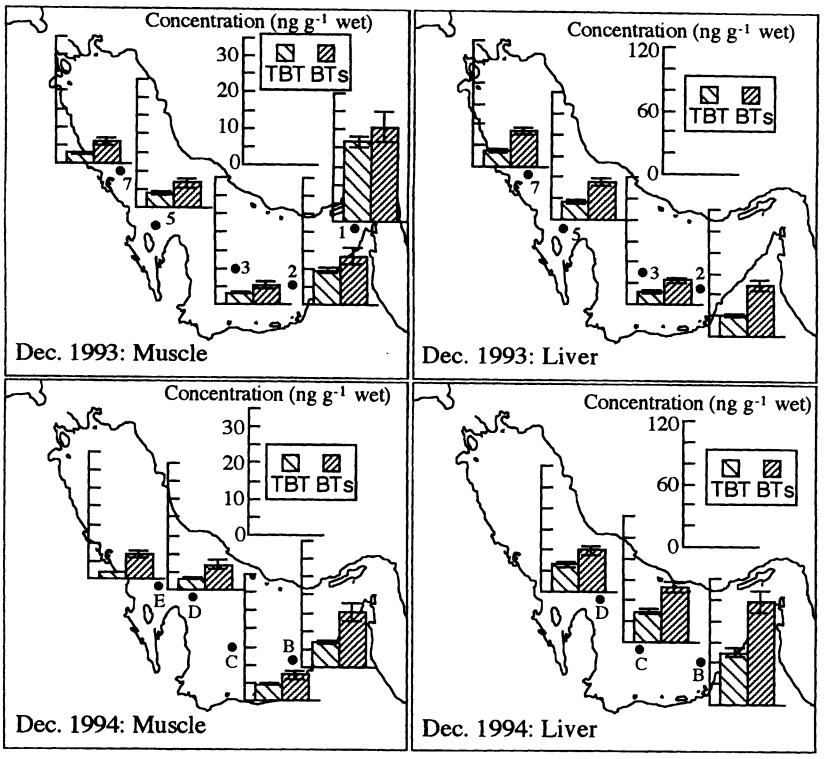

Fig. 6. Concentrations of TBT and total butyltin compounds (BTs) in muscle and liver samples of bigeye scad (*selar crumenophthalmus*) in December 1993 and 1994.

weight), respectively, and those in fish liver samples were in the range from below the detection limit to 50 and below the detection limit to 40 ppb, respectively. The concentrations of organotin compounds in fish in December 1994 were almost the same as those in December 1993.

Distribution of organotin compounds in the ROPME Sea Area

Since bigeye scad (*Selar crumenophthalmus*) could be collected at almost all sampling stations in December 1993 and 1994 in this area, we used the concentrations of organotin compounds in this species to evaluate the distribution of organotin contamination in this area.

The concentrations of TBT and total butyltin compounds (BTs) in muscle and liver samples of bigeye scad in this area in December 1993 and 1994 increased to inside of the Strait of Hormuz along the Arabian shores (Fig. 6), suggesting that the inside of the Strait on the side of UAE was the area most contaminated with butyltin compounds. The distributions of butyltin compounds in the other fish species showed a similar tendency. These results can be explained reasonably by the following 2 possibilities: the high concentrations of

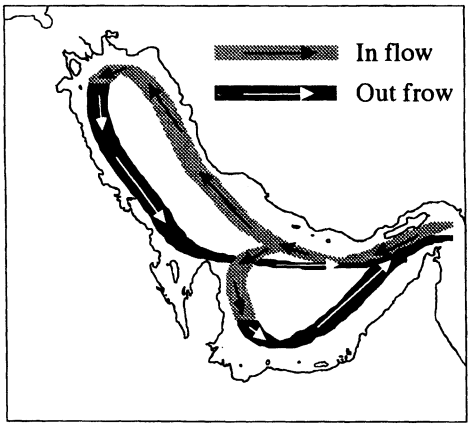

Fig. 7. Hypothesized currents in the RSA added to the original figure by Reynolds(1993). Black bands were newly added.

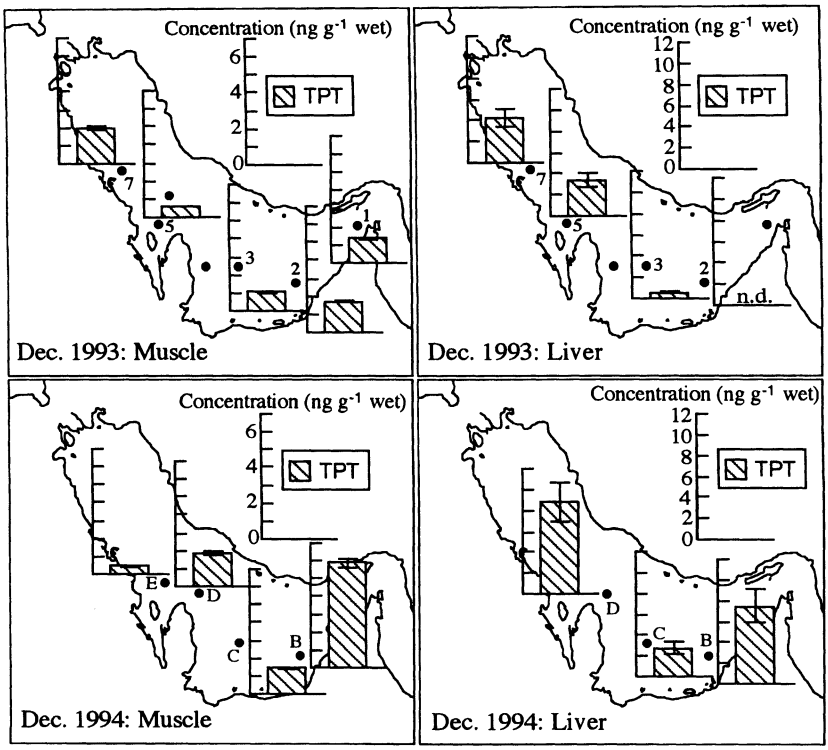

Fig. 8. Concentrations of TPT in muscle and liver samples of bigeye scad (*selar crumenophthalmus*) in December 1993 and 1994.

butyltin compounds near the inside of the Strait on the side of UAE were due to either the high volume of tankers traffic there (see Fig. 2), or older seawater contaminated with organotin compounds flowing along the Arabian coast and out from the Strait. Based on CTD data (Yoshida *et al.*, this book), organotin concentrations in fish, and the original current scheme proposed by Reynolds (1993), we hypothesize a revised current scheme for this area. Surface water enters the Gulf from Oman Bay and flows in a generally counter-clockwise circulation pattern, moving north-west along the Iranian coast, with part of the flow turning back south-east along the Arabian coast. Salinity gradually increases with flow and the high salinity water eventually sinks along the Qatar's shore (Abuzinada and Krupp, 1994). The other part of the flow turns back south near the east side of Qatar and its salinity, too, gradually increases with the high salinity water sinking near the Strait of Hormuz along the UAE's shore and then moving out of the Gulf near the bottom of the Strait.

Although TPT was a dominant compound in muscle and liver samples of bigeye scad (Fig. 8), TPT concentrations in fish in this area were extremely low compared to those of butyltin compounds. However, the distributions of TPT and butyltin compounds in liver samples in this area differed, while those in muscle samples were similar.

Difference in organotin concentrations among 7 fish species

The highest average concentrations of organotin compounds were found in liver sample of seacatfish caught at station A in December 1994 (see Fig. 9). Although BTs concentrations in the seacatfish liver samples were higher than those in the livers of the other fish species, the TBT concentrations were not always markedly different among the 7 fish species. The BTs concentrations in the liver samples were 5 to 10 times higher than those in the muscle samples. TBT was the dominant organotin compound in muscle samples, while DBT was the dominant compound in liver samples. This trend was most obvious in seacatfish and lizardfish. Since seacatfish is a benthic carnivore and feeds on benthic small crabs and shrimps which accumulate organotin compounds from the sediments (Takayama *et al.*, 1994), it is reasonable that seacatfish had the highest concentrations of BTs and PTs in their livers. The present results are consistent with previous reports that fish liver can metabolize TBT to DBT (Lee, 1985). Although the PTs concentrations in liver samples of seacatfish were also much higher than those in the other fish species tested, the TPT concentrations were not markedly different among the 7 fish species, suggesting that TPT was not easily metabolized in fish livers compared with TBT (Takayama *et al.*, 1994).

Unlike the case for butyltins, among which TBT was sometimes the most abundant form and sometimes not, TPT was the dominant phenyltin compound in muscle and liver samples from all the species tested. While the BTs concentrations in liver samples were much higher than those in muscle samples, the PTs concentrations in liver samples were not much higher than those in muscle samples, except in the case of seacatfish. These results agreed with those of other

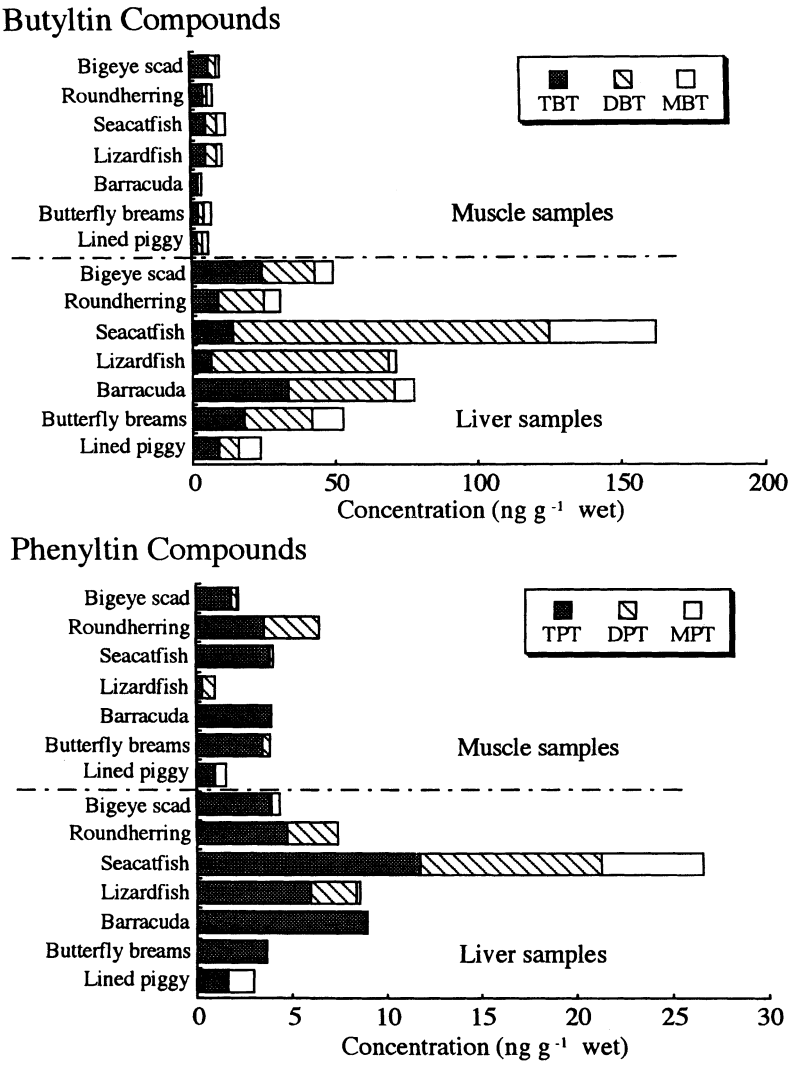

Fig. 9. Concentrations of organotin compounds in muscle and liver samples of fish caught. Average concentrations for each species.

reports of organotin contamination in fish (Krone *et al.*, 1989, 1991; Takayama *et al.*, 1995). .

Comparison of organotin concentrations in the ROPME Sea Area and Tokyo Bay

BTs concentrations in muscle samples from Tokyo Bay fish were 8 to 10 times higher than those from this central area (Fig. 10). PTs concentrations in

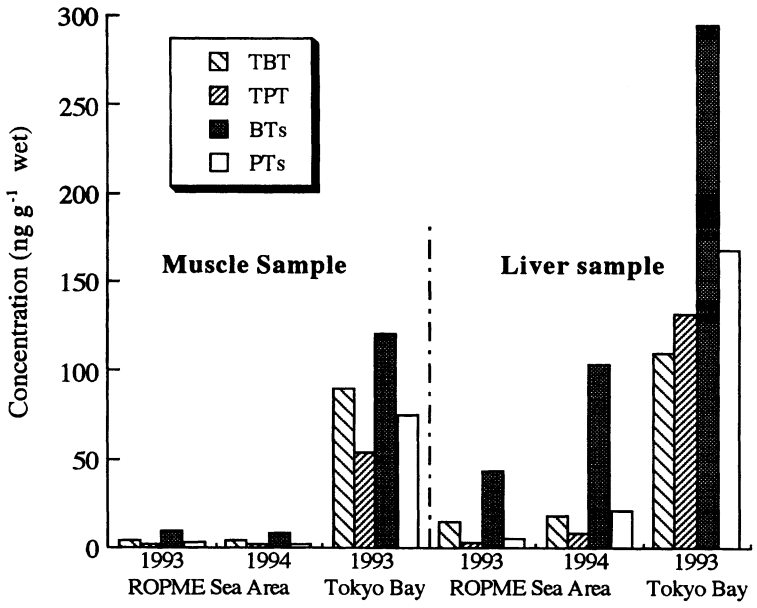

Fig. 10. Organotin concentrations in fish from the ROPME sea area and Tokyo Bay, given as the average concentrations of all fish samples. Organotin concentrations in Tokyo Bay were cited from Takayama *et al.* (1995).

muscle samples from Tokyo Bay were also 10 to 15 times higher than those from this central area. Organotin concentrations in fish from this central area were all much lower than those from Tokyo Bay except for BTs from seacatfish liver samples. These results were expected not only because of the large difference in industrial activities between the ROPME Sea Area and Tokyo Bay area, but also because Tokyo Bay has much heavier ship traffic.

Comparison of PTs/Total organotin ratio between the ROPME Sea Area and Tokyo Bay

Oil tankers are the main organotin source in this central area. Since Japan has been the only major country recently producing triphenyltin compound as an antifouling agent, it would be reasonable to assume that large vessels built in Japan are the only source of phenyltin compounds in this central area. For this reason, we calculated the ratio of PTs to total organotin in fish to estimate the contribution of organotin contamination by oil tankers built in Japan to the total organotin contamination of this central area. We expressed these concentrations in units of ng Sn g^{-1} wet weight of fish muscle or liver when PTs/total organotin in fish was calculated.

Table 3 shows the PTs/total organotin ratios from fish muscle and liver samples in the ROPME Sea Area and Tokyo Bay. In Tokyo Bay, the contribution

Table 3. PTs/total organotin ratios from muscle and liver samples of fish from the RSA and Tokyo Bay.

	Tokyo Bay	The ROPME Sea	
	1993	1993	1994
Muscle	0.35	0.24	0.19
Liver	0.32	0.09	0.11

- Total Org-Sn : BTs+PTs.
- Organotin compounds concentrations were expressed as ng Sn g^{-1}wet weight.

of phenyltin comprised about 30% of total organotin contamination, whereas it accounted for only 10–20% in this central area (Table 3). The PTs/total organotin ratios were clearly lower than those in Tokyo Bay. These reasonable results also suggested that the PTs/total organotin ratio in fish muscle may be a reliable index of the contribution of oil tankers built in Japan to the total organotin contamination in this central area. We estimated the contribution of organotin contamination from oil tankers built in Japan to the total organotin contamination in this central area using PTs/total organotin ratios for fish muscle from Tokyo Bay and from the central area, because Japanese ship-builders can still use antifouling paints containing tributyltin compounds or triphenyltin compounds on large vessels.

Here we can set up the following equation:

$$\text{PTs(J)/Total Organotin} = \text{PTs(J)}/[\text{BTs(O)} + \text{BTs(J)} + \text{PTs(J)}] \quad (1)$$

where PTs(J): Contribution of total phenyltin compounds from large vessels built in Japan, BTs(O): Contribution of total butyltin compounds from large vessels built in other countries, BTs(J): Contribution of total butyltin compounds from large vessels built in Japan.

We assumed the followings:

(1) The release rate of butyltin and phenyltin compounds from large vessels built in Japan were nearly constant.

(2) In the ROPME Sea Area, the large vessels built in Japan released butyltin and phenyltin compounds at the same rate as they do in Tokyo Bay.

(3) The biomagnification factor of butyltin compounds in fish was approximately the same as that of phenyltin compounds.

(4) The contribution by vessels built in other countries to total organotin contamination of Tokyo Bay was negligible, implying that PTs(J) plus BTs(J) equals one.

Based on these assumptions, the contribution by large vessels built in Japan to total organotin contamination in this area was calculated using the PTs/Total organotin ratio in fish muscle samples by solving Eq. (1). We used fish muscle

rather than liver samples because fish muscle would more slowly metabolize organotin compounds.

Substituting the fish muscle values from Table 3 into Eq. (1), we estimated the proportion of organotin contamination from oil tankers built in other countries (BTs(O)) to be 0.59. Because the contribution of organotin contamination from oil tankers built in Japan was 1, the proportion of organotin contamination in the ROPME Sea Area from oil tankers built in Japan was estimated to be about 60%. The production of triphenyltin compounds was banned in 1990, in 1990 and 1992 Japan has occupied 40–45% of tonnage and number of newly launched ships (gross tonnage above 100 tons) in the world, of which oil tankers comprised about 20% (Ministry of transport, 1994). Therefore, this estimate would not be unreasonable.

CONCLUSIONS

Although organotin contamination of fish in the ROPME Sea Area was clearly light compared to that in Tokyo Bay, it was detected in all fish throughout the central area. Butyltin compounds increased from the inner part of the ROPME Sea Area toward the Strait of Hormuz, unlike the distribution of phenyltin compounds. The present results suggested that butyltin contamination was the heaviest inside of the Strait of Hormuz near the UAE. The present results also suggested that about 60% of total organotin contamination of the ROPME Sea Area might be from oil tankers built in Japan, demonstrating the need for international control of the use of antifouling paints containing organotin compounds.

Acknowledgements

We thank the captain and crew of the R/V Umitaka-Maru for sample collection.

REFERENCES

Abuzinada, A. H. and Krupp, F. (1994). The Arabian Gulf environment and the consequences of the 1991 oil spill. Cour. Forsch.-Senchenberg. 166, 3–10.

Adelman, D., Hinga, K. R. and Pilson, M. E. Q. (1990). Biogeochemistry of butyltins in an enclosed marine ecosystem. Environ. Sci. Technol. 24, 1027–1032.

Alzieu, C. (1991). Environmental problems caused by TBT in France: assessment, regulations, prospects. Mar. Environ. Res. 32, 7–17.

Alzieu, C., Sanjuan, J., Deltreil, J. P. and Borel, M. (1986). Tin contamination in Arcachon Bay: effects on oyster shell anomalies. Mar. Pollut. Bull. 17, 494–498.

Alzieu, C., Sanjuan, J., Michael, P., Borel, M. and Dreno, J. P. (1989). Monitoring and assessment of butyltins in atlantic coastal waters. Mar. Pollut. Bull. 20, 22–26.

Bryan, G. W., Gibbs, P. E., Huggett, R. J., Curtis, L. A., Bailey, D. S. and Dauer, D. M. (1989). Effects of tributyltin pollution on the Mud snail, Ilyanassa obsoleta, from York River and Sarah Creek, Chesapreak Bay. Mar. Pollut. Bull. 20, 458–462.

de Mora, S. J., Stewart, C. and Phillips, D. (1995). Sources and rate of degradation of tri(n-butyl)tin in marine sediments near Auckland, New Zealand. Mar. Pollut. Bull. 30, 50–57.

Dowson, P. H., Bubb, J. M. and Lester, J. N. (1993). Temporal distribution of organotins in the aquatic environment: five years after the 1987 UK retail ban on TBT based antifouling paints. Mar. Pollut. Bull. 26, 487–494.

Dyrynda, E. A. (1992). Incidence of abnormal shell thichening in the Pacific oyster Crassostrea gigas in Poole Harbour (UK), subsequent to the 1987 TBT restrictions. Mar. Pollut. Bull. 24, 156–163.

Evans, S. M., Leksono, T. and Mckinnell, P. D. (1995a). Tributyltin pollution: a diminishing problem following legislation limiting the use of TBT-based anti-fouling paints. Mar. Pollut. Bull. 30, 14–21.

Evans, S. M., Dawson, M., Day, J., Frid, C. L. J., Gill, M. E., Pattisina, L. A. and Porter, J. (1995b). Domestic waste and TBT pollution in coastal area of Ambon Island (Eastern Indonesia). Mar. Pollut. Bull. 30, 109–115.

Gabrielides, G. P., Alzieu, C., Readman, J. W., Bacci, E., Dhab, O. A. and Salihoglu, I. (1990). MED POL survey of organotins in the Mediterranean. Mar. Pollut. Bull. 21, 233–237.

Gupta, R. S. and Kureishy, T. W. (1981). Present state of oil pollution in the northern Indian Ocean. Mar. Pollut. Bull. 12, 295–301.

Huggett, R. J., Unger, M. A., Seligman, P. F. and Valkirs, A. O. (1992). The marine biocide tributyltin: assessing and managing the environmental risks. Environ. *Sci. Technol.* 26, 232–237.

Krone, C. A., Brown, D. W., Burrows, D. G., Bogar, R. G., Chan, Sin-Lam and Varanasi, U. (1989). A method for analysis of butyltin species and measurement of butyltins in sediments and English sole livers from Puget Sound. Mar. Environ. Res. 27, 1–18.

Krone, C. A., Chan, Sin-Lam and Varanasi, U. (1991). Butyltins in sediments and bentic fish tissues from the east, Gulf and Pacific coast of the United States. Oceans *'91*, 1054–1059.

Lee, R. F. (1985). Metabolism of tributyltin oxide by crabs, oysters and fish. Mar. *Environ. Res.* 17, 145–148.

Lee, R. F., Valkirs, A. O. and Seligman, P. F. (1989). Importance of microalgae in the biodegradation of tributyltin in estuarine waters. Environ. Sci. Technol. 23, 1515–1518.

Minchin, D., Oehlmann, J., Duggun, C. B., Stroben, E. and Keatinge, M. (1995). Marine TBT antifouling contamination in Ireland, following legislation in 1987. Mar. Pollut. Bull. 30, 633–639.

Ministry of transport (1994). Production, and transport statistics of the world. In National T*ransportation Statistics Handbook* (Ministry of transport policy bureau information and research department, ed.), pp. 114–115 and 188–189. Japan Transport Economics Research Center, Tokyo.

Reynolds, R. M. (1993). Physical ocaenography of the Gulf, Strait of Hormuz, and the Gulf of Oman—results from the Mt. Mitchell expedition. Mar. Pollut. Bull. 27, 35–59.

Sarradin, P. M., Astruc, A., Sabrier, R. and Astruc, M. (1994). Survey of Butyltin compounds in Arcachon Bay sediments. Mar. Pollut. Bull. 28, 621–628.

Seligman, P. F., Valkirs, A. O., Stang, P. M. and Lee, R. F. (1988). Evidence for rapid degradation of tributyltin in a marina. Mar. Pollut. Bull. 19, 531–534.

Stewart, C., de Mora, S. J., Jones, M. R. L. and Miller M. C. (1992). Imposex in New Zealand Neogastropods. Mar. Pollut. Bull. 24, 204–209.

Takayama, T., Hashimoto, S., Tokai, T. and Otsuki, A. (1995). Measurements of organic tin compounds in fish and crustacean of Tokyo Bay. Environmental *Science* 8, 1–9 (in Japanese).

Wade, T. L., Garcia-Romero, B. and Brooks, J. M. (1990). Butyltins in sediments and bivalves from U.S. coastal areas. Chemosphere 20, 647–662.

Wade, T. L. and Garcia-Romero, B. (1991). Oyster as biomonitors of butyltins in the Gulf of Mexico. Mar. Environ. Res. 32, 233–241.

Offshore Environment of the ROPME Sea Area after the War-Related Oil Spill,Eds. A. Otsuki *et al.*, pp. 245–256.

Toxicity of dibenzothiophene and its distribution in the eastern coast of Japan and northwestern coast of the ROPME Sea Area

Jiro KOYAMA and Ryosuke KUROSIMA

Environmental Conservation Division, National Research Institute of Fisheries Science,
6-31-1, Nagai, Yokosuka, Kanagawa 238-03, Japan

Abstract—Experimental study suggested that dibenzothiophene (DB) and phenanthrene (PH) which are crude oil components, have persistency in the marine environment and also have a high toxicity for some marine organisms. Thus, the distributions of DB, PH and their alkyl derivatives (DBs and PHs) were investigated along the eastern coast of Japan and the northwestern coast of the ROPME Sea Area (RSA).

The total concentrations of DB and PH including DBs and PHs in seawater were less than 22 and 61 ng l^{-1}, respectively in both areas. While their highest total concentrations in sediment were 33.3 and 92.9 ng g^{-1} wet weight along Japanese coastal area, these were 127000 and 14000 ng g^{-1} wet weight in the RSA. Although DB, PH, DBs and PHs in seawater seemed not to affect survival of the marine organisms, the DB, PH, DBs and PHs in the sediment in the RSA seemed to have serious effect on survival of benthic animals.

INTRODUCTION

Since the huge amount of Kuwait crude oil was spilled into the ROPME Sea Area (RSA), the closed area, during War-related oil spill, serious effects on the RSA ecosystem were worried. Especially, some components in crude oil dissolve into seawater and seem to be toxic for marine organisms (Anderson *et al.*, 1974). In the present study, we identified which components in crude oil dissolve and remain in seawater and also examined the toxicity of these components for two species of marine organisms. Furthermore, we investigated the environmental distributions of dibenzothiophene (DB) and phenanthrene (PH), one of the representative component of crude oil, along the northeastern coast of the RSA. Their distributions were also investigated along Japanese eastern coast because of shipping of the huge amount of Kuwait crude oil to Japan.

MATERIALS AND METHODS

Analysis of the major components of seawater soluble fractions of Kuwait crude oil

To analyze the soluble components of crude oil in seawater, the seawater soluble fractions of Kuwait crude oil (sample No. 1) were prepared following

Anderson et al. (1974) by carefully layering 0.5 l oil on the top of 4.5 l seawater held in a 5-l glass beaker covered with a polyethylene film. The seawater soluble fraction was stirred without Kuwait crude oil for further 24 hours (sample No. 2) to examine the decreases of the crude oil components concentrations. The soluble components of crude oil were extracted with *n*-hexane and the concentrations of their main components were measured with GC/MS, HP5980 equipped with DB-1 capillary column of 0.25 mm × 30 m just after preparations. The oven temperature was programmed from 50°C to 300°C at 8°C min^{-1} and held at 300°C for 10 minutes. The injection and detector temperatures were kept at 320°C. The helium flow rate was 50 ml min^{-1}.

As some field surveys showed the persistency of organic sulfur substances of crude oil in the sediment (Michel and Hayes, 1993) and organisms (Kira et al., 1983), we also measured their concentrations in seawater soluble fractions by GC/AED, HP5921A equipped with HP-1 capillary column of 0.32 mm × 25 m after extraction with *n*-hexane. The oven temperature was programmed from 50°C to 300°C at 8°C min^{-1} and held at 300°C for 10 minutes. The injection and detector temperatures were kept at 320°C. The helium flow rate was 50 ml min^{-1}. Because of low solubilities of some organic sulfur substances, Kuwait crude oil was mixed with seawater for 240 hours (sample No. 3). The seawater soluble fraction of sample No. 3 was stirred without the crude oil for further 240 hours (sample No. 4) to examine the decreases of organic sulfur substances. The organic sulfur substances having low boiling points were analyzes by head space technique while the organic sulfur substances having high boiling points were analyzed by extraction with *n*-hexane. Although each organic sulfur substance was not separated sufficiently in GC analysis, the concentrations were shown as total concentrations of sulfur in seawater using dimethyl disulfide for the substances having low boiling point and DB for the substances having high boiling point as standard, respectively.

Acute toxicity and bioconcentration test of aromatic hydrocarbons and DB

Because little information regarding the toxicity of benzene, toluene and naphthalene which are main components of aromatic hydrocarbons, for marine organisms was available, their acute toxicity tests for red sea bream *Pagrus major* (BW: 0.19–1.08 g) and prawn *Penaeus japonicus* (BW: 0.06–0.35 g) were carried out. Furthermore, because of their persistency of organic sulfur substances having high boiling points, the acute toxicity tests of DB which is one of the representative organic sulfur substances of crude oil, were also carried out. Five or six concentrations of aromatic hydrocarbons and DB were prepared as acute toxicity test solutions. In each test solution, 10 red sea bream or 6 prawn were used and the test solutions were newly prepared every 24 hours. Temperature and salinity were kept about 23°C and 33‰, respectively. Dissolved oxygen concentration were kept above 4 mg l^{-1}. From cumulative mortality and nominal concentration of each substance, LC_{50} (median lethal concentration) were calculated by the probit method (APHA, 1985).

To determine the bioconcentration factor of DB, red sea bream (mean BW:

6 g) and prawn (mean BW: 0.7 g) were exposed to DB for 42 days by flow-through method using 60 l glass aquarium. Red sea bream and prawn were sampled at 14th, 28th and last day. DB concentration of seawater were measured at 14th and 28th day. In both bioconcentration tests, dimethyl sulfoxide was used to disperse DB into seawater and DB concentrations in the seawaters and organisms were measured by the method mentioned below.

Analysis of DB, PH and their alkyl derivatives (DBs and PHs) in seawater, sediment and organisms

Figure 1 shows sampling stations. Surface seawaters were collected in glass bottles and sediments were collected by dragging can or a core sampler. The organisms were sampled at most of sediment sampling stations. The samples of the RSA were collected by an investigation group of Tokyo University of Fisheries. Water samples were stored in a refrigerator, and sediments and organisms were stored at –30°C until analysis. DB, PH, DBs and PHs of seawater were extracted by *n*-hexane. After dehydration by anhydrous sodium sulfate and concentration by rotary evaporator, DB, PH, DBs and PHs were analyzed using GC-MS, HP5980. The homogenates of organisms (soft tissue of shellfish and fish meal) and sediments were saponified by 1N KOH/ethanol in boiling water bath, and then, DB, PH, DBs and PHs were extracted by *n*-hexane. The concentrations of them were measured by GC/MS, HP5980 after dehydration, concentration and clean up by a Sep-Pak florisil cartridge (Waters, Millipore Corp.). Since the standard substances of DBs and PHs were not available, their concentrations were estimated by the DB and PH standards following Ogata and Fujisawa (1985).

GC/MS conditions were mentioned above. The percent recoveries of DB from water, soft tissue of oyster and sediment were 96.1, 82.1 and 86.1%, respectively, while the recovery of PH were not examined.

RESULTS AND DISCUSSION

Major components of seawater soluble fractions in Kuwait crude oil

As shown in Table 1, the concentrations of alkanes and aromatic hydrocarbons were lower than 0.5 and 1.1 mg l^{-1} in the seawater soluble fractions of Kuwait crude oil after 24 hours preparation (sample No. 1) and were lower than 0.073 and 0.06 mg l^{-1} after 24 hours stirring of sample No. 1 without oil (sample No. 2). The concentrations of most alkanes and aromatic hydrocarbons in sample No. 1 decreased by more than 90% after 24 hours stirring without the crude oil. The total concentrations of organic sulfur substances having low boiling points and high boiling points were 8.7 and 340 μgS l^{-1}, respectively after 240 hours preparation of seawater soluble fractions (Fig. 2, sample No. 3). These concentrations of seawater soluble fractions decreased to ND (<0.1 μgS l^{-1}) and 292 μgS l^{-1} after 240 hours stirring without the crude oil (Fig. 2, sample No. 4). While the greater part of aromatic hydrocarbons in the seawater soluble fractions seem to volatilize or be decomposed within 24 hours, organic sulfur substances having high boiling points seem to persist in the seawater.

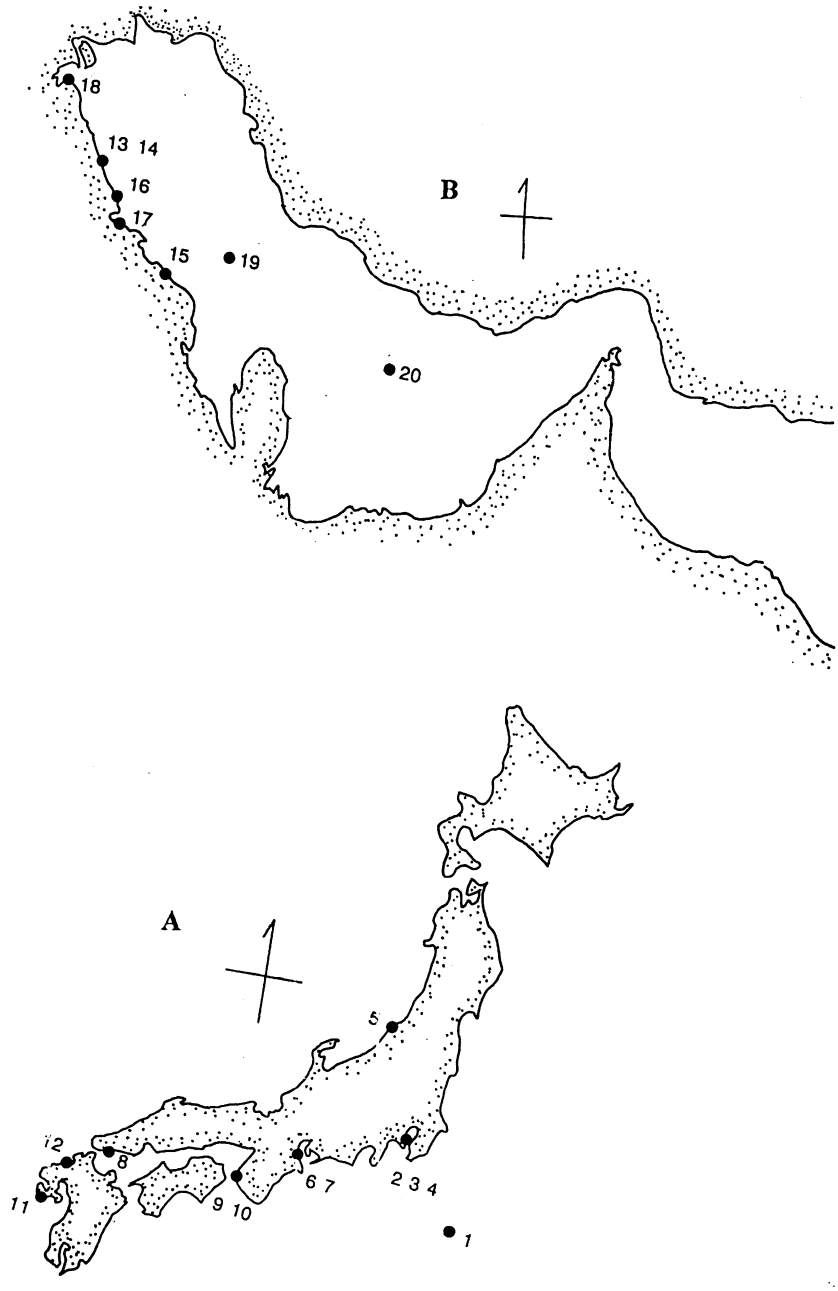

Fig. 1. The location of sampling stations in Japan (A) and the ROPME Sea Area (B).

Table 1. Chemical compositions of seawater soluble fractions in Kuwait crude oil stirred for different periods (mg l^{-1}).

	sample No.1	sample No.2	No.2/No1(%)
Alkanes			
Ethane	0.052	0.002	3.8
Propane	0.28	0.009	3.2
Isobutane	0.091	0.004	4.4
Butane	0.43	0.013	3.0
Isopentane	0.18	0.008	4.4
Pentane	0.27	0.010	3.7
Cyclopentane	0.13	0.008	6.2
2-Methylpentane	0.047	0.003	6.4
n-Hexane	0.096	0.003	3.1
Methylcyclopentane	0.073	0.005	6.8
Cyclohexane	0.085	0.005	5.9
Methylcyclohexane	0.037	0.003	8.1
$C_{8\text{-}34}$ *n*-paraffin	0.295	0.073	24.7
Aromatics			
Benzene	0.90	0.056	6.2
Toluene	1.1	0.060	5.5
Ethylbenzene	0.18	0.011	6.1
m, p-Xylene	0.42	0.026	6.2
o-Xylene	0.26	0.23	88.0
2-Ethyltoluene	0.11	0.004	3.6
4-Ethyltoluene	0.082	0.006	7.3
Trimethylbenzene	0.22	0.012	5.5
Tetramethylbenzene	0.12	0.018	15.0
Naphthalene	0.033	0.005	15.2
2-Methylnaphthalene	0.021	0.004	19.0
1-Methylnaphthalene	0.022	0.006	27.3
Dimethylnaphthalene	0.033	0.006	18.2
Phenanthrene	0.004	ND(<0.001)	-

Sample No.1: Stirred with oil for 24 hours; Sample No.2: Stirred without oil for 24 hours after No.1 preparation.

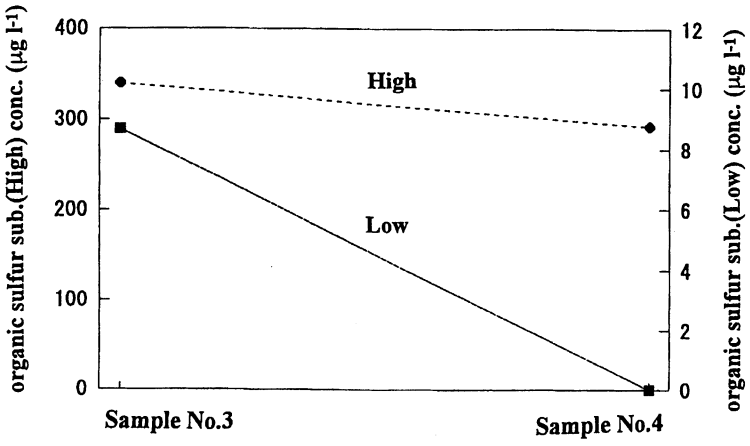

Fig.2. Organic sulfur substances concentrations having low boiling point and high boiling points (Low and High) in seawater soluble fractions of Kuwait crude oil stirred for different periods (μgS l^{-1}). Sample No.3 :Stirred with the crude oil for 240 hours. Sample No.4 :Stirred without the crude oil for 240 hours after preparation of No.3.

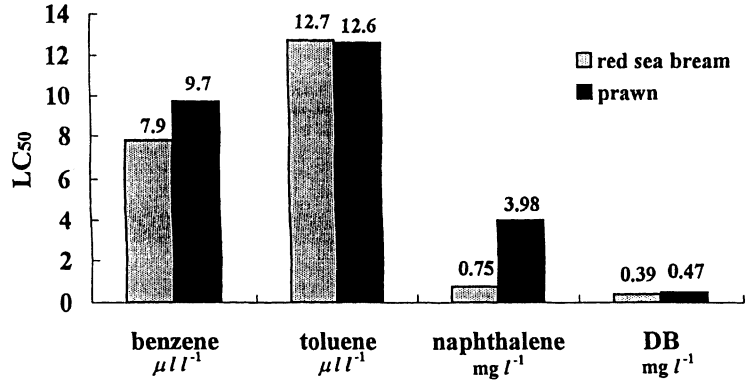

Fig. 3. Twenty-four hours LC_{50} of aromatic hydrocarbons and DB.

Acute toxicity and bioconcentration test of aromatic hydrocarbons and DB

Although aromatic hydrocarbons like benzene and naphthalene have acute toxicity to aquatic organisms, they seemed to volatilize or be decomposed easily and their concentrations decreased quickly. However, organic sulfur substances having high boiling points still remained in the seawater. Since we did not have any data on the toxicity of organic sulfur substances for marine organisms, we focused on the toxicity of DB which is one of the representative organic sulfur substances in crude oil.

Table 2. Ranges of acute toxicities of benzene, toluene, naphthalene and DB (mg l^{-1}).

	Freshwater organisms	Marine organisms
benzene[1)]	5.3 - 620	5.1 - 924
toluene[1)]	12.7 - 313	3.7 - 1050
naphthalene[1)]	2.3 - 150	2.35 - 199
DB	0.42[2)]- 106[3)]	0.15 - 0.47

1)US EPA (1980), 2)Maas (1990), 3)Chemials Inspection and Testing Institute Japan (1992)

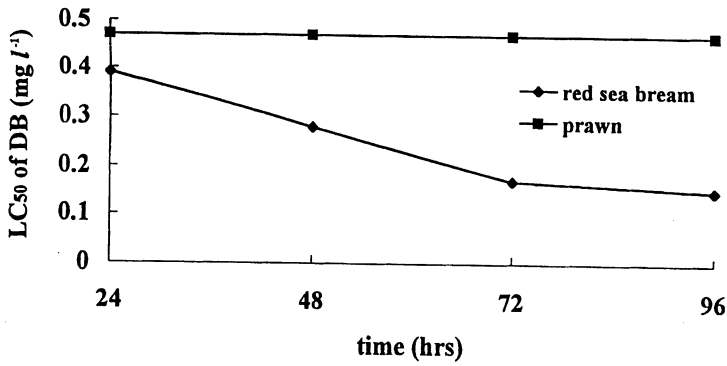

Fig. 4. LC_{50} of DB for red sea bream and prawn.

Twenty-four hours LC_{50} (median lethal concentration) of benzene, toluene, naphthalene and DB for red sea bream (*Pagrus major*) and prawn (*Penaeus japonicus*) are shown in Fig. 3. DB showed the highest toxicity among them. Furthermore, DB LC_{50} at 24–96 hours for red sea bream and prawn can be seen in Fig. 4. While LC_{50} of DB for prawn did not change with time, LC_{50} of DB for red sea bream changed till 72 hours. Thus, the incipient LC_{50} of DB for prawn and red sea bream were 0.47 and 0.15 mg l^{-1}, respectively. There seemed to be no differences regarding the toxicities of benzene, toluene and naphthalene between freshwater and marine organisms (Table 2). However, the toxicity of DB for red sea bream and prawn seemed to be higher than it for freshwater organisms.

As shown in Fig. 4, DB concentrations of red sea bream and prawn exposed to 4 and 3.5 μgDB l^{-1} for 6 weeks were 3700 μgDB g^{-1} and 640 μgDB g^{-1},respectively. The DB bioconcentration factors (BCFs) for red sea bream and prawn at 42nd day were 930 and 180, respectively. Ogata and Fujisawa (1985) reported that the BCFs of DB by oysters, mussels, eels and short neck clams were 550, 1300, 110 and 260, respectively. These results suggest that DB have a higher

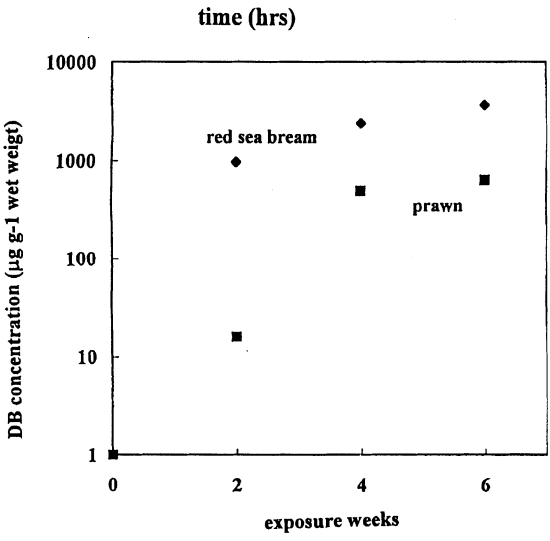

Fig.5. Bioconcentration of DB by red sea bream and prawn.

toxicity for marine organisms than other components in crude oil and also have higher BCF for marine organisms. Thus, we investigated the distribution of DB and its alkyl derivatives in seawater, sediment and organisms along the eastern coastal area of Japan and the northwestern coast of the RSA. At the same time, we also analyzed phenanthrene (PH) and its alkyl derivatives because of their persistency in environment.

DB, PH, DBs and PHs concentrations in the coastal seawaters of Japan and RSA

Table 3 shows the concentrations of DB, PH, DBs and PHs in the coastal seawaters. Each concentration of DB and DBs was lower than 8.8 ng l^{-1} in coastal seawaters along the eastern coast of Japan and northwestern coast of the RSA. The total concentrations of DB and DBs ranged from 1.5 (Stn. 8, Ube) to 21.4 ng l^{-1} (Stn. 6, Yokkaichi 1st Wharf) in Japan and from 0.5 (Stn. 20) to 3.4 ng l^{-1} (Stn. 19) in the RSA. Each concentration of PH and PHs was lower than 55 ng l^{-1} in the coastal seawaters of Japan and the RSA. The total concentrations of PH and PHs ranged from 12.2 (Stn. 8, Ube) to 61 ng l^{-1} (Stn. 4, Kamome-Tokyo Bay) in Japan and ranged from 17.1 (Stn. 20) to 30.4 ng l^{-1} (Stn. 19) in the RSA. The ninety six hours LC_{50} of DB for red sea bream and prawn were 0.15 and 0.47 mg l^{-1}, respectively. While there is little information on the toxicity of PH for marine organisms, the 48 hours LC_{50} of PH for freshwater organisms, *Daphnia pulex*, was reported 0.96–1.28 mg l^{-1} (Geiger and Buikeman Jr., 1982). The concentrations of DB, PH, DBs and PHs in coastal seawaters were much lower than their acute toxicity values for aquatic organisms. Therefore, DB, PH, DBs and PHs in coastal seawaters did not seem to affect the survival of marine

Table 3. Concentrations of DB, PH and their alkyl derivatives (DBs and PHs) in the coastal waters of Japan and the RSA (ng l^{-1}).

St.	date			DBs					PHs		
		Total	DB	1-Me*2	2-Me*3	Me-3*4	Total	PH	1-Me*5	2-Me*6	Me-3*7
1	Dec.'94	*1	0.6								
2	Dec.'94		0.9								
3	Jan.'95	13.4	0.7	6.2	6.5	<0.1	49.7	4.6	3.8	32	9.3
4	Jan.'95	7.8	0.3	5.4	2.1	<0.1	61.0	3.7	2.3	55	<0.1
5	Feb.'95	1.7	<0.1	1.7	<0.1	<0.1	33.1	3.4	2.7	27	<0.1
6	Feb.'95	21.4	0.8	6.6	8.8	5.2	45.2	5.7	3.5	33	3.0
7	Feb.'95	4	0.9	3.1	<0.1	<0.1	30.8	5.7	2.3	20	2.8
8	Feb.'95	1.5	<0.1	0.8	0.7	<0.1	12.2	3.2	<0.1	7.2	1.8
9	Oct.'94		3.3								
	Dec.'94		<0.1								
10	Oct.'94		3.5								
11	May'94		1								
13	Nov.'94		3.0								
14	Oct.'94		1.0								
15	Nov.'94		1.1								
19	Dec.'94	3.4	0.4	3.0	<0.1	<0.1	30.4	4.7	2.7	21	2.0
20	Dec.'94	0.5	0.5	<0.1	<0.1	<0.1	17.1	3.8	1.3	12	<0.1

*1: not measured

*2, 3, 4: mono-, di- and trimethyl DB, *5, 6, 7: mono-, di- and trimethyl PH

organisms along the eastern coast of Japan and northwestern coast of the RSA.

Concentrations of DB, PH, DBs and PHs in the coastal sediments of Japan and the RSA

The features of the sediments collected were as follows: Stns. 3, 4 and 11: muddy sand; Stn. 5: sand; Stns. 6, 7, 8 and 12: mud. All the sediments collected in the RSA were sand. The concentrations of DB, PH, DBs and PHs in the sediments are shown in Table 4. Each concentrations of DB and DBs in the sediments ranged from 0.2 (Stn. 5, Niigata) to 6.6 ng g^{-1} wet weight (Stn. 3, Honmoku-Tokyo Bay) in Japan. The total concentrations of DB and DBs ranged from 1.2 (Stn. 5, Niigata) to 33.3 ng g^{-1} wet weight (Stn. 12, Hakata Bay). While sand sample collected at Stn. 5 showed the lowest concentration, the mud sample collected at Stn. 12 showed the highest concentration and mud samples (Stns. 6, 7, 8 and 12) showed higher concentrations. These differences in the particle sizes among the sediments seem to cause the differences in DB and DBs concentration in the sediments because of their adsorption on the particles of sediments.

Table 4. Concentrations of DB, PH, DBs and PHs in the coastal sediments along Japan and the RSA (ng gl^{-1} wet weight).

St.	date	DBs					PHs				
		total	DB	1-Me	2-Me	3-Me	total	PH	1-Me	2-Me	3-Me
3	Jan.'95	33	6.6	10	10	6.4	64.2	46.5	12	4.1	1.6
4	Jan.'95	5.0	1.0	1.8	1.6	0.6	22.8	11.0	9.8	1.4	0.6
5	Feb.'95	1.2	0.2	0.3	0.4	0.3	2.4	1.6	0.7	<0.1	0.1
6	Feb.'95	23.1	0.5	5.6	10	7.0	63	35.1	19	5.4	3.5
7	Feb.'95	13.0	0.4	3.3	5.8	3.5	35.5	16.7	12	5.2	1.6
8	Feb.'95	16.6	2.8	4.6	4.9	4.3	92.9	19.9	33	24	16
11	May'95	2.3	0.2	0.6	0.9	0.6	4.9	2.7	1.6	0.4	0.2
12	Nov.'94	33.3	5.3	10	11	7.0	75.3	25.4	34	12	3.9
13	Nov.'94	*	1.9								
14	Aug.'93	3900	8	100	700	3100	354	4	47	43	260
(2-6cm)**											
(0cm)	Oct.'94		1.8								
15	Nov.'94		3.1								
16	Feb.'92	127000	6	1200	6200	120000	3200	2	470	820	1900
17(0cm)	Feb.'92	72000	3	2400	13000	57000	8600	1	1400	2400	4800
(5-10cm)	Aug.'93	25000	157	2800	7900	14000	8300	<0.1	3000	3200	2100
(0-3cm)	Nov.'94	630	2	11	210	410	60	2	8	27	23
(6-9cm)	Nov.'94	13000	43	330	2600	9700	1400	12	33	200	1200
(9-12cm)	Nov.'94	42000	143	2400	13000	26000	14000	23	1500	5700	7200
18	Aug.'93	75	1	7	18	49	49	4	<0.1	45	<0.1

*: not measured, **:the depth of sediment.

Although trimethyl DB generally shows the highest concentration among DBs in the marine environment (Berthou and Vignier, 1986), the concentrations of dimethyl DB in most sediments were the highest among DBs. The distribution of PH and PHs in the sediment were similar to the distribution of DB and DBs. However, the highest total concentration of PH and PHs, 92.9 ng g^{-1} wet weight was observed at Stn. 8 (Ube).

The concentrations of DB, PH, DBs and PHs in the sediment of the RSA were much higher than those in Japan (Table 4). The concentrations of DB and DBs ranged from 1 (Stn. 18, '93 Kuwait) to 1.2×10^5 ng g^{-1} wet weight (Stn. 16, '92 Al-Safaniya). Their total concentrations ranged from 75 (Stn. 18, '93 Kuwait) to 127000 ng g^{-1} wet weight (Stn. 16, '92 Al-Safaniya). The distribution of PH and PHs were similar to that of DB and DBs and their total concentrations ranged from 49 (Stn. 18, '93 Kuwait) to 14000 ng g^{-1} wet weight (Stn. 17, '94 Manifah 9–12 cm). At Stn. 17, '94 Manifah, the total concentrations of DB and DBs, PH and PHs at deeper layers of sediment were higher than that at surface of sediment. In each

Table 5. Concentrations of DB, PH, DBs and PHs in the organisms of Japanese and the RSA coastal areas (ng gl^{-1} wet weight).

St.	DBs					PHs					organisms
	total	DB	1-Me	2-Me	3-Me	total	PH	1-Me	2-Me	3-Me	
3	6.8	0.5	1.4	2.8	2.1	12.4	3.6	3.2	5.1	0.5	blue mussel
	19.8	0.5	0.9	2.1	3.2	4.4	2.3	0.6	0.2	1.3	goby
4	2.1	0.3	0.6	1.0	0.2	7.7	3.0	2.5	2.2	-	blue mussel
	22.4	0.5	5.6	15	1.3	14.6	2.9	3.0	5.6	3.1	mussel
5	77.0	1.0	15	32	29	19.2	7.0	4.1	5.3	2.8	oyster
6	69.5	1.6	12	52	3.9	17.9	7.9	6.2	3.8	<0.1	oyster
7	95.7	2.7	14	48	31	11.7	7.5	3.2	1.0	<0.1	oyster
8	37.9	1.1	3.7	7.2	3.5	11.1	5.2	3.6	1.7	0.6	oyster
9	4.5	0.7	1.2	1.8	0.8	13.8	5.8	4.5	3.1	0.4	snail-1
	51.8	1.1	5.7	23	22	32.1	6.4	6.8	11	7.9	snail-1
	115.9	1.9	11	55	48	38.0	12.8	7.7	9.4	8.1	mussel
	285	4.0	51	120	110	752	22	150	340	240	snail-2
11	207.8	1.8	33	96	77	71.8	6.8	22	30	13	oyster
12	35.6	0.6	5.0	18	12	9.4	2.8	3.2	2.6	0.8	mussel
13	88.7	1.9	14	39	34	13.5	10.7	2.8	<0.1	<0.1	snail-3
14	58.3	1.8	9.4	23	24	16.0	4.6	3.9	5.8	1.7	snail-4
15	58.1	3.1	15	30	10	21.1	12.4	7.6	1.1	<0.1	snail-4

snail-1: *Thais clavigera*, snail-2: *Tegula basilirata*,
snail-3: *Clypeomorus bifasciata* snail-4: *Cerithideopsilla cingulata*

layer, trimethyl DB and PH showed the highest concentrations. DB and DBs are decomposed by photolysis and the half-life of trimethyl DB is longer than mono- and dimethyl DB (Berthou and Vignier, 1986). Therefore, the concentrations of trimethyl DB and PH showed the highest concentration among DBs and PHs. The decreases of DB, PH, DBs and PHs concentrations in the surface sediment of Stn. 17 seem to be caused by photo oxidation (Berthou and Vignier, 1986) and new sand covering (personal communication from the investigation group of Tokyo Univ. Fish.).

Concentrations of DB, PH, DBs and PHs in organisms along Japanese and the RSA coastal areas

The concentrations of DB, PH, DBs and PHs in organisms are shown in Table 5. Mussel *Mytilus edulis*, oyster *Crassostrea gigas* and snail *Thais clavigera* were collected in the eastern coast of Japan. The highest total concentration of DB and DBs, 285 ng g^{-1} wet weight, was found in snails collected in Wakayama (Stn. 9) because of crude oil spill from tanker one week before the sampling. The highest total concentration of PH and PHs, 753 ng g^{-1} wet weight, was also found

in snails collected in Wakayama (Stn. 9). At Stn. 11 (Nagasaki), higher concentration of them were detected in oysters and it seems to be due to high ship activities.

In the investigation of the RSA in 1994, two kinds of snails, *Cerithideopsilla cingulata* and *Clpeomorus bifasciata*, were collected. The total concentrations of DB and DBs among them ranged from 58.1 (Stn. 15, Al-Jubayl) to 88.7 ng g^{-1} wet weight (Stn. 13, Al-Khafji). The total concentrations of PH and PHs among them ranged from 13.5 (Stn. 13, Al-Khafji oil refinery) to 21.1 ng g^{-1} wet weight (Stn. 15, Al-Jubayl). However, no living organisms were found at Stns. 16 and 17 in which much higher concentrations of DB, PH and their alkyl derivatives were detected.

These results suggest that DB, PH, DBs and PHs in the seawater did not have any effect on the survival of marine organisms, but DB, PH, DBs and PHs in the sediments along the northwestern coast of RSA probably affected the survival of benthic organisms.

Acknowledgements

We would like to thank Professors A. Ohtsuki and H. Takashima, Associate Professor H. Sato and Assistant Professor K. Tsuchiya, Tokyo University of Fisheries, for collection of samples.

REFERENCES

American Public Health Association, American Water Works Association and Water Pollution Control Federation (1986) *Standard Methods*, sixteenth edition, pp. 715–719.

Anderson, J. W., Neff, J. M., Cox, B. A., Taten, H. E. and Hightower, G. M. (1974) Characteristics of dispersions and water-soluble extractions of crude and refined oils and their toxicity to esturine crustaceans and fish. *Mar. Biol.* 27, 75–88.

Berthou, F. and Vignier, V. (1986) Analysis and fate of dibenzothiophene derivatives in the marine environment. Inter. *J. Environ. Anal. Chem.* 27, 81–96.

Chemicals Inspection and Testing Institute Japan (1992) *Biodegradation and Bioaccumulation Data of Existing Chemicals Based on the CSCL Japan*. Section 5, pp. 46.

Geiger, J. G. and Buikema, A. L., Jr. (1982) Hydrocarbons depress growth and reproduction of *Daphnia pulex* (Cladocera). *Can. J. Fish. Aquat. Sci.* 39, 830–836.

Kira, S., Izumi, T. and Ogata, M. (1983) Detection of dibenzothiophene in mussel, *Mytilus edulis*, as a marker of pollution by organosulfur compounds in a marine environment. *Bull. Envviron. Contam. Toxicol.* 31, 518–525.

Maas, J. L. (1990) *Toxicity Research with Thiourea*. Laboratory for Ecotoxicology, Institute for Inland Water Management and Waste Water Treatment. Report No. AOCE, 4 pp.

Michel, J. and Hayes, M. O. (1993) Persistence and weathering of Exxon Valdez oil in the intertidal zone-3.5 years later. In *Proceeding of 1993 Oil Spill Conference*. American Petroleum Institute, Washington, D.C., pp. 279–285.

Ogata, M. and Fujisawa, K. (1985) Organic sulfur compound and polycyclic hydrocarbons transferred to oyster and mussel from petroleum suspension. *Water Res.* 19, 107–118.

US.EPA (1980) *Ambient Water Quality Criteria for Benzene*. EPA-440/5-80-018. U.S. Environmental Protection Agency, Washington, D.C., USA.

US.EPA (1980) *Ambient Water Quality Criteria for Toluene*. EPA-440/5-80-075. U.S. Environmental Protection Agency, Washington, D.C., USA.

US.EPA (1980) *Ambient Water Quality Criteria for Naphthalene*. EPA-440/5-80-018. U.S. Environmental Protection Agency, Washington, D.C., USA.

Offshore Environment of the ROPME Sea Area after the War-Related Oil Spill, Eds. A. Otsuki *et al.*, pp. 257–279.

Levels of trace metals and hydrocarbons in fish from the ROPME Sea Area

Nahida B. AL-MAJED, Fuad AL-SAFAR, Wajdi A. RAJAB, Mohamed S. FARHAN and Eqbal AL-RUQAAB

Environment Protection Department, Ministry of Health, Kuwait
P.O.Box. 24395 Safat, Postal Code 13104 Kuwait

Abstract—The purpose of this study is to determine the levels of trace metals and organic pollutants in different fish species collected along the ROPME Sea Area as a part of Umitaka Maru Cruise.

Samples were prepared and analyzed in accordance with MOOPAM methods. The obtained ranges in fish species based on dry weight were as follows: (1) Trace metals: Cd 0.01 - 0.28 μg/g, Pb 0.46–2.67 μg/g, Cu 0.83–18.14 μg/g, Ni 0.05–6.07 μg/g, Zn 11.88–67.30 μg/g, V 0.05–0.4 μg/g, Mn 0.05–3.03 μg/g and Fe 0.05–57.45 μg/g. (2) Trace organic; PHC's 1.86–125.49 μg/g, total n-alkanes 4.42–183.96 μg/g, pristane 0.15–14.28 μg/g, phytane 0.18–23.33 μg/g and total PAH's 14.1–150.0 ng/g.

The obtained levels of trace metals and trace organics in fish samples do not represent serious risk to human health. The obtained levels of petroleum hydrocarbons were found to be comparable to reported levels in other regional seas.

INTRODUCTION

1.1 Trace metals

It has been shown that the concentration of heavy metals have increased in some marine environment, especially in coastal zones where they frequently display relatively high levels of toxic metals in sediment and the concentrations globally decrease towards the open sea areas.

Detection of heavy metals in human diets is of a great concern to scientist and public health authorities. This is in lieu of numerous reports of exposure of populations to heavy metals. Some metals are essential for life, others have known biologic function, either favorable or toxic, and some others have the potential to cause disease. Those causing toxicity are the ones which accumulate in the body through the food chain, water and air (Lucas, 1975; Tsoukali *et al.*, 1989; Morris, 1970).

Among the metals that receive more public health concern are mercury, cadmium, lead and nickel. Cadmium damages liver and kidney while lead causes encephalopathy and anemia renal problems (FAO/WHO 1972; Nauen 1983).

Mercury and other trace metals have been observed to accumulate within the highest levels of marine food chains (Ratkowsky *et al.*, 1975; Marcovecchio *et al.*, 1986 & Eisler,1984). Zinc, iron and some other essential elements usually do not increase in concentration with the age or size for the marine organisms, because they are thought to be under homeostatic control (Thompson, 1990). The toxicity of lead is now well stated (Vernberg *et al.*, 1974, Subramanian & Connor, 1991). In the water body, lead divides into three parts; remains soluble, assimilated by planktonic organism and bound to particulate matter, which settles in the sea bottom (Francois & Christophe, 1994). Bottom feeders will take up particulate lead from the sediment by ingestion. Lead is also absorbed though the gills and body surface and ingested with food (Donald *et al.*, 1981). In many developed countries, limits of concentration in fish and other foods have been set in order to safeguard public health (Nauen, 1983). Although elevated levels of cadmium in sea water do not necessarily present a marine ecological problem, the ability of edible marine organisms to bioaccumulate cadmium can be of human toxicological concern (Francesconi *et al.*, 1994). Nickel concentration are reported to decrease with distance from shore (Kremling, 1985). Levels of nickel in sea-foods are worth investigating, since the excessive contamination of nickel in edible marine mollusc may pose hazard to human health. The excess may inhibit many enzymatic reactions which could lead to deleterious effects (Peck & Ray, 1969). Chromium, manganese, iron and zinc are all essential as micronutrient in humans, but at high concentrations they become toxic. However, the occurrence of these metals along with cadmium, cobalt, copper and chromium, metals, whose main anthropogenic sources are wastes of industrial origin, at the relatively high levels in fish samples, indicates the existence of point sources (Okoye, 1991).

1.2 Petroleum hydrocarbons

Hydrocarbons are natural constituents of sea water since they are produced by both phytoplankton and zooplankton. n-Alkanes and isoprenoids; e.g., pristane and squalene tend to predominate in organisms although unsaturated hydrocarbons may be significant in bacteria and algae (Ackman 1972; Kolatukudy 1976 & Koons *et al.*, 1965).

Polycyclic aromatic hydrocarbons (PAH) contain two or more benzene rings. There are three main routes of their formation in the environment; pyrolysis of organic matter, generation in sedimentary organic matter and fossil fuels and biosynthesis by organisms (Hites *et al.*, 1977, LaFlamme & Hites 1978). PAH are known to be absorbed and accumulated by marine organisms from polluted waters. Their monitoring in the marine environment is a must due to their carcinogenic and mutagenic effects. The most important anthropogenic source of petroleum hydrocarbons entering the marine environment is from transportation and surface runoff from land (National Academy of Sciences, 1975). The presence of hydrocarbons in a marine sample is not by it self an indication of pollution from urban, industrial or petroleum sources. However, high levels, particularly of aromatic and high molecular weight aliphatic hydro-

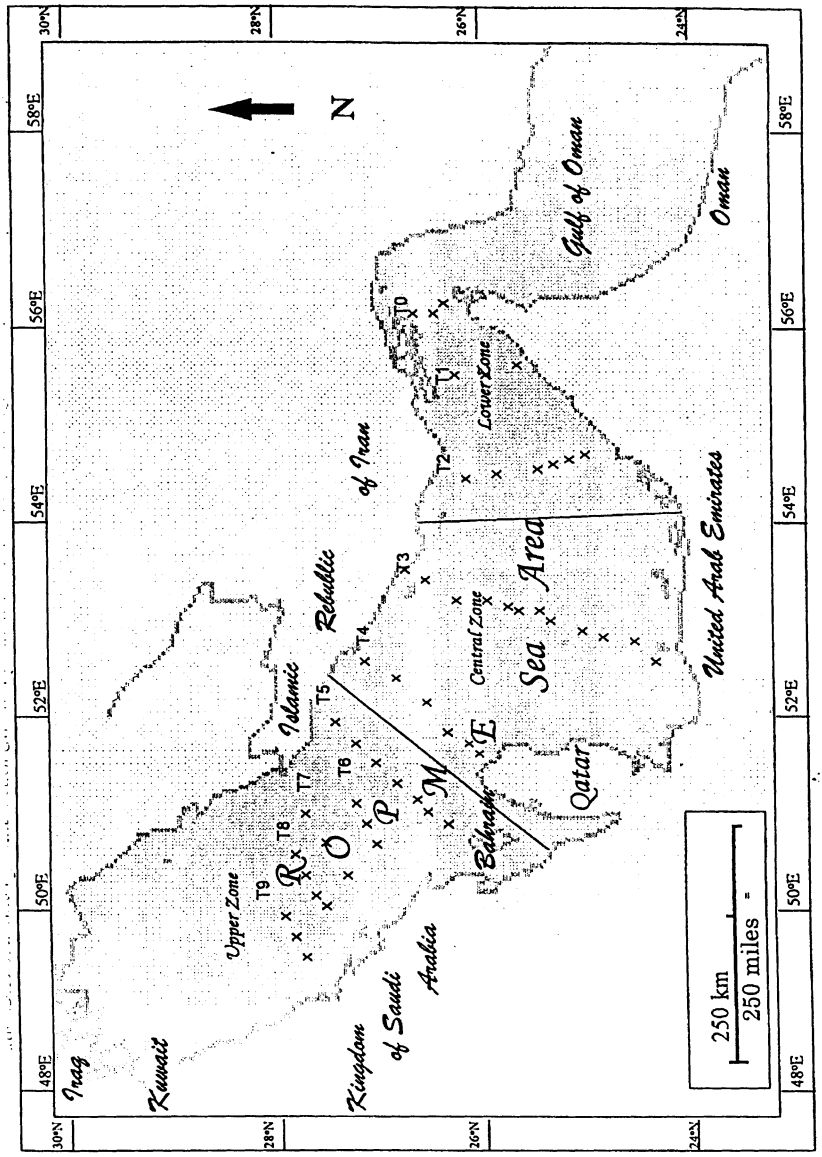

Fig. 1. The distribution of the main sampling transects in the area ROPME Sea Area (1993-1994).

carbons, are often indicative of petroleum pollution (Hites, 1976).

R/V UMITAKA MARU CRUISES IN THE ROPME SEA AREA

The R/V Umitaka Maru cruises were confined to the inner part of ROPME Sea Area, extending from the Straits of Hormuz to the approaches of Kuwait Bay. The inner part of ROPME Sea Area is semi-enclosed body of shallow water. It is 1000 km long, 300 km wide with an average depth of 35 meters. The area has been exposed to chronic and acute input of contaminants from domestic waste on the shoreline and industrial activities. Oil enters the marine environment mainly during terminal operations. Oil spills resulting from accidents at the sea although episodic in nature, result in extensive environmental damage. Nowruz oil spill in 1983 was considered one of the largest spills in the ROPME Sea Area at that time resulting in the release of 80–185 million gallons of oil during the Iraq - Iran war. This was followed by the Gulf war oil spill in 1991 when 252–336 million gallons were released from different sources in Kuwait and Iraq.

Assessment of the environmental impact of the influx of these pollutants to the marine environment has been carried out by several regional and international organizations. One of these was the Umitaka Maru cruises which were organized by the Regional Organization of the Marine Protection Environment (ROPME) in collaboration with Tokyo University of Fisheries, Japan. The first cruise was conducted during the period from 15–25 January 1993, the second cruise was conducted during the period from 14–26 December 1993, while the third cruise was conducted during the period from 14–26 December 1994. As a part of these cruises different fish species were collected for the assessment of their content of trace metals and organic pollutants. Sampling locations of the Umitaka Maru cruises in the ROPME Sea Area during the period (1993–1994) are shown in Fig. 1.

MATERIALS AND METHODS

3.1 Sampling

A total of 74 fish samples representing 26 species was collected from 15 stations during the first two Umitaka Maru cruises. Eleven samples of *Lethrinus kallpoterus* representing 16% of the total analyzed fish samples and 10 samples of *Caranx leptolepis* were analyzed (12% of the total catch). Other samples include 6 *Pelates quadrilineatus*, 5 *Loxodon macrorhinus*, 4 of each of *Arius thalassinus*, *Therapon jarbua* and *Therapon thraps*. Three samples of each of *Trachrurus trachrurus*, *Saurida lndosquamis* and *Tylosurus leiurus* and two samples of each of *Dentex nufar*, *Etrumeas tera*, *Nemitterus tolu* and *Scolopsis phaeops* were only analyzed. However, only single sample were available for *Argyrops filamentosus*, *Argyrops spinifer*, *Cephalopholis miniatus*, *Gnathandon speciosus*, *Lethrinus horak*, *Parupeneus cyclostomus*, *Platax orbicularis*, *Platycephalus indicus*, *Plectorhynchus cincuts*, *Rochycentron canadus*, *Saurida unvosqamis*, *Scolopsis bimaculatus* and *Scolopsis ghanam*.

Fishing was carried out usually from sun-set to sun-rise, using various

fishing gears that were available on the vessel (long-line, traps, rod and line and gill-net). The total catch was randomly distributed among the concerned scientists.

Total weight, total length, fork length and standard length were carried out on board for all samples. Taxonomic tasks for identification of the scientific and local name and sex were also carried out on board (Katsuzo and Yoshitaka, 1986). Samples were also dissected for fillets, then the fillets were wrapped with sterilized aluminum foil labelled and stored in deep freezer (–20°C) until the time of analysis. The species name, length expressed in centimeters (cm), fresh weight expressed in grams (g), dry weight/fresh weight ratio, sex and location for the analyzed fish samples are summarized in Table 1.

3.2 Analysis

3.2.1 Trace metals

The samples were freeze-dried, ground on Retsch and homogenized before chemical analysis. Cd, Pb, Cu, Ni, Zn, V, Mn and Fe were analyzed in fish and sediment samples in accordance with ROPME's Manual of Oceanographic Observations and Pollutant Analyses Methods (MOOPAM, 1989). Determination of trace metals in fish was obtained by a Shimadzu AA-680 Atomic Absorption fitted with GFA-4B Graphite Furnace for each of Cd, Pb, Cu, Ni, V, Cr and Mn. Whereas, a Perkin Elmer 5000 Atomic Absorption using the flame technique was used to obtain the concentrations of Zn and Fe in fish.

3.2.2 Petroleum hydrocarbons

Petroleum hydrocarbons (PHC's) in fish samples were analyzed in accordance to the MOOPAM Manual. Determination of total PHC's was carried on a Shimadzu RF-510 Spectrofluorophotometer using Kuwait crude oil as a standard. n-Alkanes ($C_{10}-C_{32}$) were obtained by a Shimadzu gas chromatograph GC-14A provided with flame ionization detector (FID), AOC-14 Auto injector and HP-Chemstation to collect and analyze the obtained results. Polycyclic aromatic hydrocarbons (PAH's) were determined on a Hewlett Packard Series II Model 5890 gas chromatograph provided with a HP 5970 Series Mass Selective Detector (MSD) and a 7673 GC/SFC Automatic injector. Selective ion monitoring (SIM) mode was used for qualitative and quantitative determination of PAH compounds.

3.3 Quality control

3.3.1 Trace metals

Triplicate analysis were carried out for each sample to determine the concentration of trace metals. Quality control was also carried out with each set of samples to check the performance of the analysis by running blanks and reference standard material. The International Atomic Energy Agency (IAEA) reference materials; Trace Metals In Tuna Fish, IAEA 350 and Trace Metals in ROPME Fish, MA-ROPME-1 were analyzed with each set of fish samples.

3.3.2 Petroleum hydrocarbons

Quality control was also carried out for petroleum hydrocarbon analysis

Table 1. Characteristics and location of fish species collected from ROPME Sea Area.(*Umitaka Maru Cruise* No.1 & 2, 1993)

Sample Code	Species Name		Length (cm)		Fresh wt. (g)		DW/FW	Sex	Location	
	Latin	Local	Total	Fork	Fish	Fillets			Long.	Lat
10FC2	*Aegyrops filamentosus*	Andug	28	25	420	92	0.22	M	49°50.60'E	27°22.10'N
08FC2	*Argyrops spinifer*	Andug	35	32	750	158	0.23	F	54°14.80'E	25°12.80'N
34FC2	*Arius thalassinus*	Chim	43	35	700	101	0.23	M	50°54.90'E	26°34.90'N
11FC1	*Arius thalassinus*	Chim	38	31	424	89	0.27	F	52°56.10'E	25°37.60'N
09FC2	*Arius thalassinus*	Chim	58	48	1540	299	0.22	M	55°00.00'E	25°59.80'N
38FC1	*Arius thalassinus*	Chim	56	48	1700	511	0.14	F	55°30.20'E	25°39.20'N
02FC2	*Caranx leptolepis*	Curfa	21	19	110	20	0.24	M	49°50.60'E	27°22.10'N
04FC2	*Caranx leptolepis*	Curfa	23	19	100	23	0.23	M	49°50.60'E	27°22.10'N
31FC1	*Caranx leptolepis*	Curfa	20	18	88	23	0.23	F	51°23.10'E	26°44.60'N
25FC1	*Caranx leptolepis*	Curfa	21	19	96	26	0.24	F	51°39.90'E	26°40.59'N
26FC1	*Caranx leptolepis*	Curfa	20	17	80	21	0.23	F	51°39.90'E	26°40.59'N
14FC2	*Caranx leptolepis*	Curfa	24	21	150	39	0.24	MD	51°45.40'E	25°36.20'N
15FC1	*Caranx leptolepis*	Curfa	20	17	74	19	0.25	F	52°56.10'E	25°37.60'N
17FC1	*Caranx leptolepis*	Curfa	21	18	104	26	0.26	F	52°56.10'E	25°37.60'N
19FC1	*Caranx leptolepis*	Curfa	20	18	98	17	0.26	M	52°56.10'E	25°37.60'N
09FC1	*Caranx leptolepis*	Curfa	21	18	101	28	0.25	M	53°15.27'E	25°51.85'N
08FC1	*Cephalopholis miniatus*	Shanamwa	27	*	273	82	0.21	F	53°15.27'E	25°51.85'N
29FC1	*Dentex nufar*	Nahash	18	16	90	22	0.19	F	51°23.10'E	26°44.60'N
27FC1	*Dentex nufar*	Nahash	15	13	46	12	0.22	F	51°39.90'E	26°40.59'N
14FC1	*Etrumeas tera*	Oom	16	15	38	12	0.24	F	52°56.10'E	25°37.60'N
16FC1	*Etrumeas tera*	Oom	18	17	56	12	0.24	F	52°56.10'E	25°37.60'N
18FC2	*Gnathandon speciosus*	Rebeeb	23	20	150	39	0.21	MD	51°45.40'E	25°36.20'N
10FC1	*Lethrinus horak*	Sha'ary	30	28	392	130	0.23	F	53°15.27'E	25°51.85'N
03FC2	*Lethrinus kallopterus*	Sha'ary	24	22	200	39	0.22	M	49°50.60'E	27°22.10'N
01FC2	*Lethrinus kallopterus*	Sha'ary	22	20	170	134	0.81	M	50°42.80'E	26°45.60'N
05FC2	*Lethrinus kallopterus*	Sha'ary	22	20	150	30	0.22	M	50°42.80'E	26°45.60'N
26FC2	*Lethrinus kallopterus*	Sha'ary	22	20	160	28	0.22	M	51°26.00'E	26°09.50'N
27FC2	*Lethrinus kallopterus*	Sha'ary	23	21	195	15	0.25	M	51°26.00'E	26°09.50'N
28FC2	*Lethrinus kallopterus*	Sha'ary	22	24	190	39	0.22	M	51°26.00'E	26°09.50'N
29FC2	*Lethrinus kallopterus*	Sha'ary	23	22	210	19	0.23	M	51°26.00'E	26°09.50'N
30FC2	*Lethrinus kallopterus*	Sha'ary	24	21	205	32	0.23	M	51°26.00'E	26°09.50'N
31FC2	*Lethrinus kallopterus*	Sha'ary	23	21	200	31	0.19	M	51°26.00'E	26°09.50'N
06FC1	*Lethrinus kallopterus*	Sha'ary	28	26	360	131	0.22	M	53°15.27'E	25°51.85'N
07FC1	*Lethrinus kallopterus*	Sha'ary	36	33	530	185	0.23	F	53°15.27'E	25°51.85'N
28FC1	*Loxodon macrorhinus*	Jarjoor	59	46	692	69	0.26	F	51°23.10'E	26°44.60'N
32FC1	*Loxodon macrorhinus*	Jarjoor	51	48	592	88	0.26	F	51°40.00'E	26°10.00'N
35FC1	*Loxodon macrorhinus*	Jarjoor	57	44	534	77	0.26	F	51°44.00'E	26°09.70'N
13FC1	*Loxodon macrorhinus*	Jarjoor	65	51	966	121	0.25	F	52°56.10'E	25°37.60'N
01FC1	*Loxodon macrorhinus*	Jarjoor	65	52	1212	302	0.26	M	54°34.70'E	25°09.18'N
30FC1	*Nemipetrus tolu*	Bassy	20	17	86	24	0.21	F	51°23.10'E	26°44.60'N
15FC2	*Nemiterus tolu*	Bassy	21	19	125	26	0.23	MD	51°45.40'E	25°36.20'N
13FC2	*Parupeneus cyclostomus*	Heddi	22	20	140	35	0.23	M	49°50.60'E	27°22.10'N
33FC1	*Pelates quadrilineatus*	Yamyam	16	15	56	11	0.21	F	51°40.00'E	26°10.00'N
02FC1	*Pelates quadrilineatus*	Yamyam	18	17	90	19	0.23	M	54°34.70'E	25°09.18'N
03FC1	*Pelates quadrilineatus*	Yamyam	20	19	120	28	0.21	F	54°34.70'E	25°09.18'N
04FC1	*Pelates quadrilineatus*	Yamyam	20	19	110	24	0.22	F	54°34.70'E	25°09.18'N
05FC1	*Pelates quadrilineatus*	Yamyam	19	18	102	20	0.22	M	54°34.70'E	25°09.18'N
39FC1	*Pelates quadrilineatus*	Yamyam	20	19	102	28	0.21	F	55°30.20'E	25°39.20'N
33FC2	*Platax orbicularis*	[illegible]	13	13	100	17	0.24	FM	50°54.90'E	26°34.90'N
23FC2	*Platycephalus indicus*	Wahra	34	34	250	41	0.23	M	51°45.40'E	25°36.20'N
11FC2	*Plectorhynchus cinctus*	Fersh	21	21	140	23	0.23	M	49°50.60'E	27°22.10'N
06FC2	*Rochycentron canadus*	Sikin	70	62	2300	350	0.23	M	49°50.60'E	27°22.10'N
34FC1	*Saurida lndosquamis*	Turr	21	20	70	21	0.22	M	51°40.00'E	26°10.00'N
36FC1	*Saurida lndosquamis*	Turr	31	29	184	48	0.20	F	51°44.00'E	26°09.70'N
37FC1	*Saurida lndosquamis*	Turr	30	28	152	144	0.20	F	51°44.00'E	26°09.70'N
16FC2	*Saurida unvosqamis*	Hasoom	28	26	190	30	0.24	M	51°45.40'E	25°36.20'N
20FC2	*Scolopsis bimaculatus*	Bzeemi	24	21	140	18	0.22	MD	55°00.00'E	25°59.80'N
12FC2	*Scolopsis ghanam*	Bzeemi	25	22	180	43	0.21	M	49°50.60'E	27°22.10'N
35FC2	*Scolopsis phaeops*	Bzeemi	24	21	160	22	0.21	M	50°54.90'E	26°34.90'N
32FC2	*Scolopsis phaeops*	Bzeemi	23	203	140	15	0.21	F	51°26.00'E	26°09.50'N
17FC2	*Therapon jarbua*	Theeb	31	30	420	83	0.23	F	51°45.40'E	25°36.20'N
19FC2	*Therapon jarbua*	Theeb	18	17	80	5	0.25	F	51°45.40'E	25°36.20'N
21FC2	*Therapon jarbua*	Theeb	18	17	75	7	0.24	MD	51°45.40'E	25°36.20'N
22FC2	*Therapon jarbua*	Theeb	23	21	190	24	0.23	MD	51°45.40'E	25°36.20'N
24FC1	*Therapon thraps*	Theeb	17	16	86	20	0.22	F	51°39.90'E	26°40.59'N
21FC1	*Therapon thraps*	Theeb	27	24	230	62	0.22	F	52°09.50'E	25°57.05'N
22FC1	*Therapon thraps*	Theeb	26	24	244	66	0.24	F	52°09.50'E	25°57.05'N
12FC1	*Therapon thraps*	Theeb	20	19	120	29	0.23	F	52°56.10'E	25°37.60'N
23FC1	*Trachrurus trachrurus*	Curfa	20	18	72	21	0.21	M	51°39.90'E	26°40.59'N
18FC1	*Trachrurus trachrurus*	Curfa	20	17	74	19	0.22	F	52°56.10'E	25°37.60'N
20FC1	*Trachrurus trachrurus*	Curfa	20	18	76	21	0.22	F	52°56.10'E	25°37.60'N
24FC2	*Tylosurus leiurus*	Hageol	105	93	1600	304	0.25	F	51°45.40'E	25°36.20'N
25FC2	*Tylosurus leiurus*	Hageol	103	88	1650	377	0.26	FM	51°45.40'E	25°36.20'N
07FC2	*Tylosurus leiurus*	Hageol	62	51	300	82	0.24	M	54°14.80'E	25°12.80'N

MD = Missing Data

whereas, the IAEA reference sample, MA-K-2, was used with each set of fish samples. The addition of internal standards, $C_{18.1}$ (n-octadecene) and C_{32}, was also carried out for all the analyzed fish as well as blank samples. The reference materials analysis gave results within ± 7–10% of the certified values.

RESULTS AND DISCUSSION

4.1 Trace metals

A total of 61 fish specimen was analyzed for Cd, Pb, Cu, Ni, Zn, V, Mn and Fe. The obtained levels expressed as mg/g (dry weight) are summarized in Table 2. It can be seen that Cd was detected in 95% of the analyzed samples. The highest value was recorded for *Therapon thraps* (0.28 µg/g), whereas the lowest value was recorded for *Tylosurus leiurus* (0.01 µg/g). Generally most of the detected values of Cd in the various analyzed fish species fluctuated around the same mean value 0.07 µg/g. Pb was also detected in all of the analyzed samples. The highest value was recorded for *Lethrinus kallopterus* (2.67 µg/g), whereas the lowest value was recorded for *Pelates quadrilineatus* (0.46 µg/g). Cu was detected in all the analyzed samples, with a maximum value of 18.14 µg/g recorded for *Lethrinus kallopterus* and a lowest value of 0.83 µg/g recorded for *Loxodon macrorhinus*. Ni was detected in 90% of the analyzed samples. The highest value (6.07 µg/g) was recorded for *Plectorhynchus cincuts,* whereas the lowest value (0.05 µg/g) was recorded for *Pelates quadrilineatus*. Zn was detected in all the analyzed samples. The highest value was recorded for *Arius thalassinus* (67.30 µg/g), whereas the lowest value was recorded for *Loxodon macrorhinus* (11.88 µg/g). V was detected in 42% of the analyzed samples. The highest value was recorded for *Therapon thraps* (0.40 µg/g), whereas the lowest value was recorded for *Arius thalassinus* (0.05 µg/g). Mn was detected in 93% of the analyzed samples. The highest value of 3.03 µg/g was recorded for *Loxodon macrorhinus* and the lowest value of 0.05 µg/g was recorded for *Pelates quadrilineatus*. Fe was detected in all the analyzed samples. The highest value was recorded for *Caranx leptolepis* (57.45 µg/g), whereas the lowest value was recorded for *Nemitterus tolu* (0.05 µg/g).

In general, the variation in all metal values, as shown in Table 2, could not be obviously ascribed to fish type. Metals concentrations do not differ significantly among the species in the sampled areas. The physiological features of fish were excluded from the statistical analysis due to the limited number of samples. The overall mean values of trace metals in some of the frequently sampled species are shown in Fig. 2. Maximum overall mean value of some of the more toxic metals such as Cd, Pb and V were 0.15 µg/g, 1.55 mg/g and 0.14 µg/g, respectively, which were recorded for non edible species, *Therapon thraps*. Whereas, the highest overall mean values for Pb and Ni were 1.60 µg/g and 2.44 mg/g recorded for *Lethrinus kallopterus* which is an edible species.

Pearson correlation analysis were performed on the absolute values of metals for all various fish species. Results shown in Table 2.1 indicate that Cd is highly correlated with Mn ($p = 0.001$), Ni ($p = 0.005$) and Cu ($p = 0.031$). Ni was

Table 2. Levels of trace metals in µg/g dry weight (DW) in fish species collected from ROPME Sea Area.(*Umitaka Maru Cruises* No.1 and 2, 1993)

Species Name	Cd	Pb	Cu	Ni	Zn	V	Mn	Fe
Argyrops filamentosus	0.03	1.80	4.76	5.02	44.81	0.00	0.00	41.16
Argyrops spinifer	0.02	0.58	1.95	4.33	44.81	0.00	0.42	34.73
Arius thaalassinus (4*)	0.02 - 0.13	0.77 - 1.36	2.27 - 12.53	0.00 - 4.62	33.11 - 67.30	0.00 - 0.30	19.43 - 48.37	19.43 - 48.37
Carnx leptolepis (8*)	0.02 - 0.10	0.74 - 1.89	3.48 - 6.77	0.15 - 6.01	15.68 - 48.33	0.00 - 0.30	0.37 - 1.05	16.25 - 57.45
Cephalopholis miniatus	0.12	0.18	2.82	0.15	35.48	0.00	0.45	17.95
Dentex mufar (2*)	0.05 - 0.06	1.54 - 1.55	2.65 - 3.75	0.05 - 0.15	14.90 - 16.28	0.08 - 0.30	0.03 -1.70	7.30 - 10.50
Etrumeas tera	0.10	1.31	4.14	0.10	37.75	0.00	1.15	52.56
Gnathandon speciosus	0.02	1.54	8.11	4.09	30.65	0.00	0.41	54.37
Lethrinus kallopterus (9*)	0.02 - 0.11	0.91 - 2.67	1.49 - 18.14	0.15 - 4.68	17.54 - 41.04	0.00 - 0.00	0.33 - 0.80	20.70 - 47.95
Loxodon macrorhinus (5*)	0.06 - 0.12	0.73 - 1.94	0.83 - 3.48	0.08 - 0.23	11.88 - 30.83	0.0 -0.20	0.08 - 3.03	6.50 - 41.88
Nemitterus tolu (2*)	0.04	0.77 - 1.31	1.49 - 11.11	0.05 - 4.27	15.60 - 19.29	0.0 - 0.35	0.15 - 0.38	3.45 - 38.05
Parupeneus cyclostomus	0.00	0.96	8.39	5.49	19.20	0.00	0.33	43.99
Pelates quadrilineatus (6*)	0.05 - 0.13	0.46 - 1.50	4.14 - 7.29	0.05 - 0.25	23.25 - 40.25	0.00 - 0.33	0.60 - 1.10	21.85 - 48.50
Platycephalus indicus	0.06	0.98	2.81	0.00	15.29	0.00	0.36	29.20
Plectorhynchus cincuts	0.03	1.52	13.86	6.07	35.82	0.00	0.00	46.58
Rochycentron canadus	0.05	0.96	16.99	3.69	39.35	0.00	0.43	40.26
Saurida indosquamis (2*)	0.07 - 0.08	0.92 - 1.18	1.82 - 3.14	0.06 - 0.28	13.93 - 15.35	0.00 - 0.20	0.30 - 0.93	5.78 - 16.13
Saurida unvosqamis	0.00	0.78	3.49	4.16	35.82	0.00	0.55	29.87
Scolopsis ghanam (2*)	0.02 - 0.03	0.80 - 1.60	6.95 - 14.66	0.00	21.22 - 30.65	0.00	0.00 - 0.39	38.99 - 41.16
Therapon jarbua (5*)	0.08 - 0.28	0.98 - 2.06	3.02 - 9.86	0.08 - 3.98	20.83 - 49.43	0.00 - 0.40	0.55 - 2.20	7.90 - 46.05
Trachrurus trachrurus (3*)	0.0 - 0.17	1.27 - 1.60	2.67 - 4.11	0.08 - 0.23	12.40 - 16.18	0.00	0.40 - 0.90	25.35 - 49.25
Tylosurus leiurus (3*)	0.01 - 0.07	0.83 - 1.03	2.35 - 8.58	0.0 - 4.39	17.28 - 25.55	0.00	0.33 - 0.48	29.20 - 39.94

*No. of samples analyzed

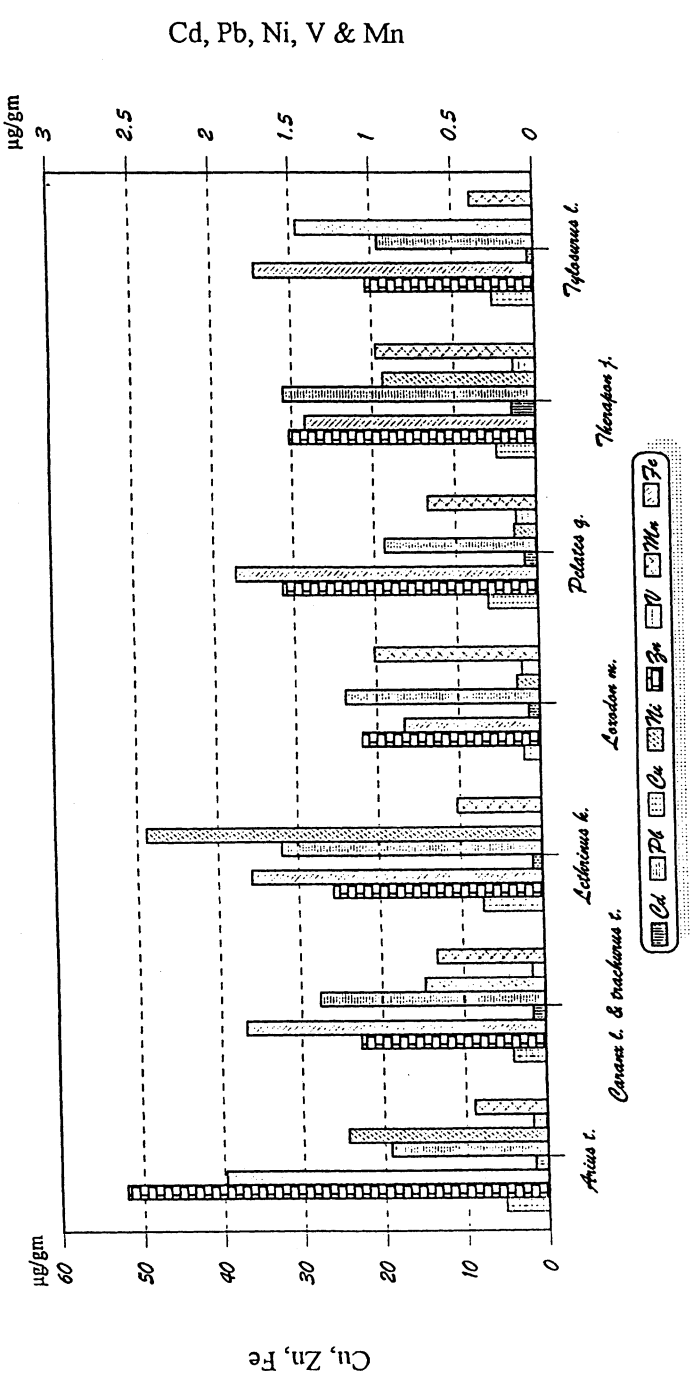

Fig. 2. Overall mean levels of trace metals in fish from the ROPME Sea Area. (*Umitaka Maru Cruises*, 1993)

Table 2.1. Pearson correlation coefficients between metals in fish species.

	Cd	Cu	Fe	Mn	Ni	Pb	V	Zn
Cd	1.0000	-0.2773	-0.1108	0.4281	-0.3538	0.1599	0.2301	0.0613
	61	61	61	61	61	61	61	61
	P=.	P=.031	P=.395	P=.001	P=.005	P=.218	P=.074	P=.639
Cu	-0.2773	1.0000	0.4443	-0.2258	0.3836	0.1008	-0.2804	0.1626
	61	61	61	61	61	61	61	61
	P=.031	P=.	P=.000	P=.080	P=.002	P=.439	P=.029	P=.211
Fe	-0.1108	0.4443	1.0000	-0.1017	0.4331	0.0920	-0.3717	0.2562
	61	61	61	61	61	61	61	61
	P=.395	P=.000	P=.	P=.436	P=.000	P=.481	P=.003	P=.046
Mn	0.4281	-0.2258	-0.1017	1.0000	-0.2748	0.1494	0.3567	-0.0134
	61	61	61	61	61	61	61	61
	P=.001	P=.080	P=.436	P=.	P=.032	P=.251	P=.005	P=.918
Ni	-0.3538	0.3836	0.4331	-0.2748	1.0000	0.0118	-0.3569	0.1019
	61	61	61	61	61	61	61	61
	P=.005	P=.002	P=.000	P=.032	P=.	P=.928	P=.005	P=.435
Pb	0.1599	0.1008	0.0920	0.1494	0.0118	1.0000	0.0101	0.0312
	61	61	61	61	61	61	61	61
	P=.218	P=.439	P=.481	P=.251	P=.928	P=.	P=.938	P=.812
V	0.2301	-0.2804	-0.3717	0.3567	-0.3569	0.0101	1.0000	0.0118
	61	61	61	61	61	61	61	61
	P=.074	P=.029	P=.003	P=.005	P=.005	P=.938	P=.	P=.928
Zn	0.0613	0.1626	0.2562	-0.0134	0.1019	0.0312	0.0118	1.0000
	61	61	61	61	61	61	61	61
	P=.639	P=.211	P=.046	P=.918	P=.435	P=.812	P=.928	P=.

highly correlated with Fe (p = 0.000), Cu (p = 0.002), V (p = 0.005) and Mn (p = 0.032) and this could be attributed to anthropogenic input whereas the most important association is found between Ni and V which could be related to spilled oil and/or oil droplet fallout during the oil fires. Pb levels do not show any significant correlation with any of the measured metals which indicate other source for the elevated lead in the marine environment and this could be related to the contribution of lead fallout.

The obtained mean values of various metals in mg/g dry weight for the analyzed fish species were recalculated on fresh weight bases and compared with other obtained values from other regions as well as some international standards as summarized in Table 2.2. Results show that the overall mean values for the

Table 2.2. Mean levels of trace metals in µg/g fresh weight (FW) in fish species from the present study and values obtained from other studies and international standards.

	a	b	c	d	e	* f	g		h		i	j	k	l	m
Metals	FDA Limits (1992) & Nauen (1983)	WHO (1987)	WHO (1972)	Limits in Malaysia (1994)	ROPME Sea Area (1993) N=61	ROPME Sea Area (1992) N=18	I. South Carolina, USA (1994) N=(4 - 35)	II. South Carolina, USA (1994) N=(6 - 11)	1. Liverpool Bay & Irish Sea (1991) N=13	II. Liverpool Bay & Irish Sea (1991) N=7	Kelang Estury Malaysia (1991) N=3	Setiu Estury Malaysia (1991) N=3	Egypt Lake (1987)	Nigeria (1994)	Kenya Lake (1987)
Cd	0.5	2.0	0.2	1.0	0.02		0.04	0.16	0.78	0.08			0.00	0.07	0.08
Pb	0.5	2.0	1.3	2.0	0.29	0.01	0.80	0.33	1.88	0.16	0.29	0.10	0.67	1.68	0.74
Cu	15.0	30.0	2.0	30.0	1.23		0.86	2.33	0.39	0.22	1.05	0.51	1.77	0.46	0.34
Ni			2.0		0.31	0.36	0.24	1.95	1.70	1.41			7.40		
Zn			50.0		6.28						10.45	5.50		5.95	4.60
V					0.02	0.94									
Cr	1.0		2.0		0.20		0.12	0.07						0.26	0.43
Mn					0.14				2.07	< 0.02				2.18	2.60
Fe					7.46				7.89	1.99				8.76	

* Original values in dry wt.x 0.23, fresh wt., based on 77% moisture content obtained in fish samples

a: FAD (1992) & Nauen (1983). b: Kakulu et al., (1987) c: Taylor (1972) d: Mat (1994) e: This Study f: Habashi et al., (1993)

g: Mathews (1994) h: Philip (1991) i& j : Hamilton (1991) k: ElNabawi et al., (1987) l: Okoye (1994) m: Wandiga et al., (1987)

determined metals are almost comparable with the reported values from other studies. Generally the mean values of trace metals are found to lie well within the international permissible limits and thus may not pose serious consequences to human health.

4.2 Petroleum hydrocarbons

The levels of total extractable lipids, hexane extractable organic matter (HEOM) in μg/g and PHC's in μg/g for the various analyzed species are summarized in Table 3. Results show that lipids levels varied between 5.0 μg/g recorded for *Pelates quadrilineatus* and 52.0 μg/g recorded for *Therapon jarbua.* The levels of HEOM varied between 300 μg/g recorded for different species and 6000 μg/g recorded for *Arius thalassinus.* PHC's levels varied between 1.86 mg/g recorded for *Loxodon macrorhinus* and 125.49 mg/g recorded for *Pelates quadrilineatus.* The overall mean values of PHC's in some frequently sampled fish species are shown in Fig. 3. The highest overall mean value of 55.30 μg/g was recorded for *Pelates quadrilineatus,* whereas the lowest mean 3.24 μg/g was recorded for *Loxodon macrorhinus.*

Pearson correlation analysis were performed on the obtained levels of hydrocarbons and the measured length and weight for all fish species as summarized in Table 3.1. Results indicate that PHC's levels are highly correlated with the levels of lipids in fish species. However, it shows that there is no correlation with other measured variables. The same analyses were performed on the results of some of the frequently sampled fish species; *Loxodon macrorhinus, Caranx leptolepis, Therapon jarbua, Pelates quadrilineatus* and *Loxodon macrorhinus* as summarized in Table 3.1.1 to Table 3.1.5. The results indicate similar trend for the first three species, whereas for *Pelates quadrilineatus* and *Loxodon macrorhinus* there was no significant correlation between the levels of PHC's and the lipid content of tissues. Whether the diet of these species has an effect on this phenomenon is difficult to ascertain.

Aliphatic hydrocarbons: series of n-alkanes from $C_{10}-C_{30}$ as well as the two isoprenoid; pristane and phytane, were measured in the analyzed samples as shown in Table 4. The results show that the obtained levels of total n-alkanes (sum of all quantified compounds) varied between 4.42 μg/g in *Caranx leptolepis* and 183.96 μg/g in *Pelates quadrilineatus,* and this variation may be attributed to the feeding habits, sex, length and weight (age of species). C_{10} was detected in only 17% of the analyzed samples, and the levels varied between 0.12 μg/g in *Aegyrops filamentosus* and 1.88 μg/g in *Lethrinus kallopterus.* C_{12} was detected in two samples with concentrations of 0.14 μg/g and 0.15 μg/g. Other n-alkane compounds were obtained in most of the analyzed samples. Isoprenoid compound (pristane) was obtained in 55% of the analyzed samples with levels varied between 0.15 μg/g in *Platycephalus indicus* and 14.28 mg/g in *Parupeneus cyclostomus.* Phytane was obtained in 52% of the analyzed samples and the levels varied between 0.18 μg/g *Caranx leptolepis* and 23.33 μg/g in *Parupeneus cyclostomus.*

Table 3. Levels of hydrocarbons in fish species collected from ROPME Sea Area. (*Umitaka Maru Cruises* No.1 and 2, 1993)

Species Name	Length (cm)	Weight (g)	DW/FW	Lipids (mg/g)	HEOM (ug/g)	PHC's (ug/g)
Argyrops filamentosus	28	420	0.22	16	900	9.47
Argyrops spinifer	35	750	0.23	26.5	2000	10.02
Arius thaalassinus (4*)	38 - 58	424 - 1700	0.14 - 0.27	13.0 - 25.0	600 - 6000	2.97 - 4.91
Carnx leptolepis (10*)	20 - 24	74 - 150	0.23 - 0.26	8.0 - 21.0	300 - 1421	2.42 - 30.49
Cephalopholis miniatus	27	273	0.21	18	300	9.33
Dentex nufar (2*)	15 -18	46 - 90	0.19 - 0.22	18 - 20	1793 - 2450	22.86 - 28.49
Etrumeas tera (2*)	16 - 18	38 - 56	0.24	11 - 13	689 - 725	8.10 - 8.84
Gnathandon speciosus	23	150	0.21	18.0	1200	3.52
Lethrinus kallopterus (12*)	22 - 36	150 - 530	0.19 - 0.81	11.0 - 35.0	300 - 900	2.83 - 30.90
Loxodon macrorhinus (5*)	51 - 65	534 - 1212	0.25 - 0.26	16 - 19	598 - 900	1.86 - 4.47
Nemitterus tolu (2*)	20 - 21	86 - 125	0.21 - 0.23	18 - 31	900 - 1242	19.89 - 46.25
Parupeneus cyclostomus	22	140	0.23	23.0	300	8.92
Pelates quadrilineatus (5*)	16 - 20	56 - 120	0.21 - 0.22	5.0 - 35.0	600 - 4020	10.44 - 125.49
Platax orbicularis	13	100	0.24	71.0	300	8.09
Platcephalus indicus	34	250	0.23	15.0	900	12.37
Plectorhynchus cincuts	21	140	0.23	22	300	4.21
Rochycentron canadus	70	2300	0.23	29.1	3000	11.54
Saurida indosquamis (3*)	21 - 31	29 - 152	0.20 - 0.22	12 - 23	600 - 900	4.62 - 11.82
Saurida unvosqamis	28	190	0.24	17.0	900	6.29
Scolopsis ghanam (4*)	23 - 25	140 - 180	0.21 - 0.22	15 -28	467 - 1534	6.01 - 33.98
Therapon jarbua (8*)	17 - 31	75 - 420	0.22 - 0.25	19 - 52	600 - 2841	2.97 - 24.97
Trachrurus trachrurus	20	76	0.22	17.0	1199	14.22
Tylosurus leiurus (3*)	62 - 105	300 - 1650	0.24 - 0.26	19 - 24	600 - 200	5.73 - 15.55

*No. of samples analyzed

Table 3.1. Pearson correlation coefficients between hydrocarbons in fish species.

	HEOM	Length	Lipids	PHC	Weight
HEOM	1.0000	0.0560	0.0282	0.1332	0.1403
	71	71	71	71	71
	P= .	P= .643	P= .816	P= .268	P= .243
Length	0.0560	1.0000	-0.1191	-0.1793	0.8675
	71	71	71	71	71
	P=.643	P= .	P= .323	P= .135	P= .000
Lipids	0.0282	-0.1191	1.0000	0.3368	-0.0373
	71	71	71	71	71
	P= .816	P= .323	P= .	P= .004	P= .758
PHC	0.1332	-0.1793	0.3368	1.0000	-0.1585
	71	71	71	71	71
	P= .268	P= .135	P= .004	P= .	P= .187
Weight	0.1403	0.8675	-0.0373	-0.1585	1.0000
	71	71	71	71	71
	P= .243	P= .000	P= .758	P= .187	P= .

Table 3.1.1. Pearson correlation coefficients between hydrocarbons in *Lethrinus kallopterus* species.

	HEOM	Length	Lipids	PHC	Weight
HEOM	1.0000	-0.3066	0.4827	0.5569	-0.3024
	12	12	12	12	12
	P= .	P= . 332	P= .112	P= .060	P= .339
Length	-0.3066	1.0000	-0.5179	-0.3040	0.9896
	12	12	12	12	12
	P= . 332	P= .	P= .085	P= .337	P= .000
Lipids	0.4827	-0.5179	1.0000	0.8318	-0.5761
	12	12	12	12	12
	P= . 112	P= .085	P= .	P= .001	P= .050
PHC	0.5569	-0.3040	0.8318	1.0000	-0.3191
	12	12	12	12	12
	P= .060	P= .337	P= .001	P= .	P= .312
Weight	-0.3024	0.9896	-0.5761	-0.3191	1.0000
	12	12	12	12	12
	P= .339	P= .000	P= .050	P= .312	P= .

Table 3.1.2. Pearson correlation coefficients between hydrocarbons in *Caranx leptolepis* species.

	Length	Weight	Lipids	HEOM	PHC
Length	1.0000	0.8822	0.5801	0.1943	0.4187
	10	10	10	10	10
	P= .	P= .004	P= .079	P= .591	P= .228
Weight	0.8221	1.0000	0.3274	0.0880	-0.0225
	10	10	10	10	10
	P= .004	P= .	P= .356	P= .809	P= .951
Lipids	0.5801	0.3274	1.0000	0.3708	0.6981
	10	10	10	10	10
	P= .079	P= .356	P= .	P= .291	P= .025
HEOM	0.1943	0.0880	0.3708	1.0000	0.3811
	10	10	10	10	10
	P= .591	P= .809	P= .291	P= .	P= .277
PHC	0.4187	-0.0225	0.6981	0.3811	1.0000
	10	10	10	10	10
	P= .228	P= .951	P= .025	P= .277	P= .

Table 3.1.3. Pearson correlation coefficients between hydrocarbons in *Therapon* species.

	HEOM	Length	Lipids	PHC	Weight
HEOM	1.0000	-0.5351	-0.3162	-0.3129	-0.4508
	8	8	8	8	8
	P= .	P= .172	P= .445	P= .450	P= .262
Length	-0.5351	1.0000	-0.2930	-0.2139	0.9681
	8	8	8	8	8
	P= .172	P= .	P= .482	P= .611	P= .000
Lipids	-0.3162	-0.2930	1.0000	0.8079	-0.2910
	8	8	8	8	8
	P= .445	P= .482	P= .	P= .015	P= .484
PHC	-0.3129	-0.2139	0.8079	1.0000	-0.1691
	8	8	8	8	8
	P= .450	P= .611	P= .015	P= .	P= .689
Weight	-0.4508	0.9681	-0.2910	-0.1691	1.0000
	8	8	8	8	8
	P= .262	P= .000	P= .484	P= .689	P= .

Table 3.1.4. Pearson correlation coefficients between hydrocarbons in *Pelates quadrilineatus* species.

	HEOM	Length	Lipids	PHC	Weight
HEOM	1.0000	-0.7685	0.4324	-0.2205	-0.6725
	5	5	5	5	5
	P= .	P= .129	P= .467	P= .722	P= .214
Length	-0.7685	1.0000	-0.4270	0.1122	0.9616
	5	5	5	5	5
	P= .129	P= .	P= .473	P= .857	P= .009
Lipids	0.4324	-0.4270	1.0000	0.7742	-0.1683
	5	5	5	5	5
	P= .467	P= .473	P= .	P= .124	P= .787
PHC	-0.2205	0.1122	0.7742	1.0000	0.3325
	5	5	5	5	5
	P= .722	P= .857	P= .124	P= .	P= .585
Weight	-0.6725	0.9616	-0.1683	0.3325	1.0000
	5	5	5	5	5
	P= .214	P= .009	P= .787	P= .585	P= .

Table 3.1.5. Pearson correlation coefficients between hydrocarbons in *Loxodon macrorhinus* species.

	HEOM	Length	Lipids	PHC	Weight
HEOM	1.0000	0.8030	-0.7844	-0.5711	0.4179
	5	5	5	5	5
	P= .	P= .102	P= .116	P= .315	P= .484
Length	0.8030	1.0000	-0.8474	-0.5746	0.8450
	5	5	5	5	5
	P= .102	P= .	P= .070	P= .311	P= .072
Lipids	-0.7844	-0.8474	1.0000	0.4156	-0.5312
	5	5	5	5	5
	P= .116	P= .070	P= .	P= .486	P= .357
PHC	-0.5711	-0.5746	0.4156	1.0000	-0.2810
	5	5	5	5	5
	P= .315	P= .311	P= .486	P= .	P= .647
Weight	0.4179	0.8450	-0.5312	-0.2810	1.0000
	5	5	5	5	5
	P= .484	P= .072	P= .357	P= .647	P= .

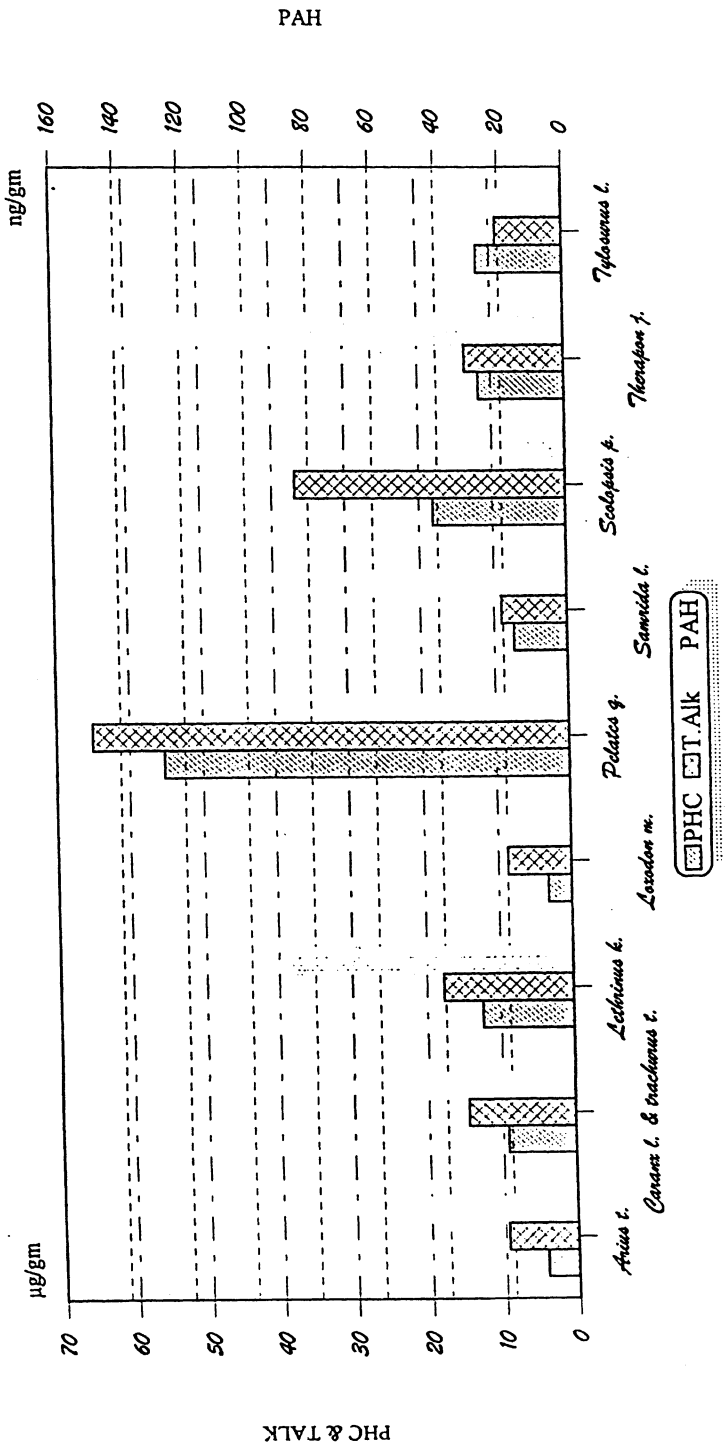

Fig. 3. Overall mean levels of hydrocarbons in fish from the ROPME Sea Area. (*Umitaka Maru Cruises*, 1993)

Table 4. Levels of aliphatic hydrocarbons (μg/g dry weight) in fish species collected from ROPME Sea Area.(*Umitaka Maru Cruises* No.1 and 2, 1993)

Species Name	Aliphatic hydrocarbons (ug/gm dry weight)															Total Alk	Pris: Phy	C17: Pris	C18: Phy
	C10	C12	C14	C16	C17	Prist	C18	Phyt	C20	C21	C22	C24	C26	C28	C30				
Argyrops filamentosus	0.12	0.00	0.22	0.54	0.68	0.30	0.54	0.37	0.31	0.45	0.61	0.97	1.47	2.86	3.38	12.15	0.8	2.3	1.5
Argyrops spinifer	0.00	0.00	0.21	0.36	0.51	0.25	0.48	0.25	0.41	0.31	0.32	0.49	1.22	2.17	0	6.48	1	2	1.9
Arius thalassinus (4*)	0.0 - 0.44	0.00	0.20 - 0.88	0.31 - 0.54	0.22 - 0.83	0.0 -0.31	0.0 - 0.53	0.0 - 0.29	0.28 - 0.51	0.17 - 0.38	0.23 - 0.46	0.40 - 0.99	1.10 - 1.76	2.73 - 6.10	0.0 - 2.72	6.87 - 11.45	1.2	2.7	2.1
Carax lepiolepis (10*)	0.0 - 1.68	0.00	0.0 - 0.61	0.22 - 1.09	0.17 - 4.48	0.0 - 3.73	0.0 - 2.14	0.0 - 2.01	0.24 - 0.86	0.22 - 1.53	0.23 - 1.06	0.39 - 1.35	1.09 - 6.45	1.86 - 8.86	0.0 - 13.38	4.42 - 32.81	0.05 - 10.1	0.5 - 11.2	1.1 - 2.0
Cephalopholis miniatus	0.00	0.00	0.59	0.89	0.91	0.79	0.61	0.00	1.27	1.46	1.48	1.34	2.78	5.81	8.72	25.86	nd	1.2	nd
Dentex rafar (2*)	0.00	0.00	0.29 - 0.66	0.58 - 1.20	0.97 - 1.07	0.0 - 1.38	0.45 - 0.76	0.0 - 0.20	0.54 - 1.07	0.76 - 1.28	0.39 - 2.05	0.36- 6.11	3.36 - 6.11	1.82 - 7.85	0.0 - 24.65	25.65 - 34.26	nd	7	2.3
Etrumeus teres (2*)	0.00	0.00	0.0 - 0.98	1.0 - 1.62	1.98 - 7.05	0.0 - 1.04	0.65 - 0.86	0.0 - 0.44	1.06 - 1.44	1.46 - 1.63	1.28 - 1.45	1.02 - 2.54	0.0 - 10.09	16.08 - 23.86	0.0 - 17.52	36.19 - 57.38	2.4	6.8	1.5
Gnathanodon speciosus	0.00	0.00	0.73	1.28	1.34	0.78	0.60	0.00	0.73	0.74	0.73	1.07	2.62	4.4	0	14.24	nd	1.7	nd
Lethrinus borak	0.00	0.00	0.23	0.56	0.70	0.38	0.58	0.27	0.38	0.35	0.32	0.48	1.15	2.88	0	7.63	1.4	1.8	2.1
Lethrinus kallopterus (11*)	0.0 - 1.88	0.00	0.0 - 0.32	0.18 - 1.55	0.18 - 4.15	0.0 - 1.93	0.21 - 4.70	0.0 - 3.60	0.26 - 55.0	0.32 - 1.51	0.22 - 8.44	0.42 - 1.17	1.08 - 5.98	1.90 - 9.51	0.0 - 8.97	6.13 - 82.52	0.5 - 1.6	1.4 - 2.4	1.3 - 2.4
Loxodon macrorhinus (5*)	0.0 - 0.34	0.0 - 0.14	0.0 - 0.29	0.31 - 0.48	0.14 - 0.28	0.00	0.0 - 0.25	0.0 - 0.25	0.26 - 0.49	0.27 - 0.64	0.21 - 0.44	0.41 - 1.07	1.07 - 2.81	2.38 - 4.80	0.0 - 3.71	5.64 - 14.85	nd	nd	0.0 - 1.3
Nemitterus tolu (2*)	0.00	0.00	0.28 - 0.41	0.32 - 0.87	0.28 - 0.56	0.00	0.20 - 0.61	0.00	0.35 - 1.74	0.29 - 1.89	0.26 - 1.65	0.38 - 0.99	1.08 - 2.26	2.53 - 3.79	0	5.97 - 14.77	nd	nd	nd
Parupeneus cyclostomus	0.22	0.00	0.49	14.30	29.39	14.28	18.84	23.33	1.10	0.86	0.43	0.56	1.34	6.77	2.26	76.56	0.6	2.1	0.8
Pelates quadrilineatus (5*)	0.00	0.00	0.25 - 1.05	0.67 - 1.92	1.10 - 10.98	0.0 - 2.51	0.81 - 1.45	0.0 - 0.64	0.78 - 2.06	0.69 - 2.14	0.88 - 1.93	1.21 - 6.84	1.64 - 22.40	3.63 - 53.0	0.0 - 82.68	6.20 - 183.96	1	1.8 - 5.1	1.4
Platycephalus orbicularis	0.00	0.00	0.21	0.59	0.77	0.00	0.67	0.35	0.51	0.28	0.19	0.97	1.7	2.08	2.93	10.9	nd	nd	1.9
Platycephalus indicus	0.00	0.00	0.21	0.67	0.85	0.15	0.00	0.42	0.53	1.22	1.32	0.74	8.35	14.01	16.18	44.08	0.4	5.7	nd
Plectorhynchus cinctus	0.00	0.00	0.29	0.43	0.57	0.41	0.55	0.24	0.34	0.34	0.38	0.56	1.24	2.63	2.78	10.11	1.7	1.4	2.3
Rochycentron canadus	0.00	0.00	0.00	0.24	0.40	0.00	0.24	0.00	0.25	0.24	0.36	0.68	1.2	2.12	1.95	7.68	nd	nd	nd
Saurida Indosquamis (3*)	0.0 - 0.13	0.0 - 0.15	0.19 - 0.41	0.34 - 0.71	0.25 - 1.27	0.0 - 0.68	0.25 - 0.73	0.0 - 0.38	0.42 - 0.61	0.37 - 0.75	0.36 - 0.79	0.39 - 0.52	1.12 - 1.23	2.29 - 7.98	0	7.22 - 14.02	1.8	1.8	1.9
Saurida tervesquamis	0.00	0.00	0.26	0.48	0.57	0.00	0.26	0.00	0.36	0.31	0.3	0.4	1.06	2.6	0	6.6	nd	nd	nd
Scolopsis bimaculatus	0.48	0.00	0.26	0.41	2.49	0.47	0.55	0.24	0.35	0.32	0.34	0.45	1.13	3.13	0	9.91	2	5.3	2.3
Scolopsis ghanam	1.81	0.00	0.00	0.46	0.78	0.36	1.00	0.54	2.05	1.75	1.97	2.29	3.67	6.91	16.29	38.98	0.7	2.2	1.9
Scolopsis phasops (2*)	0.0 - 0.20	0.00	0.18 - 0.53	0.32 - 0.80	0.43 - 0.44	0.00	0.33 - 0.50	0.00	0.30 - 0.84	0.39 - 1.76	0.64 - 1.63	1.03 - 1.17	1.46 - 12.13	3.98 - 19.09	3.03 - 20.32	12.09 - 59.41	nd	nd	nd
Therapon jarbua (8*)	0.00	0.00	0.0 - 0.57	0.0 - 0.97	0.0 - 1.37	0.0 - 1.58	0.0 - 0.83	0.0 - 0.40	0.0 - 0.91	0.0 - 1.72	0.0 - 1.13	0.0 - 1.32	0.0 - 8.83	0.0 - 8.79	0.0 - 10.24	0.0 - 31.61	1.4 -2.4	0.5 - 1.4	1.2 - 2.3
Trachurus trachurus	0.00	0.00	0.00	0.00	0.00	0.00	0.00	0.00	0.00	0.00	0.00	0.00	0.00	0.00	0.00	0.00	nd	nd	nd
Tylosurus leiurus (3*)	0.00	0.00	0.0 - 0.33	0.0 - 0.52	0.0 - 2.02	0.0 - 6.92	0.0 - 0.80	0.0 - 0.31	0.0 - 0.38	0.0 - 0.34	0.0 - 0.37	0.0 - 0.52	0.0 - 1.23	0.0 - 11.44	0.0 - 2.41	0.0 - 16.42	3.3 - 27.7	0.3 - 0.7	1.9 - 2.4

*No. of samples analyzed

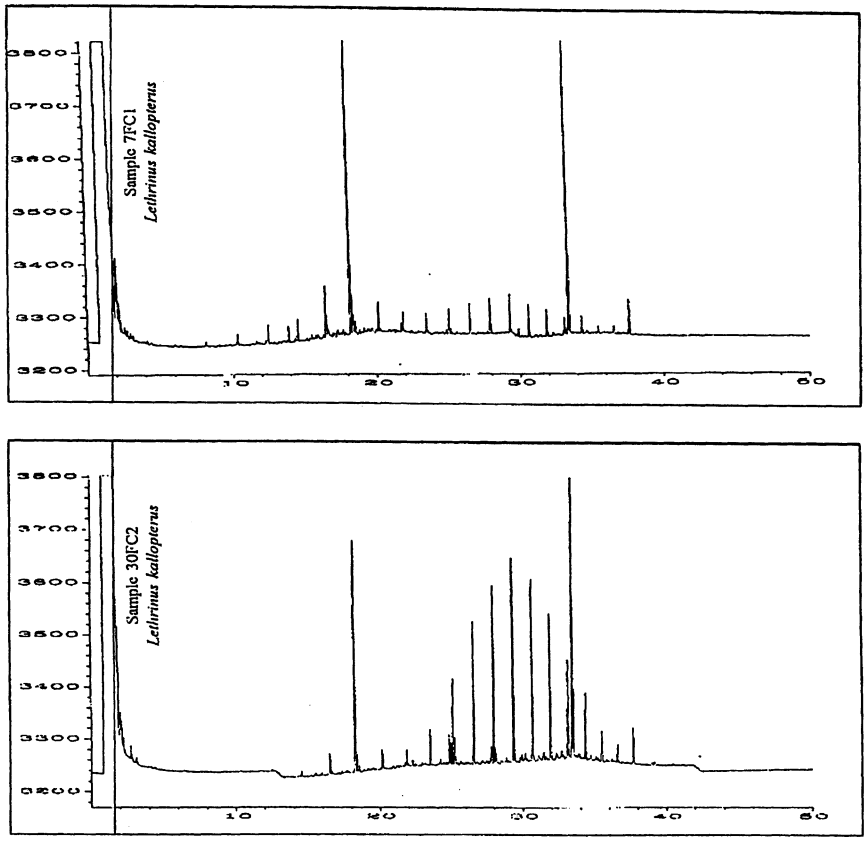

Fig. 4. The GC chromatograms of two fish samples.

The presence of pristane in fish species could be attributed to biogenic origin of hydrocarbons synthesized by zooplankton and fish. The pristane and phytane were present in the same fish species only in 38% of the samples analyzed. Pristane : phytane ratio was highly variable, ranging from 0.36 to 27.68. However the pristane : phytane ratio of ≤ 1.0 was recorded only in 10 samples, indicating a petrochemical origin of these aliphatic hydrocarbons, whereas a pristane : phytane ratio »1 would indicate a planktonic source. This was found in two *Caranx leptolepis* samples (6.27 and 10.08) and 27.68 in *Tylosurus leiurus*.

Total n-alkanes in frequently sampled species was found to vary between 8.70 µg/g in *Loxodon macrorhinus* and 65.10 µg/g in *Pelates quadrilineatus*. Similar trend was also found for PHC's as shown in Fig. 3. The absence of the unresolved complex mixture (UCM) in the analyzed samples as shown for example in Fig. 4 is a good indicator for PHC's free samples. The obtained levels of the present study were found within normal levels for areas considered to be

Table 5. Range of levels of aromatic hydrocarbons (ng/g dry weight) in fish species collected from ROPME Sea Area.(*Umitaka Maru Cruises* No.1 and 2, 1993)

Species Name	Aliphatic hydrocarbons (ug/gm dry weight)																Total PAH
	1	2.0	3.0	4	5.0	6.0	7.0	8.0	9.0	10.0	11.0	12.0	13.0	14.0	15.0	16.0	
Argyrops filamentosus	nd	nd	1.1	nd	nd	nd	nd	3.3	nd	nd	6.5	nd	nd	nd	nd	nd	10.9
Argyrops spinifer	nd	17.7	nd	nd	nd	nd	nd	4.8	16.2	nd	nd	nd	nd	nd	nd	nd	38.7
Arius thaalassinus (4)*	nd	0.0 - 15.7	0.6	nd	nd	nd	nd	0.6 - 15.1	10 - 43.8	8.4	4.6 - 5.5	10.6	nd	nd	7.8 - 33.4	4.5	5.7 - 135.5
Carnx leptolepis (10)*	nd	3.0 - 18.8	0.5 - 24.2	nd	2.6 - 60.9	11.8 - 12.7	nd	1.1 - 36.2	13.1	nd	0.8 - 4.8	nd	nd	nd	2.9	25.9	11.8 - 83.7
Trachrurus trachrurus	nd	0.8	1.9	nd	125.2	25.4	nd	40.5	nd	nd	2.9	nd	nd	nd	nd	nd	196.5
Dentex nufar (2)*	nd	nd	nd	nd	nd	50.1	nd	17.1 - 23.4	nd	nd	nd	nd	nd	nd	nd	nd	23.4 - 67.3
Etrumeas tera (2)*	nd	7.4	31.5	nd	58.0	28.2	nd	9.3	nd	nd	50.1	nd	nd	nd	nd	nd	68 - 101
Gnathandon speciosus	nd	nd	1.6	nd	nd	12.5	nd	9.8	nd	nd	4.6	nd	nd	nd	4.1	28.7	61.1
Lethrinus horak	nd	11.4	0.5	nd	nd	nd	nd	0.9	nd	nd	9.0	nd	nd	nd	nd	nd	21.8
Lethrinus kallopterus (11)*	nd	0.4 - 12.9	1.1 - 8.9	nd	37.9 - 300.8	12.2 - 20.8	nd	2.1 - 38.7	nd	nd	0.9 - 14.2	nd	3.2	nd	5.0	3.5	4.4 - 353.5
Lazodon macrorhinus (5)*	nd	nd	nd	nd	17.2 - 54.4	nd	nd	2.4 - 5.7	nd	8.1	1.9 - 15.50	nd	nd	nd	nd	nd	0.0 - 61.2
Nemitterus tolu (2)*	nd	nd	0.9	nd	nd	11.7	nd	7.1 - 37.5	nd	nd	nd	nd	nd	nd	nd	13.6	33.3 - 37.5
Parupeneus cyclostomus	nd	nd	2.1	nd	11.2	12.0	13.5	35.5	nd	nd	nd	nd	nd	nd	nd	nd	74.2
Pelates quadrilineatus (5)*	nd	2.7 - 63.5	6.1	nd	126.6	12.7	nd	13.4 - 40.0	1.3	nd	14.1 - 17.4	nd	nd	nd	nd	nd	0.0 - 250.2
Platax orbicularis	nd	0.9	nd	nd	nd	nd	nd	4.4	nd	nd	8.7	nd	3.6	nd	nd	5.0	22.7
Platycephalus indicus	nd	nd	nd	nd	56.3	nd	nd	7.3	nd	9.7	nd	nd	nd	nd	nd	nd	73.2
Plectorhynchus cinctus	nd	nd	nd	nd	nd	nd	nd	16.8	nd	nd	nd	nd	nd	nd	nd	nd	16.8
Rochycentron canadus	nd	8.4	nd	nd	nd	nd	nd	nd	9.4	nd	nd	nd	nd	nd	nd	nd	17.8
Saurida indosquamis (3)*	nd	4.2 - 12.30	0.6 - 06	nd	18.6 - 56.0	nd	nd	6.6 - 19.3	nd	nd	1.1 - 3.9	1.0	nd	nd	nd	nd	29.5 - 80.8
Saurida urvosqamis	nd	nd	nd	nd	nd	nd	nd	12.3	nd	8.6	nd	nd	nd	nd	nd	36.3	57.2
Scolopsis bimaculatus	nd	nd	nd	nd	nd	nd	nd	3.0	nd	nd	2.7	nd	nd	nd	13.5	nd	19.1
Scolopsis ghanam	nd	nd	0.7	nd	nd	nd	nd	8.6	nd	nd	nd	nd	nd	nd	nd	nd	9.3
Scolopsis phaeops (2)*	nd	0.4 - 0.7	nd	nd	nd	nd	nd	3.0 - 3.6	nd	nd	nd	nd	nd	nd	nd	8.2 - 22.8	3.7 - 24.2
Therapon jarbua (8)*	nd	0.1 - 21.5	0.4 - 3.7	nd	3.0 - 519.4	12.4 - 21.2	54.3	7.2 - 117.1	nd	12.6 - 33.5	2.8 - 8.0	nd	nd	nd	nd	22.8 - 727.9	22.8 - 727.9
Tylosurus leiurus (3)*	nd	1.0 - 19.3	1.0 - 1.1	nd	nd	12.0	nd	4.5	0.7 - 42.2	5.4	10.6	nd	nd	nd	2.8	nd	13.5 - 72.1

*No. of samples analyzed

mildly polluted and the reported n-alkanes ranged between 12.0 μg/g and 46.0 mg/g wet weight (Alzieu *et al.*, 1976 & Hermide *et al.*, 1994). Generally, the degree of pollution with aliphatic compound in fish species is low.

Polycyclic aromatic hydrocarbon: Sixteen PAH compounds were investigated, naphthalene, acenaphthylene, acenaphthene, fluorene, phenanthrene, anthracene, fluoranthene, pyrene, benzo (a) anthracene, chrysene, benzo (b) fluoranthene, benzo (k) fluoranthene, benzo (a) pyrene, dibenzo (ah) anthracene, indeno (1,2,3-cd) pyrene, and benzo (ghi) perylene. The results of PAH analysis in different species are summarized in Table 5. The total PAH's levels varied between 2.7 ng/g in *Pelates quadrilineatus* and 729.9 ng/g in *Therapon thraps*.

Of the sixteen PAH compounds, naphthalene, fluorene and dibenzo (ah) anthracene were not detected in any of the analyzed samples. Among the investigated PAH's pyrene was the dominant compound and it was measured in a detectable levels in 87% of the analyzed samples. The levels of pyrene varied between 0.6 ng/g in *Arius thalassinus* and 117.1 ng/g in *Therapon jarbua*. It may be worth noting that pyrene is also the dominant in suspended particulate analyzed during the oil fires (Al-Majed, 1991). Benzo (b) fluoranthene was detected in 50% of the analyzed samples in levels varied between 0.9 ng/g in *Lethrinus kallopterus* and 50.1 ng/g in *Etrumeas tera*. Acenaphthylene and acenaphthene were detected in about 46% of the analyzed samples in levels varied between 0.1–63.5 ng/g and 0.4–24.2 ng/g for each compound, respectively. Phenanthrene was detected in 31% of the analyzed samples. The levels varied between 2.6 ng/g in *Caranx leptolepis* and 300.8 ng/g in *Therapon thraps*. Anthracene was detected in 24% of the analyzed species in levels varied between 11.7 ng/g in *Nemitterus tolu* and 50.1 ng/g in *Dentex nufar*. Indeno (1,2,3-cd) pyrene was detected in 10% of the analyzed species. The levels varied between 2.8 ng/g in *Tylosurus leiurus* and 33.4 ng/g in *Arius thalassinus*. Benzo (ghi) perylene was detected in 14% of the analyzed samples in levels varied between 3.5 ng/g in *Lethrinus kallopterus* and 36.3 ng/g in *Saurida unvosqamis*. The most toxic carcinogenic compound, benzo (a) pyrene, was detected only in two species, 3.2 ng/g recorded for *Lethrinus kallopterus* and 3.6 ng/g in *Platax orbicularis*.

The overall mean values of total PAH's in frequently sampled species are shown in Fig. 3. Results show that the overall mean levels varied between 14.1 ng/g in *Scolopsis phaeops* and 150.0 ng/g in the non edible species, *Therapon thraps*. The detectable levels of PAH compounds do not show a regular distribution among various analyzed species and found to be comparable with the obtained levels < 0.5–148 ng/g (wet weight) recorded in unpolluted zones (Renata *et al.*, 1990) after recalculated on the bases of 75% water content .

As a general conclusion, the obtained levels of trace metals and trace organic in fish tissues were observed to have a wide range within the various fish species as well as within the same group. This variation was expected and could be attributed to several factors related to environmental conditions, e.g. temperature, water quality, type of pollutant and its mass loading to the marine environment, as well as the nature of the tested species which include its tendency to

accumulate contaminants, feeding habits and other biological parameters. Hence, the limited number of the analyzed samples can not be used to assess the monitoring trend in ROPME Sea Area. A continuous studies should be carried on taking into consideration all other biological parameters to improve the understanding of metals and petroleum hydrocarbons accumulation.

Acknowledgement

We would like to acknowledge the Environment Protection Council and ROPME for the financial support to conducting this study. We would like to thank Francis Picardo for typing this manuscript.

REFERENCES

Ackman R. G. (1972): Pristanc and other hydrocarbons in some fresh water and marine fish oils. *Lipids*, 6, 520.

AL–Majed N. (1991): Assessment of polycyclic hydrocarbons in air suspended particulate. EPD–Kuwait.

Alzieu C., Michel P. and Thibaud Y. (1976): Presence of micropollutants in mussels. Science et Peche. *Bull. Inst. Peches Marit*, 264, 1–18.

Ameijeiras, H. A., Gandara, S. J. *et al.* (1994): Aliphatic hydrocarbons levels in farmed and free–living mussels from Galicia (N.W.Spain). *Mar. Pollut. Bull.*, 28, 178–181.

Coochire, R. A., Aruese, A. and Minicuca, A. M. (1990): Polycyclie aromatic hydrocarbons in marine organisms from Italian central Mediterranean coasts. *Mar. Pollut. Bull.*, 21, 15–18.

Eisler, R. (1981): Trace metal concentrations in marine organisms. Pergamon Press, New York.

FAO/WHO Food and Agriculture Organization / World Health Organization (1972): Evaluation of certain food additives and of contaminants IIg, Pb and Cd. 16th report, Rome, p.84.

Fernex, F. and Migon, C. (1991): Tomprorary and definitive fixation of atmospheric lead in deep–sea sediment of western Mediterranean sea. *Mar. Pollur. Bull.*, 28, 727–734.

Francesconi K. A., Moore E. J. and Edmonds J. S. (1994): Cadmium up take from sea water and food by the western Rock Lobster *Panuliru Cygmus. Environ. Contam. Toxicol.*, 53, 219–223.

Habashi, B. A., Al–Majed, N. B. *et al.* (1992): Levels of major trace pollutants in fish from the western part of ROPME Sea Area. Proceeding of the Scientific workshop on results of R/V Mt. Mitchell Cruise, Kuwait.

Hamilton, E. I. (1991): Relationship between heavy metal content and body weight of fish from the Kelang Estuary, Malaysia. *Mar. Pollut. Bull.*, 22, 86–89.

Hites, R. A., LaFlamme, R. E. and Farrington, J. W. (1977): Sedim entary polycyclic aromatic hydrocarbons: The historical record. *Science*, 198, 829–831.

Hites, R. A. (1976): Sources of polycyclic aromatic hydrocarbons in the aquatic environment. In: Sources, Effects and Sinks of Hydrocarbons in the Aquatic Environment. American Institute of Biological Sciences, Washington, DC, p.325.

Katsuzo, K. and Yoshitaka, A. (1986): Fishes of the Arabian Gulf, Kuwait Institute for Scientific Research.

Kolattukudy, P. E. (1976): Biogenesis of non–isoprenoid aliphatic hydrocarbons. In Sources, Effects and Skins of Hydrocarbons in the Aquatic Environment. The American Institute of Biological Sciences, Washington, D.C., p.120.

Koons, C. B., Jamieson, G. W. and Cieroszko, L. S. (1965): Normal alkane distributions in marine organisms. Possible significance to petroleum origin. *Bull. Am. Assoc. Pet. Geol.* 49, 301–309.

Kremling, K. (1985): The distribution of cadmium, copper, nickel, manganese and aluminum in surface waters of the open Atlantic and European Shelf area. *Deep Sea Res.* 32, 531–555.

LaFlammc, R. E. and Hites, R. A. (1978): The global distribution of polycyclic aromatic hydrocarbons in recent sediment. *Geochim. Cosmochim. Acta*, 42, 289-303.

Lynam, D. R., Piantanida, L. G. and Jerome, F. (1981): Environmental Lead. Academic Press, Int.

Lucas, J. (1975): Our polluted food. Charles Knight and Company Ltd, London.

Marcovecchio, J. E., Moreno, V. J. and Perez, A. (1986): Biomagnification of total mercury in Bahia

Blanca estuary shark. *Mar. Pollut. Bull.* 17, 276–278.

MOOPAM (1989): Manual of Oceanographic Observations and Pollutant Analyses Methods, prepared by the Regional Organization for the Protection of Marine Environment (ROPME). Kuwait.

Morris, E. R. and Green, F. E. (1970): Distribution of Pb, Zn, Cd, Cr and Se in wheat and wheat products. *Fed. Proc.*, 29, 500–508.

National Academy of Sciences (1975): Effects of oil on marine organisms: a critical assessment of published data. *Water Res.*, 8, 819-827.

Nauen, C. E. (1983): Compilation of legal limits for hazardous substances in fish and fishery products. *FAO Fish Circ.* 764, Rome, 5-90.

Okoye, BCO. (1994): Lead and other metals in dried fish from Nigerian Markets. *Bull. Environ. Contam. Toxicol.*, 52, 825-832.

Pancirov, R. J. and Brown, R. A. (1977): Polycyclic aromatic hydrocarbons in marine tissues. *Envir. Sci. Technol.*, 11, 989-992.

Peck, E. J. and Ray, W. J. (1969): Role of bivalent cations in the phosphoglucomutase system 2. Metals in binding and the structure of binary enzyme metal complexes. *J. Biol. Chem.*, 244, 3718–3752.

Ratkowsky, D. A., Dix, T. G. and Wilson, K. C. (1975): Mercury in fish in Derwent Estuary. Tasmania, and its relation to the position of the fish in food chains. *Aus. J. Mar. Freshwater. Res.* 26, 223–231.

Subramamian, K. S. and Conner, J. W. (1991): Lead contamination of drinking water. *J. Environ. Health.* 54, 29–34.

Thompson, D. R. (1990): Metal levels in marine vertebrates. In Heavy Metals in the marine Environment (R. W. Furness & P. S. Rainbow eds), p. 143. CRC Press, Boca Raton, Fl.

Tsoukali–Papadopoulou, H. *et al.* (1989): Heavy metals in consumable tissues, presented at the V International Congress of Toxicology, Brighton, GB.

Vas, P. (1991): Trace metals in sharks from British and Atlantic Waters. *Mar. Pollut. Bull.*, 22, 67–72.

Verberg, W. B., Coursey, P. J. and OHara, J. (1974): Multiple environmental Factors on physiology and behavior of the fielder crab Uca pugilator. In Pollution and Physiology of Marine Organisms: Recent Advances (Vernberg W. B. & Vernberg F. J., eds). Academic Press, New York.

Wandiga, S. O. and Onyari, J. M. (1987): The concentration of heavy metals: Mn, Fe, Cu, Zn, Cd and Pb in sediment and fish from the Winam Gulf of Lake Victoria and fish bought in Mombassa town market, Kenya. *J. Sc. Ser. A.*, 8, 5–11.

Offshore Environment of the ROPME Sea Area after the War-Related Oil Spill,Eds. A. Otsuki *et al.*, pp. 281–301.

Study of phytoplankton in ROPME Sea Area

Muna HUSAIN and Shahnaz IBRAHIM

Environmental Public Authority, P.O. Box 24395, *Safat 13104, Kuwait*

Abstract—Distribution of phytoplankton in the inner part of ROPME Sea Area was studied during December 1993 and 1994. The study area covers the region from U.A.E. to Saudi Arabia including 20 stations from 5 sections, and different sections were monitored during 1994 including 24 stations. Phytoplankton was collected vertically from bottom to surface by Norpac Net (45 cm diameter, 100 micron mesh size). The higher phytoplankton counts, in December 1993, were recorded in section A (6982 cells/l), section C (6074 cells/l) and section B (5637 cells/l) and the lowest was recorded in section D (1389 cells/l). The phytoplankton population was dominated by diatoms group which constitute 83%, followed by dinoflagellates which comprise 15.4%, and finally the blue green algae which represents 1.6%.

INTRODUCTION

The ROPME Sea Areas (RSA) were subjected to acute and massive oil spill during the Gulf war in 1991. It was estimated that 1 million tonnes of oil was deliberately discharged into the Gulf waters. This was a potential threat to the marine environment. The aims of the cruise of R/V Umitaka Maru in the RSA was to monitor the possible effect of pollution by oil spill. An attempt has been made to assess the effect of such oil pollution by monitoring the standing stock of phytoplankton species and species diversity estimation. Several investigators have studied the phytoplankton population in the RSA earlier. They are Hendey (1970), Enomoto (1971), Kimor (1973), Kuronuma (1974), Al-Kaisi (1976), Jacob (1979), Dorgham (1987), Habbashi (1988) and El-Gindy (1992).

The RSA is a relatively small water body with a total area of about 240,000 square km. It is characterised by shallow waters of high temperature with little fresh water inflow and liberal evaporation resulting in highly saline conditions in some parts of the sea area. The general circulation pattern of the water in the area is counter-clockwise, and hence there is a water movement northwards along the Iranian coast and a corresponding one southwards along the southern coast (Linen *et al.*, 1990).

STUDY AREA, PHYSICAL AND CHEMICAL PARAMETERS

The present study covers the area of:

A: U.A.E. (section A)

Sampling in 4 stations (Stations, 0–3) was done during December 1993 (25°12.70′ N–25°34.19′ N and 54°14.90′ E–53°00.86′ E) (Table 1a). Samples

Table 1a. Sampling sites.

Station	Date / Time	Lat. N	Long. E	Depth (m)
St. 0	17 th / 13 : 10	25 12 . 70	54 14 . 90	25
St. 1	18 th / 13 : 22	26 14 . 60	53 11 . 60	75
St.2	18 th /16 : 50	25 54 . 38	53 07 . 86	64
St.3	18 th / 20 : 20	25 34 . 19	53 00 . 86	41
St.4	20 th / 07 : 29	26 58 . 10	52 17 . 20	72
St.5	20 th / 10 : 45	27 43 . 50	52 02 . 70	66
St.6	20 th / 14 : 00	26 27 . 90	51 48 . 50	45
St.7	20 th / 16 : 46	26 13 . 00	51 35 . 20	26
St.8	21 st / 07 : 40	27 16 . 10	51 41 . 40	43
St.9	21 st / 10 : 20	27 06 . 60	51 29 . 70	73
St.10	21 st / 12 : 38	26 56 . 90	51 19 . 90	72
St.11	21 st / 15 : 17	26 44 . 50	51 09 . 70	25
St.12	21 st / 18 : 10	26 34 . 90	50 54 . 90	16
St.13	23 rd / 06 : 55	27 32 . 60	51 06 . 50	68
St.14	23 rd / 09 : 38	27 20 . 80	50 54 . 50	52
St.15	23 rd / 12 : 27	27 07 . 80	50 41 . 70	65
St.16	24 th / 05 : 57	27 52 . 60	50 46 . 70	63
St.17	24 th / 09 : 03	27 43 . 50	50 33 . 20	57
St.18	24 th / 11 : 41	27 36 . 00	50 17 . 80	62
St.19	24 th / 14 : 25	27 27 . 70	50 03 . 70	57

Table 1b. Sampling sites.

Station	*Date / Time*	*Lat. N*	*Long. E*	*Depth (m)*
RO9401	*15th / 15:14*	*25 00. 30*	*54 35. 80*	*26*
RO9402	*16th / 09:01*	*25 14. 00*	*54 33. 00*	*28*
RO9403	*16th / 13:34*	*25 31. 94*	*54 35. 92*	*47*
RO9404	*17th / 12:26*	*25 52. 38*	*55 28. 99*	*48*
RO9405	*17th / 14:20*	*25 46. 14*	*55 29. 49*	*37*
RO9406	*17th / 16:19*	*25 39. 00*	*55 30. 25*	*21*
RO9407	*18th / 08:05*	*26 14. 36*	*53 11. 73*	*73*
RO9408	*18th / 11:41*	*25 55. 40*	*53 05. 93*	*63*
RO9409	*18th / 14:41*	*25 35. 53*	*53 00. 98*	*39*
RO9410	*19th / 09:01*	*25 15. 73*	*52 45. 24*	*28*
RO9411	*19th / 16:38*	*26 13. 85*	*51 34. 89*	*25*
RO9412	*20th / 08:19*	*26 28. 12*	*51 48. 45*	*45*
RO9413	*20th / 10:45*	*26 42. 69*	*52 02. 18*	*70*
RO9414	*20th / 13:29*	*26 57. 34*	*52 14. 41*	*64*
RO9415	*21th / 08:06*	*26 41. 69*	*51 07. 20*	*22*
RO9416	*23th / 10:08*	*26 50. 37*	*51 17. 43*	*46*
RO9417	*23th / 13:11*	*27 01. 82*	*51 29. 74*	*72*
RO9418	*23th / 16:03*	*27 12. 43*	*51 38. 30*	*57*
RO9419	*24th / 11:39*	*27 15. 14*	*50 19. 29*	*53*
RO9420	*24th / 15:05*	*27 30. 81*	*50 37. 23*	*56*
RO9421	*24th / 17:42*	*27 42. 44*	*50 54. 50*	*68*
RO9422	*25th / 09:23*	*27 56. 99*	*49 49. 77*	*45*
RO9423	*25th / 11:50*	*27 53. 67*	*49 36. 47*	*33*

Table 2a. Physical & chemical parameter.

Station	Water Depth (m)	Temperature C	Salinity (psu)	Oxygen (ml/L)	PH
St. 0	25m	25.56	40.35	—	8.2
St. 1	75m	23.65	39.9	3.3	6
St.2	64m	24.4	39.6	4.3	8.3
St.3	41m	24.89	40	4.4	8.2
St.4	72m	22.9	39.6	2.8	8
St.5	66m	23.37	39.58	2.76	8.15
St.6	45m	23.36	40	4.4	8.2
St.7	26m	22.4	40.77	4.68	8.3
St.8	43m	24.26	39.37	3.9	8.15
St.9	73m	23.4	39.6	4.37	8.2
St.10	72m	23.6	39.8	3.18	8.19
St.11	25m	23.1	39.9	4.6	8.2
St.12	16m	22.2	40.2	4.66	8.2
St.13	68m	22.59	39.8	4.4	8.16
St.14	52m	23	39.86	4.4	8.19
St.15	65m	23.2	39.1	4.4	8.2
St.16	63m	22	39.9	4.47	8.16
St.17	57m	22.5	39.89	4.3	8.1
St.18	62m	23.1	40.15	4.4	8.18
St.19	57m	22.29	40.2	4.5	8.19

were taken from different depths (24 m–64 m), and mean water temperature varied from 23.65 to 25.56°C. Salinity ranged between 39.63–40.35, pH of water was in the range of 8.07–8.32, and dissolved oxygen was in the range of 3.38–4.34 ml/l (Table 2a). A total of 10 samples was collected from 10 stations (RO9401–

Table 2b. Physical & chemical parameters during 1994.

Station	Water Depth (m)	Temperature (C)	Salinity (psu)	Oxygen (ml/L)	PH
1	26.00	23.74	41.75	4.52	8.14
2	28.00	24.19	41.16	4.29	8.23
3	47.00	24.79	40.51	4.30	7.99
4	48.00	25.34	39.06	4.10	8.22
5	37.00	25.29	39.14	4.05	7.88
6	21.00	23.76	38.92	4.53	7.96
7	73.00	24.08	39.44	3.62	7.92
8	63.00	24.82	39.97	4.17	7.91
9	39.00	24.79	40.06	4.20	7.82
10	28.00	23.75	40.93	4.44	8.14
11	25.00	22.41	40.58	4.66	8.24
12	45.00	23.89	39.95	4.34	8.18
13	70.00	23.90	39.97	4.28	8.10
14	64.00	23.62	39.71	4.31	8.12
15	22.00	23.25	40.23	2.95	8.21
16	46.00	22.81	40.20	4.66	8.20
17	72.00	23.00	40.05	4.53	8.17
18	57.00	23.00	39.70	4.53	8.18
19	53.00	22.36	33.66	3.79	6.69
20	56.00	23.07	40.24	4.50	8.15
21	68.00	22.38	39.96	4.65	8.13
22	45.00	21.80	40.45	4.69	8.17
23	33.00	21.48	40.54	4.69	8.12
24	24.00	19.90	40.72	5.02	8.12

9410) during 15th to 19th December 1994 (25°00.30′ N–25°15.73′ N and 54°35.80′ E–52°45.24′ E) (Table 1b). Sampling depth varied between 21 m–73 m, and water temperature was in the range of 23.74 to 25.34°C. Salinity value was in the range of 38.92 to 41.75. pH value of sea water was in the range of 7.82 to 8.23, and dissolved oxygen ranged between 3.62–4.53 ml/l (Table 2b).

B: Qatar (section B)

Four samples from 4 stations of Qatari waters were collected in December 1993 (26°58.10′ N–26°13.00′ N and 52°17.20′ E–51°35.20′ E). Water tempera-

ture varied between 22.4–23.3°C. Sampling depth was in the range of 23 m–62 m, salinity was in the range of 39.6–40.77 and pH value varied between 8.07–8.30. In 1994, 4 samples were collected from 4 stations (RO9411–14) during December 1994 (26°13.85′ N–26°57.34′ N and 51°34.89′ E–52°14.41′ E). Sampling depths varied between 25 m–69 m. Water temperature varied between 22.41–23.9°C, salinity was in the range of 39.71–40.58, and pH of water varied between 8.18–8.24.

C: Bahrain (section C)

Five samples from 5 stations (Sts. 8–12) were collected on a single day on 21 December 1993 (27°16.10′ N–26°34.90′ N and 51°41.40′ E–50°54.90′ E). Depth values were in the range of 15 m–70 m. Water temperature varied between 22.2–24.26°C, salinity was in the range of 39.37–40.2 pH value varied between 8.15–8.2 and dissolved oxygen was in the range of 3.9–4.66 ml/l. Chlorophyll concentration was in the range of 0.46–1.7 ug/l.

Four samples were collected from 4 stations during 1994 (RO9415–18) (26°41.69′ N–27°12.43′ N and 51°07.20′ E–51°38.30′ E). Sampling depth ranged between 22 m–72 m and temperature varied between 22.81–23.25°C, whereas salinity was in the range of 37.70–40.23 pH was in the range of 8.17–8.21, and dissolved oxygen ranged between 2.95–4.66 ml/l. Chlorophyll concentration varied between 0.29–1.05 ug/l.

D: KSA (sections D and E)

Seven samples were collected from 7 different stations (Sts. 13–19) during 23rd and 24th December 1993 (27°32.60′ N–27°27.70′ N and 51°06.50′ E–50°03.70′ E). Sampling depth was in the range of 51 m–64 m. Water temperature varied between 22.0–23°C. Salinity was in the range of 39.1–40.2. Dissolved oxygen ranged between 4.3–4.5 ml/l, and pH value was in the range of 8.1–8.2.

Six samples were collected from 6 stations (RO9419–23) during 1994 (27°15.14′ N–27°47.88′ N and 50°19.29′ E–49°23.70′ E). Sampling depth was in the range of 25 m–68 m. Water temperature varied between 19.9–23.0°C. pH value was in the range of 8.03–8.15 and salinity was in the range of 33.66–40.72. The maximum value of dissolved oxygen was 5.02 ml/l and the minimum value was 3.79 ml/l.

MATERIAL AND METHODS

A total of 44 samples (20 in 1993 and 24 in 1994) was collected by the R/V Umitaka Maru during its cruise in the waters of U.A.E., Qatar, Bahrain and Saudi Arabia (Figs. 1a and 1b) using Norpac Plankton Net which has a mesh size of 100 micron. The net was towed vertically from the bottom to the surface with different depth among stations. In 1993 depth values ranged between 15–70 m, while in 1994 they ranged between 21–73 m. A calibrated flowmeter was used to determine the amount of water filtered by the net. The samples were fixed and preserved in 5% buffered formaline. Aliquot samples were counted using a compound microscope and the results were computed to number/litter (cells/l).

The total number of phytoplankton groups such as diatoms, dinoflagellates,

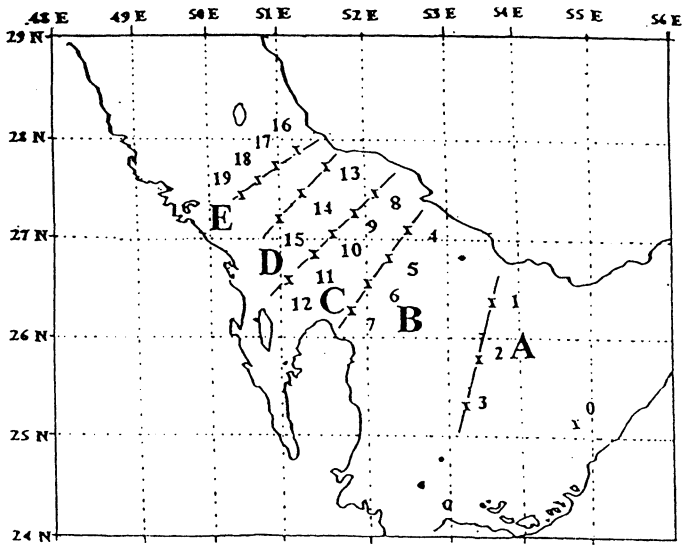

Fig. 1a. The arrangement of the sampling transects (A, B, C, D, and E) along the study area in December 1993.

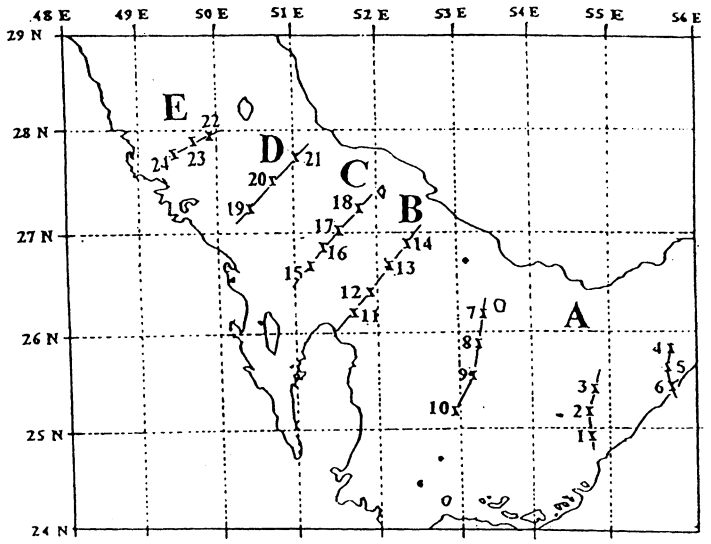

Fig. 1b. The arrangement of the sampling transects (A, B, C, D, and E) along the study area in December 1994.

Table 3a,b. Chlorophyll value and biomass (wet weight) during December 1993-1994.

ST	CHLOROPHYLL (uM/l)	BIOMASS (gm/m3)	TOTAL COUNT cells/l
0	0.82	0.8	6982
1	0.54	0.3	1366
2	0.37	0.2	1478
3	0.82	0.3	3029
4	0.84	0.6	5188
5	1.3	0.5	3296
6	0.64	0.5	2487
7	0.71	0.5	5637
8	1.1	0.4	3904
9	1.7	0.6	3092
10	0.46	0.3	2076
11	1.1	0.8	6627
12	0.59	0.6	6074
13	0.75	0.2	1389
14	0.67	0.2	1514
15	0.53	0.5	2132
16	0.63	0.5	3671
17	0.44	0.3	2114
18	0.65	0.4	2261
19	0.9	0.5	3028

(a)

ST	CHLOROPHYLL (uM/l)	BIOMASS (gm/m3)	TOTAL COUNT cells/l
1	0.56	0.8	6782
2	0.67	0.78	7912
3	0.75	1.02	8974
4	0.61	0.64	6254
5	0.68	0.34	3808
6	1.81	0.46	6280
7	0.83	0.48	4894
8	1.13	0.5	5434
9	0.83	0.28	3694
10	0.84	0.88	8590
11	0.87	0.16	1746
12	0.34	0.6	5930
13	0.47	0.56	6308
14	1.05	1.14	11160
15	0.68	0.92	8376
16	0.97	1.48	7630
17	0.29	0.4	1946
18	1.7	1.48	5166
19	0.61	0.4	1576
20	0.5	0.46	3446
21	0.63	0.2	2304
22	0.96	0.2	2302
23	1.21	0.66	6674
24	1.76	1.24	9928

(b)

blue green algae and silicoflagellates together with its wet weight biomass (displacement method) were also estimated and recorded in all the areas under investigation.

The physical and chemical parameters such as temperature, pH, salinity and nutrients were measured by Umitaka Maru staff members, and compared with

standing crops of phytoplankton species. An attempt has been made to compare the standing stock of phytoplankton with its corresponding area's physical and chemical parameters.

RESULTS

A total number of 44 samples in 1993 and 1994 was analysed and counted to estimate the population density of phytoplankton. The several species of phytoplankton found in this study in 1993 survey were classified into 3 groups (diatoms, dinoflagellates and blue green algae) and in 1994 they were classified into 4 groups including silicoflagellates as an additional group. The dominant species found in both years have been listed (Tables 4a and 4b). The highest diversity of 54 species was recorded at the station 3 (U.A.E.) in 1993, while the highest diversity of 65 species was recorded at the station 24 (Saudi Arabia) in 1994. A total number of 39 genera, 73 species, was recorded during the 1993 study, whereas 55 genera and 86 species were recorded during the 1994 study.

Chlorophyll–*a* value suggested to be related with the standing stock of phytoplankton. In 1994, a very high biomass value, 1.05 µg/l, was recorded at the station 14 (Qatar) and the highest count, 11160 cells/l, was also recorded at this station, while the lowest chlorophyll value, 0.29 µg/l, was recorded at the station 17 (Bahrain) and its count was 1946 cells/l, although this result was not the lowest but it showed a poor primary productivity at this station. The results of chlorophyll *a* and biomass showed that there were a definite correlation among the biomass and chlorophyll values (Table 3, Fig. 2). A distinct relationship occurs at specific time during the season, depending on the thermal characteristics of the water column (Billington, 1991).

The diatoms formed the main bulk of phytoplankton groups (84%) in 1993 and (79%) in 1994. *Cerataulina pelagica* was dominant species recorded during this study. This species was recorded at 17/20 stations (85%) in 1993 and 21/24 (87.5%) in 1994. The most common diatoms were *Climacodium fraunfeldianum*, *Thalassiothrix nitzchoioides*, *Chaetoceros coarctatus*, C. *lorenzianum*, C. *pseudocurvisetum*, *Coscinodiscus spp*, *Biddulphia sinensis*, B. *mobiliensis*, *Rhizosolenia spp.*, *Navicula* spp., and *Nitzschia* spp.

Dinoflagellates (mostly *Ceratium* species) formed 14% in 1993 and 17% in 1994. The most abundant species were *Ceratium trichoceros*, C. *massilense*, C. *carrienses*, C. *tripos*, C. *pennatum*, C. *furca*, and C. *fusus*. Blue green algae (mostly Oscillatoria *thiebauti*, Anabaena sp) formed 1.6% in 1993 and 3.3% in 1994, respectively. Silicoflagellates (*Dichtyocha* sp) were recorded during 1994 in all the 4 areas namely United Arab Emirates, Qatar, Bahrain and Saudi Arabia. Their abundance was insignificantly low (0.028%) of the total phytoplankton groups.

Fifty species of diatoms, 20 species of dinoflagellates and 3 species of blue green algae were recorded in all the 5 areas under study during December 1993, whereas 56 species of diatoms, 24 species of dinoflagellates, 6 species of blue green algae and 1 species of silicoflagellates were recorded in all the 5 areas under

Table 4a. Distribution of phytoplankton groups in investigated stations. During December 1993.

Station	DIATOMS		DINOFLAGELLATES		BLUE GREEN ALGAE		Total No.	Diversity	Biomass	DOMINANT SPECIES
	NO	%	NO.	%	NO.	%	Cells / l	sp.	µg /l	
St. 0	5305	76	1570	22.5	107	1.5	6982	34	0.8	Cerataulina pelagica
St. 1	1040	76.1	299	22	27	1.9	1366	31	0.3	Cerataulina pelagica
St. 2	940	63.6	510	34.5	28	1.9	1478	31	0.2	Cerataulina pelagica
St. 3	2800	92.4	200	6.6	29	1	3029	54	0.3	Cerataulina pelagica
St. 4	5001	96.4	158	3	29	0.6	5188	43	0.6	Cerataulina pelagica
St. 5	2950	89.5	320	9.7	26	0.8	3296	47	0.5	Cerataulina pelagica
St. 6	2252	90.5	200	8.1	35	1.4	2487	34	0.5	Cerataulina pelagica
St. 7	4878	86.5	673	12	86	1.5	5637	43	0.5	Cerataulina pelagica
St. 8	3428	87.8	403	10.3	73	1.9	3904	34	0.4	Cerataulina pelagica
St. 9	2808	90.8	234	7.6	50	1.6	3092	34	0.6	Cerataulina pelagica
St. 10	1890	91.1	156	7.5	30	1.4	2076	31	0.3	Cerataulina pelagica
St. 11	5960	90	585	8.8	82	1.2	6627	30	0.8	Cerataulina pelagica
St. 12	4940	81.3	1092	18	42	0.7	6074	40	0.6	Climacodium fraunfeldianum
St. 13	1226	88.3	135	9.7	28	2	1389	42	0.2	Cerataulina pelagica
St. 14	1216	80.3	249	16.5	49	3.2	1514	32	0.2	Cerataulina pelagica
St. 15	1583	74.3	472	22.1	77	3.6	2132	35	0.5	Climacodium fraunfeldianum
St. 16	2772	75.5	854	23.3	45	1.2	3671	37	0.5	Cerataulina pelagica
St. 17	1916	90.6	152	7.2	46	2.2	2114	29	0.3	Cerataulina pelagica
St. 18	1637	72.4	587	26	37	1.6	2261	36	0.4	Cerataulina pelagica
St. 19	2608	86.1	396	13.1	24	0.8	3028	46	0.5	Climacodium fraunfeldianum

Table 4b. Distribution of phytoplankton Sp. in Ropme Sea area during December 1994.

Station	DIATOM		DINOFLAGELLATES		SILICOFLAGELLATES		BLUE GREEN ALGAE		Total No.	Diversity	Biomass	Dominant
	NO.	%	NO.	%	NO.	%	NO.	%	C/L	SP.	mg/L	sp.
1	4758	70.00	1758	26.00	0	0.00	266	4.00	6782	45	0.80	Chaetoceros coarctatus
2	6372	80.50	1290	16.30	26	0.30	224	2.90	7912	54	0.78	Thalassiothrix nitzch.
3	7246	80.74	1358	15.13	8	0.09	362	4.04	8974	43	1.02	Cerataulina pelagica
4	4536	72.53	1594	25.49	14	0.22	110	1.76	6254	34	0.64	Cerataulina pelagica
5	2856	75.00	872	22.90	8	0.20	72	1.90	3808	46	0.34	Cerataulina pelagica
6	5000	78.62	1076	17.13	28	0.45	176	2.80	6280	53	0.46	Cerataulina pelagica
7	4002	81.80	784	16.00	0	0.00	108	2.20	4894	37	0.48	Cerataulina pelagica
8	4676	86.00	622	11.50	6	0.10	130	2.40	5434	47	0.50	Cerataulina pelagica
9	2620	71.00	936	25.30	0	0.00	138	3.70	3694	46	0.28	Cerataulina pelagica
10	5766	67.00	1772	20.70	14	0.20	1038	12.10	8590	54	0.88	Cerataulina pelagica
11	1246	71.00	358	21.00	0	0.00	142	8.00	1746	39	0.16	Cerataulina pelagica
12	4342	73.20	1468	24.80	10	0.10	110	1.90	5930	45	0.60	Cerataulina pelagica
13	5286	84.00	812	13.00	0	0.00	210	3.00	6308	34	0.56	Cerataulina pelagica
14	9880	88.50	1120	10.03	8	0.07	152	1.40	11160	54	1.14	Cerataulina pelagica
15	5262	62.80	2832	33.80	0	0.00	282	3.40	8376	27	0.92	Cerataulina pelagica
16	6484	85.00	1008	13.20	0	0.00	138	1.80	7630	36	1.48	Cerataulina pelagica
17	1598	82.10	302	15.50	0	0.00	46	2.40	1946	39	0.40	Cerataulina pelagica
18	4640	89.80	428	8.30	8	0.15	90	1.75	5166	59	1.48	Cerataulina pelagica
19	1278	81.10	242	15.30	0	0.00	56	3.60	1576	35	0.40	Cerataulina pelagica
20	2982	87.00	360	10.00	0	0.00	104	3.00	3446	36	0.46	Cerataulina pelagica
21	1940	84.20	296	12.80	0	0.00	68	3.00	2304	35	0.20	Cerataulina pelagica
22	2016	87.60	232	10.10	0	0.00	54	2.30	2302	48	0.20	Cerataulina pelagica
23	5900	88.40	584	8.80	0	0.00	190	2.80	6674	42	0.66	Cerataulina pelagica
24	7792	78.80	1900	19.20	0	0.00	200	2.00	9928	65	1.24	Thalassiothrix nitzcho.

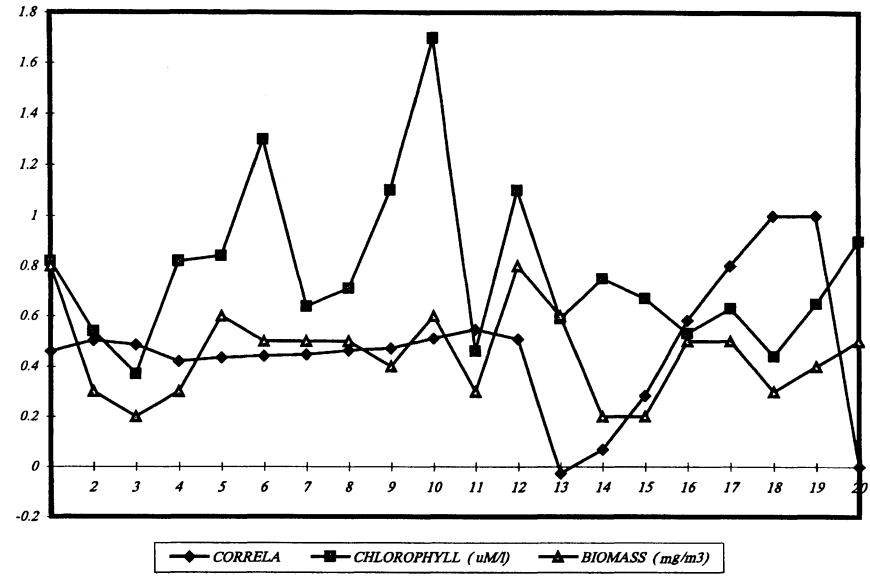

Fig. 2a. Correlation between chl. and biomass during 1993.

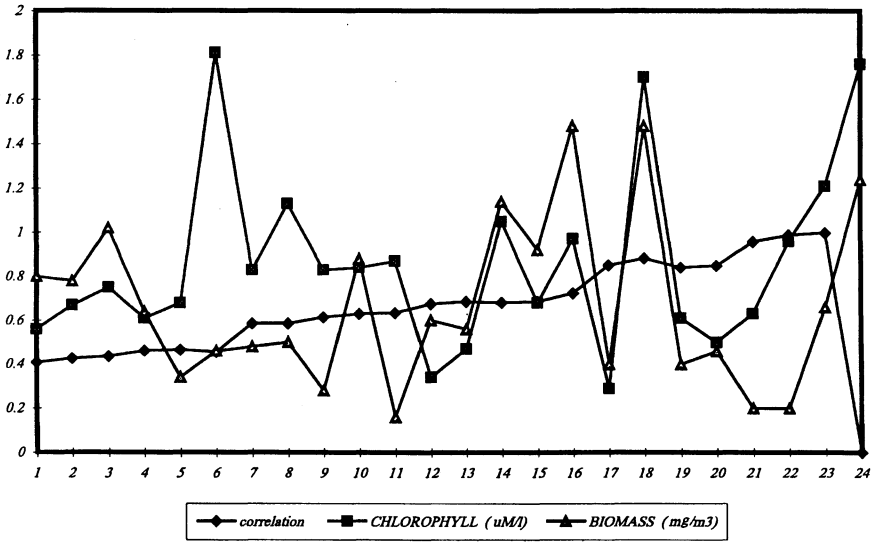

Fig. 2b. Correlation between chl. and biomass during 1994.

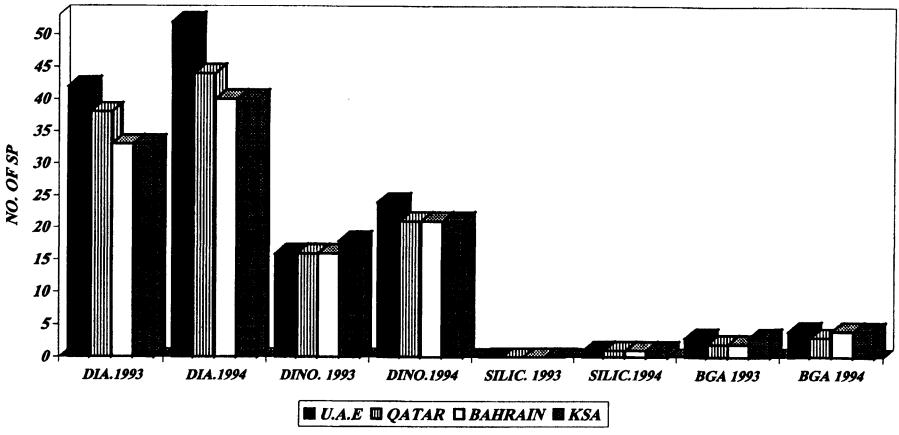

Fig. 3. Distribution of species diversity of phytoplankton recorded in Dec. 1993 & 1994.

study during December 1994.

Biddulphia mobiliensis at station 3 (U.A.E.), *Closterium* species at station 6 (U.A.E.), *Lyngbya* sp at station 9 (U.A.E.), *Merismopdia* sp. at station 17 (Bahrain) and *Rivularia* sp. at station 24 (Saudi Arabia) were recorded only once in the areas mentioned between brackets during December 1994. Silicoflagellates, *Dichtyocha* spp, were recorded in all the 4 areas during December 1994.

There was a slight difference on the distribution of phytoplankton species during the 1993 and 1994 study. The followings are the species which occurred only once in each area, they were not recorded at other stations. *Bacteriastrum* sp. 6 cells/l at the station 4 (Qatar), *Chaetoceros* lavae 4 cells/l at station 5 (Qatar) and 14 cells/l at station 7 (Qatar), *Eucampia zoodiacus* 5 cells/l at station 3 (U.A.E.), *Nitzschia longissima* 5 cells/l at station 3 (U.A.E.) and *Noctiluca miliaris* 3 cells/l at the station 6 (Qatar).

The mean of species diversity found in each area both in 1993 and 1994 is listed in the Table 6, and Fig. 3. A key point to be mentioned here is that some of the species may not occur at all in certain years; the number of individuals present may be very low; and some of them may occur earlier or later to the expected period (Sabrabmoniyan and Viswanatha Sarma, 1959).

The highest phytoplankton counts, in December 1993, were recorded at station 0 (U.A.E.), 6982 cells/l, 6074 cell/l at station 11 (Bahrain) and 5637 cells/l at station 7 (Qatar), and the lowest, 1366 cells/l, was recorded at station 1 (U.A.E.), whereas 1994 results showed that the highest phytoplankton counts 11160 cells/l were found at station 14 (Qatar), 9928 cells/l, at station 24 (Saudi Arabia) 8974 cells/l, at station 3 (U.A.E.) and the lowest, 1576 cells/l was recorded at station 19 (Saudi Arabia) (Tables 4a and 4b).

The area wise distribution of mean phytoplankton counts during December

Table 5a. Distribution of phytoplankton groups in investigated sections. During December 1993.

SECTION	DIATOMS		DINOFLAGELLATES		BLUE GREEN ALGEA		TOTAL NO.	DIVERSITY	BIOMASS
	NO.	%	NO.	%	NO.	%	Cell /l	Sp.	mg/l
A	2521	77	645	21.4	47	1.6	3214	37	0.4
B	3770	90.7	338	8.2	44	1.1	4152	42	0.5
C	3805	88.2	494	10.4	55	1.4	4354	34	0.5
D	1342	80.9	285	16.1	51	2.9	1678	36	0.3
E	2233	81.1	497	17.4	38	1.4	2768	37	0.4

Table 5b. Distribution of phytoplankton groups in investigated sections. During December 1994.

SECTION	DIATOM		DINOFLAGELLATES		SILICOFLAGELLATES		BLUE GREEN ALGA		TOTAL NO.	DIVERSITY	BIOMASS
	NO.	%	NO.	%	NO.	%	NO.	%	C/L	SP.	gm/l
A	4783	76.40	1206	19.64	10	0.16	262	3.80	6261	46	0.62
B	5189	79.20	940	17.20	5	0.04	154	3.56	6288	43	0.6
C	4496	79.93	1143	17.70	2	0.03	139	2.34	5780	40	1.07
D	2067	84.10	299	12.70	0	0.00	76	3.20	2442	35	0.35
E	5236	84.90	905	12.70	0	0.00	148	2.40	6289	52	0.7

Table 6. Distribution of species diversity of phytoplankton recorded in Dec. 1993 & 1994.

AREA	DIAT.		DINOF.		SILICO.		BLUE GREEN ALGAE	
	DIA.1993	DIA.1994	DINO. 1993	DINO.1994	SILIC. 1993	SILIC.1994	BGA 1993	BGA 1994
U.A.E	42	52	16	24	-	1	3	4
QATAR	38	44	16	21	-	1	2	3
BAHRAIN	33	40	16	21	-	1	2	4
KSA	33	40	18	21	-	1	3	4

1993 showed that the higher mean count were recorded at section C (Bahrain), 4354 cells/l, followed by section B (Qatar), 4152 cells/l, and section A (U.A.E.), 3214 cells/l, and the lowest was recorded at section E (Saudi Arabia), 1678 cells/l. On the other hand the higher mean phytoplankton counts were found at section E (Saudi Arabia), 6289 cells/l, 6288 cells/l at section B (Qatar), and 6261 cells/l at section A (U.A.E.). The lowest count was recorded at section D (Saudi Arabia), 2442 cells/l (Tables 5a and 5b).

DISCUSSION AND CONCLUSION

The present study showed that there was a tendency of occurring more density of phytoplankton groups in the northern parts of the Gulf (Figs. 1a and 1b) including the areas of Saudi Arabia which was exposed to the threat of oil spill during the Gulf crises. In spite of the highly localized short term oil spill, this study revealed that the standing stock appeared to be increasing. It is believed that, during the 24–48 hours of the spill, there is a likelihood of reducing the highly volatile toxic hydrocarbons through the process of evaporation. But the Gulf war and eventual spillages of oil occurred during the winter months. The temperature during winter months appears to be low and hence the intensity of evaporation was comparatively lesser. The sampling activities started in Kuwait 7 months after liberation of Kuwait. Meanwhile the greater part of toxic hydrocarbons either was evaporated or withered away and transported to other areas through wave action. This means that some amount of toxic hydrocarbon was distributed into the wider areas of the Gulf waters and eventually the intensity of toxic effects of hydrocarbon were recorded lesser. This lead us to believe that the more the time passes the less toxic effect of oil spill occurs.

Faraj *et al.* (1994) has studied the pre-war and post-war results of phytoplankton samples. The samples were collected nearly 7 months after liberation of Kuwait (post) and monthly EPD's biomonitoring results before the crises (pre) were compared. She has revealed that there was a considerable variation in the phytoplankton abundance between pre-crises and post-crises results. This is in agreement with the results of the similar studies in this area. Therefore, the damage occurred to the planktonic life due to the oil spill was a short term process and the study of planktonic organisms in the affected areas showed that erstwhile richness of the marine life has already restored. "Time has healed the wound" as far as planktonic life is concerned.

In conclusion, the investigators are of the opinion that the phytoplankton samples collected twice in 2 years just during the month of December is not enough to reveal the accurate standing stock of the region. A continuous plankton sampling in this area for a considerable period of time will pave the way for obtaining a clear understanding of the standing stock of phytoplankton population.

Acknowledgements

The authors are thankful to Dr. Saude Al-Rasheed, Director of Environment Protection Department for his encouragement and facilities to carry out this work and Ms. Mona

Faraj, Superintendent of soil pollution and biological resources for her kind advice and critical review of the manuscript. we are also thankful to Mr. A.M. Fahmi for his taxonomic help.

REFERENCES

Al-Kaisi, K. A.: On the phytoplankton of the Arabian Gulf. 2nd Joint Oceanography Assembly. 13–24 Sept. Edinburgh. U.K. (1976).

Al-Yamani, F. and A. M. Fahmi: Gulf war impacts on zooplankton species, diversity and its implication on Fisheries. The International Conference on the Effects of the Iraqi Aggression on the State of Kuwait. April 2–6, 1994. Kuwait (1994).

Billington, N.: A copmarison of the three methods of measuring phytoplankton biomass on a daily and seasonal basis. Hydrobiologia, 226, 1–5 (1991).

Danish Scientific investigations in Iran: Einar Marks gaard, Copenhagen (1935–38).

Dotgham, M. M., A. Muftah and K. Z. El-Deeb: Plankton Studies in the Arabian Gulf. II. The Autumn Phytoplankton in the North western Area. Arab Gulf *J. Scient. Res. Biol. Sci Bs*, 2, 215–235 (1987).

El-Gindy, A. A. and M. M Dorgham: Interrelations of phytoplankton, chlorophyll and physico-chemical factors in Arabian Gulf and Gulf of Oman during Summer. Indian Journal of Marine Sciences (1992).

Enomoto, Y.: Oceanographic survey and biological study of shrimps in the water adjacent to the eastern coast of the state of Kuwait (1971).

EPD, Environmental Protection Dept. Ministry of Public Health, Kuwait: Annual Report (1982–1990) (1992–1994).

Fahmi, A. M., B. Habbashi and M. Abdulraheem: Monthly Variations of Zooplankton in the Coastal Waters of Kuwait. The 9th Shrimp and Fin Fisheries Management Work Shop. KISR, 7–9 Dec. 1987 (1986).

Faraj, M. and H. Morad: Impacts of the Gulf environmental catastrophy on fishery resources of Kuwait. The International Conference on the Effects of the Iraqi Aggression on the State of Kuwait. April 2–6, 1994, Kuwait (1994).

Habbashi, B. B., F. Najeeb and M. Faraj: Distribution of Phytoplankton Cell Abundance of Chlorophyll with Certain Environmental Factors in the ROPME Sea Areas. Scientific Work Shop on Results of the R/V Mt. Mitchell Cruise 24–28, Jan. 1992. Kuwait (1992).

Hendey, N. I.: Some literal Diatoms of Kuwait. Nova Hedwigia, supplement: Diatomacea II pp. 110–167 (1970).

Jacob, P. G., M. A. Zarba and V. Anderlini: Hydrology, Chlorophyll and Plankton of the Kuwaiti Coastal Waters (1979).

Kimor, B.: Plankton relation of the Red sea, Persian Gulf and Arabian sea. In The *Biology of the Indian Ocean*, B. Zeitzchel (ed.), pp. 221–232, Chapman & Hall Ltd, London (1973).

Kuronuma, K.: Arabian Gulf Fishery-Oceanography survey by the Umitaka maru, training research vessel, Tokyo University of Fisheries with collaboration of Kuwait Institute for Scientific Research (1974).

Linden, O., M. Y. Abdelraheem *et al.*: State of Marine Environment in the ROPME Sea Areas. UNEP Regional Seas Report and Studies No. 112, Rev. I. UNEP (1990).

Michel, H. B, M. Behbehani *et al.*: Zooplankton Diversity, Distribution and Abundance in Kuwaiti Waters. MFD, KISR (1981).

Najeeb, F., B. B. Habbashi *et al.*: Abundance and Monthly Distribution of Phytoplankton in the Coastal Waters of Kuwait. meeting of expert on marine productivity in the Arab Region. Alexandria, Egypt. 24–26 Oct (1988).

Sabrabmoniyan, R. and A. H. Viswanatha Sarma: Studies on the phytoplankton of the west coast of India. Part III. Seasonal variation of the phytoplankton and environmental factors. *Proc. Indian Acad. Sci.*, 50B, 87–113, 189–252 (1959).

Senichkina, L. G., A. S. Mikaelyan and L. V Georgiyevich: Phytoplankton communities of surface waters in different climatic zones of the world ocean. Hydrobiological Journal, 30(4) (1994).

Appendix. Names of phytoplankton species occured

No.	SP.	0	1	2	3	4	5	6	7	8	9	10	11	12	13	14	15	16	17	18	19
	DIATOMS																				
1	*Amphi.sp.*				*			*								*	*		*	*	
2	*Bact. spp.*					*															
3	*Bid. sins.*	*	*		*	*		*	*	*	*		*	*	*	*		*			*
4	*Chae. atlen.*				*		*		*				*	*							
5	*Chae. brev.*		*																		
6	*Chae.coar.*	*	*		*	*	*		*			*	*	*	*			*	*	*	*
7	*Chae.dent.*		*	*						*	*							*			*
8	*Chae. lae.*						*		*												
9	*Chae.loren.*				*		*		*		*				*	*					
10	*Chea.peru.*																				*
11	*Chae.pseudo.*			*	*	*	*		*	*	*	*			*			*			*
12	*Chae.teres.*				*									*							
13	*Chae.torti.*						*														
14	*Ceratau.pela.*	*	*	*	*	*	*	*	*	*	*	*	*	*	*	*	*	*	*	*	*
15	*Clima. frauenfel.*	*	*	*	*	*	*	*	*	*	*	*	*	*	*	*	*	*	*	*	*
16	*Cosci.spp.*	*	*	*	*	*	*	*	*	*	*	*	*	*	*	*	*	*	*	*	*
17	*Eucam.zoodi.*				*																
18	*Guin.flac.*			*	*	*	*		*	*		*		*	*	*	*				*
19	*Hemia. sinensis*			*	*	*	*	*	*	*	*	*	*	*	*		*				*
20	*Hemid.hard.*														*			*			
21	*Laud.annu.*				*	*	*		*						*			*			*
22	*Lepto.dani.*				*			*	*												
23	*Melosi.sp.*	*			*			*					*	*							
24	*Navi.spp.*	*	*	*	*	*	*	*	*	*	*	*	*	*	*	*	*	*	*	*	*
25	*Nitz.clo.*				*		*														
26	*Nitz.long.*				*																
27	*Nitz.para.*			*	*										*	*		*			
28	*Nitz.seriata*				*	*	*			*	*		*								*
29	*Nitz. sp.*																	*			
30	*Plan.sol.*		*			*	*		*			*			*	*	*	*			
31	*Pleu.spp.*	*	*	*	*	*	*		*		*	*	*	*	*	*	*	*	*	*	*
32	*Rh.alata.*	*	*	*	*	*	*	*	*	*	*				*	*			*		*	*
33	*Rh.berg.*	*		*	*	*	*	*	*	*		*	*	*	*			*			*	*
34	*Rh.calca.*			*	*	*		*	*		*	*		*		*					*	*
35	*Rh.clev.*	*	*	*		*	*	*	*	*	*			*	*		*	*		*	*
36	*Rh.cylin.*	*				*							*				*				*
37	*Rh.cochi.*				*			*	*					*	*					*	*
38	*Rh.hebea.*	*	*	*	*	*	*	*	*					*	*		*				*
39	*Rh.imbri.*	*	*	*	*	*	*		*	*	*		*	*	*					*	*
40	*Rh.robu.*		*		*		*								*		*	*	*	*	*
41	*Rh.seti.*									*	*	*									
42	*Rh.stolt.*				*	*	*		*						*	*					
43	*Step.palm.*											*									
44	*Step.thum.*	*			*	*	*	*	*	*	*			*	*			*		*	
45	*Suriella.sp.*				*	*	*														
46	*Thala.coram.*				*	*	*	*													
47	*Thala.frauen.*	*	*	*	*	*	*	*	*	*	*	*	*	*	*	*	*	*	*	*	*

in all areas uncer study during Dec, 1993.

	SP.	0	1	2	3	4	5	6	7	8	9	10	11	12	13	14	15	16	17	18	19
48	*Thala. longis.*	*	*		*	*	*	*	*	*	*	*	*	*	*	*	*	*	*	*	*
49	*Thala.nitz.*		*		*	*	*		*	*	*		*	*	*	*	*	*	*	*	*
50	*Tricer.furca.*				*	*			*			*			*				*	*	
	DINOFLAGELLATES																				
51	*Cera.belon.*																	*		*	
52	*Cera. carriense*									*	*			*	*	*	*	*		*	*
53	*Cera. exten.*	*																	*	*	*
54	*Cera.furca.*	*	*	*	*	*	*	*	*	*	*	*	*		*	*	*	*	*	*	*
55	*Cera.fusus.*	*	*	*	*	*	*	*	*	*	*	*	*	*	*	*	*	*	*	*	*
56	*Cera. horri.*																*				
57	*Cera.kofoi.*				*	*	*	*	*					*			*		*		*
58	*Cera.massi.*	*	*	*	*	*	*	*	*	*	*	*	*	*	*	*	*	*	*	*	*
59	*Cera.penn.*	*			*	*	*		*			*		*		*	*		*	*	*
60	*Cera.tricho.*	*	*	*	*	*	*	*	*	*	*	*	*	*	*	*	*	*	*	*	*
61	*Cera.tripos.*	*	*	*	*	*	*	*	*	*	*	*	*	*	*	*	*	*	*	*	*
62	*Cera.vulture.*	*	*	*	*	*	*	*	*	*	*	*	*	*			*	*		*	*
63	*Dino.caud.*	*	*	*	*	*	*	*	*	*	*	*	*	*	*	*	*	*	*	*	*
64	*Gonian.spp.*	*	*	*	*	*	*	*	*	*	*	*	*	*	*	*	*	*	*	*	*
65	*Noct.mil.*							*													
66	*Orni.thumi.*				*		*	*		*					*	*		*	*		
67	*Peri.spp.*	*	*	*	*	*	*	*	*	*	*	*	*	*	*	*	*	*	*	*	*
68	*Proroc.sp.*	*		*	*		*							*	*						
69	*Pyro.sp.*	*	*	*	*		*	*		*	*	*	*	*	*	*	*	*		*	*
70	*Pyroh.horo.*	*	*	*	*	*	*	*	*	*	*	*	*	*	*	*	*	*	*	*	*
	BLUE GREEN ALGAE																				
71	*Anabea.sp.*	*	*	*	*	*	*	*	*	*	*	*	*	*		*	*		*	*	*
72	*Chroococus. sp*	*													*	*	*	*	*	*	
73	*Osci. thieb.*	*	*	*	*	*	*	*	*	*	*	*	*	*	*	*	*	*	*	*	*

Appendix. Names of phytoplankton species occured

No.	SP.	1	2	3	4	5	6	7	8	9	10	11	12	13	14	15	16	17	18	19	20	21	22	23	24
	DIATOMS																								
1	*Amphi.sp.*														*				*						*
2	*Bact. spp.*		*										*										*		*
3	*Bid. mobiliensis*		*	*							*														
4	*Bid. sins.*	*	*	*	*	*	*	*	*	*	*	*	*	*	*		*	*	*	*	*	*	*	*	*
5	*Chae. affinis*	*	*	*															*						*
6	*Chae. atlen.*	*	*							*					*				*						
7	*Chae.coar.*	*	*	*	*	*	*		*	*	*	*	*		*		*	*	*				*	*	*
8	*Chae.dent.*	*							*		*				*								*		*
9	*Chae. diversus*	*		*							*				*										*
10	*Chae. lacin.*																		*						
11	*Chae.loren.*	*	*	*	*				*	*	*		*		*				*		*	*	*	*	*
12	*Chea.peru.*		*												*										
13	*Chae.pseudo.*	*	*	*	*	*	*		*	*			*	*	*		*		*	*	*	*	*	*	*
14	*Chae.teres.*		*												*				*						
15	*Chae.torti.*					*	*				*		*	*			*								*
16	*Ceratau.pela.*		*	*	*	*	*	*	*	*	*	*	*	*	*	*	*	*	*	*	*	*	*	*	*
17	*Clima. frauenfel.*	*	*	*	*	*	*	*	*	*	*	*	*	*	*	*	*	*	*	*	*	*	*	*	*
18	*Closterium sp.*						*	*			*														
19	*Cosci.spp.*	*	*	*	*	*	*	*	*	*	*	*	*	*	*	*	*	*	*	*	*	*	*	*	*
20	*Cyclotella sp.*	*										*													*
21	*Ditylum sol*																								*
22	*Eucam.zoodi.*										*											*	*		*
23	*Fragillaria sp.*																								*
24	*Guin.flac.*	*	*	*			*							*	*				*						*
25	*Hemia. sinensis*	*	*																*				*		*
26	*Hemid.hard.*	*				*	*					*													*
27	*Laud.annu.*		*							*	*								*					*	*
28	*Lepto.dani.*				*															*			*		
29	*Melosi.sp.*		*	*		*	*	*	*		*	*	*	*	*	*			*			*			*
30	*Navi.spp.*	*	*	*	*	*	*	*	*		*	*	*	*	*	*	*	*	*	*	*	*	*	*	*
31	*Nitz.clo.*		*				*			*	*								*	*	*	*	*		
32	*Nitz.long.*		*	*		*	*			*	*	*							*					*	*
33	*Nitz.para.*														*		*		*	*	*	*	*	*	*
34	*Nitz.seriata*	*					*				*	*	*		*	*		*	*			*	*	*	*
35	*Plan.sol.*		*			*	*	*		*		*			*			*							
36	*Pleu.spp.*	*	*	*	*	*	*	*	*	*	*	*	*	*	*	*	*	*	*	*	*	*	*	*	*
37	*Rh.alata.*	*	*	*			*	*	*	*	*		*		*				*	*	*	*	*	*	*
38	*Rh.berg.*	*	*	*		*	*		*	*	*	*			*		*	*	*	*	*		*	*	*
39	*Rh.calca.*					*													*	*			*		*
40	*Rh.clev.*	*								*	*		*	*	*	*	*		*		*		*		*
41	*Rh.cylin.*						*	*										*							
42	*Rh.cochi.*	*				*	*		*						*			*	*				*	*	*
43	*Rh.hebea.*	*	*						*	*	*	*	*		*		*			*			*		*
44	*Rh.imbri.*	*	*	*					*	*	*	*	*		*				*				*	*	*
45	*Rh.robu.*	*	*				*	*	*	*	*	*			*	*			*	*	*	*	*	*	*
46	*Rh.seti.*	*		*					*		*				*				*	*			*		*
47	*Rh.stolt.*										*														*
48	*Step.palm.*									*															*
49	*Step.thum.*	*	*	*		*	*	*	*	*	*	*	*	*	*	*	*	*	*	*	*	*	*	*	*
50	*Suriella.sp.*		*				*		*																
51	*Thala.coram.*		*			*	*	*	*		*				*				*		*			*	*
52	*Thala.frauen.*	*	*	*		*	*						*				*	*	*	*	*	*	*	*	*

in all areas uncer study during Dec, 1994.

53	*Thala. hyalina*																						*
	SP.	1	2	3	4	5	6	7	8	9	10	11	12	13	14	15	16	17	18	19	20	21	22	23	24
55	*Thala. longis.*	*	*	*			*	*	*	*	*	*	*	*	*	*	*	*	*	*		*	*	*	*
56	*Thala.nitz.*	*	*	*	*	*	*	*	*	*	*	*	*	*	*			*	*	*	*	*	*	*	*
57	*Tricer.furca.*			*		*	*			*	*	*												*	*
	DINOFLAGELLATES																								
58	*Amphi. biden.*					*	*	*	*	*		*	*												
60	*Cera.belon.*			*	*	*	*	*	*	*									*		*				*
61	*Cera. candelab.*				*	*	*		*	*			*		*		*		*						
62	*Cera. carriense*			*		*	*	*	*	*			*	*	*		*		*						*
63	*Cera.dens*			*	*	*	*	*	*	*	*	*	*	*	*	*	*	*	*		*	*		*	*	*
64	*Cera.furca.*	*	*	*	*	*	*	*	*	*	*	*	*	*	*	*	*	*	*		*	*				*
65	*Cera.fusus.*	*	*	*	*	*	*	*	*	*	*	*	*		*	*	*	*	*	*	*	*	*	*	*	*
66	*Cera. gibberum*					*	*	*		*	*	*	*						*	*	*	*		*	*	*
67	*Cera.horri.*				*	*		*	*	*			*		*				*		*	*	*	*	*	*
68	*Cera.kofoi.*	*			*		*		*		*	*		*	*				*	*			*			*
69	*Cera.massi.*	*	*	*	*	*	*	*	*	*	*	*	*	*	*	*	*	*	*	*	*	*	*	*	*	*
70	*Cera.penn.*	*	*	*	*	*	*	*	*	*	*	*	*	*	*	*	*	*	*	*	*	*	*	*	*	*
71	*Cera.tricho.*	*	*	*	*	*	*	*	*	*	*	*	*	*	*	*	*	*	*	*	*	*	*	*	*	*
72	*Cera.tripos.*	*	*	*	*	*	*	*	*	*	*	*	*	*	*	*	*	*	*	*	*	*	*	*	*	*
73	*Cera.vulture.*	*	*	*	*	*	*	*	*	*	*	*	*	*	*	*	*	*	*	*	*	*	*	*	*	*
74	*Dino.caud.*	*	*	*	*	*	*	*	*	*	*	*	*	*	*	*	*	*	*	*	*	*	*	*	*	*
75	*Gonian.spp.*	*	*	*	*	*	*	*	*	*	*	*	*	*	*	*	*	*	*	*	*	*	*	*	*	*
76	*Noct.mil.*	*	*	*	*	*					*								*	*				*		*
77	*Orni.thumi.*		*		*	*	*	*	*	*	*	*	*	*	*	*	*			*	*	*					*
78	*Peri.spp.*	*	*	*	*	*	*	*	*	*	*	*	*	*	*	*	*	*	*	*	*	*	*	*	*	*
79	*Phalac. rapa*				*																					
80	*Proroc.sp.*	*	*	*			*			*	*		*	*					*			*			*	
81	*Pyro.sp.*	*	*		*	*	*	*	*	*	*	*	*	*	*	*	*	*	*	*	*	*	*	*	*	*
82	*Pyroh.horo.*		*	*	*	*	*	*	*	*	*	*	*	*	*	*		*	*	*	*	*		*		*
	SILICOFLAGELLATES																								
83	*Dichtyocha spp.*		*	*	*	*	*		*		*		*		*				*						
	BLUE GREEN ALGAE																								
84	*Anabea.sp.*	*	*	*		*	*	*	*		*	*	*	*	*	*	*		*	*	*		*	*	*
85	*Chroococus. sp*		*	*		*	*	*	*	*	*		*	*	*	*	*		*	*	*	*	*	*	*
86	*Lyngbya sp.*									*															
87	*Merismop. sp.*																	*							*
88	*Osci. thieb.*	*	*	*	*	*	*	*	*	*	*	*	*	*	*	*	*	*	*	*	*	*	*	*	*
89	*Rivularia sp.*																								*

Offshore Environment of the ROPME Sea Area after the War-Related Oil Spill, Eds. A. Otsuki *et al.*, pp. 303–318.

Distribution of Copepoda in the ROPME Sea Area 1994

M. AL-KHABBAZ and A. M. FAHMI

Environment Public Authority, P.O. Box 3043, Salmeiyah 22031, Kuwait

Abstract–Zooplankton distribution was studied in the inner part of ROPME Sea Area, during the cruise of R/V Umitaka Maru (15–27, December 1994). Twenty four plankton samples were collected vertically from four areas (seven transacts) viz. United Arab Emirates (U.A.E.), Qatar, Bahrain and Kingdom of Saudi Arabia (K.S.A.) using 100 μm. Norpac Net. The distribution of zooplankton community was studied both quantitatively and qualitatively with special reference to copepod abundance and diversity. The results showed that the highest dry weight biomass was recorded in Bahrain waters (St. 18; 102 mg/m^3) and the lowest was recorded in K.S.A. (St. 21; 17 mg/m^3). The mean biomass value for the 24 stations was 50 mg/m^3. The U.A.E. St. 1 showed the highest number, 19055 /m^3, while the lowest recorded was 906 /m^3 at St. 22 (K.S.A.). The total mean number of zooplankton for the twenty four stations was 6349 /m^3. In composition, copepods dominated the other zooplankton groups (66.6%) followed by the planktonic larvae (16.6%), crustacea (8.6%) and non-crustacea (8.2%). Of the twenty four different copepod genera recorded, *Oithona spp.* (15.8%) was the most abundant followed by *Oncaea spp.* (15.1%) and *Paracalanus spp.* (14.3%).

INTRODUCTION

The ROPME Sea Area has a water surface area of 240,000 sq. km. This shallow water body supports a rich collection of marine life, but the Gulf crises and the acute oil spill (Jan.–Feb., 1991) threatened the marine environment and affected 660 km. of the Saudi Arabian coast line. Six to eight million barrels of crude oil might have spilled into northern area of the Gulf. The EPD's annual reports (1992) indicated a significant reduction in plankton productivity. It is worth mentioning here that their study was carried out during the period when the threat of oil pollution was still in the marine environment they could start plankton sampling in October 1991 only (nine months after liberation of Kuwait). Price (1992) revealed that the mean zooplankton abundance showed no significant changes at one of the Saudi Arabian coastal stations (Ras Tanura) but at Safaniya, another station in Saudi Arabia showed low abundance of zooplankton biomass and *Penaeid* larvae. No numerical abundance of zooplankton was recorded in their study. Matthews *et al.* (1993) said that the war had a major impact on spawning stock size, which was reduced to a very low level in 1992. Mt. Mitchell had cruised for 100 days in the Gulf in 1992 to monitor the impact of oil spill. The results of this survey published by Al-Yamani *et al.* (1993) showed that there was no serious threat on zooplankton community as a result of oil spill.

Many research papers are available on the distribution and abundance of zooplankton in the Gulf waters (Fronter, 1963; Kimor, 1973; Yamazi *et al.*, 1974; Jacob *et al.*, 1979, 1982; Gibson *et al.*, 1980; E.P.D Annual Reports, 1982–1990, 1991–1994; Mitchell *et al.*, 1986; Fahmi *et al.*, 1986; Price, 1979, 1982, 1991; Matthews *et al.*, 1992; Al-Yamani *et al.*, 1994a, b; Faraj, 1993).

STUDY SITES, NUTRIENTS, PHYSICAL AND CHEMICAL PARAMETERS

Areas off U.A.E.: (25°00.30′ N–25°15.73′ N and 54°35.80′ E–52°45.24′ E)

Ten samples were collected from Stns. 1–10 during 15–19 Dec. 1994. Sampling depth varied between 21–73 m. Water temperature was in the range of 23.74–25.34°C, salinity value was in the range of 38.92–41.75, pH value of sea water was in the range of 7.82–8.23, silicate value ranged between 1.82–3.76 µmol/l, while phosphate and nitrate values were in range of 0.41–0.64 µmol/l and 0.15–2.28 µmol/l, respectively, Chlorophyll *a* value varied between 0.56–1.81 µg/l and dissolved oxygen ranged between 3.62–4.53 ml/l.

Areas off Qatar: (26°13.85′ N–26°57.34′ N and 51°34.89′ E–52°14.41′ E)

Four samples were collected from Stns. 11–14 during 19–20 Dec. 1994. Sample depths varied between 25–70 m. Water temperature varied from 22.41–23.9°C, salinity was in the range of 39.71–40.58, pH varied between 8.18–8.24, silicate was in the range of 2.28–3.28 µmol/l, while phosphate and nitrate ranged between 0.39–0.56 µmol/l and 0.11–1.45 µmol/l, respectively, and Chlorophyll *a* values were in the range of 0.34–1.05 µg/l.

Areas off Bahrain: (26°16.10′ N–26°34.90′ N and 51°41.40′ E–50°54.90′ E)

Four samples were collected from Stns. 15–18 during 21–23 Dec. 1994. Sampling depths varied from 22–72 m. Water temperature varied between 22.81–23.25°C, whereas salinity was in the range of 37.70–40.23, pH was in the range of 8.17–8.21, dissolved oxygen ranged between 2.95–4.66 ml/l, phosphate values were in the range of 0.45–0.56 µmol/l, and also the nitrate value ranged between 0.63–0.98 µmol/l, while the silicate value was in the range of 2.74–4.20 µmol/l and Chlorophyll *a* concentration varied between 0.29–1.05µg/l.

Areas off Kingdom of Saudi Arabia: (27°15.14′ N–27°47.88′ N and 50°19.29′ E–49°23.70′ E)

Six samples were collected from Stns. 19–24 during 24–25 Dec. 1994. Sampling depths were in the range of 24–68 m. Water temperature varied between 19.9–23.0°C, pH value was in the range of 8.03–8.15, salinity was in the range of 33.66–40.72, dissolved oxygen values ranged from 3.79–5.02 ml/l, and phosphate values were in the range of 0.40–0.58 µmol/l, whereas the silicate values ranged from 2.89–5.21 µmol/l, nitrate values were in the range of 0.07–2.08 µmol/l and chlorophyll *a* values were in the range of 0.50–1.76 µg/l.

The above parameters, shown in the areas (A–D), were analysed in situ in the R/V Umitaka Maru and the results were supplied to all participants (for the

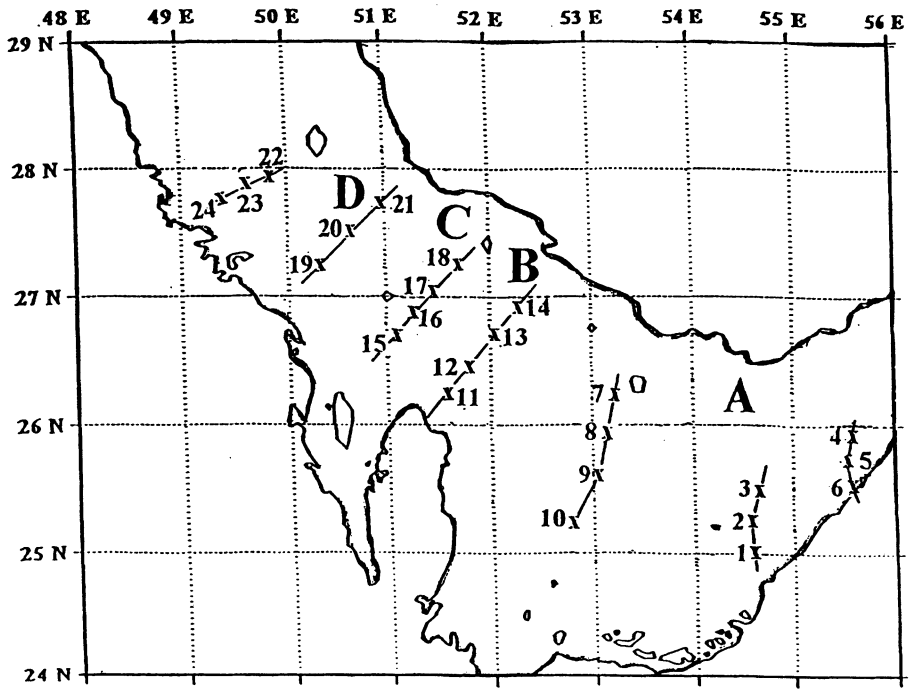

Fig. 1. Distribution of sampling sites in the ROPME Sea Area, 1994.

methedology, refer to the Cruise Report).

MATERIAL AND METHODS

The twenty four samples collected from twenty four stations belonged to four ROPME Sea Areas viz, United Arab Emirates (U.A.E.), Qatar, Bahrain and Kingdom of Saudi Arabia (K.S.A.) (Fig. 1). The sampling time was during the day hours between 15–27 Dec., 1994. The samples were collected vertically with a Norpac Plankton Net having a mesh size of 100 μm. and its mouth diameter was 45 cm. The volume of sea water filtered was measured with a flow meter fitted to the net mouth. The collected samples were preserved in 5% formalin solution. Motoda plankton sample splitter was used for splitting the sample (Motoda, 1959), one part was used for identification and counting (no./m^3), while the other part was filtered and measured for dry weight biomass (mg/m^3) (EPA, 1983).

RESULT AND DISCUSSION

A total of twenty four copepod genera was recorded during this study of which sixteen were calanoids, five were cyclopoids and three were harpacticoid copepods. The calanoid copepods were the dominant group constituting (42.5%),

Table 1. Vertical distribution of zooplankton, biomass and chlorophyll *a* in ROPME Sea Area, Dec. 1994.

St.	COPEPODA		O. CRUST.		NON - CRUST.		PLANKT. LAR.		TOTAL	BIOM.	Chl. *a*
	no./m3	%	no./m3	%	no./m3	%	no./m3	%	no./m3	mg./m3	*uM/l*
1	12192	64	645	3.4	3611	19	2607	13.6	19055	61	0.56
2	9135	69.4	358	2.7	1654	12.6	2011	15.3	13158	91	0.67
3	6865	62.6	1397	12.7	986	9	1726	15.7	10974	54	0.75
4	5202	73	469	6.6	609	8.6	843	11.8	7123	41	0.61
5	5472	56.9	1254	13	872	9.1	2017	21	9615	22	0.68
6	7856	66.6	557	4.7	557	4.7	2829	24	11799	53	1.81
7	3199	57.3	962	17.2	178	3.2	1247	22.3	5586	42	0.83
8	4863	78.6	401	6.5	320	5.2	601	9.7	6185	43	1.13
9	3824	70.4	425	7.8	299	5.5	882	16.3	5430	31	0.83
10	4714	69.6	376	5.6	627	9.3	1053	15.5	6770	66	0.84
11	4093	65	85	1.4	212	3.4	1910	30.2	6300	54	0.87
12	2901	64	766	16.9	340	7.5	528	11.6	4535	57	0.34
13	3088	80.1	310	8	162	4.2	297	7.7	3857	42	0.47
14	8444	75.8	676	6.1	394	3.5	1632	14.6	11146	101	1.05
15	2886	65.7	552	12.6	257	5.8	699	15.9	4394	54	0.68
16	3676	59.9	955	15.6	215	3.5	1289	21	6135	70	0.97
17	1862	57.1	793	24.3	147	4.5	458	14.1	3260	23	0.29
18	3429	71.6	509	10.6	170	3.6	679	14.2	4787	102	1.7
19	835	68.5	192	15.8	57	4.7	135	11	1219	21	0.61
20	679	54	361	28.7	63	5	155	12.3	1258	25	0.5
21	1038	65.9	284	18	83	5.3	170	10.8	1575	17	0.63
22	568	62.7	116	12.8	74	8.2	148	16.3	906	24	0.96
23	1819	58.9	623	20.2	204	6.6	444	14.3	3090	56	1.21
24	2828	67.2	118	2.8	382	9.1	882	20.9	4210	47	1.76
MEA.	4228	66.6	549	8.6	520	8.2	1052	16.6	6349	50	0.86

followed by the cyclopoids (40.0%) and the harpaticoids (9.6%). The dominant copepod genera was *Oithona spp.* (15.8%) followed by *Oncaea spp.* (15.1%) and *Paracalanus spp.* (14.3%) (Table 2, Figs. 2 and 3). The copepods recorded in the area of U.A.E. (St. 1; 12192/m^3) were the highest in the ROPME Sea Area, while the lowest was recorded in K.S.A. (St. 22; 568/m^3) (Fig. 4), whereas the mean total number for the 24 stations was 4228/m^3. The biomass (dry wt.) value was measured high in Bahrain area (St. 18; 102 mg/m^3), while it was recorded low in K.S.A. (St. 21; 17 mg/m^3) (Table 1).

The copepod population at U.A.E. stations was in the range of 3199/m^3–

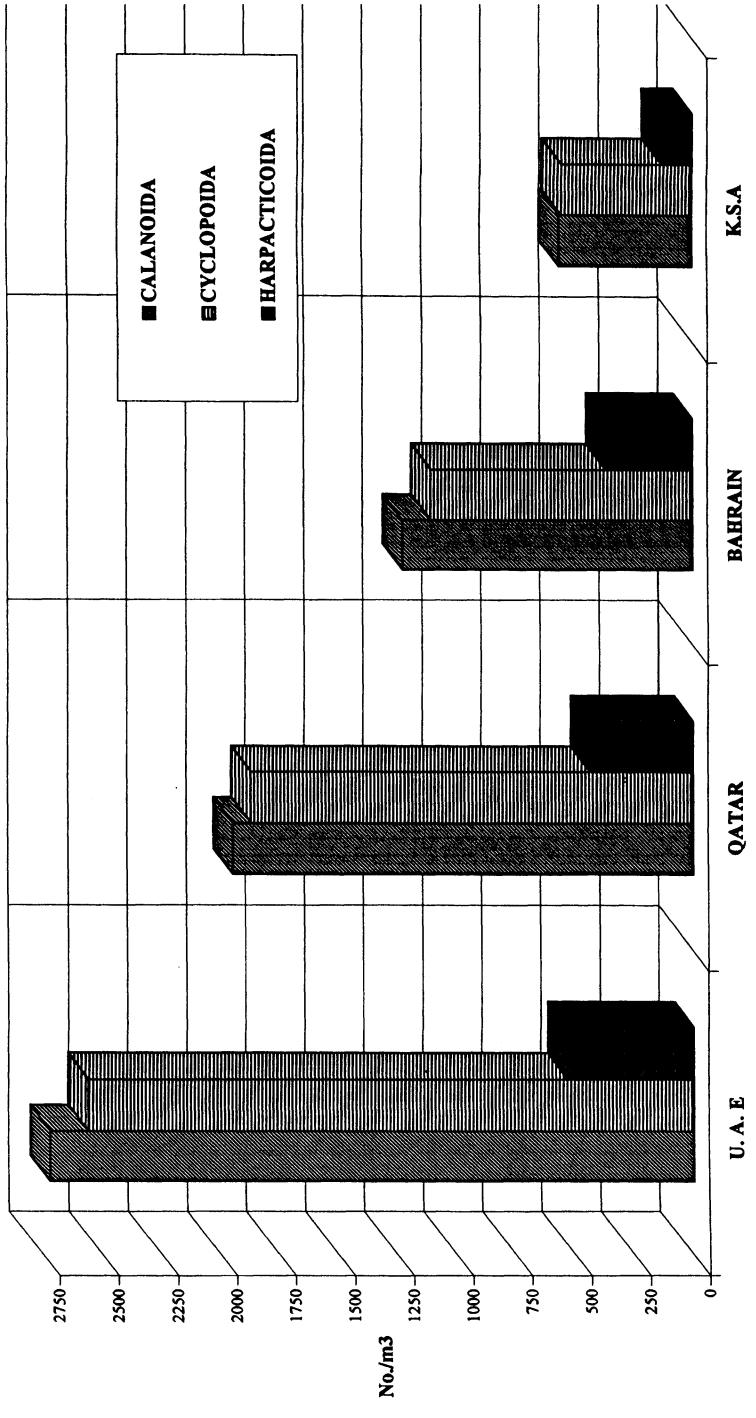

Fig. 2. The mean total number of copepod groups recorded in the investigated areas.

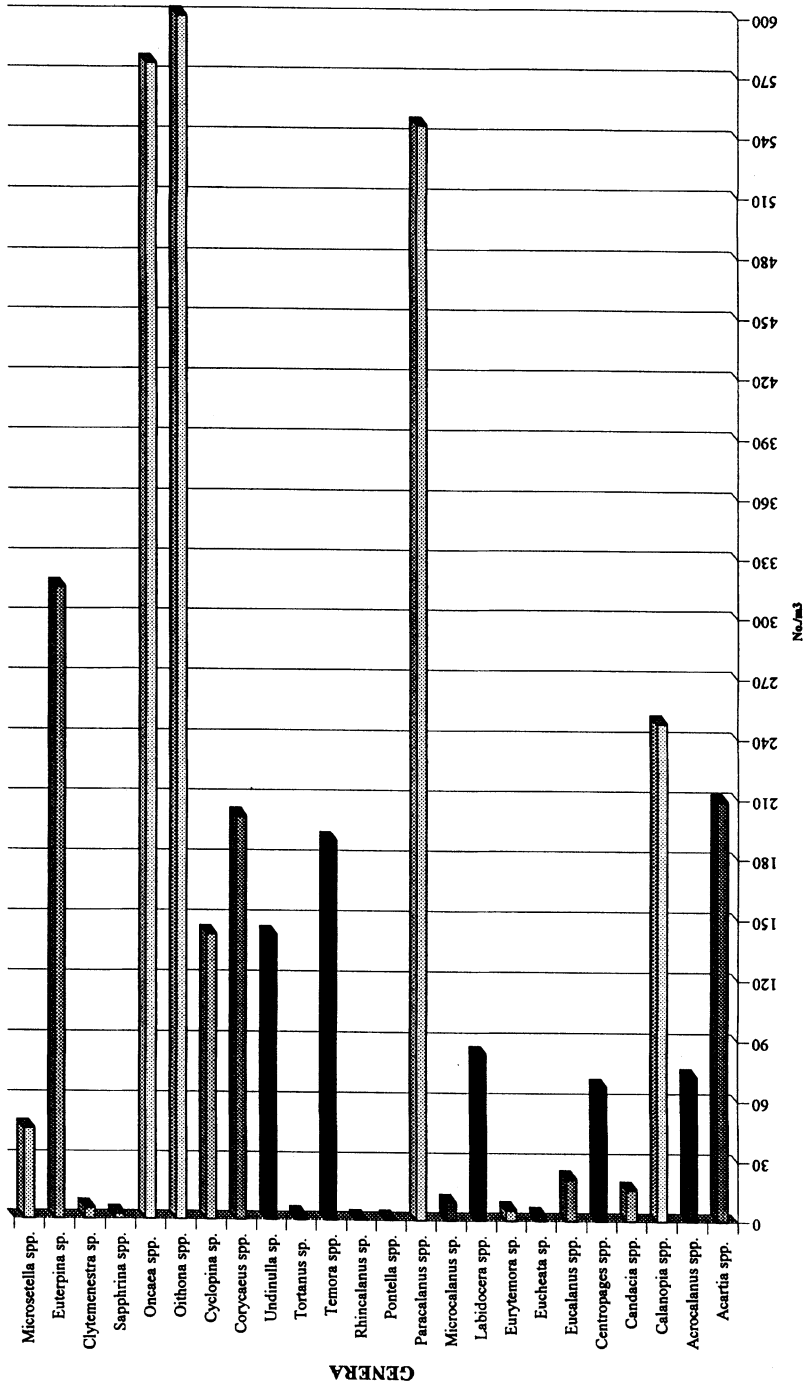

Fig. 3. Mean number of copepod genera recorded in the ROPME Sea Area.

Table 2. Mean distribution of copepod genera in ROPME Sea Area, Dec. 1994.

NO	GENERA	COMMON COPEPODS	U. A. E		QATAR		BAHRAIN		K.S.A		MEAN	
			no./m3	%	no./m3	%	no./m3	%	no./m3	%	no./m3	%
1	*Acartia spp.*	**	384	6.1	253	5.4	88	3	111	8.6	209	5.5
2	*Acrocalanus spp.*	**	193	3.1	17	0.4	55	1.9	24	1.9	72	1.9
3	*Calanopia spp.*		203	3.2	407	8.8	290	9.8	95	7.3	248	6.5
4	*Candacia spp.*	**	25	0.4	21	0.5	13	0.4	4	0.3	16	0.4
5	*Centropages spp.*	**	93	1.5	96	2.1	68	2.3	12	0.9	67	1.7
6	*Eucalanus spp.*	**	30	0.5	43	0.9	9	0.3	3	0.2	21	0.6
7	*Eucheata sp.*		0	0	0	0	0	0	11	0.9	3	0.1
8	*Eurytemora sp.*		6	0.1	0	0	0	0	16	1.2	6	0.2
9	*Labidocera spp.*	**	145	2.3	104	2.2	66	2.2	17	1.3	83	2.2
10	*Microcalanus sp.*		36	0.6	0	0	0	0	0	0	9	0.2
11	*Paracalanus spp.*	****	1163	18.4	538	11.6	375	12.6	107	8.3	546	14.3
12	*Pontella spp.*		3	0.1	0	0	0	0	0	0	1	0.1
13	*Rhincalanus sp.*		0	0	4	0.1	0	0	0	0	1	0.1
14	*Temora spp.*	**	283	4.5	233	5	152	5.1	90	6.9	189	5.0
15	*Tortanus sp.*		6	0.1	3	0.1	0	0	1	0.1	3	0.1
16	*Undinulla sp.*		154	2.4	230	5	112	3.8	72	5.6	142	3.7
	TOTAL CALANOIDA		2724	43.3	1949	42.1	1228	41.4	563	43.5	1616	42.5
17	*Corycaeus spp.*	**	413	6.5	152	3.3	144	4.9	95	7.3	201	5.3
18	*Cyclopina sp.*	**	237	3.7	202	4.3	98	3.3	32	2.5	142	3.7
19	*Oithona spp.*	****	1126	17.8	748	16.1	310	10.5	225	17.4	602	15.8
20	*Oncaea spp.*	****	780	12.3	770	16.6	555	18.7	200	15.4	576	15.1
21	*Sapphrina spp.*		9	0.1	0	0	0	0	1	0.1	3	0.1
	TOTAL CYCLOPOIDA		2565	40.4	1872	40.3	1107	37.4	553	42.7	1524	40.0
22	*Clytemenestra sp.*		0	0	17	0.4	0	0	5	0.4	6	0.2
23	*Euterpina sp.*	**	463	7.3	373	8.1	334	11.3	90	6.9	315	8.2
24	*Microsetella spp.*	**	72	1.1	45	1	32	1.1	34	2.6	46	1.2
	TOTAL HARPACTIPOIDA		535	8.4	435	9.5	366	12.4	129	9.9	367	9.6
	Copepodites		509	8	377	8.1	262	8.8	50	3.9	299	7.9
	TOTAL no./m3		6333		4633		2963		1295		3806	
	DIVERSITY		21		19		16		21		24	

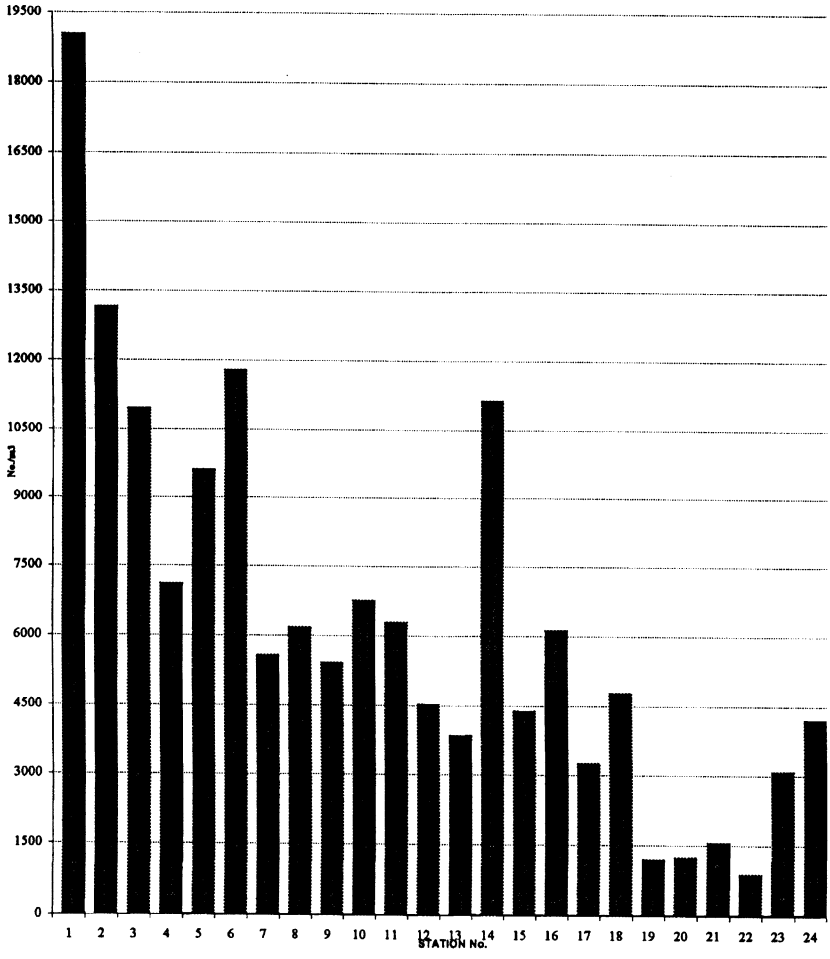

Fig. 4. Total number of zooplankton recorded in ROPME Sea Area, 1994.

12192/m³ (St. 7 and 1). *Paracalanus spp.*, *Corecaeous sp.*, *Euterpina sp.*, *Oncaea sp.* and *Oithona spp.* were found present in all the stations. This result showed that *Paracalanus spp.* (1163/m³) were the most dominant genera in U.A.E. waters closely followed by *Oithona spp.* (1126/m³) (Fig. 5a). The biomass values ranged between 22–91 mg/m³ and the diversity was 21 (Tables 1 and 2). Chlorophyll *a* value was higher (0.56–1.81 µg/l). Inspite of oil spill in the Gulf waters, the zooplankton population did not show any significant low abundance. This finding is in agreement with the other investigators in this area viz, Al-Yamani *et al.* (1994).

Table 3. Correlations between zooplankton counts and biomass, also with chlorophyll *a*.

St.	TOTAL	BIOM.	Chl. *a*	T.TEST		
	no./m3	mg./m3	*uM/l*	TOT/BIO	TOT/CHL	BIO/CHL
1	19055	61	0.56	1.73E-07	1.53E-07	3.86E-10
2	13158	91	0.67	4.08E-08	3.55E-08	1.47E-09
3	10974	54	0.75	4.66E-08	4.06E-08	2.77E-09
4	7123	41	0.61	8.53E-08	7.44E-08	1.02E-08
5	9615	22	0.68	2.81E-07	2.47E-07	3.01E-08
6	11799	53	1.81	6.51E-07	5.7E-07	4.15E-08
7	5586	42	0.83	4.38E-07	3.8E-07	1.46E-07
8	6185	43	1.13	1.49E-06	1.3E-06	4.21E-07
9	5430	31	0.83	4.88E-06	4.29E-06	1.21E-06
10	6770	66	0.84	1.56E-05	1.38E-05	2.39E-06
11	6300	54	0.87	4.6E-05	4.11E-05	8.42E-06
12	4535	57	0.34	0.000136	0.000123	2.73E-05
13	3857	42	0.47	0.000373	0.00034	8.83E-05
14	11146	101	1.05	0.000902	0.000829	0.000224
15	4394	54	0.68	0.000231	0.00021	0.00039
16	6135	70	0.97	0.000756	0.000693	0.001214
17	3260	23	0.29	0.001069	0.000984	0.003476
18	4787	102	1.7	0.003567	0.003304	0.006009
19	1219	21	0.61	0.006599	0.006223	0.002564
20	1258	25	0.5	0.012619	0.012036	0.005941
21	1575	17	0.63	0.024015	0.023185	0.016309
22	906	24	0.96	0.054477	0.053111	0.024927
23	3090	56	1.21	0.049132	0.048478	0.028146
24	4210	47	1.76	#DIV/0!	#DIV/0!	#DIV/0!

There were 19 copepod genera recorded in the areas off Qatar. The highest number of copepod genera *Oncaea spp.* (2195/m^3) was recorded at St. 14 followed by *Oithona spp.* (1689/m^3) and *Calanopia sp.* (1126/m^3). The highest number of total copepods (8444/m^3) was also recorded at this station. The mean total of copepods for the four stations of Qatar was 4633/m^3. The highest biomass value was 101 mg/m^3 and the highest zooplankton count was 11,146/m^3 (Tables 1 and 2, and Fig. 5b).

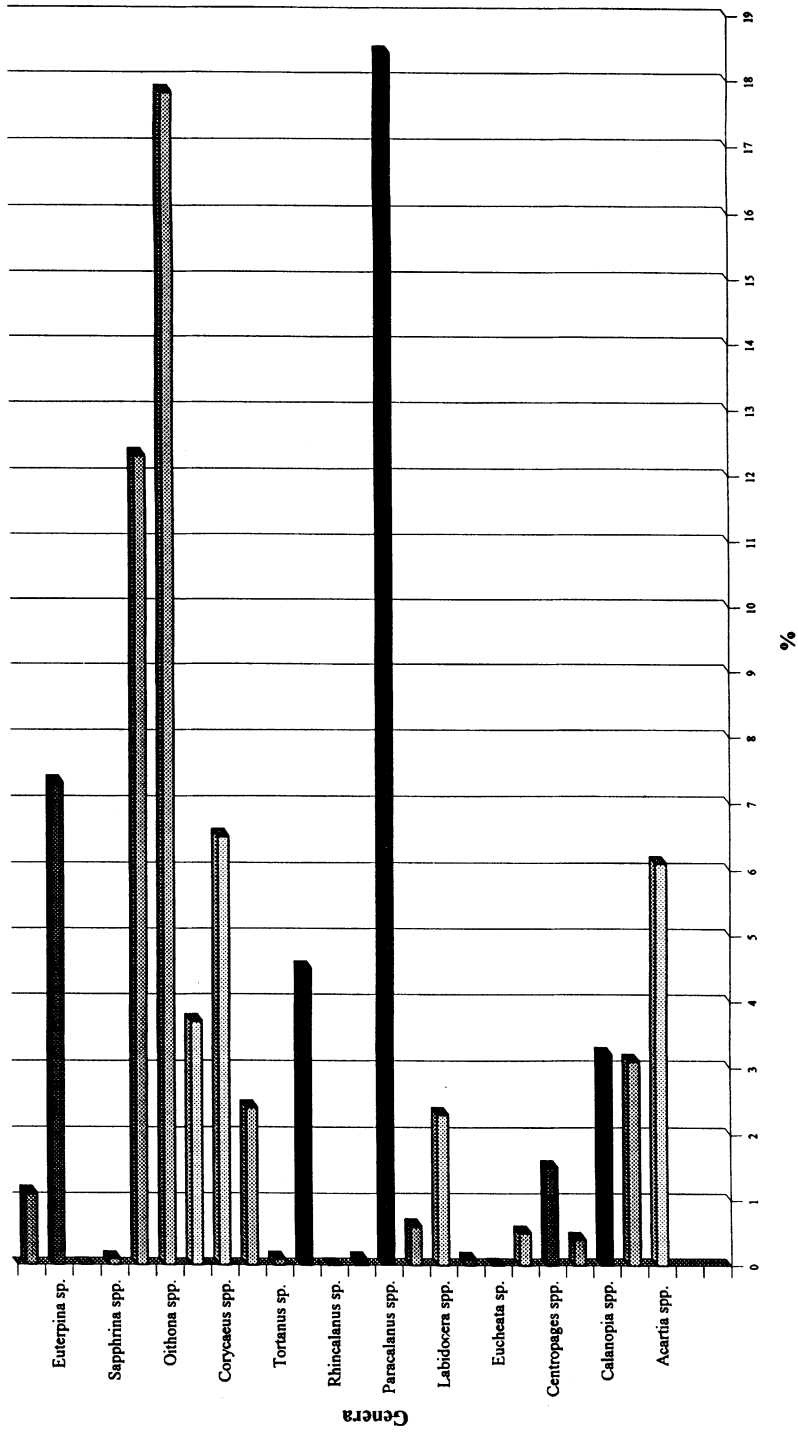

Fig. 5(a). Percent composition of copepod genera in areas off Qatar 1994.

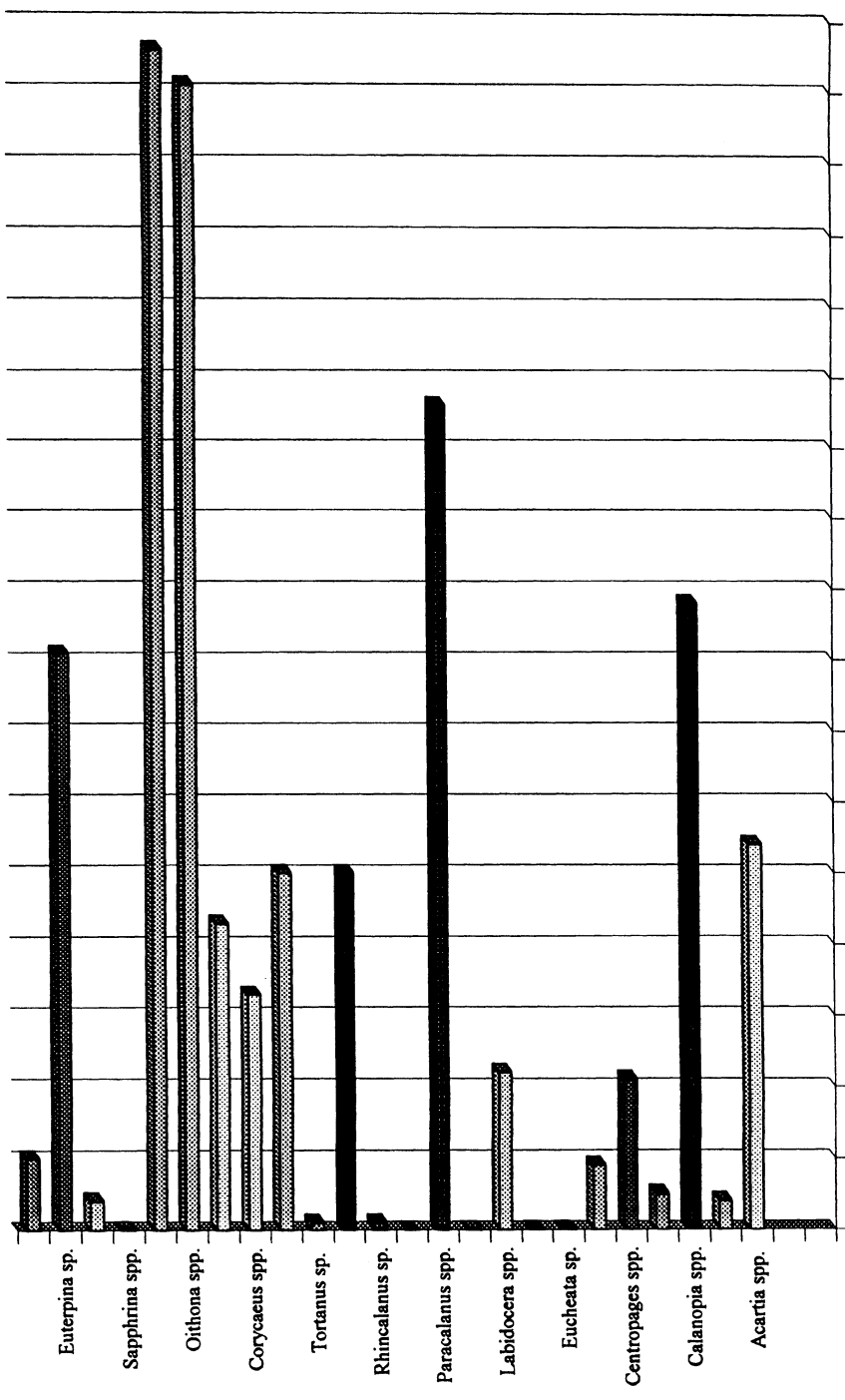

Fig. 5(b). Percent composition of copepod genera in areas off Qatar 1994.

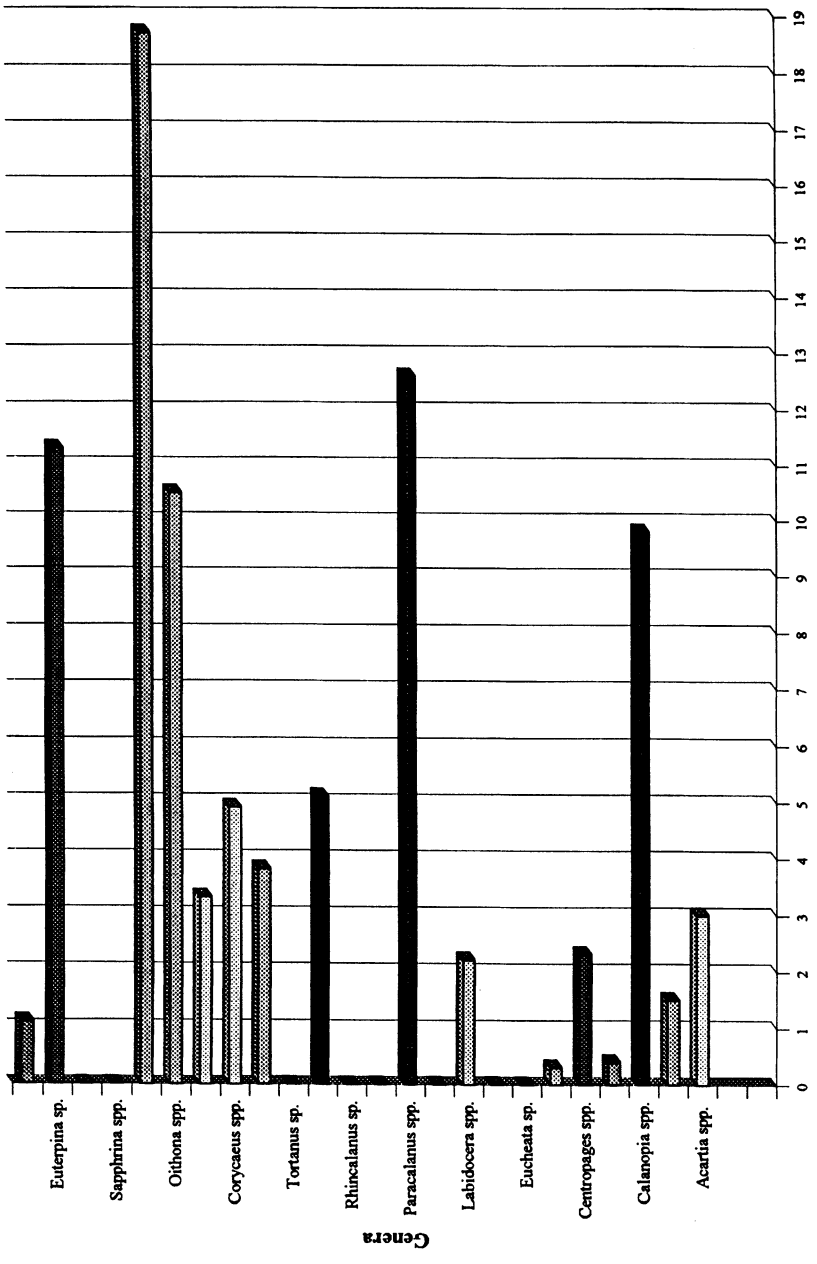

Fig. 5(c). Percent composition of copepod genera in areas off Bahrain 1994.

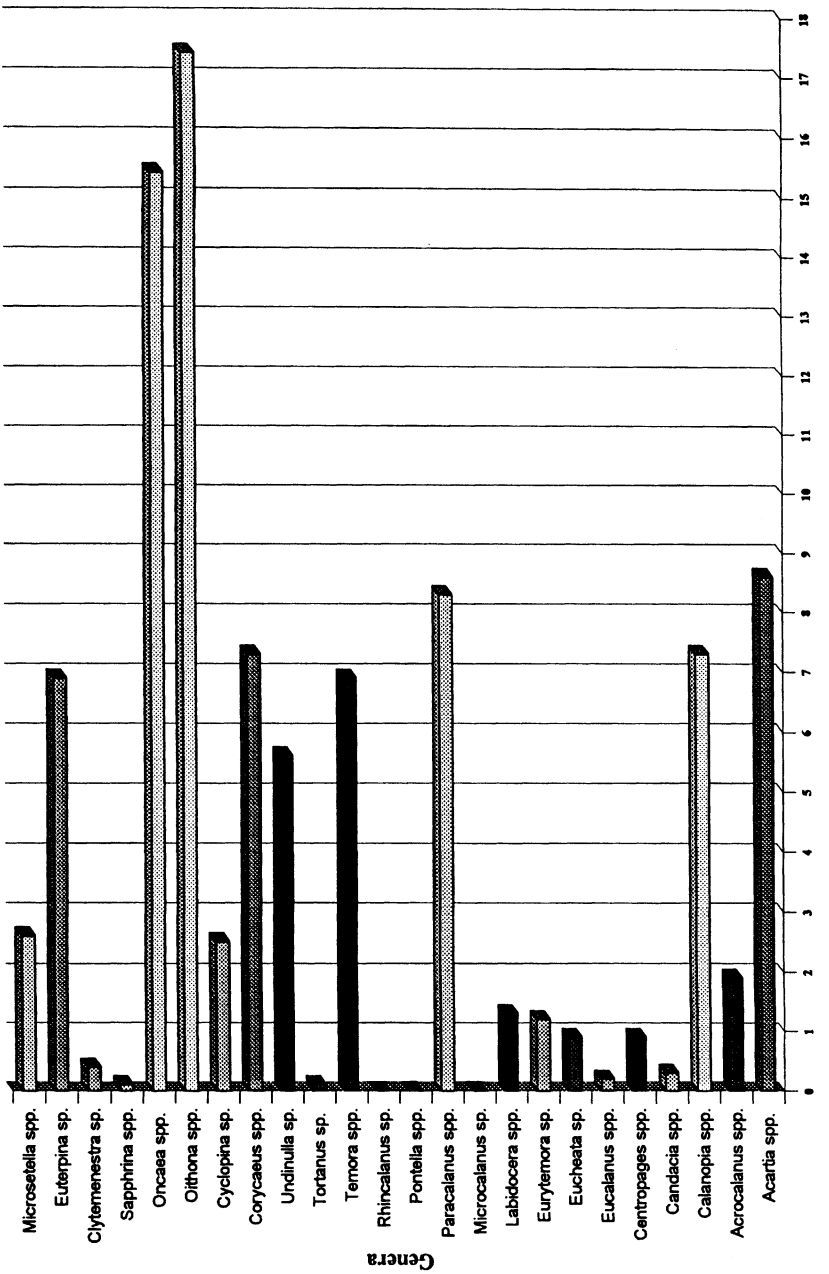

Fig. 5(d). Percent composition of copepod genera in areas off K.S.A. 1994.

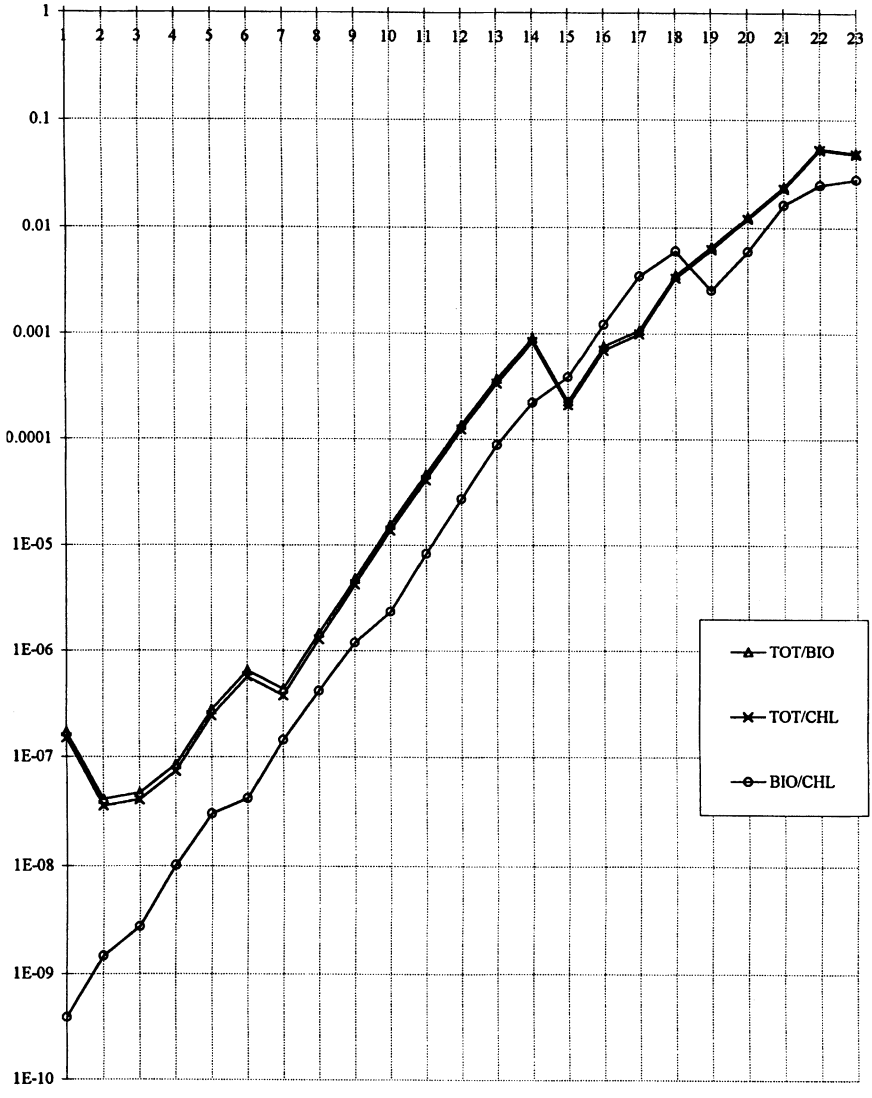

Fig. 6. T. Test correlations curves.

The results at the four stations of Bahrain revealed that copepod population was in the range of 8–788/m³. The lowest No. 8/m³ (*Candacia sp.*) was recorded at St. 17, and the highest No. 788/m³ (*Oncaea spp.*) was recorded at St. 16. A total of 16 genera was recorded in the areas off Bahrain. The mean value of biomass was 62.25 mg/m³ (range of 23–102 mg/m³). The total zooplankton counts were in

the range of 1862–3676/m³ (St. 17 and 16, respectively) (Tables 1 and 2, and Fig. 5c).

The total number of copepod genera receded in the areas off K.S.A. were 21 of which the common copepods were *Acartia spp.*, *Calanopia spp.*, *Centropages spp.*, *Paracalanus spp.*, *Undinulla sp.*, *Corycaeus spp.*, *Oithona spp.*, and *Oncaea spp.* They ranged from 568/m³ (St. 22)–2828/m³ (St. 24). The mean value of biomass recorded was 5.5 mg/m³ (range of 17.0 mg/m³ (St. 21)–56.0 mg/m³ (St. 23)) (Table 2 and Fig. 5d).

This study showed a significant correlation (T. Test) between the total number of zooplankton and biomass, and also showed a similar correlation between total number and chlorophyll *a* (Table 3 and Fig. 6).

The oil spill that occurred in the Kuwait area was during Jan.–Feb. 1991 and EPD's biomonitoring and plankton sampling started nine months after the liberation of Kuwait, meanwhile a major part of volatile toxic hydrocabons might have evaporated with approach of heat during the hotter months. Secondly, the currents of water and wave action might have transported the pollutants to the other areas of the Gulf. All of these factors might have helped to reduce the intensity of toxic effect of oil spill.

In conclusion, the aim of this study was to find out the general distribution of copepods at this specific short period (15–27 Dec. 1994) only. No attempt has been made to record all the copepod genera present in the areas under study. The number of copepod genera recorded during this study doesn't reflect all the copepod genera present in the area, and there may be more than what were recorded here. To get a more clear picture of the standing stock of copepods in ROPME Sea Area, a regular monitoring of the zooplankton population in their species level is suggested.

Acknowledgements

We are thankful to Dr. Saud Al-Rasheed, head of the Environment Protection Department for his encouragement during the study. We are indebted to Ms. Mona Faraj, superintendent of Soil Pollution and Biological Resources of EPD for her kind advice and critical review of the manuscript. We are thankful to all the colleagues of Plankton laboratory for their co-operation.

REFERENCES

Al-Yamani, F. Y. *et al*: Post-spill zooplankton distribution in the North-West Gulf. *Mar. Poll. Bull.* 27: 239–243 (1993).

Al-Yamani, F. Y., A. M. Fahmi, W. Ismail, K. Al-Rifaie and H. Al-Mutairi: MFD, KISR: Gulf war impact on zooplankton species diversity and its implication to fisheries. The International Conference on the Effects of the Iraqi Aggression on the State of Kuwait. 2–6 Apr., Kuwait (1994a).

Al-Yamani, F. Y., A. M. Fahmi, W. Ismail and K. Al-Rifaie: Post oil spill parasitism of copepods from North-Western Arabian Gulf, including first record of Ellobiopsis (1994b).

Environmental Protection Department (EPD): Ministry of Public Health, Kuwait. Annual Reports of EPD (1982–1990) and (1991–1994).

Fahmi, A. M., B. Habashi and M. Y. Abdul Raheem (Environmental Protection Department,

Ministry of Public Health, Kuwait): Monthly variations of zooplankton in the coastal waters of Kuwait. The Ninth Shrimp and Fin Fisheries Management Workshop, Kuwait. 7–9 Dec. (1987).

Faraj, M., H. Murad, M. Al-Moak, H. Al-Qallaf and S. Bu-Ramanah: Impacts of the Gulf environmental catastrophe on Fishery Resources of Kuwait. Paper presented in the international conference on the effects of the Iraqi aggression on the state of Kuwait. 2–6 Apr. (1994).

Jacob, P. G.: Report on Chlorophyll *a*, phytoplankton and zooplankton investigations in the coastal waters of Kuwait. Marine Pollution Program. EES, KISR (1978).

Jacob, P. G. and M. A. Zarba: Observations on plankton and related features of Kuwait waters. Marine Pollution Program. EES, KISR (1979).

Kimor, B.: Plankton relations of the Red Sea, Persian Gulf and Arabian Sea. pp. 221–232. In: *The Biology of the Indian Ocean*, B. Zeitschel (ed.). Springer-Verlag, N.Y. (1973).

Lindon, O., M. Y. Abdul Raheem *et al.*: State of marine environment in the ROPME Sea Areas. UNEP. Regional Seas Report and Studies No. 112 Rev. 1 UNEP (1990).

Matthews, C. P., Kedidl, S., Fitta, N. I., Al-Yahya, A. A. and Al-Rasheed: A preliminary assessment of the effects of the 1991 Gulf war on Saudi Arabia Prawn stock. *Mar. Poll. Bull.* 27: 251–271 (1991).

Michel, H. B., M. Behbehani, M. Herring, D. Arar, M. Shoushani, and T. C. Brakoniecki: Zooplankton of the western Arabian Gulf South of Kuwait waters. *Kuwait Bull. Mar. Science* 8: 1–86 (1986).

Motoda, S.: Devices of simple plankton apparatus. Memoirs of the Faculty of Fisheries, Hokkaido University 7: 73-94 (1959).

Price, A. R. G.: Temporal variations in abundance of Penaeid shrimp larvae and oceanographic conditions of Ras Tanura. *Western Arabian Gulf. East and Coast Mar.* 4: 451–465 (1979).

Price, A. R. G.: Distribution of Penaeid shrimp larvae along the Arabian Gulf Coast of Saudi Arabia. *J. Nat. Hist.* 16: 745–757 (1982).

Price, A. R. G., C. P. Matthews, R. W. Ingle and K. Al-Rashed: Abundance of zooplankton and Penaeid shrimp larvae in the western Gulf: Analysis of pre-war and post-war data (1991).

Index